

3rd YEAR'S REPORT
(June 1, 1993-September, 1994)
(Sections I and II)

ON

*DESIGN AND PROCESSING
OF MATERIALS
BY BIOMIMICKING*

(AFOSR-91-0281)
SECTION - II: PUBLICATIONS

Submitted to
Air Force Office of Scientific Research
Bolling Air Force Base
Washington, DC.

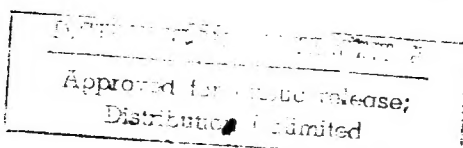
Attn. Dr. Frederick Hedberg

by

19941128 038

Mehmet Sarikaya* and James T. Staley#

*Department of Materials Science and Engineering
and #Department of Microbiology
University of Washington, Seattle, WA 98195



REPORT DOCUMENTATION PAGE

Form Approved
OMB No. 0704-0188

Public reporting burden for this collection of information is estimated to average 1 hour per response, including the time for reviewing instructions, searching existing data sources, gathering and maintaining the data needed, and completing and reviewing the collection of information. Send comments regarding this burden estimate or any other aspect of this collection of information, including suggestions for reducing this burden, to Washington Headquarters Services, Directorate for Information Operations and Reports, 1215 Jefferson Davis Highway, Suite 1204, Arlington, VA 22202-4302, and to the Office of Management and Budget, Paperwork Reduction Project (0704-0188), Washington, DC 20503.

1. AGENCY USE ONLY (Leave blank)	2. REPORT DATE	3. REPORT TYPE AND DATES COVERED FINAL 01 Jun 91 TO 31 May 94
4. TITLE AND SUBTITLE	5. FUNDING NUMBERS	

MATERIALS DESIGN AND PROCESSING BY BIOMIMICKING

AFOSR-91-0281

6. AUTHOR(S)

Dr Mehmet Sarikaya and James T. Staley

61102F

2303/DS

7. PERFORMING ORGANIZATION NAME(S) AND ADDRESS(ES)

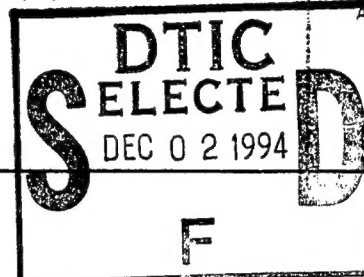
Dept of Materials Science & Engineering
University of Washington
Roberts Hall, FB-10
Seattle WA 98195

8. PERFORMING ORGANIZATION
REPORT NUMBER

AFOSR-TR 94 0694

9. SPONSORING/MONITORING AGENCY NAME(S) AND ADDRESS(ES)

AFOSR/NL
110 Duncan Ave Suite B115
Bolling AFB DC 20332-0001
Dr Hedberg

10. SPONSORING/MONITORING
AGENCY REPORT NUMBER

11. SUPPLEMENTARY NOTES

12a. DISTRIBUTION/AVAILABILITY STATEMENT

Approved for public release;
distribution unlimited.

12b. DISTRIBUTION CODE

A

13. ABSTRACT (Maximum 200 words)

The goal of this research has been to find dispersants for ceramic processing applications. The polyelectrolytes currently in use in the industry are synthesized from toxic precursors which present health hazards to workers. We have investigated polyelectrolytes produced from natural sources such as bacteria and kelp, as well as some polymers which have been produced synthetically. The polyelectrolytes which we have investigated include polysaccharides (alginate and dextran) and polypeptides (polyglutamic acid and polyaspartic acid). Some have been obtained from cultures of bacteria grown in our laboratories, others have been obtained from chemical supply houses. In addition, we have investigated the feasibility of using an in situ process by which we incubate the polymer-producing bacteria in the presence of ceramic powders. In this system, polymer adsorbs to the powder in a high affinity state, allowing subsequent washing to remove the bacterial cells, while retaining the adsorbed polymer.

DTIC QUALITY INSPECTED 5

14. SUBJECT TERMS	15. NUMBER OF PAGES		
17. SECURITY CLASSIFICATION OF REPORT (U)	18. SECURITY CLASSIFICATION OF THIS PAGE (U)	19. SECURITY CLASSIFICATION OF ABSTRACT (U)	20. LIMITATION OF ABSTRACT (U)

Section - II

(Section-I includes Research Results,
Publications, Presentations, and Talks)

Accesion For	
NTIS	CRA&I
DTIC	TAB
Unannounced	
Justification _____	
By _____	
Distribution / _____	
Availability Codes	
Dist	Avail and/or Special
A-1	

***DESIGN AND PROCESSING OF MATERIALS
BY BIOMIMICKING***

CONTENTS	Page
1. Summary	3
2. Brief Description of Research Accomplishments and Future Studies	4
2.1 Use of Biopolymers in Ceramic Processing	4
2.1.1 Selection and Biological Production of Biopolymers -- Tao Ren	4
2.1.2 Processing of Ceramics with Biopolymers -- Hsien-Liang Ker	11
2.2 The Use of Citric Acid in Ceramic Processing -- Tao Ren	18
2.3 The Use of Polymers in Ceramic Processing: A Comparison of Synthetic and Bio-Polymers for Safety Concerns - Sima F. Hashemifar	22
2.4 Mechanical properties of Biological Composites -- Bejamin Shapiro	29
2.5 Biological Synthesis of Ultrafine Magnetite Particles - Nancy Pellerin	38
2.6 Lessons From Biology: Structures and Properties of Biocomposites	42
Daniel Frech	
3. Publications and Presentations	53
3.1 Publications	53
3.2 Presentations: Invited Talks, Conferences, Workshops	57
3.3 Patents	62
3.4 News Clippings	62
4. Personnel	63
5. Appendices	64
Copies (reprints and preprints) of publications, tables of contents of edited proceedings, and news clippings	

3. Publications and Presentations

3.1 Publications

Proceedings Edited:

1. **Hierarchically Structured Materials**, Proceedings of an MRS Symposium, edited by Ilhan A. Aksay, E. Baer, M. Sarikaya, and D. A. Tirrell, Vol. 228, 1-450 (Materials Research Society, Pittsburgh, PA, 1992).
2. **Resolution in Microscopy**, Special Issue of *Ultramicroscopy*, 47, [1-3] 1-306 (Elsevier, Amsterdam, 1992); edited by M. Sarikaya.
3. **Determination of Nanoscale Physical Properties of Materials by Microscopy and Spectroscopy**, Proc. of MRS Symposium, edited by M. Sarikaya, K. Wickramasinghe, and M. Isaacson, Vol. 332 (Materials Research Society, Pittsburgh, PA, 1994) (80 papers and 700 pages).

Published Manuscripts and Those in the Works:

1. M. Sarikaya and I. A. Aksay, "Nacre of Abalone Shell: A Natural Multifunctional Nanolaminated Ceramic-Polymer Composite Material," Chapter 1, in *RESULTS AND PROBLEMS IN CELL DIFFERENTIATION*, Vol. 19: *Structure, Cellular Synthesis, and Assembly of Biopolymers*, edited by Steven Case (Springer and Verlag, Amsterdam, 1992) pp. 1-25.
2. I. A. Aksay and M. Sarikaya, "Bioinspired Processing of Composite Materials," in *Ceramics: Toward the 21st Century, Centennial International Symposium*, edited by N. Soga and A. Kato (Ceramic Society of Japan, Tokyo, 1991) pp. 136-149.
3. J. Liu, M. Sarikaya, and I. A. Aksay, "Hierarchical twin Structures in the Nacre of Red Abalone Shell," *49th Ann. Meeting of Electron Microscopy Society of America*, edited by G. W. Bailey (San Francisco Press, San Francisco, 1991) pp. 848-849.
4. M. Sarikaya and I. A. Aksay, "Synthetic and Biological Nanocomposites," *Proc. of 5th Intl. Conf. on Ultrastructure Processing*, edited by L. L. Hench and J. K. West (Wiley, New York, 1991) pp. 543-550.
5. M. Sarikaya, "Evolution of Resolution in Microscopy," *Ultramicroscopy*, 47 [1-3] 1-16 (1992).
6. N. B. Pellerin, G. L. Graff, D. R. Treadwell, J. T. Staley, and I. A. Aksay, "Alginate as a Ceramic Processing Aid," *Biomimetics*, 1 [2] 119-130 (1992).

7. T. Ren, N. B. Pellerin, G. L. Graff, I. A. Aksay, and J. T. Staley, "Dispersion of Small Ceramic Particles (Al_2O_3) with *Azotobacter vinelandii*," *Appl. Environmental Microbiol.*, **58** [9] 3130-3135 (1992).
8. K. Gunnison, M. Sarikaya, J. Liu, and I. A. Aksay, "Structure-Mechanical Property Relationships in a Biological Ceramic-Polymer Composite: Nacre," in *Proc. of Hierarchically Structure Materials*, Symposium-Z, edited by I. A. Aksay, E. Baer, M. Sarikaya, and D. Tirrell (Materials Research Society, Pittsburgh, PA, 1992) pp. 171-184.
9. J. Liu, M. Sarikaya, and I. A. Aksay, "A Hierarchically Structured Model Composite: A TEM Study of Hard Tissue of Red Abalone Shell," in *Proc. of Hierarchically Structure Materials*, Symposium-Z, edited by I. A. Aksay, E. Baer, M. Sarikaya, and D. Tirrell (Materials Research Society, Pittsburgh, PA, 1992) pp. 9-18.
10. M. Sarikaya and I. A. Aksay, "Imaging of Hierarchically Structured Materials," in *Proc of Hierarchically Structure Materials*, Symposium-Z, edited by I. A. Aksay, E. Baer, M. Sarikaya, and D. Tirrell (Materials Research Society, Pittsburgh, PA, 1992) pp. 293-308.
11. M. Sarikaya, "Biomimetic Materials: An Introduction," 50th Annual Meeting of Electron Microscopy Society of America, edited by G. W. Bailey, J. Bentley, and J. A. Small (San Francisco Press, San Francisco, CA, 1992) pp. 1020-1021.
12. J. Liu, K. E. Gunnison, M. Sarikaya, "A TEM Study of Interface between Organic Matrix and Aragonite in a Biological Hard Tissue, Nacre," 50th Annual Meeting of Electron Microscopy Society of America, edited by G. W. Bailey, J. Bentley, and J. A. Small (San Francisco Press, San Francisco, CA, 1992) pp. 1024-1025.
13. M. Sarikaya, "Tailoring Microstructures of Materials via Biomimetics," Proc. 51st Ann. Meeting of Microscopy Society of America, edited by G. W. Bailey and C. L. Reider (San Francisco Press, San Francisco, CA, 1993) pp. 500-501.
14. M. Sarikaya and I. A. Aksay, "An Introduction to Biomimetics: A Structural Viewpoint," in *Microstructure of Materials*, edited by K. M. Krishnan (San Francisco Press, San Francisco, CA, 1993) pp. 141-148.
15. M. Sarikaya, "An Introduction to Biomimetics: Structural Viewpoint," *Microsc. Res. Tech.*, **27** [5] 361-375 (1994).
16. R. Humbert, M. Sarikaya, I. A. Aksay, and C. E. Furlong, "Characterization of Organic Nucleator and Framework Macromolecules in Mollusk Shells," in Proceedings of Materials Research Society Symposium, Vol. 330, entitled: *Biomolecular Materials by Design*, edited by: H. Bayley, D. Kaplan, M. Navia, and M. Alper (Materials Research Society, Pittsburgh, PA, 1993).

17. M. Sarikaya, "Biological Composites: Ultimate Self-Assembled Materials," Proceedings of XIIIth International Congress of Electron Microscopy, ICEM 13, Paris, Vol. 3B: Applications in Biological Sciences (Les éditions de Physique, Paris, France, 1994) pp. 889-890.
18. M. Sarikaya, "Organic-Inorganic Interfaces In Layered Biological Composites," Proceedings of 52nd Microscopy Society of America, J. Bailey (ed.) (San Francisco Press, San Francisco, CA, 1994) pp. .
19. M. Sarikaya, J. T. Staley, and C. E. Furlong, "Nanodesigning and Properties of Biological Composites," Proc. American Society of Mechanical Engineers, Chicago, IL, November 6-8, 1994 (to be published).
20. M. Sarikaya, "Nanodesign and Properties of a Biocomposite for Biomimetics," Proc. of *Segundo Congreso Mexicano de Microscopi Electronica*, edited by F. Gasga (1994) pp. SP2.
21. M. Sarikaya, J. Liu, and I. A. Aksay, "Nacre of Abalone: Its Mechanical Properties, Morphology, Crystallography, and Formation," in: *Biomimetics: Design and Processing of Materials*, Edited by M. Sarikaya and I. A. Aksay (American Institutes of Physics, New York, 1994).
22. R. Humbert, M. Sarikaya, and C. E. Furlong, "Layered Aragonitic Particles from Mollusk Shell Extracts," Submitted to *Nature* (July 1994).
23. M. Sarikaya and J. Liu, "Mechanism of Formation of Nacre in Mullusks," to be submitted to *Nature* (Autumn, 1994).
24. M. Sarikaya and D. Frech, "Comparison of Crystallography of Biogenic and Geological Aragonite," to be submitted to *Acta Cryst.* (Autumn, 1994).
25. S. F. Hashemifar, J. T. Staley, and M. Sarikaya, "The Degree of Environmental Damage in the Use of Synthetic and Biological Polymers in Ceramic Processing," to be submitted to *Biomimetics* (Fall 1994).
26. M. Sarikaya, "Biomimetic Ceramics," in: *Bioceramics*, edited by James Shackelford (Trans. Tech. Publ, Ltd., Lousanne, Switzerland, 1995).

Thesis:**Completed:**

1. K. E. Gunnison, "Structure-Mechanical property Relationships in a Biological Ceramic-Polymer Composite: Nacre," M.S. thesis (June 1991, University of Washington, 1991).
2. G. L. Graff, "Biopolymers as Aids in Ceramic Processing," M.S. Thesis (June 1991, University of Washington, 1991).
3. Sima F. Hashemifar, "The Use of Polymers in Ceramic Processing: A Comparison of Synthetic and Biopolymers for Safety Concerns," M.S. Thesis (June 1994).
4. Tao Ren, "Magnetosome Structure in Magnetite Formation in Magnetotactice Bacteria" M.S. Thesis (September, 1994).

Continuing:

1. Daniel Frech, "Crystallography and Formation of Biogenic and Geological Calcite and Biomineralization," Ph.D. Thesis (started Fall 1992).
2. Benjamin Shapiro, "Mechanical Properties of Mollusk Shells: Model for Biomimetics of Impact Resistant Materials," M.S. Thesis (Started Fall 1994).
3. Sima F. Hashemifar, "In-Situ Processing of Ceramics in the Presence of Bacteria: Environmentally-benign Processing of Materials" Ph.D. (started Fall 1994).

3.2 Presentations: Invited Talks, Conferences, Workshops

a. Invited Talks:

1. M. Sarikaya and Ilhan A. Aksay, "Electron-Optical Characterization of Hierarchically Structured Materials," Materials Research Society Fall Meeting, Boston, MA, Dec. 2-6, 1991.
2. M. Sarikaya, J. Liu, and I. A. Aksay, "Hierarchical Structures of Seashells and Exoskeletons for Biomimetics," Mater. Res. Soc. Fall Meeting, Boston, Dec. 2-6, 1991.
3. Ilhan A. Aksay and M. Sarikaya, "Processing of Synthetic Hierarchically Structured Ceramic-Based Materials," Mater. Res. Soc. Fall Meeting, Boston, MA, Dec. 2-6, 1991.
4. James T. Staley, M. Sarikaya, and I. A. Aksay, "Biomimicking with Organisms," Materials Research Society Fall Meeting, Boston, MA, Dec. 2-6, 1991.
5. M. Sarikaya, J. Liu, and I. A. Aksay, "Crystallography of the Hard Tissue in Nacre of Abalone," 4th Intl. Conf. on Miner. Tissues, Coronado Peninsula, CA, Feb. 5-10, 1992.
6. M. Sarikaya, J. Liu, and I. A. Aksay, "Characterization of Hierarchically Structured Natural Ceramic-Polymer Composites," 15th Asilomar Conference on Polymeric Materials, Org. by Eric Baer and Anne Hiltner, Pacific Grove, CA, Feb. 9-12, 1992.
7. I. A. Aksay and M. Sarikaya, "Procesing of Nanocomposites by Biomimicking," The Minerals, Metals, and Materials Society and American Society of Materials, International, TMS/ASM Annual Meeting, San Diego, CA, March 1-5, 1992.
8. M. Sarikaya, "Introduction to Biomimicking and Structures of Biological Hard Tissues with Reference to Mollusca," March Meeting of American Physical Society, Indianapolis, IN, March 16-20, 1992.
9. M. Sarikaya, "Hierarchically Structured Natural Ceramic-Polymer Composites," Invitational Lecture Series, Allied-Signal, Inc., Morristown, NJ, June 25, 1992.
10. I. A. Aksay, "Bioinspired Processing of Ceramics and Composite Materials," Ceramics: Today and Tomorrow, Japan's 100th Anniversary Intl. Conf., Yokohama, Japan, Oct. 16-18, 1991.
11. I. A. Aksay, "Dispersion of Ceramic Nanosized Particles in Biological Systems," Plenary Lect., Engineering Foundation Conference, Palm Coast, FL, March 15-20. 1992.
12. I. A. Aksay, "Processing of Ceramics by Biomimicking," March Meeting of American Physical Society, Indianapolis, IN, March 16-20, 1992.
13. I. A. Aksay, "Trends in Processing of Ceramic-Polymer Composites with Colloids," 3M Technical Forum, St. Paul, MN, April 17, 1992.

14. M. Sarikaya, "Biomimetics: Design and Processing of Materials," Pfizer International, Morristown, NJ, September 2, 1992.
15. M. Sarikaya, "Nanodesign of Materials by Biomimetics," 1st International Conference on Nanocomposite Materials, Cancun, Mexico, September 22-25, 1992.
16. M. Sarikaya, "Nanodesigning of Materials by Biomimetics," 1st International Conference on Nanocomposite Materials, Cancun, Mexico, September, 22-25, 1992.
17. M. Sarikaya, "Materials Design by Biomimetics: Critical Issues," Tutorial Presentation, March Meeting of American Physical Society, Seattle, WA, March 15-19, 1993.
18. M. Sarikaya, "Biomimetics: An Introduction," National Technological University Broadcast, March 19, 1993 (Seattle, WA).
19. M. Sarikaya, "Biomimetics," Syracuse Univ., Syracuse, NY, April 5, 1993.
20. M. Sarikaya, "Biomimetic Design of Materials," National Institutes of Standard and Technology, Bethesda, MD, April 23, 1993.
21. M. Sarikaya, "Biomimetics," IBM, T. J. Watson Research Center, Yorktown Heights, NY, May 10, 1993.
22. M. Sarikaya, "An Introduction to Biomimetics," A Tutorial Lecture at 51th Annual Meeting of Microscopy Society of America, Cincinnati, OH, August 2, 1993.
23. M. Sarikaya, "Design and Processing of Materials by Biomimetics," AFOSR Workshop on Biomimetic Materials, Wright Laboratories, Wright-Patterson Air Force Base, Dayton, OH, August 12, 1993.
24. M. Sarikaya, "Biomimetics: Critical Issues," AT&T Bell Labs, Holmdel, NJ, 9/13/1993.
25. M. Sarikaya, "Growth And Shape Formation of Mollusc Shells: Hierarchical Morphogenesis," in Symposium S entitled Biomimetics, Materials Research Society Fall Meeting, Boston, MA, November 27 - Decemeber 3, 1993.
26. M. Sarikaya, Tutorial Lecture entitled: "Lessons from Biology: Structure-Property Relations in Hierarchically Structured Hard Biocomposites," Tutorial Lectures on Biomimetics, Materials Research Society Fall Meeting, Boston, MA, November 27 - Decemeber 3, 1993.
27. M. Sarikaya, Biomimetics: Current Issues and Future Prospects, Department of Materials Science and Engineering, University of Washington, Seattle, WA, January 10, 1994.
28. M. Sarikaya, Faculty of Science, Bilkent University, "Biomimetics: Rsearch Interests and Challenges," January 26, 1994.
29. M. Sarikaya, "Organic-Inorganic Interfaces in Layered Biological Composites," 16th Annual Asilomar Workshop on Advanced Polymers, Pacific Growe, CA, February 9-12, 1994.
30. M. Sarikaya, "Nanodesigning in Biological Composites," Spring Meeting of Materials Research Society, San Francisco, April 4-9, 1994.

31. M. Sarikaya, "Inorganic-Organic Interfaces in Biological Composites," in Workshop entitled: *Nanofabriaction and Biosystems: Frontiers and Challenges*, Kona, Hawaii, May 8-12, 1994.
31. M. Sarikaya, "Biomimetics," Gordon Conference entitled: *Model Membranes: From Biophysics to Materials Science*, Ventura, CA, Feb. 27 - March 4, 1994.
32. M. Sarikaya, "Organic-Inorganic Interfaces in Biocomposites," 52nd Annual Meeting of Microscopy Society of America, New Orleans, LA, August 5-9, 1994.
33. M. Sarikaya, Planary Lecture entitled: "Nanodesign and Properties of a Biocomposite for Biomimetics," 2nd Mexican Society of Electron Microscopy, Cancun, Mexico, September 26-28, 1994.
34. M. Sarikaya, "Structures and Properties of Biological Composites," ASME, Chicago, November 6-8, 1994.
35. M. Sarikaya, "Biomineralization: From Biology to Technology," in Symposium S, entitled "Biomimetics and Biomolecularly Prepared Materials," Materials Research Society Fall Meeting, November 27 - December 2, 1994.
36. M. Sarikaya, "Biomimetics: Hard Tissues," Tutorial Lecture, Fall Meeting of Materials Research Society, Boston, MA, Nov. 27, 1994.

b. Conference Presentations (contributed talks)

A partial list of conference presentations is as follows:

1. J. Liu, M. Sarikaya, and I. A. Aksay, "Hierarchical Twin Structure in the Nacre of Red Abalone Shell," 49th Mtg. of Electron Microscopy Society of America, San Jose, CA, Aug. 4-9, 1991.
2. K. E. Gunnison, M. Sarikaya, and I. A. Aksay, "Structure-Mechanical Property Relationships in a Biological Ceramic-Polymer Composite," Materials Research Society Fall Meeting, Boston, MA, Dec. 2-6, 1991.
3. B. Flinn, M. Sarikaya, and I. A. Aksay, "Deformation Mechanisms in Biolaminates," 94th Annual Meeting of American Ceramic Society, Minneapolis, MN, April 12-16, 1992.
4. T. Ren, J. T. Staley, N. B. Pellerin, and I. A. Aksay, "Bacterial Polyglutamic Acid as an Aid in Ceramic Processing," 92nd Ann. Meeting of American Society of Microbiology, May 1992.
5. M. Sarikaya and I. A. Aksay, "Shape Formation in Biological Systems," MRS Fall Meeting, Nov. 28 - Dec. 4, 1992, Boston, MA.
6. M. Sarikaya and I. A. Aksay, "Shape Formation in Biological Systems," MRS Fall Meeting, Nov. 28 - Dec. 4, 1992, Boston, MA.

7. M. Sarikaya, "Biological Composites: Ultimate Self-Assembled Materials," XIIIth International Congress of Electron Microscopy, ICEM'94, Paris, July 17-22, France.
8. M. Sarikaya, "Organic-Inorganic Interfaces in Biological Composites," Proceedings of 52nd Microscopy Society of America, New Orleans, Aug. 5-9, 1994.
9. Daniel Frech and M. Sarikaya, "Formation, Crystallography, and Morphology of Biogenic and Geological Aragonite" Symposium S, entitled: Biomimetics ??, Materials Research Society Fall Meeting, Boston, MA, November 27 - December 2, 1994.
10. R. Humbert, G. Lancaster, C. Furlong, and M. Sarikaya, "Bioduplicated Pearls: Layered Aragonitic Particles Using Organic Shell Extracts" Symposium S, entitled: Biomimetics ?, Materials Research Society Fall Meeting, Boston, MA, November 27 - December 2, 1994.
11. Sima F. Hashemifar, M. Sarikaya, and J. T. Staley, "Environmental Aspects of Using Synthetic- and Bio-Polymers in Ceramic Processing," Symposium S, entitled: Biomimetics ??, Materials Research Society Fall Meeting, Boston, MA, November 27 - December 2, 1994.

c. Organization of Symposia and Workshops

1. **Design and Processing of Materials by Biomimetics**, M. Sarikaya and I. A. Aksay, Workshop, held in Seattle, WA, April 1-3, 1991 (held during the continuation of the first 3-year portion of the current project; 12 papers by the invited speakers are being edited for publication as a book by American Institute of Physics (300 pages).
2. **Resolution in the Microscope**, Special Intl. Symposium, organized by M. Sarikaya, held during the 49th Annual Meeting of Electron Microscopy Society of America, San Jose, CA, Aug. 1-6, 1991, and the proceedings were published as a special issue of Ultramicroscopy, Vol. 47 [1-3] (1992) (24 papers; 300 pages)
3. **Hierarchically Structured Materials**, Symposium Z, organized by Ilhan A. Aksay, E. Baer, M. Sarikaya, and D. Tirrell, Fall Meeting of the Materials Research Society, Boston, MA, Dec. 1-6, 1991 (Papers in this symposium were published as MRS Proceedings, Vol. 255, 1992) (45 papers, 447 pages)
4. **Fundamental Materials Problems and Challenges in Biomimetics**, S-5, Organized by M. Sarikaya and e. A. Stern, Symposium of the Division of Condensed Physics, March Meeting of the American Physical Society, Indianapolis, IN, March 16-20, 1992.
5. **Microscopy of Self Assembled Materials and Biomimetics**, 49th Annual Meeting of Electron Microscopy Society of America, August 16-20, 1992, Boston, Mass. (Proceedings will be published as a special issue of Journal of Microscopy Techniques and Research, 1993).
6. **Determination of Nanoscale Physical Properties of Materials by Microscopy and Spectroscopy**, Proc. of MRS Symposium, edited by M. sarikaya, K. Wickramasinghe, and M. Isaacson, Vol. 332 (Materials Research Society, Pittsburgh, PA, 1994) (80 papers and 700 pages).
7. **Biominerization: From Biology to Technology**, Symposium S, Materials Research Society Fall Meeting, 1995, Boston (planned).

4.3 Patents

Patent Application: "Process for Suspension of Ceramic or Metal Particles Using Biologically Produced Polymers," U. S. Patent Appl., Serial No. 071699.970.

4.4 News Clippings

(Some examples from popular science magazines and from the science sections of newspapers and newsmagazines)

1. "Mollusk Teaches Ceramics to Scientists," by Ivan Amato, *Science News, Materials Science Section*, December 9 (1989) p. 383.
2. Chemical Processing of Ceramics, by D. Ulrich, *C&EN*, January 1 (1990) pp. 28-40.
3. Nanostructured Materials, by Robert Cahn, in *News and Views Section, Nature*, 348 389-390 (1990).
4. "Biomimetics: Creating Materials From Nature's Blueprints," by Robin Eisner, *The Scientist*, July 8, 1991.
5. "The New Alchemy," Cover Story, *Business Weekly*, , July 29 (1991) pp. 48-55.
6. "Heeding the Call of the Wild," by Ivan Amato, *Science*, August 30 (1991).
7. "Natureworks: Making Minerals the Biological Way," by Elizabeth Pennisi, *Science News*, Feature Article, 141, May 16 (1992) pp. 328-332 (Cover Story).
8. "Biomimetics," Cable News Network, National Broadcast in *Science and Technology Program* on December 15, 16, 19, and 20, 1992.
9. "Nature at the Patent Office," by Sharon Begley and Carolyn Friday, in Technology Section of *Newsweek*, December 14, 1992.
10. "Science Takes a Lesson from Nature, Imitating Abalone and Spider Silk," by Warren Leary, *The New York Times*, Science Section, Aug. 31, 1993
11. "The Mother of All Pearls," by D. Clery, in the Technology Section of *New Scientist*, 28 March 1992.
12. "Su licenza di Dio," In Section: Technolgoia/I nuovi materiali, Science Section in *PANORAMA*, 21 March(1993) pp. 153-154.
13. "Doing What Comes Naturally," by L. G. Blanchard, Columns, Sept. (1993) 20-23.
14. "Nature's Building Blocks," by T. Campbell, *POPULAR SCIENCE*, Oct. (1993) 74-77.
15. "Nature's Materials: Unlocking the Secrets of Charlotte's Web," by L. G. Blanchard, *IEEE Potentials*, (quarterly magazine) February 1994 (The Institute of Electrical and Electronics Engineers, Inc.) pp. 34-37.
16. "Biomimetics," in *Private Eye: Looking/Thinking by Analogy*, by Kerry Ruef (Seattle, 1993) (This is a book written for the elementary school students as a guide to developing the interdisciplinary mind, hands-on thinking skills, creativity, and scientific literacy. It has been adapted by many schools around Seattle).
17. *Curiosities: A Book of Scientific Trivia*, by Sharon McGayne (John Wiley, New York, 1994).
18. *Sky Magazine*, Delta Airlines, April 1994.

4. Personnel

Principal Investigators:

Mehmet Sarikaya (UW)

James T. Staley (UW) and

Ilhan A. Aksay (UW, now at PU; no contribution after September 1993)

Research Scientists:

Daniel M. Dabbs (Materials Science and Engineering) (UW, now at PU)
(no contribution after 1993)

Jun Liu (Materials science and Engineering) (UW, now at Battelle Pacific
Northwest Laboratories, Richland, WA; no contribution after December 1992)

Nancy B. Pellerin (Microbiology) (UW; left in June 1994)

Brian Flinn (Materials science and Engineering) (UW, left in January 1993)

Maoxu Qian (Materials Science and Engineering) (UW; continuing)

Graduate Students:

Tao Ren (Microbiology) (UW; Graduated in September 1994)

Hsien-Liang Kerr (Materials Science and Engineering)
(UW and PU; no longer in the program))

Katie Gunnison (Materials science and Engineering) (UW) (Graduated 1991)

Gordon L. Graff (Materials Science and Eng.) (UW) (Graduated 1991)

Daniel Frech (Materials Science and Engineering) (UW, continuing)

Benjamin Shapiro (Materials Science and Engineering, UW, continuing)

Sima F. Hasemifar (Materials Science and Engineering, UW; completed MS June
1994; started Ph.D. in Fall 1994).

Undergraduate Students:

Jeffrey Frawley (graduated) (Materials Science and Eng.) (UW)

Myeung Lee (graduated) (Materials Science and Eng.) (UW)

Bill Wang (graduated) (Chemical Eng.) (UW)

Susan Sawyer (graduated) (Microbiology) (UW)

Sean Mallony (graduated) (Microbiology) (UW)

Gretchen Wahl (graduated) (Chemical Engineering) (UW)

Demetria Webster (continuing) (Materials Science and Engineering)

Mary Katchur (continuing) (Materials Science and Engineering)

Colleen Lasley (continuing) (Chemical Engineering)

APPENDICES-A

Publications

Hierarchically Structured Materials

edited by

Ilhan A. Aksay, E. Baer, M. Sarikaya, and D. A. Tirrell
Vol. 255, 1-450

(Materials Research Society, Pittsburgh, PA, 1992).
(only the list of contents is included)

Hierarchically Structured Materials

Symposium held December 2-6, 1991, Boston, Massachusetts, U.S.A.

EDITORS:

Ilhan A. Aksay

Princeton University, Princeton, New Jersey, U.S.A.

Formerly at University of Washington, Seattle, Washington, U.S.A.

Eric Baer

Case Western Reserve University, Cleveland, Ohio, U.S.A.

Mehmet Sarikaya

University of Washington, Seattle, Washington, U.S.A.

David A. Tirrell

University of Massachusetts, Amherst, Massachusetts, U.S.A.



MATERIALS RESEARCH SOCIETY
Pittsburgh, Pennsylvania

"Nacre of Abalone Shell: A Natural Multifunctional
Nanolaminated Ceramic-Polymer Composite Material,"

M. Sarikaya and I. A. Aksay

Chapter 1, in *Structure, Cellular
Synthesis, and Assembly of Biopolymers*

edited by Steven Case
(Springer and Verlag, Amsterdam, 1992)
pp. 1-25.

Chapter 1

Nacre of Abalone Shell: a Natural Multifunctional Nanolaminated Ceramic-Polymer Composite Material

Mehmet Sarikaya¹ and Ilhan A. Aksay^{1, 2}

1 Introduction: Nanocomposite Materials and Biological Composites

When materials are manufactured with an emphasis on tailoring their properties through microstructural control, the extent of this control is generally at a specific length scale. For instance, the mechanical properties of most metallic materials are controlled through the manipulation of dislocation dynamics at the nanometer length scale (Cottrell 1953), whereas the mechanical properties of ceramic materials are controlled through the propagation of cracks that are initiated from defects of micrometer length scale (Evans and Marshall 1989).

In contrast, the approach used by organisms in processing materials is in many ways more controlled than synthetic methods because biological materials are dynamic systems (Lowenstam and Weiner 1989; Mann et al. 1989; Simkiss and Wilbur 1989). In the formation of biological materials, organisms efficiently design and produce complex and hierarchical microstructures with unique properties at spatial dimensions from the molecular to the centimeter, and with greater structural control. The dynamism of these systems allows the collection and transport of the raw constituents; the nucleation, configuration, and growth of new structures (self-assembly) (see, for instance, Wasserman et al. 1989); and the repair and replacement of old or damaged components. These materials include all organic components, such as spiders' webs (Gosline et al. 1986) and insect cuticles (Bouligand 1965); inorganic-organic composites, such as seashells (Currey 1987) and bones (Glimcher 1981); all ceramic composites, such as sea urchin teeth and spines (Berman et al. 1990); and inorganic, ultrafine particles, such as magnetic (Blakemore 1975; Frankel et al. 1979; Blakemore 1982; Frankel and Blakemore 1991) and semiconducting (see, for instance, in biological systems, Dameron et al. 1989; and in synthetic systems, Fendler 1987) particles produced by bacteria and algae, respectively. In addition, in certain cases, byproducts, such as enzymes (Alper 1991), proteins (see, for instance, Haggis 1988), and other macromolecules (Crueger

¹ Department of Materials Science and Engineering, Roberts Hall, FB-10, University of Washington, Seattle WA 98195, USA and Advanced Materials Technology Center, Washington Technology Center, University of Washington, Seattle, WA 98195, USA

² Current address: Department of Chemical Engineering, Princeton University, Princeton, NJ 08544-0563 USA

and Crueger 1982), have chemical or physical properties superior to their synthetic counterparts.

Biological systems can be a source of inspiration for design and processing concepts for novel synthetic materials where structural control can be established through a continuous length scale. An approach based on biological systems can be divided into two categories (Aksay and Sarikaya 1991). First, by studying the structures of biocrystals using various microscopy techniques at all scales of spatial resolution, the fundamentals of their unique structural designs can be acquired and then mimicked by techniques that are currently available to materials scientists — an approach that we will refer to as *biomimicking*. Second, by learning the molecular synthesis and processing mechanisms of biomaterials and using these hitherto unknown methodologies, new technological materials superior to those presently available can be produced — an approach we call *bioduplication*. The bioduplication approach is much more involved and requires a long-term commitment (probably tens of years) to learn not only the intricacies of bioprocessing used by organisms but also to develop new strategies to synthetically process materials at the molecular level with the same size, shape, multifunctional and hierarchical complexity as the biomaterials. The first approach, i.e., biomimicking, can be relatively short term (10 years or less), although by no means simple. Biomimicking involves exploring the structures of biomaterials, which are often hierarchical with each level having a different functionality, and correlating that functionality with the unique microstructural design and multifunctional properties of the biomaterial. Although our research is directed towards both categories, this chapter describes some of our findings on the design of the nacre of abalone shell and answers several questions surrounding this unique, but relatively simple, microstructure, particularly the organization of the inorganic component and its possible relation to the organic matrix.

In this chapter, specifically, the mechanical properties and structure of nacre, a composite of ceramic and proteins, are discussed. The significance of nacre as a structural material is that its mechanical properties, such as fracture toughness and strength, are unprecedentedly high and comparable to those of the high-technology structural ceramics (Sarikaya et al. 1990a,b; Yasrebi et al. 1990). Yet in nacre, the structure is mostly composed of CaCO_3 , a material that has limited engineering value for materials applications. The unique structure of nacre, which is composed of alternating nanometer-scale laminated layers of thin biomacromolecules and CaCO_3 platelets, is highly organized to produce an excellent multifunctional material (armor) for the organism (Currey 1974, 1976; Jackson et al. 1988; Sarikaya et al. 1990a). It has recently been shown that crystallographic defect formation, in particular twins, in the inorganic phase takes place in a hierarchical fashion and can be attributed to the ability of the organism to control defect structures in a hierarchical manner which results in a composite structure with excellent properties (Sarikaya et al. 1992).

Other known facts about nacre are: (1) the overall shell composite is over 5 vol% inorganic material (CaCO_3 in the form of aragonite) (Currey 1987); (2) the composite has a "brick and mortar" microarchitecture (Currey 1987; Jackson et al. 1988; Sarikaya et al. 1990a,b) with aragonite forming thin, hexagonally shaped

bricks within an organic matrix which is thought to be composed of three distinct layers (Watabe 1965; Bevelander and Nakahara 1968; Towe and Hamilton 1968; Mutvei 1970; Nakahara et al. 1982; Weiner and Traub 1984; Weiner 1986); and (3) the inorganic material consists of highly oriented aragonite platelets (Weiner and Traub 1984).

Despite these findings, however, much more needs to be known about the microstructure if the desired synthetically laminated materials are to be produced through biomimicking nacre. Some of these issues are: (1) the nature of the crystallographic defects and their distribution in the inorganic phase; (2) the crystallographic relationship between aragonite platelets to explain the high degree of organization and structural integrity of nacre; (3) the direct analysis of the possible stereochemistry between the organic and inorganic phases; (4) the nature of the organic phase(s) in the thin film matrix between the aragonite platelets, their size and distribution throughout nacre; and (5) the influence of the aragonite platelets on the formation and resultant functionality of the organic matrix in the overall behavior of the composite. Answers to these questions will shed more light on the mechanisms of formation and particularly the degree of control that the organism has over the growth of the highly ordered biocomposite.

This paper specifically concentrates on points (1) and (2) raised above, and indirectly discusses points (3), (4), and (5). Therefore, we first present a detailed analysis of the mechanical properties of nacre. Second, from the analysis of the toughening and strengthening mechanisms in nacre, we derive a set of criteria for the structural design of synthetic laminated materials via biomimetics. These are followed by a description of our current understanding of the structure of nacre in terms of morphology, composition, and crystallography, its hierarchy (in both the hard and the soft tissues), and possible structural relationships between the organic and inorganic components. Finally, we discuss possible directions for future studies that will lead to a better understanding of the biological and chemical basis of the formation of the relatively simple but highly efficient nacre structure and its significance in terms of designing and processing nanolaminated multifunctional materials for engineering applications.

2 Mechanical Properties of Nacre

2.1 Toughness and Strength in Nacre

The nacre structure is found in many families of mollusks, such as the red abalone (*Haliotis rufescens*) of the gastropod family, cephalopods such as nautilus (*Nautilus pompilius*), and bivalves such as black-lipped pearl oysters (*Pinctada margaritifera*) (Nicol 1960; Grégoire 1972; Morton 1979; Currey 1987). We used red abalone in our studies, since the diameter and the thickness of the shell containing the nacre in this species were large enough to perform standard mechanical tests (Brown and Srawley 1966), allowing direct comparison of nacre with engineering structural ceramics and ceramic-based materials. Mechanical properties were

evaluated in terms of fracture toughness, K_{IC} , and fracture strength, σ_F , in three-point straight notched and four-point bend bars, respectively, in the transverse point direction perpendicular to the laminated layers through which a crack is normally expected to propagate in the shell of the organism in its natural environment (Currey 1977). Red abalones were collected in Baja California, Mexico, and we estimated that the specimens were about 10–12 years old with a shell diameter of 25–30 cm and a thickness of about 1.5 cm, including the prismatic and nacreous layers. Although it was inevitable that the samples had curved layers, the test samples satisfied the size requirements for American Standards for Testing of Materials (ASTM) standards and allowed for the comparison of test results between nacre and structural ceramics, such as Al_2O_3 , which were prepared for this purpose (Gunnison 1991). Hardness indentations were made with a Vickers microhardness indenter with a load of 1 kg.

The results of the mechanical tests of nacre and some of the well-studied ceramics and ceramic-based composites (cermets) are plotted in Fig. 1 in terms of K_{IC} versus σ_F , specific strength (Sarikaya et al. 1990a,b; Yasarbi et al. 1990; Aksay and Sarikaya 1991).

The average values for the toughness and strength of nacre are $7 \pm 3 \text{ MPa}\text{m}^{1/2}$, and $180 \pm 20 \text{ MPa}$, respectively. As seen from the figure, fracture strength and, especially, fracture toughness values show a high degree of scatter. This may be due to the presence of yearly growth layers that are intrinsic to abalone nacre (Currey 1987). The yearly growth layers are absent in other types of nacre, such as pearl oyster; however, the samples are too thin to perform standard tests, requiring tests with undersized samples (Jackson et al. 1988).

Nevertheless, *P. margaritifera* nacre is also commonly used for mechanical tests (Currey 1977; Jackson et al. 1988; Sawyer S, Sarikaya M, Aksay IA, unpubl.).

research). The test results from our laboratory on *P. margaritifera* nacre produced values for K_{IC} and σ_F of $10 \pm 6 \text{ MPa}\text{m}^{1/2}$ and $220 \pm 60 \text{ MPa}$, respectively (Sawyer S, Sarikaya M, Aksay IA, unpubl. research). It has been reported that mechanical tests performed on "dry" samples produced much lower results (Currey 1977; Jackson et al. 1988). In the present case, there was no intentional drying, and the samples, kept under laboratory conditions, were tested within 1 to 3 months after the removal of the animal from the ocean. Therefore, the results given above may be slightly higher than those reported in the literature; however, these results should be more representative of the true properties of nacre since they are from relatively fresh samples and are more similar to the organism in its natural environment.

2.2 Toughening Mechanisms

The crack propagation behavior in nacre was studied by microindentation in the edge-on configuration to understand possible toughening mechanisms (Sarikaya et al. 1990a,b). It was revealed that there is a high degree of tortuosity not seen in the more traditional brittle ceramics, such as Al_2O_3 , or in high toughness ceramics, such as ZrO_2 (see, for example, Tressler and Bradt 1984; Evans 1988). A microstructure showing the tortuous crack propagation in the nacre is displayed in Fig. 2. The most apparent features of the crack propagation seen in the scanning electron microscopy (SEM) images are crack blunting/branching and microcrack formation. A closer examination of these images reveals that microcracks advance both on planes parallel to the CaCO_3 layers and on those perpendicular to them. It is not clear, however, whether the cracks propagate inside the organic layer or through the interface plane between the organic and the inorganic components. The surfaces of fractured samples indicate that a major crack has meandered around the CaCO_3 layers, exposing them through the organic surroundings, resulting in a very rough fractured surface that is similar to that seen in fiber-reinforced ceramic composites where a pull-out mechanism operates (Evans and Marshall 1989). In micrographs recorded at much higher magnifications, separation of the CaCO_3 layers in both x and y directions (in-layer plane) is clearly seen; see, for instance, Fig. 3a. The "bricks" have been left intact, indicating they slide on the organic layer (Sarikaya et al. 1990a,b). The micrograph in Fig. 3b, on the other hand, shows organic ligaments stretched in the perpendicular direction, i.e., the z direction, between the CaCO_3 platelets. This stretching indicates that the interface between the organic and the inorganic phases is strong and that the organic phase acts as a strong binder (Jackson et al. 1988; Sarikaya et al. 1990a).

By a close analysis of many fractured surfaces and indentation cracks, several toughening mechanisms may be proposed (Sarikaya et al. 1990a,b): (1) crack blunting/branching, (2) microcrack formation, (3) plate pull-out, (4) crack bridging (ligament formation), and (5) sliding of CaCO_3 layers. In general, it would be desirable to have all of these energy-absorbing mechanisms operative in a composite material in order to increase the overall fracture toughness of the brittle

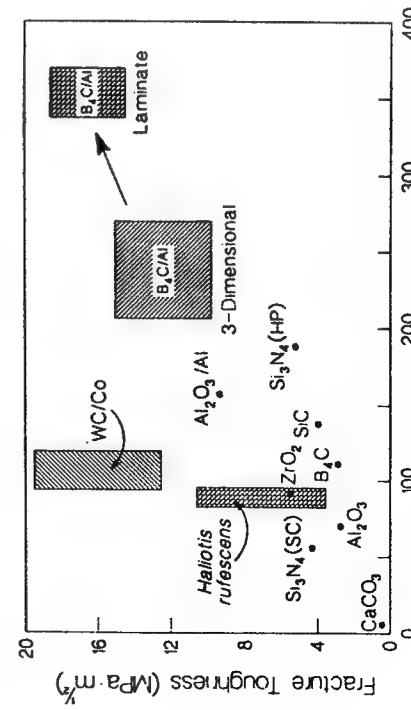


Fig. 1. Mechanical properties of nacre of abalone shell plotted with respect to the mechanical properties of ceramics and ceramic-metal composites

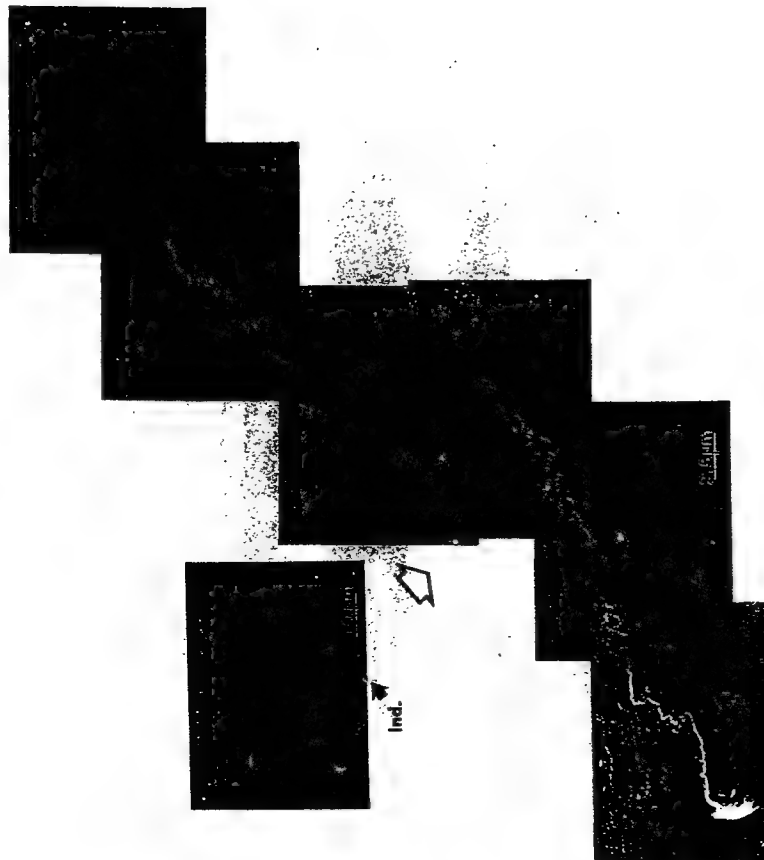


Fig. 2. Secondary electron (SE) image of crack propagation behavior in nacre in edge-on orientation (indentation is indicated by *Ind.* in the inset)

material (Evans and Marshall 1989). The high degree of tortuosity seen in crack propagation is due mainly to crack blunting and branching. However, tortuosity alone is not a major toughening mechanism in these composites because it cannot account for the many orders of magnitude increase seen in toughness. Our studies showed that the linear tortuosity, determined from a number of indentation cracks, indicates only a 30–50% toughening value of a polycrystalline pure CaCO_3 material. The major toughening mechanisms are, therefore, thought to be sliding and ligament formation (Sarikaya et al. 1990a,b).

With reference to the sliding mechanism, similarities exist between the deformation of a nacreous seashell and a metal, and these may be stated as follows: (1) Around the periphery of the indentation, as seen in Fig. 3, the material exhibits deformation features, such as sliding of the CaCO_3 layers to accommodate the strain caused by the indenter. These deformation features resemble Luders bands (or slip bands) encountered in metals (Honeycombe 1968; Engel and Klingele 1981), such as in face-centered cubic Ni and Al, in which the lattice is plastically

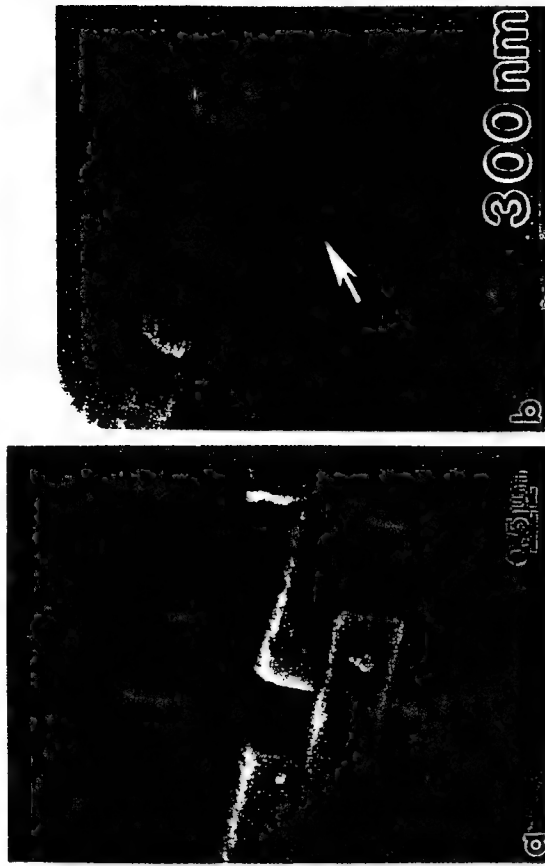


Fig. 3a, b. SEM images illustrate **a** sliding of the platelets (direction of arrows) and **b** pull-out (in the direction of arrows) of the organic matrix during crack propagation. (Sarikaya et al. 1990a)

deformed from the dislocation movement in order to accommodate the applied stress by slipping on high atomic density planes such as $\{111\}^1$. It is also noted that the amount of sliding near the indentation is higher and decreases with distance from the indentation. (2) When sliding occurs in nacre, there is no cracking through the layers except for microcrack formation. This is again similar to the process of crack formation in metals, where deformation is associated with a high degree of dislocation activity which causes an increase in dislocation density in local regions ahead of the major crack, which then becomes sites of microcracks. The microcracks eventually line up and grow to form the major crack. This phenomenon indicates that the biocomposite is not brittle and the strain accommodation mostly takes place between CaCO_3 layers, not through the ceramic layers. We do not yet know whether the interface is ruptured or the rupturing takes place within the biopolymer itself. Nonetheless, it is likely that this complex deformation mode, similar to that in metals, may be the main mechanism of energy absorption during the application of stress and may be responsible for the many orders of magnitude increase in the toughness of the composite.

Sliding takes place when there is a resolved shear stress acting in the plane of the layers. However, if the resolved shear stress has a tensile component, i.e.,

¹[hkl] refers to a family of crystallographic planes, hkl being the indices of these planes. $\langle UVW \rangle$ refers to a specific direction, $\langle UVW \rangle$ refers to a family of directions.

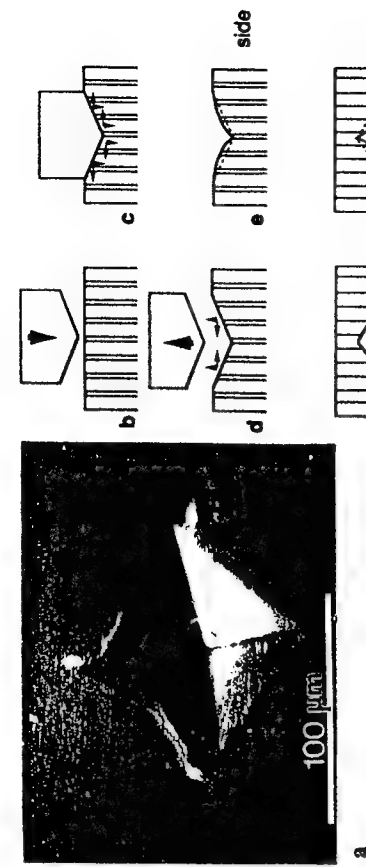


Fig. 4. a) SE image of indentation in nacre in edge-on configuration, displaying inward bulging, and b-g) schematic illustration of the structural changes that might occur in nacre during indentation. (Courtesy of K.E. Gunnison)

normal to the layers, then the CaCO_3 layers are forced to separate. This separation is resisted by the formation of organic ligaments that stretch across the organic layer to form bridges, anchored to the platelets, between the inorganics layers. It has been suggested that the organic matrix has a chitin component in the center (Watabe 1965; Weiner 1986); if so, chitin would have a plywood or an accordion-type structure which would then allow stretching during the bridging process (Sarikaya et al. 1990a,b; Gunnison 1991). The fact that there is more than 1000% stretching of the ligaments and that the organic layer is still intact is a strong indication that the interface between the organic and inorganic components of nacre is strong. Still another significant factor is that the organic layer allows either sliding or ligament formation, depending on the condition of the resolved applied stress (Sarikaya et al. 1990a,b), indicating that the ultra-architecture of the organic layer is a critical design parameter in the making of this ceramic-polymer composite and thus a subject of detailed studies (Crenshaw 1972; Weiner and Hood 1975; Weiner and Traub 1980; Greenfield et al. 1984; Addadi and Weiner 1985; Mann 1988).

2.3 Strengthening Mechanisms

The strength of nacre may be related to several factors, including the size and structure of the aragonitic platelets and the interfaces between the inorganic and the organic components. If the size of the aragonite platelets is compared to the overall toughness of the nacre, it can be seen that from the limited thickness of the largest flaw, i.e., the thickness of the platelet, 0.5 μm, (Griffith 1920) the increase in the fracture strength of aragonite would be < 50 MPa. This value is not high enough to account for the fracture strength of 185 MPa of nacre measured in our studies. Nor can the rule of mixtures account for the value of the strength measurement (Hull 1981).

The best explanation that we can presently put forward for the high strength of nacre is that the tensile stress applied to nacre is transferred to compressive stress during loading. This may be evident from the inward bulging of the edges of the microindentation (Laraya and Heuer 1990; Gunnison 1991). This energy stored in the organic component results in dilation during load release. The failure of the composite, therefore, seems to take place during unloading. The overall cycle of loading/unloading is schematically represented in Fig. 4 (Gunnison 1991). During loading of the indentor, the sample is placed in the edge-on configuration and, hence, the applied stress is distributed in the directions indicated in the figure: One component, σ_2 , in the direction parallel to the platelets and the other, $\bar{\sigma}_x$, perpendicular to them. The former is dissipated by the sliding of the aragonite platelets on the organic matrix, as depicted in Fig. 4 c, d and f. The perpendicular stress is absorbed by the compression of the organic matrix, and hence, reduces the actual stress applied to the platelets. The compression of the organic matrix acts as an energy storage mechanism during the application of the force, and the energy is released during the removal of the indentor, thus displacing the aragonitic crystals

Nacre of Abalone Shell

towards the indentation opening (Fig. 4d and e). This would then result in inward bulging of the sides of the indentation (Fig. 4a and g), at which time failure might occur. As seen in Fig. 4a, the side of the indentation which displays the largest bulging is also the side which possesses the largest crack. In the present system, this failure mechanism could effectively increase the overall strength of the composite many orders of magnitude as the major stress applied to the inorganic component is actually compressive. Such increases are a common occurrence in the strength of ceramics if the applied stress is compressive (Dawridge 1979). To ensure the transferrability of stress, further studies are necessary to elucidate the exact mechanism of strengthening in nacre.

3 Design Guidelines for Processing Biomimetic Laminated Composites

The unusual mechanical properties of nacre as compared to synthetic ceramics and composites may be due to: (1) the intrinsic properties of the constituent phases (brittle inorganic and soft organic phases); (2) the highly ordered organization of ceramic and biopolymer layers, and their detailed structures, including the interface structures and properties; and (3) the sizes of the ceramic and biopolymer layers. Despite the fact that many of the structural features in abalone, especially in the soft tissue, are not yet known, from our knowledge of their excellent mechanical properties and our knowledge of their structural architecture at the micro- and submicron levels, some guidelines may be drawn to aid in the processing of

synthetic microstructures via biomimicking. These biomimicked synthetic laminated composites are expected to have superior properties over those that were achieved in synthetic composites prepared by traditional processing approaches. Based on studies of nacre (Jackson et al. 1988; Sarikaya et al. 1990a,b), the design of high-fracture/high-toughness synthetic composites should incorporate the following:

1. a laminate thickness of the hard and brittle component of less than 1 μm and a soft component of less than 1000 Å, with an approximate ratio between 5:1 and 10:1;
2. a highly plastic soft phase (deformability $>100\%$);
3. strong interfaces between the soft and the hard phases (so that the interface does not fail during crack propagation); and
4. the ability of the soft phase to bind to the surfaces of the hard component (strong interfacial bonding) and provide either plasticity to the overall composite structure (for sliding and, hence, metal-like deformation behavior) or form ligaments to constrain crack opening (through crack bridging), depending on the resolved applied stress.

For the practical processing of laminated composites, these guidelines may be difficult to apply. For example, there is no practical way of producing structural laminates with laminate layer thicknesses thinner than about 10 μm (Yasrebi et al. 1990). Also, it is difficult, if not impossible, to control the thickness ratio of the hard and soft components at these small dimensions. However, the guidelines stated above are still useful in the sense that they present the ultimate structural features that should be achieved for the submicron and nanolaminate design. In the design of synthetic laminates, high hardness ceramics, such as BN, B_4C , TiC, ZrO_2 , and Al_2O_3 , can be used as the brittle component. Highly plastic (superplastic) metals and alloys, such as Al and Cu (and their alloys), or organic polymers, such as polyethylene and polypropylene, may be good candidates for the soft phases. Those constituent phases which give the best combination of properties, with emphasis on strong interfaces, can be used provided that they can be processed.

Some of the property requirements stated above were met to a certain degree in the B_4C -Al (Yasrebi et al. 1990; Aksay and Sarikaya 1991; Aksay and Sarikaya 1991) laminated systems designed to be used as impact-resistant materials. In one synthesis strategy for processing of B_4C -Al composites, porous B_4C layers, with thicknesses below 100 μm and as low as 15 μm , were tape cast with thin Al sheets in between. The stacks were then heated to induce infiltration and to allow bonding between Al and B_4C without an excessive reaction. The resulting composite displays a structure where both the Al-infiltrated B_4C layers and pure Al layers in between are in the form of continuous films (Yasrebi et al. 1990). The overall architecture provides alternating layers of hard and soft components and strong interfaces. As a result, mechanical properties in terms of fracture toughness and fracture strength both show a 30–40% increase over the monolithic B_4C -Al composite with the same Al composition (Fig. 1), and a structure where Al and B_4C have a three-dimensional interpenetrating network (Halverson et al. 1989). The

properties in B_4C -Al laminates are currently the best that can be achieved among the present cermet systems.

As seen from the above example, despite the fact that improvements were achieved in the mechanical properties of laminated composites based on biomimetic architecture, these improvements have not been as extraordinary as when nacre is compared to monolithic CaCO_3 . This may be due mainly to the fact that the laminate layers are not thin enough; thicknesses below 1 μm in the inorganic layers and below 100 nm in the layers of the organic or the soft phase are needed. Second, as will be clear from the discussion in the following section, both the inorganic and organic layers have complex structures, in terms of their crystallography, substructures, and morphology. In particular, it has been suggested that the organic matrix might actually have a sandwich structure containing three organic sub-layers, each having its own unique composition and molecular conformation (Watabe and Wilbur 1960; Weiner and Traub 1981, 1984; Nakahara et al. 1982). Neither the composition of these layers nor their structure have yet been clearly identified (Lowenstam and Weiner 1989; Mann et al. 1989; Simkiss and Wilbur 1989). In addition, identification of the structural relationship between the organic and the inorganic layers is far from complete (Greenfield et al. 1984; Addadi and Weiner 1985; Addadi et al. 1986; Mann 1988). Therefore, a part of our research has been directed towards the study of the structure of nacre at the nanometer scale in order to answer some of these questions (Sarikaya et al. 1992). In the following sections, we summarize the current understanding of the structural relationships in nacre. First, we present a summary of the crystallographic and morphological relationships between the building blocks which make up the inorganic component of nacre. From this study, we construct a possible structure of the underlying organic matrix, which we believe will shed more light on the areas where future studies should be focused in order to understand the structural relationships at the molecular scale.

4 Structure of the Red Abalone Shell: Prismatic and Nacreous Layers

4.1 Structure of the Shell at the Macro Level

Red abalone; *H. rufescens*, belongs to the mollusk species in the family of gastropods. Gastropods first evolved about 500 million years ago and have very successfully survived to the present time with little change (abalone is thus considered a "living fossil") (Wilbur and Yonge 1964; Morton 1979). The shell of the abalone is ear-shaped, with a large opening and a small spire. The dorsal surface is convex and exhibits growth rings. The inner surface has two scars at the position of muscle attachment and is iridescent as it consists of nacreous layers. The shell has respiratory pores (about 20 in the adult) but only the last four to five are open at a given age. The organism has a large foot with which it grabs onto



Fig. 5. SE image of a cross-section of abalone reveals the outer prismatic (PR) and inner nacreous (NC) layers

a rock when it is juvenile and forages as a bottom-dwelling mollusk on algae and plants. The shell grows about 2.5 cm per year and the diameter of the shell can reach 30 cm, after which the shell only thickens (more than 1 cm).

A longitudinal cross-section of the red abalone shell displays two types of microstructures: an outer prismatic layer and inner nacreous layer (Fig. 5). Two forms of CaCO_3 , calcite (rhombohedral, R 3 c) and aragonite (orthorhombic, Pmn₂1), constitute the inorganic phase of the composite in the prismatic and nacreous layers, respectively. The structure and properties of the nacreous layer are described in this chapter, since it is this part of the shell that displays an excellent combination of mechanical properties as a result of its highly ordered hierarchical structure (Currey 1987; Jackson et al. 1988; Sarikaya et al. 1990a,b). Furthermore, the structure of nacre is comparatively simple, having alternating layers of organic and inorganic components. This microarchitecture, especially the highly ordered inorganic component, i.e., the aragonite platelets, is more straightforward for studying crystallography with the aid of transmission electron microscopy (TEM).



Fig. 6. A TEM image showing edge-on view of the nacre section of red abalone shell with aragonite (CaCO_3) platelets, P, and thin film organic matrix, O

forming the mortar in between. As illustrated by the TEM image recorded in an edge-on configuration in Fig. 6, the thickness of the platelets is about $0.25\ \mu\text{m}$ and the organic matrix is between 10 and 50 nm in thickness, depending on the site of the shell from which the sample is extracted. As described by other researchers (Nakahara et al. 1982; Greenfield et al. 1984; Weiner and Traub 1984), the organic matrix is thought to have a sandwich form, with chitin in the middle, acidic macromolecules surrounding it, and soluble macromolecules as the outer layers adjacent to the platelets. There is some speculation on the conformation of the organic matrix and its composition (Crenshaw 1972; Addadi and Weiner 1985); however, neither direct evidence of the conformation of the macromolecules nor a quantitative analysis of the macromolecules has been possible to date.

4.2 Structure of the Nacre at the Nanometer Level

4.2.1 Morphology of Inorganic Phase: Aragonite

The general structure of nacre is seen in Fig. 5, which shows a secondary electron image of an obliquely broken sample recorded by SEM. The nacre is composed of stacked platelets throughout the thickness of the sample. Of the two types, columnar or sheet forms, nacre in abalone belongs to the former (Wilbur and Simkiss 1968; Wisc 1970; Currey 1987). The stacking is not random and in a fully grown specimen resembles a "brick and mortar" microarchitecture with the aragonite phase in the form of platelets forming the bricks and the organic matrix

4.2.2 Crystallography of Aragonite Platelets

Fundamental knowledge of the overall structural relationships between the organic and inorganic components in the closely knit structure of nacre (and in other hard tissues) is essential from the point of view of understanding, first, its mechanical properties, and second, its mechanism of formation (see, for example, Degens 1976; Mann 1988; Weissbuch et al. 1991). A more direct way to achieve such an understanding is to decipher the crystallographic relationships between the inorganic phase and organic matrix if the organic matrix also forms a crystalline lattice. Crystallinity of the organic matrix has been postulated in previous studies from the fact that it contains chitin and silk fibroin-like proteins as the outer and middle sublayers in the sandwich structure and are known to self-assemble in crystalline arrangements (Nakahara et al. 1982; Weiner and Traub 1984). In the

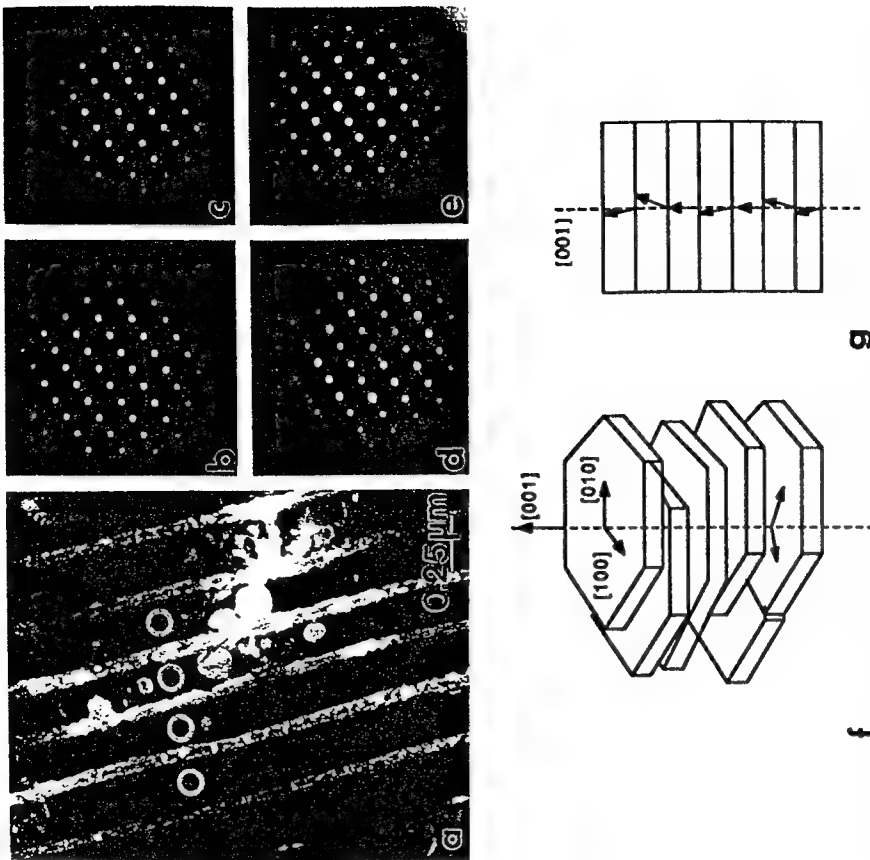


Fig. 7. Electron microdiffraction patterns (**b-e**) taken from each of the aragonite platelets in edge-on configuration shown in **a**. **f** and **g** are schematic illustrations of the misorientation of each platelet along the [001] direction

organic matrix, the outermost sublayer, the one in contact with CaCO_3 , consists mostly of soluble charged macromolecules (proteins) and presumably acts as the binder to the inorganic phase. In this scheme, it is suggested that active sites on the matrix align with those on the CaCO_3 , i.e., either Ca^{2+} ions (Weiner 1986) or CO_3^{2-} sites (ionotropy mechanism) (Greenfield et al. 1984). To date, it has been impossible to study both the organic and inorganic crystals simultaneously, and the structural relationships between the components of the nacre exist only as a conjecture (Watabe and Wilbur 1960; Meenakshi et al. 1974; Weiner and Hood 1975; Weiner and Traub 1980, 1984; Nakahara et al. 1982). Bulk studies performed by X-ray diffraction on the nacre revealed that the aragonite platelets are organized with their [001] axis perpendicular to the layers (Crenshaw 1972; Weiner and Traub 1984; Addadi and Weiner 1985). It has been postulated that the \bar{a} and \bar{b} axes, within the layer plane, are randomly oriented in each platelet. Furthermore, from this scheme, it was assumed that each aragonite platelet grows on the crystallographically related organic template, which itself has a local random orientation (Addadi and Weiner 1985; Weiner 1986). From the composition of the insoluble fraction of the organic matrix, i.e., the inner crystalline sublayers, which contain a high fraction of aspartic and glutamic acid, it might be possible to deduce a self-assembled structure that would be related epitaxially to the aragonite lattice along the [001] projection (Weiner et al. 1983; Weiner and Traub 1984).

In our studies, we followed an approach in which each aragonite crystallite was analyzed separately and its crystallographic orientation relationship was established with respect to its neighbors, both on the same layer and across the thickness of the nacre (Sarikaya et al. 1992). This was accomplished by high spatial resolution electron microdiffraction in a TEM which allowed isolated diffraction patterns from individual aragonite crystals (electron probe size as small as 50 nm diam). By such an approach, the overall crystallography of the inorganic component of the composite was established in three directions. Assuming that there is a structural relationship between the inorganic and organic components, the organic matrix, which surrounds the aragonite platelets on all sides throughout the nacre, may provide a framework by retaining all the crystallographic relationships. This scheme would then imply a lattice structure within the organic layer itself that retains the crystallographic relationship throughout the nacre structure (Sarikaya et al. 1992). To establish the crystallographic orientation relationship between the adjacent aragonite platelets, microdiffraction studies were performed both in the edge-on and face-on configurations of nacre (Sarikaya et al. unpubl.). The diffraction patterns shown in Fig. 7b-e are from regions circled in the bright field (BF) image in Fig. 7a which was recorded from nacre in the edge-on configuration. It can be seen that all the patterns belong to the same zone axis, or electron beam direction, i.e., [010] of the orthorhombic crystal. However, there is a slight orientation change between them, ranging from 0 to 5°. This misalignment is with respect to the [001] axis which is perpendicular to the flat faces of the platelets, as shown by the arrow in Fig. 7a. Therefore, the platelets are slightly rotated with respect to the [001] axis through the centers of their flat faces. It should be noted that this rotation does not follow a regular pattern but it is random, following a zig-zag pattern as depicted in the schematic illustration in Fig. 7f-g.

In the face-on view, each layer of the nacre is composed of closely packed platelets having four, five, or six edges, which may be curved rather than straight. Our study focused on the microstructure of these platelets and their crystallographic and spatial organization with respect to each other on the same layer of the nacre to draw a conclusion from their crystallographic relationships about the nature of the underlying organic matrix.

As analyzed above, adjacent platelets belong to the same [001] zone axis, but there is a slight rotation among the platelets about this axis with respect to each other. The question remains whether there is any crystallographic relationship between the \bar{a} and \bar{b} axes in each of the platelets on the same layer. The



Fig. 8a, b. Face-on image of nacre showing twin-related (A to F) aragonite platelets before (a) and after (b) slight tilting. (Sarikaya et al. 1992)

crystallographic relationship among the adjacent platelets in the face-on configuration was also analyzed by electron diffraction, which revealed that each platelet is actually twin related to the one next to it. An example is presented in Fig. 8, where six platelets from a hexagonal arrangement with an approximate 60° angle between each pair. The analysis of the electron diffraction patterns taken from each platelet indicated that they all have approximately the same zone axis. The diffraction patterns taken from the boundaries between each pair of platelets, however, reveal that each platelet is twin-related to the other in a given pair and that the twin plane is of the {110} type. Therefore, in this figure, the platelets A, C, and E are twin-related with platelets B, D, and F, respectively. The images in Fig. 8a and b were taken by slightly tilting the sample (a few degrees) to bring each of the three platelets into a strongly diffracting condition so that they give a dark diffraction contrast, respectively, in each image. This brings about the platelets which are all in the same orientation, and the remaining three in twin orientation. This arrangement would indicate that all the platelets on the same layer are twin-related to each other whether they share a boundary or not. Twinning among the platelets is called *first generation twins* since this twinning takes place at the largest spatial scale. Close analysis indicates that each platelet actually consists of several domains which are crystallographically oriented specifically with respect to each other, as shown in the BF images in Fig. 9a and b, which were recorded before and after slightly tilting the sample about the [001] zone axis. Electron diffraction patterns

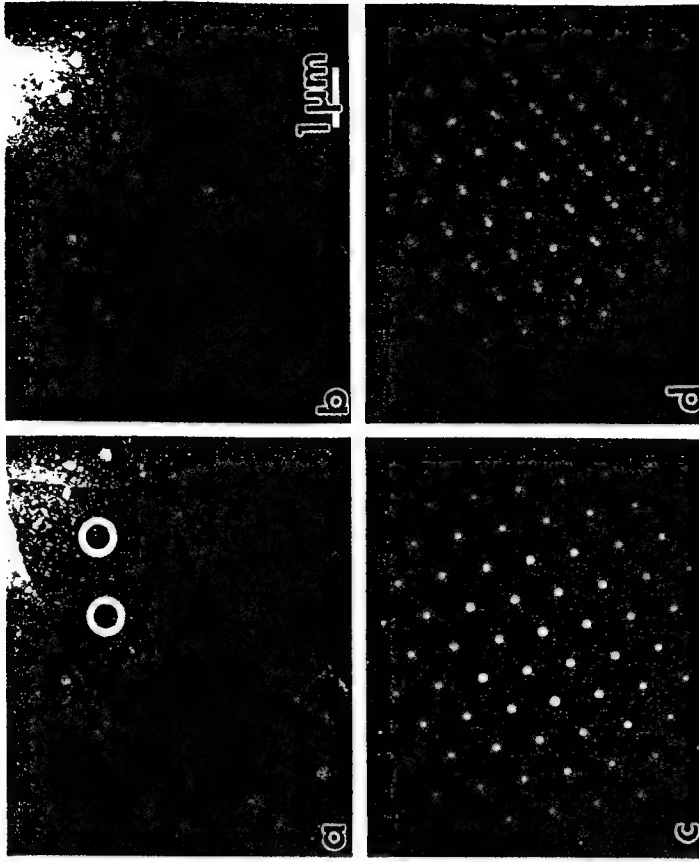


Fig. 9a and b. TEM BF images illustrating twin formation between 90° domains in a platelet. c and d. Electron diffraction patterns from the interior and boundary, respectively, of a domain. (Sarikaya et al. 1992)

taken from the interior and from the interfaces of the domains in a platelet are given in Fig. 9c and d. The single crystalline pattern in Fig. 9c is from the interior of a domain and is indexed to be in the [001] electron beam direction. On the other hand, the pattern in Fig. 9d, which was taken from the boundary between two domains as outlined by the circle in the figure, indicates that it has two superimposed patterns. Analysis of this selected area diffraction (SAD) pattern reveals that the two superimposed patterns can be correlated to each other with a twin relationship with the twin plane being {110} parallel to [001] direction of the unit cell, i.e., either (110) or (1 $\bar{1}$ 0). In fact, the SAD pattern recorded from all of the domain boundaries shows the same twin reflections, indicating that each domain is related to the one next to it by a {110} twin relation. We call these twins *second generation twins*. The analysis of the twin relationship indicates that the {110} twin planes are parallel to the outer edges of the platelets.

The number of domains in each platelet can be either six or four. Where there are six domains in a platelet, the boundaries between each pair of domains do not follow any specific crystallographic plane and are incoherent. Four-domained platelets are also frequently observed, as shown in Fig. 9; we call these platelets

which are crystallographically oriented specifically with respect to each other, as shown in the BF images in Fig. 9a and b, which were recorded before and after slightly tilting the sample about the [001] zone axis. Electron diffraction patterns

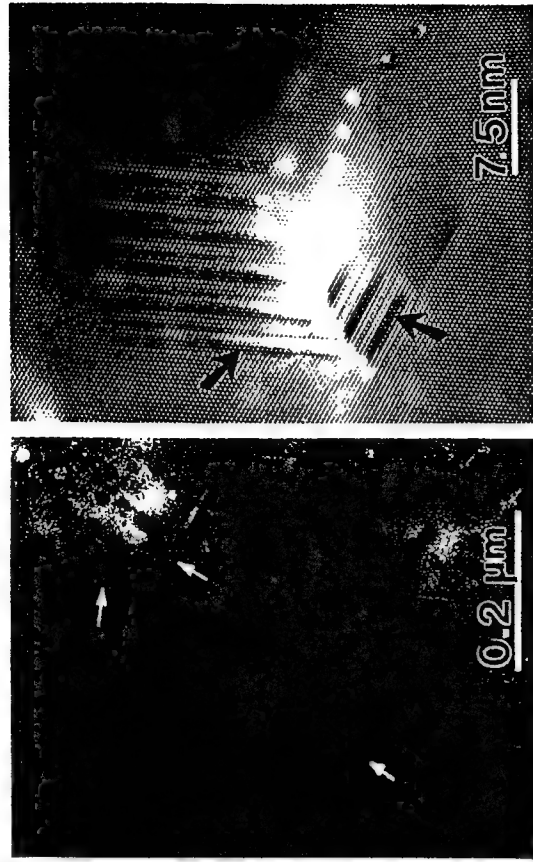


Fig. 11. **a** TEM image of domain in an aragonite platelet, showing third-generation twins. **b** Atomic resolution electron microscopy image of third-generation nanometer scale twins within a domain

-domained, as opposed to 60° -domained platelets. In the case of 90° -domained platelets, opposite domains are in the same orientation and are twin-related to the remaining two, with two of the four boundaries being atomically coherent. In an ideal hexagonally shaped platelet having six twin-related domains, the angle between each pair of domains must be 60° , with six domains completing 360° the whole platelet, as schematically illustrated in Fig. 10a. This is not possible since the outer edges of the platelets are parallel to $\{110\}$ planes and the angle between each pair of planes, for example between (110) and $(1\bar{1}0)$, is 63.5° (Fig. 10b). It leaves 3.5° unaccounted for and, as this induces strain into the aragonite matrix, therefore it must be accommodated by some structural deformation. Rather imaging of the microstructure at higher magnifications shows that each main actually contains two sets of nanometer scale twins, each forming on (110) ($1\bar{1}0$) planes.

These ultrafine twins, similar to the growth twins in geological minerals, are seen in a BF image in Fig. 11a and in the atomic resolution image in Fig. 11b lying on some crystallographic planes making an angle of about 63.5° . Based on a structural model, the accommodation of the 3.5° -strain is possible by the formation of these nanometer-scale defects on $\{110\}$ planes. If so, the lattice in each nain will be plastically deformed outwards from the boundaries, i.e., towards the

periphery of the platelet. In fact, in most cases, the outer edges of the domains are curved, with the apex in the middle of the outer edge of the domains, whereas the region at the edge where two domains meet is inwardly curved. We call these ultrafine defects *third generation twins* since they occur at the smallest scale. It must be noted that some of the lattice stress created by the 3.5° -strain can also be accommodated by the misalignment of adjacent domains, as observed. However, this cannot account for all the strain accommodation, as the interfaces between the domains show a high degree of coherency. The above analysis done on 60° -twinned platelets is also correct for 90° -twinned platelets and that the stress created due to the misorientation of domains is accommodated by the formation of similar ultrafine third generation twins.

In summary, we find that there are three scales of twins in the face-on configuration of the nacre section of red abalone shell (Sarikaya et al. 1992): (1) first generation twins among platelets having incoherent boundaries, (2) second generation twins between domains having coherent boundaries within a given platelet, and (3) nanometer-scale third generation twins within the domains. These three twin structures cover a size scale of six orders of magnitude, from the nanometer to the submillimeter, and reveal for the first time a hierarchical structure for hard tissue in a biological material. In the following section, we analyze the relationship of these hierarchical twins and their organization in the form of a space-filling tiling system, a system which will further support our hypothesis of a conformation of the underlying organic matrix that takes into account all the observed crystallographic

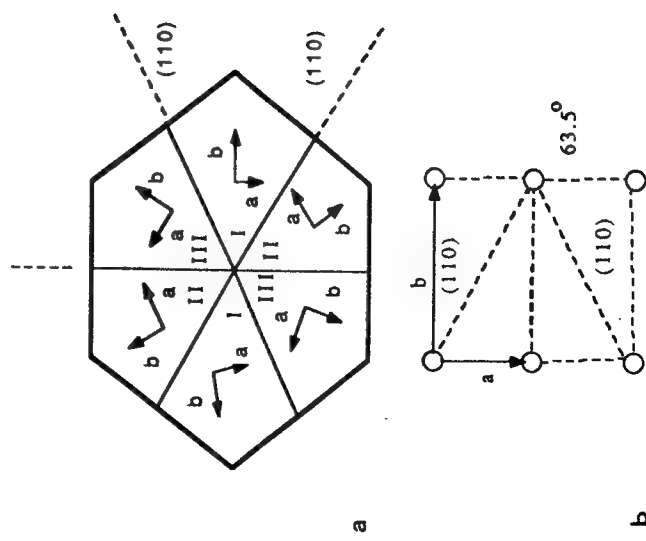


Fig. 10a, b. Schematic illustration of 60° domains in an aragonite platelet, **a** and **b**

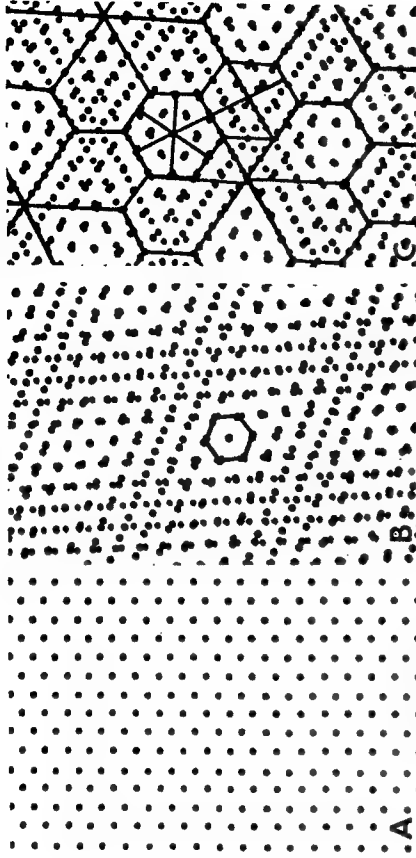


Fig. 12. A Schematic projection of the aragonite lattice in [001] orientation with Ca^{2+} ions highlighted. B Schematic illustration of the possible formation of the superstructure on the organic matrix formed by the superimposition of three aragonite lattices in [001] projection. C Possible formation of aragonite platelets (tiles) on the superstructure

As is evident from the results of the analyses in Section 4, the aragonite phase in nacre can be crystallographically correlated through three levels of twin relationships in the structural components of the nacre inorganic phase, beginning at the nanometer scale and proceeding through the millimeter scale. Although sixfold twin structures also occur in geological aragonite (Wenk et al. 1983), the hierarchical arrangement in nacre is unique in the sense that each platelet is separate from the others during the early stage of growth (Liu J., Sarikaya M., and Aksay IA; unpubl. research). On the other hand, in geological aragonite, the mimetic twin domains grow, in contact, one after another and are influenced by the presence of each other (Bragg 1924). Even after crystallization is complete, all the platelets in nacre are still separated from each other by an organic membrane (Nakahara et al. 1982; Sarikaya et al. 1990a,b). The fact that separate platelets grow simultaneously and yet have a definite crystallographic orientation relationship suggests that the growth process might be mediated by the organic template below the individual crystals, as proposed earlier (see, for example, Weiner et al. 1983; Mann 1988; Mann et al. 1988; Lowenstam and Weiner 1989; Simkiss and Wilbur 1989). In the following paragraphs, we discuss how these hierarchical twins might originate and the implication this has for the structure of the organic template on which the aragonite crystals are grown.

The interaction between the organic species and inorganic crystals must include geometrical, electrostatic, and stereochemical interactions (Addadi and Weiner 1984; Greenfield et al. 1984; Mann 1988). Therefore, the nucleation and growth of the crystals will be influenced by both the nearest and higher order interactions. The aragonite crystal structure belongs to the space group Pmcn (No. 62) with lattice parameters $a = 4.94 \text{ \AA}$, $b = 7.94 \text{ \AA}$, and $c = 5.72 \text{ \AA}$. With the number of formula units per unit cell being four, Ca^{2+} ions occupy positions $1/4, 0.08, 0.25, \text{C}$ at $0.25, 0.75, 0.08$ and $\text{O}(1)$ and $\text{O}(2)$ positions at $0.25, 0.59, 0.08$ and $0.02, 0.82, 0.08$, respectively. If the origin is taken as the center of symmetry, the mirror plane, the c-glide plane, and glide plane are at $x = 1/4, y = 1/4$ and $z = 1/4$, respectively. In the [001] projection, the Ca^{2+} ions would give the crystal a pseudo-hexagonal symmetry, as shown in Fig. 12a, and the CO_3^{2-} groups reduce the symmetry to an orthorhombic form (Sarikaya et al. unpubl.). This is physically an important characteristic in terms of the crystallographic relationships of the hierarchical twinned components of the nacre aragonite and the stereochemical relationship that might exist between the aragonite and the macromolecules in the organic matrix. The nucleation and growth of the aragonite crystals may involve both Ca^{2+} and CO_3^{2-} ions, but for simplicity, only the arrangement of Ca^{2+} ions will be illustrated in this chapter. As outlined in Fig. 12, if the array Ca^{2+} ions are considered only, they are in an approximate hexagonal closed-packed formation. True hexagonal closed-packed formation would require an axial ratio of $b/a = 1.73$; however, the observed value is 1.69. In the actual aragonite lattice, the Ca^{2+} ions are not in contact but are separated by O ions, and the pseudo-hexagonal arrangement refers to the centers of Ca^{2+} ions rather than their actual packing. Since the same $\{110\}$ twinning takes place at all length scales, superimposition of the lattices on all three possible twins with a 63.5° angle with respect to each other generates a new superlattice structure, Fig. 12B (Sarikaya et al. 1992). We call this new lattice a *superstructure*, which, in this projection, has a pseudo-hexagonal configuration of fixed lattice points. Taking the actual distance between the Ca^{2+} ions as 5.0 \AA , the distance between these lattice points would be about 30 \AA . If the nucleation and growth of the aragonite platelets take place on the underlying organic matrix, the geometrical configuration of the active sites for the binding of the Ca^{2+} ions on the organic matrix must accommodate this superlattice and, thus, all twins in the nacre. One possible solution is to assume that the binding sites on the template form a single crystalline pseudo-hexagonal lattice, or integer multiples of it, which is a reasonable assumption, since many two-dimensional membranes tend to form hexagonal lattices during self-assembly (Unwig and Henderson 1985). The hypothesis that the organic matrix may be a single crystalline is an essential feature of the structure for the formation of the highly organized tiles in nacre. A local crystalline organization of the matrix, as proposed earlier (Weiner and Traub 1984; Addadi and Weiner 1985, 1990), with no relationship between the neighboring areas and, hence, without long-range order, would result in the formation of aragonite crystals without any definite crystallographic orientation relationship among them.

and geometrical relationships among the aragonite platelets both in the face-on and in the edge-on configurations.

5 Structure of the Organic Matrix and its Relationship to the Inorganic Phase

As is evident from the results of the analyses in Section 4, the aragonite phase in nacre can be crystallographically correlated through three levels of twin relationships in the structural components of the nacre inorganic phase, beginning at the nanometer scale and proceeding through the millimeter scale. Although sixfold twin structures also occur in geological aragonite (Wenk et al. 1983), the hierarchical arrangement in nacre is unique in the sense that each platelet is separate from the others during the early stage of growth (Liu J., Sarikaya M., and Aksay IA; unpubl. research). On the other hand, in geological aragonite, the mimetic twin domains grow, in contact, one after another and are influenced by the presence of each other (Bragg 1924). Even after crystallization is complete, all the platelets in nacre are still separated from each other by an organic membrane (Nakahara et al. 1982; Sarikaya et al. 1990a,b). The fact that separate platelets grow simultaneously and yet have a definite crystallographic orientation relationship suggests that the growth process might be mediated by the organic template below the individual crystals, as proposed earlier (see, for example, Weiner et al. 1983; Mann 1988; Mann et al. 1988; Lowenstam and Weiner 1989; Simkiss and Wilbur 1989). In the following paragraphs, we discuss how these hierarchical twins might originate and the implication this has for the structure of the organic template on which the aragonite crystals are grown.

The interaction between the organic species and inorganic crystals must include geometrical, electrostatic, and stereochemical interactions (Addadi and Weiner 1984; Greenfield et al. 1984; Mann 1988). Therefore, the nucleation and growth of the crystals will be influenced by both the nearest and higher order interactions. The aragonite crystal structure belongs to the space group Pmcn (No. 62) with lattice parameters $a = 4.94 \text{ \AA}$, $b = 7.94 \text{ \AA}$, and $c = 5.72 \text{ \AA}$. With the number of formula units per unit cell being four, Ca^{2+} ions occupy positions $1/4, 0.08, 0.25, \text{C}$ at $0.25, 0.75, 0.08$ and $\text{O}(1)$ and $\text{O}(2)$ positions at $0.25, 0.59, 0.08$ and $0.02, 0.82, 0.08$, respectively. If the origin is taken as the center of symmetry, the mirror plane, the c-glide plane, and glide plane are at $x = 1/4, y = 1/4$ and $z = 1/4$, respectively. In the [001] projection, the Ca^{2+} ions would give the crystal a pseudo-hexagonal symmetry, as shown in Fig. 12a, and the CO_3^{2-} groups reduce the symmetry to an orthorhombic form (Sarikaya et al. unpubl.). This is physically an important characteristic in terms of the crystallographic relationships of the hierarchical twinned components of the nacre aragonite and the stereochemical relationship that might exist between the aragonite and the macromolecules in the organic matrix. The nucleation and growth of the aragonite crystals may involve both Ca^{2+} and CO_3^{2-} ions, but for simplicity, only the arrangement of Ca^{2+} ions will be illustrated in this chapter. As outlined in Fig. 12, if the array Ca^{2+} ions are

inorganic and organic components have a high degree of organization not encountered in synthetic materials is responsible for these superior properties. However, our current understanding of the mechanisms for toughening and strengthening is far from complete.

Morphological and crystallographical analysis by electron microdiffraction of the inorganic phase, aragonite, indicates that the individual aragonite platelets form a multiple tiling system in nacre in which twins form hierarchical defect structures which control the overall structural order. Assuming that crystal-matrix recognition is applicable, a model is forwarded for the structural conformation of the active sites in the organic matrix which may then act as the template for the formation of nacre. This model, called the superstructure, explains all the experimentally observed crystallographic and morphological relationships in the aragonite phase.

This new approach, in which the structure of an organic material is indirectly determined from detailed knowledge of the structural relationships among the subcomponents of the inorganic phase, may prove to be a viable approach for other biocomposites in which the structure of the inorganic is highly organized. This approach would not only serve as a new methodology for studying how the overall shape is determined in various species of mollusks but also for understanding general biomimeticization concepts in single and multicell organisms.

Despite considerable effort in the field, our understanding of the mechanisms that operate in nacre to make it a tough and strong composite, and our understanding of the composition and structure of the organic matrix and its structural relationship with the inorganic phase are still limited. Some of the major issues from which an agenda for future research may be formed are as follows:

1. *On Mechanical Properties.* A complete understanding of the toughening and strengthening mechanisms in nacre is necessary because of their dependence upon the structural relationships between the organic and inorganic phases. Also, mechanical property evaluation of the overall shell, particularly under the dynamic conditions in which the organism lives and makes use of its multifunctional characteristics, is essential for the design of multifunctional materials via biomimicking.
2. *On the Organic Matrix.* The protein compositions, conformations, and structural relationships of the organic matrix and its relationship to the inorganic aragonite phase are all necessary parameters for consideration in the design of synthetic materials. The relationship between the organic matrix and calcite in the prismatic layer should also be investigated.
3. *On the Mechanism of Growth.* An understanding of the nucleation of the inorganic phase in the presence of an organic matrix, beginning with the embryonic and juvenile stage of the abalone, and the degree to which the organic matrix controls growth, will assist in understanding the overall formation and shaping of the shell.
4. *On Biodegradation.* Self-assembly studies involving the *in vitro* isolation, purification, and assembly of various components of the organic matrix, separately

By tracing along the possible twin boundaries, one can see that the superlattice shown in Fig. 12C allows the generation of the overall hierarchical twin structure. One construction is illustrated in Fig. 12D, which contains all the shapes, geometry, and crystallography-related features discussed in this chapter, such as five-edged platelets with 90°-domains, sixfold symmetry of platelets, and six- and three-edged domains (Sarikaya et al. 1992). The fact that one can generate all the possible configurations in this way again illustrates that a pseudo-hexagonal template structure might be a possible solution for the structure of an organic matrix that can accommodate all the twin relationships, rather than the lattice of a single domain. The ultrastructure in the organic matrix would not only be single crystalline on the flat surface but also through the transverse direction (through-thickness direction) in nacre.

The geometrical and crystallographic model of aragonite platelets proposed in this chapter is referred to as multiple tiling in mathematics (see, for example, Grünbaum 1987). It appears that in nacre, nature utilized this mathematical technique to form a highly ordered structure that is compatible with both soft tissue and the crystalline structural constraints of hard tissue. Tiling may also play an important role in providing the overall shape of the nacre and its mechanical properties. Many mollusks, such as gastropods, cephalopods, and bivalves, have aragonite platelets as the fundamental building blocks in nacre, but have grossly different overall shapes (Nicol 1960; Wilbur and Yonge 1964; Morton 1979). For example, in red abalone, the shell is quite flat and thick, in nautilus, the shell is round and thin, forming an elegant chambered structure in which even the separation walls of the chambers are made of nacre. In all these nacre structures, aragonite platelets more or less have the same dimensions, about 0.2–0.5 μm thick and about a 5–10 μm edge length (Sarikaya et al. unpubl.). Yet the multiple tiling of the platelets and the crystallographic relationship between the platelets may be different due to slightly different structures and compositions in their underlying organic matrices. Further studies are required on various species of these organisms, both on the crystallography of the mineral component and on the structural and compositional analyses of the organic matrices, in order to decipher their structures and the unifying, underlying principles for the organization and formation of the various shapes of shell containing nacre structures. It should be clear that a fundamental understanding of these structures is essential for the possible formation of synthetic composites through biomimetics.

6 Summary and Future Directions

We have reviewed the results of most recent studies on the mechanical properties and structure of the nacre section of red abalone. Nacre, which is about 95 vol% aragonitic and about 5 vol% organic macromolecules, has fracture toughness and fracture strength properties that are orders of magnitude higher than those of monolithic aragonite. From analysis of the toughening and strengthening mechanisms, one can conclude that the unique structure of nacre in which the

and in combination, for the mineralization of CaCO_3 and other minerals under controlled conditions will lead to a fundamental understanding of how the synthesis might be controlled for the structures of hard biological components. Designing and processing novel materials similar to the multifunctional, nanolaminated composites inspired by nacre through biomimicking approaches, and eventually through bioduplication, will have to wait until we answer the crucial questions regarding the structure and function of this system.

Acknowledgments. We acknowledge the technical input by Dr. Jun Liu. This work was performed under the sponsorship of Air Force Office of Scientific Research under Grant Numbers AFOSR-89-0496, AFOSR-91-0040, and AFOSR-91-0281.

References

- Addadi L, Weiner S (1985) Interaction between acidic proteins and crystals: stereochemical requirement in biomineratization. *Proc Natl Acad Sci USA* 82:4110-4114.
- Addadi L, Weiner S (1980) Interaction between acidic macromolecules and structured crystal surfaces, stereochemistry and biomineratization. *Mol Cryst Liq Cryst* 13:305-322.
- Addadi L, Berkovich-Yellin Z, Weissbuch I, Lahav M, Leiserowitz L (1986) A link between macroscopic phenomena and molecular chirality: crystals as probes for the direct assignment of absolute configuration of chiral molecules. In: Topics in stereochemistry, vol 16. Wiley, New York, pp 1-85.
- Aksay IA, Sarikaya M (1991) Biomimic processing of composite materials. In: Soga S, Kato A (eds) Ceramics: toward the 21st century. Centennial Int Symp. Japanese Ceramic Society, Tokyo, pp 136-149.
- Alper M (1991) Enzymatic synthesis of materials: an overview. In: Alper M, Rieke PC, Frankel R, Calvert PD, Tirrell DA (eds) Materials synthesis based on biological process: proceedings of a symposium series, vol 218. Materials Research Society, Pittsburgh, pp 3-6.
- Berman A, Addadi L, Leiserowitz L, Weiner S, Nelson M, Kvirk A (1990) A synchrotron X-ray study of a unique protein-calcite composite material. *Science* 250:664-667.
- Beycheler G, Nakahara H (1968) An electron microscopy study of the formation of the nacreous layers in the shells of certain bivalve molluscs. *Calcif Tiss Res* 3:84-92.
- Blakemore RP (1975) Magnetotactic bacteria. *Annu Rev Microbiol* 36:217-238.
- Bouligand Y (1965) Sur une architecture torsadée répandue dans de nombreuses cuticules d'arthropodes. CR Hebd Seances Acad Sci Paris Ser A 261(12):3665-3668.
- Bragg WI (1924) The structures of aragonite. *Proc R Soc Lond Ser A* 17.
- Brown WF Jr, Strawley JE (1966) Plain strain fracture toughness testing of high strength metallic materials. ASTM technical publ, No 410. American Society for Testing and Materials, Philadelphia.
- Cottrell AH (1953) Dislocations and plastic flow in crystals. Oxford Univ Press, Oxford.
- Crenshaw MA (1972) Mechanism of normal biological mineralization of calcium carbonates. In: Nancollas GH (ed) Biological mineralization and demineralization. Springer, Berlin Heidelberg New York, pp 243-257.
- Crugeier W, Crugeier A (1982) Biotechnology. Sinauer Associates, Sutherland, Massachusetts.
- Currey JD (1974) The mechanical properties of some molluscan hard tissues. *J Zool (Lond)* 173:39-406.
- Currey JD (1976) Further studies on the mechanical properties of mollusc shell material. *J Zool (Lond)* 180:445-453.
- Currey JD (1977) Mechanical properties of mother of pearl in tension. *Proc R Soc Lond B* 196:443-463.
- Currey JD (1987) Biological composites. *J Mat Edu* 9[1-2]:118-296.
- Dameron CT, Reese RN, Mehra RK, Kortan AA, Carroll PJ, Steigerwald ML, Brus LE, Winge DR (1989) Biosynthesis of cadmium sulfite quantum semiconductor crystallites. *Nature* 338:596-597.
- Dowridge RW (1979) Mechanical behavior of ceramics. Cambridge Univ Press, Cambridge, p 15.
- Dogens ET (1976) Molecular mechanisms on carbonate, phosphate, and silica deposition in the living cell. *Top Curr Chem* 64: 1-112.
- Engel L, Klingele H (1981) An atlas of metal damage. Wolfe Science Books, Munich, Germany.
- Evans AG (1988) High toughness ceramics. *J Mat Sci Eng A* 105/106:65-75.
- Evans AG, Marshall DA (1989) The mechanical behavior of ceramic matrix composites. *Acta Met* 37(10):2567-2583.
- Fendler JH (1987) Atomic and molecular clusters in membrane mimetic chemistry. *Chem Rev* 87:887-899.
- Frankel RB, Blakemore RP (1991) Iron biominerals. Plenum, New York.
- Frankel RB, Blakemore RP, Wolfe RS (1979) Magnetite in freshwater magnetotactic bacteria. *Science* 203:1355-1356.
- Glimcher MJ (1981) On the form and function of bone: from molecules to organs. In: Veis A (ed) The chemistry and biology of mineralized biological tissues. Elsevier, New York.
- Anastardent, pp 617-673.
- Gosline JM, DuMont ME, Denny MW (1986) Structure and properties of spider silk. *Endeavour* 10(1):37-43.
- Greenfield EM, Wilson DC, Crenshaw MA (1984) Ionotropic nucleation of calcium carbonate by molluscan matrix. *Am Zool* 24:925-932.
- Grégoire C (1972) Structure of the molluscan shell. In: Florkin M, Scheer B (eds) *Chem Zool Academic Press*, New York, pp 45-102.
- Griffith RA (1920) The phenomena of rupture and flow in solids. *Philos Trans CCXXI-A*:163-198.
- Grünbaum B (1987) Pattern and tiling. Plenum, New York.
- Gunnison KE (1991) Structure-mechanical property relationships in a biological ceramic-polymer composite: nacre. MS Thesis, University of Washington, Seattle.
- Haggan J (1988) Membranes play growing role in small-scale industrial processing. *Chem Eng News* 66(28):25-32.
- Halverson DC, Pyzik AJ, Aksay IA, Snowden WE (1989) Processing of boron-carbide/aluminum composites. *J Am Ceram Soc* 72(5):775-780.
- Honeycombe RWK (1968) The plastic deformation of metals. St. Martin's Press, New York.
- Hull D (1981) An introduction to composite materials. Cambridge University Press, Cambridge, UK, pp 81-100.
- Jackson JP, Vincent JFV, Turner RM (1988) The mechanical design of nacre. *Proc R Soc Lond B* 314:415-440.
- Khatua S (1991) Processing of laminated B_4C -polymer laminated composites. MS Thesis, University of Washington, Seattle.
- Larrea VJ, Heuer AH (1990) The micro-indentation behavior of several mollusk shells. In: Reike PC, Calvert PD, Alper M (eds) Materials synthesis utilizing biological processes: proceedings of a symposium series, vol 174. Materials Research Society, Pittsburgh, pp 125-131.
- Lowenstein HA, Weiner S (1989) On biomineratization. Oxford University Press, New York.
- Mann S (1988) Molecular recognition in biomineratization. *Nature* 332:119-123.
- Mann S, Heywood BR, Rajjam S, Birchall D (1988) Controlled crystallization of CaCO_3 under stearic acid monolayer. *Science* 334:692-695.
- Mann S, Webb J, Williams RJ (eds) (1989) Biomineratization: chemical and biochemical perspectives. VCH publ, Weinheim.
- Meenakshi VR, Donnay G, Blackwelder PL, Wilbur KM (1974) The influence of substrata on calcification patterns in molluscan shell. *Calcif Tissue Res* 15:31-44.
- Morton JE (1979) Molluscs. 5 edn. Hutchinson, London.
- Mutvei H (1970) Ultrastructure of the mineral and organic components of molluscan nacreous layers. *Biomineratization* 2:48-72.
- Nakahara H, Bevelander G, Kakei M (1982) Electron microscopic and amino acid studies on the outer and inner shell layers of *Halitota rufescens*. *VENUS (Jpn J Malac)* 41(1):33-46.
- Nico JA (1960) The biology of marine animals. Interscience, New York.
- Sarikaya M, Gunnison KE, Yasebi M, Aksay IA (1990a) Mechanical property-microstructural relationships in abalone shell. In: Reike PC, Calvert PD, Alper M (eds) Materials synthesis utilizing biological processes: proceedings of a symposium series, vol 174. Materials Research Society, Pittsburgh, pp 109-116.
- Sarikaya M, Gunnison KE, Yasebi M, Aksay IA (1990b) Seashells as a natural model to study laminated composites. In: Proc Am Soc of Composites, Fifth Tech Conf Technomic Publ Co, Lancaster, Pennsylvania, pp 176-183.
- Sarikaya M, Liu J, Aksay IA (1992) Multiple tiling with hierarchical twins: TEM study of the nacre structure in red abalone. (submitted).
- Simkiss K, Wilbur KM (1989) Biomineratization: cell biology and mineral deposition. Academic Press, New York.

- Towe MK, Hamilton GH (1968) Ultrastructure and inferred calcification of the mature and developing nacre in bivalve mollusks. *Calcif Tissue Res* 1:306–318
- Tressler RI, Bradt RC (eds) (1984) Deformation of ceramic materials II. Materials science research, vol 18. Plenum, New York
- Unwig N, Henderson R (1984) The structure of proteins in biological membranes. *Sci Am* 250(2):78–94
- Wasserman SR, Whitesides GM, Tidswell IM, Ocko BM, Pershan PS, Axe JD (1989) The structure of self-assembled monolayers of alkylsiloxanes on silicon: a comparison of results from ellipsometry and low angle X-ray reflectivity. *J Am Chem Soc* 111:5852–5861
- Watabe N (1965) Studies in shell formation: crystal-matrix relationships in the inner layers of molluscan shells. *J Ultrastruct Res* 12:351–370
- Watabe N, Wilbur KM (1960) Influence of the organic matrix on crystal type in molluscs. *Nature* 188:334–336
- Weiner S (1986) Organization of extracellularly mineralized tissues: a comparative study of biological crystal growth. *CRC Crit Rev Biochem* 20(4):365–380
- Weiner S, Hood L, (1975) Soluble protein of the organic matrix of mollusc shells: a potential template for shell formation. *Science* 190:987–989
- Weiner S, Traub W (1980) X-ray diffraction study of the insoluble organic matrix of mollusc shells. *FEBS Lett* 111(2):311–316
- Weiner S, Traub W (1981) Organic matrix-mineral relationships in mollusc shell nacreous layers. In: Balaban M, Sussman JL, Traub W, Yonath A (eds) Structural aspects of recognition and assembly in biological macromolecules. Balaban ISS, Yehovot Philadelphia, pp 462–487
- Weiner S, Traub W (1984) Macromolecules in mollusc shells and their functions in biomimetication. *Philos Trans R Soc Lond B* 304:425–434
- Weiner S, Talmon Y, Traub W (1983) Electron diffraction studies of molluscan shell organic matrices and their relationship to the mineral phase. *Int J Biol Macromol* 5:325–328
- Weissbuch I, Addadi L, Lahav M, Leiserowitz L (1991) Molecular recognition at crystal interfaces. *Science* 253:637–645
- Wenk HR, Barber DJ, Reeder RJ (1983) Microstructures in carbonates. In: Reeder RJ (ed) Reviews in mineralogy, vol 11. Miner Soc Am, Washington DC, pp 301–367
- Wilbur KM, Simkiss K (1968) Calcified shells. *Compr Biochem* 26A:229–295
- Wilbur K, Yonge CM (eds) (1964) Physiology of Mollusca. Academic Press, New York
- Wise SW (1970) Microarchitecture and mode of formation of nacre (mother-of-pearl) in pelecypods, gastropods, and cephalopods. *Eclogae Geol Helv* 63(3):775–797
- Yasrebi M, Kim GH, Milius DL, Sarikaya M, Aksay IA (1990) Biomimetic processing of ceramics and ceramic-based composites. In: Brinker CJ, Clark DE, Ulrich DR, Zelinski BJJ (eds) Better ceramics through chemistry IV: proceedings of a symposium series, vol 180. Materials Research Society, Pittsburgh, pp 625–635

"Bioinspired Processing of Composite Materials"

I. A. Aksay and M. Sarikaya

in *Ceramics: Toward the 21st Century
Centennial International Symposium*

edited by N. Soga and A. Kato
(Ceramic Society of Japan, Tokyo, 1991) pp. 136-149

BIOINSPIRED PROCESSING OF COMPOSITE MATERIALS

Ilhan A. Aksay and Mehmet Sarikaya

Department of Materials Science and Engineering, and
Advanced Materials Technology Center, Washington Technology Center,
University of Washington, Seattle, Washington, USA 98195

*Biologically produced composites possess hierarchical architectures with synergistic variations from atomic to macroscopic dimensions. Consequently, these biocomposites display unique properties that are affected by processes operating at all levels of the length scale. As a source of inspiration for new design concepts, we examine the structure of nacre (abalone shell) and show that a similar architectural design for laminated ceramic/metal and ceramic/polymer composites, produced by totally artificial methods (biomimetics), results in improvements in the mechanical properties of the laminates compared to the same phase-composition materials of isotropic morphology. We also examine the formation of nanometer-sized particles in a microorganism (*Aquaspirillum magnetotacticum*) and illustrate process mechanisms somewhat similar to those used by this microorganism (bioduplication) that can be utilized to synthesize multiphase and nanosized particles in phospholipid vesicles.*

I. Introduction

When materials are manufactured with an emphasis on tailoring their properties through microstructural control, the extent of this control is generally at a specific length scale. For instance, the mechanical properties of most metallic materials are controlled through the manipulation of dislocation dynamics at the nanometer length scale, whereas the mechanical properties of ceramic materials are controlled through the propagation of cracks that are initiated from defects of micrometer length scales.

In contrast, many biologically produced materials are very complex in structural design at a spectrum of length scales varying from atomic to macroscopic dimensions and possess unique hierarchical architectures [1-6]. Cellulose-based aggregates in wood [7], collagen-based aggregates in skin, cartilage, and bone [1-3,5,6,8], and chitin-based aggregates in seashells [1,4,6,9-13] are excellent examples of nature's way of designing composites for multifunctional applications by efficient and ecologically balanced methodologies. These hierarchically structured materials display unique properties that are affected by processes operating at all levels of the length scale spectrum [1-13].

It is interesting to note that when we attempt to engineer composites with functions similar to those found in biological materials, the architectural design of the manmade materials

also starts to display similar hierarchical features and multifunctionality. For instance, the architecture of fiber-reinforced automobile tires, which are designed to perform a multitude of functions, is very similar to the hierarchical design observed in intestinal tissue or elephant trunk. However, it is quite unlikely that the engineers who came up with these innovative designs had any knowledge of their similarity to biological analogs.

Our contention is that if we were to utilize biological systems as a source of *inspiration* for new design and processing concepts, then more manmade materials might display these unique architectural features and thus multifunctional performance characteristics [14]. We envision two approaches to achieve this goal of *bioinspired* processing: (i) *biomimetics* and (ii) *bioduplication*. The biomimetic approach aims at designing hierarchical structures by synthesis and processing methodologies that are largely artificial with respect to the biological processing mechanisms. However, these artificially engineered composites will exhibit structural features similar to those found in biological composites. For instance the example of automobile tire mentioned above falls into this category. Conversely, the bioduplication approach aims at producing hierarchical structures by mechanisms very similar to those observed in biological synthesis and processing methodologies.

In support of this bioinspired processing concept, in this paper we provide examples from both the biomimetic and the bioduplication approaches on the synthesis and processing of ceramics and ceramic-based composites. For the biomimetic approach, we first summarize our recent studies on the structure and properties of abalone shell and illustrate that similar structures and thus properties can be modeled in laminated ceramic/metal (cermet) and ceramic/polymer (cerpoly) composites by using totally artificial process methodologies. With respect to our Japanese hosts of this symposium, we acknowledge them as the originator of this concept of artificially produced laminated ceramic/metal composites since Samurai sword appears to be the first manmade laminated ceramic/metal composite that displays striking similarities to the structure of abalone shell.

In the category of bioduplication, we use the bacterium *Aquaspirillum magnetotacticum* as an example of a microorganism that produces nanometer-sized superparamagnetic magnetite particles. We then illustrate that mechanisms somewhat similar to those used by this microorganism can be utilized to synthesize ceramic particles of different structures and compositions in phospholipid vesicles.

II. Design in Biologically Produced Ceramic/Polymer Composites

Most biologically produced composites are built upon a fibrous framework of either collagen, chitin, or cellulose and always reveal a hierarchical structure that originates at the molecular level [1-3,7,8,12,13]. In all cases, the structures are formed by groupings of discrete units in the form of fibrils, which themselves are composed of smaller subfibrils and microfibrils. These highly interacting fibrous units are organized to form a variety of oriented

hierarchical composite systems that are designed to meet a spectrum of functional requirements. For instance, a classical hierarchical system that connects muscle and bone is tendon, which in use is subjected almost exclusively to uniaxial tensile stresses along its length. The hierarchical structure of tendon displays six discrete levels of organization [2,3,8]: (i) at the molecular level, a triple helical arrangement of polypeptide chains forms the basic tropocollagen molecule at a length scale of 1.5 nm; (ii) tropocollagen molecules aggregate to form microfibrils at a length scale of 3.5 nm; (iii) microfibrils are packed into a lattice structure forming subfibrils at a length scale of 10-20 nm; (iv) the subfibrils are joined to form fibrils at a length scale of 50-500 nm; (v) these fibrils serve as the basic building blocks to form fascicles at a length scale of 50-500 μ m; and (vi) two or three fascicles together form the structure referred to as tendon. This multilevel organization then imparts both nonlinear reversible mechanical properties and toughness to the tendon. If the tendon is subjected to excessive stresses, individual elements at different levels of the hierarchical structure fail independently [2,3,6]. These elements absorb energy and protect the tendon as a whole from catastrophic failure.

In collagen, the tropocollagen molecules are arranged with a stagger that results in a 64 nm band structure and a 30-40 nm gap between the molecules [1,12]. This gap is believed to be associated with the nucleation of the hydroxyapatite mineral as the inorganic phase leading to the formation of bone [1,5,12]. Similar to the role that collagen plays in the formation of bone, a chitin-based fibrous framework acts as the template for the formation of the orthorhombic form of calcium carbonate (aragonite) crystals in nacre, or mother of pearl [4,9-13]. Here, the structure is composed of layers of aragonite platelets held together by a matrix of acidic proteins organized around the network of chitin fibrils (Fig. 1) [1,4,6,9-13].

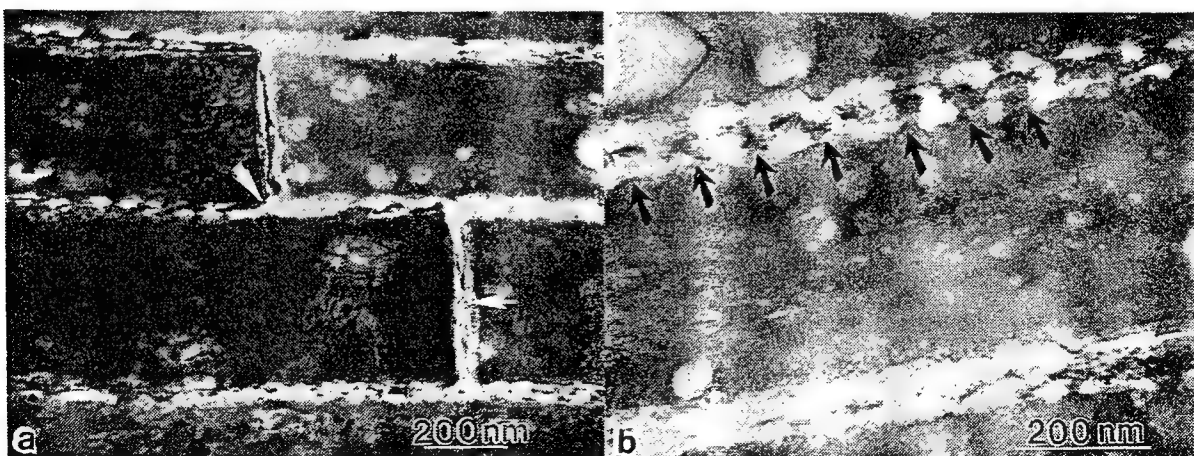


Figure 1(a) and (b). Conventional transmission electron microscopy (TEM) images of cross section of abalone shell revealing the nacre structure. Dark layers are the ceramic phase and the light color interfacial regions contain a fibrous network of organic tissue as highlighted with arrows [9].

In Figs. 1 and 2, the aragonite layers are shown to be highly regular, about 0.25-0.5 μm thick [9-11]. These layers are glued together by ultrathin, 10 nm, tough, proteinaceous composite nanoscale layers that are specifically functionalized to bond to the inorganic layers [1,12]. This rigid, predominantly inorganic (~ 95% by volume) hierarchical composite is toughened by the organic nanoscale layer, as is evident from the fact that the fracture path is both relatively wide and tortuous with inorganic platelets held by organic ligaments. There is also a significant irreversible deformation of the overall composite due to the sliding of platelets over the organic layers as shown in Fig. 2(a-b) [11].

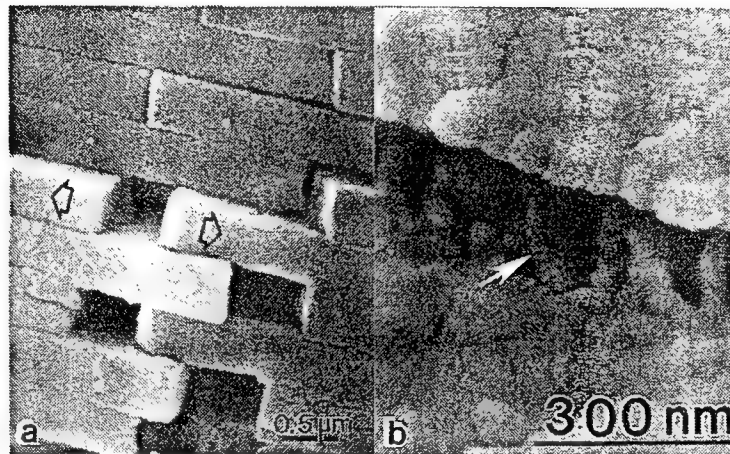


Figure 2. (a) Sliding of aragonite platelets during crack propagation in nacre and (b) ligament formation by the organic matrix between the platelets [11].

The resultant layered composite, incorporating hard inorganic layers (aragonite platelets) surrounded by a nanometer-thick organic matrix, is an excellent nanoscale layered design for a perfect impact resistant material, as evidenced from both the toughness and strength increases in nacre compared to single crystalline aragonite (Fig. 3). In the case of nacre, both the fracture toughness and fracture strength increase significantly. Unusual toughening mechanisms, in particular irreversible deformation, may be responsible for the increase in toughness in what is practically a ceramic material. Studies [11] on crack propagation behavior indicate that two mechanisms play a key role in enhancing the toughness: (i) energy dissipation during sliding of the aragonite layers, resulting in an overall plastic deformation of the composite (Fig. 2(a)); and (ii) energy dissipation during stretching of the chitin filaments (Fig. 2(b)). In both cases, the presence of an ionic bond between aragonite and the organic layer is believed to be essential for optimization of the properties. To date, however, there is no clear explanation that can account for the strength increases in these biological ceramic/polymer composites. The increase in strength cannot be explained based solely on the effect of the size of the layers and the rule of mixtures. The best explanation that we can presently put forward is that the tensile stress applied to the nacre is transferred to compressive stresses during loading. As evident from the

inward bulging of the edges of the indentation [10], this stored energy during loading results in dilation during load release; the failure of the composite appears to take place during unloading. Although not fully understood, this failure mode effectively increases the overall strength of the composite many orders of magnitude.

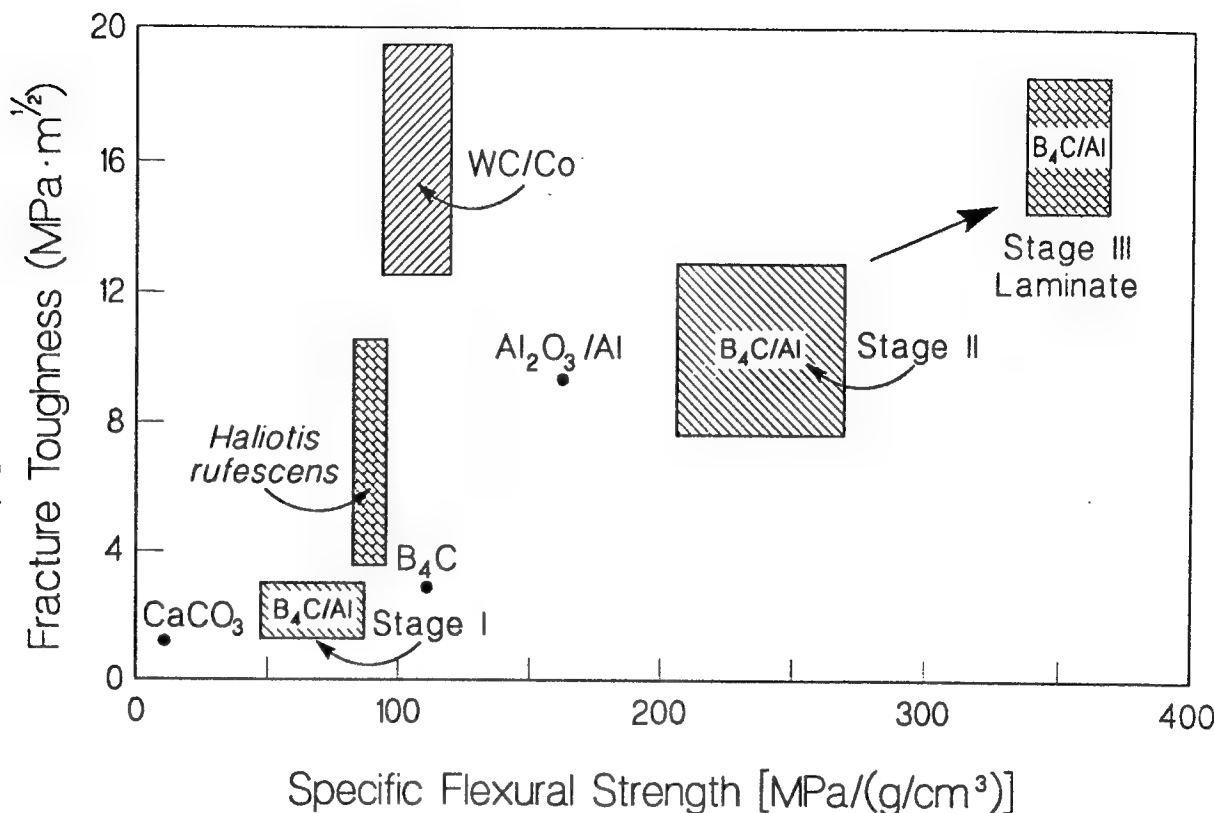


Figure 3. Mechanical properties of the nacre of red abalone (*Haliotis rufescens*) compared to ceramics and ceramic-based composites. In *Stage I*, the processing of boron carbide/aluminum was done by hot pressing of mixed powders. In *Stage II*, an infiltration technique was used to process an isotropic and bicontinuous composite. In *Stage III*, the lamination techniques described in this paper were used.

III. Synthesis and Processing of Hierarchical Structures

The example of nacre as a hierarchically structured biological ceramic/polymer composite illustrated in Section II indicates the design principles that synthetic hierarchical structures will require in order to achieve superior properties. Synthetic examples given in this section illustrate two key points: (i) by mimicking the architecture of biological composites through artificial methods, it is possible to improve upon the properties of composites even though we may not quite understand how biological composites are produced; and (ii) by realizing that the first approach will ultimately be insufficient, longer range research on bioduplication will aid in advancing the progress in biomimetics by integrating biological methodologies with synthetic ones. We also recognize that the concept of biomimetics is not a totally new concept since

many conventional composites are already produced with hierarchical structures that are similar to those found in biological counterparts.

(A) Biomimetic Approach:

Laminated Ceramic/Metal and Ceramic/Polymer Composites: Based on the design criteria derived from nacre [11], we have been working on the processing of cermet and cerpoly laminated composites through tape casting and liquid infiltration techniques, specifically with boron carbide/aluminum [15,16] and boron carbide/polymer [17] composites, respectively. In both cases, significant increases in both the fracture toughness and fracture strength have been observed (Fig. 3). Toughening mechanisms similar to those that operate in biological composites also operate in these synthetic laminates (Fig. 4). However, the improvements in the properties of synthetic laminates are still far inferior to the properties of laminated biological composite structures. The conjecture is that a major reason for our failure to achieve the values of the biological composites is because our current processing strategies do not permit processing of laminates on the micro- and nanometer scales.

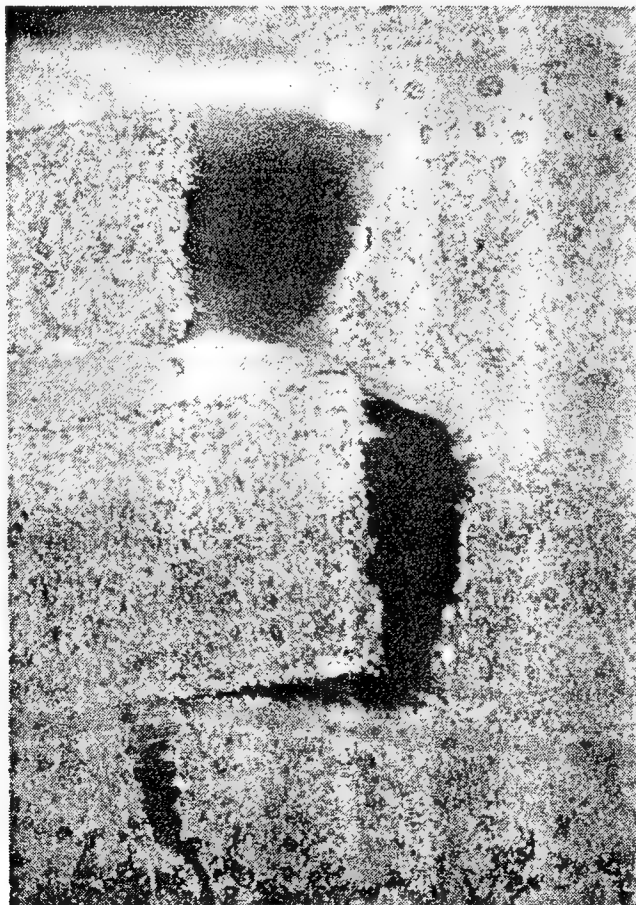


Figure 4. Fracture pattern of a laminated boron carbide/polypropylene composite illustrating polymer bridging within and between the ceramic layers ($\sim 90 \mu\text{m}$) [17].

These laminated composites can be formed by one of three basic methods: (i) partially sintered ceramic tapes are sandwiched with metal or polymer sheets and then heated to induce infiltration of the metal or the polymer; (ii) nonsintered ceramic tapes are stacked, partially sintered, and then infiltrated with metal or polymer; and (iii) nonsintered ceramic tapes of different porosity are laminated (stacked and pressed), partially sintered, and then infiltrated. In all cases, the resulting structure is a ceramic/metal or ceramic/polymer laminated composite with metal or polymer at intra- and interlayers (Fig. 4).

Mechanical property testing of laminated boron carbide/aluminum cermets in four-point bending showed increases in fracture strength and toughness over the same aluminum-content materials with an isotropic morphology (Fig. 3). When the aluminum content of laminated samples was altered by changing the ratio between the aluminum-rich and boron carbide-rich layers in the microstructure, a ratio of 6 to 1 of high-boron-carbide-content tape to low-boron-carbide tape (and hence the aluminum-rich region in the post-infiltration microstructure) with a 33.5 vol% aluminum content resulted in the highest fracture strength (945 MPa).

After the proper ratio of high boron carbide content to low boron carbide content (or aluminum-rich) laminae was determined to be 6 to 1, simultaneous changes in the size of both laminae were made while maintaining the ratio. The effect of changing the thickness of the laminae on both fracture strength and fracture toughness was in agreement with the Hall-Petch relation. The coarsening of the microstructure by increasing the tape thicknesses degraded the mechanical properties, with values approaching those for isotropic samples. Finer 6 to 1 ratio graded laminate structures have not been processed at this time due to the difficulty in casting and handling tapes thinner than 15 μm .

In the case of boron carbide/polypropylene laminates, the work of fracture of the laminates similar to the ones shown in Fig. 4 showed a 30- to 40-fold increase over monolithic and porous preforms. But no strength increase was observed.

Samurai Sword: A Laminated Nanocomposite: The practice of controlling the microstructure of materials at the nanoscale to achieve desired properties has a long history, especially in metallurgy [18]. Understanding the microstructures in successful ancient materials is essential both for developing "microarchitectural design" concepts for modern multifunctional composites as well as generating new alloy microstructures. For instance, it has been known for many centuries that laminated steels make stiff, strong, and tough swords by alternating thin layers of a stiff metal alloy with thin layers of a tough alloy. These remarkable composite structures are still being studied today [19,20]. An excellent example of this is Damascus steel, which was developed in the Middle East during the late iron age, more than 2000 years ago. The steel was used mostly for armor applications requiring high toughness as well as high strength and hardness. The metallurgy that produced Damascus steel is based on a simple thermomechanical cycle which forms a composite microstructure containing soft and hard phases. Originally "cast" high carbon steel (>1.0-2.0 wt% C) is homogenized at 1200°C,

which produces coarse austenite (γ) grains. The steel is then cooled slowly through the γ +carbide (Fe_3C) region during which pre-eutectoid carbides form at prior austenite grain boundaries. The coarse microstructure is "broken down" during forging at temperatures of 750°-900°C, and carbides spherodize to form strings of particles in refined austenite grains. Quenching into warm water (40°-80°C) from about 750°C transforms the fine austenite grains into fine needles of brittle but strong martensite, which is a supersaturated ferrite. The material is then annealed at 200°-300°C to produce tempered fine carbides (200-500Å) to form what is now still strong, but relatively tough, martensite needles. The resulting microstructure is then tough martensite containing ultrafine precipitates with hard strings of carbides decorating prior austenite grain boundaries.

Many variations of iron-based microstructures have since been developed by modifying the thermomechanical treatments and, most notably, by "composite lamination," which incorporates both pure iron (soft and tough) and high and medium carbon steels (hard and strong). An excellent example of this is Samurai sword, which is truly "nanolaminated" and is an ideal material for its purpose because of its unique combination of toughness, hardness, and rigidity [21,22]. These three properties in one material, however, are contradictory: that is, toughness implies a soft material that bends easily; hardness is associated with brittle material; and rigidity requires high strength at low strain. Apparently, Japanese smiths many centuries ago developed these composites based on techniques similar to the earlier techniques of Damascus steel-making and by knowing how thermomechanical treatments and compositional adjustments can change the steel's properties.

The final body of the Samurai sword blade is a hierarchical structure consisting of a soft inner core (ferrite) with a hard outer core (low-carbon martensite). The steel is produced first in the form of a laminated iron and steel blank with dimensions 1.5 cm thick by 5 cm wide and 15-20 cm long. The blank is inserted into pine ash (carbon source) and heated white hot (about 600°-800°C) and then doubled onto itself by hammering until it takes its original width. This process is repeated fifteen to twenty times. Four similar blanks are then welded together, and the same thermomechanical treatment is repeated five times. Eventually, the resulting blank, presumably, forms a laminate with the thickness of each lamellae equal to a few nanometers [21,22]. The surface of the blade (the laminated blank) is then scraped and ground to shape. The final blade is covered with a mixture of clay and fine sand and dried. The blade is then heated to about 900°C and quenched in a room temperature bath of oil or water by inserting the tip first and then the sharp edge horizontally. The final blade has a curved shape with the sharp edge having mostly a hard and strong martensitic structure and the back edge consisting of the relatively soft ferritic microstructure, providing ultra-rigidity to the overall material.

It should be noted here that the microstructures of lath martensitic steels and nacre are very similar. It is the martensite lath, which has dimensions similar to the aragonite platelets in nacre (both about 0-25 μm thick), that provides strength. The thin film retained austenite (50-

500 Å thick) [23] that covers the martensite platelets (laths) is similar to the organic layer (~ 200Å) covering the aragonite platelets in the nacre. Furthermore, in both cases, the interfaces are very strong between the hard and soft phases. In nacre, adjacent aragonite platelets have their [001] axis perpendicular to the platelet/organic matrix interface, with plates rotating slightly (1-5°) with respect to this axis. In martensite, similarly, the adjacent laths have a common <110> axis, perpendicular to the α'/γ interface, with laths rotating slightly (1-6°) with respect to this axis. In both cases, the matrices (organic phase in the nacre and austenite in lath martensitic structures) have the same orientation throughout. However, the difference between the two structures is that the lath martensite contains packets (three 70° variants of martensite grains, with their attendant austenite grains, randomly distributed throughout the sample) [23]. In the nacre, the local arrangement of the layered structure is repeated throughout the sample. Therefore, lath martensite is a true three-dimensional structure, with local laminated domains, resulting in isotropic mechanical properties. Nacre, on the other hand, is a true two-dimensional microstructure possessing unprecedented high anisotropic properties.

(B) Bioduplication Approach:

Vesicle-Mediated Multicomponent Processing: Intravesicular precipitation of inorganic, crystalline particles is a very common method of producing nanosized particles in biological systems [24,25]. For example, nanometer-sized magnetite particles are fabricated in intracellular vesicles by certain types of bacteria with precise control over particle morphology and orientation (Fig. 5) [24,25]. Various investigators have already demonstrated that single component particles can be precipitated within synthetic vesicles as a model system for the study of biomineralization [26]. Below, we illustrate the extension of these methods to the processing of multicomponent particles [27].

Particle precipitation within vesicles has several fundamental differences from bulk precipitation methods due to the unique properties of the lipid bilayer. In addition to forming a reaction cell, which limits the particle size, the bilayer serves as a semipermeable membrane to ion diffusion. Generally, phospholipid vesicles are nearly impermeable to cations, with typical permeability coefficients between 10^{-12} to 10^{-14} cm/s. Diffusion rates of anions, on the other hand, are usually quite low (10^{-10} cm/s for Cl⁻). This characteristic imposes a kinetic restraint on precipitation due to the diffusion restrictions across the bilayer and produces a system in which cations are essentially "trapped" within the phospholipid cage until precipitation can occur. This could potentially enhance chemical homogeneity within the system and facilitate the aqueous precipitation of water-soluble phases (such as Ba(OH)₂).

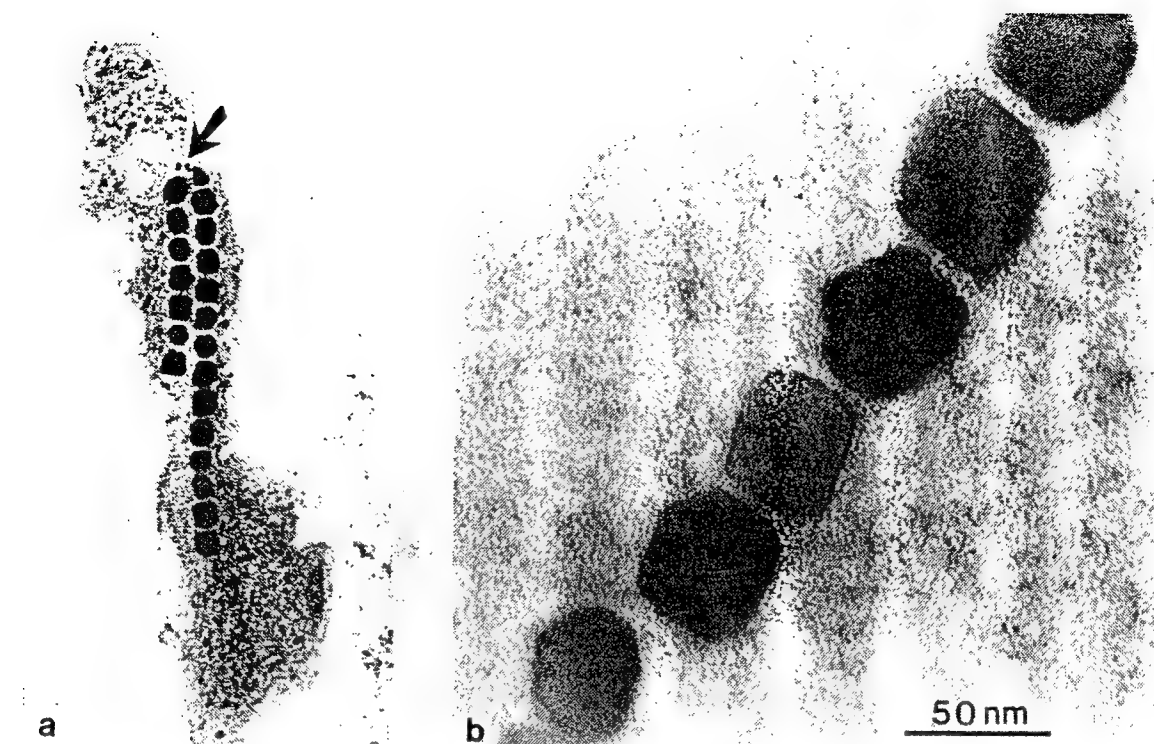


Figure 5. String of single crystalline magnetite particles in magnetic bacteria, *Aquaspirillum magnetotacticum*. Both are TEM images.

Figure 6 shows a transmission electron microscopy (TEM) image of the vesicle-formed particles using Y, Ba, Cu, and Ag nitrate precursors. The lipid membrane was not stained in these experiments and, therefore, is not visible. The particles are roughly spherical, crystalline, and well-dispersed. A mean particle diameter of 34.8 nm with a standard deviation of 13.2 nm was determined from TEM micrographs of 470 different particles. It is important to compare the particle sizes with the starting sizes of the original vesicles. Theoretically, the particle sizes should be smaller than the vesicles from which they were formed. Light-scattering experiments showed the vesicle size in deionized water to be approximately 59 nm. Since the presence of ions in solution can have pronounced effects on the morphology and phase transitions of vesicles, we also measured sizes in the presence of the nitrate salts. The vesicle size increased to 99 nm under the high ion concentrations. In both cases, the results confirm that the particle size is smaller than the corresponding vesicle size.

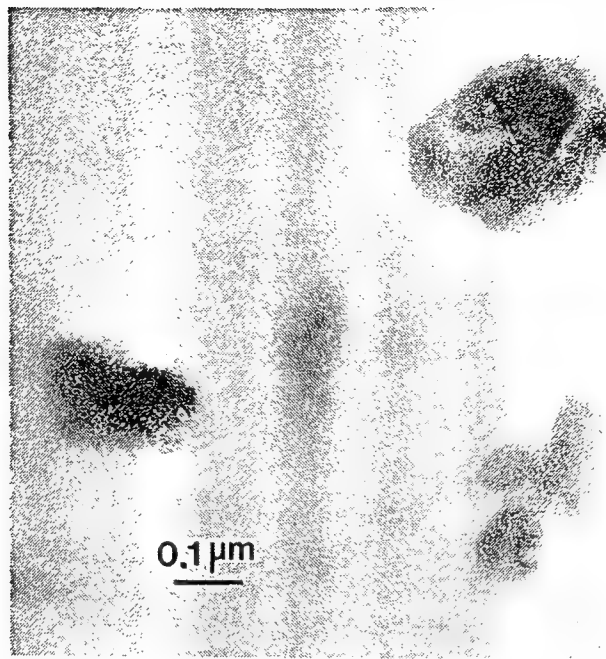


Figure 6. TEM micrograph of multicomponent particle formed within vesicle [27].

Although the vesicle-mediated particle formation system exhibits some exciting advantages over more conventional methods of powder production, there are also some distinct problems with the system. By far the most serious is that the ratio between elements in the formed particles is not consistent with the beginning solution ratios. Most pronounced is the barium to silver ratio. Although the starting solution contained eight times more barium than silver, the final particles were always rich in silver. In order to provide solutions to this problem, future research has to be directed toward understanding the association of ionic species in solution with the phospholipid bilayer by approaches discussed elsewhere [28-30].

IV. Conclusions

We have illustrated that by processing materials with architectural designs similar to those of biological composites (*biomimetics*), it is possible to improve upon their properties. The nacre of abalone shell which is a nanoscale-laminated composite of ~ 95 vol% aragonite and a chitin-based organic tissue possesses significantly higher values both in strength and toughness than its ceramic constituent phase. The microscale-laminated composites of boron carbide/aluminum discussed in this paper similarly displayed increases both in strength and toughness. Microscale-laminated boron carbide/polypropylene composites showed only a toughness increase. Since in both cases, the improvements are not yet as impressive as observed in the biological composites, we predict that nanoscale lamination may be necessary to achieve further improvements.

We have also demonstrated that phospholipid vesicles can be used as reaction vessels for the synthesis of ultrafine, well-dispersed, multicomponent ceramic particles by a processing approach which is similar to the methods used in biological systems (*bioduplication*). Here, the chemical inhomogeneity of the system can be restricted to the individual vesicle size, which is approximately 40 nm. We also found that precise control over chemical stoichiometry in multicomponent systems may be difficult to achieve due to differences in ion permeabilities, trapping efficiencies, and interactions between various cations and the vesicle membrane. This bioduplication approach to processing nanosized particles is truly multifunctional since the system simultaneously acts as: (i) a reaction cell for particle precipitation, (ii) an ion selective membrane that affects precipitation kinetics, and (iii) a barrier to prevent spontaneous agglomeration of the ultrafine particles.

Acknowledgments

The research described in this paper was sponsored by the U.S. Air Force Office of Scientific Research under Grant Nos. AFOSR-91-0040 and AFOSR-91-0281, by the U.S. Department of Energy through a subcontract by Battelle, Pacific Northwest Laboratory under Contract No. 0722348-A-F1, and by the IBM Corporation. The assistance of M. S. Wallace and D. M. Dabbs in the preparation of the manuscript is appreciated.

References

1. S. A. Wainwright, W. D. Biggs, J. D. Currey, and J. M. Gosline, *Mechanical Design in Organisms*, Princeton University Press, Princeton, New Jersey, 1976.
2. J. Kastelic, I. Palley, and E. Baer, "A Structural Mechanical Model for Tendon Crimping," *J. Biomech.*, **13** [10] 887-93 (1980).
3. J. J. Cassidy, A. Hiltner, and E. Baer, "Mechanical Properties of Biological Polymers," *Annual Rev. Materials Sci.*, **15**, 455-82 (1985).
4. A. P. Jackson, J. Vincent, R. M. Turner, "The Mechanical Design of Nacre," *Proc. Royal. Soc., B*, **234** [1277] 415-40 (1988).
5. J. Currey, *The Mechanical Adaptations of Bones*, Princeton University Press, Princeton, New Jersey, 1984.
6. J. Vincent, *Structural Biomaterials*, revised edition, Princeton University Press, Princeton, New Jersey, 1990.
7. *The Chemistry of Solid Wood, Advances in Chemistry Series, No. 207*, ed. R. M. Powell, American Chemical Society, Washington, D.C., 1984.

8. E. Baer, A. Hiltner, and H. D. Keith, "Hierarchical Structure in Polymeric Materials," *Science*, **235**, 1015-22 (1987).
9. J. Liu, M. Sarikaya, and I. A. Aksay, "Hierarchical Twins and Multiple Tiling in Nacre," unpublished work, University of Washington, Seattle, Washington.
10. K. E. Gunnison, "Structure-Mechanical Property Relationships in a Biological Ceramic Polymer Composite: Nacre," M.S. Thesis, University of Washington, Seattle, Washington, 1991.
11. M. Sarikaya, K. E. Gunnison, M. Yasrebi, and I. A. Aksay, "Mechanical Property-Microstructural Relationships in Abalone Shell," in *Materials Synthesis Utilizing Biological Processes, MRS Symp. Proc.*, Vol. 174, eds. P. C. Rieke, P. D. Calvert, and M. Alper, Materials Research Society, Pittsburgh, Pennsylvania, 1990, pp. 109-16.
12. H. A. Lowenstam and S. Weiner, *On Biomineralization*, Oxford University Press, Oxford, 1989.
13. K. Simkiss and K. M. Wilbur, *Biomineralization: Cell Biology and Mineral Deposition*, Academic Press, San Diego, California, 1990.
14. I. Amato, "Heeding the Call of the Wild," *Science*, **253** [5023] 966-68 (1991).
15. A. J. Pyzik and I. A. Aksay, "Microdesigning of B₄C-Al Cermets," in *Processing of Ceramic and Metal Matrix Composites*, ed. H. Mostaghaci, Pergamon Press, New York, 1989, pp. 169-80.
16. M. Yasrebi, G. H. Kim, K. E. Gunnison, D. L. Milius, M. Sarikaya, and I. A. Aksay, "Biomimetic Processing of Ceramics and Ceramic-Metal Composites," in *Better Ceramics Through Chemistry IV, MRS Symp. Proc.*, Vol. 180, eds. B. J. J. Zelinski, C. J. Brinker, D. E. Clark, and D. R. Ulrich, Materials Research Society, Pittsburgh, Pennsylvania, 1990, pp. 625-35.
17. S. S. Khanuja, "Processing and Structure-Property Relationships of Boron Carbide/Polymer Composites," M.S. Thesis, University of Washington, Seattle, Washington, 1991.
18. C. S. Smith, *A History of Metallography*, University of Chicago Press, Chicago, 1965.
19. J. Wadsworth and O. D. Sherby, "On the Bulat - Damascus Steels Revisited," *Progress in Materials Science*, **25** [1] 35-68 (1980).
20. J. Wadsworth, D. W. Kum, and O. D. Sherby, "Welded Damascus Steels and A New Breed of Laminated Composites," *Metal Progress*, **129** [7] 61-7 (1986).

21. E. C. Bain, "Nippon-to, An Introduction to Old Swords of Japan," *J. Iron and Steel Inst.*, **200** [2] 265-82 (1962).
22. L. Kapp, H. Kapp, and Y. Yoshihara, *The Craft of the Japanese Sword*, Kodansha Intl. Ltd., Tokyo, 1987.
23. M. Sarikaya, H. Togushige, and G. Thomas, "Lath Martensite and Bainite in Low Alloy Steels," in *Proc. Intl. Conf. Martensitic Transformations*, Japan Institute of Metals, 1986, pp. 613-18.
24. R. P. D. Blakemore, D. Maratea, and R. S. Wolfe, "Isolation and Pure Culture of a Freshwater Magnetic *Spirillum* in Chemically Defined Medium," *J. Bacteriol.*, **140** [2] 720-29 (1979).
25. S. Mann, R. B. Frankel, and P. P. Blakemore, "Structure, Morphology, and Crystal Growth of Bacterial Magnetite," *Nature*, **310** [5976] 405-07 (1985).
26. J. H. Fendler, *Membrane Mimetic Chemistry*, John Wiley, New York, 1982.
27. H. Liu, G. L. Graff, M. Hyde, M. Sarikaya, and I. A. Aksay, "Synthesis of Ultrafine, Multicomponent Particles Using Phospholipid Vesicles," in *Materials Synthesis Based on Biological Processes, MRS Symp. Proc.*, Vol. 218, eds. M. Alper, P. D. Calvert, P. C. Rieke, D. A. Tirrell, R. Frankel, Materials Research Society, Pittsburgh, Pennsylvania, 1991, in press.
28. S. Mann, "Molecular Recognition in Biomineralization," *Nature*, **332** [6159] 119-24 (1988).
29. S. Mann, B. R. Heywood, S. Rajam, and J. D. Birchall, "Controlled Crystallization of CaCO₃ under Stearic Acid Monolayers," *Nature*, **334** [6184] 692-95 (1988).
30. I. Weissbuch, L. Addadi, M. Lahav, L. Leiserowitz, "Molecular Recognition at Crystal Interfaces," *Science*, **253** [5020] 637-45 (1991).

"Hierarchical Twin Structures
in the Nacre of Red Abalone Shell"

J. Liu, M. Sarikaya, and I. A. Aksay

*49th Ann. Meeting of
Electron Microscopy Society of America*

edited by G. W. Bailey

(San Francisco Press, San Francisco, 1991) pp. 848-849

HIERARCHICAL TWIN STRUCTURES IN THE NACRE OF RED ABALONE SHELL

Jun Liu, Mehmet Sarikaya, and Ilhan A. Aksay

Department of Materials Science and Engineering, University of Washington, Seattle, WA 98195

The nacre structure of red abalone (*Haliotis rufescens*) shell has a higher strength^{1,2} and fracture toughness² at room temperature compared to some monolithic ceramics. The unusual mechanical properties may be attributed to the unique microarchitecture that can be described as a laminated composite of about 95% CaCO₃ and 5% organic matter (a combination of proteins, chitin, and other macromolecules). It is desirable to form synthetic materials having a microarchitecture similar to the nacre through a *biomimetic* approach to obtain improved mechanical properties. In order to achieve this goal, it is necessary to have a better understanding of the microstructure of the nacre at different length scales. The purpose of this work was to examine the structure of nacre in more detail. It has been found that the structure is actually composed of twins which are hierarchical from the nanometer to sub-millimeter scale.

In the edge-on configuration, the nacre is composed of aragonite platelets (thickness 0.25 to 0.5 μm) with their flat faces in [001] direction. The platelets are arranged in a "brick and mortar" microarchitecture with an organic matrix (~20 nm) forming the glue between the platelets (Fig. 1). In the face-on configuration, the structure can be described by twinning on three different length scales: first generation, incoherent twinning between platelets; second generation, coherent twinning between domains within platelets; and the third generation, nanoscale twins within domains. Both 60° or 90° twin boundaries have been observed at different length scales. Figure 2 illustrates the six-fold symmetry twin boundaries between platelets where A, C, and E platelets are twin related to platelets B, D, and F, respectively, but they are tilted slightly about the *c*-direction. Fig. 3 illustrates the 90° boundaries within a platelet, in which the four domains are related to each other by twinning, and platelets I and II which are also twin related.

Six-fold symmetry twinning within a platelet is usually observed in natural aragonite since it has an orthorhombic structure (Pmcn) with lattice parameters $a = 4.94 \text{ \AA}$, $b = 7.94 \text{ \AA}$, and $c = 5.72 \text{ \AA}$, but, 90° twin boundaries are less common in nature. It should be noted that the 90° boundary can be accounted for by forming four twin-related domains. However, to form hexagonal platelets, there should be only a 60° angle between each pair of domains, with six domains completing 360° for the whole platelet. This is not possible since the outer edges of the platelets are parallel to {110} twin planes. The angle between {110} planes is 63° and this leaves 3° unaccounted for, and, therefore, causes each domain to be highly strained. Careful analysis of each domain indicates that there are two sets of growth twins forming on {110} planes as illustrated in Fig. 4. The presence of these fine scale defects indicates that the 3°-strain is accommodated by the formation of these twins. As observed, some of the strain can also be released by a slight misalignment among the domains along the *c*-direction.

In summary, there are three scales of twins: (i) first generation twins between platelets, (ii) secondary twins between the domains in a given platelet, and (iii) nanoscale twins within domains. It is well known that the structure of biological soft tissues, such as tendon, have highly ordered hierarchical structure. To our knowledge, this is the first time it has been shown that the inorganic component of a biological structure also has a hierarchical structure. In this case, the hierarchical twin structure covers four orders of magnitude size scale ranging from nanometer to sub-millimeter, again revealing highly ordered microarchitecture in the nacre of red abalone.³

1. J. D. Currey, in *The Mechanical Properties of Biological Materials*, edited by J. F. V. Vincent and J. D. Currey, (Cambridge Univ. Press, London, 1980) pp. 75-98.
2. M. Sarikaya et al., Mater. Res. Soc. Proceedings, Vol. 174 (1990) pp. 109-116.
3. This work is supported by the Air Force Office of Scientific Research under the Grant Nos. AFOSR-87-0114 and AFOSR-89-0496.



Fig. 1 Brick-and-mortar micro-architecture of the nacre of the abalone shell.



Fig. 2 First generation twins in a six-fold configuration.

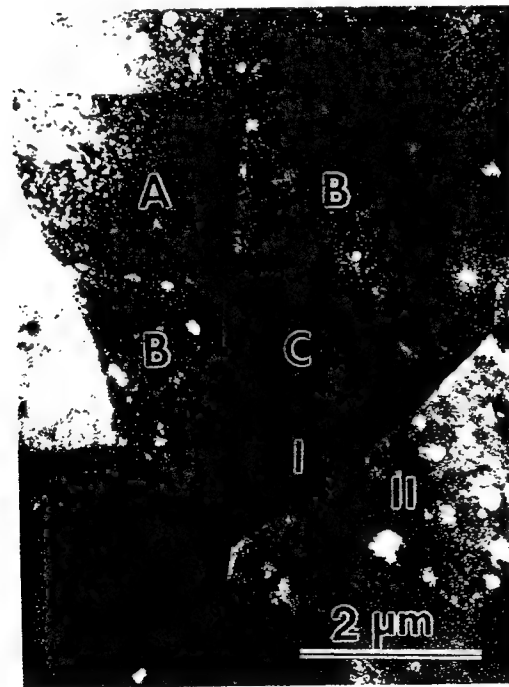


Fig. 3 Second generation twins in a four-fold configuration, and first generation twins between the platelets I and II.



Fig. 4 Third generation twins on a fine scale on (110) and (110) planes in a domain.

"Synthetic and Biological Nanocomposites"

M. Sarikaya and I. A. Aksay

*Proc. of 5th Intl. Conf.
on Ultrastructure Processing*

edited by L. L. Hench and J. K. West

(Wiley, New York, 1991) pp. 543-550.

Synthetic and Biological Nanocomposites

Mehmet Sarikaya and Ilhan A. Aksay

Department of Materials Science and Engineering, and
Advanced Materials Technology Center, Washington Technology Center,
University of Washington, Seattle, Washington 98195 USA

submitted to

1991 Ultrastructure Conference

June 20, 1991

Abstract

The effects of structures on the mechanical properties of laminated composites, with lamination at the nanometer scale, are discussed by presenting two example systems, one inorganic and the other biological. The first example is from a metallic system that forms a lath martensitic structure due to a phase transformation in the Fe-C binary alloy. In this case, the heavily dislocated martensitic units are hard and strong (supersaturated with carbon) and are surrounded by ductile retained austenite thin films. The second example is nacre, a biological composite, consisting of relatively hard (CaCO_3) platelets surrounded by a soft proteinaceous matrix, resulting in a brick and mortar micro-architecture. In both cases, the hard component has a thickness in the range of 100-500 nm and the soft component of about 10-50 nm. The unique structural organization of the components gives the overall composite an excellent combination of mechanical properties in terms of hardness, strength, and toughness. In this paper, the structures of these materials are discussed in detail and some guidelines are presented for the future synthesis of nanolaminated composites.

1.0 An Introduction to Nanocomposite Materials

Properties of materials are structure-sensitive and, hence, control of the structure on a continuous length scale from the nanometer to the micrometer to the macrometer range is essential. For instance, metallic and ceramic composites and monoliths with layered microstructures and homogeneous matrices containing nanometer scale second phases offer

significant advantages in controlling the physical properties of materials.¹ Examples include layered compound semiconductors in which both the chemistry and atomic structure of the interfaces are controlled for improved electronic properties;² high-temperature ceramic superconductors, such as $\text{YBa}_2\text{Cu}_3\text{O}_{7-x}$,³ which have ultrathin ($\sim 1.5\text{-}2.5$ nm) transformation twin boundaries with low oxygen ordering where the twin boundaries act as flux pinning sites resulting in an increase in critical current densities in high applied magnetic fields;⁴ and low-carbon/low-alloy steels that are strong but tough due to a hard lath martensitic structure and ductile thin film retained austenite.^{5,6} In the case of biological composites,⁷ the control of the structure begins at the nanometer dimension and scales up in secondary, tertiary, quarternary structures, resulting in a final structure that is often hierarchical. Hierarchical biological composites include all polymeric composites such as exoskeletons (cuticles) of insects, ceramic-polymer composites in skeletons of vertebrates and in seashells, and ultrafine paramagnetic⁸ and semiconducting⁹ particles found in bacteria and algae. Furthermore, in biological materials the resulting structure is multifunctional, conducting heat and electrical pulses and providing mechanical responses.

In this paper, we provide detailed analyses on the structures and properties of two novel nanocomposites: (i) high-strength/high-toughness lath martensitic steels and (ii) nacre of abalone shell. Our goal here is to illustrate that the nanoscale integration of metallic, ceramic, and polymeric phases in a composite can result in a unique combination of enhanced properties. We hope that these two examples will provide pathways for the processing of more novel synthetic structures.

2.0 Examples of Nanocomposite Systems

Techniques such as those used in the formation of laminated composite structures at the nanoscale have been developed through phase transformations, especially in metal alloy systems, by carefully selecting the correct alloy composition and controlling the heat treatment (cooling). An excellent example is the high-strength/high-toughness lath martensitic steels developed during the 1970s and early 1980s.¹⁰ These structures are nanocomposites in scale and have soft (austenite) and hard (martensite) phases with a uniform distribution of fine (nanometer scale) carbide precipitates, closely controlled to give the best combination of strength and toughness in the final material. This successful composite system having structural variations at the nanometer scale will be discussed in more detail in Section 2.1 and will be closely related to the biological composites in Section 2.3. In Section 2.2, an ancient technique used to make a metal/ceramic composite will be presented.

2.1 Lath Martensitic Microstructures in Steels

Low-carbon (< 0.3 wt%)/low-alloy (< 5.0 wt%) steels are used in a variety of applications from armor to heavy machinery. These steels are heat treated by a simple procedure that, with modification, gives a myriad of microstructures, resulting in a wide variation in properties (Fig. 1). Low-alloy/low-carbon steels are probably the best examples among all synthetic materials systems in terms of developing composite microstructures on a wide dimensional scale (from nanometer to micrometer) with a high degree of control over the mechanical properties.

Quenching the alloy (about 100°C/s) from a homogenization temperature (usually above 1000°C) to room temperature results in a microstructure composed of a metastable mixture of martensitic laths ($0.2\text{-}0.5 \mu\text{m} \times 2\text{-}5 \mu\text{m} \times 5\text{-}20 \mu\text{m}$) with a continuous thin film of (5-50 nm thick) retained austenite decorating the lath boundaries⁵ (Fig. 2). The Fe-C equilibrium diagram displays a eutectoid transformation at 723°C and 0.8 wt% C composition. Above 723°C austenite (γ -iron, fcc) is the stable phase. Below 723°C ferrite (α -iron, bcc) is the stable phase and has a maximum solubility of C at about 0.02 wt%. A low or a medium C steel (0.05-0.4 wt%) quenched from the austenite phase field undergoes a shear transformation resulting in a metastable martensitic phase which has supersaturated C in the lattice that orders along the c-direction, and hence, the crystal structure becomes bct, where the tetragonality changes with C in solution. What is unusual is that the microstructure contains a thin film retained austenite continuously surrounding the martensite phase which is in the form of dislocated laths (Fig. 2(a-b)). Since the bct lattice of Fe is highly strained due to the supersaturation of C, the elastic modulus and the strength of martensite are very high (50 GPa and 5 GPa, respectively).⁵ Correspondingly, martensite is brittle. On the other hand, austenite is tough (in the case of austenitic steels, K_{Ic} is about 150 MPa·m^{1/2}) but not as strong as martensite because of the easy slip in the fcc lattice resulting in plastic deformation. Therefore, the final microstructure in a low-carbon lath martensitic steel is basically a nanocomposite with component martensitic and austenitic phases that provide the strength and toughness of the material, respectively. Furthermore, in these structures the properties of component phases can further be modified by a low-temperature tempering. For example, tempering the quenched structure at 200°C for 2 h produces Widmanstätten Fe_3C (cermentite) – plate-shaped with a thickness of 10-20 nm –

which results in a substantial increase in fracture toughness without a significant loss in strength of the composite structure.

Layered structures can be readily obtained in many other metallic and ceramic systems with two or more components whose phase diagrams display eutectic or eutectoid transformations. Metallic (such as Cu-Nb),¹¹ ceramic (B₄C-SiC),¹² and intermetallic systems (Al-Ti-Nb)¹³ can form *in situ* composites. Depending on the cooling rate from the high-temperature single-phase homogenization region, a certain degree of control over the thickness of the lamellae is assured, but not usually at the nanometer level. Some of the structural features in the Fe-C system discussed above include: (i) a martensitic transformation, resulting in a metastable microstructure which contains the high-temperature parent phase, austenite, indicating that kinetics dictates the final microstructure; (ii) lamination at the nanometer level; and (iii) the thorough distribution of lath martensitic packets (or colonies), resulting in a true three-dimensional composite. The effect of adding alloys, such as Cr, Mn, Ni, and Si, is to change the kinetics, such as the martensite start temperature, which affects the C-diffusion rates and the stability of the retained austenite,¹⁰ as well as to change some of the intrinsic properties of the component phases.

The unusual presence of a high-temperature austenite phase in the form of thin films is attributed to several stabilization mechanisms:¹⁰ (i) compositional stabilization due to the high C content in austenite films (up to 1.0 wt%), (ii) mechanical stabilization due to a high degree of deformation of the austenite lattice between the martensite laths, and (iii) chemical stabilization from the locking of the α' / γ interfaces due to C saturation at the coherency dislocations forming Cottrell atmospheres. Even at high cooling rates (10,000°C/s), C atoms leaving the

α' lattice ahead of the interface move into the γ lattice and/or accumulate at the interface, stabilizing the austenite.

Each martensite lath in a given region obeys a specific crystallographic orientation relationship with the retained austenite, either a Kurdjumov-Sachs or Nishiyama-Wassermann relationship, that results in a $\{111\}\gamma$ (parallel to $\{110\}\alpha'$) habit.^{10a} In each packet, martensite laths (all having the same [110] direction) belong to the same variant, which is a 70° rotation with respect to the neighboring packet. Therefore, in a given austenite grain, there are three variants of martensite, resulting in an overall structure which is a true three-dimensional composite with local lamination of component phases at the nanometer scale. As a result of this process, a unique lath martensitic microstructure develops which displays a room temperature fracture toughness, K_{Ic} , of about 100 MPa·m^{1/2} and a tensile yield strength, σ_Y , of about 1.4 GPa.¹⁰

2.2 *Samurai Sword: An Ideal Nanocomposite Alloy*

The practice of controlling the structure of materials at the nanometer scale to achieve desired properties has a long history, especially in metallurgy. Understanding the microstructures in ancient materials can be useful both for developing "micro-architectural design" concepts for modern multifunctional composites as well as generating new alloy microstructures. An excellent example of this is Damascus steel, which was developed in the Middle East during the late iron age, more than 2000 years ago. The steel was used mostly for armor applications, which required high toughness as well as high strength and hardness. The metallurgy that

produced Damascus steel is based on a simple thermomechanical cycle that forms a composite structure containing soft and hard phases.¹⁴ Originally "cast" high-carbon steel (wt% C > 1-2%) is homogenized at 1200°C, which produces coarse austenite (γ) grains. The steel is then cooled slowly through the γ -carbide (Fe_3C) region during which pre-eutectoid carbides form at prior austenite grain boundaries. The coarse microstructure is "broken down" during forging at temperatures of 750°-900°C, and carbides spherodize to form strings of particles in refined austenite grains. Quenching into warm water (40°-80°C) from about 750°C transforms the fine austenite grains into fine needles of brittle but strong martensite, which as discussed previously is a supersaturated ferrite. The material is then annealed at 200°-300°C to produce tempered carbides (20-50 nm) in what is now still strong but relatively tough martensite needles. The resulting microstructure is then tough martensite containing ultrafine precipitates with hard strings of carbides located at prior austenite grain boundaries.

Many variations of these iron-based structures have since been developed by modifying the thermomechanical treatments, most notably by "composite lamination," which incorporates both pure iron (soft and tough) and high and medium carbon steels (hard and strong).¹⁵ An excellent example of this is the Samurai sword, which is truly "nanolaminated" and is an ideal material for its purpose because of its unique combination of toughness, hardness, and rigidity.¹⁶ These three properties in one material, however, are contradictory; that is, toughness implies a soft material that bends easily, hardness is associated with brittle material, and rigidity requires high strength. However, Japanese smiths, many centuries ago, developed these composites based on techniques similar to the earlier techniques of Damascus steel-making by

understanding how thermomechanical treatments and compositional adjustments can change the steel's properties (Fig. 3).

The final body of a sword blade is a hierarchical structure consisting of a soft inner core (ferrite) with a hard outer core (low-carbon martensite). The steel is produced first in the form of a thick, laminated iron and steel blank with dimensions 1/2" thick by 2" wide and 6 to 8" long.¹⁷ The blank is inserted into a pine ash (carbon source) and heated white hot (about 600° to 800°C) and then doubled onto itself and hammered until it again has its original dimensions (Fig. 3). This process is repeated fifteen to twenty times. Four similar blanks are then welded together, and the same thermomechanical treatment is repeated five times. The resulting blank forms a laminate with the thickness of each lamellae equal to $2''/4 \times 5 \times 2^{25}$ or a few nanometers. At this time, the surface of the blade (the laminated blank) is scraped and ground to shape. The final blade is covered with mixture of clay and fine sand, and then dried. The blade is then heated to austenitizing temperature (about 900°C) and quenched to room temperature in a bath of oil or water by inserting the tip first and then the sharp edge horizontally. The final blade has a curved shape with the sharp edge having mostly a hard and strong martensitic structure and the back edge consisting of the relatively soft ferritic microstructure. Both are nanolaminates, which provide the ultrarigidity to the overall material. Although no quantitative measurements have been made to date, the composite has been known to have an excellent combination of impact resistance, strength, and toughness in practice.¹⁸

2.3 Nacre of the Red Abalone Shell: A Natural Ceramic-Polymer Laminated Material

It is coincidental that the lath martensitic structures discussed in Section 2.1 are similar in design on a local scale to the structure of nacre, which forms the basis of many shells such as those from gastropods, cephalopods, and mollusks.¹⁹ Both the lath martensitic structures and the biologically occurring nacre structure are similar in that they (i) are laminated on a fine scale, (ii) have a hard and strong phase (martensite in steel and aragonite in nacre) that is thicker than the soft and tough phase (austenite in steel and an organic proteinaceous matrix in nacre), (iii) have a hard phase 100-500 nm thick and a soft phase 10-20 nm thick, and (iv) have soft phases in both cases of about 2-4% by volume. It is not coincidental, however, that both structures provide a good combination of strength and toughness with adequate hardness in the overall composite. For the purposes of micro-architectural design, the structure of nacre is described in detail below.

The method used by organisms in processing materials is in many ways more controlled than synthetic methods. In the formation of biological materials, therefore, organisms can efficiently produce complex and hierarchical microstructures with unique properties at spatial levels ranging from the molecular (10^{-10} m) to the macroscopic (10^{-3} m), and with greater control. The dynamism of these systems allows the collection and transport of the raw constituents; the nucleation, configuration, and growth of new structures (self-assembly); and the repair and replacement of old or damaged components.

Nacre, a ceramic-polymer nanocomposite of red abalone shell (*Haliotis rufescens*), for example, displays a unique structure-property correlation.²⁰ A longitudinal cross-section of the

red abalone shell displays two types of structures: the outer prismatic layer and the inner nacreous layer. Two forms of CaCO_3 , calcite (rhombohedral, $\bar{R}\bar{3}c$) and aragonite (Pmnc), constitute the inorganic component of the organic-inorganic composite in the prismatic and the nacreous layers, respectively.

The mechanical properties of nacre, i.e., σ_f (fracture strength) and K_{Ic} (fracture toughness), have been evaluated in the transverse direction (perpendicular to the shell plane) and exhibit values of 180 MPa and about $10 \text{ MPa}\cdot\text{m}^{1/2}$, respectively (Fig. 4). In addition to a substantial increase in strength, there is an increase in the fracture toughness of at least 40 times in nacre compared to the fracture toughness of monolithic CaCO_3 ($K_{Ic} < 0.25 \text{ MPa}\cdot\text{m}^{1/2}$) based on a straight notch three-point bend test. In terms of specific strength, nacre is comparable to many monolithic ceramics; in terms of toughness, nacre is a better material. It is surpassed by only the most successful ceramic-metal composites (cermets): WC-Co (density 14.5 g/cc),²¹ Al_2O_3 -Al (density 2.8 g/cc),²² and B_4C -Al (density 2.65 g/cc),²³ all of which have the form of a three-dimensional network and, hence, have isotropic properties.

The study of crack propagation behavior in nacre reveals a high degree of tortuosity not seen in traditional brittle (such as Al_2O_3) and tough (ZrO_2) ceramics, indicating that certain toughening mechanisms, such as crack blunting, branching, and "layer pullout," operate in the shell. A closer examination of the microstructure reveals that cracks mostly advance through the organic layer and with difficulty as this process is accompanied by sliding of the CaCO_3 layers (when there is a shear component of the resolved stress) and by the bridging of the organic ligaments (when there is a normal stress component), as shown in Fig. 5(a-b). It is these last two mechanisms that contribute most to the toughening of nacre. These processes

absorb considerable energy that would otherwise be used in the propagation of cracks through the material, resulting in controlled crack propagation and hence a damage tolerant composite.

The superior mechanical properties of the nacre section of abalone shell (which is 96-98% CaCO₃ and about 2-4% organic matter) over those of synthetic ceramics and their composites come from the unique "brick and mortar" micro-architecture. Figure 6 shows the alternating layers of the hexagonally shaped 100-500 nm-thick aragonite crystals (platelets) that form the hard component and the thin (10-20 nm) organic substance (a nanolaminate of chitin, proteins, and macromolecules) that provides the "ductile" component of the microstructure. It appears, therefore, that the organic matrix not only acts as the lifeline of the shell but also is an indispensable structural component of the resultant ceramic-polymer composite. The conclusion that can be drawn from these observations is that in the composite (i) the biopolymer component has to be soft and sticky, and (ii) the inorganic component has to be hard, and (iii) interfaces between the soft and the hard components must be strong. These guidelines may serve as a design basis for enhancing impact and wear resistance in future nanolaminated engineering materials, such as cerpolys (ceramic-polymers) and cermets (ceramic-metals), incorporating soft and hard components.

3.0 Summary

From the above, it is clear that structures of lath martensitic steels and nacre are very similar. In steels, it is the martensite lath, which has dimensions similar to CaCO₃ in nacre (both about 200-500 nm thick), that provides strength. The thin film retained austenite (5-50

nm thick) that covers the martensite platelets (laths) is similar to the organic layer (10-20 nm) covering the aragonite platelets in the nacre. Furthermore, in both cases, the interfaces are very strong between the hard and soft phases. In terms of crystallographic relationships in nacre, adjacent CaCO_3 platelets have their [001] axis perpendicular to the platelet/organic matrix interface, with plates rotating slightly ($1\text{-}5^\circ$) with respect to this axis. In martensite, similarly, the adjacent laths have a common $<110>$ axis, perpendicular to the α'/γ interface, with laths rotating slightly ($1\text{-}6^\circ$) with respect to this axis. In both cases, the matrices (organic phase in the nacre and austenite in lath martensitic structures) have the same orientation throughout. However, the difference between the two structures is that the lath martensite contains packets (three 70° -variants of martensite crystals) within each pre-austenite grain that are randomly distributed throughout the sample. In nacre, the local arrangement of the layered structure is repeated throughout the thickness of the sample. Therefore, lath martensite is a true three-dimensional microstructure with local laminated domains that produce its isotropic mechanical properties. Nacre, on the other hand, is a true two-dimensional microstructure possessing high anisotropic properties.

Unfortunately, other than expensive techniques such as molecular beam epitaxy, presently we do not have commercially viable techniques to produce nanolaminated structures as good as the two novel examples discussed in this paper. We hope that future research will provide more practical processing schemes to accomplish the goal of achieving cermet and cerpoly composites.

4.0 Acknowledgments

The work was supported by the Air Force Office of Scientific Research (AFOSR) and was monitored under Grant Nos. AFOSR-88-0135, AFOSR-89-0496, AFOSR-⁴₁-004, and AFOSR-NC-003.

5.0 References

1. R. P. Anders et al., Research Opportunities on Cluster and Cluster-assembled Materials--A Department of Energy, Council on Materials Science Panel Report, *J. Mater. Res.*, 4 (3) 707 (1989).
2. T. P. Pearsall, Silicon-Germanium Alloys and Heterostructures: Optical and Electronic Properties, *CRC Critical Reviews in Solid State and Materials Science*, 15 (6) 551 (1989).
3. M. Sarikaya, R. Kikuchi, and I. A. Aksay, Structure and Formation of Twins in Orthorhombic $\text{YBa}_2\text{Cu}_3\text{O}_{7-x}$, *Physica C*, 152, 161 (1989).
4. U. Welp, W. K. Kwok, G. W. Crabtree, and K. G. Vandervorst, Magnetization Hysteresis and Flux Pinning in Twinned and Untwinned $\text{YBa}_2\text{Cu}_3\text{O}_{7-x}$, Single Crystals, *Appl. Phys. Lett.*, 57 (1) 84 (1990).

5. (a) J. McMahon, Ph.D. Thesis, University of California, Berkeley (1973).
(b) R. Raghavan, Ph.D. Thesis, University of California, Berkeley (1976).
(c) R. V. Narasinha Rao, Ph.D. Thesis, University of California, Berkeley (1978).
(d) M. Sarikaya, Ph.D. Thesis, University of California, Berkeley (1982).
6. M. Sarikaya, H. Togushige, and G. Thomas, Lath Martensite and Bainite in Low Alloy Steels, in *Proc. Intl. Conf. Martensitic Transformations*, Japan Institute of Metals, 1986, p. 613.
7. (a) H. A. Lowenstam, Minerals Formed by Organisms, *Science*, **211**, 1126 (1981);
(b) J. A. Currey, Biological Composites, *J. Mater. Edu.*, **9** (1/2) 118 (1987).
8. R. P. Blakemore, Magnetotactic Bacteria, *Science*, **190**, 377 (1975).
9. C. T. Dameron, Biosynthesis of Cadmium Sulphite Quantum Semiconductor Crystallites, *Nature*, **338**, 596 (1989).
10. (a) M. Sarikaya and G. Thomas, Lath Martensites in Low Carbon Steels, *J. de Physique*, Colloque (4) supplement au no. 12, Tome 43, 1982 Decembre, p. C4-563-568;
(b) M. Sarikaya, G. Thomas, J. W. Steeds, S. J. Barnard, and G. D. W. Smith, Solute Element Partitioning and Austenite Stabilization in Steels, in *Proc. Intl. Conf. Solid-Solid*

Phase Transformations, H. I. Aaronson and C. M. Wayman, Eds., American Society of Metals, 1982, p. 1421.

11. J. Berk, J. P. Harbison, and J. L. Bell, Anomalous Increase in Strength of In-Situ Formed Cu-Nb Multifilamentary Composites, *J. Appl. Phys.*, **49** (12) 6031 (1979).
12. W. J. Minford, F. L. Kennards, R. C. Bradt, and V. S. Stubican, Directionally Solidified Ceramic Eutectics: Microstructures, Crystallography, and Mechanical Properties, in *Ceramic Microstructures '76*, R. M. Fulrath and J. A. Pask, Eds., Westview Press, Boulder, Colorado, 1977, p. 456.
13. E. Ense and H. Margolin, *Trans. Metall. Soc. AIME*, **221**, 151 (1960).
14. J. Wadsworth and O. D. Sherby, "On the Bulat. Damascus Steel Revisited," in *Progress in Mater. Sci.*, Vol. 25, 1980, p. 15.
15. C. S. Smith, *A History of Metallography*, University of Chicago Press, Chicago, 1965.
16. E. C. Bain, Nippon-to, An Introduction to Old Swords of Japan, *J. Iron and Steel Inst.* London, 200, 265 (1962).

17. L. Kapp, H. Kapp, Y. Yoshihara, *The Craft of the Japanese Sword*, Kodansha Intl. Ltd., Tokyo, 1987.
18. B. S. Lyman, Metallurgical and Other Features of Japanese Swords, *J. of the Franklin Institute*, 13 (January 1896).
19. J. Currey, Biological Composites, *J. Materials Edu.*, 9 (1-2) 118 (1987).
20. M. Sarikaya, K. E. Gunnison, M. Yasrebi, and I. A. Aksay, Mechanical Property-Microstructural Relationships in Abalone Shell, in *Materials Synthesis Utilizing Biological Processes*, *MRS Symp. Proc.*, Vol. 174, P. C. Rieke, P. D. Calvert, and M. Alper, Eds., Materials Research Society, Pittsburgh, Pennsylvania, 1990, p. 109.
21. H. E. Exner and J. Garland, A Review of Parameters Influencing Some Mechanical Properties of WC-Co Alloys, *Powder Metallurgy*, 13, 13 (1970).
22. M. S. Newkirk, A. W. Urquhart, H. R. Zwicker, and E. Bretal, Formation of Lanxide™ Ceramic Composite Material, *J. Mater. Res.*, 1 (1) 81 (1986).
23. D. C. Halverson, A. J. Pyzik, I. A. Aksay, and W. E. Snowden, Processing of B₄C-Al Composites, *J. Am. Ceram. Soc.*, 72 (5) 775 (1989).

Table I. Natural and Synthetic Nanocomposite Materials

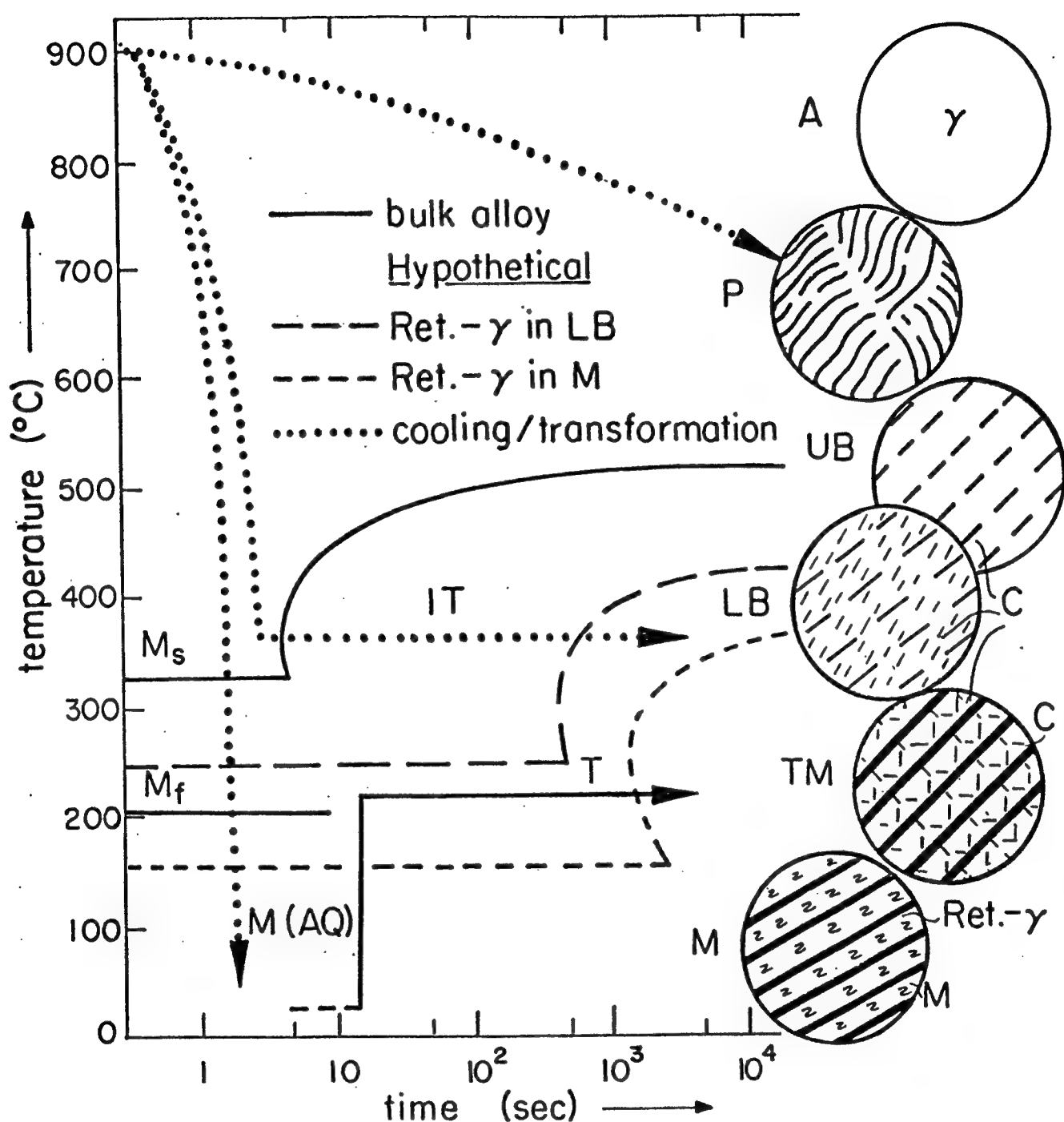
Natural	Dimension of the Second Phase	Synthetic	Dimension of the Second Phase
clays (2-D)	~ 1 nm	semiconductor heterostructures (2-D)	1 nm layers
opal (2-D)	~ 1 nm	high-temperature superconductors (2-D)	1 nm layers
seashells (2-D)	1-100 nm	lath martensite (3-D) samurai sword (2-D)	5 – 50 nm layers 1 – 3 nm layers (calculated)
		Ti-C multilayers (2-D)	2 – 10 nm

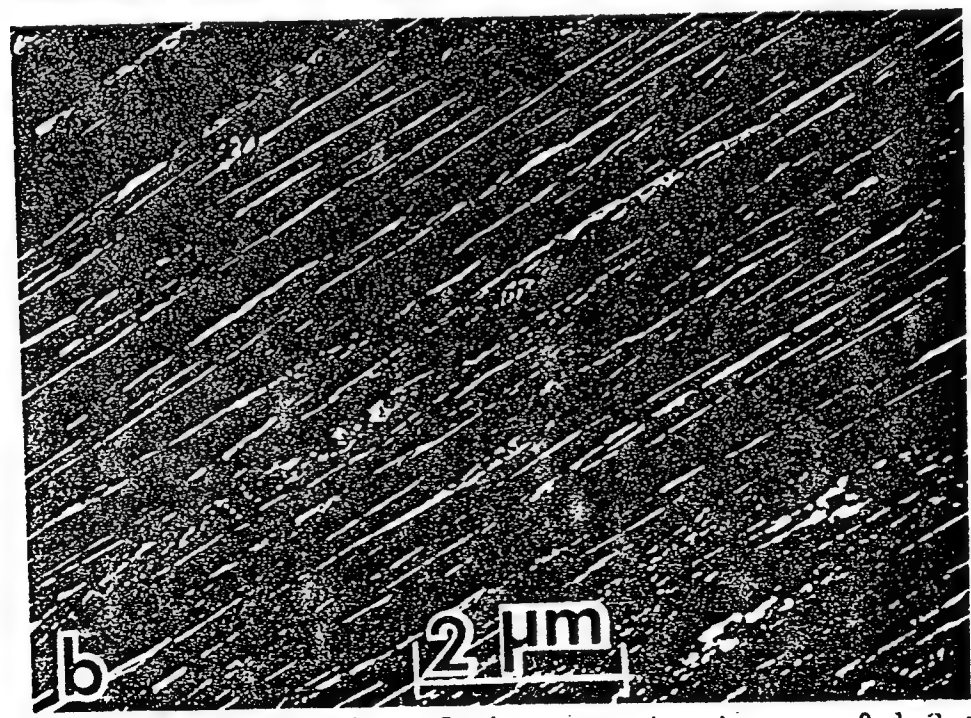
Figure Captions

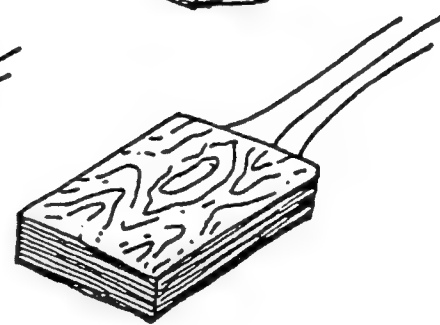
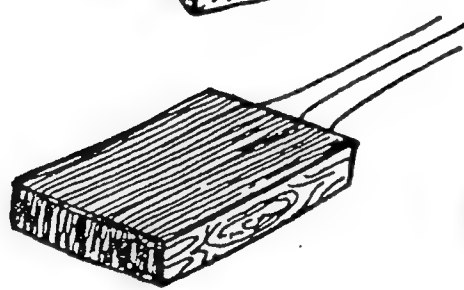
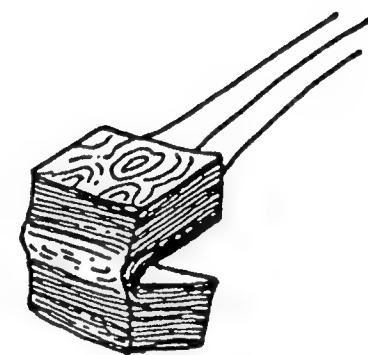
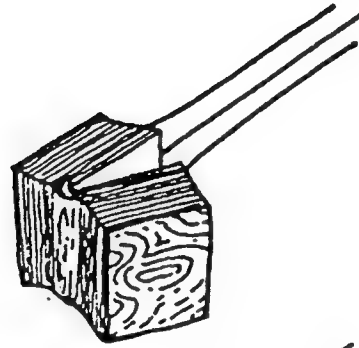
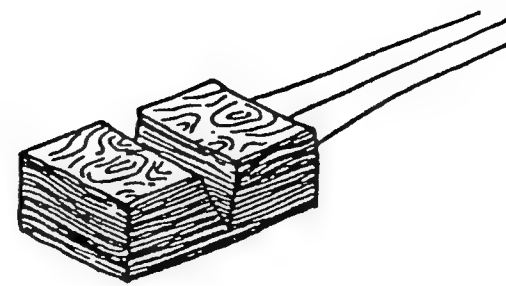
- Figure 1.** TTT diagrams for bulk steel and hypothetical steels having the compositions of retained austenite ($\text{Ret}-\gamma$) phases in lower bainite (LB) and martensite (M), respectively. Microstructures produced by different cooling routes from austenite phase field are also schematically indicated (A: austenite; C: carbide; IT: isothermal transformation; T: tempering; P: pearlite; TM: tempered martensite; and UB: upper bainite.;
- Figure 2.** (a) Bright field and (b) dark field images, the latter recorded by using the retained austenite reflection, reveal dislocated martensite laths, with a common $<110>_M$ direction, and thin film retained austenite, with $<111>_A$ parallel to $<110>_M$ in each packet.
- Figure 3.** The making of samurai swords: two Jihada. Masame grain is produced when the unhammered face of the forged block of steel is used to form the surface of the blade. Itame is made by using the hammered face, creating a laminated appearance resembling nacre or a wood surface.
- Figure 4.** Mechanical properties of the nacre section of the red abalone shell (96% CaCO_3 , 4% organic) as compared to common high-technology ceramics and cermets. Note the increase of properties in nacre compared to monolithic CaCO_3 .

Figure 5. (a) and (b) are secondary electron images in SEM revealing crack propagation characteristics in the nacre structure; and sliding of CaCO_3 platelets and ligament formation in the organic matrix, respectively.

Figure 6. TEM BF image in cross-section revealing the "brick and mortar" micro-architecture of CaCO_3 platelets, C, and organic matrix, OM, in the nacre section of red abalone shell.







Masame

Itame

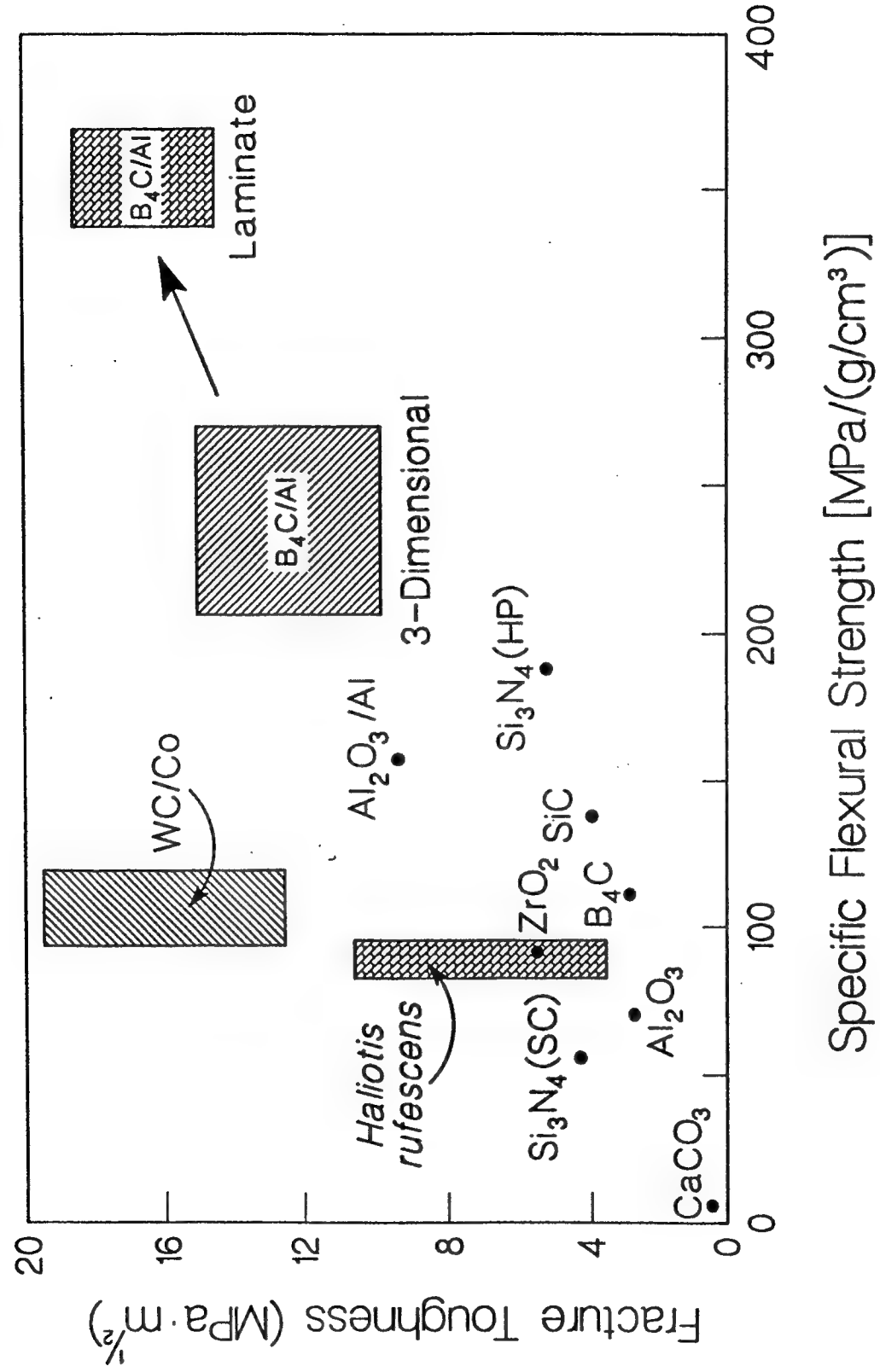
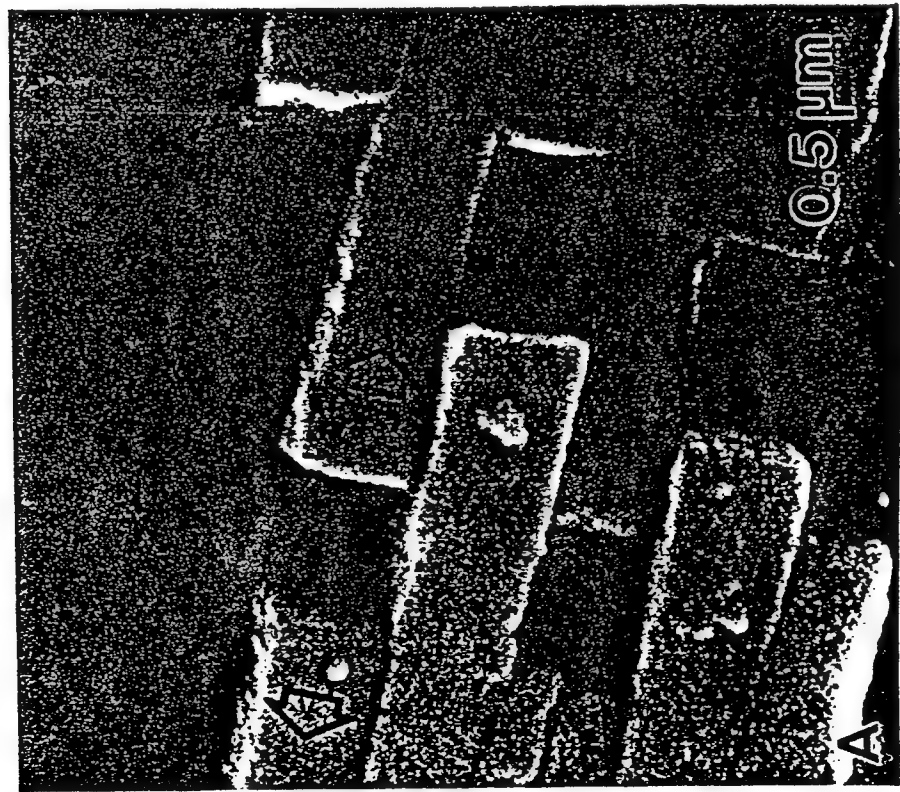
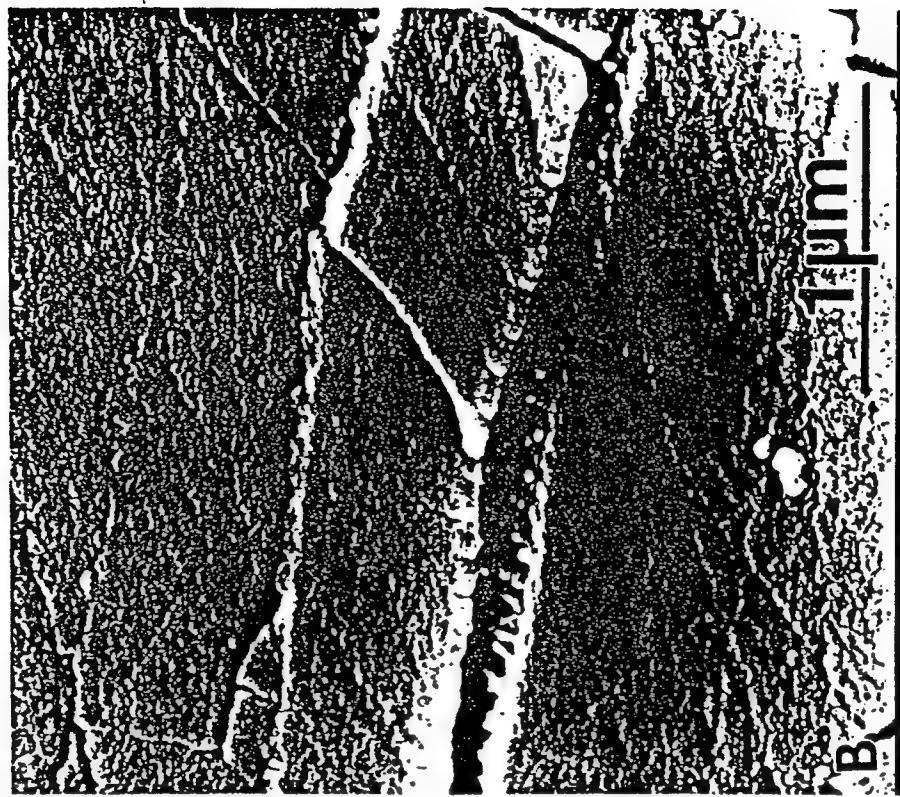


Fig. 5
Lankau & Akai



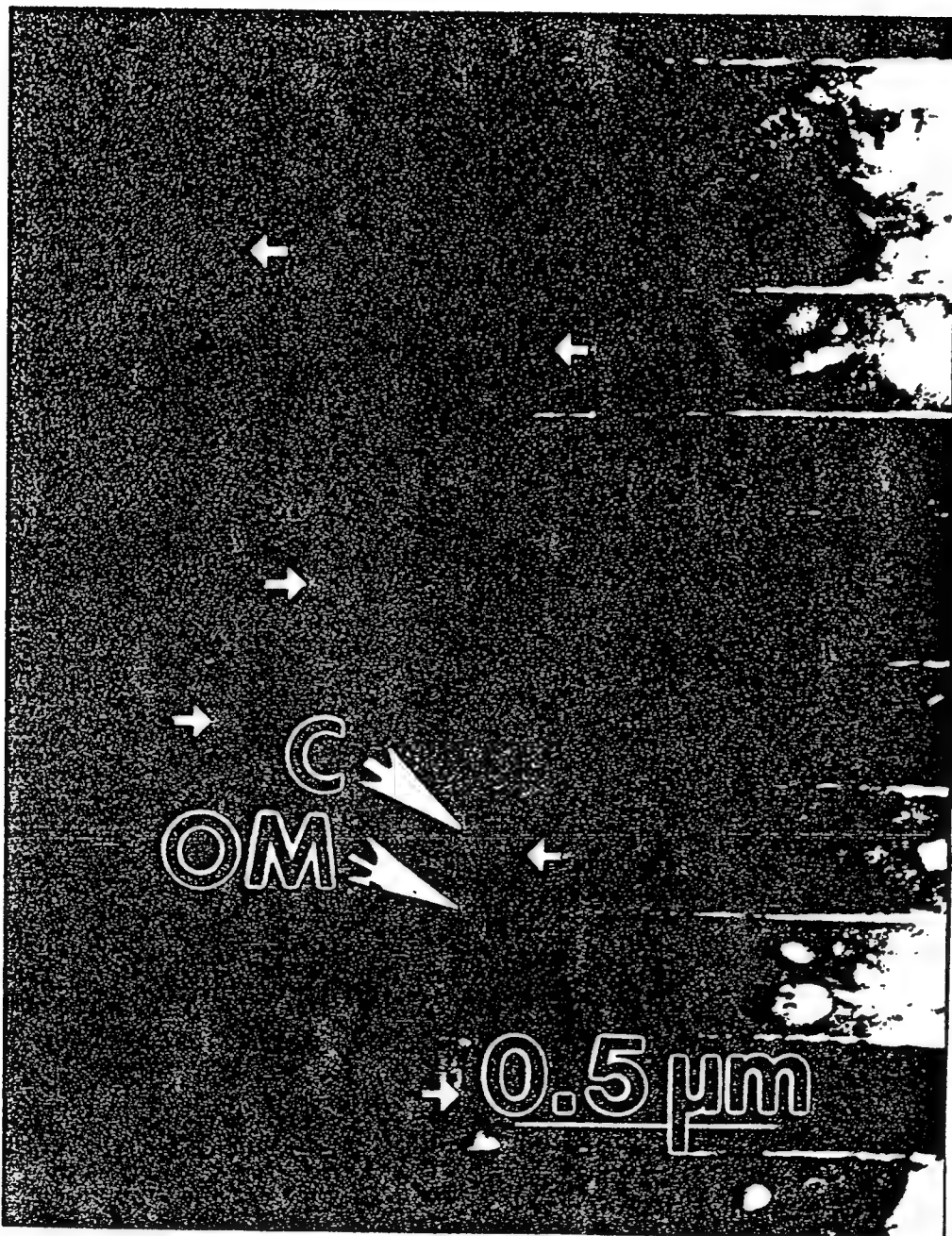


Fig. 3
Surface and

"Structure-Mechanical Property Relationships
in a Biological Ceramic-Polymer Composite: Nacre"

K. Gunnison, M. Sarikaya, J. Liu, and I. A. Aksay

in Proc. of *Hierarchically Structured Materials*

edited by I. A. Aksay, E. Baer, M. Sarikaya, and D. Tirrell

(Materials Research Society, Pittsburgh, PA, 1992)
Vol. 255, pp. 171-183

STRUCTURE-MECHANICAL PROPERTY RELATIONSHIPS IN A BIOLOGICAL CERAMIC-POLYMER COMPOSITE: NACRE

KATIE E. GUNNISON, MEHMET SARIKAYA, JUN LIU, and ILHAN A. AKSAY
Department of Materials Science and Engineering, and
Advanced Materials Technology Center, Washington Technology Center,
University of Washington, Seattle, WA 98195

ABSTRACT

The structure-mechanical property relationships were studied in nacre, a laminated ceramic-polymer biocomposite found in seashell. Four-point bending strength and three-point bend fracture toughness tests were performed, and the results averaged 180 ± 30 MPa and 9 ± 3 MPa·m^{1/2}, respectively, indicating that the composite is many orders of magnitude stronger and tougher than monolithic CaCO₃, which is the primary component of nacre. Fractographic studies conducted with a scanning electron microscope identified two significant toughening mechanisms in the well-known "brick and mortar" microstructure of nacre: (i) sliding of the aragonite platelets and (ii) ligament formation in the organic matrix. These toughening mechanisms allow for high energy absorption and damage tolerance and thereby prevent catastrophic failure of the composite. The structure of the organic matrix and the interfacial structure between the organic and inorganic components were studied with transmission electron microscopy by using both ion milled and ultramicrotomed sections with and without the intact aragonite platelets. We found that the organic matrix is indeed a multilayered composite at the nanometer scale but is thinner (about 100 Å) than reported in the literature. The morphology of the interfacial region between the organic and the inorganic layers suggests the presence of a structural "transitory" region that interlocks the two dissimilar phases.⁵

1. INTRODUCTION

In designing and processing materials for technological applications, valuable lessons can be learned from biological soft and hard tissues.¹⁻³ Biologically formed materials almost exclusively have composite structures⁴ and the individual phases of these structures are often arranged in complex and highly ordered units to form hierarchically organized architectures.^{2,4,5} The design of biological structures developed over time in order to meet specific materials requirements for the organism. Since biological systems have a limited supply of raw materials at their disposal, they must use the available raw materials in the most efficient manner possible to achieve the structures and the properties that are required for survival in their habitat.⁶ The formation of biological materials systems, and the relationships between the structures and their resulting properties, can provide important information for the development of synthetic materials.⁷

We chose to study the property-structure relationship in the nacre of the red abalone, *Haliothis rufescens*, because it has been shown to display a higher strength and toughness than other mollusk shell structures.⁸⁻¹¹ Nacre in mollusk shells is a unique biocomposite similar in some respects to synthetic laminated composites.¹⁰ Mollusk shells are composed of various crystallographic and morphological forms of CaCO_3 in conjunction with a variety of macromolecules and can be laid up to form many different architectures.^{2-4,6,12} Nacre is just one part of the whole structure and usually is the inside portion of the shell. Nacre is found in the shells of various molluskan species including bivalves, gastropods, and cephalopods and is often referred to as mother-of-pearl,¹³ which has become fashionable in jewelry because of its opalescence and brilliant coloring. As is now well known, the nacreous structure consists of thin CaCO_3 crystals and an organic matrix arranged in a "brick and mortar" structure¹³ with the organic matrix serving as the mortar. The CaCO_3 platelets take the form of crystalline aragonite and make up 95 to 98% of the composite.⁸⁻¹⁰ The aragonite platelets are approximately 5 to 10 μm in diameter and 0.25 to 0.5 μm thick. An example of the nacre structure as viewed in the edge-on orientation, i.e., in a direction perpendicular to the c axis of the aragonite platelets, is shown in Figure 1, which was taken from a *Pinctada margarifera* shell (the so-called pearl oyster).¹ The figure displays relatively thicker aragonite platelets, about 0.5 μm , compared to those of the *Haliothis rufescens*. Although the red abalone platelets are thinner, they have a similar architectural design but a different mode of growth.^{2,10}



Figure 2. Secondary electron image of the pallial myostracum layer in the nacre of red abalone.

2. EXPERIMENTAL PROCEDURE

2.1 Mechanical Testing

Mechanical tests were performed on *Haliothis rufescens* specimens in which the original nacre portion of the shell was approximately 1 cm thick. Specimens were stored and tested at ambient temperature and humidity.¹⁹ Samples of abalone that were sufficiently thick and large were prepared for notched three-point and four-point bend tests according to the specifications



Figure 1. Bright field (BF) TEM image of the nacre section of pearl oyster viewed in the edge-on configuration. The crystallographic c axis, i.e., [001] of the aragonite crystals is shown. The constituent phases, i.e., CaCO_3 and organic matrix are indicated by CaCO_3 and OM in the image. The sample was low-temperature ion-milled and the image was recorded with a 300 kV TEM.

of ASTM standards²⁰ for fracture toughness and fracture strength, respectively. The specimens were cut with a cooled diamond blade into parallel-sided rectangular blocks and polished prior to testing. Flexural strength and fracture toughness tests were performed using an Instron Universal Testing Instrument. All specimens were mounted in the testing apparatus so that crack propagation would occur across the laminates.

Vickers and Knoop microhardness tests were performed on polished sections of nacre from *Halivis rufescens* and *Pinctada margaritifera* using a Shimadzu Type M Micro Hardness Tester. The nacre layers were oriented both at an acute angle and perpendicular to the surface of indentation.¹⁹

2.2 Electron Microscopy

The bulk specimens of seashell were coated with gold-palladium and observed in a Philips 515 scanning electron microscope (SEM) operating at 25 kV. Thin sections of the shell were prepared for transmission electron microscopy (TEM) by cryogenic ion beam milling (sample temperature of about 130K) and room-temperature ultramicrotomy. Uranyl acetate was used on some of the ultramicrotomed samples to enhance the contrast of the organic component for TEM analysis.¹⁹ Samples were viewed in a Philips EM 300 at 100 kV and in a Philips EM 430T operating at between 150 and 300 kV using a liquid nitrogen holder (sample temperature of about 150K).

3. RESULTS

3.1 Mechanical Property-Structure Correlations

The three-point bend tests showed an average fracture toughness of approximately 9 ± 3 MPa·m^{1/2}. The four-point bend tests resulted in a measured fracture strength of approximately 180 ± 30 MPa. Most of the samples failed in mixed mode behavior.^{10,19} Due to the inherent curvature of the layers within the test specimens, slightly wider scatter was observed in the data. As mentioned earlier, the nacre of *Halivis rufescens* contains a relatively thick periodic layer of organic material which runs parallel to the long axis of the aragonite platelets (Figure 2). This thick organic layer, thought to be related to the yearly growth front, acts as a weak region, and samples often fail by shear within this region.^{2,17}

As discussed in earlier publications,⁷ the relative values of the mechanical properties of the composite shell compared to those of the individual components which make up the shell are of interest from an engineering standpoint with regard to the possible mimicking of nacre for technological applications. Considering that the shell is 95 to 98% CaCO₃, the mechanical properties of the composite structure would be expected to be near those of CaCO₃. It is clear, however, that the incorporation of an organic component and the highly ordered lamination of the nacre structure produce properties which are substantially enhanced with respect to those of synthetic and geological aragonite.^{5,8-10}

We also investigated the response of the nacre structure to microhardness indentations with SEM to determine the process(es) by which cracks travel through the composite. The most



Figure 3. Secondary electron image of the nacre structure near a microhardness indentation displaying the sliding of the aragonite platelets in red abalone.

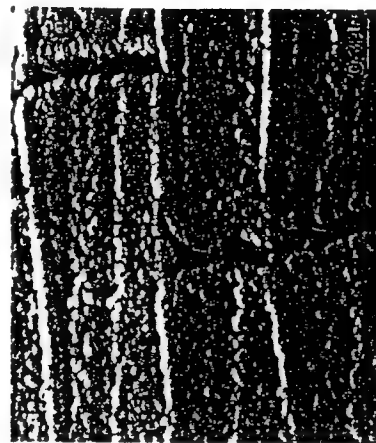


Figure 4. A close-up secondary electron image of the deformed region of the sample showing ligament formation by the organic matrix extending across the edges of platelets.



Figure 5. An SEM image of the microhardness indentation in an edge-on configuration in the nacre of abalone. Note that the indentation involves considerable deformation in the composite without extensive formation of cracks, indicating ductile behavior, as opposed to brittle cracks that usually form at the tips of the indentation.

obvious fracture feature is that crack propagation generally occurs in a tortuous manner across the laminates, with the weakest region being the organic matrix. The tortuosity increases the surface area of the crack and, thus, the amount of energy absorbed during fracture. However, measurements of tortuosity show that increased fracture surface (up to 50%) is not sufficient by itself to account for the toughness value of the composite.

In many instances, aragonite platelets slide over the organic layers, leading to overall deformation of the composite without causing total failure (Figure 3).¹⁹ Through this deformation process, a large amount of energy is absorbed within the organic matrix and at the organic-inorganic interface. In addition, during deformation, the organic matrix and at the organic-inorganic interface. In addition, during deformation, the organic matrix was observed to bridge the crack between layers of aragonite platelets by the formation and extension of ligaments. This was shown earlier to take place within the matrix between the broad faces of the aragonite platelets, i.e., in the transverse direction.¹⁰ Figure 4 shows that bridging also takes place in the longitudinal direction (i.e., in the direction parallel to the plane of the platelets). The formation and extension of organic ligaments slows or prevents the propagation of the crack within the organic matrix by absorbing the energy that would have propagated the crack. Although other toughening mechanisms are usually encountered in brittle materials,²¹ such as microcrack formation, crack blunting and branching, it is the sliding of platelets that provides the two major toughening mechanisms most effective in the prevention of catastrophic failure: the deformation of the overall composite and the formation of ligaments to bridge cracks. These mechanisms can be seen in Figure 5, which shows the deformation, rather than brittle failure, around a microhardness indentation made on a sample with the aragonite crystals at an acute angle to the polished surface.

The fact that aragonite platelets slide over the organic matrix while, at the same time, the organic matrix forms ligaments, each under appropriate applied stress conditions, suggests that both the structure of the interface between the macromolecules and the aragonite platelets, as well as the structure of the organic matrix, play significant roles in allowing deformation and thereby preventing catastrophic failure of the composite. Both of the processes, i.e., the sliding of the aragonite platelets over the organic matrix and organic ligament formation between the platelets, seem to indicate that the interface between these highly dissimilar ceramic and organic materials might be strong enough not to fail in either mode of deformation. Sliding may either happen between the platelets and the top layer of the organic matrix or within the layers of organic matrix. On the other hand, ligament formation clearly takes place within the organic matrix, although it is not yet known which component of the organic matrix plays the most significant role during the deformation process. It is obvious that the ligaments are anchored to the aragonite platelets, suggesting the presence of a strong interface between the organic matrix and CaCO_3 platelets. A strong interface would allow the transfer of stresses between the rigid ceramic crystals and the pliant organic matrix, in addition to allowing the deformation of the overall composite to take place. With synthetic composites such as cermets (ceramic-metal composites) and cerpolys (ceramic-polymer composites), it is usually difficult to achieve strong interfaces between such dissimilar phases.²² Therefore, the structure of the interface in nacre might possibly play a part in its superior properties as compared to synthetic composites. Interface design may be an important design criteria for future biomimetic applications.

In the following section, we provide a more detailed analysis of the structures at the interface region in nacre in order to gain further insight into the deformation processes that take place during the structural response of the composite material to stress. First, we discuss the structure of the organic matrix and then the structure of the interface region between the two phases.

3.2 Study of the Microstructure at the Interfacial Region: Results and Discussions

Structural analysis of the interfacial region was performed by TEM as this technique provides the resolution necessary for imaging the details in both the organic and inorganic phases of nacre. Particular attention was given to the preparation and handling of the samples to ensure that they did not deteriorate. Generally, TEM samples, which consist primarily of the aragonitic phase, are prepared by ion-beam milling, as was demonstrated by us¹⁰ (see, for example, Figure 1) and other earlier studies.²³ During a typical milling process, the sample is inadvertently heated, which can lead to structural damage of both the crystalline and the organic components. Structural damage to the samples can be minimized by performing the milling process under cryogenic conditions (about -130° C in our case). However, even with cryogenic ion beam milling, the organic components of the structure are highly sensitive to ion bombardment and, thus, to knock-on and radiolysis degradation. For this reason, the ion milling method of sample preparation was used only when the structure of the organic region was not of great interest. (Even in ion milled samples, most of the organic material, particularly the innermost layer, stayed intact. This permitted limited analysis of the organic matrix, as discussed below.)

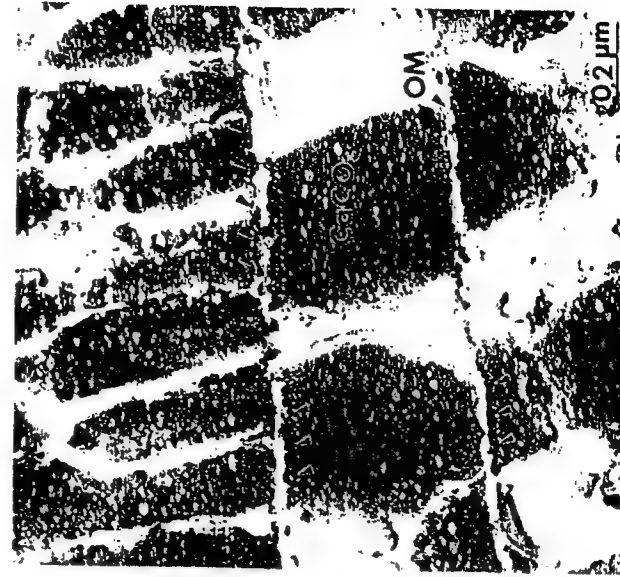


Figure 6. A BF TEM image of the nacre of red abalone prepared by ultramicrotoming. Rough interface between the organic matrix and aragonite crystals and the frothed structure in the aragonite are clearly seen (small arrows).

Ultramicrotoming can be used to preserve both the structure of the crystalline and the organic regions simultaneously (Figure 6) with some sacrifice to the sample.¹⁹ Due to the brittle nature of the crystals and the presence of mechanical instabilities in the experimental set-up, however, the microtomed samples displayed periodic chatter in the aragonite crystals. As shown in Figure 6, the chatters run perpendicular to the aragonite crystals and appear roughly vertical in the image. Even so, local regions of the aragonite crystal-organic matrix interface remain intact (arrows in the image) and leave sufficiently large areas for imaging, diffraction, and high-resolution analysis, as described below.

Uranyl acetate was applied to some microtomed sections to demonstrate that the organic matrix was indeed undisturbed by the microtoming process and that it is composed of a layered structure. Figure 7 shows the structure of the organic matrix in decalcified nacre as observed in an edge-on configuration (note that, due to the application of uranyl acetate staining solution, the aragonite crystals are dissolved and, thus, not present in the image). As indicated by the arrows, the five-layer structure of the organic matrix is clearly visible. This layered, sandwich structure of the organic matrix was proposed earlier in the literature.^{15-17,24} According to the hypothesis, the middle layer is thought to be structural polysaccharide, most likely chitin. On either side of the middle layer are structural proteins, such as silk-fibronilike proteins, which are thought to be stereochemically related to the aragonite matrix, and, therefore, more directly involved in the biomineratilization process.²⁴ Finally, the outer layer that is in contact with the aragonite is assumed to be acidic macromolecules containing mostly aspartic and glutamic acids, its function being secondary.²⁴

Despite extensive research, neither the composition nor the structure of each of the organic layers have been quantitatively analyzed.⁴ Both the structural interrelationship of the organic matrix and the aragonite crystals in nacre and its effect on the overall mechanical properties of the composite structure require an understanding of the structure and composition of the organic matrix in detail at the nanometer scale. Such knowledge is also essential for a fundamental understanding of the control of the organic matrix over the biocrystallization process in this and other similar hard tissues. (Along with efforts by other groups working in this area,²⁵ a part of our current research focuses on the analysis of each of these layers by protein purification and antibody generation and decoration procedures.²⁶)

In addition to the organic matrix, it is clear that the detailed structure of the interface between the aragonite crystals and the organic matrix has to be investigated in order to describe the mechanical properties of nacre and its fractographic features. Obtaining this information on the interface structure has not yet been possible mainly because of the difficulties in the simultaneous imaging of both the aragonite platelets and the organic matrix with TEM. Despite these difficulties, however, our TEM investigation indicates periodic contrast fluctuations that run parallel to the aragonite/organic matrix interface both in the ion milled and the microtomed thin sections, as displayed in Figures 1 and 6, respectively. These images indicate that there is a string of small pores approximately 8 to 12 nm in diameter and spaced 20 to 32 nm apart (measuring center to center) parallel to the organic matrix. The nature of these pores has not yet been clarified, but it is assumed that they contain either water or organic material or both.¹⁹ Because these features are present in samples prepared by both techniques, they are considered to be representative of the structure and are not an artifact developed during sample preparation.



Figure 7. A TEM image of the organic matrix displaying a five-layer sandwich structure of the composite. This section was stained with uranyl acetate and the aragonite crystals were dissolved by the staining solution.



Figure 8. TEM image of a gold citrate stained section of nacre which was originally ion-beam milled. Two major features of interest are dark bands (DB) within the organic layer and the preferential etching characteristics of the aragonite crystals (ST) which give a saw-tooth angle of about 46° in this projection.

These features were observed both in *Haliois rufescens* and *Pinctada margarifera*,¹⁹ and they are similar to those that were reported in bivalve mollusks.²³ Therefore, they appear to be a common feature, characteristic of the nacre structure in general and not specific to a single molluskan species.

A closer examination of the interface between the organic and the aragonite platelets indicates that the interface does not have a flat surface but rather is rough and the edges of the aragonite crystals near the interface are "frothed" in addition to containing the aforementioned "pores." As shown in the ultramicrotomed sample in Figure 7, these features suggest a "transitory region," whose structural characteristics are quite different from the substructure of the aragonite in the interior of the platelets. This transitory region is even more apparent in Figure 8, which was recorded from an ion milled sample in which parts of the aragonite crystals near the interface have been partially dissolved by the colloidal gold solution containing citric acid. As shown in the image, thin dark bands run parallel to the aragonite platelets in the interface region previously occupied by the organic matrix. If these bands are a surviving portion of the organic matrix, or what remains of it after ion beam milling, they are very likely structural polysaccharides, or the hypothesized¹⁶ "chitin" section of the organic sandwich structure.^{15,17} In addition, as can be seen in the image, the CaCO₃ crystals are etched preferentially, making a $46 \pm 1^\circ$ angle with respect to the plane of the interface which is parallel to the (001) plane of the aragonite lattice. This produces a characteristic "saw-tooth" shaped etching of the transitory region, suggesting that the organic matrix may have infiltrated through the interface into the inorganic crystals. At this stage of our research, this conclusion is only a conjecture and remains to be proven by other means.

Nonetheless, this transitory region in the aragonite phase near the interface (which is effectively a "composite" of CaCO₃ and organic material as schematically depicted in Figure 9) may have a significant effect on the mechanical properties of the overall composite. First of all, a spatial interlocking of the organic matrix and the aragonite crystals would be expected based on the assumption that part of the organic matrix is occluded in the aragonite crystals. This would increase the effective surface area and thus the adhesive strength between these dissimilar phases. Our mechanical test results and fractographic analysis have some parallelism with these observations of the detailed structure of the interfacial region.

4. CONCLUSIONS

The nacre portion of mollusk shell has been shown to display greater toughness and strength than CaCO₃, which makes up 95 to 98% of the nacre structure. The increase in toughness has been attributed to a variety of fracture mechanisms that increase energy absorption during failure, the main mechanisms being sliding of the inorganic crystals and ligament formation in the organic phase. An essential feature critical to several of these energy-absorbing mechanisms is the presence of a strong interface between the aragonite crystals and the organic matrix. This strong interface is necessary for the transfer of stress from the crystals to the organic matrix and subsequent energy absorption within the organic matrix. Factors leading to higher strength are not yet understood.

We determined that the interface between the organic matrix and the aragonite crystalites is not planar but is what we call a transitory region, which seems to be an interlocking of the organic matrix into the aragonite, as suggested by the structural features. Although the true nature of this region has not yet been clarified, it appears to increase the surface area between the two phases and thereby increases the strength of the bond across the interface, thereby resulting in a composite structure with desirable mechanical properties.

ACKNOWLEDGEMENTS

This work was supported by the Air Force Office of Scientific Research under Grant Nos. 89-0496 and 91-0281. The assistance of D. L. Milius is gratefully acknowledged.

REFERENCE

1. R. T. Abbott, *Sea Shells of the World* (Plenum, New York, 1962).
2. J. D. Currey, "Biological Composites," *J. Mater. Edu.*, **9** [1-2] 118-296 (1987).
3. P. D. Calvert and S. Mann, "Synthetic and Biological Composites Formed by In Situ Precipitation," *J. Mater. Sci.*, **5**, 309-14 (1987).
4. (a) K. Simkiss and K. M. Wilbur, *Biomineralization* (Academic Press, New York, 1989); (b) H. A. Lowenstein and S. Weiner, *On Biominerilization* (Oxford University Press, New York, 1989); (c) *Biominerilization: Chemical and Biochemical Properties*,

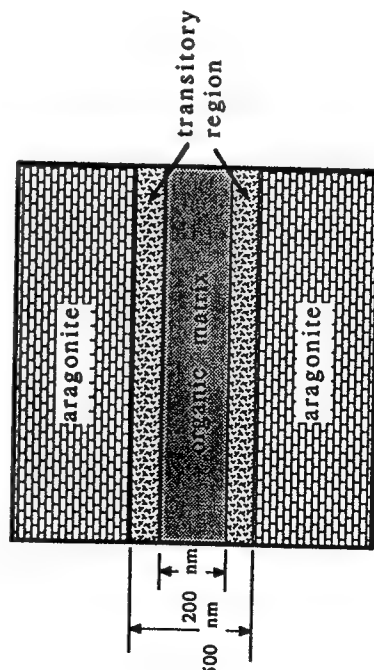


Figure 9. Schematic illustration of the transitory region in the CaCO₃ crystals near the organic matrix.

- edited by S. Mann, J. Webb, and R. J. Williams (VCH Publisher, Weinheim, Germany, 1989).
5. M. Sarikaya and I. A. Aksay, "Nacre of Abalone: A Natural Ceramic-Polymer Composite Material," Chapter 1 in *Structure, Cellular Synthesis, and Assembly of Biopolymers*, edited by Steven Case (Springer-Verlag, New York, 1992).
 6. S. W. Wise, "Microarchitecture and Deposition of Gastropod Nacre," *Science*, **167**, 1486-87 (1970).
 7. *Design and Processing of Materials by Biomimicking*, edited by M. Sarikaya and I. A. Aksay (Springer-Verlag, New York, to be published 1992).
 8. (a) J. D. Currey, "Mechanical Properties of Some Molluscan Hard Tissues," *J. Zool., Lond.*, **173**, 395-406 (1974); (b) J. D. Currey, "Further Studies on the Mechanical Properties of Mollusk Shell Materials," *J. Zool., Lond.*, **180**, 445-53 (1976).
 9. (a) A. P. Jackson, J. F. V. Vincent, and R. M. Turner, "The Mechanical Design of Nacre," *Proc. R. Soc. Lond.*, **234**, 415-40 (1988); (b) A. P. Jackson, J. F. V. Vincent, and R. M. Turner, "A Physical Model of Nacre," *Composites Science and Technology*, **36**, 255-66 (1989).
 10. M. Sarikaya, K. E. Gunnison, M. Yasarbi, and I. A. Aksay, "Mechanical Property-Microstructural Relationships in Abalone Shell," in *Materials Synthesis Utilizing Biological Processes, MRS Symp. Proc.*, Vol. 174, edited by P. C. Rieke, P. D. Calvert, and M. Alper (Materials Research Society, Pittsburgh, 1989), pp. 109-16.
 11. V. J. Laraia and A. H. Heuer, "Novel Composite Microstructure and Mechanical Behavior of Mollusk Shell," *J. Am. Ceram. Soc.*, **72** [11] 2177-79 (1989).
 12. S. Weiner and H. A. Lowenstam, "Organization of Extracellularly Mineralized Tissues: A Comparative Study of Biological Crystal Growth," *CRC Crit. Rev. Biochem. B*, **20**, 365-98 (1986).
 13. C. Gregorie, "Topography of the Organic Components in Mother-of-Pearl," *J. Biophys. Biochem. Cytol.*, **3**, 797-804 (1957).
 14. J. Liu, M. Sarikaya, and I. A. Aksay, "A Hierarchically Structured Model Composite: A TEM Study of the Hard Tissue of Red Abalone," see this volume.
 15. S. Weiner and W. Traub, "X-Ray Diffracton Study of the Insoluble Organic Matrix of Mollusk Shells," *FEBS Lett.*, **111** [2] 311-16 (1980).
 16. G. Bevelander and H. Nakahara, "An Electron Microscope Study of the Formation of the Nacreous Layer in the Shell of Certain Bivalve Molluscs," *Calc. Tiss. Res.*, **3**, 84-92 (1969).

17. N. Watabe, "Studies on Shell Formation: XI. Crystal-Matrix Relationship in the Inner Layers of Mollusk Shells," *J. Ultrastructure Research*, **12**, 351-70 (1965).

18. R. A. Lutz and D. C. Rhoads, "Anaerobiosis and a Theory of Growth Line Formation," *Science*, **198**, 1222-27 (1977).

19. K. E. Gunnison, "Structure-Mechanical Property Relationships in a Biological Ceramic-Polymer Composite: Nacre," M.S. Thesis, University of Washington, 1991.

20. W. F. Brown, Jr., and J. E. Strawley, "Plain Strain Crack Toughness Testing of High Strength Metallic Materials," *ASTM Special Publ. No. 410* (1967).

21. *Deformation of Ceramic Materials II, Materials Science Research*, Vol. 18, edited by R. E. Tressler and R. C. Bradt (Plenum, New York, 1984).

22. *Interfacial Phenomena in Composites: Processing, Characterization, and Mechanical Properties*, edited by S. Suresh and A. Needleman (Elsevier, London, 1989); also, *Mater. Sci. Eng.*, A107 [1-2] 1-280 (1989).

23. (a) K. M. Towe and G. H. Hamilton, "Ultrastructure of Inferred Calcification of the Mature and Developing Nacre in Bivalve Mollusks," *Calc. Tiss. Res.*, **1**, 306-318 (1968); (b) K. M. Towe and G. R. Thompson, "The Structure of Some Bivalve Carbonates Prepared by Ion-Beam Thinning," *Calc. Tiss. Res.*, **10**, 38-48 (1972).

24. (a) S. Weiner, "Organization of Extracellularly Mineralized Tissues: A Comparative Study of Biological Crystal Growth," *CRC Crit. Rev. in Biochem.*, **20** [4] 365-80 (1986); (b) L. Addadi and S. Weiner, "Interactions Between Acidic Macromolecules and Structured Crystal Surfaces: Stereochemistry and Biomineratization," *Mol. Liq. Cryst.*, **134**, 305-22 (1986).

25. J. A. Keith, S. A. Stockwell, D. H. Ball, W. S. Muller, D. L. Kaplan, T. W. Thanhouser, and R. W. Sherwood, "Characterization of the Complex Matrix of the *Mytilus edulis* Shell and the Implications of Biomimetic Ceramics," this volume.

26. C. Furlong, M. Sarikaya, and I. A. Aksay, unpublished research; also see, for preliminary studies, C. E. Furlong and R. Humbert, "Design of Protein-Producing Bioreactors for Self-Assembling Systems," this volume.

"A Hierarchically Structured Model Composite:
A TEM Study of Hard Tissue of Red Abalone Shell,"

J. Liu, M. Sarikaya, and I. A. Aksay

in

Proc. of *Hierarchically Structured Materials*

edited by I. A. Aksay, E. Baer, M. Sarikaya, and D. Tirrell

(Materials Research Society, Pittsburgh, PA, 1992)
Vol. 255, pp. 9-18

**A HIERARCHICALLY STRUCTURED MODEL COMPOSITE:
A TEM STUDY OF THE HARD TISSUE OF RED ABALONE**

JUN LIU, MEHMET SARIKAYA, and ILHAN A. AKSAY

Department of Materials Science and Engineering, and
Advanced Materials Technology Center, Washington Technology Center,
University of Washington, Seattle, WA 98195

ABSTRACT

The structure and crystallography of the nacre of red abalone, *Haliotis rufescens*, was studied by transmission electron microscopy imaging and diffraction. We found that the nacre structure is based upon hierarchical {110} twinning in aragonite with the following organization: (i) first generation twins between platelets having incoherent boundaries, (ii) second generation twins between domains having coherent boundaries within a given platelet, and (iii) nanometer-scale third generation twins within domains. Since the aragonite platelets nucleate and grow as separate crystals, this long-range crystallographic relationship between the inorganic units of a biological hard tissue indicates that the nucleation and growth process of crystals may be mediated by the organic matrix and that the organic template structure may also be long-range ordered. We propose a superlattice structure based on the possible twin variants compatible with the superlattice. Multiple tiling based upon this superlattice allows all of the crystallographic and morphological platelet configurations observed in nacre.

INTRODUCTION

Nacre is a laminated ceramic-polymer composite material found in mollusk shells.¹⁻⁶ It has a highly ordered structure on a continuous scale¹ from the nanometer to the millimeter and has unique mechanical properties, such as high fracture toughness and strength.³⁻⁴ Understanding its structure, in particular the growth process and the interrelationships between the microstructure and properties, is valuable to biological sciences, materials science and engineering, and the electronic industry. Previous studies have suggested that the formation of the inorganic crystals was regulated by the organic matrix through epitaxial growth.⁶⁻⁹ But to date neither the structure of the inorganic phase with its detailed architecture nor the organic phase have been fully understood. In nacre, the inorganic phase, CaCO_3 in the aragonite form (Pmcn, No. 62), and the organic phase, a mixture of proteins and polysaccharides,⁸⁻⁹ are arranged in a "brick and mortar" microarchitecture (Figure 1).¹⁻⁵ The aragonite platelets, with hexagonal or square faces, are about 5 μm in edge length and 0.25 to 0.5 μm in thickness, and the organic phase is about 100-200 \AA thick.¹⁰ Previous diffraction studies¹¹ illustrated that the platelets on a given layer are aligned in the *c* direction of the orthorhombic unit cell of the aragonite lattice. It was further suggested that the platelets are arranged in a "mosaic pattern" without definite crystallographic relationships between them in the *a-b* plane.¹² Similarly, it was suggested that only local ordering existed in the organic matrix, which was thought to be responsible for the mosaic polycrystalline pattern in the aragonite crystals.¹²

sample a few degrees to bring each of the three alternate platelets into a strongly diffracting condition so that they exhibit a dark diffraction contrast. The platelets A, C, and E, therefore, are all in the same orientation and the remaining three, B, D, and F, are in a twin orientation with the first set. Although the diffraction patterns are slightly misaligned about the c direction, the twin relationships between them are preserved. In fact, the selected area diffraction (SAD) pattern recorded from all platelet boundaries shown in Figure 2 reveals the same twin reflections, indicating that each platelet is related to the one next to it by a $\{110\}$ twin relation. In this paper, we refer to the twinning between aragonite platelets as *incoherent first generation twinning*.



Figure 1. Secondary electron image of fractured surface of nacre reveals the brick and mortar microarchitecture. Nacre is from a pearl oyster sample (*Pinctada margaritifera*). Courtesy of Katie E. Gunnison.

Contrary to these earlier studies, in the following sections, we summarize our recent electron microscopic studies to show that platelets have definite crystallographic relationships to each other and are arranged with levels of hierarchical twins. Our findings also suggest the existence of a long-range order in the organic matrix.

CRYSTALLOGRAPHY OF ARAGONITE PLATELETS: HIERARCHICAL TILING IN THE NACRE STRUCTURE

We first studied both the geometrical arrangement of and the crystallographic relationship among the aragonite platelets.^{1,13} In the face-on view, each layer of the nacre is composed of closely packed platelets (Figures 2(a) and 2(b)). The platelets have either three, four, five, or six edges. The geometrical organization of the platelets often exhibits sixfold symmetry as shown in Figures 2(a) and 2(b) where six platelets are arranged with an approximate 60° angle between each pair (60° twin boundaries). The crystallographic orientations between the platelets on the a - b plane are not random, contrary to previous assumptions,¹¹⁻¹² but generally relate to one another by twinning, as shown by the diffraction patterns in Figures 2(c) and 2(d). The [001] single crystalline pattern in Figure 2(c) is from the interior of a platelet; the pattern in Figure 2(d), which was recorded from the boundary between two platelets, incorporates two superimposed patterns. Analysis of the two patterns reveals that they are correlated to each other by a twin relationship, with the twin plane $\{110\}$ parallel to the [001] direction of the crystal, i.e., either $\{110\}$ or $\{1\bar{1}0\}$. The images in Figures 2(a) and 2(b) were recorded by tilting the

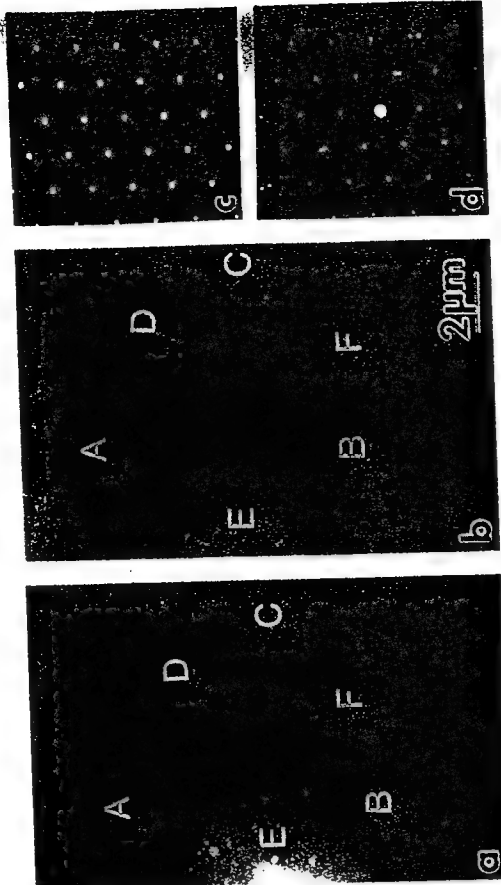


Figure 2. (a) and (b) show the face on view of nacre and were recorded by slightly tilting the specimen along the c direction. The nacreous layer consists of closely packed 3-, 4-, 5-, and 6-edged platelets, which often exhibit sixfold symmetry. In (c) and (d), diffraction revealed that the platelets are related to one another on $\{110\}$ planes. (c) is a single crystalline diffraction pattern from one platelet. (d) is the diffraction pattern from boundaries between platelets, showing twin relationships.

Further studies revealed that many of the platelets are not single crystals but are comprised of several domains, and that the domains are related to each other by twinning as well. Figure 3(a) shows a four-domain platelet with 90° domains. The diffraction pattern in Figure 3(b), recorded from the interior of one of the domains, indicates that the platelet is again perpendicular to the [001] electron beam direction. The diffraction pattern in Figure 3(c) recorded from the boundary of one of the domains, exhibits twin splitting of $\{110\}$ reflections. A close examination of the crystal structure of aragonite shows that the 90° twin boundaries can be accommodated by including two atomically flat $\{110\}$ twin planes (reflection twins) and two zig-zag boundaries

In summary, we found that there are three levels of twinning in the face-on configuration of the nacre section of red abalone shell: (i) first generation twins between platelets that have incoherent boundaries, (ii) second generation twins between domains with coherent boundaries within a given platelet, and (iii) nanometer-scale third generation twins within a domain. It should be noted that both twin and domain boundaries can be either 60° or 90° , although we only show examples of 60° twin boundaries and 90° domain boundaries. Therefore, these twin structures encompass a six-order magnitude size scale covering a range from the nanometer to



Figure 3. (a) shows the domain structures within platelets; (b) single crystalline diffraction pattern from one domain; (c) twin diffraction pattern from domain boundaries.

180° -rotation twins). This kind of twinning is called *second generation coherent twins*, and there is no misalignment in the c direction among the domains within a platelet.

In an ideal hexagonally shaped platelet having six twin-related domains, the angle between each pair of domains must be 60° , with the six domains completing 360° for the whole platelet. This is not possible in aragonite since the outer edges of the platelets are parallel to $\{110\}$ planes and the angle between each pair of $\{110\}$ planes is 63.5° . This discrepancy, therefore, must be accommodated by lattice deformation during the formation of twin-related domains in an aragonite platelet and can be accomplished by either slipping (dislocation formation) or by twinning,¹ with the latter preferred in ionic crystals.¹ Imaging of the microstructure at higher magnifications shows that each domain in a given platelet actually contains two sets of nanometer-scale twins, each forming $\{110\}$ planes. Figure 4 shows two variants of ultrafine twins forming angles of about 63.5° or 127° , which are similar to growth twins in geological minerals.¹⁴ The accommodation of the 3.5° strain is possible by the formation of these nanometer scale defects on the $\{110\}$ planes, which allows the lattice to be deformed towards the periphery of the platelet. In fact, in most cases, the outer periphery of the platelets has a convex shape, the apex being in the middle of the edge, and the region of the edge where the two domains meet inwardly curved. We call these ultrafine twins *third generation nanometer-scale twins* as they take place at the smallest dimensional scale.



Figure 4. Nanotwins within domains.

the submillimeter and reveal a hierarchical structure for hard tissue in a biological material. Although sixfold twin structures also occur in geological aragonite, the hierarchical arrangement of twins in nacre is unique in the sense that each platelet is completely separate from the others during the early stage of growth. Even after crystallization is complete, the platelets are still separated from one another by an organic membrane. On the other hand, in geological aragonite¹⁹ the mimetic twin domains always grow one after another. The fact that the separate platelets grow simultaneously and yet retain a certain crystallographic relationship suggests that the growth process is mediated by the organic template beneath the crystals, and that the organic matrix also has long-range ordering.¹ In the following section we discuss how these hierarchical twins originate and the implications for the structure of the organic template on which the aragonite crystals are grown.

CONFORMATION OF MATRIX MACROMOLECULES

The interaction between the organic template and the crystals may include both electrostatic and stereochemical forces.^{8,15-17} If that is the case, then the nucleation and growth of the crystals will be influenced by both the nearest and higher order interactions. In aragonite, calcium ions give the crystal a pseudohexagonal symmetry in the [001] projection, but the CO_3^{2-} ions reduce the symmetry to an orthorhombic form.¹⁴ Although nucleation and growth may involve both the calcium²⁺ and the CO_3^{2-} ions,¹² for simplicity, in this study only the arrangement of the calcium ions is examined in the [001] projection. To understand the origin of the hierarchical twins, we superimposed the lattices of all three possible twins with a 63.5° rotation with respect to each other and generated a new, higher-order structure, which we call the *superstructure* (Figure 5(a)). If the nucleation and growth of aragonite platelets takes place on this spatial configuration of the active sites for the binding of the Ca^{2+} ions, then the organic matrix must accommodate this superlattice and, thus, all twins in nacre, since the organic template structure should also be aligned over all length scales. The most likely solution to this problem is that the organic matrix, or the arrangement of the active nucleation sites on it, has a single crystalline lattice structure over a wide area that is compatible with the superlattice. A local crystalline organization of the organic matrix, with no relationship between the neighboring areas, and, hence, without long-range order, would result in the formation of

aragonite crystals without any definite crystallographic relationship among the platelets. For example, a pseudohexagonal arrangement, which is indicated by the circles in Figure 5(a), would satisfy the requirement for the organic matrix. The crystalline pseudohexagonal lattice is a possible solution since many two-dimensional protein lattices assume this organization during self-assembly.¹⁸

The superlattice shown in Figure 5(a) allows the generation of the overall hierarchical twin structures by tracing along the possible twin boundaries. One construction is illustrated in Figure 5(b) which contains all the shapes, geometry, and crystallography-related features discussed in this paper, such as five-edged platelets with 90° domains, sixfold symmetry of platelets, and six- and three-edged domains. The fact that all the possible configurations can be generated this way again illustrates the need for a compatible organic matrix with a wide range of length scales to accommodate all the twin relationships, rather than the lattice of a single domain or a single platelet.

The construction of the aragonite platelets discussed in this paper is the subject of multiple tiling in mathematics.¹⁹ Nature uses this technique to form a highly ordered structure compatible with both the soft tissue and the crystalline structural constraints of the hard tissue. This unique ordering, originating from the atomic or molecular structures of both the organic and inorganic tissues, extends from the molecular to the millimeter scales to form different shapes of shells.^{1,13}

ACKNOWLEDGEMENT

This work was supported by the Air Force Office of Scientific Research under Grant No. AFOSR-91-0281.

REFERENCES

- M. Sariyaka and I. A. Aksay, "Nacre of Abalone: A Natural Multifunctional Nanolaminated Ceramic-Polymer Composite Material," in *Structure, Cellular Synthesis and Assembly of Biopolymers*, edited by Steven T. Case (Springer-Verlag, New York, 1992) in press.
- S. M. Wise, "Microarchitecture and Mode of Formation of Nacre (Mother-of-Pearl) in Pelecypods, Gastropods, and Cephalopods," *Ecloae Geol. Helv.*, **63** [3] 775-95 (1970).
- J. D. Currey, "Biological Composites," *J. Mater. Edu.*, **9** [1-2] 118-96 (1987).
- A. P. Jackson, J. F. V. Vincent, and R. M. Turner, "The Mechanical Design of Nacre," *Proc. Roy. Soc. London*, **B234**, 415-40 (1988).
- M. Sariyaka, K. E. Gunnison, M. Yastrebi, and I. A. Aksay, "Mechanical Property-Microstructural Relationships in Abalone Shell," in *Materials Synthesis Using*

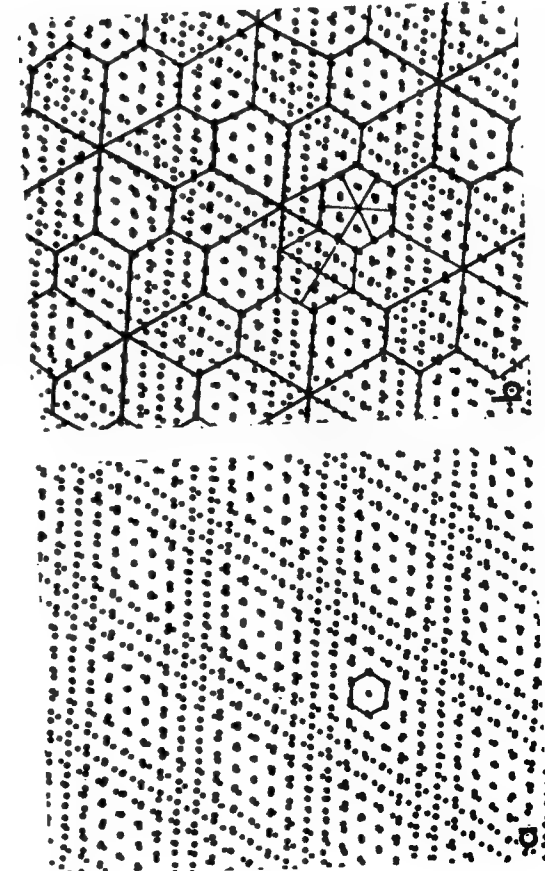


Figure 5. (a) Superlattice generated by superimposing possible twin crystal lattice structures. The circles are an imaginary lattice structure of the organic matrix; (b) All tiling patterns can be constructed on the superlattice by tracing along possible twin boundaries.

- Biological Processes**, edited by P. C. Rieke, P. D. Calvert, and M. Alper (Materials Research Society, Pittsburgh, 1990), pp. 109-16.
6. **Design and Processing of Materials by Biomimicking**, edited by M. Sarikaya and I. A. Aksoy, (Springer-Verlag, New York, to be published 1992).
7. G. Bevelander and H. Nakahara, "An Electron Microscope Study of the Formation of the Nacreous Layer in the Shell of Certain Bivalve Molluscs," *Calc. Tiss. Res.*, **3**, 84-92 (1969).
8. E. M. Greenfeld, D. C. Wilson, and M. A. Crenshaw, "Ionotropic Nucleation of Calcium Carbonate by Molluscan Matrix," *Amer. Zool.*, **24**, 925-32 (1984).
9. (a) K. Simkiss and K. M. Wilbur, **Biomineralization**, (Academic Press, New York, 1989); (b) H. A. Lowenstein and S. Weiner, *On Biominerization*, (Oxford University Press, New York, 1989).
10. K. E. Gunnison, M. Sarikaya, J. Liu, and I. A. Aksoy, "Structure-Mechanical Property Relationships in a Biological Ceramic-Polymer Composite: Nacre," in *Hierarchically Structured Materials, MRS Symp. Proc.*, Vol. 255, (Material Research Society, Pittsburgh, 1992).
11. (a) S. Weiner and W. Traub, "X-ray Study of the Insoluble Organic Matrix of Mollusk Shells," *FEBS Letters*, **111**, 311-16 (1980); (b) S. Weiner, Y. Talmon, and W. Traub, "Electron Diffraction of Mollusc Shell Organic Matrix and Their Relationships to the Mineral Phases," *Int. J. Biological Macromolecules*, **5**, 326-28 (1983); (c) S. Weiner and W. Traub, "Macromolecules in Mollusc Shells and Their Functions in Biominerization," *Phil. Trans. R. Soc. Lond.*, **B304**, 425-34 (1984).
12. L. Addadi and S. Weiner, "Interaction between Acidic Proteins and Crystals: Stereochemical Requirement in Biominerization," *Proc. Natl. Acad. Sci.*, **82**, 4110-14 (1985).
13. M. Sarikaya, J. Liu, and I. A. Aksoy, "Multiple Tiling with Hierarchical Twins in Nacre: A TEM Study in *Haliotis rufescens*," to be submitted (1992).
14. A. D. Negro and L. Ungaretti, "Refinement of the Crystal Structure of Aragonite," *American Mineralogist*, **56**, 769-72 (1971).
15. S. Weiner, "Organization of Extracellularly Mineralized Tissues: A Comparative Study of Biological Crystal Growth," *CRC Critical Reviews in Biochemistry*, **20** [4] 365-80 (1986).
16. S. Mann, "Molecular Recognition in Biominerization," *Nature*, **332** [11] 119-23 (1988).
17. I. Weissbuch, L. Addadi, M. Lahar, and L. Leiserowitz, "Molecular Recognition at Crystal Interfaces," *Science*, **253**, 637-95 (1991).
18. N. Unwin and R. Henderson, "The Structure of Proteins in Biological Membranes," *Scientific American*, **250** [2] 78-94 (1985).
19. For a review, see B. Grunbaum in *Tilings and Patterns* (W. H. Freeman, New York, 1987).

"Imaging of Hierarchically Structured Materials"

M. Sarikaya and I. A. Aksay

in Proc. of *Hierarchically Structured Materials*
Vol. 255, pp. 193-308

edited by I. A. Aksay, E. Baer, M. Sarikaya, and D. Tirrell
(Materials Research Society, Pittsburgh, PA, 1992)

IMAGING OF HIERARCHICALLY STRUCTURED MATERIALS

MEHMET SARIKAYA and ILHAN A. AKSAY

Department of Materials Science and Engineering, and
Advanced Materials Technology Center, The Washington Technology Center,
University of Washington, Seattle, WA 98195

ABSTRACT

We describe techniques used to characterize hierarchically structured synthetic and biological materials. These techniques decipher the structures through the dimensional spectrum from the molecular and atomic scales (10^{-10} m) to the macro scales (10^{-3} m) where the overall shape of the material emerges. Techniques used to image surfaces and internal structures can be categorized according to their wavelength and thus spatial resolution as light, x-ray, and electron microscopy. We also discuss newly emerging microscopy techniques that image surfaces at the atomic level without a focusing lens, such as scanning tunneling and atomic force microscopies, with the aid of field ion microscope and scanned probe microscopes. Transmission electron microscopy (TEM), a unique tool for multipurpose imaging, provides structural information through direct imaging, diffraction, and spectroscopic analysis. We illustrate the major TEM techniques used to analyze structural hierarchy with examples of synthetic and biological materials. We also describe light optical microscopy and scanning probe microscopy techniques, which cover the opposite ranges of the dimensional spectrum at the micrometer and subangstrom levels.

1. INTRODUCTION AND BACKGROUND ON HIERARCHICAL STRUCTURES

Hierarchically structured materials display distinct architectural designs at successively varying length scales, with each level of structure a self-forming entity.¹ In this definition, each level of structure is locally diverse, yet interactive through successive levels, thereby generating a larger overarching structure with unique properties that reflect the contribution of phenomena taking place at various levels of the hierarchy. Although the internal structures in each level of the hierarchy provide the intrinsic properties of material, it is the interfaces between the hierarchical levels that allow interaction between levels and provide continuity at each step throughout the entire structure.

In synthetic materials,^{1,2} such as crystalline ceramics or metals, the hierarchy may include the levels summarized in Figures 1 and 2, with the smallest level a few angstroms containing a single atom. The next scale in the hierarchy would be the unit cell which represents the smallest crystallographic entity. In a single crystalline material, the unit cell would repeat itself through the entire material in three dimensions with no higher level of hierarchy. In the single crystalline state, thermodynamically dictated imperfections such as vacancies, interstitials, and dislocations constitute the first level of structural features in the hierarchical ladder.³ Most materials of technological importance, though, are not single crystalline, but instead are aggregates of finite size single crystalline grains (Figure 1).³ In some cases, these grains may exhibit domain structures. Second phase precipitates within grains are also commonly observed features.² Higher level aggregation of grains can deliberately be introduced when it is essential to design more complex structures.⁴ Figure 3 is a set of transmission electron microscope (TEM) images from a nanoparticle colloidal-gold system in which the different levels of the structure are revealed. The individual particles, their aggregation, the formation of first generation voids, clusters of particles, second and higher generation voids, and cluster of aggregates clearly demonstrate the formation of a structural hierarchy on a wide dimensional scale.⁴

Hierarchy in biological materials is much more organized and well studied.^{5,6} Almost all soft tissues are made up of hierarchical structures that start at the molecular level as organic molecules, usually as molecules formed of C, H, N, O, and sometimes S and P.⁵ Macromolecules in the secondary structures are long-chain organic molecules. At the third level, organic structures are composed of these macromolecules as aggregates in the form of enzymes, which themselves self-assemble into specific shapes forming quaternary structures, such as structural proteins and polysaccharides. Specific functions of the proteins and other macromolecular aggregates are defined by these quaternary structures. At higher levels of hierarchy, the structures of biological soft tissues successively form membranes, organelles, cells, tissues, and organs, as indicated in the chart shown in Figure 4.⁵

In tendon, a classic example of hierarchy in a biological material,⁶ the structure resembles a common engineering fiber composite in which the fibers are uniaxially embedded in a binding matrix. The hierarchy in tendon, however, is much more established and the structure is highly ordered.⁶ The primary and secondary structures are ions and molecules. At the tertiary level, long chains of molecules form and, in groups of three, wind in helices to form individual collagen fibrils. Tropocollagen fibrils are triple helices of collagen fibrils a few nanometers thick.⁵ In the next layer up, these fibrils wind together in groups of three or more (similar to the previous level) to form microfibrils (3–4 nm in diameter). Higher levels of structure incorporate subfibril, fibril, fascicles, and finally tendon through the dimensional hierarchy from 10 nm, 100 nm, 50 μm, and 0.5 mm in diameter, respectively. A similar hierarchy forms in many biological tissues, including hair and skin.⁵

Like soft tissues, biological hard tissues also have a hierarchical structure that starts at the molecular level. But here it is much less defined and is difficult to infer. For example, the hierarchy in bone above the micrometer dimension has been well established,⁷ but at lower levels, the hierarchy in the inorganic component is not yet well established.⁸ Even in this case, however, some new evidence illuminates the nature of the structural units that make up the calcium phosphate component of the tissue.⁹ In an accompanying paper, we discuss the structural hierarchy of nacre, a hard tissue found in mollusks, beginning at the nanometer level and extending to the macroscale.¹⁰ The nacre section of the red abalone shell contains CaCO₃ in the form of aragonite platelets organized as "bricks" held together by an organic matrix.^{11–13} At the microscale, the platelets are crystallographically related to each other in that each one is twin-related to the one next to it (first generation twins). Each platelet, furthermore has three, four, or six domains that are themselves twin-related to each other (second generation twins). The integrity of the structure in a given single crystalline platelet is maintained by the formation of {110} twins at the nanometer scale (third generation twins). The crystallographic, morphological, and geometrical configuration of the platelets suggest that they are space filling tiles with multiple twins.¹⁴ We find that the space filling is accomplished by the formation of local spirals, which themselves form spirals that continue up the scale to finally form the shape of the shell.¹⁴

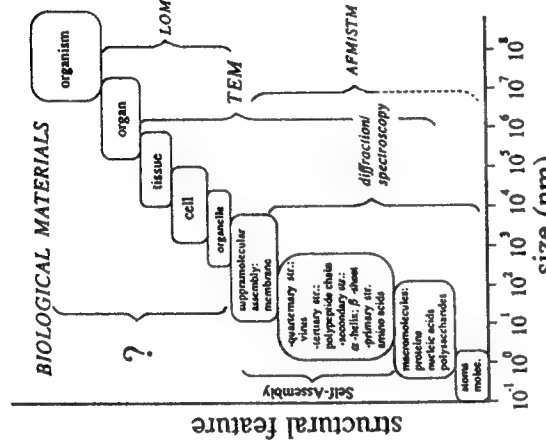


Figure 4. Hierarchical structures in biological materials.

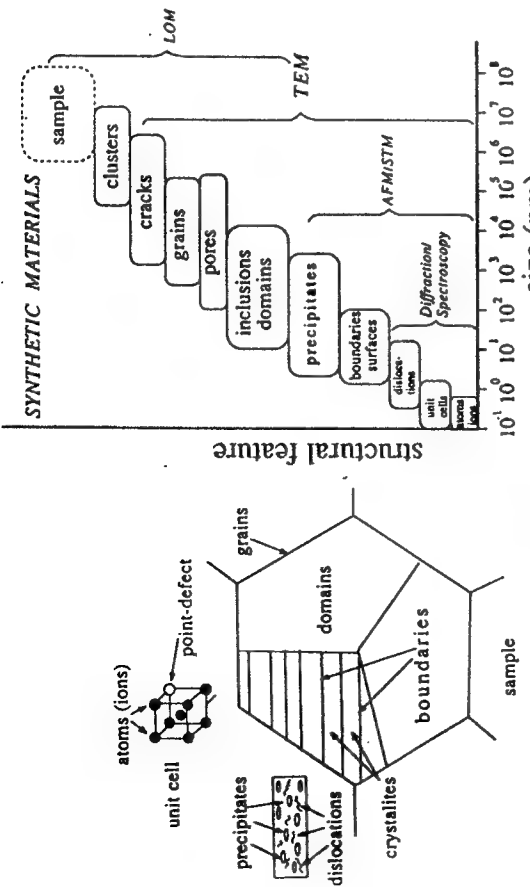


Figure 1. Schematic illustration of hierarchy in synthetic materials.

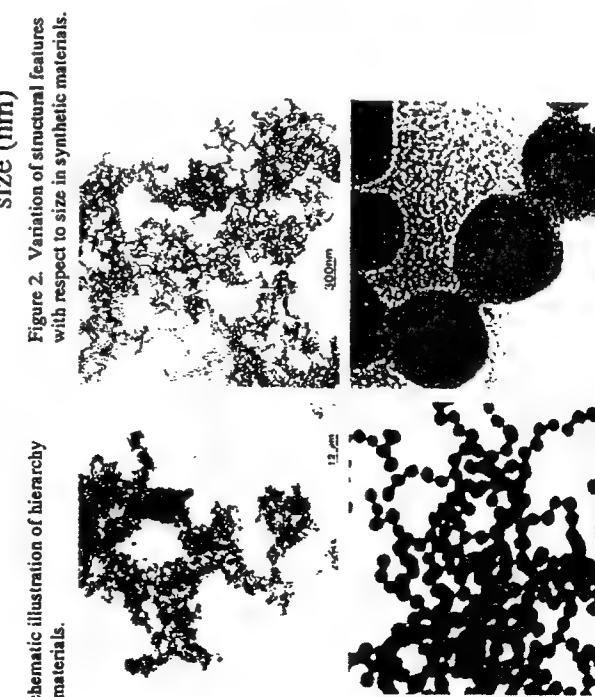


Figure 2. Variation of structural features with respect to size in synthetic materials.

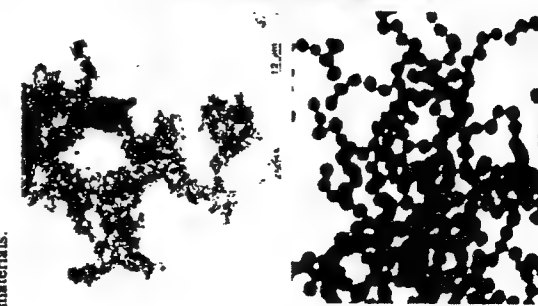


Figure 3. TEM images of colloidal gold particles suspended on a carbon film. At low magnification, only the shape of the cluster is apparent (a); at higher magnifications, smaller pores and the individual particles are revealed (b and c). Lattice and interface structures of particles are resolved at the highest magnification (d) (from Ref. 4(b)).

In order to discern the hierarchy in a given synthetic or biological structure, it is essential to use techniques that give structural information at many dimensional levels, from atomic to macro-scales. There are many imaging, spectroscopy, scattering, and diffraction techniques that provide structural information.¹⁵ Our objective in this paper is to provide a concise description of imaging techniques that provide the most direct visual investigation of the structures. We limit our discussion only to the length scale from atomic to micron dimensions since it is the architecture of this range that most directly influences the architecture and the properties of larger structures.

2. MICROSCOPIES TO INVESTIGATE HIERARCHY IN MATERIALS STRUCTURES

Two classes of microscopy techniques are used to image hierarchical structures (Table I). The first, surface imaging, uses radiation reflected from the surface of a sample or uses the interaction of a scanning tip with a surface. The technique, therefore, allows imaging of only surfaces or surface layers of materials. With the second class, internal structure imaging, primary radiation passes through and interacts with the matter and produces an image of the bulk structures, internal interfaces, lattice and microstructural defects, and second phase particles. In the following sections, these microscopy techniques are described in order of their capability to resolve hierarchical structures at increasingly smaller length scales.

Table I. A Summary of Microscopies

Microscopy	Resolution	Surface Imaging	Bulk Imaging	Wet
light optical (LOM)	0.5 μm, 50 nm (NFOM)	—	0.2 μm (CM)	Y
x-ray (XRM)	—	50 nm	Y	Y
electron	5 nm (1 nm) (SEM)	1.5 Å (FIREM)	N	N
field ion	<1 nm (FIM)	2 nm (ion probe)	N	N
scanning probe:				
atomic force (AFM)	0.5 nm (lateral), <1 Å (vertical)	—	Y	—
tunneling (STM)	1 Å (lateral), <<1 Å (vertical)	—	—	N

2.1 Light Optical Microscopy

Light optical microscopy (LOM) has traditionally been used to image surface structures of biological and physical materials at about the 500 nm resolution level.¹⁶ Figure 5 is an LOM image of a low carbon/low alloy steel showing the hierarchical structure in a synthetic material.¹⁷ The microstructure displays a single pre austenite grain (original phase) containing domains, or packets, of martensitic (product phase) that are rotated with respect to each other at 70° or 110°, i.e., four {111} variants of an austenite (face-centered cubic) crystal.¹⁸ Each packet is actually composed of lath-shaped martensite crystallites (parallelopiped-shaped crystallites are 0.5 μm thick, 2–5 μm wide, and 5–20 μm long) all in the same crystallographic orientation belonging to the same {111} austenite variant. Therefore, the image in Figure 5 actually shows three levels of hierarchy and compares well with the model described in Figure 1.

The resolution in LOM can be improved to several hundred nanometers in the transmission mode, for example in confocal microscopy (CM). In CM, the image is obtained by scanning a rastered sample with a laser beam focused to a certain depth that allows three-dimensional imaging of the sample with improved resolution since the light scattered from parts other than the portion of the specimen being illuminated is rejected from the optical system.¹⁹ In the newly developed near-field optical microscopy (NFOM) technique, the resolution is not limited by diffraction from the aperture, and, therefore, is not limited by the wavelength of light.²⁰ A focusing lens is not used in this technique; instead the light wave

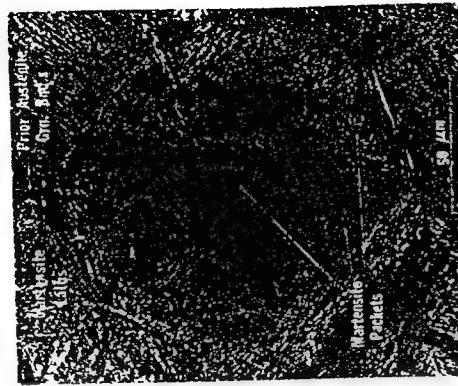


Figure 5. LOM image reveals hierarchy in the structure of a low-alloy steel (from Ref. 17).

probe that illuminates the sample is a geometrical projection of the aperture and not its Fourier transform, unlike the far-field case, and, thus, diffraction from the aperture is not allowed, so Abbe's diffraction limited resolution limitation does not apply. High spatial frequencies of the sample can be imaged, limited only by the size of the illuminating (imaging) aperture and by the material of which it is made (opacity). This pushes the limits of resolution in light optical imaging to 50 nm as demonstrated experimentally, and theoretically to levels less than 10 nm.²⁰

2.2 X-ray Microscopy

It is possible to increase resolution in the image beyond that provided by visible LOM using shorter wavelengths of x-rays. X-rays are also preferable to electrons because of their usefulness in studying biological materials in their natural states under wet or gaseous atmospheres. Because x-rays can neither be reflected nor refracted, focusing them is very difficult; magnified imaging, in the past, has been impossible. Recently, however, x-rays have been successfully focused using Fresnel zone plates to obtain magnified images at resolutions down to 500 Å in imaging or scanning x-ray microscopes.²¹ The zone plates are analogous to glass lenses in LOM and magnetic lenses in EM. To reduce radiation damage, soft x-rays (a 20–40 Å wavelength) are used and the sample is scanned with an x-ray probe,²¹ building the image one picture element at a time, which significantly reduces exposure of the sample to the beam, as in the scanning transmission electron microscope.²² The best resolution depends largely upon the finest zone spacing (now about several hundred angstroms) but is still limited to diffraction aberration from the rings.²³

2.3 Electron Microscopy

Electron microscopy imaging techniques can be divided into three major areas according to their specific image forming means. These three areas are described below with examples.

2.3.1 Scanning and Scanning Transmission Electron Microscopy

In scanning electron microscopy (SEM), a small electron probe formed by a convergent lens is scanned over the surface of a sample by the use of scan coils. The interaction of the incoming electrons with the sample produces secondary electrons from the surface layers that are then collected by a solid-state detector (Figure 6).²⁴ In SEM, the smaller the area scanned, the higher the magnification of the final image. In all scanning microscopy systems, the resolution depends on the effective size of the probe, i.e., the original size of the probe modified by the aberrations of the probe-forming lenses and the modifications that arise from sample-probe interactions. In terms of resolution, electrons at high voltages (20-30 kV) have wavelengths in the subangstrom range (fraction of an angstrom) and hence provide much better resolution than what can be achieved with LOM. Resolution in SEM, roughly defined by

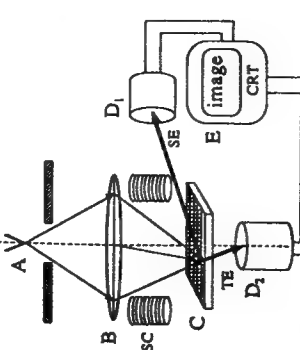


Figure 6. Simplified schematic of the electron microscope. A: electron source, B: objective lens, SC: scan coils, C: sample, TE: transmitted electrons, SE: secondary electrons, D₁ and D₂: detectors, and E: imaging system. The configuration ABCD₁ corresponds to SEM and ABCD₂ to scanning transmission electron microscopy (STEM) (the latter also to TEM if the illumination is parallel).

the size of the electron probe, can now be at the nanometer level, and the smallest point detectable on the surface of a sample typically falls between 50 and 100 Å. Smaller electron probes can be achieved in systems with a high-flux electron source (e.g., a field emission gun system) or a probe-forming lens with a low spherical aberration; resolution in the subnanometer range is not difficult to achieve.²⁵

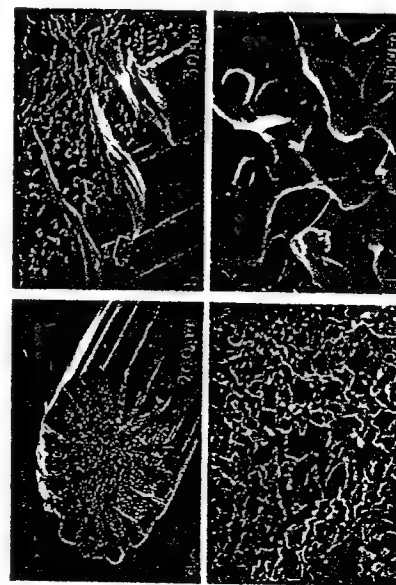


Figure 7. SEM images from fractured sea urchin spine reveal structural detail at different magnifications.

The primary benefit of SEM in imaging surfaces is its large depth of field, which allows examination of rough sample surfaces with large disparities. In LOM, by contrast, only optically polished surfaces can be focused and studied. The value of depth of field is illustrated in Figure 7, where a cross-sectional view of the fractured surface of a sea urchin spine is analyzed. Sea urchin spine is thought to be a single crystalline calcitic (rhombohedral CaCO_3) structure, and yet it has an elaborate microarchitecture. A general view of the fractured surface is seen in Figure 7(a), which illustrates a central hard and "spongy" structure surrounded by the 18 wedge-shaped columns radiating from the center. Both these columns and the spongy structure are seen in detail in Figure 7(c). Finally, in Figure 7(d), a higher magnification image shows the details of the fractured surface of calcite in the spongy portion of the sample, revealing a concoidal fracture.

In the scanning transmission electron microscope (STEM) mode,²² imaging is accomplished by scanning a small electron probe formed by a strong condenser lens over a sample, just as in SEM. In STEM, however, the sample is thin enough for electron transparency, so images are formed with detectors placed at appropriate positions along the optic axis. In the dark field (DF) mode, STEM can image a single heavy atom or cluster of atoms suspended on a thin amorphous film.²⁶ Atomic resolution images can be achieved with annular DF imaging, obtained using a sufficiently small ($\sim 2 \text{ \AA}$ in diameter) and highly coherent electron probe. This technique has been demonstrated to display atomic number contrast, and hence the ability to distinguish compositional fluctuations at high resolution due to the differences in the scattering powers of different atomic species constituting the sample.²⁶

2.3.2 Transmission Electron Microscopy

The transmission electron microscope is a multipurpose instrument that permits investigation of synthetic and biological samples in three modes of analysis: (i) imaging, (ii) diffraction, and (iii) spectroscopy.²⁷ The fundamental principle of TEM is the same as that of LOM. The primary electrons reach a thin sample in the parallel illumination mode, travel through the sample and are diffracted. A

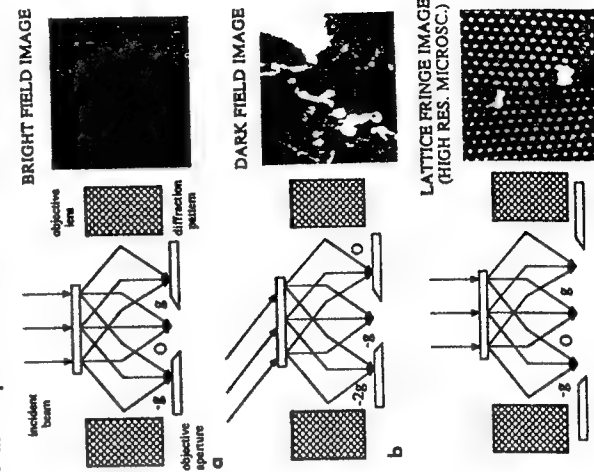


Figure 8. Schematic of TEM bright field (BF) (a), dark field (DF) (b), and high-resolution electron microscopy (HREM) (c) images with corresponding experimental images (from Ref. 28).

magnetic lens (called objective lens, analogous to the glass objective lens in the LOM) focuses the scattered electrons to form the diffraction pattern and the image. In the imaging mode, conventional TEM (CTEM) limits the formation of the image to only one of the diffracted beams. The detail in a CTEM image is produced by many contrast mechanisms arising from amplitude variations in a single electron wave,²⁸ which are introduced because of the interaction of the incoming wave with the sample. The elastically scattered transmitted and diffracted beams are used for bright field (BF) and dark field (DF), respectively. CTEM techniques are used in many imaging studies in synthetic materials and biological tissues to investigate morphology and distribution of the constituent phases at an image resolution of about several nanometers. Figures 8(a and b) show BF and DF images where dislocations are revealed in the matrix of Al.²⁸

In the case of high-resolution TEM (HREM), imaging is performed using many beams, including the central beam (Figure 8(c)).²⁹ The image formed at the back focal plane of the objective lens is an interference pattern, which under ideal circumstances (i.e., small spherical aberration of the objective lens and its defocus) may represent the projected potential of an ultrathin (<10 nm) crystalline sample in the particular orientation in which it is observed.³⁰ Therefore, HREM provides direct imaging of crystalline structures to investigate their atomic configurations at the site of defects, such as dislocations, interfaces, and boundaries³¹ and their long-range ordered structures.³² For instance, Figure 8(c) shows an image of a low-angle boundary in a biogenic aragonitic CaCO₃ crystal where dots represent atomic columns in the structure in the reverse contrast. Edge dislocations at the boundary and the bending of atomic planes near the core of the dislocations are clearly visible.²⁸

In the diffraction mode, diffraction patterns form at the back focal plane of the objective lens through either parallel illumination or convergent illumination of the sample by the beam.²⁷ In the former case, a spot pattern forms, which is generally used to identify crystallographic zone axes and lattice parameters of an examined crystalline sample. The sampled area that gives rise to the diffraction pattern is selected by a field limiting aperture and can be as small as 0.5 μm in diameter. With convergent beam electron diffraction (CBED), the sampled area can be as small as 1 nm, making the CBED technique the highest spatial resolution diffraction technique available.

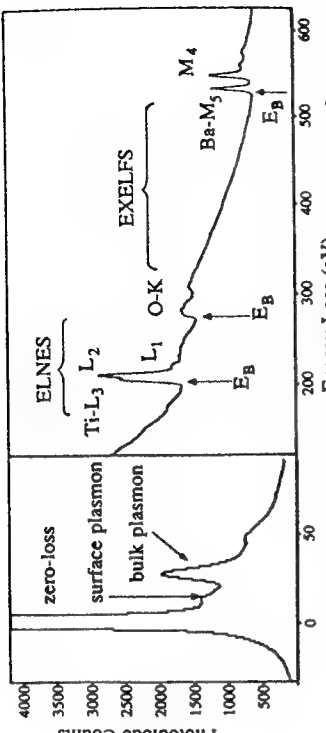


Figure 10. A characteristic EEL spectrum illustrates various regions used for spectroscopic analysis from a sample of BaTiO₃ (spectrum was taken with a parallel detection system at 200 kV).

Due to the finite convergence of the beam, diffracted beams in this case form disks instead of spots, the centers of which are located at the Bragg positions.³³ Because of the interaction of the upper Laue layers, diffraction lines form in the central and diffracted beams (Figure 9). The position of these so-called high-order Laue zone (HOLZ) lines or their absence provides information about the constituent atoms in the unit cell, the unit cell geometry and its lattice parameters, symmetry groups (point and space groups),^{34,35} and internal stresses; CBED, therefore, can be used for analysis of crystalline structures at varying length scales.³³

Spectroscopy, the third mode of operation of TEM, includes energy dispersive x-ray spectroscopy (EDS) and electron energy loss spectroscopy (EELS).³⁶ When an incoming electron probe strikes a TEM sample, it produces x-rays with specific energies characteristic of the constituent elements in the sample. Quantification of these x-rays can provide compositional analysis of the sample from areas defined by the probe diameter, areas as small as a few nanometers.³⁷ Low energy x-rays may be trapped at the window of the x-ray detectors and, thus, limit the compositional analysis to elements with atomic number Z > 10, i.e., Na and up.

Electrons passing through the sample will lose some of their initial energy through beam-sample interaction, including the process of x-ray production.³⁸ In EELS, these electrons are examined with respect to their loss in energy, as plotted in Figure 10. The sharp peak at the "zero" position corresponds to those electrons that did not lose any of their energy and corresponds to the zero-loss peak. The low-loss energy region, up to 50 eV, corresponds to the plasmon excitation, including surface and bulk plasmon. From the positions of these peaks, plasmon energies or frequencies can be determined, allowing the estimation of, for example, complex dielectric function. At high losses, edges appear due to inner shell excitations, whose threshold values correspond to the binding energies of the electrons of the K, L, etc., shells (K-edges, L_{2,3} edges). In addition, the shape of the near-edge structure represents the density of states for the empty orbitals and therefore the oxidation state of the element (i.e., near-edge fine structure analysis, ELNES).³⁹ Beyond about 50 eV from the threshold, fine structure in the tail of an edge gives variations similar those found in soft x-ray absorption edges.⁴⁰ This means that the information from the fine structure can be used to deduce near-neighbor interactions and short-range order (e.g., coordination number) that are similar to extended x-ray fine structure (EXELFS).⁴⁰ Such an analysis in EELS is called extended energy loss fine structure analysis (EXELFS).⁴¹ In the sense of providing bonding and electronic information of the structure with or without long-range order (i.e., crystalline or amorphous samples) the EELS technique permits hierarchical structural analysis at the lower end of the structural spectrum.



Figure 9. CBED pattern recorded in [001] zone axis orientation from β-SiC (hexagonal) shows details of crystallographic features and symmetries in the zero and higher order Laue zone layers (courtesy of G. H. Kim).

2.4 Field Ion Microscopy

The formation of an image in the field ion microscope (FIM) is based on the tunneling principle and does not require an image-forming lens.⁴² When an imaging gas, He, for example, is ionized (at 10^{-3} torr) near a positively charged, cryogenically cooled tip of a specimen at a certain voltage, ions are accelerated radially onto a channel plate/fluorescent screen assembly to form an image, which is the magnified projection of the tip. The mechanism by which the imaging gas is ionized is known as field ionization and is based on the electron tunneling process.⁴² At the atomic protrusions on the tip, local field strength is raised, which preferentially ionizes atoms at these positions, and corresponding bright spots form the image. The visible image formed on the screen is a projection of the sample tip and roughly resembles the stereographic projection of the crystalline sample in the direction of the specimen axis.⁴³ The magnification (M) on the screen is determined by the ratio of the distance between the tip and the screen (L) to the radius of the tip (R); for example, for $R = 5 \text{ nm}$ and $L = 5 \text{ cm}$, then $M = 10^6$. When the tip radius is less than 500 \AA , and the tip is kept at the temperature of liquid He, the atomic structure of a conductive sample becomes resolvable. An FIM image consists of an array of bright spots, each of which corresponds to an atom; the atoms are lined at the periphery of concentric terraces centered around crystallographic axes that make up the tip surface. When the temperature of the tip is low (<10K) and imaging gas atoms of small diameter are used (e.g., He), then resolution as small as 2 \AA can be achieved.⁴⁴

2.5 Scanning Probe Microscopy

The scanning probe microscopy system (SPM) uses a probe tip, held by a piezoelectric cantilever, scanned above the sample.⁴⁵ Either the tunneling current between a conductive sample and the tip (in the case of scanning tunneling microscopy (STM))⁴⁵ or the deflection of the cantilever caused by the forces acting between the sample and the tip as it scans above the sample (in the case of atomic force microscopy (AFM))⁴⁶ is measured as a function of the distance traveled by the probe in the x and y directions. Measurement of the current or the deflection is sufficiently accurate to resolve atomic or molecular corrugations on the surface of the sample and allow topographical analysis of the sample at the atomic resolution. The interaction (in terms of tunneling current or atomic force) between the probe tip and the sample varies exponentially with distance between the sample and the very extreme point on the

probe tip; in the STM, for example, the atom at the extreme point of the probe tip allows the tunneling current to pass through. Spatial confinement of the tunneling current into a small cross section allows this technique to image the electron cloud on the surface of the sample in the form of contours around each atom. The resolution in the image, which is only a surface or subsurface image, is defined both vertically and laterally on the plane of the sample. Under favorable experimental conditions, lateral resolution is less than the diameter of the atoms on the surface and easily reaches a fraction of an angstrom. The STM technique has been successfully applied to conductive samples, such as metals and semiconductors but, despite great effort, has not yet successfully imaged biological membranes or protein tissues.^{45,47}

In AFM, the interaction forces between the tip material and the sample thin film or substrate can be measured. These forces, attractive or repulsive, may be as small as a few nanonewtons, and the sample may or may not be an electrical conductor.^{46,48} The sample can thus be imaged in its natural state, biological samples, for example, in an aqueous environment. In the case of repulsive forces, the tip actually touches the surface and can trace over the atoms without damaging the surface of the sample. In AFM, unlike STM, the sample moves with respect to a fixed force sensor containing the tip. The deflection of the cantilever, hence the force between the tip and the sample, can be measured by the aid of a laser beam that is reflected to a detector (Figure 11). Like STM, under favorable conditions (flat crystalline surfaces of graphite, mica, or CaCO_3 , for example) AFM images with atomic corrugations can be produced. Atomic resolution images of more complex surfaces, however, including biological membranes or protein complexes such as DNA, have not yet been reproducibly imaged.⁴⁸

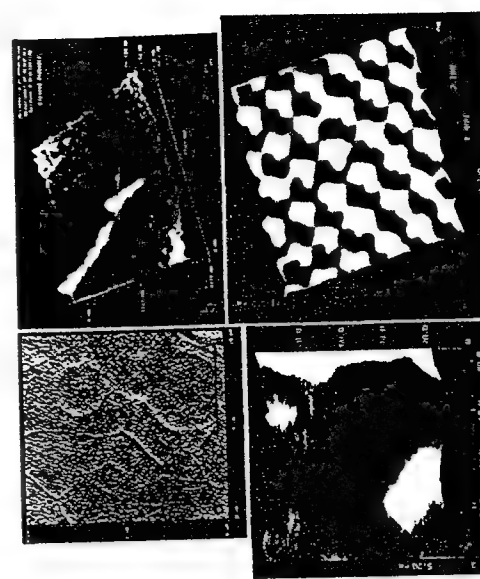


Figure 12. AFM images (a to c) show details of the structure on the cleaved surface of the nacre of a red abalone recorded in water. (d) AFM image of calcite reveals atomic packing on the basal plane (courtesy of Kevin Kjolar, Digital Instruments).

In summary, the usefulness of AFM is threefold: (i) no limitation on samples, (ii) imaging under various environmental conditions, and (iii) a wide range of magnification. The example given in Figure 12 illustrates this point with images recorded in water from the cleaved surface of the nacre of red abalone at increasing higher magnifications. In Figure 12(e), a scan over the surface covering an area $10 \mu\text{m} \times 10 \mu\text{m}$ reveals multi-edged CaCO_3 (aragonite) platelets in a face-on configuration separated by

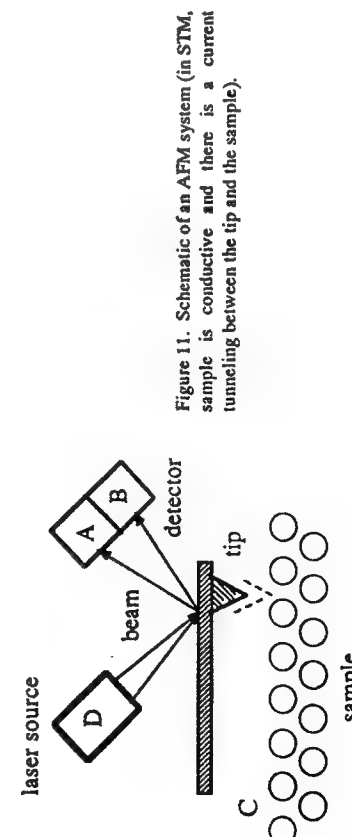


Figure 11. Schematic of an AFM system (in STM, sample is conductive and there is a current tunneling between the tip and the sample).

grooves of organic matrix. In Figure 12(b), a scan of $2 \mu\text{m} \times 2 \mu\text{m}$ reveals that the organic matrix that separates each layer of platelets and over which the cleavage took place is still attached to the surface. Note that the surface is rough and decorated with semispherical beads of organic matrix probably due to deformation during cleavage. In the image, however, the interfaces between the platelets are clearly seen, significantly more deformed than the organic matrix in the interior of the platelets. At higher magnification, or in a smaller scan of $80 \text{ nm} \times 80 \text{ nm}$, the details on the surfaces of the organic beads can be seen in Figure 12(c). Although there is regular image variation on the organic surface, which may be due to the original conformation of the proteins in the organic matrix, the image is not detailed enough to confirm any kind of regular structure. Finally, in Figure 12(d) the atomic resolution in the image of synthetic CaCO_3 (calcite) is sufficient to clearly reveal the lattice of the rhombohedral structure on the basal plane.

3. CONCLUSIONS

Many scattering, spectroscopy, and imaging techniques can provide valuable information, but no single technique is capable of providing all the hierarchical structural information from the atomic to the macro scale. Among the structural characterization techniques, however, the information gathered by TEM may be the most comprehensive. The TEM instrument can simultaneously provide information at all modes of analysis, including imaging, diffraction, and spectroscopy, all from the same region with spatial resolutions at the subnanometer and atomic levels. A combination of techniques from the TEM can provide information about the atomic species (CBED, EELS, STEM, HREM); atomic bonding and oxidation states (ELNES); unit cell and its dimensions (HREM, CBED); short-range order (EXELFS); long-range order (CBED and HREM); and defect and morphological analysis (CTEM). TEM, therefore, can truly provide hierarchical information from organic and inorganic samples. TEM, however, is not without limitations, the major ones being that since it is a high vacuum technique, samples in the "wet" state cannot be observed, and because of highly energetic primary electrons, radiation damage can be a problem (especially for biological and amorphous materials). So it is clear that for a comprehensive analysis of structures of materials an arsenal of techniques is required, from light, x-ray, and electron to scanning probe microscopes.

ACKNOWLEDGEMENTS

This work was performed under the sponsorship of the Air Force Office of Scientific Research under Grant Numbers AFOSR-91-0281 and AFOSR-91-0040.

REFERENCES

- C. S. Smith, "Structural Hierarchy in Science, Art, and History," in *Aesthetics in Science*, J. Wechsler (ed.) (MIT Press, Cambridge, Massachusetts, 1978), pp. 9-53.
- F. A. Kroger, *The Chemistry of Imperfect Crystals*, Vol. 2 (North-Holland, Amsterdam, 1974).
- I. A. Aksay, "Molecular and Colloidal Engineering of Ceramics," *Ceramics International*, 17 [5] 267-74 (1991); (b) M. Sarikaya, "Atomic Resolution Microscopies in Materials," in *Advanced Characterization techniques in Ceramics*, *Ceramic Transactions*, Vol. 5 (American Ceramic Society, Westerville, Ohio, 1990), pp. 247-86.
- C. K. Mathews and K. E. van Holde, *Biochemistry* (Benjamin/Cummins Publ., Redwood City, California, 1990).
- E. Baer, J. J. Cassidy, and A. Hiltner, "Hierarchical Structure of Collagen and Its Relationship to the Physical Properties of Tendon," Chapter 9 in *Collagen: Biochemistry and Biomechanics*, Vol. II, edited by M. E. Nini (CRC Press, Boca Raton, Florida, 1988), pp. 177-99.
- M. J. Glimcher, "On the Form and Function of Bone; from Molecules to Organs," *The Chemistry and Function of Mineralized Tissues*, edited by A. Veis (Elsevier, Amsterdam, 1981), pp. 617-73.
- S. Weiner and W. Traub, "Mineralized Tendon, Bone, and Dentin," *Connect. Tissue Res.*, 27 [2-3] 86 (1992).
- H. A. Lowenstein and S. Weiner, *On Biominerilization* (Oxford University Press, New York, 1989).
- J. Liu, M. Sarikaya, and I. A. Aksay, "A Hierarchically Structured Model Composite: A TEM Study of the Hard Tissue of Red Abalone," this volume.
- J. D. Currey, "Biological Composites," *J. Mater. Edu.*, 9 [1-2] 118-296 (1987).
- A. P. Jackson, J. F. V. Vincent, and R. M. Turner, "The Mechanical Design of Nacre," *Proc. Roy. Soc., London*, B234, 415-40 (1988).
- M. Sarikaya and I. A. Aksay, "Nacre of Abalone Shell: A Natural Multifunctional Nanoamidated Ceramic-Polymer Composite Material," Chapter 1 in *Structure, Cellular Synthesis, and Assembly of Biopolymers*, edited by S. Cuse (Springer-Verlag, New York, 1992).
- J. Liu, M. Sarikaya, and I. A. Aksay, unpublished work.
- J. P. Sibilia, *Materials Characterization and Chemical Analysis* (VCH, New York, 1988).
- R. Hooke, *Micrographia* (Royal Society, London, 1665).
- M. Sarikaya, Ph.D. Thesis (University of California, Berkeley, LBL Rep. # 15211, 1982).
- (a) M. Sarikaya and G. Thomas, "Lath Martensites in Low Carbon Steels," *J. Phys., Colloid* (4) supp. 12, Tome 43, C4-563-68 (1982); (b) M. Sarikaya, H. Togushige, and G. Thomas, "Lath Martensite and Bainite in Low Alloy Steels," in *Proc. of Int'l. Conf. on Martensitic Transformations* (Japan Institute of Metals, Tokyo, 1986), pp. 613-18.
- The Handbook of Biological Confocal Microscopy*, edited by J. Pawley (IMR, Madison, Wisconsin, 1989).
- M. Isaacson, "Resolution in Near-Field Optical Microscopy," in *Resolution in the Microscope, Ultramicroscopy*, special issue, edited by M. Sarikaya, in press (1992).
- M. Howells, J. Kirz, and D. Sayre, "X-ray Microscopes," *Sci. Amer.*, 264 [2] 88-94 (1991).

22. A. V. Crewe, J. P. Langmore, and M. Isaacson, "Resolution and Contrast in the Scanning Transmission Electron Microscope," Chapter 4 in *Physical Aspects of Electron Microscopy and Microbeam Analysis*, edited by B. M. Siegel and D. K. Beaman (Wiley, New York, 1975), pp. 47-62.
23. C. Jacobsen, J. Kirz, and S. Williams, "Resolution in X-ray Microscopes," in *Resolution in the Microscope, Ultramicroscopy*, special issue, edited by M. Sarikaya, in press (1992).
24. *Practical Scanning Electron Microscopy: Electron and Ion Microanalysis*, J. I. Goldstein and edited by H. Yakowitz (Plenum, New York, 1975).
25. D. C. Joy and J. Pawley, "Resolution in the SEM," in *Resolution in the Microscope, Ultramicroscopy*, special issue, edited by M. Sarikaya, in press (1992).
26. S. J. Pennycook, "Z-Contrast STEM for Materials Science," *Ultramicroscopy*, **30**, 58-69 (1989).
27. L. Reimer, *Transmission Electron Microscopy* (Springer-Verlag, Berlin, 1984).
28. M. Sarikaya and J. M. Howie, "Resolution in CTEM," in *Resolution in the Microscope, Ultramicroscopy*, special issue, edited by M. Sarikaya, in press (1992).
29. J. C. H. Spence, *Experimental High Resolution Electron Microscopy* (Oxford University Press, Oxford, 1986).
30. M. A. O'Keeffe, "Resolution in High Resolution Electron Microscopy," in *Resolution in the Microscope, Ultramicroscopy*, special issue, edited by M. Sarikaya, in press (1992).
31. O. L. Krivanek, "High Resolution Imaging of Grain Boundaries and Interfaces," *Chemica Scripta*, **14**, 213-20 (1979).
32. J. M. Cowley and D. J. Smith, "High Resolution Transmission Electron Microscopy," *Acta Cryst.*, **A 43**, 739-48 (1989).
33. J. W. Steeds, "Convergent Beam Electron Diffraction," in *Introduction to Analytical Electron Microscopy*, edited by J. J. Hen, J. I. Goldstein, and D. C. Joy (Plenum, New York, 1979), pp. 387-422.
34. M. Tanaka, R. Sito, and H. Sekii, "Point Group Determination by Convergent Beam Electron Diffraction," *Acta Cryst.*, **A39**, 357-68 (1983).
35. J. W. Steeds and R. Vincent, "Use of High Symmetry Zone Axis in Electron Diffraction in Determining Crystal Point and Space Groups," *J. App. Cryst.*, **16**, 317-24 (1983).
36. J. I. Goldstein, "Principles of Thin Film Microanalysis," Chapter 3, pp. 83-120, and N. Zaluzec, "Quantitative X-ray Microanalysis: Instrumental Considerations and Applications to Materials Science," Chapter 4, pp. 121-68, in *Introduction to Analytical Electron Microscopy*, edited by J. J. Hen, J. I. Goldstein, and D. C. Joy (Plenum, New York, 1979).
37. D. B. Williams et al., "Resolution in Energy Dispersive X-ray Spectroscopy," in *Resolution in the Microscope, Ultramicroscopy*, edited by special issue, M. Sarikaya, in press (1992).
38. R. F. Egerton, *Electron Energy Loss Spectroscopy in the Electron Microscope* (Plenum, New York, 1986).
39. R. Brydson, "Interpretation of Near Edge Structure in the Electron Energy Loss Spectrum," *EMSA Bulletin*, **21** [2] 57-67 (1991).
40. E. A. Stern and S. M. Heald, "Basic Principles and Applications of EXAFS," Chapter 10 in *Handbook on Synchrotron Radiation*, Vol. 1, edited by E. E. Koch (North-Holland, Amsterdam, 1983).
41. S. Chilag, D. A. Johnson, and E. A. Stern, "Extended Energy Loss Fine Structure Studies in the Electron Microscope," in *EXAFS Spectroscopy: Techniques and Applications*, edited by F. K. Teo and D. C. Joy (Plenum, New York, 1981), pp. 241-54.
42. R. H. Good and E. W. Muller, "Field Emission," in *Handbuch der physik*, Vol. 21 (Springer-Verlag, Berlin, 1956), pp. 176-231.
43. M. K. Miller and G. D. W. Smith, *Atom Probe Microanalysis: Principles and Applications to Materials Research* (Materials Research Society, Pittsburgh, Pennsylvania, 1989).
44. C. R. M. Grovenor et al., "Ultrahigh-Resolution Chemical Analysis by Field-Ion Microscopy, Atom Probe, and Position Sensitive Atom Probe Techniques," in *Resolution in the Microscope, Ultramicroscopy*, special issue, edited by M. Sarikaya, in press (1992).
45. G. Binnig and H. Rohrer, "Scanning Tunneling Microscopy," *Helv. Phys. Acta*, **55**, 726-35 (1992).
46. G. Binnig, C. Quate, and C. Gerber, "Atomic Force Microscope," *Phys. Rev. Lett.*, **56**, 930-32 (1986).
47. J. A. Givachenko, "The Tunneling Microscope: A New Look at the Atomic World," *Science*, **232**, 48-53 (1986).
48. P. K. Hansma, V. B. Ellings, O. Marti, and C. E. Bracker, "Scanning Tunneling Microscopy and Atomic Tunneling Microscopy: Applications to Biology and Technology," *Science*, **242**, 209-16 (1988).

"Evolution of Resolution in Microscopy,"

M. Sarikaya

Ultramicroscopy

(Vol. 47 [1-3] pp. 1-306, 1992)

NORTH-HOLLAND
PHYSICS
PUBLISHING



Evolution of resolution in microscopy

Mehmet Sarikaya

*Department of Materials Science and Engineering and Washington Technology Center, University of Washington,
Seattle, WA 98195, USA*

Received at Editorial Office 26 June 1992

This paper discusses resolution, or the capability of an optical imaging instrument to discern the closest distance between points in an image, in terms of its conceptual evolution. The original definition of resolution in telescope and light-optical microscope is given, followed by a summary of early attempts to achieve resolution limits in the transmission electron microscope, the effects of lens aberrations and defocusing, and the concepts of contrast transfer. The second section of the paper addresses types of resolution in microscopies that use a probe (light, electron, or X-ray probe), those that use ion and electron tunneling (field-ion microscopy and scanning tunneling microscopies), and those that measure force exerted on a tip (atomic force microscopy).

Reprinted from ULTRAMICROSCOPY

Evolution of resolution in microscopy

Mehmet Sarikaya

*Department of Materials Science and Engineering and Washington Technology Center, University of Washington,
Seattle, WA 98195, USA*

Received at Editorial Office 26 June 1992

This paper discusses resolution, or the capability of an optical imaging instrument to discern the closest distance between points in an image, in terms of its conceptual evolution. The original definition of resolution in telescope and light-optical microscope is given, followed by a summary of early attempts to achieve resolution limits in the transmission electron microscope, the effects of lens aberrations and defocusing, and the concepts of contrast transfer. The second section of the paper addresses types of resolution in microscopies that use a probe (light, electron, or X-ray probe), those that use ion and electron tunneling (field-ion microscopy and scanning tunneling microscopies), and those that measure force exerted on a tip (atomic force microscopy).

1. Historical background

Since the day Galilei discovered the telescope [1] and Hooke discovered the light-optical microscope [2], these instruments have been used to examine objects increasingly distant in space and smaller in size of a given sample, respectively. At the same time, researchers have sought to improve the capability of the instrument to resolve closely spaced objects, those farthest away with the telescope, those smallest in size with the microscope [1-5]. Defining spatial resolution and improving it remain major objectives in the present time, along with improvements in the imaging instruments themselves.

Scientists have debated both the theoretical definition of resolution and the practical ways of measuring its predicted values for centuries. With the discovery of new microscopy techniques—i.e. those that do not use a focusing lens, which otherwise constitutes a major part of traditional imaging systems—the issue of what resolution actually is in a given instrument has become even more pressing. The object points seen with these new imaging systems are now in the atomic dimension. It should be obvious that the interpreta-

tion of the image detail, or description of what has actually been seen, depends largely on the smallest and closest objects that can be seen in the image, along with the contrast generated by these object points. In the following sections, we briefly summarize how the concept of resolution and its measurement have evolved over the years, emphasizing the historical perspective. In touching upon a number of microscopy techniques in this paper, we hope to set the stage for the more rigorous discussions that follow in this special issue.

2. Resolution in imaging

2.1. Light-optical instruments

In the broadest terms, the resolution of an image formed in an optical instrument is defined by the smallest distinguishable distance between two closely spaced features in the sample. Each point source in the object, absorbing or self-luminous, produces a corresponding image point at the focal plane of an objective lens. Based on the wave theory [3], each image point has an

intensity distribution given approximately by a Gaussian function and consists of a central bright disk surrounded by alternating dark and bright rings of eventually decreasing intensity (Airy disks [6]), shown schematically in fig. 1a. The angular radius of the central disk is given by:

$$\theta = 1.2197 \lambda / 2R, \quad (1)$$

where λ is wavelength of light and $2R$ is the diameter of the objective aperture. Contrast in the image, then, arises from the differences in the

magnitude of the intensities within these disks, and the information in the image is limited by the amount of overlap between them (fig. 1b). The ability to distinguish between two closely spaced object points is, therefore, limited by the ability to distinguish intensity maxima, in the case of luminous, and minima, in the case of absorbing points, in the Airy disks.

If we consider two object points separated by distance d , the centers of their diffraction disks will be a distance Md apart, where M is the

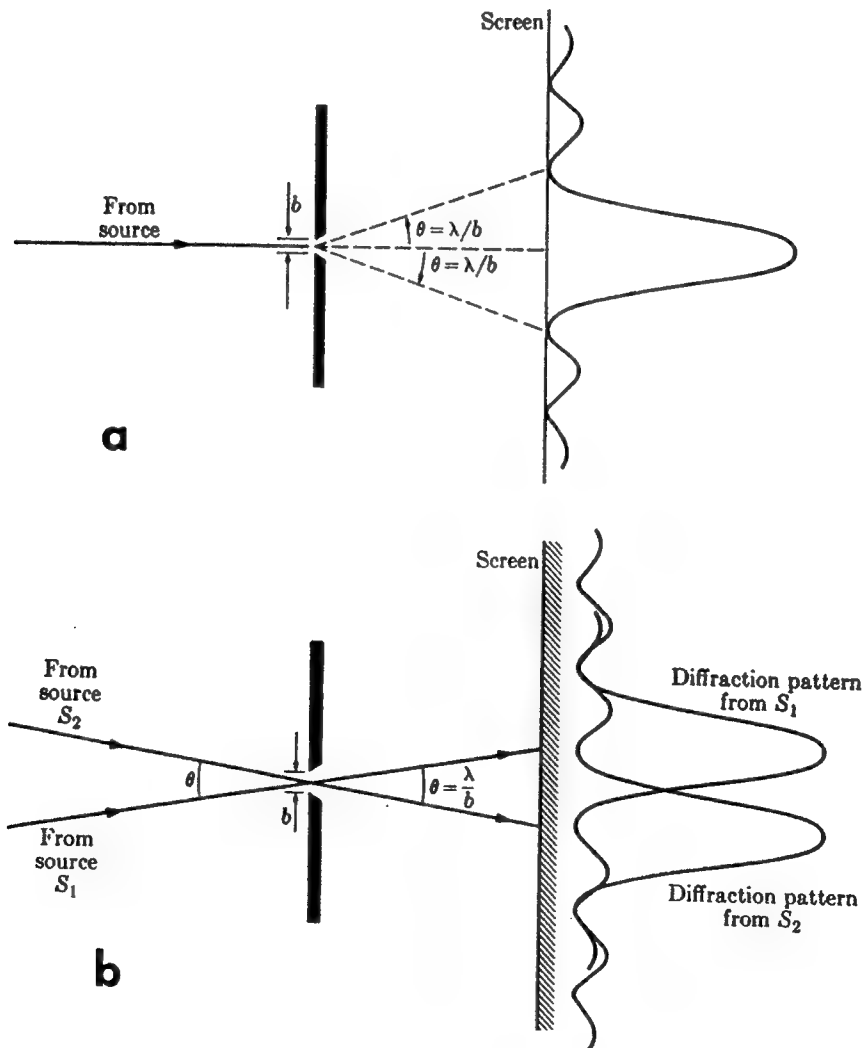


Fig. 1. (a) Angle subtended by the central intensity peak of the diffraction pattern of a single slit. (b) Rayleigh's criterion for resolving power of a slit.

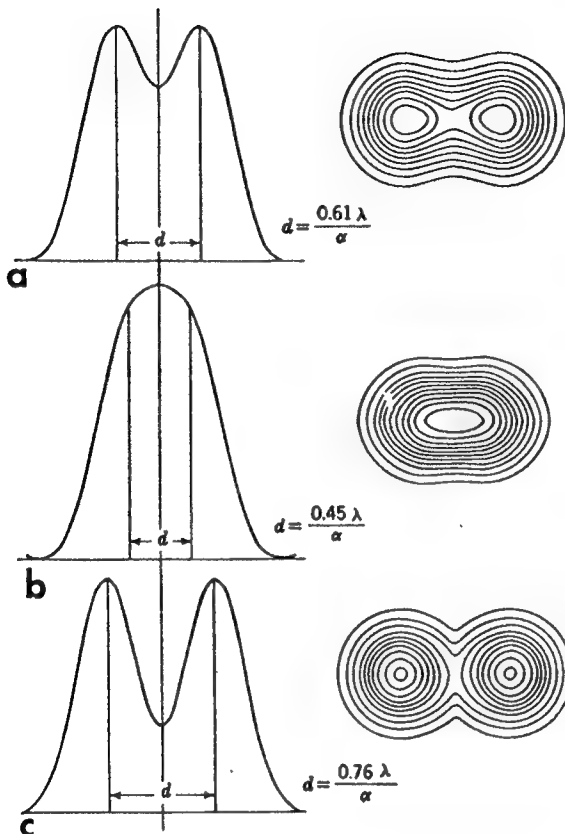


Fig. 2. (a)-(c) Intensity distribution in an aberration-free image of two neighboring point sources (from ref. [7]).

magnification (fig. 2). If Md is greater than the distance between the center and the first minimum (or zero) of the diffraction figure, a dip will appear between the two intensity peaks, allowing their separation (fig. 2a). If, however, the disks are closer together, the two diffraction figures will appear to coalesce since the maximum of the intensity would fall halfway between the centers of two diffraction patterns (fig. 2b) and the dip in intensity will eventually disappear. The limit of resolution, then, can arbitrarily be defined as the point at which the peak of one diffraction figure coincides with the first minimum of the other (fig. 2c). This establishes the smallest separation between two points of the object that will still allow the observer to distinguish the two points as separate entities [8].

If α is the half angle subtended by the aperture at the object, i.e., the objective aperture, and n_i and n_0 are indexes of refraction of the image space and the medium in which the object is placed, respectively, then the theorem of Helmholtz-Lagrange requires that:

$$n_0 \sin \alpha = M n_i r \alpha / b. \quad (2)$$

The condition under which the diffraction maximum for one point coincides with the first minimum for the other takes the form:

$$(2\pi M d / \lambda_i) (n_0 \sin \alpha / n_i M) = 1.22 \pi, \quad (3)$$

or

$$d = 0.61 \lambda_0 / \sin \alpha, \quad (4)$$

where $\lambda_0 = (n_i / n_0) \lambda_i$ and λ_i is the wavelength of the imaging radiation at the object.

The effective angular aperture of the imaging beams is determined not by the size of the aperture but by the degree of scattering in the object. If a coherent radiation of any kind strikes a periodic structure, such as a line grating with line separation d , some of the incident radiation will be scattered producing diffracted beams. Abbe's theory of the imaging of non-self-luminous objects by the microscope tells us that in addition to the primary beam at least one of the two diffracted beams must pass through the objective lens to produce an image of the structure. This image is the result of the interference of the direct beam with the diffracted beams in the image plane. The angles d which the diffracted beams form with the primary beam are given by $\sin \theta = n\lambda/d$; the condition that at least one diffracted beam be admitted in addition to the central beam takes the form:

$$d \geq \lambda / \sin \alpha, \quad \text{for illumination parallel to the axis;} \quad (5a)$$

$$d \geq \lambda / 2 \sin \alpha, \quad \text{for oblique illumination.} \quad (5b)$$

These relationships typically define the resolving power of the microscope for non-luminous objects and the conclusion is essentially the same as for the imaging of self-luminous point objects discussed above [9].

For the simplest example of diffraction phenomena, we take a very long and narrow rectangular slit (ignoring the effect at the ends) with a normal incident wave of wavelength λ (fig. 1b). According to Huygens' principle, when the incident wave falls onto the slit, all points of its plane become secondary sources of waves, emitting new (diffracted) waves. At certain angles θ with respect to the incidence, the intensity becomes zero according to $b \sin \theta = n\lambda$, $n \neq 0$ ($n = 0$ is the maximum illumination), where b is the width of the slit, i.e., $\sin \theta = \pm \lambda/b, \pm 2\lambda/b, \pm 3\lambda/b$, with decreasing intensity maxima. The resolving power of a rectangular slit, defined by Rayleigh, is the minimum angle subtended by two incident waves coming from two distant points of self-luminous sources which permit their respective diffraction patterns to be distinguished [9]. As shown in fig. 1b, the sources S_1 and S_2 form an angle θ , and the waves pass through the same slit reducing superimposed diffraction patterns. The patterns become distinguishable when the central maximum of one falls on the first zero on either side of the central maximum of the other, for which $\theta = \lambda/\beta$, which gives the resolving power.

The diffraction pattern produced by a circular aperture of radius R consists of a bright disk surrounded by alternating dark and bright rings of decreasing intensity. As in the case of the rectangular slit, the angle corresponding to the first dark ring is given by:

$$2R \sin \theta/\lambda = 1.21987$$

or

$$\sin \theta \sim \theta \sim 1.22\lambda/2R. \quad (6)$$

Here the angle θ , the angle subtended by the image, defines the resolution, a circumstance extensively discussed in the literature as the resolving power of telescopes [5,9].

The magnification of the optical instrument is limited by the resolving power of the objective lens and the eye of the observer. According to fig. 3, the resolving power of the eye is about 0.2 mm, or the angle subtended by the image $\beta = 0.02 \text{ cm}/25 \text{ cm} = 4 \times 10^{-4} \text{ rad} = 1.36''$. For an objective with a diameter D , the maximum useful magnification, M , for a telescope would be:

$$M = \beta/\theta, \\ M = 4 \times 10^{-4} D / 1.22\lambda = 3.3 \times 10^{-4} D/\lambda. \quad (7)$$

Larger magnification would result in either a smaller value for α , which would mean less detail in the image, or a larger value of β , which essentially does not reveal any new detail in the image. For light, $\lambda \approx 500 \text{ nm}$ and $M \approx 660D$, where D is measured in meters. In the new Keck telescope built at Mauna Kea in Hawaii, for example, $D = 10 \text{ m}$; for a magnification of about 660, the resolving power is 10^{-3} seconds of arc, sufficient to resolve a double-star with the same angular separation (assuming no scattering in the atmosphere, which actually is true only for the Hubble telescope [10]).

Similarly, in the light-optical microscope, the useful magnification is also limited by the resolution; from eq. (4):

$$d = \lambda/2n \sin \theta, \quad (8)$$

where λ and θ have the usual meaning and n is the index of refraction of the medium in which the object is immersed. In general ($2n \sin \theta$) is

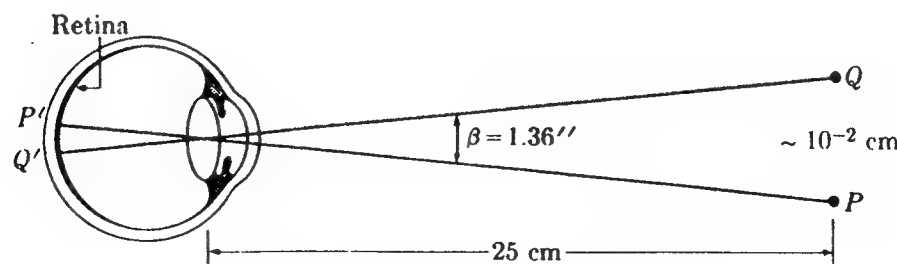


Fig. 3. Resolving power of the human eye.

about 3, so that $d = \lambda/3$. The maximum magnification, from $M = d_e/d_m = 10^{-2}/(\lambda/3)$, therefore, is $\sim 600 \times$, similar to that of a telescope [9].

2.2. Transmission electron microscopy

After the discovery of electrons [11] and theoretical [12,13] and experimental [14,15] verification of their wave nature and fundamental understanding of wave propagation through matter [16], it was realized that magnetic or electrostatic lenses could be used to focus electrons diffracted from thin transparent samples [17]. Based on the principles set forth by Abbe [8] on the wavelength diffraction limitation, i.e., that resolution is proportional to the wavelength of radiation used, electron microscopes were developed to increase resolution based on the shortness of electron wavelength. Until the introduction of electron microscopes, however, the lenses used in light-optical microscopes were nearly perfect, and the images were aberration-free. It was realized [18] that wave static aberration (i.e., spherical aberration) limits the size of the objective aperture, α , that can be used in the electron microscope. The rays that originate from a single point on the object and then pass through the lens would be focused at different locations along the optic axis before and after the image plane, creating a disc of confusion. The diameter, d_s , of the disc of confusion is given by:

$$d_s = C_s f \alpha^3, \quad (9)$$

where C_s is called the spherical aberration coefficient and f is the focal length in mm. In this relationship, the disc of confusion, which provides no structural information but is merely an optical confusion, has a cubic relationship with α . As a result, large objective apertures significantly worsen the possibility of observing image detail. From eqs. (1) and (2) the optimum value of α is then given by:

$$\alpha_{\text{opt}} = (1/2C_s f)^{1/4}. \quad (10)$$

Substituting this value in eq. (1), the resolution value, δ , in the electron microscope becomes:

$$\delta = 1/q = 0.67 C_s^{1/4} \lambda^{3/4}. \quad (11)$$

As in the case of light-optical microscopy, there is a direct relationship between δ and λ , but in electron microscopy a convolution of aberration coefficient decreases the ability to distinguish image detail.

Due primarily to the axial symmetry in the magnetic field of the lenses and partly to a confusion about how to measure a separation between small particles or edges (e.g., distance between centers of just resolved particles, half the width of a contour of a sharp edge taken from external maximum to internal minimum, and the estimated minimum possible separation between Fresnel fringes in the image of a sharp edge), theoretical predictions of resolution in the electron microscope were not demonstrated for a long period of time [7].

Along with the studies of resolution and its experimental measurement, it was realized that contrast in the image also affects the resolution [17–23]. In actual practice, the contrast in the image of an atom (or cluster of atoms) of low-Z elements, $Z \approx 25$, is greatly reduced by (i) the presence of nearby atoms, (ii) the use of non-parallel illumination, (iii) the presence of supporting film, and (iv) lens aberrations. Hillier concluded that even in the optimum case of ultrafine “free” particles (hypothetical case of particles suspended in space at the object plane), the contrast obtainable from a light particle would set the limit of the size of the particle that could be discerned with the electron microscope, and that these particles could be observed only in the presence of a lens error [21,22].

Scherzer formulated the resolving power of the electron microscope in a well known resolution equation, structurally similar to that in eq. (1) but based on lens aberration and defocus; he also obtained a resolution limit for incoherent illumination and lens aberration alone [24]. His analysis stated first, as was by then already known [18–20], that all electron lenses exhibit spherical aberration caused by those electrons passing through the edge of the lens that cannot be focused at the Gaussian plane and hence do not contribute to the resolution; rather, the spherical aberration does. Second, contrary to the assumption that contrast derived from absorption of

electrons in the self-luminous sample. Scherzer maintained that only a small fraction of electrons is actually absorbed; contrast is caused mainly by the phase delay of the electrons passing through the sample. Third, Scherzer concluded that, because of the low scattering angles, the electrons that form the image do not fill the objective aperture, so the resolution power is not affected by the size of the aperture.

Introducing the spherical aberration and all the defocusing corrections of the lens an additional phase shift $\chi(u,v)$ is introduced into every diffracted beam at the back focal plane of the objective lens:

$$\chi(u,v) = \frac{\lambda}{2\pi} (C_s \lambda^4 q^4 - 2\Delta f \lambda^2 q^2). \quad (12)$$

In this contrast transfer function (CTF) q is the reciprocal lattice vector (components u and v) and Δf is the total value of defocusing errors. This complex function is added to the phase function that is formed at the diffraction plane [24]. For bright-field (BF) imaging, only the $\sin \chi$ is involved; therefore, only in those reflections whose q vectors give a value of unity for $\sin \chi$ will the information be faithfully transferred to the image. The behavior of $\sin \chi$ for q values greater than this cut-off value oscillates considerably and therefore does not contribute to the resolution. The cut-off value is found by taking

$$d\chi/d\theta = 0 \text{ at } \chi = -3\pi/4, \quad (13)$$

which corresponds to a defocus value of the objective lens as:

$$\Delta f = -1.22(C_s \lambda)^{1/2}. \quad (14)$$

The value for q , i.e., the resolution δ , is found by inserting these values in eq. (12) and eq. (11) is again achieved; it gives the same dependence on C_s and λ in the ideal case of complete transfer of the information, i.e., $\chi(u,v) = 1$.

In reality, it is not possible to achieve the value of χ . In most cases the samples are treated as weak phase objects, i.e., only the periodic potential field of the sample is considered and no absorption is allowed (correct for very thin samples, < 5 nm, with low atomic weight) [25]. In

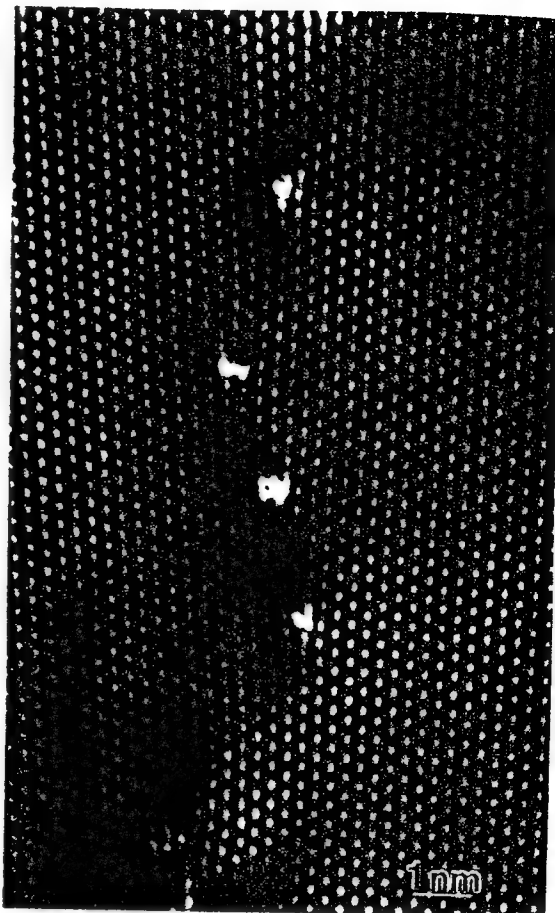


Fig. 4. High resolution transmission electron microscopy image of aragonite (orthorhombic) lattice in the [001] direction. Image clearly reveals structural dislocations in the image that has a reverse contrast (i.e., atomic columns are bright).

practical cases, beam divergence, α , chromatic aberration, C_s , and aperture functions (convolutions) are also added to the transfer function which, in effect, causes a damping of the CTF, making it impossible to observe higher periodicities (or higher frequencies of q) in the image [26,27].

An example of the current limit of resolution is illustrated in fig. 4, which was recorded from a biological aragonite (nacre section of red abalone). The image shows the organization of atomic columns around dislocation cores in the [001] projection of the lattice with the objective lens defocus set such that the atoms appear bright

(reverse contrast). The thickness of the sampled area is estimated to be about 10 nm and the resolution of the microscope to be about 1.6 Å (at 400 kV and $C_s = 1.0$ mm).

3. Microscopy using probes

Using the imaging methods discussed above in both light-optical (LOM) and transmission electron microscopy (TEM), the sample is illuminated by the light or electron source and a large area of the sample is imaged at once. It is also possible to image the sample with a small probe that scans only a small portion of the image area; the observer records the intensity of one image point at a time as the probe scans the sample to obtain the overall image of the area of interest. With this method the smaller the area scanned, the higher will be the magnification of the final image. In all the scanning microscopy systems, the resolution depends on the effective size of the probe, which includes the original size of the probe modified by the aberrations of the lenses (used to form the probe) and the modifications that arise from sample-probe interactions.

3.1. Scanning electron microscopy

The idea of forming a focused electron probe and using the secondary emission to image surface topography of materials was first realized by Zworykin et al. [28]. The formation of the image in a scanning electron microscope (SEM) is schematically described in fig. 5. By the focusing action of a strong convergent lens, an electron probe is formed and scanned over the surface of a thick sample (not electron transparent). Secondary electrons produced are then collected by a detector connected to a scintillator so that the resulting photocurrent is amplified and recorded with respect to position of the probe, thereby forming the scanned image of the surface. SEMs did not, however, come into widespread use until Everhart and Thornley designed a new detector to increase the signal-to-noise ratio [29].

The resolution in SEM, in the simplest terms, is related to the size of the electron probe that

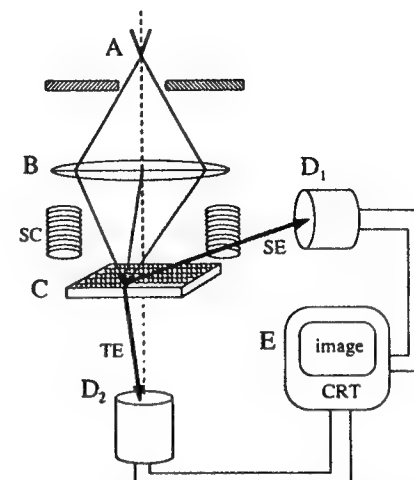


Fig. 5. Schematic illustration of SEM (configuration ABCD₁ with thick sample) and STEM (ABCD₂ with electron-transparent sample). A is electron source, B probe forming lens, C is a sample, D₁ is an SEM detector that collects secondary electrons (SE) and D₂ is a STEM detector that collects transmitted electrons (TE).

contains a sufficient amount of current, which, to a certain extent, is dictated by the spherical and chromatic aberrations as well as the diffraction limitation [30]. Resolution in SEM, however, is deteriorated by the interaction of the probe with the sample, and the subsequent beam spreading. This limitation becomes more significant at high emission voltages (20–30 kV) which are necessary to obtain sufficient brightness in conventional electron sources. The use of high-brightness field emission sources in SEM allows the use of lower voltages (1–5 kV) providing the currently achievable resolution values smaller than 1 nm [31].

3.2. Scanning transmission electron microscopy

In the scanning transmission electron microscopy (STEM) mode, similar to SEM, imaging is accomplished by scanning a small electron probe, which is formed by a strong condenser lens, over a thin sample (fig. 5). This was first realized by von Ardenne in 1938 [32]. Both the bright field (BF) and dark field (DF) images are produced by using detectors placed at appropriate positions along the optic axis [33–36]. STEM

imaging may be performed either as an attachment to a conventional TEM instrument or as an independent dedicated instrument.

In the case of dedicated STEMs, most of which use field emission sources with sufficient current, the point resolution, to a first approximation, may be taken as the full-width at half-maximum of the probe or its diameter to the first zero in the modified Airy disk [33–36]. In the DF mode, for example, a single heavy atom or cluster of atoms suspended on a thin amorphous film can be imaged.

Another definition of resolution in STEM would be the degree to which it can resolve lattice images, similar to high-resolution TEM imaging. In the case of annular DF imaging, for example, the signal is a convolution of specimen object function with a point spread function and includes the diameter of the probe modified by lens aberrations and diffraction [33,35]. In contrast to TEM atomic-resolution imaging, the dark spots that represent atomic columns in this case do not change significantly in either intensity or position with respect to thickness and defocus of the objective lens. With a sufficiently small ($\sim 2 \text{ \AA}$ diameter) and highly coherent electron probe, atomic-resolution images obtained by this technique in zone-axis orientations have been demonstrated to display atomic-number contrast, and hence the ability to distinguish compositional fluctuations at the atomic resolution, because of the differences in the scattering powers of different atomic species constituting the sample [37,38].

3.3. Near-field light-optical microscopy

In the above analysis of an image formed by incoherent radiation (using illumination and image-forming lenses and an aperture of known convergence angle), the resolution, defined by the size of the first minimum in the modulation transfer function, is limited by the convolution of the aperture function (diffraction) with the image detail and the wavelength of the radiation [39,40]. In the case of near-field optical microscopy, on the other hand, a focusing lens is not used; instead the light wave is confined to a pipe with an exit aperture radius less than the wavelength of

radiation used [41]. The sample is placed at the near field, i.e., at a distance less than the diameter of the aperture. The size of the probe that illuminates the sample is a geometrical projection of the aperture and not its Fourier transform, in contrast to far-field techniques, and diffraction from the aperture, therefore, is not allowed. Thus, Abbe's diffraction-limited resolution restriction does not apply. Based on a similar definition of resolution, the first minimum in the near-field modulation transfer function is given by [42]:

$$d = 0.61/R, \quad (15)$$

so, in this optical system resolution is not limited by the wavelength of radiation. Instead, high spatial frequencies of the sample can be imaged, limited only by the size of the illuminating/imaging aperture size and the material of which it is made (opacity). This pushes the limits of resolution in light-optical imaging to sub-100 nm (or smaller) dimensions, demonstrated experimentally, and to sub-10 nm levels, predicted theoretically [42].

3.4. X-ray microscopy

Since Röntgen scientists dreamed of increasing the resolution in the image beyond the limits of visible light-optical microscopy by using the shorter wavelengths of X-rays [43,44]. X-rays have additional advantages over electrons because of their potential use for studying materials, biological materials in particular, in their natural wet or dry states under special atmospheres (wet or gaseous). X-rays, however, can neither be reflected nor refracted, making focusing very difficult. So magnified imaging has, for a long time, been impossible. From the beginning, though, in addition to their use in well known X-ray diffraction studies for crystallographic analysis, X-rays have been used to image structures of materials as maps of density distributions in contact microscopy. It was not until recently that scientists were able to focus X-rays to obtain magnified images with resolution down to 500 Å levels. In imaging or scanning X-ray microscopes, the focusing of the X-rays is accomplished by using

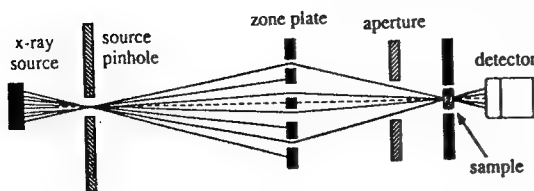


Fig. 6. Schematic illustration of an XRM (adapted from ref. [46]).

Fresnel zone plates [45,46]. These plates are concentric circular gratings that consist of transparent and opaque rings whose spacing diminishes with distance from the center. This allows the X-ray waves to be diffracted as they pass through the transparent rings and are focused to a common point (fig. 6) [46]. In this sense, the zone plates are analogous to glass lenses in light-optical microscopy and magnetic lenses in electron microscopy. In order to reduce radiation damage, soft X-rays (20–40 Å wavelength) can be used as the sample is scanned by the X-ray probe; the image is created one picture element at a time, significantly reducing the exposure of the sample to the beam, as in STEM [46]. The best resolution depends largely on the finest zone spacing (now about several hundred Å) but is still limited to diffraction aberration from the rings [47].

3.5. Field-ion microscopy

The formation of an image in the field-ion microscope (FIM) is based on the tunneling principle and does not require an image-forming lens. This instrument is schematically illustrated in fig. 7, and the image formation takes place as follows. As an imaging gas—He for example—is ionized (at 10^{-3} Torr) near the positively charged, cryogenically cooled tip of a specimen at a certain voltage, ions are accelerated radially onto a channel plate/fluorescent screen assembly to form an image, which is magnified as a projection of the tip. The mechanism by which the imaging gas is ionized is known as field ionization and is based on the electron tunneling process [48]. At the atomic protrusions on the tip, local field strength is raised, preferentially ionizing atoms at these positions, and corresponding bright spots form on the

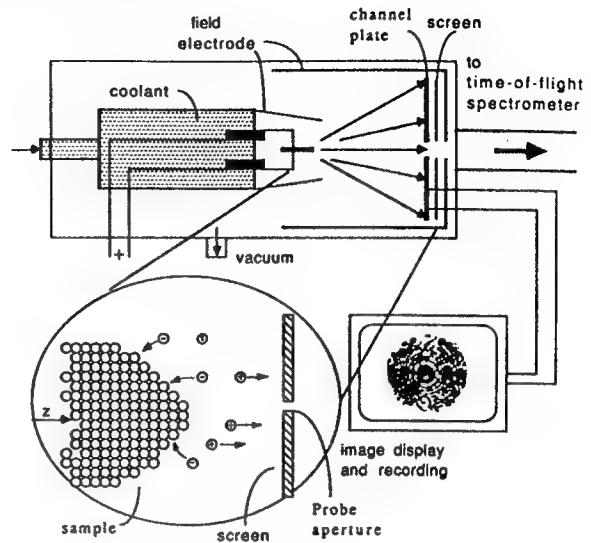


Fig. 7. Schematic cross-section of FIM/AP instrument. AP analyzer is fitted to the plate beyond the screen. Inset illustrates the ion evaporation at the tip of the sample.

image. The visible image formed on the screen is a projection of the tip of the sample and roughly resembles the stereographic projection of the crystalline sample in the direction of the specimen axis [49–51]. The magnification on the screen is determined by the ratio of the distance between the tip, L , and the screen to the radius of the tip, R ; for example, for $R = 5$ nm and $L = 5$ cm, $M = 10^6$ times. When the tip radius is less than 500 Å and the tip is kept at liquid He temperature, the atomic structure of a conductive sample becomes resolvable. An FIM image consists of an array of bright spots, each of which corresponds to an atom. The atoms are lined at the periphery of concentric terraces centered around crystallographic axes that make up the tip surface. When the temperature of the tip is low (< 10 K) and imaging gas atoms of small diameter are used (e.g., He), then a resolution as small as 2 Å can be achieved [52].

The correlation between the image spots on an FIM image and the chemical nature of the corresponding atoms is possible with a time-of-flight spectrometer that is attached beyond the screen, an arrangement called an atom probe (AP) analyzer [53,54]. The ions evaporated from the tip of

the sample are allowed to pass through a selected-area aperture (with a diameter of 1 to 5 nm) placed on the screen and analyzed by a mass spectrometer. The lateral spatial resolution of the analyzed ions on the surface of the sample is roughly equal to the size of the aperture and dictates the lateral resolution. Since the ions are stripped off the sample layer-by-layer during field evaporation, the depth resolution in compositional analysis of an atom probe is practically given as the interplanar spacing along the axis of the sample. This resolution, in conjunction with the lateral resolution, is the highest of any spectroscopy technique in performing compositional analysis and thus makes the atom probe analyzer, although restricted mostly to conductive samples, one of the highly valuable instruments in materials science [55].

3.6. Scanning probe microscopy

In a scanning probe microscopy system (SPM) a probe tip held by a piezoelectric cantilever is scanned above the sample. Either the tunneling current between a conductive sample and the tip

(in the case of scanning tunneling microscopy, STM) [56] or the deflection of the cantilever caused by the forces acting between the sample and the tip as it scans above the sample (in the case of atomic force microscopy (AFM)) [57] is measured as a function of the distance travelled by the probe in the x and y directions. Measurement of the current or the deflection is sufficiently accurate to resolve atomic or molecular corrugations on the surface of the sample. This allows topographical analysis of the sample at the atomic resolution. The interaction (i.e., the tunneling current or the atomic force) between the probe tip and the sample varies exponentially with the distance between the sample and the most extreme point on the probe tip; in the STM, for example, the atom at the extreme point at the tip of the probe allows the tunneling current to pass through (fig. 8).

Spatial confinement of the tunneling current into a small cross-section allows the STM technique to image the electron cloud on the surface of the sample in the form of contours around each atom. The resolution in the image, which is only a surface or subsurface image, is defined

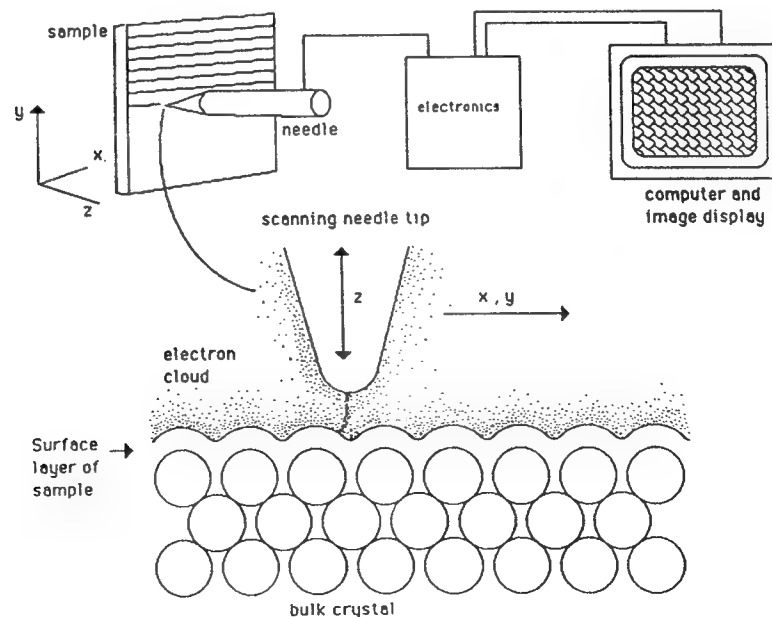


Fig. 8. A schematic illustration of the principle of image formation in STM.

NACRE: PROPERTIES, CRYSTALLOGRAPHY, MORPHOLOGY, AND FORMATION

Mehmet Sarikaya,⁺ Jun Liu,⁺ and Ilhan A. Aksay^{*}

⁺Department of Materials Science and Engineering
University of Washington, Seattle, WA 98195, and

^{*}Department of Chemical Engineering, Princeton University, Princeton, NJ 08544, USA

Biological hard tissues are composite materials incorporating both the inorganic component (phosphates and carbonates) and organic component (macromolecular structural units including proteins and polysaccharides). These materials have excellent physical properties mainly because of their highly ordered structures through the dimensional scale from molecular to submeter. Biological composites are a source of inspiration for design and processing of synthetic materials based on both their structure (biomimicking) and processing (bioduplication). In this paper, we give a general overview of some biological hard and stiff tissues in biomimetics research. Furthermore, we specifically discuss mechanical properties of nacre section of mollusk shells which is a composite structure consisting of CaCO_3 platelets surrounded by an organic matrix, an ideal nanolaminated composite material. The current understanding of micro- and nano-structures of CaCO_3 and the organic matrix, crystallographic relationship between them, and finally, the morphology and shape formation of the shell are discussed.

1.0 INTRODUCTION

1.1 NANOCOMPOSITE MATERIALS

Technological materials are rarely used in their "pure" or "perfect" forms since their physical and chemical properties depend primarily on their microstructures.¹ The object in designing and processing materials, therefore, is to tailor their properties for specific application(s) through structural control. In practice, however, this control is generally limited to a specific length scale: for example, lattice structure, impurities and defects at the atomic scale;

interface structure, precipitates, and second phase particles at the nanometer scale; grain structure, size, and shape at the micrometer scale; and finally overall architecture of the sample at the macro scale. A classic example of a composite material system is Fe-C steel, in which equilibrium and metastable equilibrium microstructures can be produced through relatively simple thermal and thermo-mechanical treatments. Countless different steels have been produced since the eighteenth-century Industrial Revolution, and many are still in use today (in fact, tough and strong steels were produced for thousands of years earlier as materials for armor, for example Damascus and samurai swords, and simple instruments).²

Recently, materials scientists have discovered that materials with controlled structural variations at the nanometer scale (i.e., size range from 1 to 100 nm, hence the name nanocrystalline or mesoscopic)³ exhibit unprecedented physical properties, including optical, electronic, magnetic, and elastic characteristics. Fundamental reasons for property improvements, however, are not well understood. Nanocrystalline materials are somewhat a natural extension of extensive work and progress that took place throughout this century, especially right before and after World War II, based on the understanding of the structural effects and their practical uses on many Fe-C⁴ and Al alloys,⁵ cemented carbides,⁶ and superalloys.⁷ In each of these cases, toughness increases associated without a loss of strength and, in fact, concurrent with a hardness increase. This is because of controlled precipitation of nanometer-sized metastable precipitates in the matrix through tempering.⁴⁻⁶ Recently, for example, in laminated single or multiphase composites, it was discovered that elastic modulus (or hardness) of the material increases as the thickness of each laminate is decreased to below 10 nm, the so-called supermodulus effect.⁸ High temperature superconductors, such as in $\text{YBa}_2\text{Cu}_3\text{O}_{7-x}$, may be considered laminated composites with alternating oxide and metallic layers (Cu-O and Y or Ba) within a dimension of little more than one nanometer.⁹ In non-linear optical materials, such as Lead Zirconate Titanate,¹⁰ controlled variation of the structure at the nanometer scale changes the second- and third-order parameters and creates non-linear optical effects and novel electrical properties.¹¹

Although some current synthetic techniques can achieve controlled composite microstructures in a limited extend, it is, however, still difficult to produce materials structures with desirable interface properties and with a high degree of control of the lattice and defect

structures at the nanometer scale, in practical and energy efficient ways and in large quantities. Some of these problems may be circumvented and certain control of micro-structures may be achieved, for example, in the synthesis of semiconductive multilayer quantum-well structures, such as Si-Ge and GaAs-GaAlAs. In this case, ion- or molecular-beam techniques are used to control structural development truly at the atomic scale.^{12,13} Even here, however, the size of the material produced is limited and the processing is performed under the strictest conditions of temperature, pressure, and environment. As a result, these techniques do not have widespread structural application except in areas that require small and critical components. Manufacturing of almost all large technological materials presents more difficulties. First, high temperature processing and consequent energy inefficiency are typical. Second, structural design is usually accomplished at a single length scale, with possible full control, and over several scales in synthesis, with limited control. Third, these materials are processed for one particular property, such as for certain mechanical properties, or electrical or optical properties, so they are rarely multifunctional for more than two properties. Finally, technological materials do not actively respond to external stimuli and are not damage tolerant.¹⁴⁻¹⁷ In order to meet the demands of current and future technologies for materials with superior physical properties, however, materials scientists will need more practical and energy-efficient strategies for producing larger components with more complex shapes for multipurpose uses.

Materials scientists may look into biological systems for model materials strategies. Biological systems are a rich source of inspiration for design and processing concepts for developing novel synthetic materials where structural control is established over a wide length scale.¹⁸⁻²² Among many novel features, from the materials scientist's perspective, some features are that biological materials are synthesized at room temperature under ambient conditions in aqueous environment; their structural make-up is controlled at a continuous length scale from molecule to final tissue in a hierarchical manner; and they are multifunctional and self-healing. The approach used by organisms in processing materials is, in many ways, more controlled than synthetic methods because biological materials are dynamic systems.²³ In the formation of biological materials, organisms efficiently design and produce complex and hierarchical microstructures, with unique properties at spatial dimensions, from the molecular to the centimeter level, and with great structural control.²¹⁻

²⁴ The dynamics of these systems allow the collection and transport of the raw constituents;²⁵ self-assembly,²⁶ nucleation, configuration, and growth of new structures;^{27,28} and the repair and replacement of old or damaged components.²⁹

We divide design approaches based on biological systems into two categories (Figure 1).³⁰ First, by investigating the structures of biomaterials at all possible scales of spatial resolution, the fundamentals of their unique structural designs can be deduced and then mimicked by techniques currently available to materials scientists - an approach we refer to as *biomimicking*. Second, by mastering the molecular synthesis and processing mechanisms of biomaterials and these hitherto unknown methodologies may be applied to produce new technological materials, superior to those presently available - an approach we call *bioduplication*. The bioduplication approach is much more complex than biomimicking and will require a long-term commitment (probably decades of research), not only to learn the intricacies of bioprocessing used by organisms but also to develop new strategies to process materials synthetically from the molecular level up with the same size, shape, complexity, and multifunctionality as the biocomposites. The biomimicking approach, although by no means simple, will require a shorter time commitment (ten years of research or less). Biomimicking involves exploring the structures of biomaterials, which are often hierarchical with each level having its own unique function, correlating these multifunctional properties with the specific microstructural features. Although the research in the authors' groups is directed toward both categories, to meet the objectives of this book, this chapter focuses on the biomimicking approach.

In this paper, we describe some of our findings on structural design of the nacre of abalone shell and answer several questions about this unique, but relatively simple, microstructure. In particular, we focus on the organization of the inorganic component, its possible structural relation to the organic matrix, and the growth mechanism of the shell. Before describing detailed microstructure of nacre, certain unique aspects of some of the other biological composites will be discussed. We intend to set the stage and justify further and detailed investigation of these unique composites. Our goal is to obtain lessons and design guidelines for synthesis of future technological materials via biomimetics which, to us, is a natural

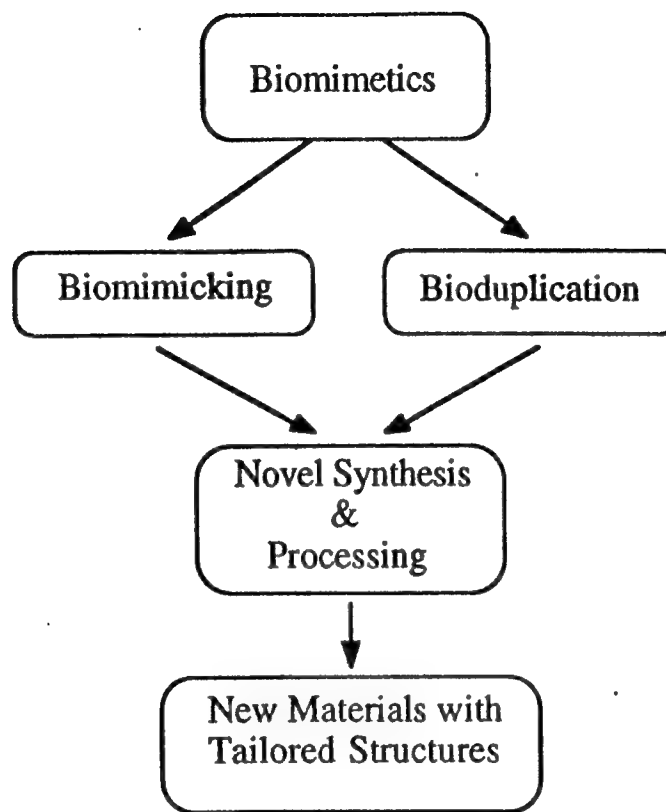


Figure 1 - Schematic description of methods of materials design based on biomimetics.

extension of the materials revolution that is taking place today and is expected to continue well into the next century.

1.2 AN OVERVIEW OF MICRO- AND NANO-STRUCTURAL DESIGN IN BIOLOGICAL HARD TISSUES

Biological materials of materials science and engineering interest are mostly hard and stiff tissues and small particles. With respect to hard and stiff tissues, the structure is composed of an organic matrix (mostly proteins and polysaccharides) with the inorganic phase interspersed

throughout. The formation, morphological development, and crystallography of the inorganic particles are assumed to be controlled by the organic matrix, a hypothesis which has not been undisputably established.^{21,31} In the case of stiff tissues, such as insect cuticles,³² all the components of the composite are organic macromolecules in which the matrix is usually composed of proteins. The stiffness comes from fibrillar polysaccharides, such as collagen and chitin, organized at the nano-, submicro-, micro- or higher-scales.³³ Some lower organisms, such as bacteria and alga, produce fine inorganic particles with unique physical properties.³⁴ As listed in Table-I with their corresponding properties, biological composite materials include all organic components, such as spiders' webs,³⁵ mucus,³⁶ and insect cuticles;^{32,33} inorganic-organic composites, including seashells,⁴¹ teeth,⁴² and bones⁴³; mostly ceramic composites, such as sea urchin teeth⁴⁴ and spines;⁴⁵ and inorganic materials, ultrafine particles, such as magnetic^{34,46} and semiconducting⁴⁷ particles produced by bacteria and algae, respectively. In some cases, byproducts and enzymes,⁴⁸ proteins,⁴⁹ and other macromolecules⁵⁰ have chemical or physical properties superior to their synthetic counterparts.

Small inorganic particles of biological origin offer analogies with synthetic nanoparticles¹¹ and mesoscopic systems.⁵¹ There are many organisms that produce ultrafine inorganic particles that perform various functions.³⁴ One notable example of this is iron clusters that form at the center of ferritin molecular cages (or vesicles) in organisms.⁵² In some cases, metal clusters are accumulated as foreign entities that might otherwise be harmful to the host organism, such as CdS in algae (which, however, have excellent optical properties).⁴⁷ Another example, as discussed above, is ultrafine magnetic particles that are found in bacteria.^{34,46,53,54} Some species of bacteria that live anaerobically in freshwater and salt swamps move about to seek oxygen and food by a mechanism that make use of a string of magnetic particles (Fe_3O_4 or Fe_3S_4) as a compass.⁴⁶ In *Aquaspirillum magnetotacticum*,⁵⁵ for example, each bacterium has about 20-25 particles that are oriented along a string with their magnetization axis along the long axis of the bacterium (Figure 2). Bacteria can move either forward or backward, depending on their configuration with respect to the Earth's magnetic field. In terms of biomimetic applications, some of the significant materials

Table-I: Categorization of various biological composites, their micro-/nano-design, and physical properties

material/ composite	example	micro- or nano-level	properties
small particles	<i>bacterial algal</i>	N N	magnetic electronic, optical
ceramic/ceramic	<i>sea-urchin</i>	B	mechanical (wear resistant)
ceramic/polymer	<i>mollusk</i>	N, H	mechanical, (tough, strong) ferroelastic
	<i>bone dentin</i>	" "	" "
polymer/polymer		N, H	mechanical, ferroelastic, optical
laminated	<i>cuticle</i>	N, H	mechanical, optical
fiber/matrix	<i>tendon</i>	N, H	mechanical, ferroelastic
fiber/fiber	<i>silk</i>	N	mechanical (tensile props.)
liquid crystalline /matrix	<i>mucus</i>	N	rheological

N: nano, M: micro, B: both M and N, H: hierarchical

characteristics of these particles are: (i) they are single crystalline (no lattice defects, such as dislocations, twins, or stacking faults),^{54,56,57} (ii) they have a uniform particle size of about 500-600 Å, and, thus, are in the single domain region (superparamagnetic),^{55,58} (iii) particle shape is species specific, and can be dodecahedral, cubo-octahedral or hexagonal,⁵⁶ (iv) they are aligned as a single string of particles (and occasionally, as double strings)^{54,59} (v) they form in biological sacks, called magnetosomes.⁵⁴ In S-rich regions, some species are known to form isomorphic form of magnetite, i.e. Fe₃S₄.⁶⁰

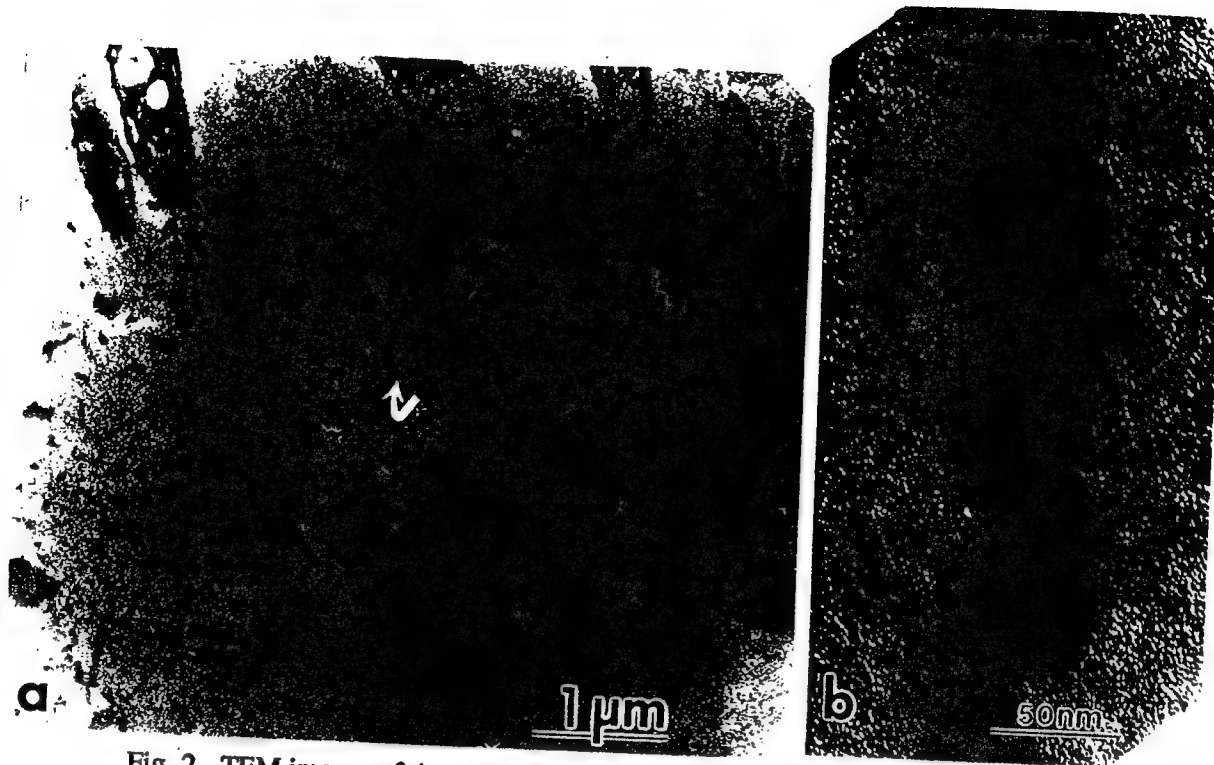


Fig. 2 - TEM images of *A. magnetotacticum* show a string of fine Fe_3O_4 particles.

The formation of magnetic particles within magnetosomes membranes is of great interest especially with respect to forming small synthetic particles under closely controlled synthesis conditions.⁶¹ Small magnetic particles can be formed synthetically in several ways including solution precipitation from precursors, in microemulsions, and using vesicles.⁶² In each of these cases, however, the particles formed are non-uniform, they often are not fully crystalline, they are compositionally nonhomogeneous, and, more importantly, they are in an agglomerated state which imposes problems in processing.⁶³ Processing of small magnetic and other inorganic ultrafine particles via biological routes, therefore, promises advantages in terms of controlling synthesis and morphological properties. The most critical point in the understanding of particle formation in magnetosomes, however, is mechanism(s) by which organic matrix allows the nucleation and controls the growth of these particles. The investigation of structure and composition of the magnetosome membrane and its protein organization, therefore, are important for understanding transport of ions through the membrane and the early stages of formation of particles. Current knowledge of the

membrane demonstrates that it is a bilayer and is likely to contain proteins that are found in the outer membrane of the bacteria.⁶⁴ Other questions involve details of the early stage of formation of particles (amorphous or crystalline and, possibly, in the hydrated form), selection of their chemistry (Fe_3O_4 vs Fe_3S_4), the control of their growth, and finally, factors that affect particle morphology, as discussed by Frankel and Bazylinsky in this book.⁶⁵

While only a small particle may be wholly inorganic in bacterial magnetite, in some organisms, such as echinoderms^{66,67} skeletal components display unique composite microstructures also involving mostly inorganic phases. It is assumed in biocomposites, such as sea shells and bones, that an organic phase is usually associated with an inorganic phase in an easily recognizable way, with each phase in close proximity to the other.^{20,21} In sea urchin skeletal units, however, inorganic phase(s) appears to be present alone and constitutes the overall component of the skeleton. (In these systems, organic matrix may cover the overall skeletal unit as a sheath (teeth) that may control the growth, or may be present within holes of the spongy-structured inorganic phase (spine) and which is dissolved during sample preparation for observation.) These biocomposites, therefore, also provide potential examples in biomimetic applications for ceramic/-ceramic composites. In the body and the spine of sea-urchin [Figure 3(a)], the mineral is calcitic single crystal forming intricate architectural design.⁶⁸ The most interesting among the structural composites in sea urchin, however, is its teeth.⁶⁹ It has five pieces in the lower center of the body that the organism uses to scrape its food from the surface of rocks. A cross-section at the cutting edge of a tooth is composed of a matrix of amorphous CaCO_3 with crystalline calcitic CaCO_3 fibers embedded in it with their long axes perpendicular to the cutting surface as to increase the wear resistance^{69,70} of the tooth [Figure 3(b)]. Irrespective of sea urchin teeth, this design has been in use in synthetic fiber-reinforced composites.⁷¹

Recent studies reported that organic macromolecules may be occluded within certain sea urchin skeletal units.⁶⁷ With respect to biomimetics, the major questions involve the presence, types, and spatial distribution of organic macromolecules that constitute less than 1 vol. % of the structure. If there exist occluded proteins, or their fractions, then these hard tissues may be regarded as molecular composites, i.e., analog of nanocomposites.³ Investigation of sea-urchin at high spatial resolution (in imaging) and elemental resolution (in

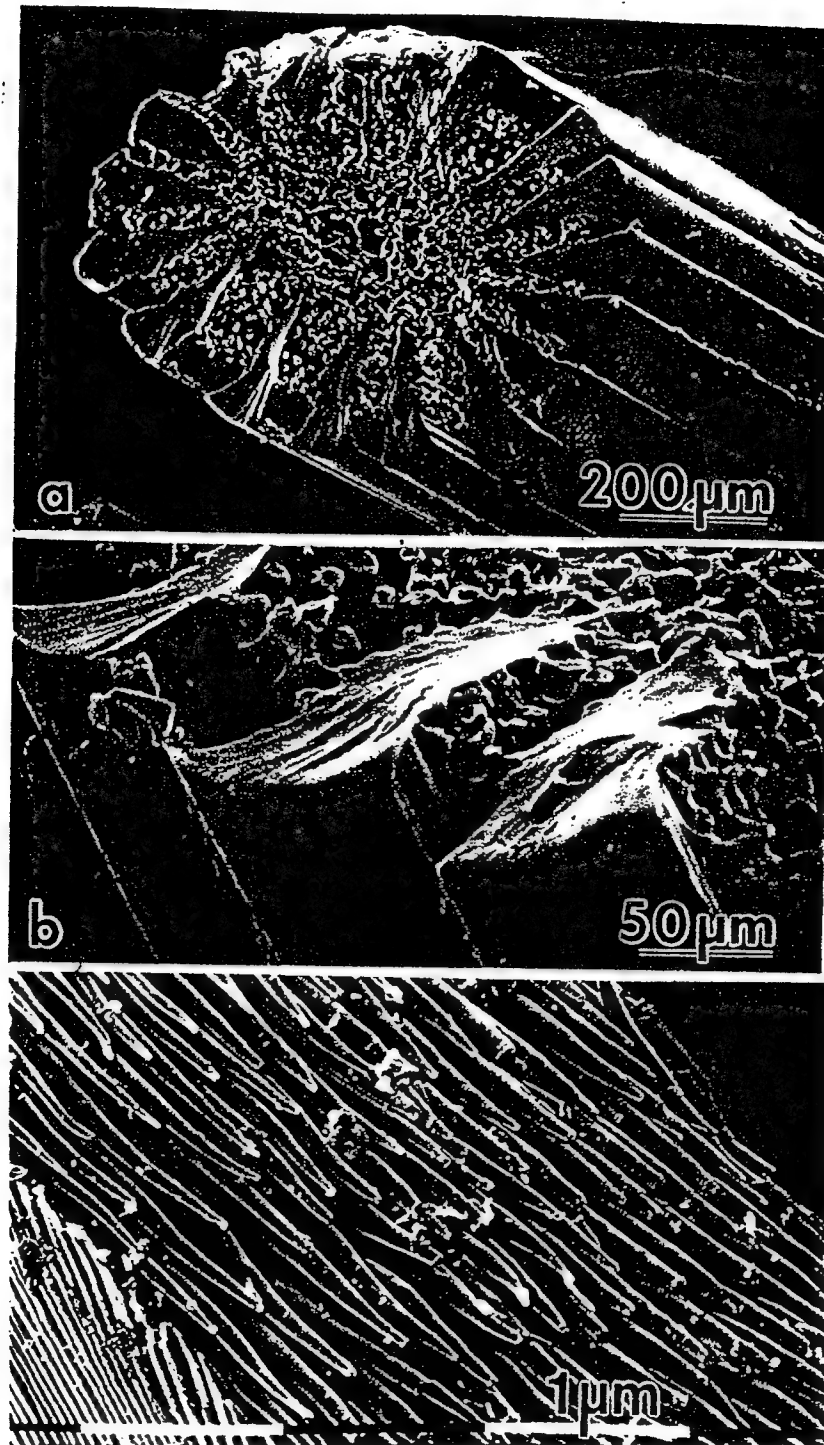


Figure 3 - SEM images of a sea-urchin (a-b) spine, showing its intricate structure, and (c) tooth, displaying its composite structure consisting of calcite fibers embedded in an amorphous CaCO_3 matrix.

spectroscopy), therefore, is expected to provide better insights into the understanding of these unique structures and new lessons for biomimetics.

Organic/Organic Biological Composites constitute numerous stiff biological tissues, composites of fibrous organic components embedded in a soft organic matrix, that are analogs of fiber- or particle-reinforced polymeric composites.⁷¹ Tendon,^{38,72} which connects muscle and bone, is a classic example. It has six discrete levels of structures organized in a hierarchical manner from molecular to centimeter-scale. Silk, found in cocoons of silk moths and webs of spiders, is another structural material.^{35,73i} These unique structures consist of silk fibroin proteins (pleated sheets) organized in a liquid crystalline fashion in an amorphous protein matrix. These are designed, by the organisms, to withstand stresses much higher than those encountered by high tensile strength-metallic or polymeric fibers (see also the paper by Gosline et al.).⁷³ⁱⁱ

One of the major classes of organic biocomposites is cuticles.^{32,74} Arthropods, such as insects, crustaceans, spiders, millipedes, and others, are evolutionarily very successful, probably because their cuticles cover their bodies from "head to toe." The cuticle, therefore, is the skeleton, for example, of an insect. Its structure resembles that of fiber-reinforced polymer matrix; the fibers are chitin (polysaccharides), and the matrix consists mostly of proteins.^{74,75} The composite has a sheet structure in which chitin fibers are arranged in layers. In each layer, the fibers are oriented parallel to each other.^{32,33,75} In successive layers, however, there is a rotation of these parallel fibers only a few degrees, i.e., helicoidal (discussed by Gunderson and Schiavoni in this book and references therein).⁷⁶ The unique microstructure of the insect cuticle, as well as cuticles of other classes, may serve as an example for the design of composite materials in which all the components are polymers.

Exoskeletons, in addition to serving as protective "armor" for insects, also form intricate surface structures which give optical effects. For example, in butterfly wings, although the origin of color for the most part is pigmentary, nevertheless some colors such as blues and violets come from scattering of light from highly ordered surface structures.⁷⁷ The structural details on surfaces can take an intricate and ordered combination of layers, scales, and ridges which are arranged to produce optical effects through the interference of light. Coloring

mechanical properties better than existing ones using nanoscale lamination based on lessons from biology.^{30,85}

The major component of nacre is CaCO₃, a material with limited engineering value in the bulk form for structural applications (although it is heavily used as a filler in the powder form in cements, papers, paints, and plastics).⁸⁶ This unique structure is composed of alternating nanometer-scale laminated layers of thin biomacromolecular matrix and CaCO₃ platelets, all highly organized to produce an excellent multifunctional material (armor) for the organism.⁸³⁻⁸⁵ Some of the other known facts about nacre include:^{83-85,87-89} (i) the overall shell composite is more than 95 vol% inorganic material--CaCO₃ in the form of aragonite; (ii) the composite has a brick and mortar (Figure 4) microarchitecture with aragonite forming thin, hexagonally shaped multi-edged bricks^{30,90} and an organic matrix that is a composite of proteins and polysaccharides;⁹⁰ and (iii) the inorganic phase consists of crystallographically highly oriented aragonitic platelets.^{30,90i} If the desired synthetically laminated materials based on nacre are to be produced through biomimicking and bioduplication, further knowledge is needed about this unique microstructure. The areas of investigation may be divided into several categories: (a) micro- and nano-structural variations, including: (i) lattice and interface defect structures within the aragonitic phase; (ii) composition and structural organization of the organic matrix; (iii) interface structural and compositional relationship between aragonite and the organic matrix; (b) structure-property relationships, including: (i) cooperative and separate structural responses of phases (aronite, organic matrix, and interfaces) under various mechanical stresses, (ii) toughening, strengthening, and hardening mechanisms, (iii) size, lamination, and organizational effects (nanocomposite behavior and source(s) of multifunctionality); (c) biomineralization, including: (i) identification of the active units within the organic matrix (nucleator proteins), (ii) mechanism of self-assembly of the organic macromolecules (also of construction of framework macromolecules), and (iii) mechanisms of nucleation and growth; (d) shape formation (morphogenesis) including (i) hierarchy in structural units, and (ii) growth mechanism of the shell (based on geometry, crystallography, and size); (e) biomimicking, including (i) detailed structural build-up of the shell from the molecular level to macro-scale and (ii) its mimicry through novel materials processing strategies; bioduplication, including (i) separation, purification, compositional (amino acid) and

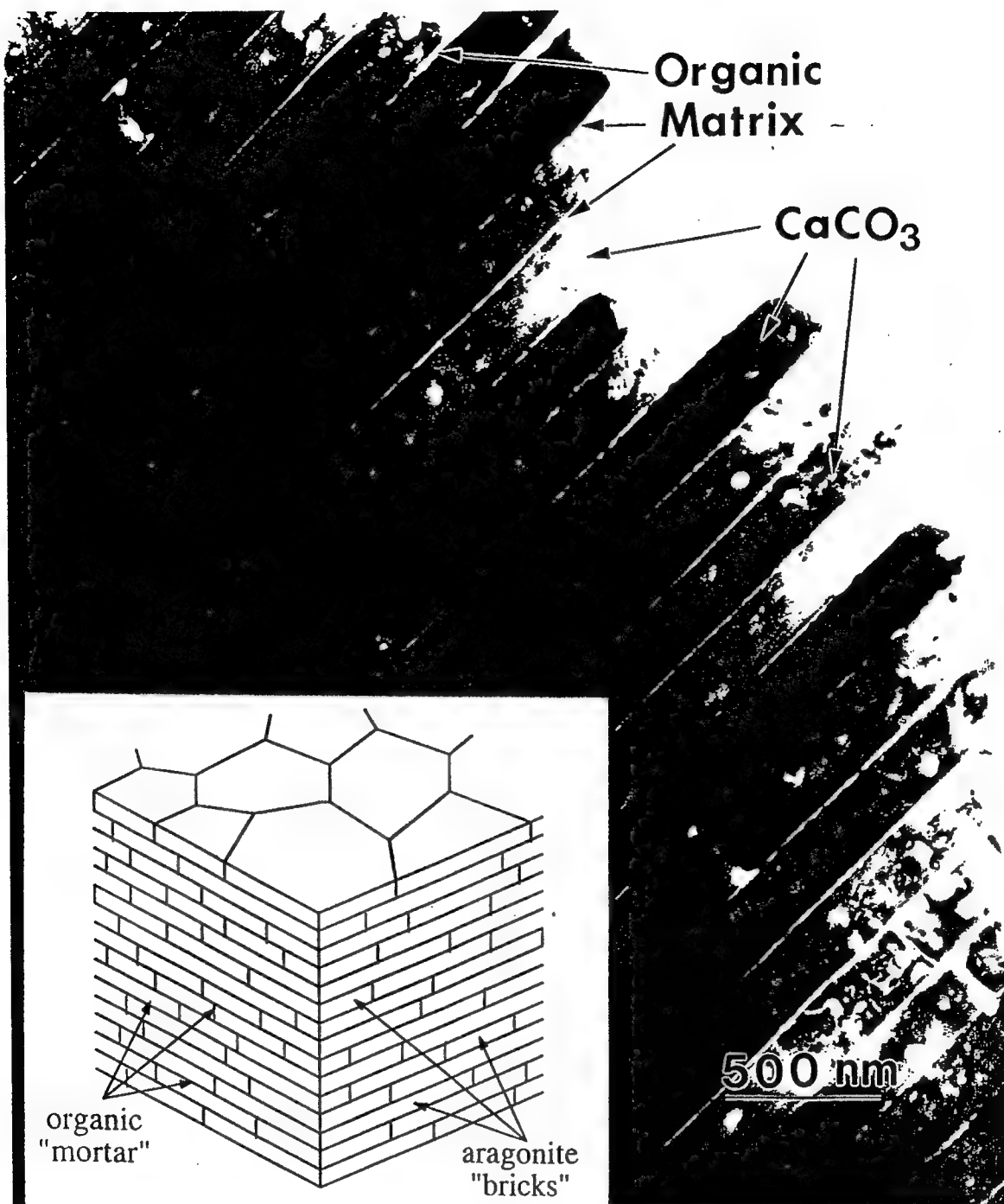


Figure 4 - A cross-sectional image of nacre (edge-on configuration) of red abalone. The inset is a schematic three-dimensional view of the structure.

structural identification of each of the macromolecular units in the organic matrix; (ii) cloning, reproduction, and self-assembly of structural macromolecules, and (iii) processing new materials by using these macromolecules based on both biomimeticization and morphogenesis principles. Answers to these questions will shed more light not only on the basis for nanocomposite behavior of nacre but also on the mechanisms of its formation and particularly the degree of control that the organism has over the growth of this highly ordered biocomposite, and their use in the processing of future biomimetic materials.

This paper discusses the areas on microstructural aspects, structure-property relationships, and biomimicking of nacre, and touches upon the other points, in particular shape formation. Although discussed in our earlier papers, for completeness of this book, we begin with a summary analysis of the mechanical properties of nacre. A set of criteria is developed for the structural design of synthetic laminated materials using the principles of biomimetics. This is followed by a description of the current understanding of the structure of nacre in terms of morphology, composition, and crystallography. Its hierarchy is also discussed in both the hard and soft tissues that leads to a possible structural relationships between the organic and inorganic components. Finally, an assessment is made of current knowledge, with possible directions, for future studies. It is believed that these studies will lead to a better understanding of the biological and chemical basis of the formation of this relatively simple, but highly efficient, structure. Its significance as a model system will appear for designing and processing nanolaminated multifunctional materials for current and future engineering applications.

2.0 MECHANICAL PROPERTIES OF NACRE: A NANOLAMINATED CERAMIC-POLYMER COMPOSITE

Nacre structure is found in many families of mollusks, including abalone (*Haliotidae*) of the gastropod family, cephalopods such as nautilus (*Nautilus pompilius*), bivalves such as pearl oysters (*Pinctada*), and blue mussels (*Mytilus edulis Linne*).⁹¹⁻⁹⁴ A transverse cross-section of each of these shells display two types of microstructures: an outer prismatic layer (calcite) and inner nacreous layer (aragonite) (Figure 7). We focused our work on the structure and properties of the nacreous layer since this is the part of the shell that displays an excellent

combination of mechanical properties as a result of its highly ordered laminated structure. We mostly used red abalone (*Haliotis rufescens*) because in this species the diameter and thickness of the shell containing the nacre are large enough to perform standard mechanical tests.⁹⁵ This allows a direct comparison of nacre with engineering structural ceramics and ceramic-based materials. Black-lipped pearl oyster (*Pinctada margaritifera*) shells were also used. Although relatively thin (1 to 5 mm), these shells are much more uniform through the thickness and relatively flat, and, therefore, exhibit less scatter in mechanical tests.

Red abalone samples were collected in Baja California, Mexico. The specimens were estimated to be 10 to 12 years old, had shell diameters of 25 to 30 cm, and shell thickness of about 1.5 cm, including the prismatic and nacreous layers. Mechanical properties in terms of fracture toughness (K_{IC}) and fracture strength (S_F) in three-point straight notched and four-point bend bars, respectively, were evaluated in the transverse direction--perpendicular to the laminated layers through which a crack is normally expected to propagate in the shell of the mollusk in its natural environment.⁹⁶ Fracture toughness and fracture strength of nacre of both abalone and pinctada, and those of some of the well-known ceramics and ceramic-based composites (cermets) are plotted in Figure 5. The average K_{IC} and S_F values of nacre are approximately 20-30 times that of synthetically produced monolithic CaCO_3 .^{84,85}

The investigation on crack propagation behavior in nacre^{84,85} reveals that there is a high degree of tortuosity not seen in the more traditional brittle ceramics, such as Al_2O_3 , or in high toughness ceramics, such as in fiber-reinforced SiC ⁹⁷ and particulate-reinforced ZrO_2 ⁹⁸ composites. The surfaces of fractured samples indicate that a major crack has meandered around the CaCO_3 layers resulting in a rough fractured surface, similar to that seen in fiber-reinforced ceramic composites where a pull-out mechanism operates.⁹⁹ Examination of micrographs recorded at higher magnifications indicates either sliding of the CaCO_3 layers upon organic matrix, suggesting the resolved stresses are lateral to the layers, or formation of organic ligaments between the layers, when the stresses are normal to the layers (Figure 6). The latter case, stretching, indicates that the interface between the organic and the inorganic phases is strong and that the organic phase acts as a strong binder.^{84,85} (This "smart" behavior, i.e., sliding or bridging, of the macromolecular assemblages that make up the composite organic matrix under different modes of stresses is an excellent example of the

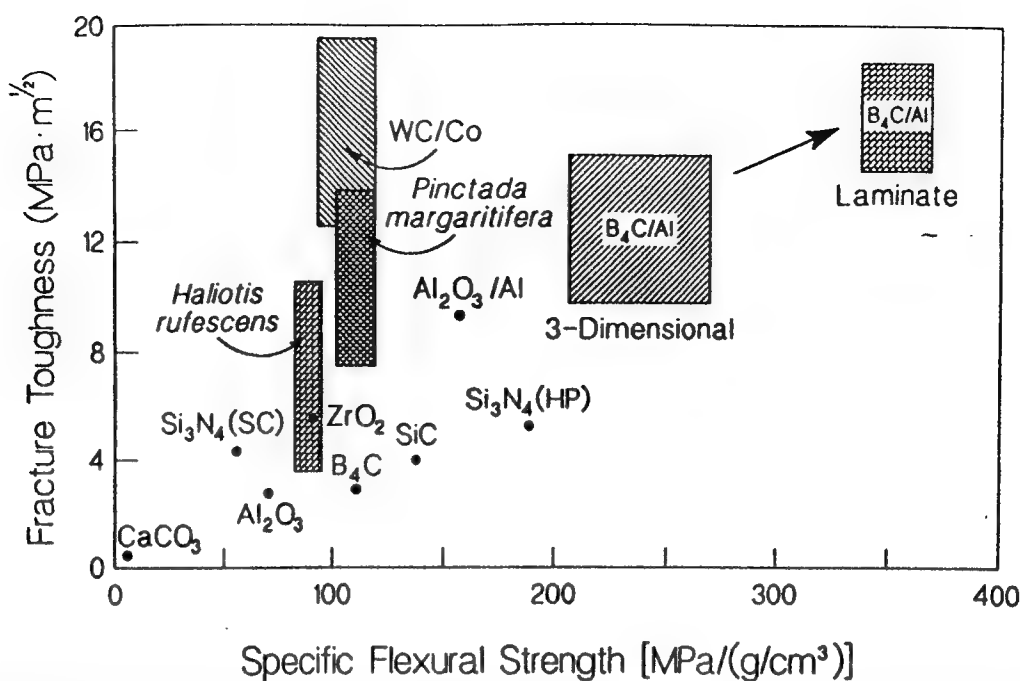


Figure 5 - Mechanical properties of nacre of abalone and pinctada (pearl oyster) compared to some major ceramic and cermet materials.

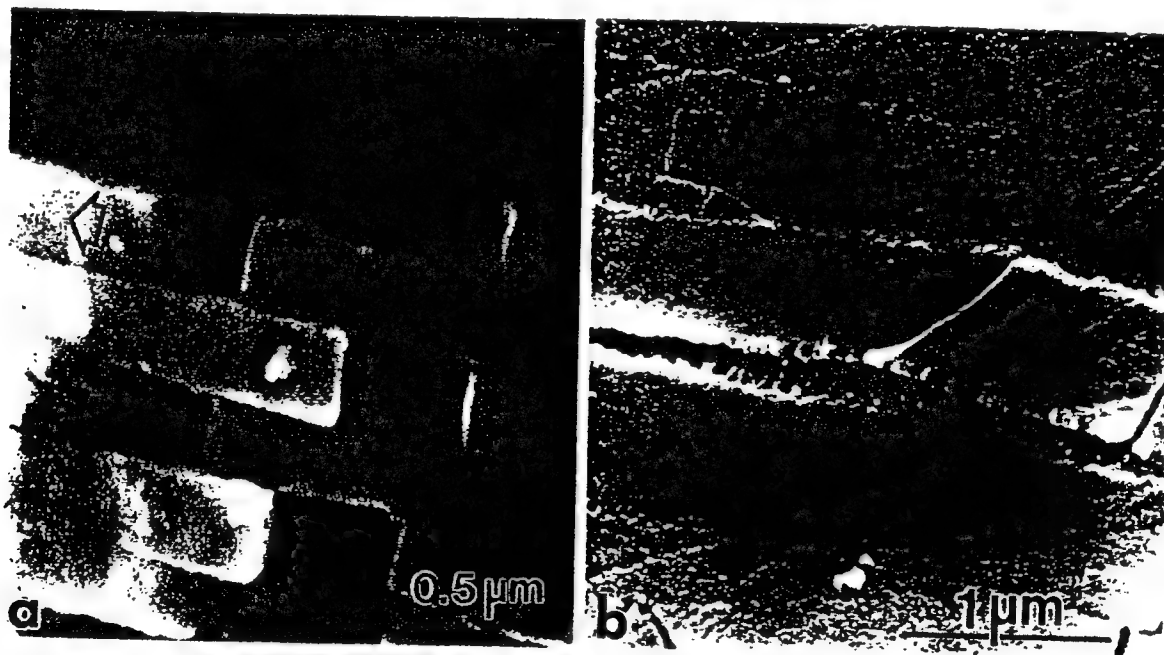


Fig. 6 - SEM images recorded near an indentation performed on an edge-on configuration in nacre of abalone. Either sliding of aragonite platelets (a) or ligament formation by the organic phase (b) takes place depending on the resolved applied stress (longitudinal and transverse, respectively). Both mechanisms are responsible for the high toughness of the nacre.

unique quality of biological materials in terms of their structures and resulting properties.) Several toughening mechanisms, therefore, may be proposed:¹⁰⁰ (i) crack blunting/branching, (ii) microcrack formation, (iii) plate pull-out, (iv) crack bridging (ligament formation), and (v) sliding of CaCO₃ layers. The high degree of tortuosity seen in crack propagation⁸⁵ may be due mainly to crack blunting and branching.^{97,99} Tortuosity alone, however, is not a major toughening mechanism in these composites, because it cannot account for the many orders of magnitude increase in toughness. The major toughening mechanisms, therefore, are sliding and ligament formation.⁸⁵ Similarities exist between the deformation of a nacreous seashell^{30,85} and a metal¹⁰¹ in the sliding mechanism in terms of forming deformation bands in the bulk that appear as striations on the surface. It is likely that this complex deformation mode may be the main mechanism of energy absorption during the propagation of cracks, which needs to be further investigated quantitatively in terms of its energetics.

The strength of nacre, on the other hand, may be related to several factors, including the size and structure of the aragonite platelets and the interfaces between the inorganic and the organic components. From the limited thickness of the largest flaw (i.e., the thickness of the platelet) 0.5 mm, the increase in the theoretical fracture strength¹⁰² of aragonite would be about 200 MPa, comparable to the measured value of 185 - 220 MPa in our studies.⁸⁵ Therefore, the rule-of-mixtures¹⁰³ may account, at least, for part of the value of the measured strength.^{83-85,100}

3.0 DESIGN GUIDELINES FOR PROCESSING BIOMIMETIC LAMINATED COMPOSITES

The lamination microarchitecture of presentday impact resistance materials originates from ancient armor.¹⁰⁴ Biological structures, such as those in insects,³² eggs,¹⁰⁵ and sea shells⁹¹⁻⁹⁴ also have similar architecture, but at much smaller dimensional scale. In fact, the best armor has a double-architectural design in which the front section is hard, for the effective stopping of the projectile, and the back section is soft (but strong) for the absorption and dissipation of the kinetic energy from the projectile.¹⁰⁴ This is basically analogous to the shell of abalone. In cross-section, the hard front consists of long calcite crystals perpen-

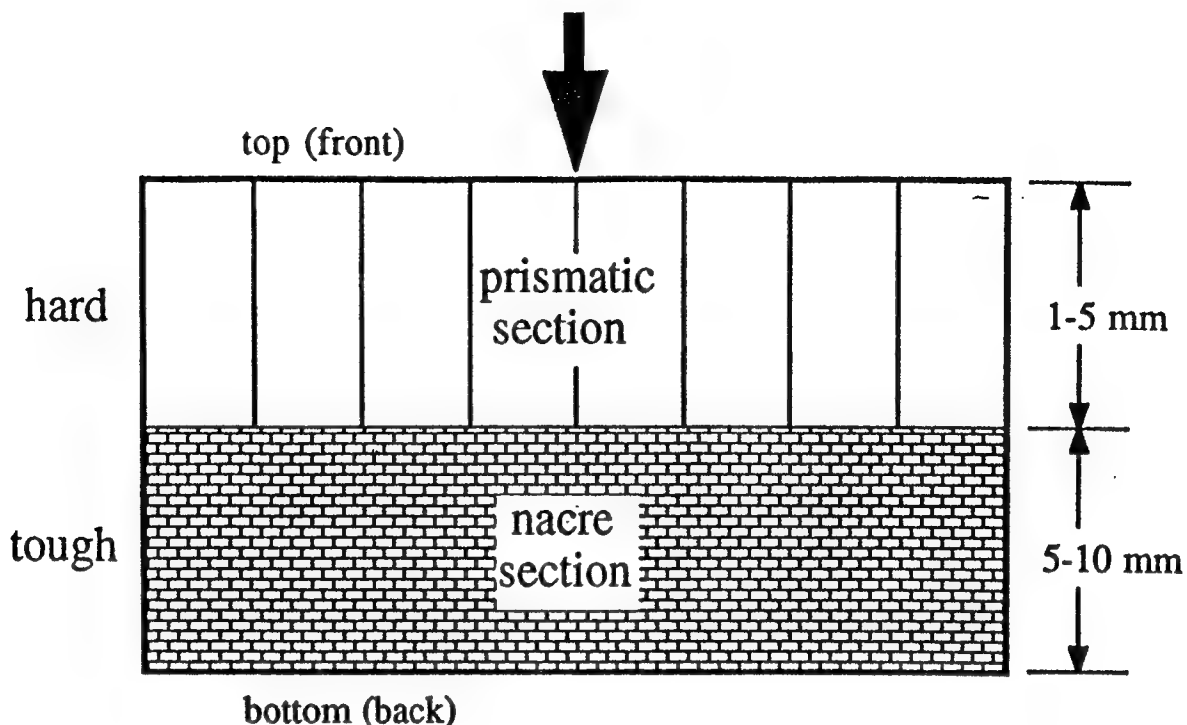


Figure 7 - Schematic illustration of the cross-section of the abalone or pinctada shell, an ideal armor material with hard front and tough back.

dicular to the shell plane (and in the direction of the projectile, ready to confronting it), and the back is tough nacre (laminated aragonite and organic matrix) as schematically illustrated in Figure 7 (also see Figure 10). In ceramic/ceramic composite design, on the other hand, even in laminated architecture, weak interfaces are a necessary condition for the toughness increase, with a sacrifice in the expected deterioration of the overall strength of the composite.^{106,107} Contrary to the accepted materials design criteria in the role of interfacial strength in synthetic materials (as described in the previous section) in the structural design of biological materials such opposing affects are circumvented by the role of macromolecules due to their composite structures and resulting multifunctionality. Hence, there seems to be no need for a sacrifice in any of the properties, and therefore, both the toughness and the strength of the biocomposite increase, as seen in the laminated structure of nacre.

The unusual mechanical properties of nacre, absent in synthetic ceramics and composites, may, therefore, derive from: (i) the intrinsic properties of the constituent phases (brittle inorganic phase and soft organic matrix); (ii) the highly ordered organization of ceramic and

biopolymer layers and their detailed structures, including the interface structures and properties; and (iii) the size of the ceramic and biopolymer layers which may be critical factors due to the intrinsic properties of biogenic aragonite and the organic matrix. Despite the fact that many of the structural features of abalone remain a mystery (especially of the soft tissue), we can distinguish some guidelines using the knowledge of their excellent mechanical properties and structural architecture at the micro- and submicron levels to aid us in the processing of synthetic microstructures through biomimicking. We expect these biomimicked synthetic laminated composites to have superior properties over those achieved in synthetic composites prepared by traditional processing methods and having common microstructures. Based on the previous studies of nacre,^{30,85} the design of high-strength/high-toughness synthetic composites should incorporate the following:

- (i) A laminate thickness of the hard and brittle component of less than 1 mm and a soft component of less than 1000 Å, with an approximate ratio between 5:1 and 10:1
- (ii) A highly plastic soft phase (deformability > 100%)
- (iii) Strong interfaces between the soft and hard phases (so that the interface does not fail during crack propagation)
- (iv) A soft phase able to bind to the surfaces of the hard component (strong interfacial bonding) and provide plasticity to the overall composite structure (for sliding and metal-like deformation behavior) or form ligaments to constrain crack opening (through crack bridging), depending on the state of resolved applied stress.

In actual processing of laminated composites, these guidelines may be difficult to apply. For example, there is no practical current way to produce structural laminates with layer thicknesses thinner than about 10 mm^{108,109} (except in *in-situ* laminates formed through phase transformations in which overall architectural design is somewhat limited due to thermodynamics or kinetics limitations).⁸ It is also difficult, if not impossible, to control the thickness ratio of the hard and soft components at these small dimensions. The guidelines stated above, nevertheless, remain useful as they present the ultimate structural features to achieve and it is a goal in materials design at submicron and nano-scale levels. In the design of synthetic laminates, high hardness ceramics such as BN, B₄C, TiC, ZrO₂, and Al₂O₃ can be used as the brittle component. Highly plastic (superplastic) metals, such as Al and Cu

(and their alloys), or organic polymers, such as polyethylene and polypropylene, may be good candidates for the soft phases. These constituent phases which give the best combination of properties, with emphasis on strong interfaces, can be used if they can be processed.

Some of the property requirements stated above were met to a certain degree in the B_4C -Al^{100,109} and B_4C -polymer¹⁰⁸ laminated systems designed for use as impact resistant materials. In one synthesis strategy for processing of B_4C -Al composites, porous B_4C layers with thicknesses below 100 mm, and as low as 15 mm, were tape-cast between thin sheets of Al. The stacks were heated to induce infiltration and to allow bonding between Al and B_4C without an excessive reaction. The resulting composite displays a structure in which both the Al-infiltrated B_4C and the alternating layers of pure Al form continuous films.^{109,110} The overall architecture provides alternating layers of hard and soft components and strong interfaces. As a result, fracture toughness and fracture strength both show a 30 to 40 % increase over the monolithic B_4C -Al composite with the same Al composition (Figure 6), as well as structure in which Al and B_4C have a three-dimensional interpenetrating network.¹⁰⁹ The mechanical properties of B_4C -Al laminates, in terms of K_{IC} and specific fracture strength, are currently the best that can be achieved among the present cermet systems.

Despite the fact that improvements have been achieved in the mechanical properties of laminated composites based on biomimetic architecture, as in the example of B_4C -Al, these improvements have not yet come close to the superior properties of nacre over monolithic $CaCO_3$. This may be due primarily to insufficiently thin laminate layers. Thicknesses below 1 mm in the inorganic layers and below 100 nm in the organic layers (soft phase) are needed. Second, as will be clear from the discussion in the following section, both the inorganic and organic layers have complex structures, in terms of their crystallography, substructures, and morphology.

4.0 DETAILED STRUCTURE OF NACRE

In a layered composite design,¹¹⁰ the most significant structural features are: (i) properties of hard and soft components, (ii) interface structures and properties, (iii) thicknesses of the



Figure 8 - (a) Platelets of biological aragonite in an edge-on view of nacre of *pinctada*, and (b) geological aragonite (sample from Aragon, Spain) display substructural details. Note high dislocation density (in this orientation) in (a) but only antiphase boundaries in (b). (Twins in (a) are in face-on configuration and, hence, are not seen).

lamellae and their ratio, and (iv) geometry of the lamellae. In the case of nacre, although many structural factors are known, some of the most significant questions are still unanswered. In nacre, for example, it is possible that the aragonite lattice may incorporate organic molecules.⁹⁰ If this is so, then the bulk properties (e.g., moduli) of the biogenic aragonite will differ significantly from those of geological aragonite.³⁰ As shown in Figure 8, biogenic aragonite contains significant density of dislocations (in addition to other substructural features),¹¹¹ contrary to geological aragonite (an ionic crystal) in which dislocation could not be observed.¹¹² In nacre, the lamellae do not form simple continuous layers; instead the inorganic component, in the form of platelets (bricks), interrupts the continuity of a given layer with each platelet surrounded by a thin film of organic matrix. Even less is known about the composition and molecular and conformational structure of the organic matrix.^{86,89,90,113-118}

Among all the features of nacre, the interface structure and properties are the least understood. As we have seen, interfaces not only allow sliding of aragonite platelets and formation of

organic ligament under stress, (both necessary conditions for the excellent properties), but they are also the sites of the nucleation and growth of the aragonite layers.^{113-115,118,119} For these reasons, structural correlation of aragonite and the organic matrix deserve closer examination. In order to answer some of these questions, we have directed a portion of our research toward the study of the structure of nacre at submicron and nanometer scales.³⁰

In the following sections we summarize the current understanding of morphological and crystallographic relationships among the structural components of nacre. First, we present an overview of these relationships between the inorganic building blocks. From this, we construct a model for the possible molecular conformation of the underlying organic matrix. We find that the model not only allows the crystallographic but also the morphological relationships among building units in nacre, and forms a basis for shape formation and growth of the shell.

4.1 MICROSTRUCTURE OF NACRE

Red abalone (*Haliotis rufescens*) belongs to the mollusk species in the family of gastropods. Gastropods first evolved about 500 million years ago, and, with little change, they have survived to the present time (abalone is, thus, considered a "living fossil").^{21,91-94} The shell of the abalone is ear-shaped, with a large opening and a small spire (Figure 9). The shell has respiratory pores (about 20 in the adult) but only the last 4 to 5 are open at a given age. The organism has a large foot which, in the juvenile period, grabs onto a rock, allowing adult mollusk to forage for algae and plants on the bottom. Although other abalone species are much smaller, the shell of *H. rufescens* grows by about 2.5 cm per year and can reach 30 cm in diameter; after which it only thickens (becoming more than a cm).

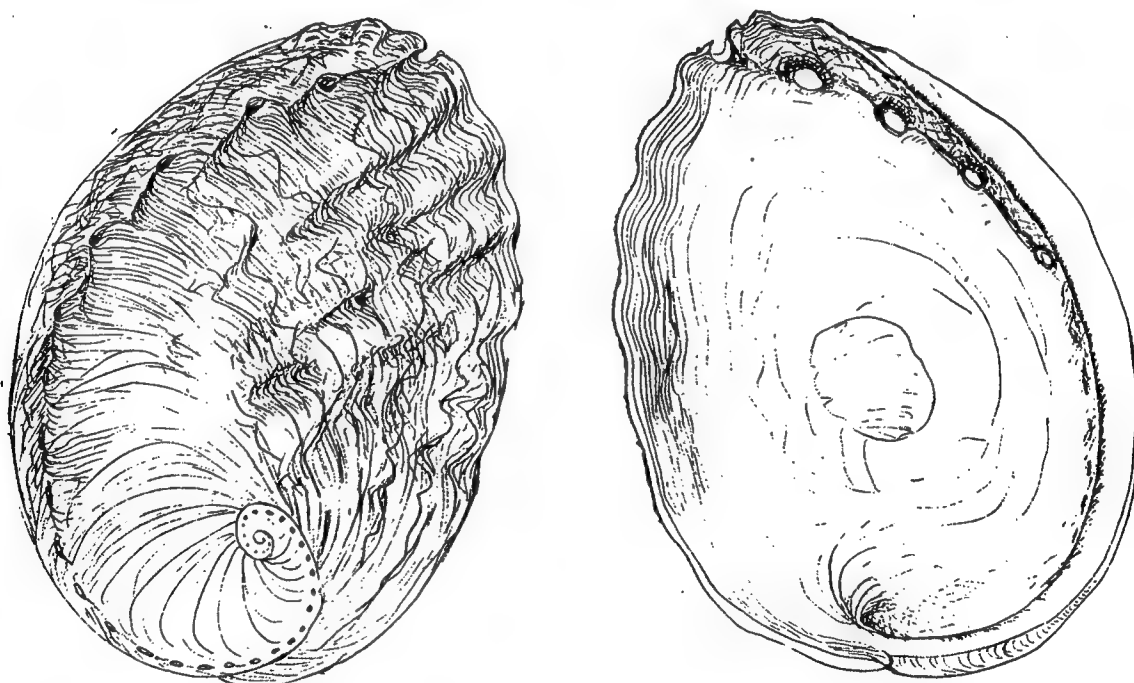


Figure 9 - Schematic drawing of (a) a top view and (b) an inside view of *Haliotis rufescens*.

A longitudinal cross-section of the red abalone shell displays two types of microstructures: an outer prismatic layer and inner nacreous layer (see Figures 7, 9, and 10). Two forms of CaCO_3 , calcite (rhombohedral, R3m) and aragonite (orthorhombic, Pmnc), constitute the inorganic phase of the composite in the prismatic and nacreous layers, respectively. This paper focuses on the structure and properties of the nacreous layer, since, as discussed above, this part of the shell displays an excellent combination of mechanical properties that derive from its highly ordered and comparatively simple hierarchical structure having alternating layers of organic and inorganic components.³⁰ This microarchitecture, especially the highly ordered inorganic component (aragonite platelets), is possible to study crystallographically with the aid of electron microscopy directly and in great detail. This is mainly because electron radiation damage poses less of a threat during the observation of the CaCO_3 crystals than does the organic matrix.

The structures of shells are seen in the SEM images in Figure 10, from the fractured surfaces of red-abalone and nautilus. The images display stacked platelets (aragonite) in nacre on the inner portion, and elongated crystallites (calcite) in the prismatic section on the outer portion. Platelets in nacre are typically arranged in either columns (abalone and nautilus) or sheets (pinctada). The stacking is not random and, in a fully grown specimen, resembles a brick and mortar microarchitecture as discussed. The platelets vary in thickness; an average of 0.25 mm, 0.4 mm, and 0.5 mm in red abalone, nautilus, and pinctada, respectively, and edge length is 5-10 mm. Organic matrix is between 10 and 50 nm thick. The dimensions of the aragonite platelets and the organic matrix vary depending on the site of the shell from which the sample is extracted and the species of the mollusks.

The following sections describe the structure of the organic matrix and the crystallographic and geometrical relationships between the CaCO_3 platelets throughout the nacre of abalone. Based on the structural relationships in the inorganic component, a possible correlations between the structures of aragonite platelets and organic matrix will be proposed in a later section.³⁰ First, the current knowledge on the organic matrix is summarized below.

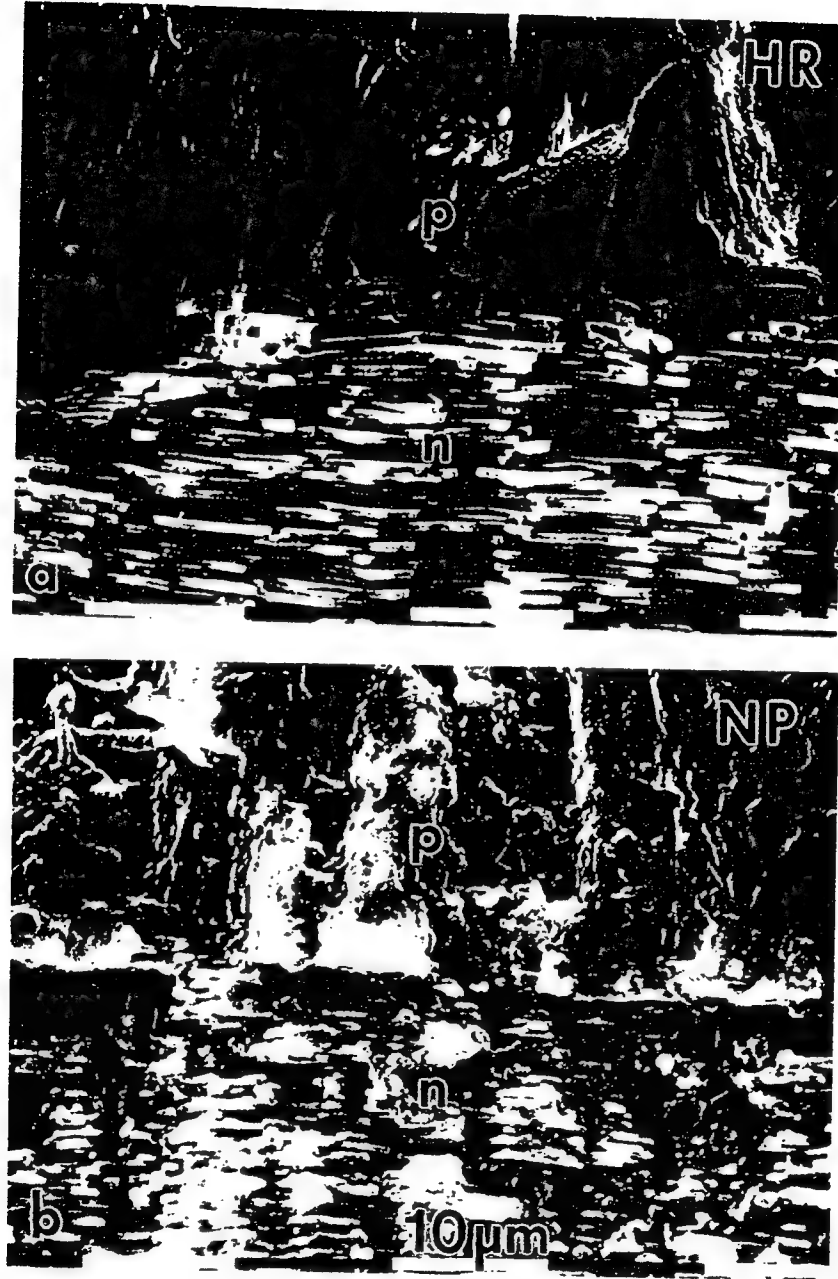


Figure 10 - Images of fractured surfaces of abalone (a) and nautilus (b) exhibit both the prismatic (p) and the nacre (n) sections.

4.2 STRUCTURE OF THE ORGANIC MATRIX

As described by other researchers,^{90,119,120} the organic matrix is thought to be a composite of macromolecules stacked in a sandwich form. This is based mostly on indirect investigation of the characteristics of the biological macromolecules that are extracted from the shell through decalcification.^{90,114,119,120} Macromolecules are divided into two groups: those soluble in weak acids, and those that are not.⁹⁰ In the former case, the proteins extracted were found to contain aspartic and glutamic acids (see references in Table-II). These amino acids are known to be major components of structural proteins that form sheet-like structures, such as in β -pleated sheets, that are found throughout the animal kingdom.²³ An extensive literature survey reveals the major amino acid compositions of the proteins in various species of mollusks given in Table-II. There is also speculation of the composition of the insoluble portion of the organic matrix, but it is probably much less accurate. It is possible, based on many investigations, that this portion of the matrix may constitute polysaccharides in addition to proteins (see Table-II).

The major flaw in each of these studies has been that the macromolecules extracted from the shell have not been specific to a certain section in the shell. In fact, the shell is often pulverized, with both the calcitic (prismatic) and aragonitic (nacre) sections intermixed before decalcification. The organic macromolecules are expected to have different stoichiometric compositions, and hence different conformations with respect to each other. These differences may, in turn, greatly affect the structure, crystallography, and the geometry of the inorganic crystals. The analysis which gives a mixture of all the biological macromolecules in a shell, therefore, has so far not been adequate in describing the true composition and the structure of the macromolecules that make up the nacre structure. (Several investigators - D. Morse,¹²¹ⁱ University of California, Santa Barbara, D. Kaplan,¹²¹ⁱⁱ Natick Research Center, ARO Lab, including those in our laboratory,¹²¹ⁱⁱⁱ are working towards isolating macromolecules from different portions of the shell).

Nevertheless, based on the findings so far, and limited direct analysis, the organic matrix may

Table - II: Amino acid compositions of the mollusk shells used in this study
(table is made using the literature data)

		Asx	Thr	Ser	Glx	Pro	Gly	Ala	Val	Tyr	ref.
<i>H. rufescens</i>	W	25.0	?	10.2	8.2	?	48.5	4.52	?	?	i
	N	20.0	2.0	9.2	4.3	3.6	18.4	17.1	?	?	ii.
	P	20.0	11.0	6.8	5.7	5.7	11.0	6.8	?	?	ii
<i>N. pompilius</i>	WI	7.1	1.3	9.8	4.5	0.5	35.3	25.0	1.4	0.6	iii/iv
	N	2.0	1.3	6.3	6.7	0.0	19.7	48.0	2.3	0.0	v
	NS	26.1	4.8	7.9	6.6	4.6	23.6	4.4	1.5	6.4	vi
<i>P. margaritifera</i>	P	9.4	2.9	3.9	2.2	5.6	22.3	3.2	?	5.5	vii

N: Nacre only, P: prismatic only; NS: nacre-soluble proteins; W: whole shell; WI: whole shell, insoluble only.

- i. M. Cariolu and D. E. Morse, "Purification and Characterization of Calcium-binding Conchiolin Shell Peptides from the Mollusc, *Haliotis rufescens*, as a Function of Development," *J. Comp. Biol. B*, **157**, 717-729 (1988).
- ii. N. Nakahara, G. Bevelander, and M. Kakei, "Electron Microscopic and Amino Acid Studies of the Outer and Inner Shell Layers of *Haliotis rufescens*, *Venus*, **41** [1] 34-46 (1982).
- iii. M. F. Voss-Foucart, "Assais de solubilization et de fractionnement d'une conchioline (nacre mulaire de *Nautilus pompelius*, mollusque céphalopode), *Comp. Biochem.*, **26**, 877-886 (1968).
- iv. E. T. Degens, D. W. Spencer, and R. H. Parker, "Pleobiochemistry of Molluscan Shell Proteins," *Comp. Biochem. Physiol.*, **20**, 553-579 (1967).
- v. S. Weiner and L. Hood, "Soluble Protein of the Organic Matrix of Mollusk Shells: A Potential Template for Shell Formation," *Science*, **190**, 987-989 (1975).
- vi. G. Goffinet and C. Jeuniaux, "Composition chimique de la fonction "nacrpine" de la conchioline de nacre de *Nautilus pompelius* Lamarck," *Comp. Biochem. Physiol.*, **29**, 277-282 (1969).
- vii. S. Tanaka, H. Hatano, and O. Itasaka, Biochemical Studies on Pearl. IX. Amino Acid Composition of Conchiolin in Pearl and Shell," *Bull. Chem. Soc. Japan*, **33**, 543-545 "(1960).
- viii. H. Nakahara, M. Kakei, and G. Bevelander, "Fine Structure and Amino Acid Composition of the Organic Envelope in the Prismatic Layer of Some Bivalve Shells," *Venus*, **39** [3] 167-177 (1980).

actually have a sandwich structure containing three organic sublayers, each with its own unique composition and molecular conformation.¹¹⁴ According to this scheme, the central portion of the organic matrix is composed of chitin (polysaccharides), which is surrounded on both sides by β -pleated protein sheets. The layer next to the inorganic is then composed of acidic proteins. In this scheme, while the chitin provides the structural (mechanical) stability

to the composite forming a back-bone (framework macromolecules), the b-pleated sheets act as the substrate and provides the biomineralization sites (nucleator macromolecules). The acidic proteins are there to fill in the gaps between the organic matrix and the aragonite crystals. Neither the composition of these layers nor their structure has yet been clearly identified. The investigation of the structural relationship between the organic and the inorganic layers is, therefore, far from complete.³⁰

Similarly, it may be possible to directly study the organic macromolecules in the TEM if proper molecular markers are developed.^{122,123} For this, isolation of each of the major macromolecules from the organic matrix seems to be necessary. Once this is done development of antibodies and proper stains will follow. These stains can then be used in ultramicrotomed thin sections to identify locations and concentrations of each of the macromolecules. In our group a preliminary work is being carried out to reveal structures of the macromolecules in samples that are either ultramicrotomed or low temperature ion-beam milled.¹²⁴ Two such micrographs are displayed in Figure 11. Figure 11(a) reveals layered structure of the organic matrix in an ultramicrotomed section.¹²⁴ The contrast difference is due to differential staining of the organic sub-layers by uranyl acetate due to their differences in composition and structure. A detailed microstructure of the interface between organic layer and aragonite is shown in Figure 11 (b). The image was taken from a sample that was low-temperature ion-milled and then slightly etched by gold citrate.¹²⁴ The preferential etching of the aragonite platelets gives them a saw-tooth appearance. The light acid used that causes this feature also dissolves away the acid soluble portion of the organic sublayers. As a result, central sub-layers of the organic matrix are exposed. This is the part we think is made up of polysaccharides since they are known to be resistant to such treatment. Further studies are underway to correlate these characteristic features related to the structures of aragonite and the organic matrix.

From the point of biomimetics it is essential to understand what the function of the organic matrix in nacre is in controlling nucleation of the inorganic crystals, their shape formation and growth. In future crystal engineering, in making nanostructures and laminated composites based on biological hierarchical composites using either synthetic or biological macromolecules, the first requirement is to understand the mechanism of inorganic-organic

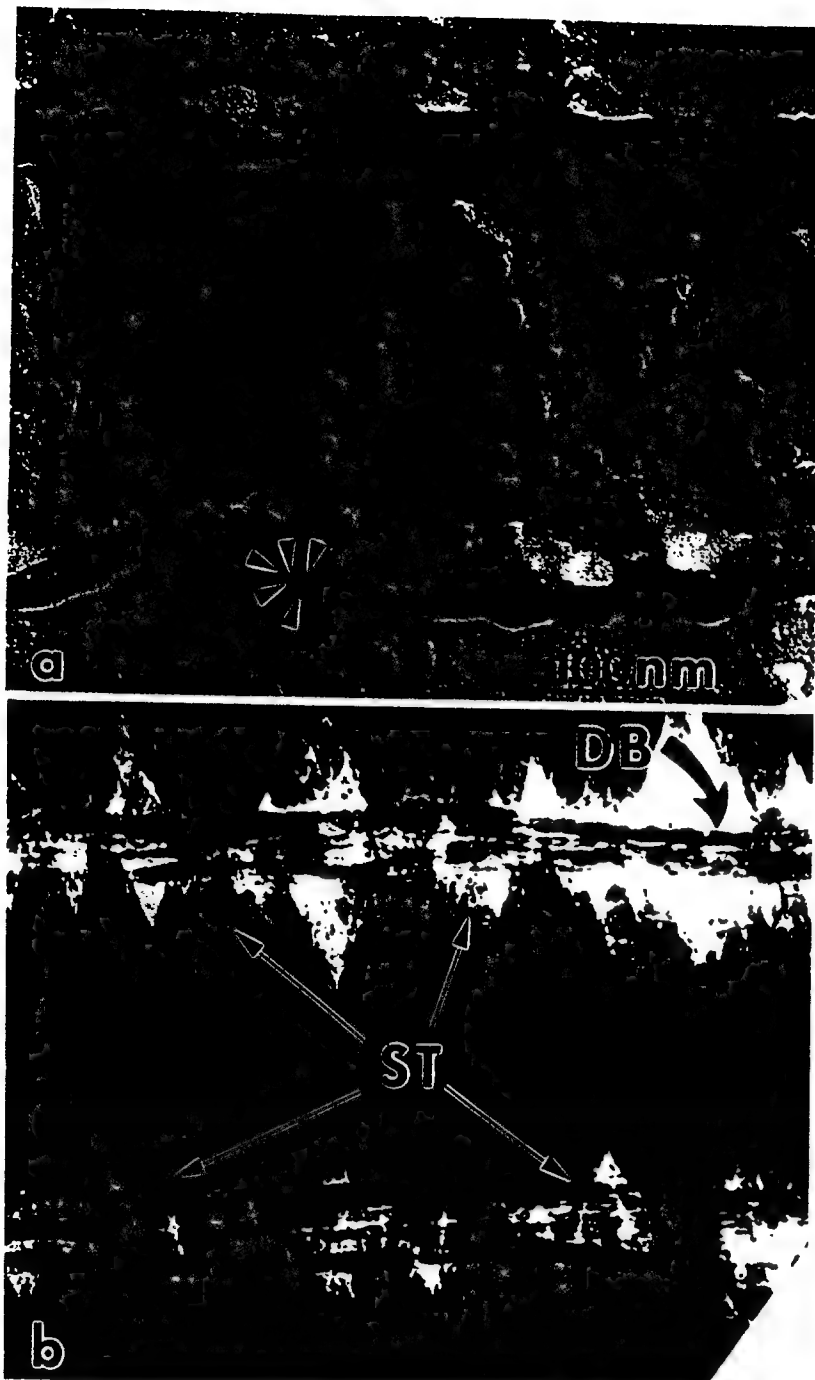


Figure 11 - Structure of the organic matrix in nacre of abalone. The sample in (a) was ultramicrotomed, decalcified, fixed, and stained. Five sub-layers (arrows) are exposed in the organic matrix, possibly due to their differential staining. The image in (b) was taken from an ion-beam milled sample that was slightly acid etched. It reveals insoluble (central) portion of the organic layer DB (dark bands) and the saw-tooth (ST) appearance of the etched aragonite/matrix interface.

interactions in biological systems. Further detailed investigation, especially in a hard tissue like nacre having a relatively simple structure, therefore, appears to be well warranted. The following section will attempt to address this issue.

4.3 CRYSTALLOGRAPHY OF ARAGONITE PLATELETS

As discussed above, a fundamental knowledge of the overall structural relationships between the organic and inorganic components in the closely knit structure of nacre (and other hard tissues) is essential to understanding, first, its mechanical properties, second, relationship with the organic matrix, and third, its mechanism of formation. Prior studies have postulated the crystallinity of the organic matrix from the fact that it contains chitin and silk fibrion-like proteins as the outer and middle sublayers of a sandwich structure and that these macromolecules are known to self-assemble in crystalline arrangements.^{90,114-115,119,120} The outermost sublayer in the organic matrix, the one in contact with CaCO_3 , consists mostly of soluble charged macromolecules (proteins) and presumably acts as the binder to the inorganic phase. This scheme suggests that active sites on the matrix align with those on the CaCO_3 , i.e., either Ca^{2+} ions^{90,114} or CO_3^{2-} sites (ionotropy mechanism).^{113,119}

It has been impossible to study both the organic and inorganic crystals simultaneously, and the structural relationships between the components of the nacre exist only as a conjecture.^{90,113-115,119,120,125-128} Bulk studies, performed by X-ray diffraction, on the nacre revealed that the aragonite platelets are organized with their [001] axis perpendicular to the layers.^{90,114,128} It has been postulated that the axes within the layer plane in each platelet are oriented randomly.^{90,114} Furthermore, it was assumed from this scheme that each aragonite platelet grew on the crystallographically related organic template, which itself has a local random orientation.⁹⁰ From the composition of the insoluble fraction of the organic matrix, i.e., the inner crystalline sublayers which contain a high fraction of aspartic and glutamic acid, it might be possible to deduce a self-assembled structure that would be related commensurately to the aragonite lattice along the [001] projection.^{90,114,120,128}

In the present work, each aragonite crystallites was analyzed by electron diffraction separately and its crystallographic orientation relationship was established with respect to its

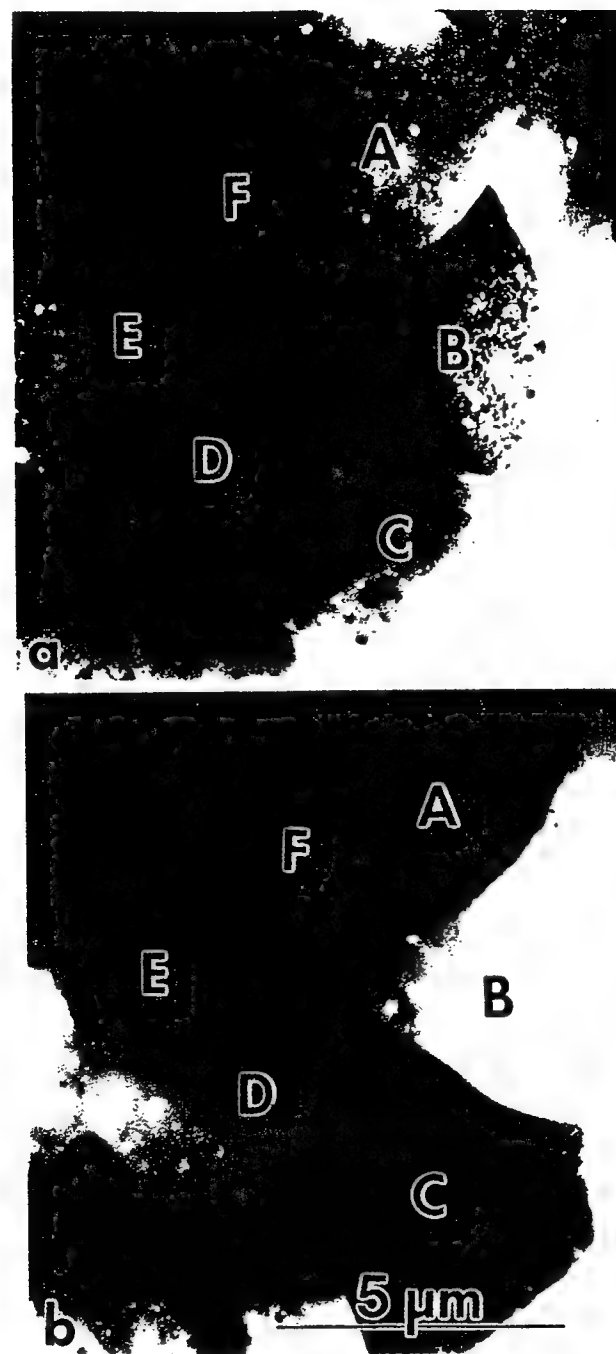


Figure 12 (a-f) - TEM images reveal crystallographic relation between aragonite platelets and domains. Images in (a) and (b) reveal that A-C-E are twin related to B-D-F, as confirmed by electron diffraction (image recorded with a slight tilt about the [001] axis that is normal to the plane of the paper).

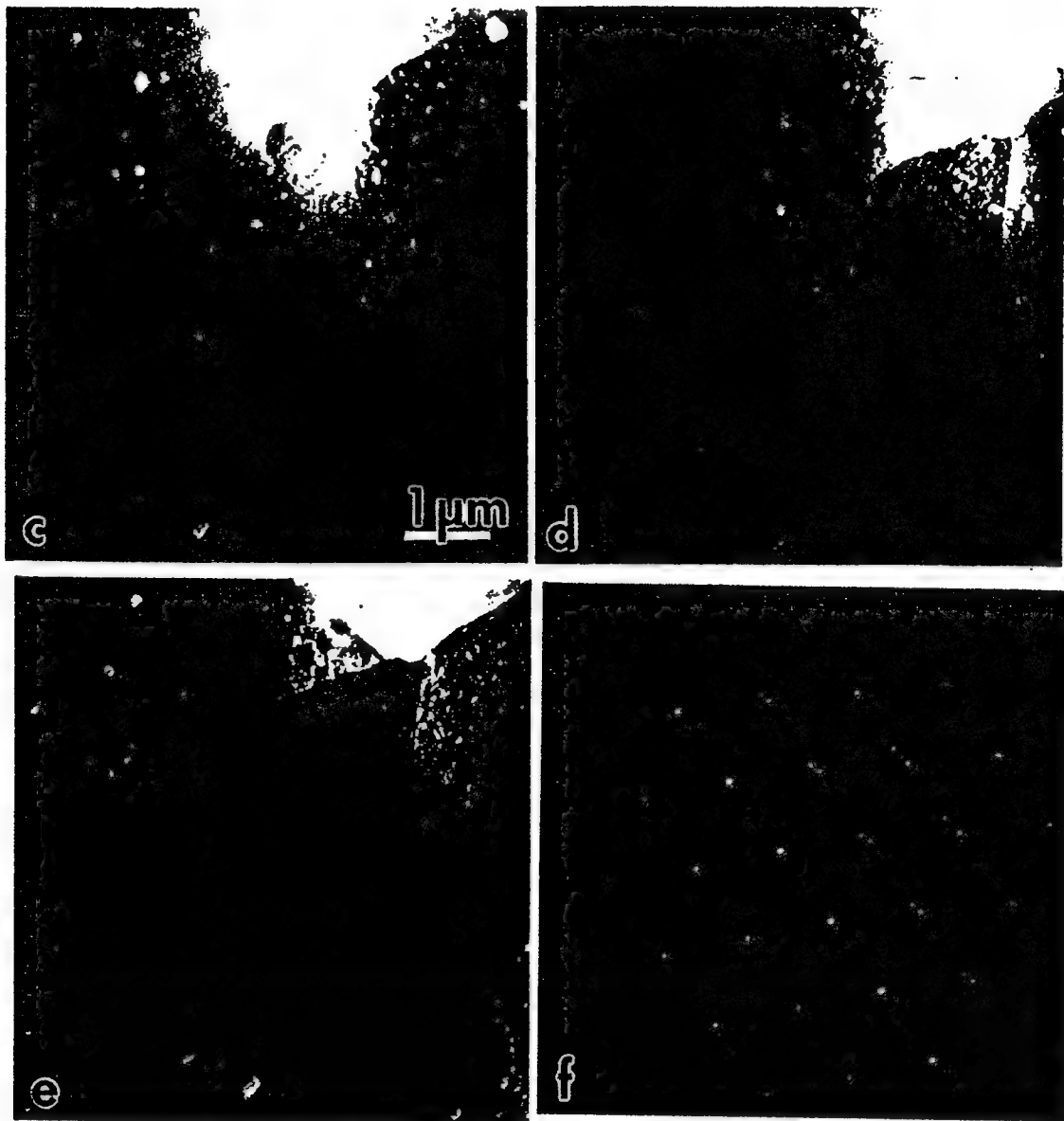


Figure 12 (cont.) Images in (c) and (d) are from a platelet in (e) containing four domains. [001] diffraction pattern (f) taken from a domain boundary in (e) reveals that the domains are twin related.

neighbors, both on the same layer and across the thickness of the nacre, hence, enabling us to complete a three-dimensional picture.³⁰ First, we found that adjacent platelets on the same layer belong to the same [001] zone axis with a slight rotation among them. The question

whether there is any crystallographic relationship between the *a* and *b* axes of platelets on the same layer was also answered; it was found that they are twin-related with a twin plane of {110} type.³⁰ In this scheme, all of the platelets on the same layer are twin-related whether they share a boundary or not, constituting *first generation twins* since this twinning takes place at the highest spatial scale (Figure 12 (a-b)). Further analysis indicated that each platelet consists of several domains which are crystallographically related (Figure 12 (c-f)). In fact, the diffraction patterns from all the domain boundaries show twin reflections with domains belonging to either (110) or (110) variant. Adjacent domains, therefore, are twin related and constitute the *second generation twins*.

The angle between each pair of domains in an ideal hexagonally-shaped platelet with six twin-related domains would be 60°. This is not possible, however, since the outer edges of the platelets are parallel to {110} planes. The angle between each pair of planes - for example, between (110) and (110) - is 63.5°; this leaves a 3.5° unaccounted for. This induces strain into the aragonite lattice and must be accommodated by some structural deformation, such as, by slip or twin formation. In the present case, nanometer-scale twins form on {110} planes, shown in Figure 12 (g), that are similar to growth twins in geological minerals. Since they occur at the smallest scale, these are called *third generation twins*.³⁰ (It was found that a portion of the lattice stress created by the 3.5°-strain can also be accommodated by the misalignment of adjacent domains, as frequently observed. This misalignment, however, cannot account for all the strain accommodation, as the interfaces between the domains show a high degree of coherency.) These three twin structures cover a size scale of six orders of magnitude, from the nanometer to the submillimeter, and reveal, for the first time, a hierarchical structure in a biological hard tissue.

4.4 A MODEL OF THE CONFORMATION OF ORGANIC MACROMOLECULES

The interaction between the species on an organic substrate and a crystalline organic phase must include geometrical, electrostatic, and stereochemical interactions.^{113-115,119,120,127-131} Therefore, the nucleation and growth of the crystals will be influenced by both the nearest neighbor interactions and those higher on the scale. The aragonite crystal structure

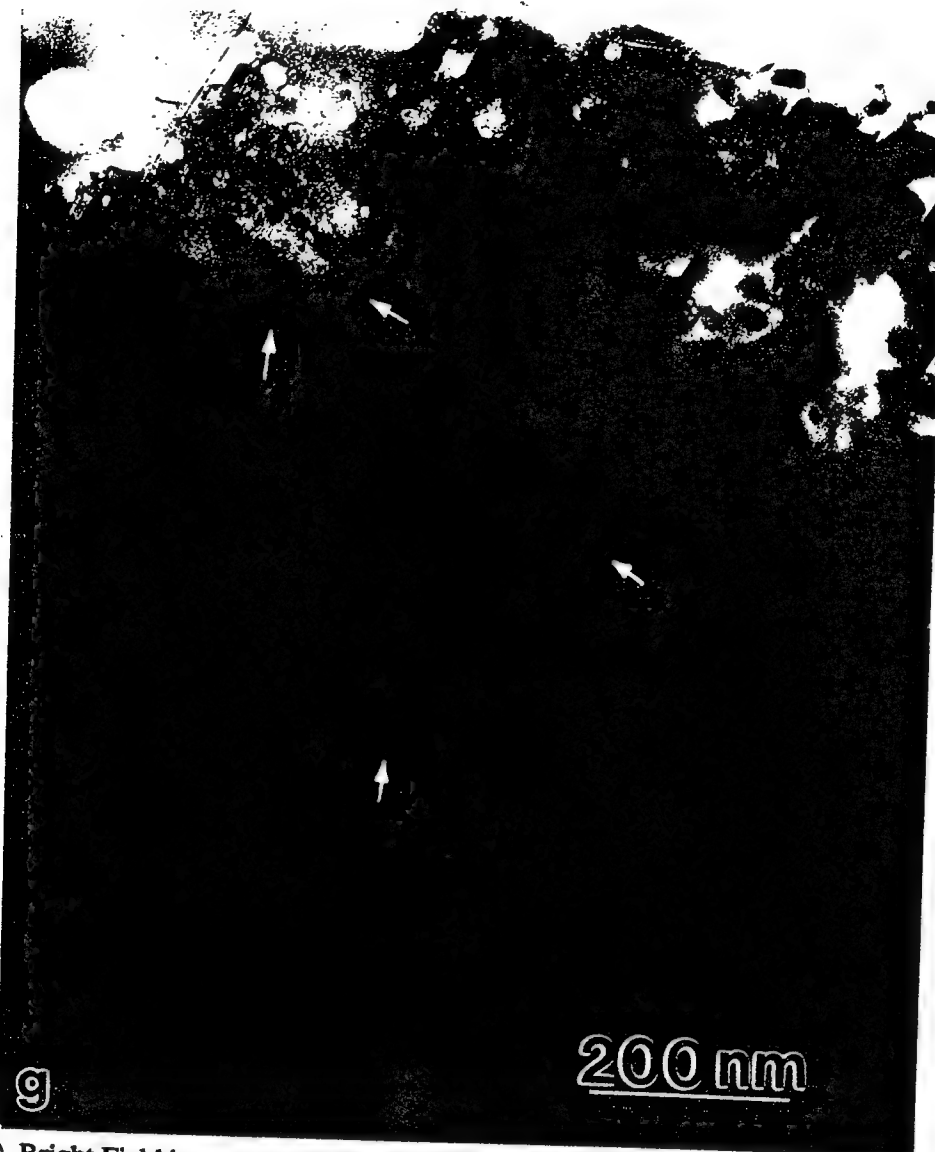


Figure 12 (g) Bright Field image taken in [001] orientation shows the ultrafine twins on two {110} variants within a domain.

belongs to the space group Pmcn (No. 62) with lattice parameters $a=4.94 \text{ \AA}$, $b=7.94 \text{ \AA}$, and $c=5.72 \text{ \AA}$.¹³² The location of Ca^{2+} ions in [001] projection is shown in Figure 12(a) giving the crystal a pseudo-hexagonal symmetry. In the unit cell, CO_3^{2-} groups would reduce the symmetry to an orthorhombic form.¹³² This is an important physical characteristic in terms of the crystallographic relationships of the hierarchical twinned components of the nacre

aragonite and the stereochemical relationship that might exist between the aragonite and the macromolecules in the organic matrix.

The nucleation and growth of the aragonite crystals may involve both Ca^{2+} and other ions, but for simplicity, only the arrangement of Ca^{2+} ions is illustrated in Figure 13. True hexagonal closed-packed formation would require an axial ratio of $b/a = 1.63$; however, the observed value is only 1.69. In the actual aragonite lattice, the Ca^{2+} ions are not in contact but are separated by O^{2-} ions, and the pseudo-hexagonal arrangement refers to the centers of Ca^{2+} ions rather than their actual packing. Since the same {110} twinning takes place at all length scales, superimposition of the lattices on all three possible twins with a 63.5° angle with respect to each other generates a new superlattice structure based on the coincidence lattice sites (LCL)¹³³ and is called *superstructure*.^{30,134} [see Figure 13(c)]. Taking the actual distance between the Ca^{2+} ions as 3.94 Å, it is calculated that the distance between these lattice points would be about 30-40 Å. If the nucleation and growth of the aragonite platelets takes place on the underlying organic matrix, then the geometric configuration of the active sites for binding Ca^{2+} ions on the organic matrix must accommodate this superlattice and thus all twins in the nacre. To explain this phenomenon, it may reasonably be assumed that the binding sites on the template form a single crystalline pseudo-hexagonal lattice, or integer multiples of it. It is known that many two-dimensional membranes tend to form hexagonal lattices during self-assembly.¹³⁵ This hypothesis (that the organic matrix may be a single crystalline) is an essential structural feature for the formation of the highly organized platelets in nacre.^{30,134} The local crystalline organization of the matrix proposed earlier,^{90,114} with no relationship between the neighboring areas and therefore no long-range order, would result in aragonite crystals with no definite crystallographic orientation relationships.

By tracing the possible twin boundaries, the superlattice allows the generation of the hierarchical twin structure and all the shapes, geometry, and crystallography-related features, including five-edged platelets with 90° -domains, sixfold symmetry of platelets, and six- and three-edged domains.^{30,134} The fact that one can generate all the possible configurations in this way illustrates again that a pseudo-hexagonal template structure (and not the lattice of a single domain) might be a possible solution for the structure of an organic matrix that can

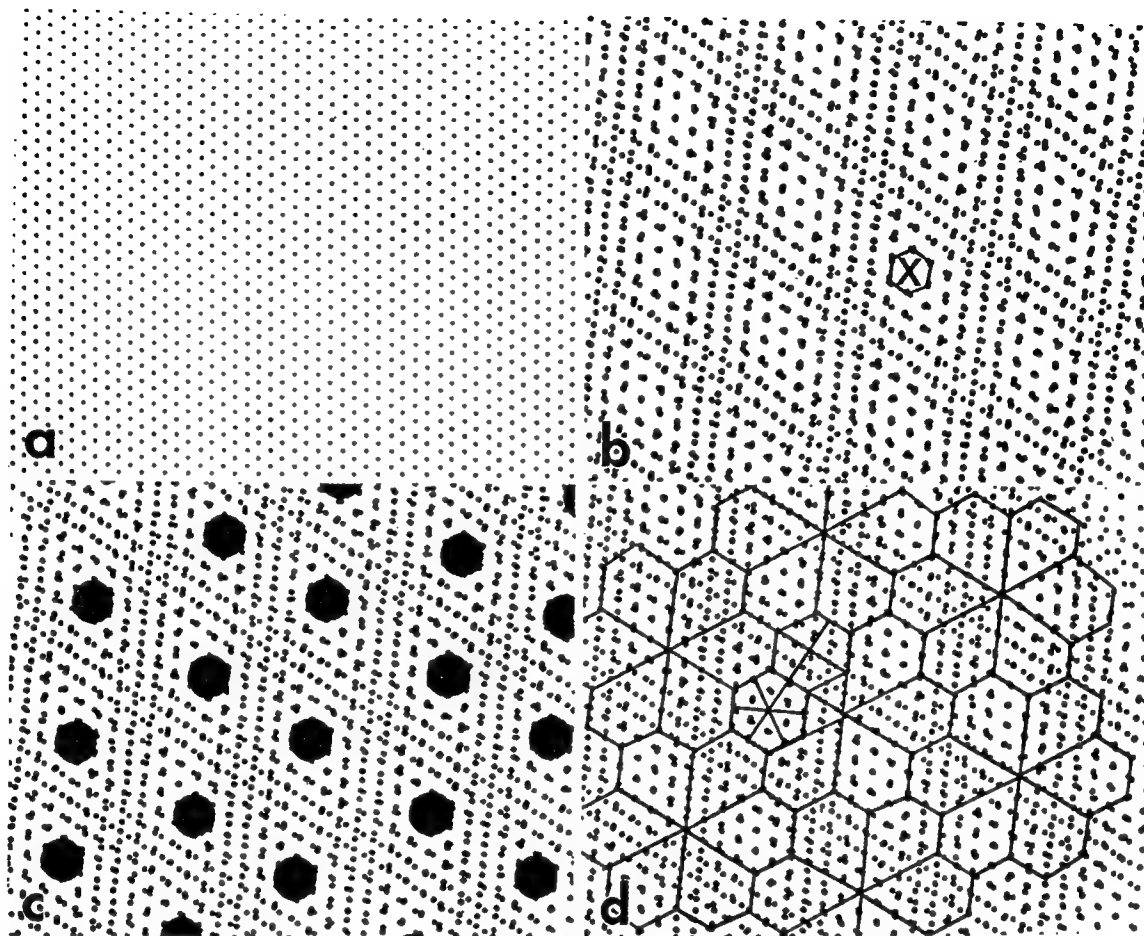


Figure 13 - (a) The model of the aragonite lattice in [001] projection with only Ca²⁺ ions highlighted. Superimposition of three lattices each with a successive rotation of 63.5° (angle between {110} planes) produces a Morie fringe pattern. (c) Highlighted coincidence lattice sites produce a pseudo-hexagonal pattern. (d) Platelets, which retain the crystallographic and morphological relations, can be drawn based on the CLS model.

accommodate all the twin relationships. The ultrastructure in the organic matrix would be single crystalline not only on the flat surface but also through the transverse direction of nacre as demonstrated from the twin orientation-relation of the crystals across the thickness direction as well.³⁰ The platelets do not leave space when packed on a given layer because of the crystallographic and geometrical requirements, whence called *space filling tiles*. The tiles (aragonite platelets) can have several different edges (3-, 4-, 5-, 6-edged) but still have

regular shape. Based on a mathematical description,¹³⁶ therefore, we call them *multiple tiles*.¹³⁷ Since the tiles also have domains at lower dimensional scale, we can call the configuration of the tiles within the nacre in three-dimensional space as multiple tiling with hierarchical twins.¹³⁷

5.0 GROWTH AND SHAPE FORMATION OF THE SHELL: MORPHOGENESIS

As discussed above, although six-fold twin structures also occur in geological aragonite,¹¹¹ the hierarchical arrangement in nacre is unique in that each platelet is separated from the others during the early stage of growth.^{134,137} This is illustrated in Figure 14 which shows the layers of aragonite are separated on the growing edge of the shell by a thin film of organic matrix, and the new platelets grow on it independently. In geological aragonite, by contrast, the mimetic twin domains grow in contact, one after the other, and each is influenced by the presence of another.^{111,112} In nacre, however, even after crystallization is complete, the platelets remain separated from each other by an organic membrane.¹³² The fact that separate platelets grow simultaneously and, yet, have a definite crystallographic orientation relationship suggests that the growth process might be mediated by the organic template beneath each of the individual crystals, as proposed earlier.^{114,115,119,120} In the following paragraphs, we discuss how these hierarchical twins might originate and the implications this has for the structure of the organic template on which the aragonite crystals are grown.

As can be determined from Figure 14, which was recorded from the growing edge of a juvenile abalone, the organic membranes actually form layers of sheet with an empty space between them which would eventually be filled with the inorganic material. Each layer occasionally separates into several sublayers, and this is repeated for many layers, seemingly in a random fashion, throughout the thickness. This suggests a hierarchical organization of the organic membrane as well. The production of further organic layers originating from a single membrane also has significant implications in terms of the mechanism of self-assembly of the macromolecules that make up the framework of the organic matrix. Although attempts have been made in the literature,^{119,126,135-137} a clear description

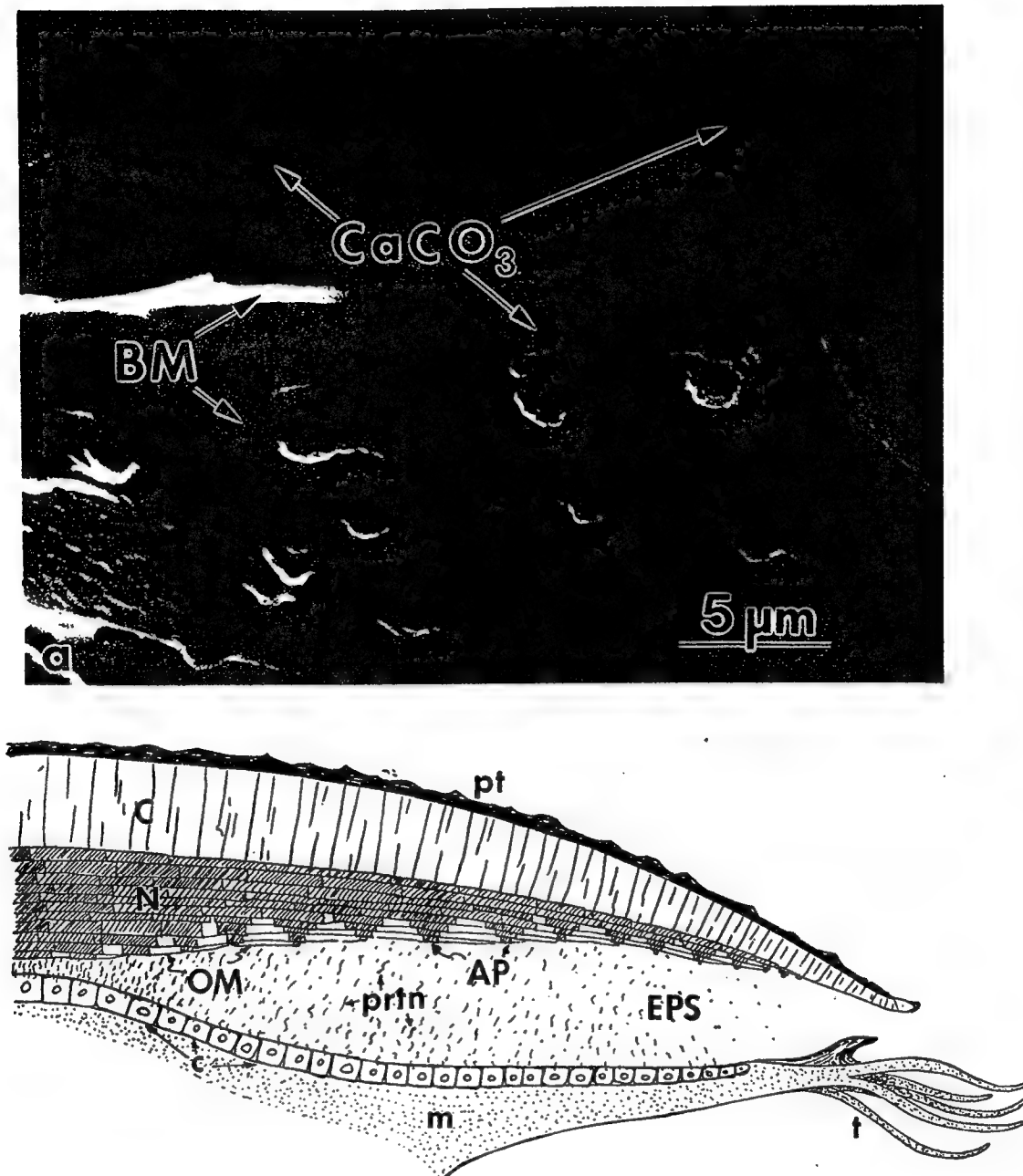


Figure 14- (a) Secondary electron image of the growing edge of a juvenile red abalone in an edge-on view shows organic matrix (BM) between the newly forming aragonite platelets (CaCO_3) in a columnar organization. Notice the bottommost organic layer with newly formed aragonite nuclei. (b) A schematic drawing illustrate the growing edge of the abalone shell. C: prismatic layer; N: nacreous layer; EPL: extrapallial space; pt: periostracum; c: cells; prtn: self assembling proteins and polysaccharides; m: muscle of the foot; t: tentacles, OP: organic matrix; and AP: aragonite platelets.

explaining how the successive single layers form in the nacre, or any other hard tissue has not been established. The best description so far has been the presence of compartments which would initially form as small boxes on top of the older, much larger. These would then eventually grow as the inorganic crystallites form within them. It has not been clear, in this scheme, called compartmentalization, how the layers actually come to being in the first place, and how each compartment would form and be enlarged.

Here, we see for the first time, that successive layers form from an original membrane as subsidiary layers, which would themselves act as originators of further subsidiary layers in a cascading fashion.¹³⁷ This mechanism is similar to reproduction of cells in organisms in making new cells and subcellular features (such as organelles). If this scheme is correct, then the layers must be in closer scrutiny by the organism than what has been hitherto thought as merely being formed through self-assembly. In other words, the cell membrane formation is a further step up in the hierarchy of making cells than the self-assembly of macromolecules which is a quaternary step in the organization of macromolecules in organisms, such as protein clusters, or structural polysaccharides. It can also be noted, in this case, that both proteins and polysaccharides are thought to be present in the organic matrix structures, adding more evidence that the organic matrix might be a membrane in the sense of the physiological terms. A membrane therefore, having proper proteins in their respective locations, both within the composite layers of the organic matrix and on certain locations of the membrane surfaces, would serve the function of being structural proteins, and of transport proteins regulating the passage of the inorganic ions in and out of the membrane for the formation of CaCO_3 on the surface. This description on the formation and the function of the organic matrix as, what we will call, a *pseudomembrane*,¹³⁷ is conjectural and requires further, careful study. These studies would be essential to find the true nature of structures and growth of hard tissues. (Future investigations may involve, for example, either *in vitro* experiments using detailed histochemical techniques, or *in vivo* observations of the growing edge of the nacre directly at the nanometer-scale to elucidate the growth process at the nanometer scale.¹³⁷)

It has been well recognized that the shapes of many mollusk shells can be described mathematically by a helico-spiral.^{138,139} This is demonstrated schematically in Figure 15(a)

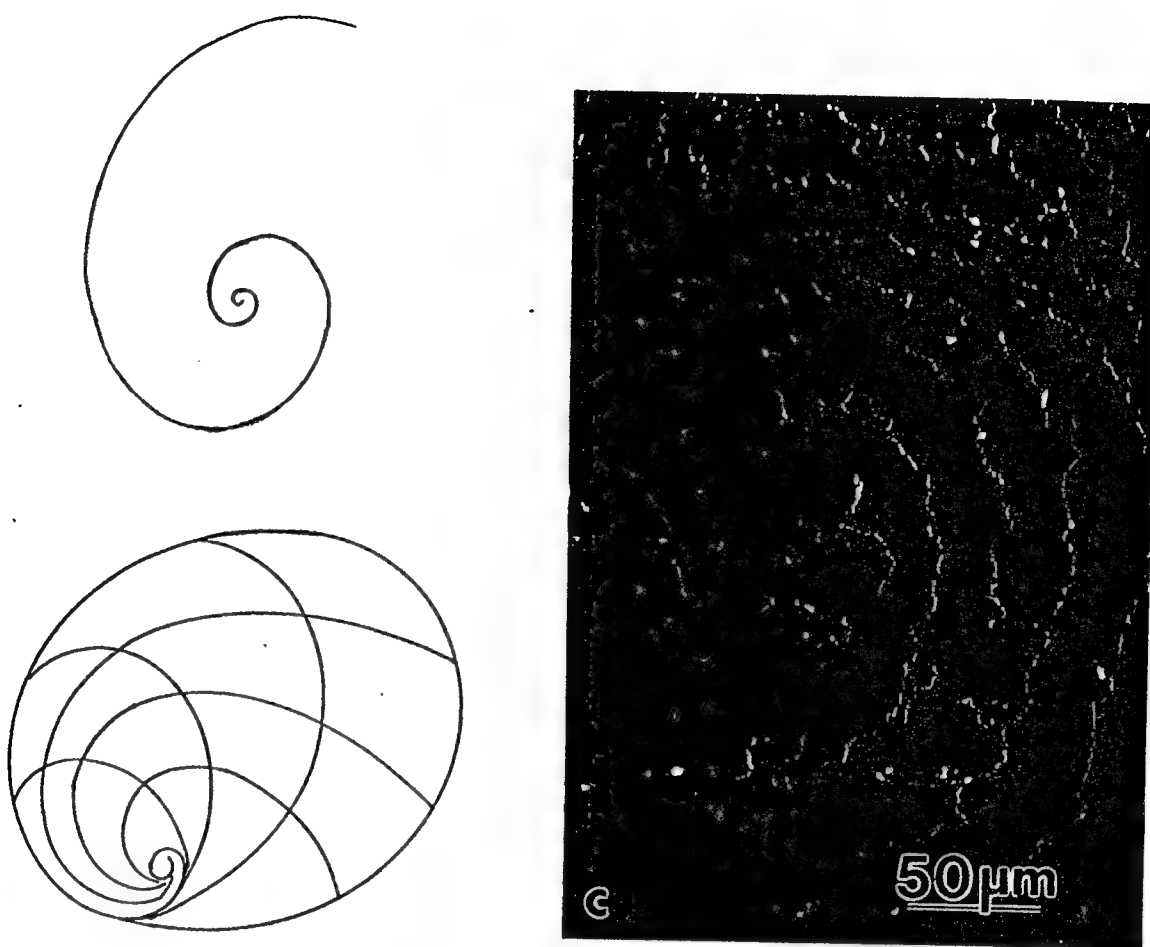


Fig. 15 - (a) Logarithmic spiral. (b) A schematic illustration of growth spirals of abalone shell. (c) Local spirals of aragonitic platelets in nacre (secondary electron image).

for abalone shell. In two-dimensions (x-y plane) the equation of the spiral is: $r = a e^\phi$ where r is the radius of the spiral at any position of the angle ϕ , a is a constant specific to a species of the mollusk. The depth is given to the shell by a variation in the third dimension, z . What has not been recognized so far, neither by biologists nor by mathematicians, however, is the possibility of the design of the overall shape of the shell based on the underlying organic matrix within the hard tissue.^{138,139} This design may be a result of the structural interrelationship between the crystallography of the aragonite lattice and the crystallographic conformation of the Ca^{2+} -binding (or CO_3^{2-} -binding) matrix nucleator

proteins. For instance, assuming that macromolecular conformation based on the proposed superstructural model above provides a template for the CaCO₃ formation, then the growth of an individual aragonite platelet follows a spiral (Figure 15(b)). Furthermore, this growth scheme may allow adjacent platelets to grow in a spiral manner, as demonstrated in the SEM image in Figure 15(c). Spiral growth of platelets in local regions along and behind the growing edge of the shell would lead to the growth of the shell at hierarchically higher scales, eventually leading to the final specific shape of each of the mollusk species. In this proposed growth scheme, therefore, the overall morphology of the shell is designed at the molecular scale by the organic matrix.¹³⁷ In terms of biomimetics, this hypothesis, if proven correct, may have implications in net-shape formation of technological ceramics, and, therefore, constitutes another important area of future investigation.¹⁴⁰

7.0 SUMMARY AND FUTURE DIRECTIONS

We have reviewed the results of some of the recent studies on mechanical properties and structure of the nacre section of mollusks. Nacre, which is about 95 vol. % aragonite and about 5 vol. % organic macromolecules, has fracture toughness and fracture strength properties that are orders of magnitude higher than those of monolithic aragonite. The inorganic and organic components in nacre have a high degree of organization not encountered in synthetic materials. From our analysis of toughening and strengthening mechanisms, we can conclude that the unique structure of nacre is responsible for these superior properties. The current understanding of these toughening and strengthening mechanisms, and their relation to the sizes of the component phases, is far from complete.

Morphological and crystallographic analyses by electron microdiffraction of the inorganic phase biogenic aragonite indicate that the individual aragonite platelets in nacre form a multiple tiling system in which twins form hierarchical defect structures to control the overall structural order. Assuming that crystal-matrix recognition is applicable, a model is forwarded for the structural conformation of the active sites in the organic matrix which may then act as the template for the formation of nacre. This model, called the *superstructure*, explains all the experimentally observed crystallographic and morphological relationships in the aragonite phase. The geometric and crystallographic model of aragonite platelets

proposed in this review is referred to as *multiple tiling*, as discussed. It appears that nature has utilized this mathematical technique in nacre to form a highly ordered structure compatible with both the soft component and the crystalline and geometrical structural constraints of the hard component. Tiling may also play an important role in determining the overall shape formation of the nacre and its mechanical properties. Many mollusks species, such as gastropods, cephalopods and bivalves have aragonite platelets as the fundamental building blocks in their nacre, but they also have grossly different overall shapes. In red abalone, for example, the shell is quite flat and thick; in nautilus, the shell is round and thin and forms an elegant chambered structure in which even the separation walls of the chambers are made of nacre. In all these nacre structures, the aragonite platelets have more or less the same dimensions, about 0.2 to 0.8 mm thick and 5 to 10 mm long on the edge. On the other hand, the multiple tiling of the platelets and the crystallographic relationship between the platelets may differ in these organisms due to slightly different structures and compositions in their underlying organic matrices. Further studies on various species of these organisms of both the crystallography of the mineral component and the structural and compositional analyses of the organic matrices, are warranted if we are to discern their structures and the unifying, underlying principles for the organization and formation of the various shapes of shell containing nacre structures. A fundamental understanding of these structures is essential for the possible formation of synthetic composites through biomimetics.

This new approach, in which the structure of an organic material is indirectly deduced from detailed knowledge of the structural relationships among the subcomponents of the inorganic phase, may prove a viable approach for studying other biocomposites that also have a highly organized inorganic structure. This approach would serve as a new methodology, not only for studying the way the overall shape is determined in various species of mollusks, but also for understanding general biomineralization concepts in single and multicell organisms, including bone and teeth in higher organisms.

Despite considerable effort in the field, our understanding of the mechanisms that operate in nacre to create such a tough composite, and of the composition and structure of the organic matrix and its structural relationship with the inorganic phase are still limited. Some of the major issues, from which an agenda for future research may be drawn, are as follows:

- i. *On Mechanical Properties:* A quantitative understanding of the toughening and strengthening mechanisms in nacre is necessary because these mechanism depend upon the structural relationships of the organic and inorganic phases. Mechanical property evaluation of the overall shell, particularly under the dynamic conditions in which the organism lives and makes use of its multifunctional characteristics, is also essential for the design of multifunctional materials through biomimicking.

Future research should include proper testing techniques for measurement including interfacial properties, analysis of paths for crack propagation, and their micromechanical analyses. For this, the knowledge of actual properties of the individual phases (organic matrix and biogenic aragonite) are essential, which, in turn, requires careful analysis of true structures (substructures and defects (Figure 16) and compositions of the component phases. The coupling between the component phases and their size (size-effect) and conformation (crystallography) need to be studied to reveal sources of nanocomposite effects.

- ii. *On the Organic Matrix:* The protein and polysaccharide compositions in nacre, their conformations, identification as nucleator and framework macromolecules, and structural relationships of the organic matrix as well as its relationship to the inorganic aragonite phase are necessary parameters for consideration in the design of synthetic materials. Similarly, the relationship between the organic matrix and calcite in the prismatic layer should also be investigated.

Items (i) and (ii) will lead to structural design rules for biomimicking new materials.

- iii. *On the Mechanism of Growth and Morphogenesis:* An investigation of the nucleation of the inorganic phase in the presence of an organic matrix, beginning at the embryonic and juvenile stages of the mollusk and comprehension of the degree to which the organic matrix controls growth will assist the understanding the overall formation and shaping of the shell.
- iv. *On Biomimicking:* New synthetic strategies are necessary to process thinner ceramic, metal, and polymeric layers for ceramic-metal and ceramic-polymer composites with

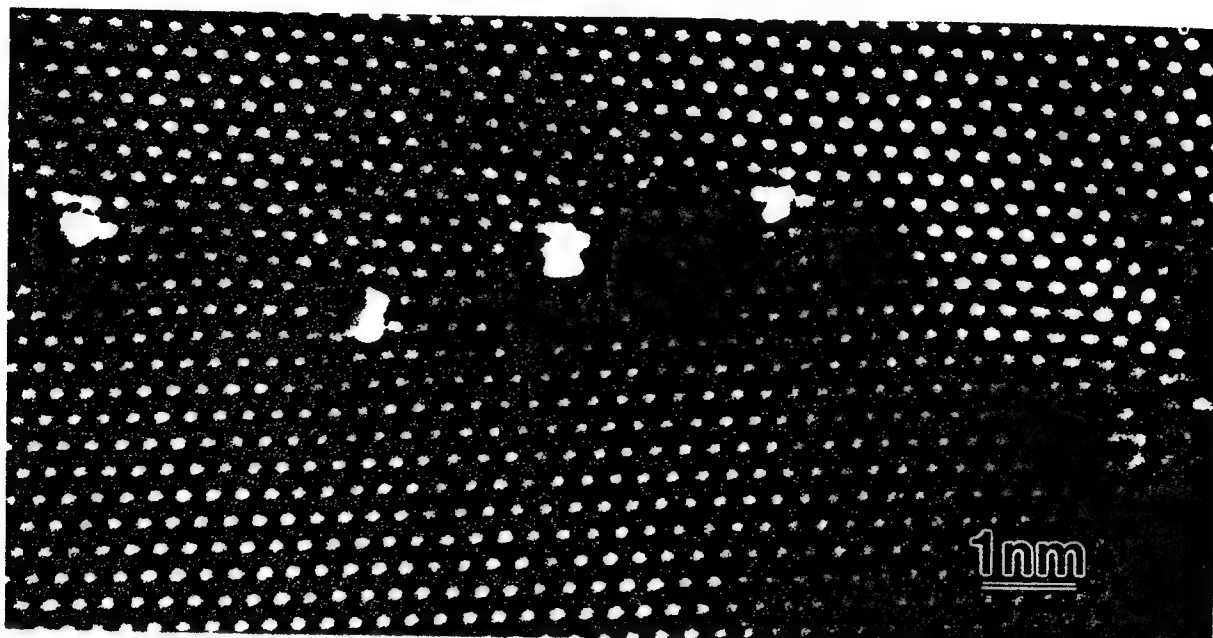


Figure 16 - Atomic resolution transmission electron micrograph of a low-angle boundary in biogenic aragonite in nacre of abalone displays dislocation core structures in the [001] electron beam direction (recorded at 400 kV). Although it is unusual for aragonitic lattice, as an ionic crystal, to have such defects, they are common substructural features in biogenic aragonite crystals.

controlled substructures and interfaces, controlled lamination to achieve novel layered composites with desired microarchitecture.

- v. *On Bioduplication:* Fundamental studies involving *in vitro* isolation, purification, and self-assembly of various components of the shell organic matrices, separately and in combination, are essential as the ground work. These would be followed by biomimetic mineralization of CaCO_3 and other biogenic ceramics on biogenic or engineered organic matrices under controlled conditions leading to a fundamental understanding of how the synthesis and structural evolution of hard biological structures might be controlled. Finally, these studies would open up new avenues in bioduplication of technologically more significant ceramics, such as Fe_3O_4 and BaTiO_3 , in various morphological forms (particles, platelets, laminates, and thin films).

Both biomimicking and, eventually, bioduplication may prove invaluable tools for the materials engineer. Using these methods to design and process novel materials similar to biogenic multifunctional, nanolaminated composites like nacre, however, will be deferred until we answer the crucial questions discussed regarding the structure and function of this and similar other biocomposite systems.

8.0 ACKNOWLEDGMENTS

This work was performed under the sponsorship of Air Force Office of Scientific Research under Grant # AFOSR-91-0281, and Army Research Office, Grant # DAAL03-92-G-0241.

9.0 REFERENCES

1. See, for instance, i. P. Haasen, *Physical Metallurgy* (Cambridge University Press, London, 1978); *Ceramic Microstructures*, R. M. Fulrath and J. A. Pask (eds.) (University of California Press, Berkeley, 1966); ii. *High Performance Polymers*, E. Baer and A. Moet (eds.) (Hanser, Munich, 1991).
2. i. Nippon-to no kagateki kenkyu, K. Tawara (Tokyo, 1953); ii. H. Tanimura, "Development of the Japanese Sword," *JOM*, 32 [2] 63-73 (1980); iii. *A Search for Structure*, C. S. Smith (MIT Press, Cambridge, 1981) pp. 66-72; iv. O. D. Sherby, T. Oyama, D. W. Kum, and J. Wadsworth, *JOM*, 37 [6] 50-56 (1985).
3. R. P. Anders et al., "Research Opportunities on Clusters and Cluster Assembled Materials," *J. Mater. Res.*, 4, 704-496 (1989).
4. See, for instance, *Decomposition of Austenite by Diffusional Processes*, V. F. Zackay and H. I. Aaronson (ed.) (Interscience, New York, 1962).
5. *Phase Transformations in Metals and Alloys*, D. A. Porter and K. E. Easterling (Van Nostrand Reinhold, Berkshire, UK, 1981) Chp. 5.
6. i. G. S. Kreimer, "Strength of Hard Alloys," Consultants Bureau, New York, 1968) pp. 1-30; ii. H. E. Exner and J. Gurland, "A Review of Parameters Influencing Some Mechanical Properties of Tungsten Carbide - Cobalt Alloys," *Powder Metallurgy*, 13, 13-31 (1970); iii. H. C. Lee and J. Gurland, "Hardness and Deformation of Cemented Tungsten Carbide," *Mater. Sci. Eng.*, 33, 125-133 (1978);

7. *Superalloys*, M. Gell, D. H. Duhl, and A. F. Giamei (ASM-International, Metals Park, OH, 1980).
8. i. D. Baral, J. B. Ketterson, and J. E. Hilliard, "Mechanical Properties of Compositionally Modulated Cu-Ni Foils," *J. Appl. Phys.*, **57** [4] 1076-1084 (1985); ii. Anomalous Increase in the Strength of In-Situ Formed Ultrafine Cu-Nb Multifilamentary Composites," *J. Appl. Phys.*, **49** [12] 6031-6038 (1979); iii. *Metallic Superlattices*, T. Shinjo and T. Takada (eds.) (Elsevier, Amsterdam, 1987).
9. See, for instance, *High Temperature Superconductors: Relationships Between Properties, Structure, and Solid-State Chemistry*, J. D. Jorgensen, K. Kitazawa, J. M. Tarascon, M. S. Thomson, and J. B. Torrance (eds.) Proc. of MRS, Vol. 156 (Materials Research Society, Pittsburgh, 1989).
10. J. F. Scott and C. A. Paz de Araujo, "Ferroelectro Memries," *Science*, **246**, 1400-1405 (1989).
11. i. R. Bringer, U. Herr, and H. Gleiter, "Nanocrystalline Materials - A First Report," *Trans. Jap. Inst. Metall.*, Suppl., **27**, 43-52 (1986); ii. *Microclusters*, S. Sugano, Y. Nishina, and S. Ohnishi (eds.) (Springer and Verlag, Amsterdam, 1987); iii. L. E. Brus, "Semiconductor Crystallites," *Acc. Chem. Res.*, **23**, 183-188 (1990).
12. See, for example, *Layered Structures, Epitaxy, and Interfaces*, J. M. Gibson and L. R. Dawson (eds.) Vol. 37 (Materials Research Society, Pittsburgh, 1984)
13. See, for instance, *Epitaxial Heterostructures*, D. W. Shaw, J. C. Bean, V. G. Keramidas, and P. S. Peercy (eds.) Proc. of MRS, Vol. 198 (Materials Research Society, Pittsburgh, 1989).
14. See, for instance, i. R. T. Bate, "The Quantum Size Effect: Tomorrow's Transistors," *Scientific American*, **258** [3] 96-106 (1988); ii. *Clusters and Cluster-assembled Materials*, R. S. Averback, D. L. Nelson, and J. Bernhole (eds.) Proc. of MRS, Vol. 206 (Materials Research Society, Pittsburgh, 1991); iii. *Microclusters*, S. Sugano, Y. Nishina, and S. Ohnishi (eds.) (Springer and Verlag, Heidelberg, 1987).
15. *Smart Structures and Materials*, 1993 North American Conference, Albuquerque, New Mexico, U.S.A., Jan. 31 - Feb. 4, 1993.
16. R. E. Newnham and G. R. Rushan, "Smart Electro-ceramics," *J. Am. Ceram. Soc.*, **74** [3] 463-480 (1991).

17. For instance, see, *Materials Research Bulletin*, **12** [3] (1987); also, ii. R. E. Newnham, S. E. McKinstry, and H. Ikawa, "Multifunctional Ferroic Nanocomposites," in: *Multifunctional Materials*, D. R. Ulrich, F. E. Karasz, A. J. Buckley, and G. Galaher-Daggitt (eds.) Proc. of MRS, Vol. 175 (Materials Research Society, Pittsburgh, 1990) pp. 161-168.
18. E. Baer, A. Hiltner, and R. J. Morgan, "Biological and Synthetic Hierarchical Composites," *Physics Today*, October, 60-67 (1992).
19. *Mechanical Design in Organisms*, S. A. Wainwright, W. D. Briggs, J. D. Currey, and J. M. Gosline (eds.) (John Wiley & Sons, New York, 1976).
20. J. D. Currey, "Biological Composites," *J. Mater. Edu.* **9** [1-2] 118-296 (1987).
21. i. *Biomineralization*, K. Simkiss and K. M. Wilbur (Academic Press, New York, 1989); ii. *On Biominerization*, H. A. Lowenstam and S. Weiner (Oxford University Press, New York, 1989); iii. *Biominerization: Chemical and Biochemical Perspectives*, S. Mann, J. Webb, and R. J. Williams (eds.) (VCH Publishers, Weinheim, 1989).
22. i. P. Calvert and S. Mann, "Synthetic and Biological Composites Formed by *in situ* Processing," *J. Mater. Sci.*, **23**, 3801-3815 (1988); ii. *Materials Synthesis Using Biological Processes*, P. C. Rieke, P. D. Calvert, and M. Alper (eds.), Proc. of MRS, Vol. 174 (Materials Research Society, Pittsburgh, 1990); iii. *Materials Synthesis Based on Biological Process*, M. Alper, P. D. Calvert, R. Frankel, P. Rieke, and D. Tirrell (eds.) Proc. of MRS, Vol. 218 (Materials Research Society, Pittsburgh, 1991); iv. *Hierarchically Structured Materials*, I. A. Aksay, E. Baer, M. Sarikaya, and D. A. Tirrell (eds.), Proc. of MRS, Vol. 255 (Materials Research Society, Pittsburgh, 1992).
23. *Biochemistry*, C. K. Mathews and K. E. van Holde (The Benjamin/Cummings Publ. Co., Redwood City, CA, 1990).
24. H. A. Lowenstam, "Biological Minerals," *Science*, **211**, 1126-128 (1981).
25. T. Degens, "Molecular Mechanisms on Carbonate, Phosphate, and Silica Deposition in the Living Cell," *Top. Curr. Chem.*, **64**, 1-112 (1976).
26. i. M. Paulsson, "Basement Membrane Proteins: Structure, Assembly, and Cellular Interactions," *Critic. Rev. in Biochem. and Molec. Bio.*, **27** [1/2] 93-120 (1992); ii. W. A. Cramer, D. M. Engleman, and G. von Heijne, "Forces Involved in the Assembly and Stabilization of Membrane Proteins," *FASEB J.*, **6** [15] 3397-3405 (1992). ii. T.

- Hashimoto, K. Kimishama, and H. Hasegawa, "Self-Assembly and Patterns in Binary Mixtures of SI Block Copolymers and PPO," *Macromol.*, **24** [20] 5604-5710 (1991).
27. L. Addadi and S. Weiner, "Interaction between Acidic Proteins and Crystals: Stereochemical Requirements in Biomineralization," *Proc. Natl. Acad. Sci., USA, Biophysics*, **82**, 4110-4114, (1985).
 28. i. H. R. Crane, "Principles and Problems of Biological Growth," *Sci. Monthly*, **70**, 376-389 (1950); ii. S. Mann, "Mineralization in Biological Systems," *Structure and Bonding*, Vol. 54 (Springer-Verlag, Berlin, 1983) pp. 125-174.
 29. K. M. Wilbur, "Shell Formation and Regeneration," in *Physiology of Mollusca*, K. M. Wilbur and C. M. Yonghe (eds.) Vol. 1 (Academic Press, New York, 1964) p. 243.
 30. M. Sarikaya and I. A. Aksay, "Nacre of Abalone Shell: a Natural Multifunctional Nanolaminated Ceramic-Polymer Composite Material," Chapter 1, in: *Results and Problems in Cell Differentiation in Biopolymers*, Steven Case (ed.) (Springer and Verlag, Amsterdam, 1992) pp. 1-25.
 31. L. Addadi and S. Weiner, "Interactions between Acidic Macromolecules and Structured Surfaces; Stereochemistry and Biomineralization," *Mol. Cryst. Liq. Cryst.*, **134**, 305-322 (1986).
 32. Y. Bouligand, "Sur une architecture torsadée repandue dans de nombreuses cuticules d'arthropodes," *C R Hebd. Sceances Acad. Sci.*, **261** [12] 3665-3668 (1965).
 33. M-M. Giraud-Guille, "Liquid Crystalline Order of Biopolymers in Cuticles and Bones," in *Microscopy of Self-Assembled Materials and Biomimetics*, Special Issue of *J. Microsc. Res. Tech.*, M. Sarikaya (ed.) (to be published in 1993).
 34. *Iron Biominerals*, B. Frankel and R. P. Blakemore (eds.) (Plenum, New York, 1991).
 35. M. Gosline, M. E. DuMont, and M. W. Denny, "Structure and Properties of Spider Silk," *Endeavour* **10** [1] 37-43 (1986).
 36. M. Denny and J. M. Gosline, "The Physical Properties of the Terrestrial Slug," *J. Exp. Biol.*, **88**, 375-393 (1980).
 37. A. I. Caplan, "Cartilage," *Sci. Amer.*, **251** [4] 84-94 (1984).

38. *Biochemistry of Collagen*, G. N. Ramachandran and R. H. Reddi (eds.) (Plenum Press, New York, 1976); ii. Y. Bouligand and M. M. Giraud-Guille, "Spatial Organization of Collagen Fibrils in Skeletal Tissues: Analogies with Liquid Crystals," in: *Biology of Invertebrate Collagens*, A. Bairati and R. Garrone (eds.) (Plenum, New York, 1985) pp. 115-134. iii. E. Baer, J. J. Cassidy, and A. Hiltner, "Hierarchical Structure of Collagen and Its Relationship to the Physical Properties of Tendon," Chapter 9, in: *Collagen: Biochemistry and Biomechanics*, M. E. Nimi (ed.) (CRC Press, Inc., New York, 1988) pp. 177-199; iv. P. Borstein and W. Traub, "The Chemistry and Biology of Collagen," in *The Proteins*, H. Neurath and R. L. Hill (eds.) 3rd Ed. (Academic Press, New York, 1979) pp. 412-632.
39. W. M. Kier and K. K. Smith, "Tongues, Tentacles, and Trunks: Biomechanics of Movement in Muscular Hydrostats," *Zool. J. Linn. Soc.*, **83**, 307-324 (1985).
40. *Introduction to Plant Biochemistry*, T. W. Goodwin and E. I. Mercer (Pergamon, Oxford, 1983).
41. See, for instance, References 20, 21, 25, and 30.
42. See, for instance, A. Boyde, "Comparative Histology of Mammalian Teeth," in *Dental Morphology and Evolution*, A. A. Dahlberg (ed.) (Chicago University Press, Chicago, 1971) pp. 81-94. Also, see Reference 43.
43. *Chemistry and Biology of Mineralized Tissues*, H. C. Slavkin and P. Price (eds.) (Excerpta Medica, Elsevier, Amsterdam, 1992).
44. K. Markel and P. Gorny, Zur Funktionellen Anatomie der Seeigelzahne (Echinodermata and Echinoidea), *Z. Morphol. Tiere*, **75**, 223-242 (1973).
45. K. M. Towe, "Echinoderm Calcite: Single Crystal or Polycrystalline Aggregate," *Science*, **157**, 1048-1050 (1967).
46. i. R. P. Blakemore, "Magnetotactic Bacteria," *Science* **190**, 377-379 (1975); ii. R. P. Blakemore, "Magnetotactic Bacteria," *Ann. Rev. of Microbiology*, **36**, 217-238 (1982).
47. C. T. Dameron, R. N. Reese, R. K. Mehra, A. R. Kortan, P. J. Carroll, M. L. Steigerwald, L. E. Brus, and D. R. Winge, "Biosynthesis of Cadmium Sulfide Quantum Semiconductor Crystallites," *Nature*, **338**, 596-597 (1989).

48. i. *Enzyme Structure and Mechanism*, A Fersht, 2nd Ed. Chps. I and II (Freeman, New York, 1985); ii. M. Alper, "Enzymatic Synthesis of Materials -- An Overview," in *Materials Synthesis Based on Biological Processes*, M. Alper, P. Calvert, R. B. Frankel, P. Rieke, and D. A. Tirrell (eds.) Proc. MRS Symp., Vol. 218 (Materials Research Society, Pittsburgh, 1991) pp. 3-6.
49. S. F. Mathews, "The Structure, Function, and Evolution of Proteins," *Prog. Biophys. Mol. Sci.*, **45**, 1-56 (1985).
50. M. Fournier, H. S. Creel, K. P. McGrath, M. T. Krejchi, E. D. T. Atkins, T. L. Mason, and D. A. Tirrell, "Genetic Synthesis of Periodic Protein Materials," *J. Biocat. Compat. Polymers*, **6**, 326-338 (1991).
51. *Research Opportunities for Materials with Ultrafine Microstructures*, National Research Council (National Academy Press, Washington, DC, 1989).
52. P. M. Harrison, P. J. Artymiuk, G. C. Ford, D. M. Lawson, J. M. A. Smith, A. Treffry, and J. L. White, "Ferritin: Function and Structural Design of an Iron-Storage Protein," in *Biomineralization: Chemical and Biochemical Perspectives*, edited by S. Mann, J. Webb, and R. J. P. Williams (eds.) (VCH, Weinheim, 1989) pp. 257-294.
53. i. B. Frankel, R. P. Blakemore, and R. S. Wolfe, "Magnetite in Freshwater Magnetotactic Bacteria," *Science*, **203**, 1355-1356 (1979); ii. R. P. Blakemore, "Magnetotactic Bacteria," *CRC Critical Rev. in Biochem.*, **20** [4] 365-380 (1986).
54. D. A. Bazylinski, R. B. Frankel, A. Garrat-Reed, and S. Mann, "Biomineralization of Iron Sulfides in Magnetotactic Bacteria from Sulfidic Environments," in *Iron Biominerals*, R. B. Frankel and R. P. Blakemore (eds.) (Plenum Press, New York, 1991) pp.239-256;
55. i. B. M. Moskowitz, R. B. Frankel, P. J. Flanders, R. P. Blakemore, and B. B. Schwartz, "Magnetic Properties of Magnetotactic Bacteria," *J. Magn and Magnetic Mater.*, **73**, 273-280 (1988); ii. S. Krieger, G. J. Olson, J. J. Rhyne, R. P. Blakemore, Y. A. Gorby, and N. Blakemore, "Small Angle Neutron and X-Ray Scattering from Magnetic Crystals in Magnetotactic Bacteria," *J. Magnetism and Mag. Maters.*, **82**, 17-28 (1989); iii. K. M. Towe and T. T. Moench, "Electron-Optical Characterization of Bacterial Magnetite," *Earth and Planetary Sci. Lett.*, **52**, 213-220 (1981).
56. i. S. Mann, R. B. Frankel, and R. P. Blakemore, "Structure, Morphology, and Crystal Growth of Bacterial Magnetite," *Nature*, **310**, 405-407 (1984); ii. S. Mann, N. H. C. Sparks, and V. J. Wade, "Crystalliochemical Control of Iron Oxide Biominerization,"

- in *Iron Biominerals*, R. B. Frankel and R. P. Blakemore (eds.) (Plenum Press, New York, 1990).
57. M. Sarikaya, N. Pellerin, J. T. Staley, and I. A. Aksay, Unpublished Results (1992).
 58. J. F. Stoltz, S-B R. Chang, and J. L. Kirschvink, "Magnetotactic Bacteria and Single-Domain Magnetite in Hemipelagic Sediments," *Nature*, **321**, 849-851 (1986).
 59. W-H Shih, M. Sarikaya, W. Y. Shih, and I. A. Aksay, "Geometrical Arrangement of Magnetosomes in Magnetotactic Bacteria," in *Materials Synthesis Based on Biological Processes*, M. Alper, P. Calvert, R. B. Frankel, P. Rieke, and D. A. Tirrell (eds.) Proc. of MRS, Vol. 218 (Materials Research Society, Pittsburgh, 1991) pp. 109-114.
 60. i. See paper by D. A. Bazylinski and R. B. Frankel, "Biomineralization of Iron Sulfides in Magnetotactic Bacteria in Sulfidic Environments," in ref. 34., pp. 239-255, and also D. A. Bazylinski, A. J. Garratt-Reed, and R. B. Frankel, "Electron Microscopic Studies in Magnetcotactic Bacteria, in: *Microscopy of Self-Assembled Materials and Biomimetics*, M. Sarikaya (ed.) *J. Microsc. Res. Tech.* (to be published, 1993).; ii. M. Farina, D. M. S. Esquivel, and H. G. P. Lins de Barros, "Magnetic Iron-Sulphur Crystals from Magnetotactic Microorganisms," *Nature*, **343**, 256-258.
 61. i. *Membranemimetic Chemistry*, J. H. Fendler (Wiley-Interscience, New York, 1982); ii. J. H. Fendler, "Atomic and Molecular Clusters in Membrane Mimetic Chemistry," *Chem. Rev.*, **87** 887-899 (1987).
 62. i. H. Liu, G. L. Graff, M. Hyde, M. Sarikaya, and I. A. Aksay, "Synthesis of Ultrafine Multicomponent Particles Using Phospholipid Vesicles," in *Materials Synthesis Based on Biological Processes*, M. Alper, P. Calvert, R. B. Frankel, P. Rieke, and D. A. Tirrell (eds.) Proc. of MRS, Vol. 218 (Materials Research Society, Pittsburgh, PA, 1991) pp. 115-121; ii. Sung Pak, "Potential Application of Microemulsions in Ceramic Processing," M.S. Thesis (University of Washington, Seattle, 1979).
 63. I. A. Aksay, W. Y. Shih, and M. Sarikaya, "Colloidal Processing of Ceramics with Ultrafine Particles," in: Proc. *Third Ultrastructure Processing of Ceramics, Glasses, and Composites*, J. Brinker and D. R. Ulrich (eds.) ().
 64. Y. A. Gorby, T. J. Beveridge, and R. P. Blakemore, "Characterization of the Bacterial Magnetosome Membrane," *J. Bacteriology*, **170** [2] 834-841 (1988).
 65. Frankel-Bazylinsky, "Structure and Function of Magnetosomes in Magnetotactic Bacteria," this book, pp. 189-215.

66. E. Kniprath, "Ultrastructure and Formation of Sea Urchin Tooth," *Calcif. Tiss. Res.*, **14**, 211-228 (1974).
67. i. S. Weiner, "Organic Matrixlike Macromolecules Associated with the Mineral Phase of Sea Urchin Skeletal Plates and Teeth" *J. Exp. Zool.*, **234**, 7-15 (1985); ii. D. J. Veis, T. M. Albinger, J. Clohisy, M. Rahima, B. Sabsay, A. Veis, "Matrix Proteins of Sea Urchin *Lytechinus variegatus*," *J. Exp. Zool.*, **240**, 35-46 (1986); iii. A. Berman, L. Addadi, L. Leiserowitz, S. Weiner, M. Nelson, and A. Kvirk, "A Synchrotron X-ray Study of a Unique Protein-Calcite Composite Material," *Science*, **250**, 664-667 (1990).
68. M. Sarikaya, J. Liu, and I. A. Aksay, "Ultratructure of the Mineral Phase in Sea-Urchin Teeth," unpublished research (1992).
69. K. Brear and J. D. Curry, "Structure of the Sea-Urchin Tooth," *J. Mater. Sci.*, **11**, 1977-1978 (1976).
70. I. A. Aksay and M. Sarikaya, "Bioinspired Processing of Composite Materials" in *Ceramics: Toward the 21st Century, Centennial International Symposium*, S. Soga and A. Kato (eds.), (Japanese Ceramic Society, Tokyo, 1991) pp. 136-149.
71. *Fundamental Principles of Fiber Reinforced Composites*, K. H. G. Ashbee (Technomic Publishing, Lanchester, PA, 1989).
72. E. Baer, J. Kastelic, and A. Galeski, " , " *J. Connective. Tiss.,Res.*, **6**, 11- (1978); ii. E. Baer, J. J. Cassidy, and A. Hiltner, "Hierarchical structure of Collagen Composite Systems: Lessons from Biology," this book, pp. 13-34.
73. i. D. L. Kaplan, S. J. Lombardi, W. S. Muller, and S. A. Fossey, "Silks," in *Biomaterials*, D. Byrom (ed.) (Stockton Press, New York, 1991) pp. 1-53; ii. J. Gosline, C. Nichols, P. Guerette, A. Cheng, and S. Katz, "The Macromolecular Design of Spiders' Silks," this book, pp. 239-263.
74. *The Biology of Anthropod Cuticle*, A. Neville (Springer, Berlin, 1975).
75. M. M. Giraud-Guille, "Liquid Crystalline Order of Biopolymers in Cuticles and Bones," in *Microscopy of Self-Assembled Materials and Biomimetics*, M. Sarikaya (ed.) Special Issue of *J. Microsc. Res. Tech.* (to be published, 1993).
76. i. S. L. Gunderson and R. C. Schiavone, "The Insect Exoskeleton: A Natrural Structural Material," *JOM*, **41** [11] 80-82 (1989); ii. S. L. Gunderson and R. C. Schiavone,

- "Microstructure of an Insect Cuticle and Applications to Advanced Composites," this book, pp. 164-197.
77. H. Ghiradella, D. Aneshansley, T. Eisner, R. E. Silberglied, and H. E. Hinton, "Ultraviolet Reflection of Male Butterfly: Interference Color Caused by Thin-Layer Elaboration of Wing Scales, *Science*, **178**, 1214-1217 (1972).
 78. i. J. Semseth, R. J. Spontak, and K. Mortensen, "The Response of Microstructure to Processing in a Series of Poly (siloxaneimide) Copolymers," *J. Poly. Sci.*, Part B, **31** [4] 467-475 (1993); ii. R. J. Spontak, S. D. Smith, and A. Ashraf, "Morphological Studies of Linear (AB)_n Multiblock Copolymers and Their Blends," in *Microscopy of Self-Assembled Materials and Biomimetics*, M. Sarikaya (ed.) Special Issue of *J. Microsc. Res. Tech.* (to be published, 1993)..
 79. E. Baer, "Advanced Polymers," *Scientific American*, **255** [4] 178-190 (1986).
 80. J. Glimcher, "On the Form and Function of Bone: from Molecules to Organs" in *The Chemistry and Biology of Mineralized Biological Tissues: Wolff's Law Revisited*, A. Veis (ed.) (Elsevier, New York and Amsterdam, 1981) pp. 617-673.
 81. *Studies in the Development, Function, and Evolution of Teeth*, P. M. Butler and K. A. Joysey (eds.) (Academic, London, 1973).
 82. C. Grégoire, "Structure of the Molluscan Shell," in: *Chem. Zoology*, M. Florkin and M. Scheer, (eds.) (Academic Press, New York, 1972) pp. 45- 102
 83. i. J. D. Currey, "The Mechanical Properties of Some Molluscan Hard Tissues," *J. Zool. London*, **173**, 39-406 (1974); ii. D. Currey, "Further Studies on the Mechanical Properties of Mollusc Shell Material," *J. Zool. London*, **180**, 445-453 (1976).
 84. A. P. Jackson, J. F. V. Vincent, and R. M. Tunner, "The Mechanical Design of Nacre," *Proc. Roy. Soc. London*, **B234**, 415-440 (1988)
 85. M. Sarikaya, K. E. Gunnison, M. Yasrebi, and I. A. Aksay, "Mechanical Property-Microstructural Relationships in Abalone Shell," *Materials Synthesis Using Biological Processes*, P. C. Rieke, P. D. Calvert, and M. Alper (eds.) Proc.of MRS, Vol. 174 (Materials Research Society, Pittsburgh, 1990) pp.109-116.
 86. W. Schober, "Precipitated Calcium Carbonate: A Quite Market Expects Excellence," *Industrial Minerals*, No. 265, October Issue, 69-81 (1989).

87. i. H. Nakahara, G. Bevelander, M. Kakei, "Electron Microscopic and Amino Acid Studies on the Outer and Inner Shell Layers of *Haliotis rufescens*," *VENUS (Japn. Jour. Malac.)* **41** [1] 33-46 (1982); ii. G. Bevelander and H. Nakahara, "An Electron Microscopy Study of the Formation of the Nacreous Layers in the Shells of Certain Bivalve Molluscs," *Calc. Tiss. Res.*, **3**, 84-92 (1968).
88. i. K. Bandel, "Übergange von der Perlmutter-Schicht zu Prismatischen Schichttypen bei Mollusken," *Biomineralization*, **2**, 28-47 (1970); ii. K. M. Wilbur and K. Simkiss, "Calcified Shells," *Comprehensive Biochemistry*, **26A**, 229-295 (1968).
89. N. Watabe, "Studies on Shell Formation: XI. Crystal-Matrix Relationship in the Inner Layers of Mollusk Shells," *Ultrastr. Res.*, **12**, 351-370 (1965).
90. i. S. Weiner, W. Traub, and H. A. Lowenstam, "Organic Matrix in Calcified Exoskeletons," in *Biomineralization and Biological Metal Accumulation*, P. Westbroek and E. W. de Jong (eds.) (Dordrecht: Reidel, 1983) pp. 205-224; ii. S. Weiner, Y. Talmon, and W. Traub, "Electron Diffraction Studies of Molluscan Shell Organic Matrices and Their Relationship to the Mineral Phase," *Int. J. Biol. Macromol.* **5**, 325-328 (1983); iii. S. Weiner and W. Traub, "Macromolecules in Mollusc Shells and Their Functions in Biominerlization," *Phil. Trans. R. Soc. Lond.*, B **304**, 425-434 (1984); iv. D. Worms and S. Weiner, "Mollusk Shell Organic Matrix: Fourier Transform Infrared Study of the Acidic Macromolecules," *J. Exp. Zool.*, **237**, 11-20 (1986);
91. *The Biology of Marine Animals*, A. Nicol (Interscience, New York, 1960).
92. *Molluscs*, E. Morton, 5th Edition (Hutchinson, London, 1979).
93. i. H. Mutvei, "Ultrastructure of the Mineral and Organic Components of Molluscan Nacreous Layers," *Biomineralization* **2**, 48-72 (1970); ii. H. Mutvei, "Ultrastructural Characteristics of the Nacre in Some Gastropods," *Zool. Scripta*, **7**, 287-296 (1978).
94. *Physiology of Mollusca*, K. Wilbur and C.M. Yonge (eds.) (Academic Press, New York, 1964).
95. i. W. F. Brown Jr. and J. E. Srawley, "Plain Strain Fracture Toughness Testing of High Strength Metallic Materials," *ASTM Technical Publ. No 410* (American Society for Testing and Materials, Philadelphia, 1966); ii. *Plane Strain Fracture Toughness Testing*, ASTM E599 (American Society for Testing and Materias, Philadelphia, 1983).

96. J. D. Currey, "Mechanical Properties of Mother of Pearl in Tension," *Proc. Roy. Soc. London*, B196, 443-463 (1977).
97. *Deformation of Ceramic Materials II*, I. Tresler and R. C. Bradt, (eds.) *Materials Science Research*, Vol. 18 (Plenum Press, New York, 1984).
98. *Science and Technology of Zirconia*, N. Claussen, M. Ruhle, and A. Heuer (eds.) (American Ceramic Society, Inc., Columbus, Ohio, 1984); ii. S. M. Wiederhorn, "Brittle Fracture and Toughening Mechanisms in Ceramics," *Ann. Rev. Mater. Sci.*, 14, 373-403 (1984).
99. See, for instance, W. Dawidge, *Mechanical Behavior of Ceramics* (Cambridge University Press, Cambridge, 1979).
100. See, for instance, i. References 30 and 85, and also, ii. M. Yasrebi, G. H. Kim, D. L. Milius, M. Sarikaya and I. A. Aksay, "Biomimetic Processing of Ceramics and Ceramic-Based Composites," in: *Better Ceramics Through Chemistry-IV*, C. J. Brinker, D. R. Ulrich, and B. J. Zelinski (eds.) Proc. of MRS, Vol. 180 (Materials Research Society, Pittsburgh, 1990) pp. 625-635.
101. See, for example, *The Plastic Deformation of Metals*, W. K. Honeycombe (St. Martin's Press, New York, 1968).
102. A. A. Griffith "The Phenomena of Rupture and Flow in Solids," *Phil. Trans. CCXI A*, 163-198 (1920).
103. *An Introduction to Composite Materials*, D. Hull (Cambridge University Press Cambridge, 1981) pp. 81-85.
104. *British and Continental Arms and Armor*, C. H. Ashdown (Dover Publications, New York, 1975); ii. *Arrows Against Steel: The History of the Bow*, (Mason/Charter, New York, 1975); iii. V. Hurley, M. L. Wilkins, C. F. Cline, and C. A. Honodel, *Light Armor*, Report UCRL-7-1817, Lawrence Livermore National Laboratory, Livermore, CA, USA, (1969).
105. H. Silyn-Robertson and R. M. Sharp, "Crystal Growth and the Role of the Organic Network in Eggshell Biomineralization," *Proc. Roy. Soc. Lond.*, B 227, 303-324 (1986).

106. R. W. Rice, "Microstructure Dependence of Mechanical Behavior," in *Treatise on Materials Science and Technology*, Vol. II, *Properties and Microstructure*, R. K. McCrone (ed.) (Academic Press, New York, 1977) pp. 199-381.
107. i. A. G. Evans and R. M. MacMeeking, "On the Toughening of Ceramics by Strong Reinforcements," *Acta Metall.*, **34** [12] 2435-2441 (1986); ii. A. G. Evans, "High Toughness Ceramics," *J. Mater. Sci. Eng.*, **A105/106**, 65-75 (1988); iii. G. Evans and D. A. Marshall, "The Mechanical Behavior of Ceramic Matrix Composites," *Acta Met.* **37**, [10] 2567-2583 (1989).
108. S. Khanuja, "Processing and Structure-Property Relationships of Laminated B₄C-Polymer Composites," *MS Thesis* (University of Washington, Seattle, 1991).
109. G. H. Kim, "The Effect of Metallic Phase and Microstructure on the Strengthening Behavior of B₄C-Al Cermets, *Ph.D. Thesis* (University of Washington, Seattle, 1993).
110. See, for example, i. P. Boch, T. Chartier, and M. Huttepain, "Tape Casting of Al₂O₃/ZrO₂ Laminated Composites," *J. Am. Ceram. Soc.*, **69** [8] C191-C192 (1986); ii. H. Takeba and K. Morinaga, "Fabrication and Mechanical Properties of Lamellar Al₂O₃ Ceramics," *J. Ceram. Soc. Jap. Interntl. Ed.*, **96**, 1122-1128 (1988); iii. D. B. Marshall, J. J. Ratto, and F. F. Lange, "Enhanced Fracture Toughness in Layered Nanocomposites of Ce-ZrO₂ and Al₂O₃," *J. Am. Ceram. Soc.*, **74** [12] 2979-2987 (1991).
111. i. K. Towe and G. H. Hamilton, "Ultrastructure and Inferred Calcification of the Mature and Developing Nacre of Bivalve Mollusks," *Calc. Tiss. Res.*, **1**, 306-318 (1968); (ii) K. M. Towe and G. R. Hamilton, "The Structure of Some Bivalve Shell Carbonates Prepared by Ion-Beam Thinning," *Calc. Tiss. Res.*, **10**, 38-48 (1972).
112. (i) W. L. Bragg, "The Structures of Aragonite," *Proc. Roy. Soc. London, Ser. A*, **17** (1928); (ii) R. Wenk, D. J. Barber, and R. J. Reeder, "Microstructures in Carbonates" in *Reviews in Mineralogy*, Vol. 11, R. J. Reeder (ed.) (Miner. Soc. Amer., Washington D.C., 1983) p.301.
113. M. A. Crenshaw and H. Ristedt, "Histochemical and Structural Study of Nautiloid Septal Nacre," *Bomineralization*, **8**, 1-8 (1975).

114. S. Weiner, "Organization of Extracellularly Mineralized Tissues: a Comparative Study of Biological Crystal Growth," *CRC Crit. Rev. in Biochem.*, **20** [4] 365-380 (1986); ii. L. Addadi and S. Weiner, "Interaction between Acidic Macromolecules and Structured Crystal Surfaces, Stereochemistry and Biominerization," *Mol. Cryst. Liq. Cryst.* **13**, 305-322 (1990); L. Addadi and S. Weiner, "Control and Design Principles in Biological Mineralization," *Angew. Chem. Intl. Ed. Engl.*, **31**, 153-169 (1992).
115. S. Mann, "Molecular Recognition in Biominerization," *Nature*, **33**, 119-123 (1988).
116. J. A. Keith, S. A. Stockwell, D. H. Ball, W. S. Muller, D. L. Kaplan, T. W. Thannhauser, and R. W. Sherwood, "Characterization of the Complex Matrix of the *Mytilus Edulis* Shell and the Implications for Biomimetic Ceramics," in *Hierarchically Structured Materials*, I. A. Aksay, E. Baer, M. Sarikaya, and D. A. Tirrell (eds.), Proc. of MRS Symp., Vol. 255 (Materials Research Society, Pittsburgh, 1992) pp. 3-8.
117. M. A. Cariolou and D. E. Morse, "Purification and Characterization of Calcium-binding Conchiolin Shell Peptides from the Mollusc, *Haliotis rufescens*, as a Function of Development," *J. Comp. Physiol B.*, **157**, 717-729 (1988).
118. i. N. Watabe, "Crystal Growth of Calcium Carbonate in the Invertabrates," *Prog. Crystal Growth Charact.*, Vol. 4 (Pergamon Press, London, 1981) pp. 99-147; ii. C. Grégoire, "Structure of the Molluscan Shell," *Chem. Zool.*, **45**, 102-130 (1972); S. W. Wise, "Microarchitecture and Mode of Formation of Nacre (mother-of-pearl) in Pelecypods, Gastrapods, and Cephalopods," *Eclogae geal Helv.*, **63** [3] 775-797 (1970).
119. i. M. Greenfield, D. C. Wilson, and M. A. Crenshaw, "Ionotropic Nucleation of Calcium Carbonate by Molluscan Matrix," *Amer. Zool.*, **24**, 925-932 (1984); ii. A. Crenshaw, "Mechanism of Normal Biological Mineralization of Calcium Carbonates" in *Biological Mineralization and Demineralization*, G. H. Nancollas (ed.) (Springer, Berlin and New York, 1972) pp. 243-257.
120. i. S. Weiner and W. Traub, "X-ray Diffraction Study of the Insoluble Organic Matrix of Mollusc Shells," *FEEBS Letters*, **111** [2] 311-316 (1980); ii. S. Weiner and W. Traub, "Organic Matrix-Mineral Relationships in Mollusc Shell Nacreous Layers" in *Structural Aspects of Recognition and Assembly in Biological Macromolecules*, M. Balaban, J. L. Sussman, W. Traub, and A. Yonath, (eds.) (Balaban ISS, Yehevot Philadelphia, 1981) pp. 462-487; iii. S. Weiner and W. Traub, "Macromolecules in

- Mollusc Shells and Their Functions in Biomineralization," *Phil. Trans. R. Soc. London B* **304**, 425-434 (1984).
121. i. D. E. Morse, University of California, Santa Barbara, CA - private communication (1992); ii. D. Kaplan, Army Research Center, Natick, MA, private communication (1992); iii. C. E. Furlong, University of Washington, private communication (1993).
 122. C. E. Furlong and R. Humbert, "Design of Protein Producing Bioreactors for Self-Assembling Systems," in *Hierarchically Structured Materials*, I. A. Aksay, E. Baer, M. Sarikaya, and D. A. Tirrell (eds.), Proc. of MRS Symp., Vol. 255 (Materials Research Society, Pittsburgh, 1992) pp. 435-442.
 123. C. E. Furlong, R. Humbert, M. Sarikaya, and I. A. Aksay (Unpublished Research, 1993).
 124. K. Gunnison, M. Sarikaya, J. Liu, and I. A. Aksay, "Structure-Mechanical Property Relationships in a Biological Ceramic-Polymer Composite: Nacre," in *Hierarchically Structured Materials*, I. A. Aksay, E. Baer, M. Sarikaya, and D. A. Tirrell (eds.), Proc. of MRS Symp., Vol. 255 (MRS, Pittsburgh, 1992) pp. 171-183.
 125. N. Watabe , K. M. Wilbur, "Influence of the Organic Matrix on Crystal type in Molluscs," *Nature*, **188**, 334-336 (1960).
 126. R. Meenakshi, G. Donnay, P. L. Blackwelder, and K. M. Wilbur, "The Influence of Substrata on Calcification Patterns in Molluscan Shell," *Calc. Tiss. Res.*, **15**, 31-44 (1974).
 127. A. Crenshaw, "Mechanism of Normal Biological Mineralization of Calcium Carbonates" in *Biological Mineralization and Demineralization*, G. H. Nancollas (ed.) (Springer, Berlin and New York, 1972) pp. 243-257.
 128. S. Weiner, "Organization of Extracellularly Mineralized Tissues: a Comparative Study of Biological Crystal Growth," *CRC Crit. Rev. in Biochem.*, **20** [4] 365-380 (1986).
 129. S. Mann, "Biogenic Inorganic Materials," in *Inorganic Materials*, D. W. Bruce and D. O'Hare (eds.) (John Wiley & Sons, New York, 1992) pp. 237-294.
 130. i. L. Addadi, Z. Berkovitch-Yellin, I. Weissbuch, M. Lahav, L. Leiserowitz, "A Link between Macroscopic Phenomena and Molecular Chirality: Crystals as Probes for the Direct Assignment of Absolute Configuration of Chiral Molecules," in *Topics in*

Stereochemistry, Vol. 16 (Wiley, New York, 1986) pp. 1-85; ii. I. Weisbuch, L. Addadi, M. Lahav, and L. Leiserowitz, "Molecular Recognition at Crystal Interfaces," *Science*, **253**, 637-645 (1991).

131. i. S. Mann, B. R. Heywood, S. Rajam, and D. Birchall, "Controlled Crystallization of CaCO_3 under Stearic Acid Monolayer," *Science*, **334**, 692-695 (1988); ii. S. Mann, B. R. Heywood, S. Rajam, and J. D. Birchall, "Interfacial Control of Calcium Carbonate Under Organized Stearic Acid Monolayers," *Proc. R. Soc. Lond.*, A, **423**, 457-471 (1989); iii. S. Mann, B. R. Heywood, S. Rajam, and J. B. A. Walker, "Structural and Stereochemical Relationships between Langmuir Monolayers and Calcium Carbonate Nucleation," *J. Phys. D: Appl. Phys.*, **24**, 154-164 (1991).
132. *Crystal Structures*, R. W. G. Wyckoff (Interscience Publ., New York, 1960).
133. See, for instance, D. Romeu, "Decagonal Phase Model with Multiple Periods and Quasiperiodic Coincidence Lattice," *J. Non-Cryst. Solids*, **153/154**, 232-240 (1993).
134. J. Liu, M. Sarikaya, and I. A. Aksay, "A Hierarchically Structured Model Composite: A TEM Study of the Hard Tissue of Red Abalone," in *Hierarchically Structured Materials*, I. A. Aksay, E. Baer, M. Sarikaya, and D. A. Tirrell (eds.), Proc. of MRS Symp., Vol. 258: (Materials Research Society, Pittsburgh, 1992) pp. 9-17.
135. N. Unwig and R. Henderson, "The Structure of Proteins in Biological Membranes," *Scientific American*, February, 78-94 (1985).
136. i. *Pattern and Tiling*, B. Grünbaum (Plenum, New York, 1987); ii. *Tilings and Patterns*, B. Grünbaum and G. C. Shephard (W. H. Freeman and Company, New York, 1987).
137. M. Sarikaya, J. Liu, and I. Aksay, submitted to *Science* (1993).
138. *On the Growth and Form*, d'Arcy Thompson (University Press, Cambridge, 1952) Cpt. XI.
139. D. R. Fowler, H. Meinhardt, and P. Prusinkiewicz, "Modelling Seashells," *Computer Graphics*, **26** [2] 379-387 (1992).
140. M. Sarikaya and I. A. Aksay, unpublished research (1993).

"Alginates as a Ceramic Processing Aid,"

N. B. Pellerin, G. L. Graff, D. R. Treadwell,
J. T. Staley, and I. A. Aksay

Biomimetics (Vol. 1, No. 2, pp. 119-130, 1991)

Alginic acid as a Ceramic Processing Aid

Nancy B. Pellerin,¹ G. L. Graff,² David R. Treadwell,²
James T. Staley,^{1,3} and Ilhan A. Aksay²

*Alginic acid obtained from *Macrocystis pyrifera* (kelp) has been used in a novel way to produce stable suspensions of $\alpha\text{-Al}_2\text{O}_3$ ceramic particles for use in producing a high (>40%) packing density in the unfired ceramic material. Native alginic acid was effective in producing low-viscosity, stable suspensions up to 20 vol% of solids; however, the higher viscosity of the polymer solution interfered with the preparation of higher-solids loading suspensions. The hydrolysis products of alginic acid, polymannuronic acid- and polyguluronic acid-rich fractions, were effective in producing stable suspensions up to 30 and 40 vol%, respectively. The higher charge density of polyguluronic acid appears to be responsible for its more effective role as a dispersant.*

KEY WORDS: ceramic processing; dispersants; alumina; alginic acid; *Macrocystis pyrifera*.

INTRODUCTION

Recent progress in the field of ceramics has focused on the development of highly dense, homogeneous materials for new applications such as ceramic engine components and superconductive composites (Ulrich, 1990). For these applications, nonclay materials such as alumina (Al_2O_3) are synthesized in very small (submicron) sizes. Submicron particle systems yield finer-grained products after sintering provided that they can first be compacted to a high-density state with a uniform pore size distribution. However, a long-standing problem is that

¹Department of Microbiology and Advanced Materials Technology Center, Washington Technology Centers, University of Washington, Seattle, Washington 98195.

²Department of Materials Science and Engineering and Advanced Materials Technology Center, Washington Technology Centers, University of Washington, Seattle, Washington 98195.

³To whom correspondence should be addressed at Department of Microbiology, SC-42, University of Washington, Seattle, Washington 98195.

these submicron-sized particles are highly attracted to each other due to van der Waals forces, causing aggregations which effectively increase the particle size and leave undesired voids in the finished product (Aksay, 1984). The prime requirement for preparation of a high density in the compact is that particles be completely dispersed in the solvent system and exhibit no agglomeration (Calvert *et al.*, 1986).

One method to overcome agglomeration and achieve dispersion is to use a polyelectrolyte to coat the particles, which creates a net repulsive force between them due to electrosteric interactions (Cesarano and Aksay, 1988; Cesarano *et al.*, 1988). The synthetic polymer, poly(methacrylic acid) (PMAA) has been commonly used to disperse alumina in aqueous suspensions. This polymer causes a decrease in the interparticle attraction as reflected by a decrease in viscosity of the suspension and, thus, in an increase in the packing density of the wet cake (Cesarano and Aksay, 1988; Cesarano *et al.*, 1988). However, PMAA and its monomer, acrylic acid, are toxic and corrosive (Merck and Co., 1989).

In this paper we report the use of a naturally occurring, polymer that can produce well-dispersed colloidal suspensions of submicron-sized alumina particles. We have demonstrated that alginate obtained from the marine alga, *Macrocystis pyrifera* (kelp), has dispersing capabilities comparable to those of PMAA. Furthermore, it is neither toxic nor corrosive.

Alginate is a copolymer of the isomers D-mannuronic (M) and L-guluronic (G) acids. The biosynthesis is thought to involve the initial formation of poly-mannuronic acid, followed by the epimerization of D-mannurosyI residues to L-gulurosyI residues (Grasdalen *et al.*, 1979). The two uronides are distributed along the chain in blocks of three types, polymannuronic acid (poly M), poly-guluronic acid (poly G), and poly-mannuronic-guluronic acid (poly MG) (Grasdalen *et al.*, 1979; Haug *et al.*, 1966, 1974; Larsen *et al.*, 1970). A similar polymer is produced extracellularly by some bacteria, including *Azotobacter vinelandii* (Pindar and Bucke, 1975) and various *Pseudomonas species* (Linker and Jones, 1966). Alginate-producing, mucoid variants of *P. aeruginosa* have been obtained from patients suffering from respiratory infections accompanying cystic fibrosis (Govan, 1976). It is thought that the production of polymer by the bacterium confers protection from antibiotics.

MATERIALS AND METHODS

Materials and Chemicals

The ceramic used in this study was a high-purity (99.99% α -Al₂O₃, with an average particle size of 0.4 μm as determined by X-ray sedigraph (AKP-30, Sumitomo Chemical America, Inc., New York).

The polymer was a low-viscosity kelp alginate (75,000 to 100,000 MW;

Sigma Chemical Company, St. Louis, Mo.). Low molecular weight fractions were prepared by hydrolysis in 0.1 N HCl under reflux for 4 h. The solution was centrifuged, after which the pellet was dissolved using NaOH. The guluronic acid fraction was obtained by lowering the pH to 2.4 and collecting the precipitate; the mannuronic acid fraction was precipitated by further lowering the pH to 1.3 (J. M. Beale, personal communication).

Reagent-grade HCl and NaOH were used for pH adjustments. Distilled water was used throughout. Mannuronic acid lactone was obtained from Sigma Chemical Company.

Sedimentation Experiments

Sedimentation columns were prepared with 2 vol% α -Al₂O₃ in aqueous solutions of polymer. The suspensions were sonicated for 5 min, then mixed on a magnetic stirrer for 0.5 h, and the pH adjusted to the experimental value before bringing the final volume to 10 ml. The suspension was decanted into a conical-bottom, graduated polystyrene tube (Falcon 2095, Becton Dickinson, Cockeysville, Md.) and left undisturbed for several weeks. Final sediment volumes were measured to ± 0.1 ml. The wet sediment density was calculated as (theoretical volume/final volume) $\times 100$.

Viscosity Measurements

Suspensions for viscosity measurements were prepared with 30 to 40 vol% α -Al₂O₃ in 0.5% (dwB) aqueous solution of polymer (pH 5 or 8) and mixed as above. Measurements were obtained by the method of Cesarano and Aksay (1988) using a digital viscometer (Model RVTD, Brookfield Engineering Laboratories, Inc., Stoughton, Mass.). Viscosities of polymer solutions were measured using parallel plates on a Rheometrics fluid spectrometer (Model 8400, Rheometrics Inc., Piscataway, N.J.).

Determination of Degree of Polymerization of Alginate Oligomers

Samples of the poly M- and poly G-rich fractions and unhydrolyzed alginic acid were each mixed with 1 ml of D₂O and dissolved by adding a few drops of 5% NaOD in D₂O dissolved in D₂O. The pH of the solutions was adjusted to slightly acidic with 1% DCI in D₂O. Na₂EDTA was added to complex any Ca²⁺ present. The ¹H NMR spectra of the samples were recorded on a Varian VXR 300 spectrometer at 300 MHz and analyzed by the method of Grasdalen *et al.*, (1979; Grasdalen, 1983). The chemical shifts are reported as parts per million downfield of internal 3-trimethylsilyl-1-propanesulfonic acid-2,2,3,3-d₄ sodium salt. The ratios of mannuronate to guluronate were determined from the integrals of the anomeric protons: M at 4.64δ and G at 5.02δ. The degrees of

Table I. MR Data for Determination of Uronide Residue Composition and Degree of Polymerization (DP) of Hydrolyzed Alginate Fractions^a

Sample	Polymer wt (mg)	Na ₂ EDTA wt (mg)	Final pD	% G	DP
Poly M	10.2	2.2	5.0	10	18
Poly G	9.0	2.0	5.3	83	>24

^aTransients collected: 128.

polymerization of the poly M- and poly G-rich fractions were estimated by the ratio of the sum of the integrals of these two peaks to that of the reducing-end protons at 5.20δ (see Table I). The linewidths of the unhydrolyzed alginic acid were too great to yield useful information.

RESULTS AND DISCUSSION

Effect of pH on the Particle Packing Density

Several factors must be considered when working with polyelectrolytes in aqueous solutions. First, the dissociation behavior of the polymer is greatly affected by the solution pH. The dissociation of a weak acid group on the polyelectrolyte depends on the overall degree of dissociation, since dissociation of a proton from an already ionized polyacid is hampered by the negative potential of such a polyacid (Hesslein, 1983). Thus the ρK_A varies for every acid site and increases as each successive site dissociates. Second, the surface charge of the alumina particles varies from highly positive at low pH to negative at high pH, with the zero point of charge (zpc) occurring at about pH 8.7 (Cesarano *et al.*, 1988). These factors result in suspensions that are extremely pH sensitive.

In order to determine the optimum pH range for the alginate/alumina system, we prepared a series of sedimentation tests under different pH conditions. At low pH (2.8) the suspension was flocculated, with a cake density of less than 10% of the theoretical packing density, similar to the cake formed when no suspending agent was used (Fig. 1). This result was expected since at low pH the polyuronic acid would be essentially nondissociated, with very few ionized groups on the polymer to interact with the alumina surface. The increase in cake densities with rising pH reflects an increasing number of ionized COO^- sites on the polymer. Interestingly, maximum sediment densities were obtained near pH 8–9 where the polymer is fully dissociated, and the surface of the alumina particles has a slight positive charge. This condition provides the maximum electrostatic contribution from the polymer while providing a driving force

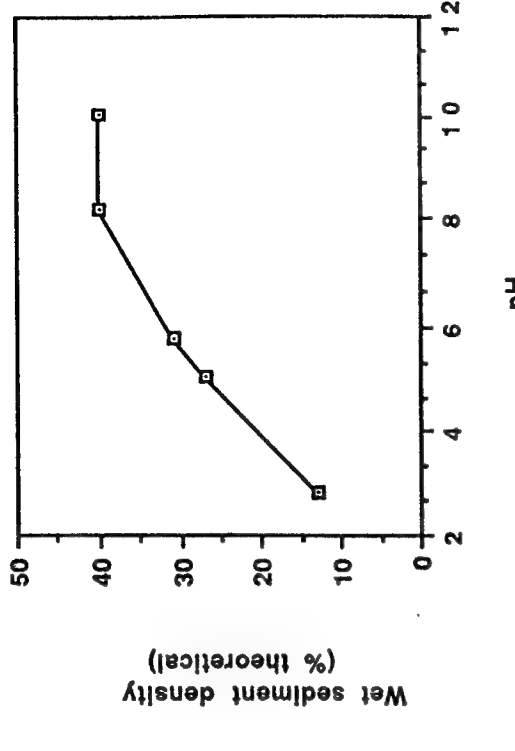


Fig. 1. Wet sediment densities of 2 vol% suspensions of alumina in alginate (0.5% dwb alumina) prepared at various pH levels.

Effect of Polymer Concentration

To determine the optimum concentration of polymer required to disperse the alumina powder, a series of sedimentation tests was performed at a fixed pH of 8.5. Dilute (2 vol%) suspensions were prepared with various concentrations of polymer relative to the dry weight of the particles (dw_b). Figure 2 shows the wet sediment densities obtained in these suspensions after several weeks of settling. In the absence of polymer, the suspension was unstable, with particles spontaneously agglomerating into poorly packed, ramified structures with packing densities of approximately 10% of the theoretical value. The addition of 0.1% polymer had no observable effect, but with slight increases in polymer concentration, the sediment densities increased dramatically. At a polymer concentration of 0.5% (dw_b), the sediment cakes reached a maximum density of greater than 40% theoretical (density). This indicates that the added polyelectrolyte is acting to stabilize the particles in suspension by creating a barrier against spontaneous flocculation of the individual particles. This facilitates particle packing upon consolidation in the sediment, resulting in the highest densities observed.

Cesarano *et al.* (1988) reported wet sediment densities of approximately

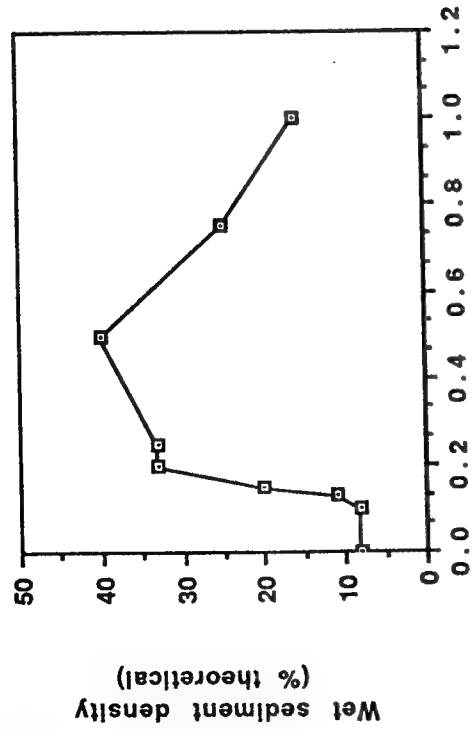


Fig. 2. Wet sediment densities of 2 vol% suspensions of alumina prepared with various concentrations of alginate (dwb alumina). The pH of the suspensions was adjusted to 8.5-8.6.

50% theoretical (density) for the poly(methacrylic acid)-Na (PMAA)-stabilized alumina suspensions. The lower packing densities (40%) observed with the alginate could be due to several effects. First, the higher molecular weight of the alginate (100,000) compared to the PMAA (15,000) would tend to create a thicker adsorbed polymer layer on each individual alumina particle (Hesselink, 1983). The increased volume occupied by the adsorbed polymer would increase the interparticle separation distance and could easily account for a 10% decrease in final sediment density. Second, the difference in charge density between the two polyelectrolytes might explain the lower packing densities. Fully dissociated PMAA has a charged COO^- site for each ethyl group along the polymer backbone. In comparison, the alginate contains a single carboxylic acid for each hexose unit. These differences in structure result in approximately twice (1.84 times) the charge density for PMAA compared to alginate, given identical molecular weight polymer segments. This lower electrostatic repulsion may result in alginate suspensions that are mildly agglomerated, with lower particle packing densities.

Figure 2 further shows a distinct maximum in sediment density at a polymer concentration of 0.5% (dwb), with a decrease in packing density at higher concentrations. This indicates that full surface coverage of the alumina particles by the alginate occurs at approximately 0.5% (dwb). The decrease in packing

Viscosities of Highly Concentrated Suspensions

To understand better the role of the alginate in controlling particle-particle interactions, we measured the viscosities of concentrated alumina suspensions prepared with the polymer. The viscosity of the suspension can give information as to the effectiveness of the polymer in stabilizing the suspension.

For our experiments we measured the viscosity of the suspension as the mixing speed was decreased from 93 to 0.47 s^{-1} for 5 min and then increased. Figure 3 shows the thixotropic loop obtained for a 30 vol% suspension of particles in alginate solution. After 5 min at a low rate of mixing, the viscosity again nearly doubled, but as the rate of mixing was increased the viscosity again decreased.

Of the possible explanations for the increase in viscosity at a low rate of mixing, two are that (i) the polymer may be forming a gel structure which is disturbed by more vigorous mixing or (ii) the suspension may be unstable, i.e.,

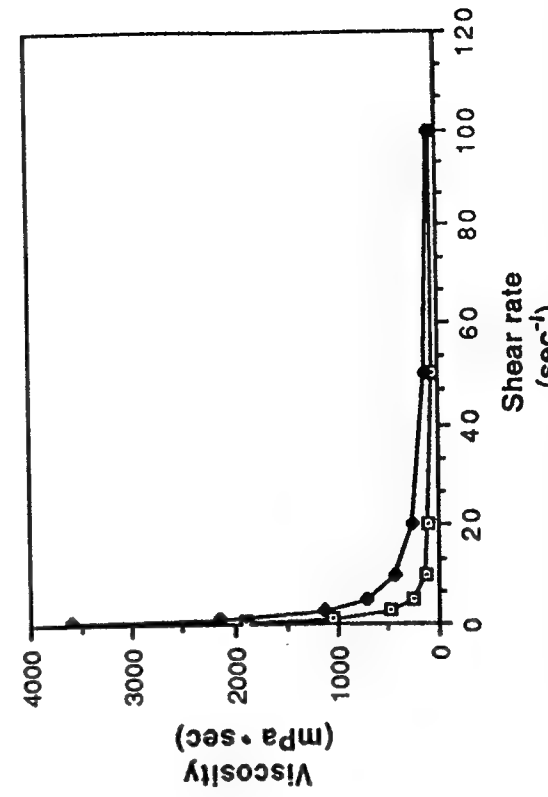


Fig. 3. Viscosity curve obtained from a 30 vol% suspension of alumina in 0.5% dwb alginate. Open squares represent values obtained during increasing shear rate. Filled squares represent values obtained during decreasing shear rates.

the particles may be flocculating (agglomerating) to form a network structure in the suspension due to insufficient stabilization.

We next prepared a 40 vol% suspension of particles in alginate solution (Fig. 4). This suspension showed characteristics different from those of the 30 vol% suspension. Here, the viscosity displayed less hysteresis, but at all rates the viscosity was 10-fold higher than that of the 30 vol% suspension. The suspension acted like a soft gel, leading us to suspect that the polymer was contributing to the high viscosity.

When we compared the viscosities of solutions of alginate in water without the particles, we found that of the polymer solution alone in the 30 vol% suspension to be 160 mPa·s and that of the solution in the 40 vol% suspension to be 341 mPa·s. This is strong evidence that the polymer forms a gel in the solution.

Low Molecular Weight Fractions as Dispersants

We next investigated whether lower molecular weight fractions would be effective as dispersants and would avoid the problem of gel formation encountered with the native polymer. Kelp alginate (75,000–100,000 MW) was hydrolyzed in 0.1 N HCl for 4 h, after which two fractions were collected by

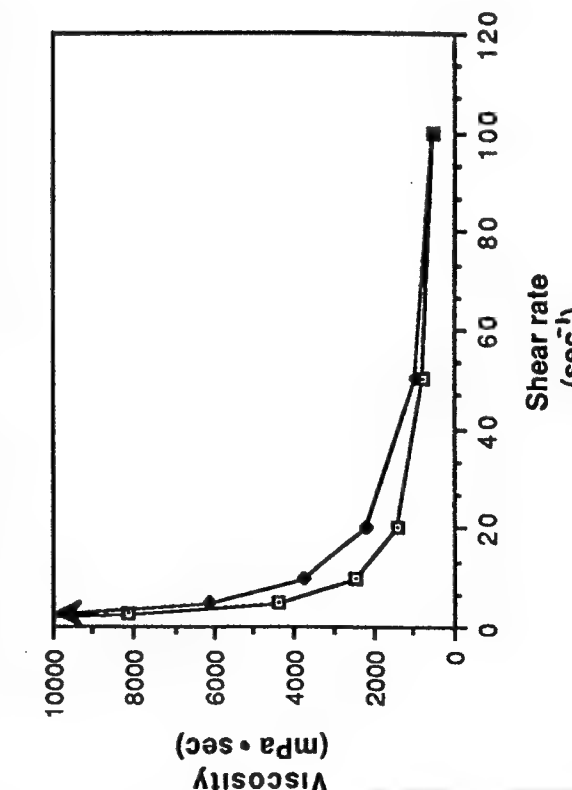


Fig. 4 Viscosity curve obtained from a 40 vol% suspension of alumina in alginate. Open squares represent values obtained during increasing shear rate. Filled circles represent values obtained during decreasing shear rates. The arrow represents an off-graph value of 10,500 mPa·s at the shear rate of 2.5 s^{-1} .

precipitation. Fraction poly G was collected by precipitation at pH 2.4. The degree of polymerization and uronide composition was determined by NMR (Table I). This fraction contained an oligomer with an average degree of polymerization greater than 24 ($\geq 4800 \text{ MW}$) and a ratio of guluronic to manno-uronic acid of 6 to 1. The viscosities of solutions of the oligomer in water were reduced approximately 100-fold as compared to the native polymer (Table II).

Fraction poly M, with an average degree of polymerization of about 18 and molecular weight ~ 3600 (Table I), was precipitated at pH 1.3. It contained more than 10 mannuronate residues to 1 guluronate residue. Viscosity measurements were not performed, but the values would be expected to be similar to or less than that of the poly G fraction since the gel-forming capacity of the polymer is directly related to the guluronic acid content (Penman and Sanderson, 1972).

We also included mannuronic acid monomer in this study to determine the effectiveness of a single uronnic acid sugar as a dispersant. This was obtained by treating commercially available mannuronic lactone with base (final pH 8.3). The packing densities obtained with these fractions show clearly that there are differences in their ability to stabilize suspensions (Fig. 5). The poly G fraction was effective over a wider concentration range than the native alginate, and slightly less oligomer was needed to produce an effect equal to the native polymer. The poly M fraction was effective only at a higher concentration (0.4 to 0.5% dwb) of oligomer to particle. The monomer had only a slight effect at very high concentrations (1% dwb) and could not be considered a useful suspension stabilizer.

The viscosities of concentrated suspensions prepared with 0.5% (dwb) of the oligomers again show a difference between the fractions (Table III). The poly M fraction stabilized suspensions at a 30 vol% solids loading, while the poly G fraction was capable of stabilizing suspensions with 40 vol% solids. A fluid ($< 1 \text{ Pa}\cdot\text{s}$) 50 vol% suspension could not be prepared with the poly M

Table II. Viscosities of Native Alginate and Polyguluronic Acid in Water*

Sample	30 vol%	40 vol%	Viscosity (mPa·s)
Poly G	0.9	4.9	160
Native alginate	160	341	

*Solutions were prepared to yield the same final concentrations as were in the 30 and 40 vol% suspensions, but the particles were omitted.

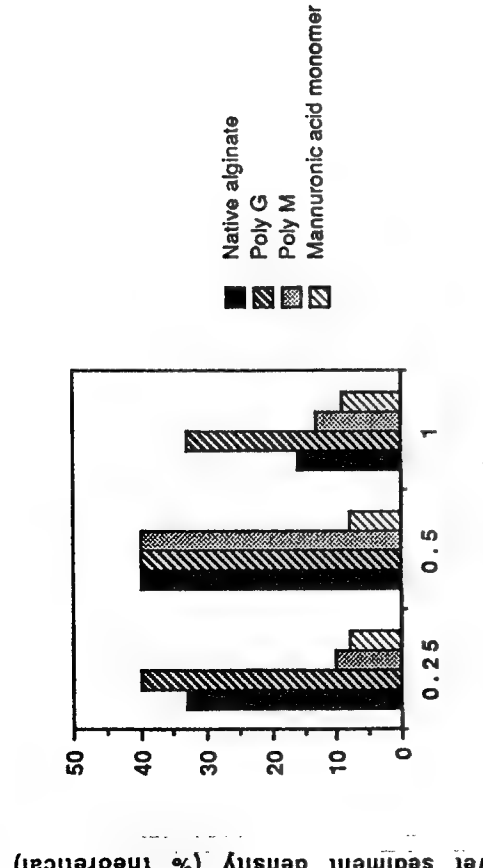


Fig. 5. Wet sediment densities of 2 vol% suspensions of alumina prepared with native alginate, polygaluronic acid (poly G), polymannuronic acid (poly M), or mannuronic acid monomer. The pH of the suspensions was adjusted to 8.3-8.6.

Table III. Viscosities (mPa·s) of Concentrated Suspensions of Alumina in Polymannuronic or Polygaluronic Acid Fractions at a Shear Rate of 9.3 s^{-1}

Fraction	pH	30 vol%	40 vol%	50 vol%
Poly G	8	40	230	470-625
Poly G	5	<20	35	Slightly flocculated 110
Poly M	8	95	465	Slightly flocculated Too high to be prepared

fraction because of particle agglomeration, yet the poly G fraction yielded a weakly flocculated, low-viscosity suspension at this solids loading. The reason for these differences may lie in the molecular configuration of the two polymers. Solution studies using NMR (Penman and Sanderson, 1972) provide evidence that the uronic acids adopt different chain forms when in solution, such that the bulky carboxyl group is in the equatorial position. The resultant glycosidic bonds at positions 1 and 4 would be equatorial in β -D-mannuronate but axial in α -L-guluronate. This would lead to a flat, ribbon-like conformation in poly M sequences, whereas poly G would adopt a buckled conformation. The buckled arrangement brings the oxygens on either side of the glycosidic bond in close proximity, leading to a localized increase in charge

CONCLUSIONS

We have demonstrated that uronic acid-containing polysaccharides are useful as dispersants in preparing concentrated, aqueous suspensions of ceramic powders. This represents an easily isolated, inexpensive, and nontoxic polymeric additive for potential commercial applications.

In addition, we have shown that oligomeric fractions of the native alginates are equally effective, or superior, as dispersants in colloidal alumina suspensions. Therefore, the undesirable gelling characteristics of the high molecular weight alginates can be eliminated while maintaining the necessary suspending properties.

ACKNOWLEDGMENTS

This work was supported in part by a grant from the United States Air Force (AFOSR-88-135). We thank John M. Beale and Blain Mimaya for helpful advice and discussions.

REFERENCES

- Aksay, I. A. (1984). Microstructure control through colloidal consolidation. In Mengel, J. A., and Messing, G. L. (eds.), *Advances in Ceramics 9, Forming of Ceramics*, Am. Ceram. Soc., Columbus, Ohio, pp. 94-104.
- Aksay, I. A. (1988). Principles of ceramic shape-forming with powder systems. In Messing, G. L., Fuller, E. R., and Hausner, H. (eds.), *Ceramic Powder Science II, Ceramic Transactions Vol. 1*, American Ceramic Society, Columbus, Ohio, pp. 663-674.
- Cesarano, J., III, and Aksay, I. A. (1988). Processing of highly concentrated alumina suspensions stabilized with polyelectrolytes. *J. Am. Ceram. Soc.* 71(12):1062-1067.
- Cesarano, J., III, Aksay, I. A., and Bleier, A. (1988). Stability of aqueous Al_2O_3 suspensions with poly(methacrylic acid) polyelectrolyte. *J. Am. Ceram. Soc.* 71(4):250-255.
- Govan, J. R. W. (1976). Antibiotic therapy and cystic fibrosis: Increased resistance of mucoid *Pseudomonas aeruginosa* to carbencillin. *J. Antimicrob. Chem.* 2:215-217.
- Grasdalen, H. (1983). High field $^1\text{H-NMR}$ spectroscopy of alginate: Sequential structure and lineage conformations. *Carbohydr. Res.* 118:255-260.
- Grasdalen, H., Larsen, B., and Smidsrød, O. (1979). A P.M.R. study of the composition and sequence of uronic residues in alginates. *Carbohydr. Res.* 68:23-31.
- Haug, A., and Larsen, B., (1971). Biosynthesis of alginate. II. Polymannuronic acid C-5-epimerases from *Azotobacter vinelandii* (Lipman). *Carbohydr. Res.* 17:297-308.
- Haug, A., Larsen, B., and Smidsrød, O. (1966). A study of the constitution of alginic acid by partial acid hydrolysis. *Acta Chem. Scand.* 20:183-190.
- Haug, A., Larsen, B., and Smidsrød, O. (1974). Uronic acid sequence in alginate from different sources. *Carbohydr. Res.* 32:217-225.
- Hesslein, F. Th. (1983). Adsorption of polyelectrolytes from dilute solution. In Parfitt, G. D., and Rochester, C. H. (eds.), *Adsorption from Solution at the Solid/Liquid Interface*, Academic Press, London; New York pp. 377-412.

- Larsen, B., Smidsrød, O., Painter, T., and Haug, A. (1970). Calculation of the nearest-neighbour frequencies in fragments of alginic acid from the yields of free monomers after partial hydrolysis. *Acta Chem. Scand.* 24:726-728.
- Linker, A., and Jones, R. S. (1966). A new polysaccharide resembling alginic acid isolated from pseudomonads. *J. Biol. Chem.* 241:3845-3851.
- Merck and Co. (1989). *The Merck Index*, 11th ed., Merck, Rahway, N.J.
- Penman, A., and Sanderson, G. R. (1972). A method for the determination of uronic acid sequence in alginates. *Carbohydr. Res.* 25:273-282.
- Pindar, D. F., and Bucke, C. (1975). The biosynthesis of alginic acid by *Azotobacter vinelandii*. *Biochem. J.* 152:617-622.
- Rees, D. A. (1972). Shapely polysaccharides. *Biochem. J.* 126:257-273.
- Ulrich, D. R. (1990). Chemical processing of ceramics. *Chem. Eng. News.* 68(1):28-40.

"Dispersion of Small Ceramic Particles with
Azetobacter vinelandii"

T. Ren, N. B. Pellerin, J. T. Staley,
G. L. Graff, and I. A. Aksay

Appl. Environmental Microbiol., 58 [9] 3130-3135 (1992).

Dispersion of Small Ceramic Particles (Al_2O_3) with *Azotobacter vinelandii*

TAO REN,¹ NANCY B. PELLERIN,¹ GORDON L. GRAFF,² ILHAN A. AKSAY,^{2,3} AND JAMES T. STALEY^{1*}

Departments of Microbiology¹ and Materials Science and Engineering² and Advanced Materials Technology Center,³ University of Washington, Seattle, Washington 98195

Received 31 March 1992/Accepted 13 July 1992

The high surface charge of small ceramic particles such as alumina particles prevents them from dispersing evenly in aqueous suspensions and forming high-density compacts. However, suspensions of 400-nm-diameter alumina particles treated with alginate from the bacterium *Azotobacter vinelandii* were well dispersed. The alginate bound firmly to the particle surface and could not be removed by repeated washing with distilled water (2.82 mg of the bacterial alginate adsorbed to 1 g of the alumina particles). Furthermore, *A. vinelandii* grew and produced alginate in the presence of up to 15% (vol/vol) alumina particles. These results suggest that an in situ process using this bacterium to coat ceramic particles with alginate might be developed. In in situ processing experiments, the particle-packing densities were significantly increased and the viscosities of 5 and 10% (vol/vol) suspensions were reduced 4- and 60-fold, respectively, over those of controls. The bacteria were readily removed from the alumina particles by washing.

Since prehistoric times, potters have prepared clay beds by amending them with organic materials such as urine, manure-water mixtures, and tannin. This practice of "aging" made the clay materials more plastic and therefore more readily workable for pottery production.

Early in the 20th century, several scientists performed experiments that implicated microorganisms in clay aging. In 1902, Stover noted that clays which were sterilized did not exhibit the plastic qualities of properly aged clays containing bacteria (23). Furthermore, when the sterilized clay was inoculated with previously aged clay, it acquired the workability properties of normally aged clays within 2 to 4 weeks. Spurrier demonstrated the growth of filamentous algae in aging clay and hypothesized that the products of their growth contributed to the increase in plasticity of the clay body (22).

Glick (7, 8) and Baker and Glick (3) noted that clays to be used in the manufacture of high-quality ceramics were aged in commercial cellars for several weeks to a year. New cellars were prepared by inoculating fresh clay material with small amounts of well-aged clays. Several bacteria were isolated from the seasoned clays and identified as species of *Bacillus* and *Pseudomonas* as well as of other genera.

One is naturally led to inquire how microorganisms are able to increase the plasticity of clays. Since current ceramic processing employs synthetic polymers as dispersants, we hypothesized that microbial exopolymers, such as polysaccharides or polypeptides, are responsible.

Advanced ceramic techniques for the production of highly dense, fine-grained products employ a system in which particles of a very small size (<1 μm in diameter) or powders are evenly dispersed within some solvent system and then concentrated to a high density in the green body (i.e., the ceramic object before firing or sintering). Particles of such small size are subject to strong interparticle interactions, such as the van der Waals force. Alumina in particular has a mixture of positive and negative surface charges which at

certain pHs (for instance, pH 8) causes agglomeration in rough aggregates and results in a porous product. To prevent this, a polyelectrolyte, which acts by providing a significant electrical repulsion between particles, may be used as a dispersant. Currently, synthetic polymers from petrochemicals, such as polymethacrylic acid (PMAA) and polyacrylic acid (PAA), are used as dispersants (5, 6). However, commercial PMAA may contain formaldehyde, and PAA may contain residual amounts of acrylic acid; both of these chemicals are toxic. Furthermore, they are produced from precursors that are toxic and/or carcinogenic. In contrast, naturally occurring polymers are nontoxic and do not pose problems of disposal, since they are readily degraded by natural processes.

Earlier studies from this laboratory showed that although the bacterial glycan dextran was ineffective as a dispersant, it became a satisfactory dispersant of alumina when it was modified chemically to produce dextran sulfate (9a). Like the acrylate polymers, dextran sulfate has an acidic side group which is thought to be the important feature for alumina dispersion. However, because of the sulfate groups, dextran sulfate is not completely removed by sintering.

Therefore, we set out to determine whether naturally occurring acidic polymers could be used as dispersants. The first naturally occurring acidic polymer that we studied was alginate, an α -1-4-linked linear copolymer of β -D-mannuronic (M) and β -D-guluronic (G) acids (10-12, 15) synthesized by several species of marine algae (4). Polymers with molecular weights of about 5,000 were found to be satisfactory dispersants for alumina processing (17a). The purpose of this study was to determine whether bacterial alginate from *Azotobacter vinelandii* (9, 18) would also serve as an effective dispersant of ceramic particles and, if so, whether an in situ process could be developed to produce bacterial alginate in the presence of ceramic particles.

MATERIALS AND METHODS

Bacterial cultivation. *A. vinelandii* NCIB 8789 (National Collection of Industrial Bacteria, Aberdeen, Scotland) was

* Corresponding author.

maintained on Larsen's broth medium (14) in cyst-stage cultures. Cyst-stage cultures (stock cultures) were subcultured every 2 months to fresh broth, grown at 30°C for 2 days, and stored at 4°C. Working cultures were subcultured from the stock culture when needed. The composition of normal Larsen's broth medium is as follows: sucrose (or mannitol), 20 g; K_2HPO_4 , 1.0 g; $\text{MgSO}_4 \cdot 7\text{H}_2\text{O}$, 1.0 g; $\text{FeSO}_4 \cdot 7\text{H}_2\text{O}$, 50 mg; $\text{Na}_2\text{MoO}_4 \cdot 2\text{H}_2\text{O}$, 5 mg; CaCl_2 , 50 mg; $\text{CH}_3\text{COONH}_4$, 2.3 g; distilled water, 1 liter; the pH is 6.5. For plate cultures, 1.8% agar was added to the broth.

Bacterial counts and cyst observations. Bacterial cells were counted by standard plate count techniques on solid Larsen's medium. Cyst formation of *A. vinelandii* was observed directly by using a phase-contrast microscope.

Determination of polysaccharide in culture suspensions. Bacteria were removed from the culture by centrifugation at $22,000 \times g$ for 40 min. Polysaccharide in the supernatant was determined by the *meta*-hydroxydiphenyl-sulfuric acid assay (17). Mannitol (20 g/liter) was used in place of sucrose as a carbon source in the growth medium because of its minimal interference with the colorimetric analysis when this assay was used. Low-viscosity kelp alginate (Sigma) was used as the standard for this assay. Spectrophotometric work was conducted with a Gilford Response II spectrophotometer (Gilford Instrument Laboratories, Oberlin, Ohio) or a Spec-tronic 20 spectrophotometer (Bausch & Lomb, Rochester, N.Y.).

Polysaccharide harvest. *A. vinelandii* NCIB 8789 was shaken in the Larsen's broth at 30°C for 5 days. Bacterial cells were removed by centrifugation at $22,000 \times g$ for 40 min. Three volumes of 2-isopropanol were then added to the supernatant for precipitation (13). The precipitate was washed two to four times with 2-isopropanol and then dissolved in distilled water before being dialyzed against distilled H_2O overnight. After dialysis, the polysaccharide was lyophilized.

Kelp alginate. The polymer used was a low-viscosity (approximately 250 cps for a 2% solution at 25°C) kelp alginate (Sigma Chemical Company, St. Louis, Mo.) produced from *Macrocystis pyrifera* (molecular weight, 75,000 to 100,000) M/G (mannuronic acid/guluronic acid) ratio of alginate from *M. pyrifera* has been reported independently as 1.56 (20).

Ceramic particles. The ceramic particles used in this study were high-purity (99.99%) Al_2O_3 , with an average particle diameter of 400 nm and a density of 3.96 g/ml (AKP-30, Sumitomo Chemical America, Inc., New York, N.Y.).

pH adjustment of particle suspensions. Because the pH of the particle suspension is affected by the extent of mixing (2), suspensions for sedimentation tests, rheological measurements, and *in situ* cultures were mixed for more than 0.5 h (in some situations, overnight) with a magnetic stirrer. The pH was initially adjusted to the experimental value and then readjusted to the same value after mixing. For sedimentation tests, the pH was adjusted to between pH 8.0 and 8.5, a pH range which is the best for observing the dispersion effects of the bacterial alginate because there is no net charge on the surfaces of the alumina particles.

Sedimentation tests. Sedimentation columns were prepared by adding 2% (vol/vol) AKP-30 powder (for the *in situ* tests, this was 5 to 10% [vol/vol]) to aqueous solutions with various concentrations of the polymer (5, 6). The suspensions were sonicated for 5 min and mixed with a magnetic stirrer for 0.5 h. The pH of the suspension was adjusted to the experimental value (8.0 to 8.5) before the final volume was brought to 10 ml. The suspension was decanted into a

conical-bottom, graduated polystyrene tube (Falcon 2095; Becton Dickinson) and left undisturbed at room temperature for 3 to 4 weeks. Final sedimentation heights (cake height in milliliters) were measured to ± 0.1 ml and converted into wet densities in the following way. The theoretical cake height of a 2% (vol/vol) AKP-30 particle suspension in 10 ml of water is 0.2 ml. One milliliter of AKP-30 particles weighs 3.96 g; therefore, the theoretical packing volume of 0.792 g of AKP-30 (2% [vol/vol]) is 0.2 ml, assuming the particles are completely packed. This value was divided by the measured cake height (in milliliters) of the samples, and the percentage was then calculated. For example, if the measured cake height of one sample is 0.5 ml, its wet density is 40% of the theoretical value ($[0.2 \text{ ml}/0.5 \text{ ml}] \times 100\%$). In highly packed ceramic suspensions, the packing density approaches 100% (theoretical) after sintering.

Viscosity measurements. Viscosity measurements were obtained by using a Rheometrics Fluid Spectrometer (model 8400; Rheometrics Inc., Piscataway, N.J.). Suspensions (about 15 ml) for viscosity measurements were prepared as described for the sedimentation tests.

Washing of the bacterial alginate from the AKP-30. A 200-ml volume of Larsen's broth with mannitol as a carbon source was inoculated with a 1-ml suspension of *A. vinelandii* cells and shaken at 30°C for 5 days. The culture was centrifuged at $22,000 \times g$ for 40 min to remove the bacterial cells. The concentration of the polymer in the suspension was determined by the *meta*-hydroxydiphenyl-sulfuric acid assay. Alumina (5% [vol/vol]) (5.94 g of AKP-30) was added to 28.5 ml of the supernatant. The mixture was then ultrasonicated (with a probe) for 2 min for complete mixing. The suspension was adjusted to pH 8, and after centrifugation the concentration of the alginate remaining in the supernatant was determined by the *meta*-hydroxydiphenyl-sulfuric acid assay. The pellet was then washed three times. After each washing, the polymer concentration of the supernatant was assayed. The amount of the polymer bound to the particles was calculated by determining the difference between the total amount of polymer and that in the supernatant.

Removal of bacterial cells from the *in situ* system. The bacterium was cultured with a 5% (vol/vol) ceramic particle suspension at 30°C for 5 days on a shaker and then centrifuged for 40 min at $22,000 \times g$. This resulted in three layers: the ceramic particle cake at the bottom, a very thin layer of bacterial cells in the middle, and the spent broth (supernatant) at the top. The supernatant was decanted, and the cell layer at the top part of the particle pellet was removed by a sterile pipette. The newly exposed surface was then washed 8 to 10 times with sterile saline solution (0.85% NaCl) to remove loosely associated bacteria before the pellet was resuspended in sterile water to the original volume. Bacterial numbers were determined in this suspension by plate counting.

Nutrient limitation tests. *A. vinelandii* was cultivated in normal Larsen's broth for about 24 h, and the cells were harvested by centrifugation. The cell pellet was washed twice and then suspended in sterile saline. A sample was removed for bacterial enumeration, and 1 ml of this suspension was inoculated into 99 ml of modified nutrient-deficient Larsen's broth. Three modified Larsen's media were used. Modified medium 1 (mannitol only) contained only mannitol (20 g/liter). All other components were deleted. Modified medium 2 (mannitol plus buffer) contained mannitol (20 g/liter), but the K_2HPO_4 was reduced to 65 mg and 32 mg of KH_2PO_4 was added; $\text{MgSO}_4 \cdot 7\text{H}_2\text{O}$ was reduced to 40 mg, and 50 mg of FeSO_4 was replaced by 1.7 mg of

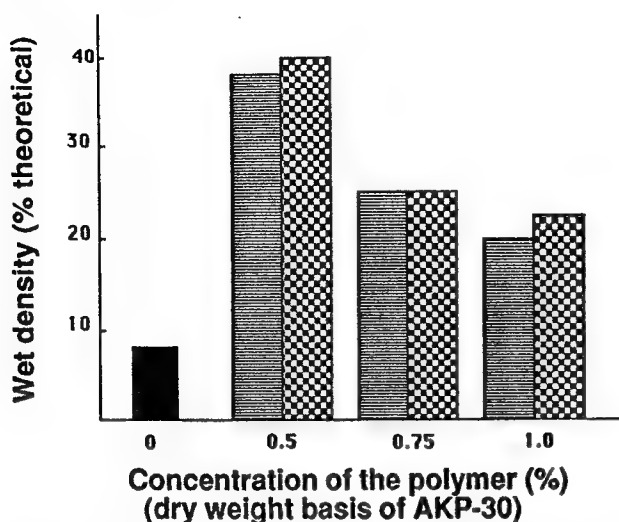


FIG. 1. Sedimentation (wet packing density) of 2% (vol/vol) suspensions of AKP-30 alumina (theoretical wet packing density, 100%) with kelp (■ [17a]) and bacterial (▨) alginate. All samples were adjusted to pH 8.0 to 8.5.

$\text{FeCl}_2 \cdot 4\text{H}_2\text{O}$. Medium 3 (mannitol plus buffer and acetate) contained the same ingredients as medium 2 but was also supplemented with 1.5 g of sodium acetate. After incubation for 96 h, the number of bacteria and the concentration of bacterial alginate were determined.

RESULTS

Production of alginate by *A. vinelandii*. The production of alginate during growth was determined by sampling batch cultures periodically and analyzing them for viable cell counts and alginate production. Bacterial cell numbers peaked after 20 to 40 h, and cyst production (19) began toward the end of logarithmic growth (between 40 to 60 h). Bacterial alginate secretion corresponded closely with the onset of cyst formation, i.e., in the late logarithmic to early stationary phase of growth. The yield of the alginate, which was harvested by precipitation from culture supernatants with 2-isopropanol, ranged from 0.8 to 1.2 g (dry weight) per liter of broth at the end of 4 days of culture.

The range of the M/G ratio of alginate from *A. vinelandii* was reported to be 0.53 to 0.58 (14), which is lower than that of the kelp alginate from *Macrocystis pyrifera*, reported to have an M/G ratio of 1.56 (20). The viscosity of the bacterial alginate was reported to be influenced by the addition of salts, the M/G ratio, and the molecular weight (16).

Bacterial alginate as a dispersant. The alginate obtained from *A. vinelandii* cultures was tested for its ability to act as a dispersant by preparation of 2% (vol/vol) suspensions of alumina particles. The resulting wet particle-packing densities showed clearly that bacterial alginate was an effective dispersant (allowing for increased wet packing density relative to the control) and acted in a manner similar to that of kelp alginate (Fig. 1). The maximum wet packing density occurred with a 0.5% concentration of the alginate (dry weight basis of polymer to particles) for both alginates.

In situ production of alginate. The foregoing results indicate that bacterial alginate can be used as a dispersant for ceramic particles. The question arises as to the most expedient method that could be used to deliver the alginate to the

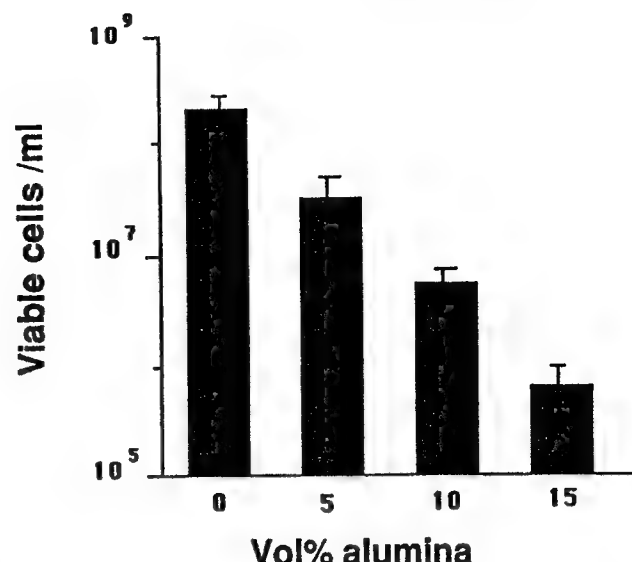


FIG. 2. Growth of *A. vinelandii* at various solids loadings of alumina inoculated with 3.4×10^3 cells per ml.

particles. The most direct means of doing this would be an in situ process in which the bacterium is grown with the particles while it produces the alginate. Therefore, we initiated work to determine whether the bacterium could be grown in the presence of the particles, while producing the alginate at the same time. This concept was tested using 5, 10, and 15% (vol/vol) alumina suspensions inoculated with 3.0×10^3 bacterial cells per ml of Larsen's medium and incubated at 30°C for 4 days. Before inoculation, the pHs of all samples were adjusted to 7.4 (for bacterial growth) and were readjusted to 8.0 to 8.5 (for sedimentation and viscosity measurements) after culturing.

Organisms grew at all concentrations of alumina, although bacterial yields were progressively reduced at higher alumina concentrations (Fig. 2). The bacterial numbers in the cultures increased to 5.1×10^7 , 7.5×10^6 , and 8.2×10^5 per ml of suspension from the inoculum concentration of 3.0×10^3 /ml for the 5, 10, and 15% (vol/vol) suspensions, respectively. A control culture without alumina increased to 3.1×10^8 /ml during the 4-day incubation period. As the concentration of the particles increased incrementally by 5% (vol/vol), the bacterial cell yield was reduced about 10-fold. This reduced yield may be attributable to reduced oxygen concentrations, to pH effects of the alumina, or to some other unknown factor. The polymer was detected in the supernatant of each culture after incubation.

We next evaluated whether the particles became coated with the polymer during growth of the bacterium. The 5 and 10% (vol/vol) suspensions which had been incubated with *A. vinelandii* and their sterile controls were adjusted to the same pH before being tested. Sedimentation test results showed that the particle packing was twice as dense as that in the untreated sterile control for the 5% (vol/vol) suspension and two and one-half times as dense than that in the untreated sterile control for the 10% (vol/vol) suspensions (Fig. 3). These results indicated that the polymer was being produced, coating the particles, and facilitating more dense packing of the particles in the sedimented cake.

Suspension viscosity is another method of assessing the effectiveness of a dispersant. Well-dispersed systems are

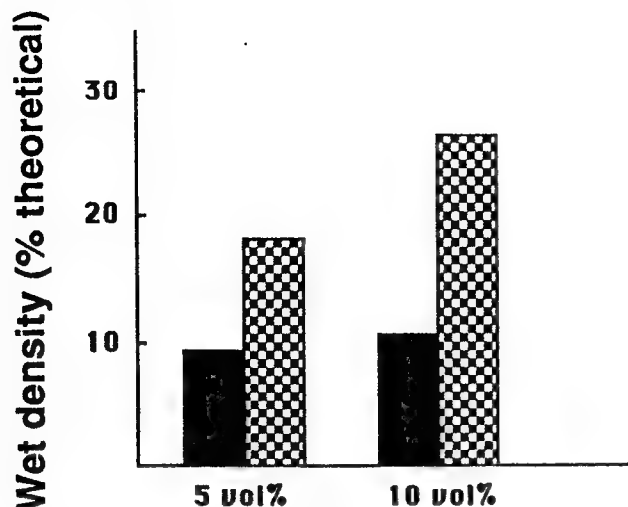


FIG. 3. Particle-packing density resulting from in situ processing of alumina particles by growing cultures of *A. vinelandii* in the presence of 5% (vol/vol) alumina (▨) versus that in the sterile control (■) and in the presence of 10% (vol/vol) alumina (▨) versus that in the sterile control (■). Before sedimentation columns were prepared, the pH was adjusted to the same value as that of the sterile control.

characterized by low viscosities due to repulsive particle-particle interactions in suspension (1, 6). The viscosities of the inoculated 5 and 10% (vol/vol) suspensions were reduced fourfold (from 0.48 to 0.12 P 10 sec⁻¹) and 60-fold (from 6.0 to 0.1 P 10 sec⁻¹) compared with those of the controls.

One of the problems encountered in the in situ processing of ceramic materials is the possible deleterious effect of the bacterial cells on the quality of the final ceramic product. Ideally, cells should be either grown separately from the particles by using a filter system or removed after they have been grown in the presence of the particles. Since we grew cells in direct contact with the particles, we were interested in determining whether cells could be readily removed without removing the polymer. To study this, successive washings were undertaken to determine whether bacterial cells could be removed from the particles (Table 1). After cultivation for 5 days at 30°C, bacterial cell numbers in the in situ system were 5.6×10^7 per ml of particle suspension (a mixture of bacterial cells, particles, and nutrient solution) before washing. Cell counts in the pellet gradually decreased after each successive washing with sterile saline solution. After the fifth washing, there were only 85 cells per ml of the pellet suspension. Therefore, the bacterial cells do not bind

TABLE 1. Removal of *A. vinelandii* cells from alumina particles by washing

Treatment stage	Viable cells per ml of suspended pellet ^a
Before washing	5.6×10^7
Wash no.:	
1	3.2×10^5
2	1.3×10^3
3	8.2×10^2
4	4.8×10^2
5	8.5×10^1

^a Viable counts are averages of three replicate plates and three repeated experiments.

TABLE 2. Adsorption of alginate to alumina particles^a

Treatment stage	Alginate (mg) in 28.5 ml of supernatant	Alginate adsorbed (%)
Before addition of alumina	26.42	
After addition of alumina ^b	9.66	
Wash no.:		
1	0.143	99.1
2	0	99.1
3	0	99.1

^a Data are averages of three tests.

^b The alumina was removed from suspension by centrifugation. The amount of alginate adsorbed by the particles was determined by subtracting the amount remaining after the alumina was removed from the amount present initially, i.e., 16.76 mg of bacterial alginate was adsorbed by 5.94 g of AKP-30 particles.

strongly to the particles and are readily removed by successive washings.

Separate experiments using particles and cell-free culture supernatant containing bacterial alginate were conducted to assay the amount of polymer adsorbed to the particles and the strength of that adsorption (Table 2). In contrast to the results obtained for the bacterial cells, washing had little effect on the removal of polymer bound to the alumina surface. Thus, when the alumina (5.94 g) was added to the supernatant containing the polymer (26.42 mg in 28.5 ml of supernatant) and removed subsequently by centrifugation, it had adsorbed 16.76 mg of the alginate. By calculation, it was determined that a total of 2.82 mg of bacterial alginate was adsorbed per g of AKP-30 particles. After the first washing of the adsorbed particles, only 0.143 mg was detected in 28.5 ml of supernatant, and none could be detected after further washing. Therefore, more than 99% of the polymer that was initially bound remained adsorbed to the particles even after three successive washes.

Use of nongrowing cells for in situ processing. One logical route to consider for in situ ceramic processing is the use of pre-grown bacterial suspensions that are capable of alginate production under nongrowing conditions. This would allow polymer production under conditions of greater control over pH, carbon source concentration, mineral base medium composition, and cell concentrations, all of which would be expected to have some influence on an in situ process. Furthermore, a condition might be found in which polymer production could be accomplished by a minimum bacterial biomass, since bacterial cells would be undesirable in the final product.

For this purpose, washed suspensions of *A. vinelandii* cells were inoculated into the three different nutrient-deficient media (Table 3). Growth did not occur in either modified medium 1 (mannitol only) or modified medium 2

TABLE 3. Production of alginate in nutrient limitation tests^a

Medium	Final cell yield (cells/ml)	Amt of polyuronic acid present [μg/ml (μg/1,000 cells)]
Larsen's	3×10^8	810 (2.7)
Modified medium:		
1	3.0×10^5	5.8 (20)
2	3.2×10^5	30.5 (100)
3	5.0×10^6	495.4 (100)

^a Experimental cultures were inoculated with 2.8×10^5 cells per ml and incubated for 96 h; data are averages of two experiments.

(mannitol plus buffer). In modified medium 1, the yield of the alginate was very low (only 5.8 µg/ml), but in modified medium 2 alginate production was 30.5 µg/ml, or 100 ng per 1,000 cells. This yield compared favorably with the yield per cell in modified medium 3 (mannitol plus buffer plus acetate); however, greater growth occurred in medium 3 because of the added acetate. In contrast, under normal growth conditions in Larsen's medium the bacterium produced only 2.7 ng of alginate per 1,000 cells. In all media tested, the bacteria lost motility and developed to the cyst stage.

DISCUSSION

Clay aging resembles other empirical processes developed by humans, such as alcoholic and lactic fermentations and bread leavening, that have unwittingly involved microorganisms. However, the actual mechanism that underlies this microbial aging process is still only poorly understood. The results of this study suggest that the production of natural acidic bacterial exopolymers is the underlying explanation for this phenomenon.

The kelp and the bacterial alginates had comparable suspension behaviors, suggesting that they have similar physicochemical properties. The alginate from *A. vinelandii* is not only structurally similar to the alginate from marine algae (both alginates contain blocks of M, blocks of G, and blocks of MG), but it also contains the same ratio of poly(G) to poly(M) that the alginate from marine algae does (21). The primary difference between the alginate from *A. vinelandii* and algae is that O-acetyl groups are associated with some of the M residues of the former. However, the ester-linked acetate groups do not contribute to the charge on the polymer (24, 25).

It is of interest that the polysaccharide concentration for best sedimentation is about 0.5% (Fig. 1), which is close to the concentration at which the polymer was fully adsorbed to the particles (0.3%) (Table 2). Too little or too much polysaccharide resulted in poorer sedimentation. This result also agrees with the results obtained with other polymers (17a). If insufficient polymer is present, dense packing cannot occur. If excess polymer is present, the polymer interacts with itself to cause gelling, leaving void spaces in the cake. Thus, the poorer packing density found at the lower concentration of alumina, i.e., 5 versus 10% (vol/vol) in the in situ growth experiment, is likely due to excess alginate production. It was also observed that the adsorption of polymer can be influenced somewhat by other experimental conditions, including ultrasonication time and the pH of the sample suspension (data not shown).

The high affinity of the polymer for the particles was demonstrated by the experiments in which the coated particles were subjected to several successive washings in distilled water (Table 2). Over 99% of the polysaccharide remained adsorbed to the particles even after three washings.

From the results of these experiments, it is possible to calculate the number of ceramic particles that can be coated with the alginate produced by a single *A. vinelandii* cell (assuming growth on modified medium 2 and an alumina particle radius [r] of 200 nm). From the polysaccharide adsorption data (Table 2), we know that about 2.82 mg of alginate are required to coat 1 g of particles and that this amount of polymer is produced by about 2.82×10^7 cells of *A. vinelandii* (Table 3). Thus, in theory, the alginate produced by a single bacterial cell from medium 2 can coat about 2.8×10^5 AKP-30 particles.

The results of this study indicate that *A. vinelandii* can be used in an in situ process. We have demonstrated that *A. vinelandii* can grow and produce the alginate in 15% (vol/vol) aqueous suspensions of alumina (60 g of particles per 100 ml of suspension). Furthermore, whereas bacterial cells do not adhere strongly to the particles and can be easily removed by washing, the alginate they produce is strongly bound to the particles and cannot be removed by repeated washings. Moreover, only a small number of nongrowing cells is required to coat a large number of particles. While it was not the intent of this study to design a specific procedure for a commercial in situ process for coating advanced ceramic materials, the results of this study should be useful for anyone who wishes to develop such a process using the alginate-producing bacterium *A. vinelandii*.

In addition, the results of this study suggest that commercial pottery manufacture with natural clays could benefit from a fuller understanding of the microbiology of the aging process. Perhaps the use of appropriate bacterial inocula, carbon sources, and other nutrients could improve polymer production, dramatically hasten the seasoning process, and make it more reproducible and efficient, like commercially controlled alcoholic and lactic fermentations.

ACKNOWLEDGMENTS

This investigation was supported in part by a grant from the U.S. Air Force Office of Scientific Research (grant no. AFOSR 88-0135) and the Washington Technology Center (WTC 09-1002). One of the investigators (T.R.) received partial support from the National Education Committee of the People's Republic of China through the Huazhong Agricultural University.

REFERENCES

1. Aksay, I. A. 1984. Microstructure control through colloidal consolidation, p. 94-104. In J. A. Mengels and G. L. Messing (ed.), Advances in ceramics, vol. 9. Forming of ceramics. American Ceramic Society, Columbus, Ohio.
2. Aksay, I. A., F. F. Lange, and B. I. Davis. 1983. Uniformity of $\text{Al}_2\text{O}_3\text{-ZrO}_2$ composites by colloidal filtration. *J. Am. Ceram. Soc.* 66:190-192.
3. Baker, D. R., and D. P. Glick. 1936. Sterilization effects on properties of clays. *J. Am. Ceram. Soc.* 19:209-212.
4. Booth, E. 1975. Seaweeds in industry, p. 219-268. In J. P. Riley and G. Skirrow (ed.), Chemical oceanography. Academic Press Ltd., London.
5. Cesaran, J., III, and I. A. Aksay. 1988. Stability of aqueous Al_2O_3 suspensions with poly(methacrylic acid) polyelectrolytes. *J. Am. Ceram. Soc.* 71:250-255.
6. Cesaran, J., III, and I. A. Aksay. 1988. Processing of highly concentrated alumina suspensions stabilized with polyelectrolytes. *J. Am. Ceram. Soc.* 71:1062-1067.
7. Glick, D. P. 1936. The microbiology of aging clays. *J. Am. Ceram. Soc.* 19:169-175.
8. Glick, D. P. 1936. The effects of various treatments upon the aging of a ceramic body. *J. Am. Ceram. Soc.* 19:240-242.
9. Gorin, P. A. J., and J. F. T. Spencer. 1966. Exocellular alginate acid from *Azotobacter vinelandii*. *Can. J. Chem.* 44:993-998.
- 9a. Graff, G. L., et al. Unpublished data.
10. Grasdalen, H., B. Larsen, and O. Smidsrød. 1979. A P.M.R. study of the composition and sequence of uronate residues in alginates. *Carbohydr. Res.* 68:23-31.
11. Haug, A., B. Larsen, and O. Smidsrød. 1966. A study of the constitution of alginic acid by partial acid hydrolysis. *Acta Chem. Scand.* 20:183-190.
12. Haug, A., B. Larsen, and O. Smidsrød. 1974. Uronic acid sequence in alginate from different sources. *Carbohydr. Res.* 32:217-225.
13. Jarman, T. R., L. Deavin, S. Slocombe, and P. C. Righelato. 1978. Investigation of the effect of environmental conditions on the rate of exopolysaccharide synthesis in *Azotobacter vinelandii*.

- dii.* J. Gen. Microbiol. **107**:59-64.
14. Larsen, B., and A. Haug. 1971. Biosynthesis of alginic, Part I. Composition and structure of alginic produced by *Azotobacter vinelandii*. Carbohydr. Res. **17**:287-296.
 15. Larsen, B., O. Smidsrød, T. Painter, and A. Haug. 1970. Calculation of the nearest-neighbour frequencies in fragments of alginic from the yields of free monomers after partial hydrolysis. Acta Chem. Scand. **24**:726-728.
 16. Matsumoto, T., and K. Mashiko. 1990. Viscoelastic properties of alginic aqueous solutions in the presence of salts. Biopolymers **29**:1707-1713.
 17. Montreuil, J. 1986. Glycoproteins, p. 175. In M. F. Chaplin and J. F. Kennedy (ed.), Carbohydrate analysis: a practical approach. IRL Press, Ltd., Oxford, England.
 - 17a. Pellerin, N. B., G. L. Graff, D. R. Treadwell, J. T. Staley, and I. A. Aksay. Alginic as a ceramic processing aid. Biomimetics, in press.
 18. Pindar, D. F., and C. Buche. 1975. The biosynthesis of alginic acid by *Azotobacter vinelandii*. Biochem. J. **152**:617-622.
 19. Sadoff, H. L. 1975. Encystment and germination in *Azotobacter vinelandii*. Bacteriol. Rev. **39**:516-539.
 20. Sandford, P. A., and J. Baird. 1983. Brown seaweed (Phaeophyceae): algin, p. 448-454. In G. O. Aspinall (ed.), The polysaccharides. Academic Press, New York.
 21. Skjæk-Bræk, G., B. Larsen, and H. Grasdalen. 1985. The role of *O*-acetyl groups in the biosynthesis of alginic by *Azotobacter vinelandii*. Carbohydr. Res. **145**:169-174.
 22. Spurrier, H. 1921. The "why" of ageing clay. J. Am. Ceram. Soc. **4**:113-118.
 23. Stover, E. C. 1902. Bacterial growth as a factor in aging clay mixtures. Trans. Am. Ceram. Soc. **4**:183-192.
 24. Sutherland, I. W. 1988. Bacterial surface polysaccharides: structure and function. Int. Rev. Cytol. **113**:187-231.
 25. Sutherland, I. W. 1989. Bacterial exopolysaccharides: their nature and production. Antibiot. Chemother. (Washington, DC) **42**:50-55.

"Structure-Mechanical Property Relationships in a Biological
Ceramic-Polymer Composite: Nacre,"

K. E. Gunnison

M.S. Thesis

(June 1991, University of Washington, 1991)

"Selection and Use of Biopolymers as an aid in Colloidal
Processing of Ceramics,"

G. L. Graff,

M.S. Thesis

(June 1991, University of Washington, 1991).

RESOLUTION IN THE MICROSCOPE

Ultramicroscopy

Vol. 47 [1-3] 1-307

Collection of Papers Presented at the 48th Annual Meeting of
Electron Microscopy Society of America
San Jose, CA, 4-9 August 1991

Guest Editor

Mehmet Sarikaya

contents

RESOLUTION IN THE MICROSCOPE

A COLLECTION OF PAPERS PRESENTED AT
THE 1991 EMSA MEETING
SAN JOSE, CALIFORNIA, 4-9 AUGUST 1991

Guest Editor:

Mehmet Sarikaya
University of Washington, Seattle



1992
NORTH-HOLLAND

ULTRAMICROSCOPY

Volume 47, Numbers 1-3, 1992

CONTENTS

RESOLUTION IN THE MICROSCOPE

**A collection of papers presented at the 1991 EMSA Meeting
San Jose, California, 4-9 August 1991**

Guest Editor:

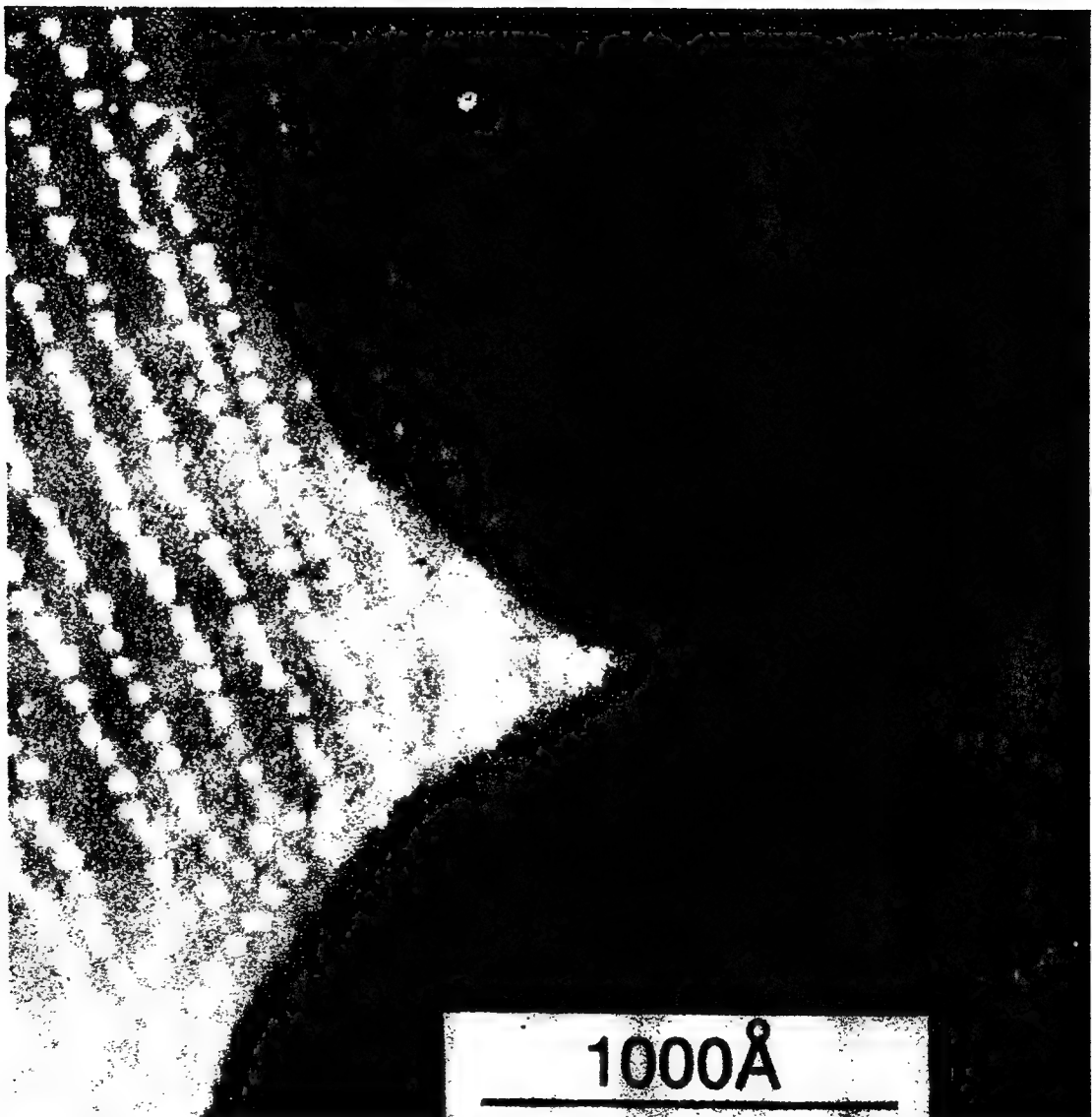
Mehmet Sarikaya

Volume 47, Nos. 1-3
November/December 1992

ISSN 0304-3991
Editor: Elmar Zeitler

ultramicroscopy

An International Journal affiliated with EMSA, ISEM, SCANDEM, NVEM, SGOEM, SIMS-SM-DGE, MSC and ASEM



NORTH-HOLLAND

ULTRDG 47(1-3) 1-306 (1992)

Contents

Preface	vii
Evolution of resolution in microscopy <i>M. Sarikaya</i>	1
Resolution in near-field optical microscopy <i>M. Isaacson, J. Cline and H. Barshatzky</i>	15
Fluorescence microscopy: a tool for studying the physical chemistry of interfaces <i>K.J. Stine and C.M. Knobler</i>	23
Emission microscopy and related techniques: resolution in photoelectron microscopy, low energy electron microscopy and mirror electron microscopy <i>G.F. Rempp and O.H. Griffith</i>	35
Resolution in soft X-ray microscopes <i>C. Jacobsen, J. Kirz and S. Williams</i>	55
High-resolution scanning electron microscopy <i>D.C. Joy and J.B. Pawley</i>	80
Magnetically filtered low-loss scanning electron microscopy <i>O.C. Wells and E. Munro</i>	101
Nanometer-resolution scanning Auger electron microscopy <i>G.G. Hembree and J.A. Venables</i>	109
Definition of the spatial resolution of X-ray microanalysis in thin foils <i>D.B. Williams, J.R. Michael, J.I. Goldstein and A.D. Romig, Jr.</i>	121
Spatial resolution in electron energy loss spectroscopy <i>P.E. Batson</i>	133
Resolution in conventional transmission electron microscopy <i>M. Sarikaya and J.M. Howe</i>	145
Prospects for convergent beam electron diffraction with 200–300 kV cold field emission transmission electron microscopes <i>J.W. Steeds and R. Vincent</i>	162
Quantitative chemical mapping: spatial resolution <i>F.H. Baumann, M. Bode, Y. Kim and A. Ourmazd</i>	167

Resolution limits in annular dark field STEM <i>J. Silcox, P. Xu and R.F. Loane</i>	173
Resolution limitation in the electron microscopy of surfaces <i>J.M. Cowley</i>	187
Ultra-high-resolution chemical analysis by field-ion microscopy, atom probe and position-sensitive atom-probe techniques <i>C.R.M. Grovenor, G.D.W. Smith, A. Cerezo, J.A. Liddle, R.A.D. Mackenzie, P.J. Warren, R.P. Setna, J.M. Hyde, J.E. Brown, I. Stark and B.A. Shollock</i>	199
Resolution in the scanning tunneling microscope <i>R.J. Wilson, P.H. Lippel, S. Chiang, D.D. Chambliss and V.M. Hallmark</i>	212
Electron holography. I. Can electron holography reach 0.1 nm resolution? <i>H. Lichte</i>	223
Electron holography. II. First steps of high resolution electron holography into materials science <i>H. Lichte, E. Völk and K. Scheerschmidt</i>	231
Methods of calculating resolution in electron microscopy: Scherzer's equation, circles of least confusion and the intensity distribution approach <i>G.F. Rempfer</i>	241
Assessment of resolution in biological electron crystallography <i>R.M. Glaeser and K.H. Downing</i>	256
Ultimate resolution and information in electron microscopy: general principles <i>D. Van Dyck and A.F. de Jong</i>	266
"Resolution" in high-resolution electron microscopy <i>M.A. O'Keefe</i>	282
Ultimate resolution: a mathematical framework <i>A. van den Bos</i>	298

**"Hydroxylated Carboxylic Acid Monomers Serve as
Dispersants for Ceramic Particles"**

Tao Ren, I. A. Aksay, M. Yasrebi, N. B. Pellerin, and J. T.
Staley

paper in preparation for a publication
(1993)

Hydroxylated Carboxylic Acid Monomers Serve as Dispersants for Ceramic Particles

**Tao Ren¹, I. A. Aksay^{2*}, M. Yasrebi³, N. B. Pellerin¹,
and J. T. Staley^{1**}**

Departments of Microbiology¹ and Material Science and Engineering²,
University of Washington, Seattle, Washington 98195
Structurals Division - Technical Center, Precision Castparts Corp.³,
Portland, Oregon, 97206

Key words: dispersion, carboxylic acids, hydroxyl group, ceramic processing, pKa value, alumina particles, sedimentation, zeta potential, adsorption, hydrogen bond

* Author's new address:

** Corresponding author

Abstract

Carboxylic acids, which contain one to three negatively charged --COO⁻ group(s), were investigated as dispersion additives in the processing of the ceramic particles. A total of 21 of these carboxylic acids were examined for dispersion by sedimentation tests in this study. Only carboxylic acids containing more than one hydroxyl group were able to disperse the Al₂O₃ particles (AKP-30 Sumitomo Co., 400 nm diameter,) in aqueous suspensions. The packing densities of the ceramic particle suspensions varied from 30 % to 50 % of the theoretical depending on the numbers of hydroxyl groups and carboxylate groups. Four carboxylic acids, citric acid, tricarballylic acid, meso-tartaric acid and fumaric acid, were studied in detail by measurements of zeta potential, particle packing, and dispersant adsorption characteristics to compare their dispersion behavior. These detailed studies further indicate that carboxylic acid groups and hydroxyl groups are both important for dispersion of the ceramic particles. Thus, organic acids containing only the negatively charged carboxylate group do not disperse ceramic particles in aqueous suspensions. Hydroxyl groups are also necessary. Citric acid was found to be an excellent dispersant by itself. Using it alone resulted in attaining a high solids loading concentration of greater than 50 vol% of AKP-30 particles and a viscosity lower than 1,000 cPs. From the study, it can be concluded that the hydroxyl group associated with the carboxylic acid increases the adsorption of the acidic monomer molecules to the ceramic particle surface (adsorption measurement) and therefore increases the surface charge of the particles (zeta potential measurement up to -68 mV). This high surface charge results in a stronger charge repulsion between the particles and therefore provides better dispersion stabilization in the aqueous suspension.

Introduction

New significant developments in the preparation of advanced ceramics have focused on improvements of materials properties (1,2). It is especially important to improve the resistance to cracking and fracture by reducing or removal of microstructure voids and defects. Therefore it is important to obtain high densities in preparation of ceramic products to reduce the weakness of the finished parts, since high packing densities can minimize void volumes and internal stress by forcing the particles to pack in a highly ordered space-filling array (3,4,5). Recent advances indicate that significant improvements in attaining high packing densities in ceramics processing can be achieved by control of dispersion and colloid rheology. However, particles of such small size are subject to strong interparticle interactions, such as the van der Waals force, which could cause agglomeration in rough aggregates and result in a porous product. To prevent this and produce a high packing densities, polyelectrolytes, which act by providing a significant electrical repulsion between particles, can be used as dispersants. Currently, synthetic polymers from petrochemicals, such as polymethacrylic acid (PMAA) and polyacrylic acid (PAA) are used as dispersants (6, 7...). Similarly, previous work from this laboratory has shown that biologically produced polyelectrolytes such as Kelp and bacterial alginate and bacterial polyglutamic acid also function as dispersants in ceramic processing (8,9,10). However, synthetic and biological polymers have several major limitations 1) polydispersant layers may be too thick to allow high packing densities; 2) the polyelectrolyte may not be compatible with useful gelling biopolymer matrices (12); 3) commercial cost; and 4) specifically, in the case of the synthetic polymers PMAA and PAA, lack of biodegradability.

Graff (11), Cesarano and Aksay (6,12), and others (check the ref. in Cesarano' thesis) indicate that polymers may form many loops and tails that away from the particle surface thereby increasing the thickness of the polymer layer on the particle surface and preventing close particle packing. In this case the lower the molecular weight of the polyelectrolyte, the better the dispersion of particles. With a molecular weight of about 5,000 D (6,7,12), PMAA produced the best dispersion behavior when compared to other polymers of higher molecular weight. Unpublished data from this laboratory also indicate that in aqueous solutions, polymers with higher molecular weights can interact with themselves to form gel structures which increase the viscosity of the suspension system and limit the otherwise good dispersion performance of the polyelectrolyte. Furthermore,

PMAA may contain formaldehyde, and PAA may contain residual amounts of acrylic acid. both are toxic and are produced from precursors that are toxic and/or carcinogenic. Additionally, all synthetic and biologically produced polymers are expensive to synthesize, harvest, isolate and purify.

This study was undertaken to investigate the use of monomers as dispersants. The compounds tested comprise a group of carboxylic acids.

Materials and Methods

(1) Materials and Chemicals

Ceramic particles. The ceramic particles used in this study were high-purity (99.99%) Al₂O₃, with an average particle diameter of 400 nm and a density of 3.96 g/ml (AKP-30, Sumitomo Chemical America, Inc., New York, N.Y.).

Carboxylic acids. Carboxylic acids and their salts used in this study are listed in Table 1. All are commercially available from Sigma Chemical Company (St. Louis, Mo) and/or Aldrich Chemical Company, Inc. (Milwaukee, WI).

The water used was distilled and deionized. The pH was adjusted with standardized analytical-grade HCl and NaOH solutions.

(2) Experimental Methods

Preparation of the suspensions. The preparation of the suspensions for all purposes in this study was performed in following manner: a specific vol% of AKP-30 particles was added to the aqueous system (distilled water or acid solution). This suspension was stirred for about half hour and its pH was roughly adjusted to the desired value. The suspension was ultrasonicated for 3-6 min at 58 W (Fisher Sonic Dismembrators Model 300) and the pH was constantly monitored and adjusted for at least 0.5 h (most samples, overnight) so that it was always within 0.05 unit of the desired pH value. This comprised the ceramic suspensions used in the experiments below.

Sedimentation tests. Sedimentation columns of 2 vol% AKP-30 powder with various concentrations and types of carboxylic acids were prepared as described above. 10 mL of each suspension was then poured into a conical-bottom, graduated polystyrene tube (Falcon 2095; Becton Dickinson) and left undisturbed at room temperature for 3 weeks. Final sedimentation heights (cake height in milliliters) were measured to +/- 0.1 mL.

Viscosity measurements. The viscosity of the suspensions with a certain volume percent of particles was measured by a Rheometrics Fluid spectrometer (Model 8400; Rheometrics Inc., Piscataway, N.J.). Suspensions (about 15 mL) for these measurements were prepared as described above.

Zeta potential measurements. Electrophoretic mobility was measured (ZETASIZER 3 from Malvern instruments, Laser Electrophoresis Analyses) and used to calculate zeta potential according to Henry's equation (ref.). These measurements can only be completed on very dilute suspensions. Therefore, the

prepared AKP-30 suspensions were centrifuged and the supernatant was carefully decanted into a beaker; subsequently, a very minute amount of the sediment was remixed with the supernatant.

Fraction dissociation determination of the carboxylic acids. A given carboxylic acid at 1 M concentration was titrated with 2 M NaOH solution (when titrating di-carboxylic acids) or 3 M (when titrating tri-carboxylic acids). The amounts of the titrant consumed at each pH point was recorded gradually from the beginning pH (about 2) to the equivalence point. From this information the fractions of titrant consumed at each point to the titrant consumed at the equivalence point were calculated and the curve of fraction dissociated versus pH was drawn.

Adsorption of acid to the particle. Suspensions of 20 ml 10 vol% Al_2O_3 were prepared with 0.5 and 1% (dry weight basis) of carboxylic acids at various pHs (4,6 and 9). The suspensions were then centrifuged for 30 min. at 10,000 rpm after the samples were stirred overnight and the pH was readjusted. 10 mL of the supernatant was then titrated to determine the amount of acid remaining in solution. From the difference between the amounts of the titrant added to the corresponding blank solution and the sample supernatant, the adsorption of the acid to the particles' surface at a specified pH was calculated.

Results

(1) Dispersion of the alumina suspension by carboxylic acids with hydroxyl groups

A total of 21 carboxylic acids were evaluated for their dispersion behavior. Most of them are acidic and have one, two, three or four carboxylate groups. Table 1 shows their molecular structures, pKa values, molecular weights and solubility data. The sedimentation results are shown in Table 2 and Figure 1. Tartaric acid, citric acid, mucic acid produced the best dispersion with the ceramic suspension and malic acid, tartronic acid, mesoxalic acid provided some dispersion effect. These results are shown schematically in Table 3. From the molecular structure, it can be seen that tartaric acid, citric acid, mucic acid, malic acid, tartronic acid and mesoxalic acid all contain hydroxyl group(s). In contrast succinic acid, maleic acid, tricarballylic acid, aconitic acid, and adipic acid do not contain this group. When the various organic acids that are structurally similar to one another are compared by molecular weight and pKa value, the hydroxyl group was the principal difference between those producing good versus poor dispersion.

The viscosity measurement gave similar results. With citric acid and tartaric acid, AKP-30 ceramic particle suspensions with solid concentrations as high as 50 vol% could be prepared with a viscosity lower than 1,000 cP.s. On other hand, it was difficult to prepare ceramic suspensions with a solids concentration higher than 20 vol% when succinic acid, malic acid, tricarballylic acid, aconic acid or adipic acid were used as dispersants.

(2) Comparison of dispersion versus the particle surface charge

Two pairs of carboxylic acids, citric acid versus tricarballylic acid, and meso-tartaric acid versus fumaric acid were chosen for more detailed investigation of sedimentation and surface charge under various acid concentrations. These two pairs were chosen because in each pair, the two acids (for example, meso-tartaric acid and fumaric acid) have similar molecular structures, molecular weights and especially close pKa values (since the difference of pKa could result in different dissociation of the acid groups in aqueous solution). In fact, the difference of the dissociation between compared carboxylic acids is not key case (will discussed below). The sedimentation and zeta potential results of citric acid and tricarballylic acid with various concentrations of the acids are shown in Figures 2, 3, 4 and 5. In Figure 2 all samples (except the samples at pH 4) at pH 6, 8, 9, and 10 produced

the lowest cake heights (about 0.5 ml in this test) when the concentration of citric acid in the suspension was increased to 0.3 % (dwb). At pH 4, the cake height was lowest without any citric acid and eventually increased as the concentration of the acid increased to achieve a maximum at 0.4 %. After this, the cake heights of the samples plateaued at about 1.2 ml. This effect was thought to be due to incomplete adsorption of the acid by the particles (6,7). Trace amounts of citric acid (<0.1%, except at pH 4) induced flocculation and resulted in large sedimentation volumes. This occurred because the binding energy between the particles is high and the particle clusters that form during consolidation behave as rigid flow units and do not pack densely. In contrast, at concentrations at and above about 0.2% citric acid, the binding energy between particles is low and the particle clusters display a relatively denser packing structure (6,12). Similar to PMAA, it can be observed that small additions (<0.2%) of citric acid neutralize charge and induce subsequent flocculation. In this regime, flocculation is mainly due to electrostatic patch model flocculation (12). This type of flocculation takes place because negatively charged patched due to the adsorbed carboxylic acid are attracted to positively charged patches of surface on other particles (12).

These dispersion behaviors correlate with and can be explained by zeta potential experiments. Figure 3 shows that with increasing citric acid concentration, the zeta potential decreases to zero (at pH 4 and 6) and then reverses sign and increases in the negative direction. With pH 8, 9, and 10, suspensions the zeta potential is near zero or already negative, so, as the concentration of the citric acid increases, the zeta potential continues to increase in negative direction. Above 0.2% acid , the zeta potential approaches a nearly constant value of -65 mV (at pH 4 this is 33 mV). This value may reflect the saturated monolayer of citric acid.

From the curve, it can also be concluded that the higher the pH of the samples, the earlier the cake height reaches its highest point (e.g., flocculation). This is because the lower the pH, the greater the number of positive sites on the particle surface (ref. from Cesarsno'). Therefore, a sample with lower pH (for instance, pH 4) needs to adsorb more acid to achieve saturation.

At pH 4 the dispersion result is different from the other pHs, and this may also be due to the surface charge property of the particles. At this pH, the particle is much more positively charged so its net surface charge is positive (about 65 mV) sufficiently high to disperse each other without any acid added. However, the mechanism why at pH 4 the suspension of citric acid - alumina particle performs

worse dispersion (in both sedimentation and zeta potential) in comparison with higher pHs is not understood. This can also be observed in tricarballylic acid - alumina particle suspension. It is contradicting to the surface charge property of the particles. At lower pH, the particle surface has more positive charge sites (ref.), the surface could adsorb more amounts of the negatively charged carboxylic acid and would result in higher repulsion forces between the particles (higher zeta potential in this case) and higher packing density (lower cake height) than at higher pHs. So, the plateau of the pH 4 shoud be lower than that of other higher pHs. The explanation of this reversed result could be attributed to the lower dissociation of the carboxylic acid in low pH.

In contrast the tricarballylic acid did not produce the same packing densities as the citric acid under the same conditions (Figure 4) and zeta potential values (Figure 5) regardless of pH. At pH 4 the zeta potential changed from 55 mV to about 5 mV and never reversed sign. The cake height increased from 0.6 mL to 3.5 mL (at 1.0%). Similar results were observed at pH 6. The zeta potential decreased from about 43 mV to zero at about 0.2% concentration and then reversed sign and decreased to about -30 mV. This result is consistent with the sedimentation tests in which the cake height is first low (0.75 mL) and reaches its summit (2.5 mL) before 0.2% concentration and then decreases to around 1.5 mL but never decrease further although the concentration of the acid was increased to 6% (result not shown). At pH 8, 9, and 10, the zeta potential varies within the range of 0-40 mV, but the cake heights changed slightly (from 2.7 mL to 2.3 mL). As mentioned in the sedimentation section, the zeta potential and packing density differences between citric acid and tricarballylic acid could be attributed to the hydroxyl group of citric acid as discussed below.

The results from another pair of the carboxylic acids, fumaric acid and meso-tartaric acid, further confirm the observations of the effect of the -OH group. Figure 7 and 8 show that like citric acid and tricarballylic acid, both the zeta potential and the cake height of the meso-tartaric acid - alumina suspensions were different from those of the fumaric acid - alumina suspensions. Using the same concentration of the acids (0.5% dwb), the cake height of the suspensions prepared with both fumaric acid and meso-tartaric acid decreases as the pH increased. The cake height of the fumaric acid suspension changed from 4 mL to 2.5 mL and the that of meso-tartaric acid suspension from 2.7 mL to 0.5 mL. However, at each pH, the cake height of the meso-tartaric acid suspension was always lower than that of the fumaric acid suspension (e.g., the meso-tartaric acid suspension was packed

more densely than the fumaric acid suspension under the same conditions). These data are also consistent with the zeta potential measurements. The zeta potential of the fumaric acid suspension decreases from 10 mV to about 40 mV when the pH of the suspension changed from 4 to 10. The zeta potential of meso-tartaric acid suspension decreases from -17 mV to -65 mV as the pH of the suspension was changed from 4 to 10. Therefore it can be concluded that at every pH, zeta potential of the meso-tartaric acid suspension was lower than that of the fumaric acid suspension.

(3) Adsorption of the carboxylic acids with -OH group on Al_2O_3

As discussed above, the different dispersion behaviors between the carboxylic acids with hydroxyl groups and the carboxylic acids without hydroxyl groups could be attributed to hydroxyl groups. According to this study, it can be concluded that the higher particle surface charge results in a higher packing density and the hydroxyl group may produce an increase in the surface charge. How do the hydroxyl groups affect the particle surface charges? Chemically, the -OH group is an electron-withdrawing group, which is defined as the group that extends to attract an electron. The more electronegative the group is, the stronger the withdrawal. Neckers and Doyle (16) explained this as an inductive effect. But this inductive effect only influences the acidity of the acid, or in other words, the acidity constant, K_a . If two acids have very closed pK_a 's, it would be difficult to explain the adsorption difference of the acid by this mechanism.

One another explanation could be that hydroxyl groups affect the adsorption of the acid to the particles. To verify this, tests evaluating adsorption of the acid to the particles were performed by titration. Figures 6 and 9 show the adsorption of citric acid, tricarballylic acid, meso-tartaric acid and fumaric acid per 3.96 gram particles. The samples were examined at 2 concentrations (0.5 % dwb and 1.0% dwb) or a single concentration (0.5%, dwb) at 3 pH's (pH 4, 6 and 9) with citric acid and tricarballylic acid. At each treatment, the adsorption of citric acid and meso-tartaric acid were always greater than that of tricarballylic acid and fumaric acid. These results clearly show that the hydroxyl group associated with the carboxylic acid can somehow increase the adsorption of the acid to the particle and this increase of the adsorption may result in the increase of the particle surface charges (zeta potential) and therefore increase the dispersion capability of the acid with the hydroxyl group. From Figure 6 and 9, it can also be seen that at lower pH values, the acids were adsorbed more than at higher pH. This agrees again with the

results from the zeta potential and sedimentation tests and it can be explained as follows: at lower pH, the surface of the particle has more positive charges than at higher pH and therefore can attract more negatively charged carboxylic acid.

Another interesting observation is seen from Figures 6 and 9. At the same pH, when the concentration of the acid increases, the adsorption of the acid also increases and no plateau was observed over the test range. These results are different from reports of other researchers (6, 11 and 12), who showed that the pattern of the adsorption curve of polyelectrolytes (PMAA and PAA) to ceramic particles produces a plateau. In their work, initially the adsorption of the polymer increases as the concentration of the polymer increases, but when the concentration of the polymer reaches a certain value, the adsorption of the polymer to the particle surface remains unchanged because the positive sites on the surface of the particle are saturated. The changing of the adsorption of the acid to the particle surface as the concentration of the acid was changed could be explained by the monomer property of the carboxylic acid. When monomers which are weak acids (pK_a around 4) were used as dispersants, their dissociations kept changing and could decrease as with an increase in the concentration of the acids (17). Therefore, if all other conditions are constant, more acid molecules would be needed to cover the same particle surface area as the concentration of the acid increases from 0.5% to 1.0% in this study. From this point, it seems that increasing the concentration of the dispersant does not affect the dispersion performance of those monomers in certain concentration range. This could be a advantage over the polymer dispersants such as PMAA, in which little increase of the PMAA concentration after satuation could result the flocculation of the suspention (12). Our further sedimentation and zeta potential tests confirmed this (data not show here). When the concentrations of citric acid and meso-tartaric acid increased to 6.0% (dwb), they still produced good dispersion of alumina particles. Of cause, this conclusion need to be confirmed by further adsorption measurements with different concentrtrions of the acid.

To confirm that the difference of adsorption between hydroxylated carboxylic acids and non-hydroxylated carboxylic acids is not due to the difference of the dissociation of the acids, the fraction dissociated, a , of four acids versus pH were obtained by titration. The results are shown in Figure 10. From the figure little difference could be seen among the four different carboxylic acids. This curve of fraction dissociated agrees also very well with the reference acidic constant data, K_a , which are in the order of fumaric acid, meso-tartaric acid, citric acid, and

tricarballylic acid from greater to the smaller. Especially, in the case of the acid pair, fumaric acid and meso-tartaric acid, at certain pH's, the dissociation of fumaric acid (pK_a are 3.03 and 4.44) was even higher than that of meso-tartaric acid (pK_a are 3.22 and 4.82) referred to the Figure 10 and Table 1, but the dispersion capability of fumaric acid is less than that of meso-tartaric acid according to the sedimentation tests, zeta potential measurements, and adsorption tests. This further supports the view that dissociation is not the reason for the difference in adsorption.

Discussion

A new group of monomers has been found that serve as excellent dispersants of alumina for the processing of aqueous ceramic suspensions. These hydroxylated carboxylic acid dispersants are mostly naturally occurring acidic compounds. These organic acid monomers are structurally simpler, commercially less expensive, and environmentally compatible, and can promote the rapid formation of stable, homogeneous aqueous suspensions of 400 nm diameter alumina particles. Torobin (15) and Pearson (14) have previously reported that citric acid and tartaric acid can serve as dispersion agents when used together with the commercial polymer, Darvon C. However, this study for the first time has shown that these organic carboxylic acids are able to serve as sole dispersants for ceramic processing.

The results of this study clearly show that all of the carboxylic acids test cannot be used as dispersants. Only those that contain hydroxyl group(s) disperse alumina particles in aqueous suspensions. Although some organic acids tested contain more than two or more carboxylate groups, they do not function well as ceramic dispersants without the presence of a hydroxyl group. Similar results were observed with monomers possessing similar acidic constants. Furthermore, it can also be stated that for compounds that contain the same number of charged groups and carbon atoms and have a similar molecular structure, the more hydroxyl groups the molecule has, the better it performs as a dispersant (group I: tartronic acid and mesoxalic acid; group II: tartaric acid, malic acid, maleic acid and succinic acid; group III: citric acid, tricarballylic acid and aconitic acid; group IV: mucic acid and adipic acid). Compared with the effect of the hydroxyl group, the effect of a double bond between the carbon atoms is insignificant.

These results were confirmed by studies using high solid loading suspensions which indicate that aqueous suspensions of AKP-30 with a concentration higher than 50 vol% can easily be obtained with citric acid, which keeps the viscosity of the suspension below 1,000 cP.s. In contrast it is difficult to prepare AKP-30 suspensions with a similar viscosity when the particle concentration is higher than 20 vol% with tricarballylic acid, nitrilotriacetic acid, or EDTA although they have the same number or more charged carboxylic groups and similar pKa values as citric acid does.

It should also be noted that the various chain lengths of the carboxylic acids does not significantly affect the dispersion behavior of the monomers, although the

lengthening of the carbon chain does reduce the solubility of some acids. For example, glutamic acid (solubility: 80-200 g/100 ml) and maleic acid (79 g/100 ml) both have greater solubilities than tartaric acid (solubility: 21 g/100 ml) and mucic acid (solubility less than 2 g/100 ml), but the latter two produce much higher dispersion capability than the former two.

The explanation of how the hydroxyl group of the carboxylic acid affects the adsorption and the dispersion behavior is not known. Rosen (13) and () suggested several possible mechanisms for surfactant adsorption to solid substrates in aqueous solution. One possibility is hydrogen bond formation between substrate and adsorbate. The hydroxyl group of the carboxylic acid could increase the adsorption by hydrogen bond formation or other mechanisms. This increase of the adsorption is accompanied by an increase in the surface charge of the particles and therefore an increase in the dispersion capability.

It is also possible that the hydroxyl group of the carboxylic acid influences the charge behavior of the --COO⁻ groups on the molecule, for instance, the --OH group next to the --COO⁻ group could cause a redistribution of the electron destiny (electron cloud) of the oxygen atoms (18). Additionally, it is also possible that a hydroxyl group associated with carboxylic acid could increase the affinity chelation of the acid to the particle surface and this could strengthen the reaction between the particle and dispersant. Or, a combination of these and other effects may play a role.

Some inorganic or organic nonbiogenic dispersion polyelectrolytes used currently, such as PMAA and PAA, are environmentally incompatible. In addition, these chemically synthesized polymers are expensive compared with simpler biogenic molecules. Biopolymers, such as alginate, polypeptides have been investigated as dispersants for ceramic processing (8,9,10.). However, all polyelectrolytes (including both synthetic and biopolymers) have the same disadvantage - steric hindrance, which has two functions: on the one hand, steric hindrance provides steric stabilization for the ceramic suspension (6,7,12); on the other hand, however, because the polymer's tails and loops extend away from the surface of the particles, steric hindrance could limit the close packing of particles in aqueous suspensions (6,11). Cesserano examined the effects of the molecular weight of the PMAA. The results showed that PMAA molecules of lower molecular weight provide better dispersion than those of larger molecular weight. This advantage could become much more significant when carboxylic acids are used with smaller nano-sized particles, such as AKP-30 alumina particles.

The chemical composition of the carboxylic acids should be suitable for and compatible with diverse industrial processes. These monodispersant (most are biogenic) contain only carbon, hydrogen, and oxygen in their molecular structure and no phosphorous, sulfur, halides, or metals. Therefore, these novel dispersants should not be corrosive, nor detrimental to product quality when used in ceramics processing or other applications.

Citric acid and other biogenic acids are currently in wide use in industry and medicine. They are inexpensive and can be readily produced by large scale microbial fermentation. They are non-toxic and readily biodegradable. Additionally, because most of them are small monomers they readily dissolve in the aqueous solution, and unlike most polymers, they do not cause gel formation and phase separation when mixed with the gelling agent in the preparation of aqueous particle suspensions, which is especially crucial in the PMAA or PAA suspension system. This means that they should be compatible with other gelling agents such as agarose. When a 0.5% (dwb) of citric acid is combined with a 0.3% (dwb) of polyglutamic acid or bacterial alginate used to disperse AKP-30 particles, no significant increase of viscosity and phase separation were observed (data not shown here), evidence which supports this contention.

Therefore, in summary, this new group of simple monomers provide several advantages over both synthetic and biologically produced polymer dispersants. In addition, besides the immediate applications of hydroxylated carboxylic acids for ceramic processing, the recognition of the importance of the hydroxyl group in combination with carboxylate groups in enhancing dispersion demonstrated by this investigation may lead to the recognition or development of new monomers and polymers as effective and useful dispersants.

Acknowledgements

This investigation was supported in part by a grant from the U.S. Air Force Office of Scientific Research (grant no. AFOSR 88-0135) and the Washington Technology Center (WTC 09-1002).

References

1. Brown, K.H., Scientific American, 255, 168 (1986).
2. Brown, K. H. Calvert, P.D., Lalanandham, R.R. Parish, M. V., Fox, J., Lee, H., Pober, R. L. and Tormey, E. S, Res. Symp. Proc., 73, 579 (1986)
3. Onoda, G.Y.Jr. and Hench, L.L., "ceramic Processing Before Firing", Jone Wiley & Sons, USA, 1978.
4. Wang, F.F.Y., "Treatise on materials science and technology", V.9, "Ceramic Fabrication Processes", Academic Press, USA, 1979.
5. S.Horowitz and J.K.Currie, J. Dispersion Science and Technology, 11(6), 637-659,1990.
6. Cesarano, J., III, and I. A. Aksay. 1988. Stability of aqueous Al₂O₃ suspensions with poly(methacrylic acid) polyelectrolytes. J. Am. Ceram. Soc. 71:250-255.
7. Cesarano, J., III, and I. A. Aksay. 1988. Processing of highly concentrated alumina suspensions stabilized with polyelectrolytes. J. Am. Ceram. Soc. 71:1062-1067.
8. Tao Ren, N. B. Pellerin, G. L. Graff, I. A. Aksay, and J. T. Staley. 1992. Dispersion of small ceramic particles (Al₂O₃) with Azotobacter vinelandii. Appl. Envir. Microb. 58: 3130-3135.
9. Pellerin, N. B., G. L. Graff, D. R. Treadwell, J. T. Staley, and I. A. Aksay. Alginate as a ceramic processing aid. Biomimetics, in press.
10. Graff, G. L., et al. Unpublished data.
11. Graff thesis for Master degree.
12. Cesarano' thesis for Ph D degree.
13. M.J. Rosen, 1975. Relationship of structure ot properties in surfactants. III. Adsorption at the solid-liquid interface from Aqueous solution. J. American Oil Chemist's Soc. 52: 431-435.
14. Alan Pearson, J. E. Marhanka, 1974. Aluminum oxide fibers. Ger. Offen., 10-
15. L.B. Torobin, 1986. Methods and apparatus for producing hollow microspheres made from dispersed particle compositions. PCT int. Appl., 98-.
16. D.C. Neckers, M.P. Doyle, 1977. Organic chemistry. pp. 459-468. John Wiley & Sons, Inc. New York.
17. W.L. Masterton, and E.J.Slowinski, 1973. Chemical Principles (third edition). pp. 459-460. W.B. Saunders Co., Philadelphia.

Table 1: Carboxylic acids investigated in this study with their molecular components, acidic constants and solubilities.

Name	Structure	pKa	Solubility (g/100 ml H ₂ O)
Mono-carboxylic acids			
Glutamic	-OOCCH(NH ₃ ⁺)(CH ₂) ₂ COOH	2.19, 4.25, 9.67	~ 80-200
Mannuronic	HOOC[CH(OH)] ₄ CHO	-	-
Di-carboxylic acids			
Adipic	HOOC(CH ₂) ₄ COOH	4.43, 4.41	2
Mucic	HOOC[CH(OH)] ₄ COOH	-	-
Fumaric (<i>trans</i>)	HOOCC=CHCOOH	3.03, 4.44	0.7
<i>meso</i> -Tartaric	HOOCCH(OH)CH(OH)COOH	3.22, 4.82	167
Succinic	HOOC(CH ₂) ₂ COOH	4.16, 5.61	6
Maleic(<i>cis</i>)	HOOCC=CHCOOH	1.83, 6.07	79
Malic	HOOCCH ₂ CH(OH)COOH	3.40, 5.11	138
<i>d,l</i> -Tartaric	HOOC[CH(OH)] ₂ COOH	2.98, 4.34	21
Malonic	HOOCCH ₂ COOH	2.83, 5.69	74
Tartronic	HOOCCH(OH)COOH	2.42, 4.54	-
Mesoxalic	HOOCOCOOH	-	-
Glutaric	HOOC(CH ₂) ₃ COOH	4.34, 5.41	64
Sebacic	HOOC(CH ₂) ₈ COOH	4.6, 5.6	-
Tri-carboxylic acids			
Tricarballylic	HOOCCH ₂ CH(COOH)CH ₂ COOH	3.6, 4.7, 5.8	-
Aconitic (<i>trans</i>)	HOOCCH ₂ (COOH)=CHCOOH	2.8, 4.6,-	-
Nitrolotriacetic	HOOCCH ₂ N(CH ₂ COOH)CH ₂ COOH	3.03, 3.07, 10.7	-
Citric	HOOCCH ₂ C(OH)(COOH)CH ₂ COOH	3.13, 4.76, 6.40	-
Tetra-carboxylic acids			
Ethylenediamine tetracetate (EDTA)	HOOCCH ₂ N(CH ₂ COOH)CH ₂ CH ₂ N(CH ₂ -COOH)CH ₂ COOH	-	-

Note: The data are from 1) --- Index, and 2) Physical and Chemical Handbook

Table 2: Sedimentation results (cake height, ml) of selected carboxylic acids at various concentrations (dry weight base of the particle)

	0	0.1 %	0.3 %	0.5 %	1.0 %	2.0 %	3.0 %	4.0 %	6.0 %
Succinic	1.85	2.40	2.45	2.7	2.7			2.40	
EDTA	1.8	1.75	2.0	2.0	2.0			1.9	
<i>d,l</i> -Tartaric	2.20	2.60	1.50	0.55	0.55			0.45	-
NTA	2.25		1.90	1.45	1.10			0.90	
Citric	2.0	2.0		0.50	0.50		0.40		0.40
TCA				1.70		1.20			
Malic				0.70		0.70			
Tartronic				0.70		0.50			
Mesoxalic				0.80		0.50			
<i>cis</i> -Aconitic				1.10		1.00			
<i>trans</i> -Aconitic				1.80		1.75			
Mucic				0.50		1.60			
Maleic				2.50		2.50			
Glutamic	1.80	1.80							
Mannuronic	1.80	1.85							
<i>meso</i> -Tartaric	0.55	0.60							
<i>trans</i> -Fumaric	3.00	3.00							
Adipic			1.80					1.75	
Malonic		2.00		2.05				1.80	
Glutaric	2.50	2.50							
Sebacic	2.00	3.50							

Table 3: Comparison of the dispersion behavior of carboxylic acids in groups according to the numbers of -OH groups.

	Satisfactory	Less satisfactory	Unsatisfactory
Group I: three carbon atoms		HOOCCH(OH)COOH (Tartronic acid) HOOCOCOOH (Mesoxalic acid)	
Group II: four carbon atoms	$\text{HOOC}[\text{CH(OH)}]_2\text{COOH}$ (Tartaric acid)	$\text{HOOCCH}_2\text{CH(OH)COOH}$ (Malic acid)	$\text{HOOCCH}_2\text{CH}_2\text{COOH}$ (Succinic acid) $\text{HOOCCH}_2\text{CH}_2\text{COOH}$ (Maleic acid)
Group III: five carbon atoms in main chain	$\text{HOOCCH}_2\text{C(OH)(COOH)COOH}$ (Citric acid)		$\text{HOOCCH}_2\text{CH(COOH)CH}_2\text{COOH}$ (Tricarballylic acid) $\text{HOOCCH}_2\text{C(COOH)=CHCOOH}$ (Aconitic acid)
Group IV: six carbon atoms in main chain	$\text{HOOC}[\text{CH(OH)}]_4\text{COOH}$ (Mucic acid)		$\text{HOOC}(\text{CH}_2)_4\text{COOH}$ (Adipic acid)

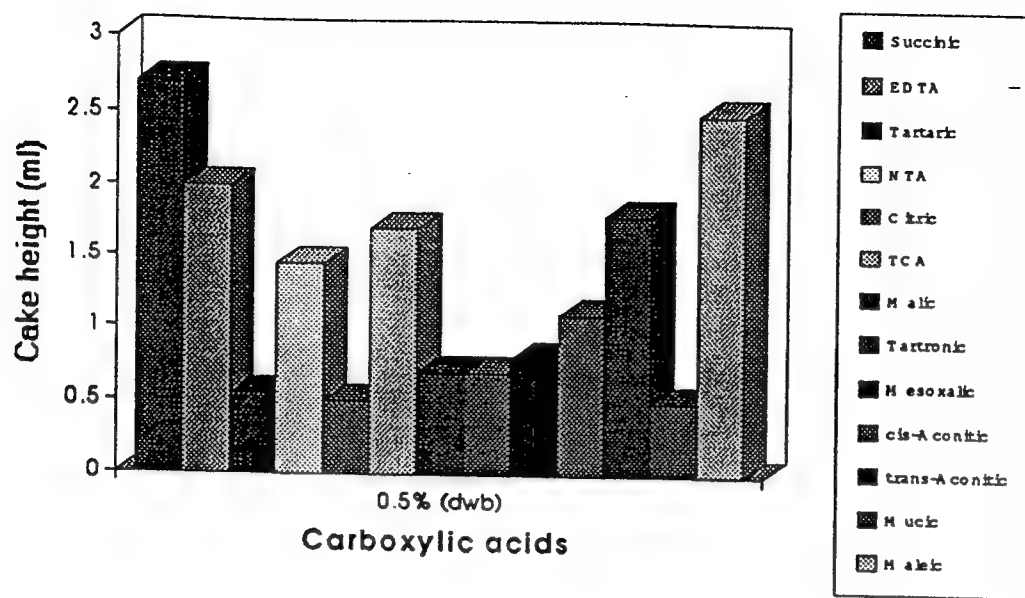


Figure 1: Sedimentation densities of the AKP-30 particle suspensions with selected carboxylic acids from Table 1 at concentration of 0.5% (dwb).

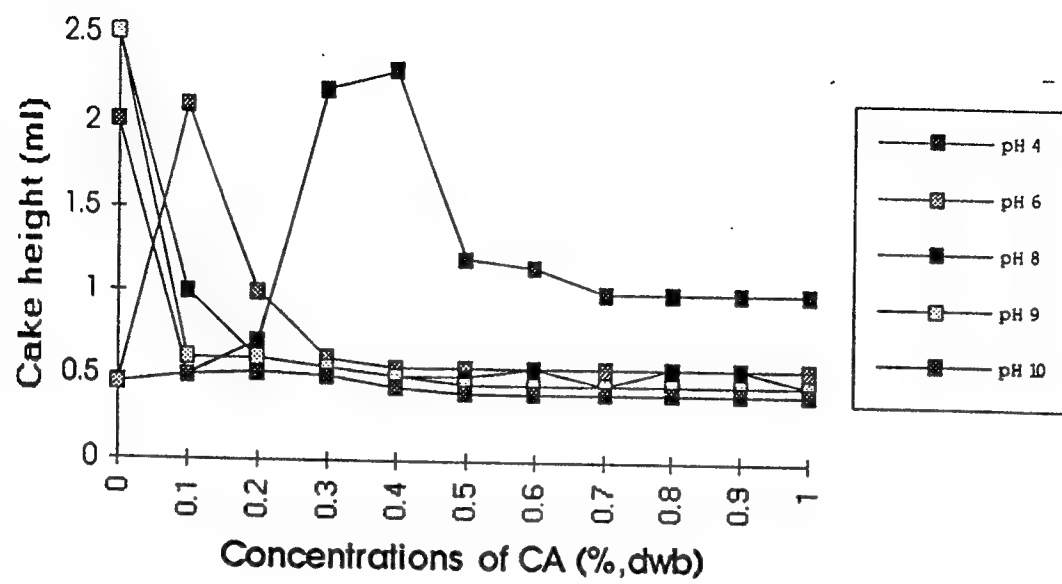


Figure 2: Sedimentation densities of AKP-30 particle suspensions when citric acid was used as a dispersant with a concentration of 0.5% (dwb) versus pHs.

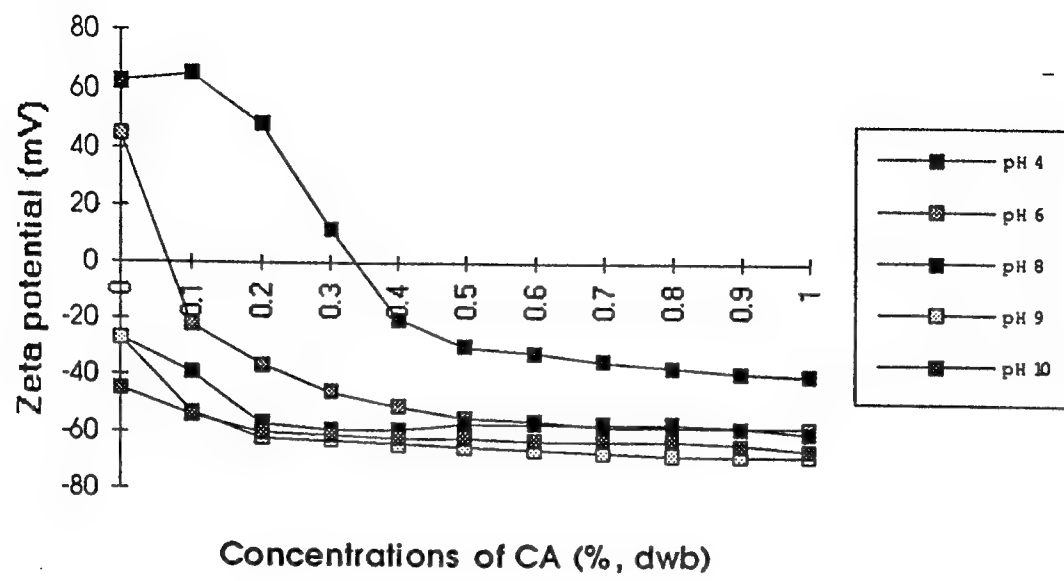


Figure 3: Surface charges of AKP-30 particles prepared with 0.5% (dwb) citric acid at different pHs.

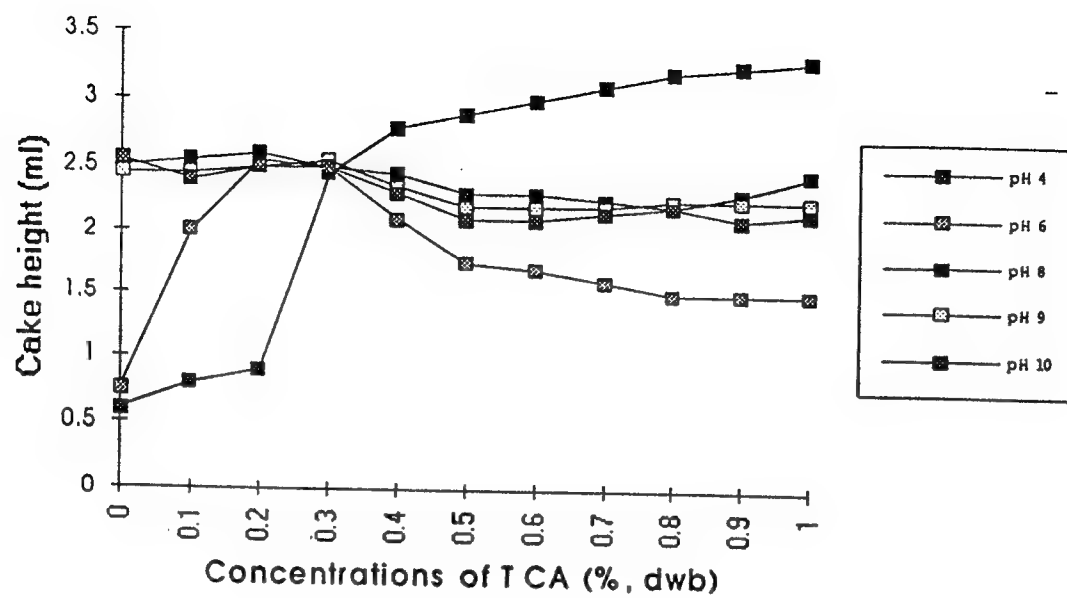


Figure 4: Sedimentation densities of AKP-30 particle suspensions when tricarballylic acid was used as a dispersant with a concentration of 0.5% (dwb) versus pHs.

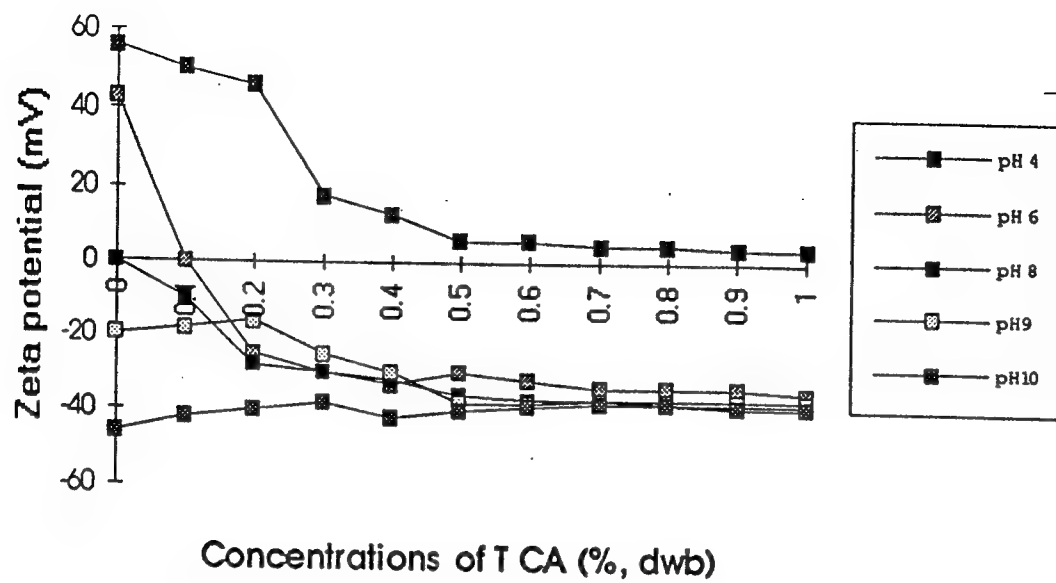


Figure 5: The surface charges of the AKP-30 particles prepared with tricarballylic acid at a concentration of 0.5% (dwb) with different pHs.

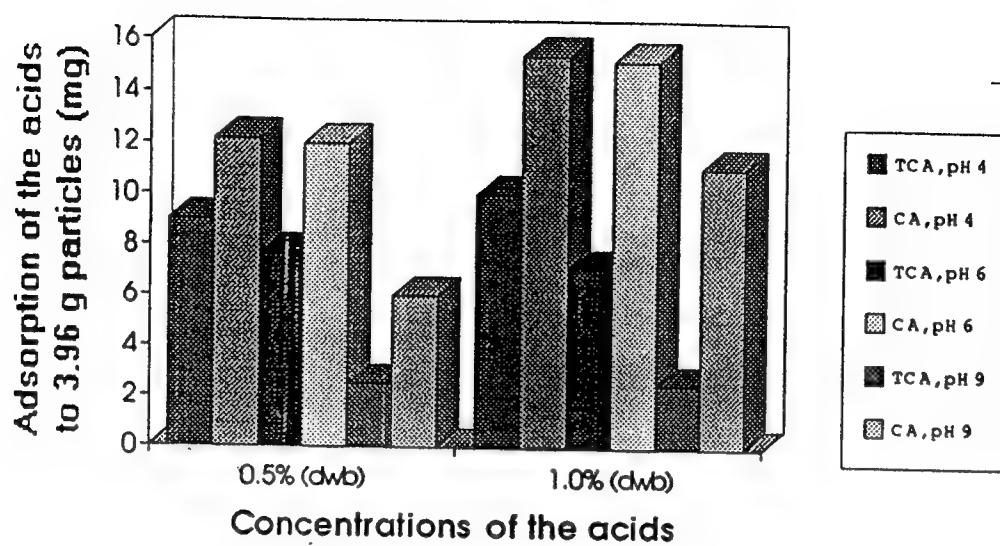


Figure 6: Comparison of the adsorptions of tracarballylic acid and citric acid to 3.96 g AKP-30 particles with different concentrations versus pHs

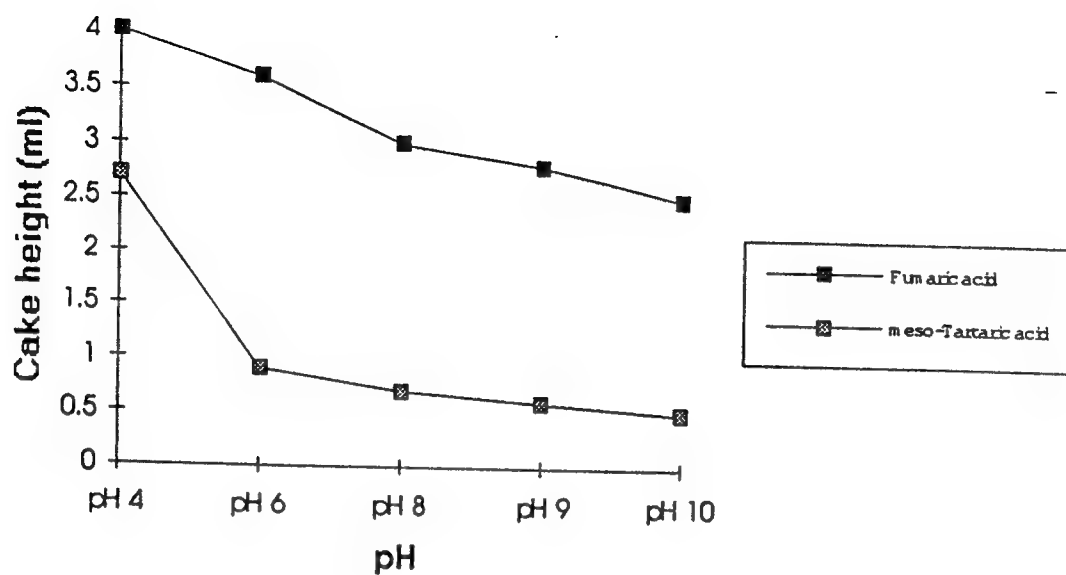


Figure 7: Sedimentation density results of the ceramic particle suspensions prepared with 0.5% (dwb) meso-tartaric acid and fumaric acid with different pHs.

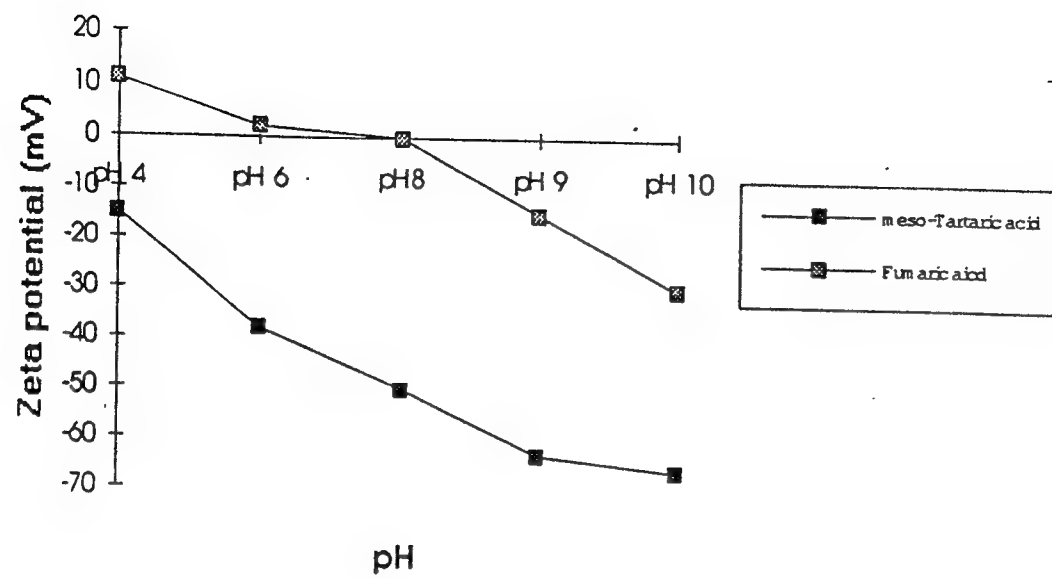


Figure 8: The surface charge of the ceramic particles when meso-tartaric acid and fumaric acid were used as dispersants at a concentration of 0.5% (dwb) with different pHs.

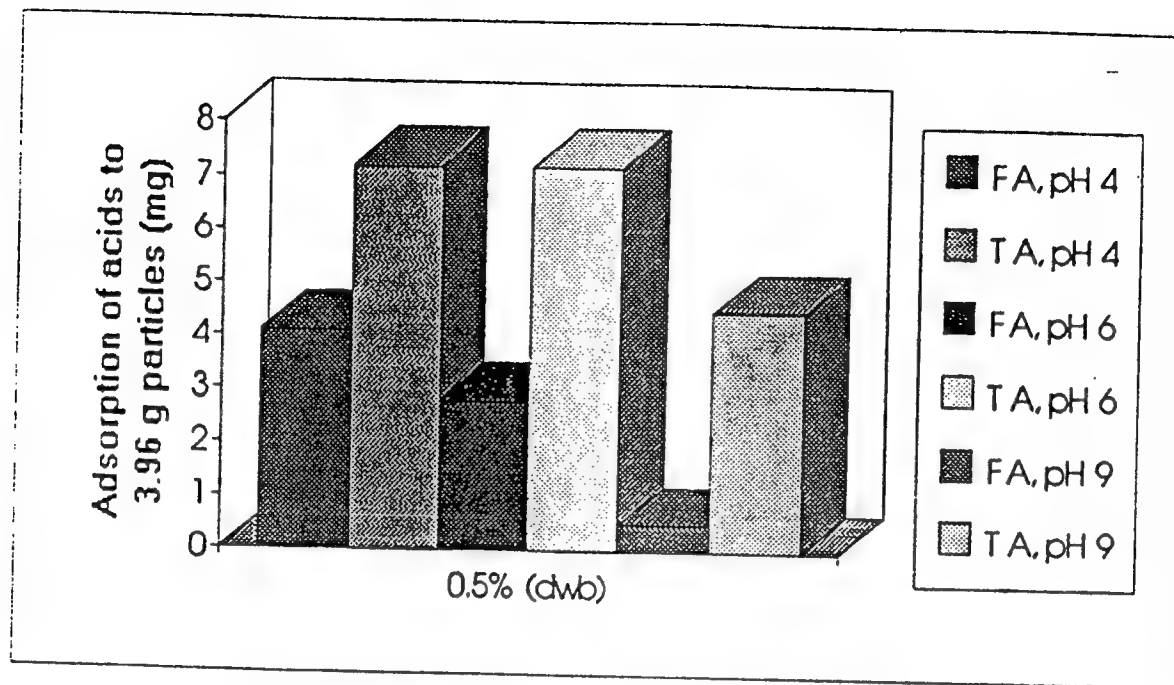


Figure 9: The comparison of the adsorptions of Fumaric acid and meso- Tartaric acid to 3.96 g AKP-30 particles at a concentration of 0.5% (dwb) with different pHs.

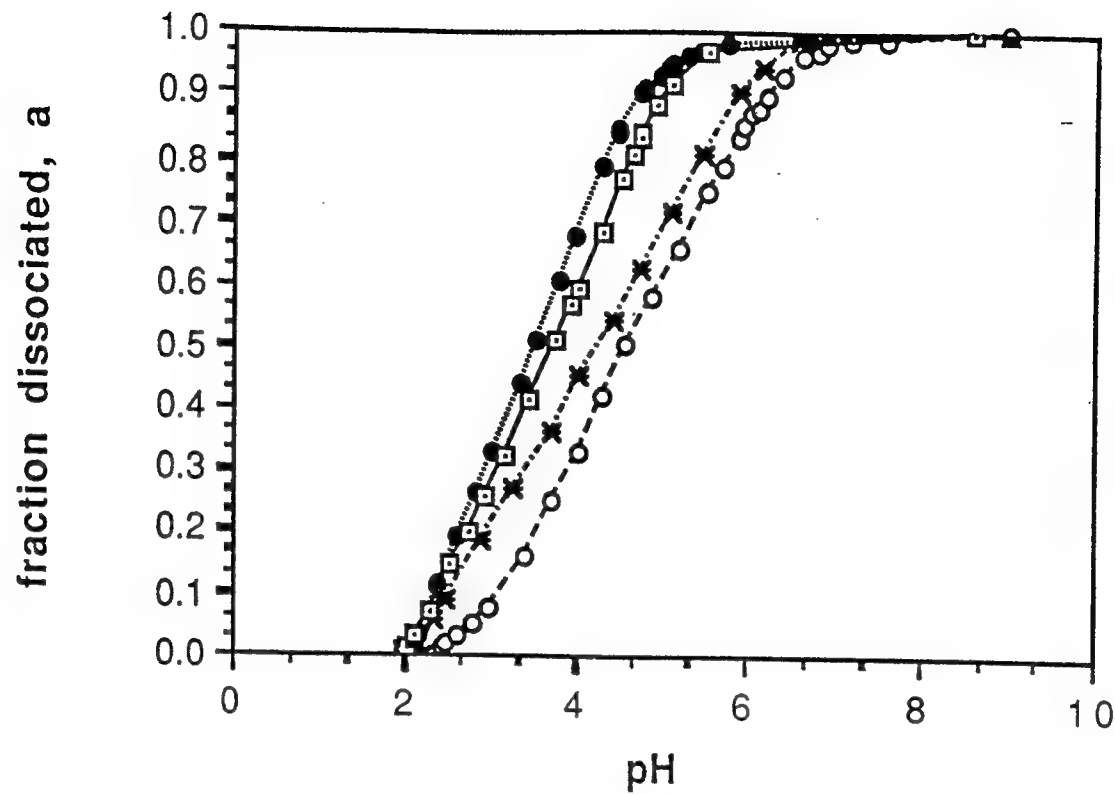


Figure 10: Fraction dissociated, a , of four carboxylic acids versus pH.
(●—● meso-tartaric acid; □—□ fumaric acid; ×—× citric acid;
○—○ tricarballylic acid)

**The Use of Polymers in Ceramic Processing: A Comparison
of Synthetic- and Bio-polymers for Safety Reasons**

M.S. Thesis

by

Sima F. Hasemifar

June 1994

The Use of Polymers in Ceramic Processing:
A Comparison of Synthetic and Biopolymers for Safety Concerns

by

Sima F. Hashemifar

A thesis submitted in partial fulfillment
of the requirements for the degree of

Master of Science in Materials Science and Engineering

University of Washington

1994

Approved by

Ronald Finlay
(Chairperson of Supervisory Committee)

Program Authorized
to Offer Degree

Materials Science and Engineering

Date

7-8-94

University of Washington

**The Use of Polymers in Ceramic Processing:
A Comparison of Synthetic and Biopolymers for Safety Concerns**

by

Sima F. Hashemifar

Chairperson of the Supervisory Committee:

Professor Mehmet Sarikaya

Department of Materials Science and Engineering

Abstract

The fundamental requirement for preparation of high density in a ceramic compact is that submicron-sized particles be completely dispersed in the solvent system and exhibit no agglomeration. Further, they should retain the state of high dispersion throughout the consolidation process. In this capacity, polyelectrolytes act as dispersants or deflocculants in colloidal processing of ceramics.

There are two major classes of these polymeric additives: synthetic polymers; e.g., PMAA, and biopolymers, such as alginates. The synthetic polymer, polymethacrylic acid, PMAA, polyelectrolyte has been widely used in steric and/or electrosteric applications.

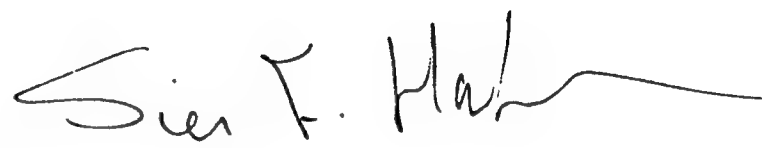
A comparison of the behaviors of PMAA and alginate, when used as a suspension-enhancing aid through electrosteric stabilization, in the polyelectrolyte/alumina system is presented. It is shown that alginate as a dispersant, has comparable properties to the PMAA and its rheological behavior, sensitivity to pH variation, polymer molecule weight, concentration and viscosity are comparable to polyelectrolytes.

Comprehensive survey of health hazards (skin and respiratory irritation and carcinogenicity), storage and handling (corrosivity, toxicity and flammability), chemical

reaction (self-reaction, water and other chemicals) and toxicity of decomposition products, data shows that the use of alginate, a naturally occurring biopolymer instead of PMAA, leads to a safer environment. This is based on the assessment of Degree of Environmental Damage (DED) factor of the polymers used as dispersants in ceramic processing. While retaining comparable processing properties, alginate has a "DED" factor of 1030 compared to 1812 for PMAA, and, hence, provides environmentally-benign processing.

In presenting this thesis in partial fulfillment of the requirements for a Master's degree at the University of Washington, I agree that the library shall make its copies freely available for inspection. I further agree that extensive copying of this thesis is allowable only for scholarly purposes, consistent with "fair use" as prescribed in the U.S. Copyright Law. Any other reproduction for any purposes or by any means shall not be allowed without my written permission.

Signature



Date

7/8/94

TABLE OF CONTENTS

	Page
List of Figures	iv
List of Tables.....	vi
Background.....	1
Chapter 1	
Introduction.....	5
Chapter 2	
Processing of Ceramics	7
2.1 Introduction.....	7
2.2 Colloidal Processing of Ceramics.....	10
Chapter 3	
Comparison of PMAA & Alginate as Aids in Ceramic Processing.....	13
3.1 Introduction	13
3.2 Effect of pH.....	14
3.2.1 PMAA.....	15
3.2.2 Alginate.....	20
3.3 Effect of Polymer Concentration.....	22
3.4 Viscosity Comparison.....	26
Chapter 4	
Properties, Production and Application of Polymethacrylic acid (PMAA).....	31
4.1 Introduction	31
4.2 Properties.....	31
4.2.1 Physical Properties.....	31
4.2.2 Chemical Properties.....	33
4.3 Production	34
4.3.1 Acetone Cyanohydrin Route	34
4.3.2 Isobutene (C-4) Route	35
4.3.3 Isobutyric Acid (C-3) Route	35
4.3.4 Ethylene (C-2) Route.....	36
4.4 Polymerization	37
4.4.1 Aqueous Solution	37
4.4.2 Nonaqueous Media.....	37
4.4.3 Inverse Phase Emulsion and Suspension.....	37

4.5 Properties of Polymethacrylic Acid (PMAA)	38
4.5.1 Viscosity.....	38
4.5.2 Chemical Properties.....	38
i) Acid Strength and Titration	38
ii) Cation Binding	38
4.5.3 Thermal Properties	39
4.5.4 Solubility.....	39
4.5.5 Precipitation Temperature.....	39
4.6 Applications	39
Chapter 5	
Properties Production and Application of Alginate	41
5.1 Introduction	41
5.2 Structure of Alginate	42
5.3 Properties of Alginate.....	48
5.3.1 Viscosity.....	48
A. Molecular Weight	48
B. Concentration	49
C. Temperature.....	50
D. pH	51
E. Calcium Ions	51
5.3.2 Water Retention	53
5.3.3 Ion Binding.....	53
5.3.4 Ability to Form Gels	53
5.3.5 Physiological Properties.....	54
5.4 Production of Alginate	55
5.4.1 Introduction.....	55
5.4.2 Process I: Calcium Alginate Process	59
5.4.2.1 Size Reduction of Raw Material.....	59
5.4.2.2 Acid Treatment	60
5.4.2.3 Formaldehyde Treatment.....	61
5.4.2.4 Alkaline Extraction	61
5.4.2.5 Separation of Insoluble Seaweed Residue.....	62
A. Flotation	62
B. Filtration	64
5.4.2.6 Precipitation of Calcium Alginate.....	64

5.4.2.7 Bleaching.....	65
5.4.2.8 Conversion of Calcium Alginate to Alginic Acid.....	65
5.4.2.9 Dewatering the Alginic Acid	66
5.4.2.10 Conversion of Alginic Acid to Sodium Alginate.....	66
5.5 Application of Alginates	67
Chapter 6	
Environmental Issues Associated With PMAA and Alginate.....	71
6.1 Production Routes and Polymerization Methods.....	71
6.2 Comparative Analysis.....	73
6.2.1 Health Hazards.....	74
6.2.2 Storage and Handling	74
6.2.3 Chemical Reactivity	76
6.2.4 Toxicity of Decomposition Products.....	76
6.2.5 Waste Disposal	76
6.2.6 Summary of the Environmental Impact of PMAA and the Alginate Preparation Processings	79
6.2.7 Degree of Environmental Damage (DED).....	84
6.3 Conclusion	86
6.3.1 Health Hazards	86
i) Skin and Respiratory Irritation.....	86
ii) Carcinogenicity.....	86
6.3.2 Storage and Handling	86
i) Corrosivity	86
ii) Toxicity	87
iii) Flammability	87
6.3.3 Chemical Reaction.....	87
i) Self-reaction and Reaction with Water.....	87
ii) Reaction with other Chemicals.....	87
6.3.4 Toxicity of Decomposition Products	87
6.4 Future Research	88
References.....	89
Appendix "A" Waste Disposal Methods.....	99

LIST OF TABLES

Table 3.1	Rheology Data at Various pH's.....	18
Table 3.2	Viscosities (mPa.s) of Concentrated Suspensions of Alumina in Polymannuronic or Polyguluronic Acid Fractions at a Shear Rate of 9.3 s^{-1} . ⁸	29
Table 4.1	Physical Properties of the monomer, Methacrylic Acid ¹	32
Table 4.2	Some of the Applications of Polymethacrylic Acid ¹	40
Table 5.1	Fractional Composition of Alginates as Determined by H-NMR ¹⁶	47
Table 5.2	Variation of viscosity (mPa.s) with concentration for Sodium Alginate solutions at 20°C ²¹	49
Table 5.3	Percentage of Mannuronic Acid and Guluronic acid, and M/G ratios, of Alginic Acid from various commercial brown seaweeds..	52
Table 5.4	Some Uses of Alginates ^{41, 10}	68
Table 5.5	Use of Alginates in Special Forms ⁴¹	69
Table 6.1	Different routes and materials involved with production of Methacrylic Acid	72
Table 6.2	Different polymerization methods of PMAA and involved materials.....	72
Table 6.3	Materials involved in different processing stages of Alginate.....	73
Table 6.4	Explanation of Health Hazards Ratings.....	75
Table 6.5	Explanation of Storage and Handling Ratings	75
Table 6.6	Explanation of Chemical Reactivity Ratings.....	77
Table 6.7	Toxicity Ratings for Decomposition Products.....	78

Figure 5.5	Proposed structure of an alginate gel chain contours ¹⁵	45
Figure 5.6	Viscosity in 1% solutions at different temperatures ²⁶	50
Figure 5.7	Process I, Production of sodium alginate, Calcium Alginate process ^{31,3457}	
Figure 5.8	Process II, Production of sodium alginate, Alginic Acid process ³¹	58

LIST OF FIGURES

Figure B.1	Schematic representation of the structure of the electric double layer ¹	3
Figure 2.1	Processing steps in powder consolidation, leading to ceramic green compact (after drying) and final multiphase composite (after sintering) ^{2,3}	9
Figure 3.1	Stability map showing the amount of adsorbed PMAA required to form stable suspensions of 20 vol % AKP 30 α -Al ₂ O ₃ as a function of pH ⁶	16
Figure 3.2	Viscosity at 9.3 S ⁻¹ versus pH for PMAA stabilized AKP 30 α -Al ₂ O ₃ suspensions from 20 to 58 vol. % solids concentrations ⁶	19
Figure 3.3	Wet sediment densities of 2 vol. % suspensions of alumina in alginate (0.5% dwb alumina) prepared at various pH levels ⁸	21
Figure 3.4	Viscosity at a shear rate of 9.3 s ⁻¹ versus pH for 50.vol% AKP-20 alumina suspensions stabilized with dextran sulfate-Na (MW 5,000), polyacrylic acid-Na (MW 6,000) and polyguluronic acid.	23
Figure 3.5	Wet sediment densities of 2 vol. % suspensions of alumina prepared with various concentrations of alginate (dwb alumina) ⁸	25
Figure 3.6	Viscosity curve obtained from a 40 vol. % suspension of alumina in alginate ⁸	27
Figure 5.1	Diagram of an adult Giant Kelp (<i>Macrocystis</i>) plant ¹²	41
Figure 5.2	The component monosaccharides of alginate; D-mannuronate and L-guluronate ¹⁰	42
Figure 5.3	Chain conformations of Poly D-mannuronate and Poly L-guluronate ¹⁰	43
Figure 5.4	Gelation of Poly L-Guluronate blocks with calcium ions ¹⁰	44

ACKNOWLEDGMENTS

I wish to express my sincere gratitude to Professor Mehmet Sarikaya, my Thesis Advisor, for his strong and continued support both moral and academic during the course of my graduate studies.

I extend heartfelt thanks to my best friend and mentor, Dr. Mansour Moinpour, for his inexhaustible patience and the kind wisdom of his guidance. None of this work, nor much of my sanity, would have been possible without his help in many unseen ways.

I am immeasurably grateful to the University of Washington's Women in Engineering Program (WIE), it's staff and particularly Dr. Suzanne G. Brainard, the Director of the program for her phenomenal, remarkable assistance and extraordinary support during my graduate studies.

I would also like to thank my advisory committee, Drs. Thomas Stoebe, Robert M. Fisher and James T. Staley and also Ms. Nancy B. Pellerin and Dr. Mehrdad Yasrebi for their guidance and advice.

Many thanks and honorable mentions are also due to:

Dr. Thomas Stoebe, Department Chairman of the Materials Science and Engineering, for his sincere care and support during the course of my study in the MSE department at the University of Washington.

Claire LeBlanc, for so kindly helping me in preparing the manuscript during all those memorable late nights and weekends.

Paula Palmer, the student reference helper at the Fisheries Library, for her amazing willingness to help me know more about seaweeds.

My beloved sister, Soheila, for all her unconditional support and love.

My ex-husband and friend of all times, Goodarz, for his support and for taking such beautiful care of our daughter during my absence.

My friends in MSE and Chemistry departments, Ademola, Farhad, Shahrzad and Sima for being with me during all those tough moments of returning to school after 12 years.

Finally, my highest praise and appreciation to:

My cherished mother, Mahin, who has been the most influential factor contributing toward the completion of this degree, for her constant unfailing faith, inspiration and sacrifice.

My precious daughter, Golbone, for her love, support, encouragement and patience during my time in graduate school. (Mommy will make it up to you!)

M. Sarikaya, "An Introduction to Biomimetics: Structural Viewpoint," *Microsc. Res. Tech.*, **27** [5] 361-375 (1994).

An Introduction to Biomimetics: A Structural Viewpoint

MEHMET SARIKAYA

Materials Science and Engineering, University of Washington, Seattle, Washington 98195

KEY WORDS Biological composites, Structural biocomposites, Microarchitecture, Materials design

ABSTRACT Biomimetics is a newly emerging interdisciplinary field in materials science and engineering and biology in which lessons learned from biology form the basis for novel technological materials. It involves investigation of both structures and physical functions of biological composites of engineering interest with the goal of designing and synthesizing new and improved materials. This paper discusses microarchitectural aspects of some structural biocomposites, presents microstructural criteria for future materials design and processing, and identifies areas of future research. © 1994 Wiley-Liss, Inc.

INTRODUCTION

Properties of materials are structure sensitive and the basis of materials design and processing, therefore, is to control microstructures so as to achieve desired physical and chemical properties in materials (see, for instance, Baer and Moet, 1991; Fulrath and Pask, 1966; Haasen, 1978). In one of the most widely used structural materials, for example, in low-alloy low-carbon structural steels, a myriad of different microstructures from pearlitic to martensitic are produced through thermal and mechanical treatments that results in countless different types of steel used in many different applications (see, for instance, Zackay and Aaronson, 1962). In a more recent example of high temperature superconductor $\text{YBa}_2\text{Cu}_3\text{O}_{7-\text{x}}$, the significance of effects of microstructural features, such as structural characteristics of transformation twins, amounts, types, and distribution of local oxygen ordering, and interface structures and chemistry on the superconducting properties, have been well realized (see, for instance, Jorgensen, et al., 1989). Despite the enormous technological possibilities, however, unlike in steels, some major difficulties are encountered in high temperature superconductors in controlling the structural features during processing. As a consequence, these new materials have been used only in constrained structural forms (like thin films) and, therefore, have so far had limited applications.

In these and many other technological materials systems microstructures consist mostly of metastable phases with morphologies that are difficult to control. In cases where nucleation and growth of the secondary phases (such as precipitates) are controlled at the atomic and molecular levels under stringent synthesis conditions, the microstructures are tailored to a large extend to produce certain desired properties. Examples are traditional alloy systems (steels, Al- and Cu-alloys, superalloys, and cemented carbides; Gell, et al., 1980; Zackay and Aaronson, 1962) and in more recent cases of nanostructural materials (Shinjo and Tanaka, 1987) and in compound semiconductor heterostructures (see, for instance, Shaw, et al., 1989).

In biological systems, on the other hand, organisms

produce soft and hard materials which have properties far beyond those can be achieved in present technological materials. Biological composites are complex in terms of composition and microstructure, but yet highly ordered, containing both inorganic and organic components in an intricate blend (Lowenstam and Weiner, 1989; Simkiss and Wilbur, 1989). Physical properties include optical, magnetic, electronic, and piezoelectric, as well as mechanical. These materials are synthesized at ambient temperatures under atmospheric conditions with the structural build-up completely controlled by the organisms.

The unique microstructures and resulting properties in biological composites have been unknown to materials scientists, and may well be inspirational sources in the development of future materials. With this in mind, this research group started investigating structures of biological composites to establish relationships with properties and to obtain processing strategies and microstructural design criteria for the development of new materials with novel properties, a field which is now called *biomimetics*. (see, for instance, Aksay, et al., 1992; Alper, et al., 1991; Rieke, et al., 1990). Biomimetics may be one of the major ways to produce next generation materials that would meet demands of the technologies of the coming century.

We divide biomimetics into two categories (Fig. 1; Sarikaya and Aksay, 1993a). First, by investigating the structures of biomaterials at all possible scales of spatial resolution, the fundamentals of their unique structural designs can be deduced and then mimicked by techniques currently available to materials scientists—an approach we refer to as *biomimicking*. The second category is mastering the molecular synthesis and processing mechanisms of biomaterials and applying these hitherto unknown methodologies to produce new technological materials superior to those presently

Received November 15, 1992; accepted in revised form March 15, 1993.

Address reprint requests to Dr. Mehmet Sarikaya, Materials Science and Engineering, Roberts Hall, FB-10, University of Washington, Seattle, WA 98195.

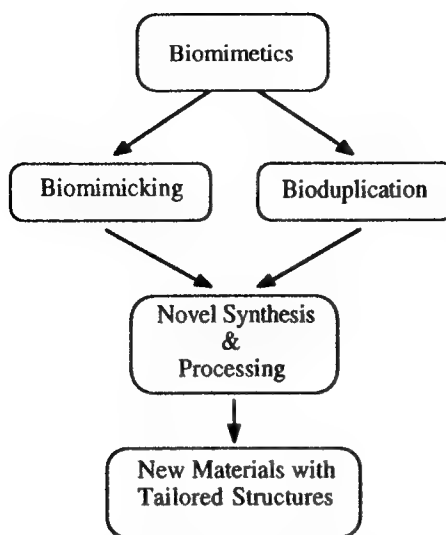


Fig. 1. The description of interdisciplinary field of biomimetics.

available—an approach we call *bioduplication*. The bioduplication approach is much more complex and will require a long-term commitment, not only to learn the intricacies of bioprocessing used by organisms but also to develop new strategies to process materials synthetically from the molecular level up with the same size, shape, complexity, and multifunctionality as the biocomposites. The biomimicking approach, although by no means simple, will require a shorter time commitment.

One of the most interesting aspects of biological materials is that their metastable microstructure is formed from the molecular to macroscales to attain a combination of certain physical properties that the organism best functions within its given environment. A particular microstructure in an organism is developed through millions of years of evolution. Biocomposites are structured in a hierarchical manner (Baer et al., 1992), from the molecular to the macro scale, they are intricately microarchitected, and they often have multifunctional properties (Currey, 1987; Wainwright et al., 1976). These materials are composites containing various structural organic macromolecules (proteins and polysaccharides) and inorganic materials (often ceramic crystals or glasses) (Currey, 1987; Frankel and Blakemore, 1991). They can be found from the most primitive organisms (such as small particles and thin films in algae and bacteria) (Frankel and Blakemore, 1991) to invertebrates (shells and cuticles in mollusks [Grégoire, 1972] and insects [Bouligand, 1965], respectively), and to the highly developed vertebrates (such as bones and teeth of mammals) (Glimcher, 1981).

Biomimetics is a wide area of research and, therefore, it requires a close collaboration between biological (biochemistry, genetics, microbiology, and zoology) and physical sciences fields (materials sciences, physics, chemistry, chemical, electrical, and mechanical engi-

neering). Commensurate with the objectives of the symposium and this special issue of the journal, this paper focuses only on the microstructural aspects of biocomposite hard and stiff tissues. The purpose is to bring about various fascinating and unique structural design in biocomposites with the aim of raising interest in microscopists—materials and biological scientists alike—who would be involved in this field in the future.

STRUCTURAL DESIGN IN SOME BIOLOGICAL HARD TISSUES

Biological materials of engineering interest are mostly hard and stiff tissues, and small particles (Table 1). In the former case, the structure is composed of an organic matrix (mostly proteins and polysaccharides) with the inorganic material interspersed throughout. The formation, morphology, and crystallography of the inorganic phase are all assumed to be controlled by the organic matrix. In hard tissues such as mollusk shells, the inorganic phase, for example calcite or aragonite form of CaCO_3 , is in the form of crystallites of various shapes, size, and morphology that are controlled by the organic matrix which constitutes only less than 5% vol. of the composite. In the case of stiff organic tissues, such as insect cuticles (Bouligand, 1965), all the components of the composite are organic macromolecules in which matrix is usually composed of proteins and polysaccharides. The stiffness comes from fibrillar polysaccharides, such as collagen and chitin, organized at the nano-, submicro-, micro- or higher scales (Baer et al., 1992). Finally, some lower organisms, such as bacteria and alga produce fine inorganic particles with unique properties (Frankel and Blakemore, 1991). These biological materials are listed in Table 1 with their corresponding properties, and will be discussed in some detail in the following examples with emphasis on the mollusk shells which have relatively simple microstructures.

Biogenic Small Inorganic Particles

From the point of obtaining lessons on characteristic materials structures and properties, small inorganic particles of biological origin offer analogies with synthetic nanoparticles and mesoscopic systems. There are many organisms that produce ultrafine inorganic particles in their bodies that perform various functions (Frankel and Blakemore, 1991). One most notable example is iron clusters that form at the center of ferritin molecular cages (or vesicles) in organisms (Harrison et al., 1989). In some cases, metals clusters are accumulated as foreign entities that might otherwise be harmful to the host organism, such as CdS in algae (which, however, have excellent optical properties; Dameron et al., 1989). Another example is ultrafine magnetic particles that are found in bacteria (Blakemore, 1982), as further discussed below.

Some species of bacteria that live anaerobically in freshwater and salt swamps move about to seek oxygen and food by a mechanism that makes use of a string of magnetic particles (Fe_3O_4 or Fe_3S_4) as a compass (Frankel and Blakemore, 1991). One of the first puri-

TABLE 1. A chart showing categorization of various biological composites, their micro-/nano-design and physical properties

Material/composite	Example	Micro- or nano-level	Properties
Small particles	Bacterial algal	N N	Magnetic Electronic, optical
Ceramic/ceramic	Sea-urchin	B	Mechanical (wear resistant)
Ceramic/polymer	Mollusk	N, H	Mechanical (tough, strong), ferroelastic
	Bone	N, H	Ferroelastic
	dentin	N, H	Ferroelastic
Polymer/polymer		N, H	Mechanical, ferroelastic, optical
Laminated	Cuticle	N, H	Mechanical, optical
Fiber/matrix	Tendon	N, H	Mechanical, ferroelastic
Fiber/fiber	Silk	N	Mechanical (tensile props.)
Liquid crystalline/matrix	Mucus	N	Rheological

N: nano, M: micro, B: both M and N, H: hierarchical.

fied strains, in *Aquaspirillum magnetotacticum* (Blakemore, 1982), for example, each bacterium has about 20–25 particles that are oriented along a string with their magnetization axis along the long axis of the bacterium (Fig. 1). These bacteria have two flagella on each end, and therefore, can move in forward or backward directions, depending on their configuration with respect to the Earth's magnetic field. In terms of biomimetic applications, some of the significant materials characteristics of these particles are listed as: (i) they are single crystalline, having no dislocations, twins, or stacking faults; (ii) have a uniform particle size of about 500–600 Å, and, thus, are in the single domain region (superparamagnetic); (iii) particle shape is species specific, and can be dodecahedral, cubo-octahedral or hexagonal; (iv) they are aligned in the form of a single string (in some isolated cases, as double strings); (v) they form in a biological sacks, called magnetosomes. In S-rich regions, some species are known to form isomorphic form of magnetite, i.e. Fe_3S_4 (Bazylinski et al., 1991; also see Bazylinski et al., this issue).

The formation of magnetic particles within magnetosome membranes is of a great interest in terms of forming small synthetic particles under closely controlled synthesis conditions (Fendler, 1982; also see Yang et al., this issue). Small magnetic particles can be formed synthetically by following several routes, e.g., solution precipitation from precursors, in microemulsions, and using vesicles. In all these cases, however, the particles formed are nonuniform, they are often not fully crystalline, compositionally nonhomogeneous, and, more importantly, in an agglomerated state which imposes problems in processing. Therefore, synthesis of small magnetic, and other inorganic ultrafine, particles via biological routes promises advantages in terms of controlling growth and morphological properties.

The most critical issue in the understanding of particle formation in magnetosomes is the mechanism(s) by which organic matrix allows the nucleation and controls the growth of particles. The investigation of structure and composition of the magnetosome membrane and its protein organization, therefore, is essential for understanding transport of ions through the membrane and the early stages of formation or particles. Current knowledge of the membrane is that it is a bi-

layer and is likely to contain proteins that are found in the outer membrane of bacteria (Gorby et al., 1988). Other questions involve details of the early stage of formation of particles (amorphous or crystalline and, possibly, in the hydrated form), selection of their chemistry (Fe_3O_4 vs. Fe_3S_4), the control of their growth, and finally factors that affect particle morphology and size (Mann et al., 1990).

Ceramic/Ceramic Biological Composites

In biological composite materials involving inorganic phases, it is usually assumed that organic macromolecules are associated with the composite in a settled way, such as described under the heading Ceramic/Organic Composites. However, there are also many cases in which mineral appears to be present alone in the structure and, therefore, constitutes the overall sample. For example, in the body and the spine (Fig. 2) of sea-urchin, the mineral which does not appear to contain any organic matrix is a calcitic single crystal (Berman et al., 1988; Veis et al., 1986). The most interesting among the composite structures in sea urchin, however, is its teeth (Brear and Curry, 1976). There are five pieces in the lower center of the body that the organism uses to scrape food from surface of rocks. Cross section at the cutting edge of a tooth exposes a composite of a matrix of amorphous CaCO_3 with crystalline calcitic CaCO_3 fibers embedded in it with their long axes perpendicular to the cutting surface as to increase the wear resistance of the tooth (Fig. 3; Sarikaya et al., 1992a). In these biomaterials, location and distribution of an organic matrix, which presumably controls calcite growth, are not clearly known.

In regards to biomimetics, therefore, the major questions about sea-urchin skeletal units are the presence, types, and spatial distribution of organic macromolecules. These, constituting less than 1% of the composite, do not appear to form spatially discernible separate phase(s) and which are, then, most likely to be occluded within the inorganic matrix (Berman et al., 1990). If there are proteins, or their fractions, are occluded within the matrix, then these hard tissues may be regarded as molecular composites, i.e., analog of nanocomposites at smaller spatial dimension. Investigation of various skeletal units of sea-urchin in detail by mi-



Fig. 2. (a,b) TEM images of *A. magnetotacticum* show string of fine Fe_3O_4 particles (a, arrow).

croscopy and spectroscopy, therefore, is expected to provide better insights into the understanding of these unique structures and new lessons for biomimetics.

Organic/Organic Biological Composites

There are numerous stiff biological tissues, composites of fibrous organic components embedded in a soft organic matrix, that are analogs of fiber- or particle-reinforced polymeric composites (Baer, 1986). Tendon, which connects muscle and bone, is a classical example (Baer et al., 1988). It has six discrete levels of structures organized in a hierarchical manner from molecular to centimeter-scale. Silk, found in cocoons of silk moths and webs of spiders, is another structural ma-

terial (Gosline et al., 1986). Its unique structure, consisting of silk fibroin proteins (β -pleated sheets) organized in a liquid crystalline fashion in an amorphous protein matrix, is designed to withstand stresses (Gosline et al., 1986) much higher than those encountered by high tensile strength metallic or polymeric fibers (Baer, 1986).

One of the major classes of organic biocomposites is formed by cuticles. Arthropods, such as insects, crustaceans, spiders, millipedes, and others, are evolutionarily very successful probably because of their cuticles that cover their body from "head to toe" (Neville, 1975). The cuticle, therefore, is the skeleton (exoskeleton) of an insect. Its structure resembles that of fiber-rein-

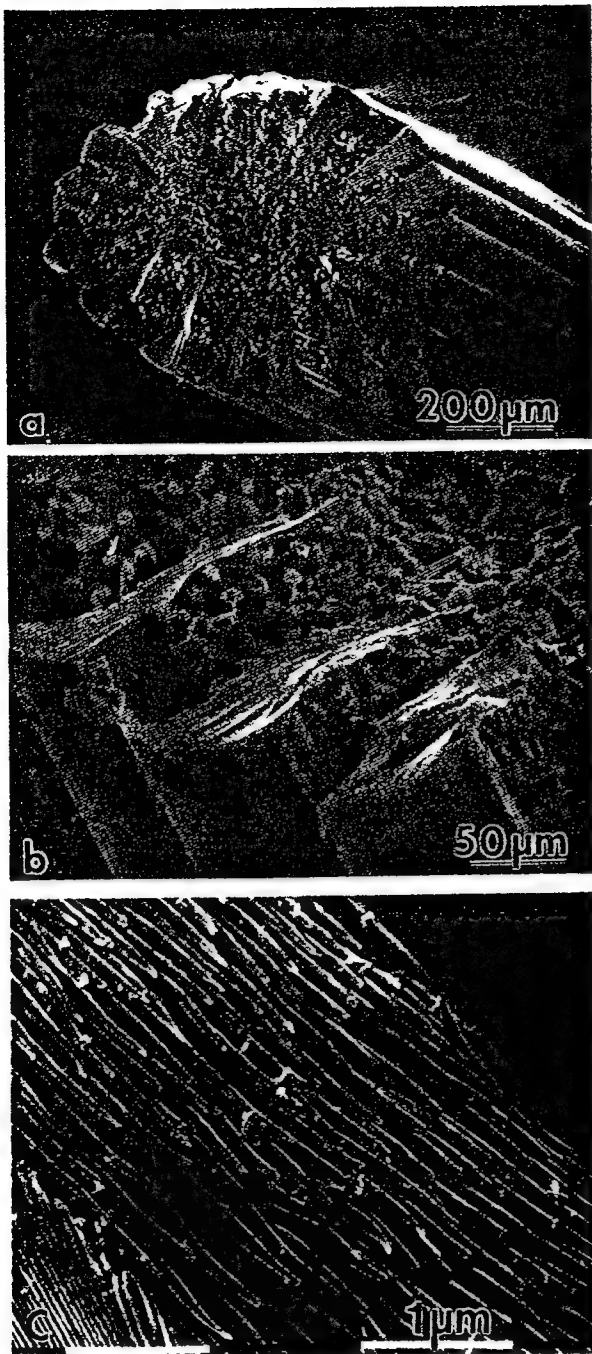


Fig. 3. (a,b) SEM images of a sea-urchin spine (single crystal) showing its intricate structure in a fractured sample. (c) Sea urchin tooth is a composite of crystalline calcite fibers in an amorphous matrix (etched; secondary electron image).

forced polymer matrix where the fibers are collagen (polysaccharides), and the matrix is mostly proteins (see, for instance, Giraud-Guille, this issue).

The composite has a sheet structure in which collagen fibers are arranged in layers. In each layer, the

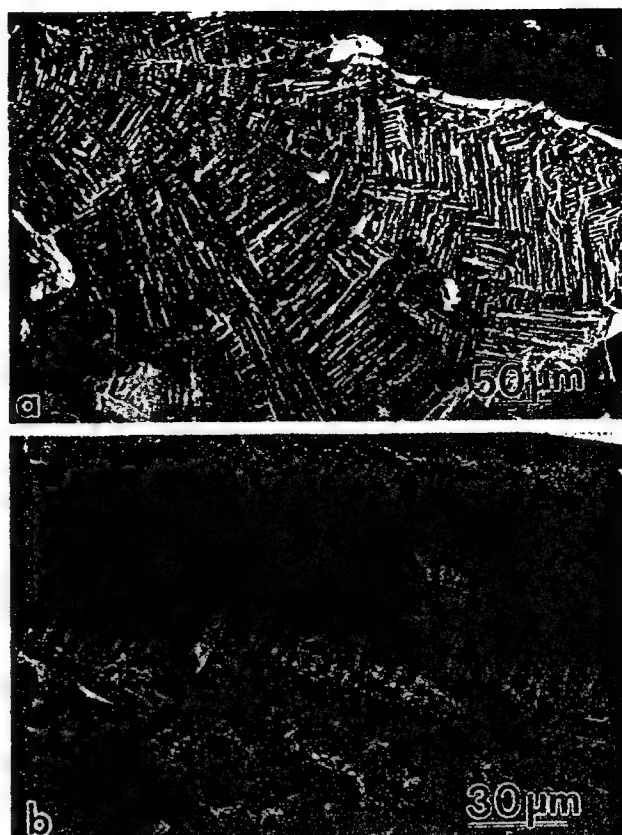


Fig. 4. (a,b) SEM images of an insect cuticle showing helicoidal organization of layers in a "ply-wood" structure (secondary electron image).

fibers are oriented parallel to each other. In successive layers, however, there is rotation of parallel fibers only few degrees, i.e., helicoidal. The thickness of each layer may be as small as 5–10 nm and the thickness of the chitin fibrils as thin as 3–5 nm in diameter (Neville, 1975). In *Odontotaenius disjunctus*, shown in Figure 4 at a higher scale of microstructure, there are two simultaneous clockwise rotations between two sets of sheets (double-helicoid). Therefore, although in each layer the fibers are isotropic, the overall composite structure is anisotropic in the cuticle. This has a significance for the composite material from its mechanics point of view (Gunderson and Schiavone, 1989). The unique microstructure of the insect cuticle, as well as cuticles of other classes, may serve as a lesson for the design of composite materials in which all the components are polymers.

Exoskeletons, in addition to serving as light, versatile, and protective "armor" for insects, also form intricate surface structures which give optical effects (Ghiradella et al., 1972). For example, in butterfly wings, although the origin of color for the most part is pigmentary, some colors such as blues and violets, come from surface structures (Ghiradella et al., 1972; Ghiradella, this issue). The structural details on surfaces can take an intricate and ordered combination of

layers, scales, and ridges which are arranged to produce optical effects through interference during scattering of light. Coloring through structural effects is an area of study in biomimetics. Furthermore, pigmentation itself is also an area of materials science interest, involving questions such as the origin of pigmentation, the nature of pigments, their size, distribution, and composition within the matrix, and their coloring (possibly, non-linear optical) effects.

In cuticles, in summary, there are both biomimicking and bioduplication possibilities for future materials formation. On the biomimicking side, questions involve the types of structural units at the nano- and micro-scales, and their spatial distribution. There are already synthetic polymers that may be used as the matrix (such as diblock copolymers and liquid crystalline polymers; Spontak et al., this issue) as well as fibrous polymers that can be used as the stiff component. On the bioduplication side, some subjects of future investigation are composition and spatial distribution of proteins in the matrix, their possible liquid crystalline order, and their synthesis. The nature of polysaccharides, its molecular structure and composition (including collagen), its structural relationship with the protein matrix, and overall hierarchy of the structure of cuticle are further areas of biomimetic interest.

Ceramic/Organic Composites

The examples of biological composites containing both ceramic and organic phase(s) in the form of macromolecules, take many different forms (Currey, 1987). They are mainly used as structural materials in skeletons or protective covers for the bodies of organisms (Lowenstam and Weiner, 1989; Simkiss and Wilbur, 1989). These include bones in vertebrates, teeth in fishes and mammals, and shells in mollusks. A representative example of the inner section of many sea-shells, namely nacre, is discussed below as this hard tissue has been a major area of investigation in the authors' laboratory (Sarikaya and Aksay, 1992).

Mechanical Properties of Nacre. The nacre structure, mother-of-pearl, is found in many families of mollusks, such as red abalone (*Haliotis rufescens*; Currey, 1987; Jackson et al., 1988; Sarikaya et al., 1990; Sarikaya and Aksay, 1992; Yasrebi et al., 1990), the gastropod family, cephalopods, such as nautilus (*Nautilus pompilius*; Grégoire, 1972) and bivalves, such as black-lipped pearl oysters (*Pinctada margaritifera*; Currey, 1987). A transverse cross-section of the red abalone shell displays two types of microstructures: an outer prismatic layer (calcite) and inner nacreous layer (aragonite). The structure and properties of the nacreous layer are described here as this is the part of the shell that displays an excellent combination of mechanical properties as a result of its highly ordered hierarchical structure (Currey, 1987; Jackson et al., 1988; Sarikaya et al., 1990; Sarikaya and Aksay, 1992; Yasrebi et al., 1990). As shown in Figure 5, nacre is composed of stacked platelets (0.2–0.5 μm thick) that are arranged in brick and mortar microarchitecture with an organic matrix (20–400 nm in thickness) form-

ing a "glue" between the platelets (Jackson et al., 1988; Sarikaya et al., 1990; Yasrebi et al., 1990).

Fracture toughness (K_{IC}) and fracture strength (σ_F) of nacre (tested in the transverse direction) (Sarikaya et al., 1990; Yasrebi et al., 1990) and those of some of the well-known ceramics and ceramic-based composites (cermets) are plotted in Figure 6. The average K_{IC} and σ_F values of nacre are some 20–30 times that of synthetically produced monolithic CaCO_3 (Jackson et al., 1988; Sarikaya et al., 1990; Yasrebi et al., 1990). This result is a major driving force in producing ceramic-based composites (cermets and cerpolys) with better mechanical properties than existing composites through nanoscale lamination based on lessons from biology (Jackson et al., 1988; Sarikaya et al., 1990; Sarikaya and Aksay, 1992; Yasrebi et al., 1990).

The investigation on crack propagation behavior in nacre (Sarikaya et al., 1990; Yasrebi et al., 1990) reveals that there is a high degree of tortuosity not seen in the more traditional brittle ceramics, such as Al_2O_3 , or in high toughness ceramics, such as ZrO_2 (see, for example, Dawridge, 1979 and Evans, 1988). The surfaces of fractured samples indicate that a major crack has meandered around the CaCO_3 layers exposing them through the organic surroundings, resulting in a highly rough fractured surface (Fig. 7). This is similar to that seen in fiber-reinforced ceramic composites where a pull-out mechanism operates (see, for example, Evans and Marshall, 1989, and Tressler and Bradt, 1983). In micrographs recorded at higher magnifications, either a sliding of the CaCO_3 layers (Fig. 8a) or organic ligaments between the layers (Fig. 8b) are seen. The latter case, stretching, indicates that the interface between the organic and the inorganic phases is strong and that the organic phase acts as a strong binder (Sarikaya et al., 1990; Sarikaya and Aksay, 1992; Yasrebi et al., 1990). Several toughening mechanisms, therefore, may be proposed (Sarikaya et al., 1990): (i) crack blunting/branching, (ii) microcrack formation, (iii) plate pull-out, (iv) crack bridging (ligament formation), and (v) sliding of CaCO_3 layers. The high degree of tortuosity seen in crack propagation (Jackson et al., 1988) may be due mainly to crack blunting and branching (Sarikaya et al., 1990; Yasrebi et al., 1990). However, tortuosity (about 40–50%) alone is not a major toughening mechanism in these composites, because it cannot account for the many orders of magnitude increase in toughness. The major toughening mechanisms, therefore, are sliding and ligament formation (Sarikaya et al., 1990; Sarikaya and Aksay, 1992; Yasrebi et al., 1990). Similarities exist between the deformation of a nacreous portion of a sea shell and a metal in the sliding mechanism, and ligament formation in nacre is similar to bridging by metal in ceramic-metal composites during crack propagation. The results strongly suggest that these complex deformation modes may be the main mechanisms of energy absorption during the propagation of a stable crack.

The strength of nacre, on the other hand, may be related to several factors, including the size and structure of the aragonite platelets and the interfaces between the inorganic and the organic components. From the limited thickness of the largest flaw (Griffith,

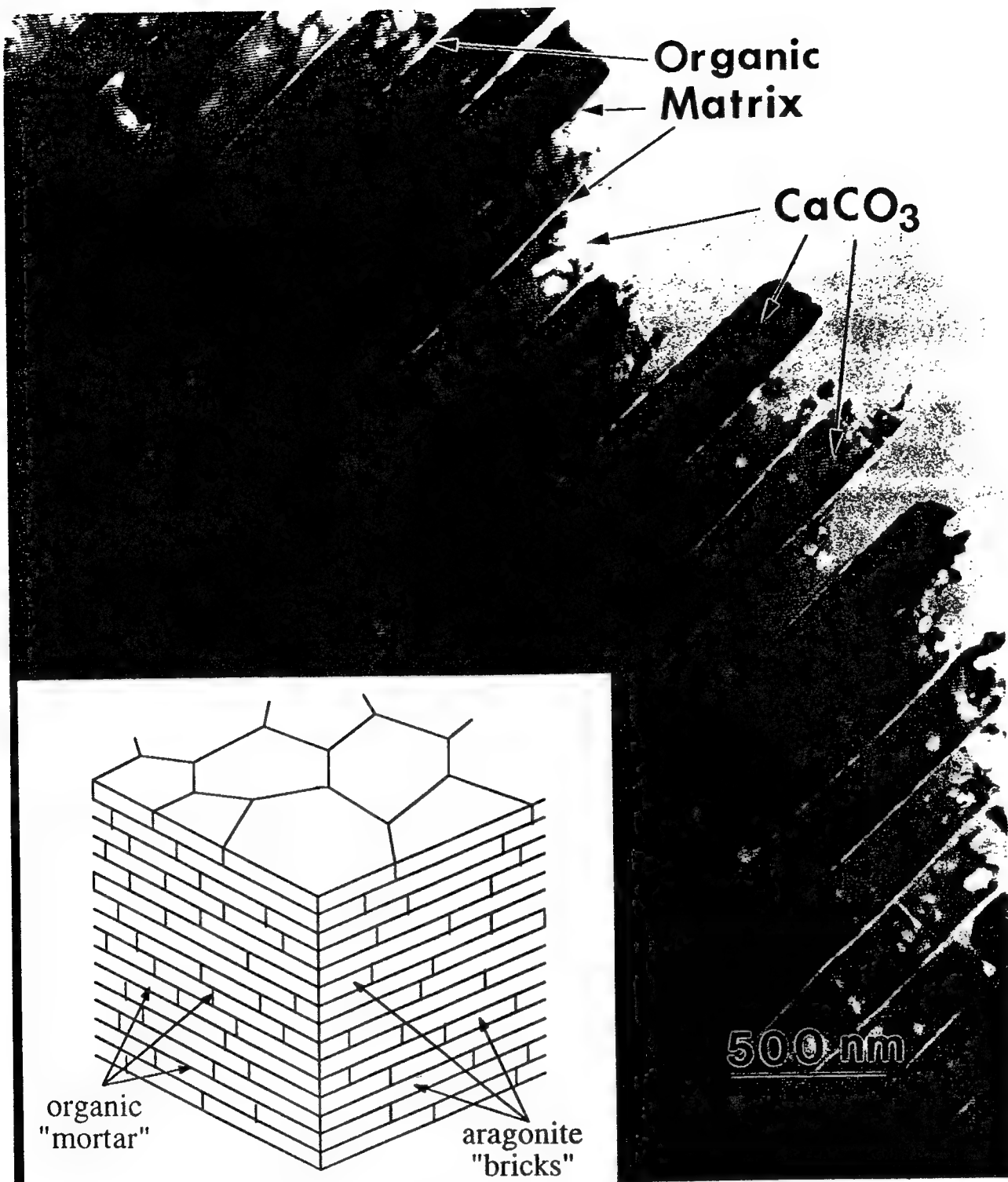


Fig. 5. TEM image of nacre in an edge-on configuration displays aragonite platelets separated by a thin film of organic matrix. The inset shows the brick and mortar microarchitecture.

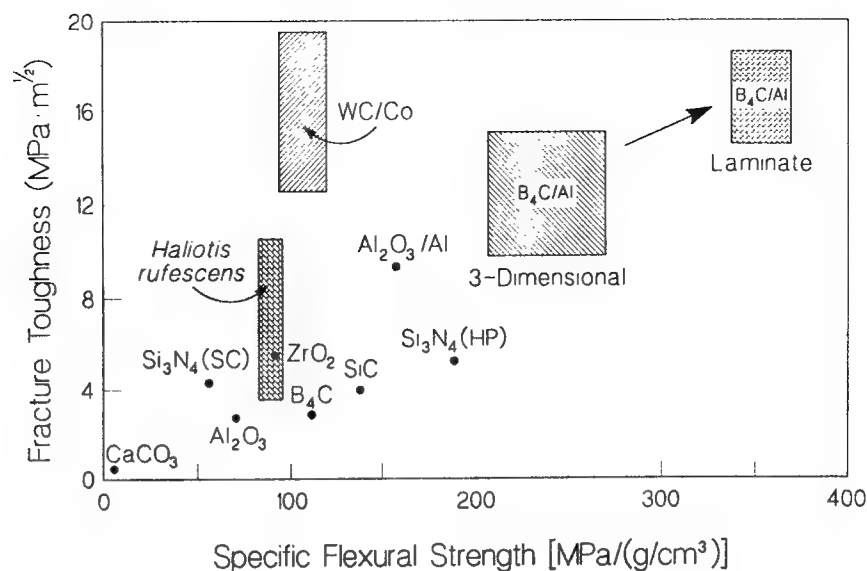


Fig. 6. Mechanical properties of nacre of abalone compared to some major ceramics and cermets. Note the property increases in laminated B₄C-Al cermet compared to that in 3-D microstructure.



Fig. 7. Highly tortuous fracture surface of nacre exposing aragonitic platelets. It is found that the tortuosity is not the main toughening mechanism.

1925), i.e., the thickness of the platelet, 0.5 μm , the increase in the fracture strength of aragonite would be about 200 MPa, comparable to the measured value of 185–220 MPa in our studies (Sarikaya et al., 1990; Sarikaya and Aksay, 1992; Yasrebi et al., 1990). Therefore, the rule of mixtures (Hull, 1981) may account for the value of the measured strength (Sarikaya and Aksay, 1992).

Although improvements were achieved in the mechanical properties of synthetic laminated composites (cermets [Yasrebi et al., 1990] and cerpolys [Khanuja,

1991]) based on biomimetic architecture, these have not been as extraordinary as when nacre is compared to monolithic CaCO₃. This may be due to limited laminate thicknesses in synthetic composites; thicknesses below 1 μm in the inorganic layers and below 100 nm in the layers of the soft phase, are needed. Secondly, both the inorganic and organic layers have complex structures, in terms of their crystallography, substructures, and morphology. In particular, the organic layer has a complex nanolaminated structure within itself (Watabe, 1965; Weiner and Traub, 1984; Weiner, et al., 1983). Neither the composition of these layers nor their structure have yet been clearly identified. Furthermore, identification of the structural relationship between the organic and the inorganic layers is far from complete and constitutes one of the most outstanding problems in biominerization.

Detailed Microstructure of Nacre. It has been impossible to study both the organic and inorganic crystals simultaneously, and the structural relationships between the components of the nacre exist only as a conjecture (Addadi and Weiner, 1990; Mann, 1988). Bulk studies performed by X-ray diffraction on the nacre revealed that the aragonite platelets are organized with their [001] axis perpendicular to the layers (Addadi and Weiner, 1990; Mann, 1988). It has been postulated that a and b axes within the layer plane in each platelet are oriented randomly. Furthermore, it was assumed from this scheme that each aragonite platelet grew on the crystallographically related organic template, which itself had a local random orientation. From the composition of the insoluble fraction of the organic matrix, i.e., the inner crystalline sublayers which contain a high fraction of aspartic and glutamic acid, it might be possible to deduce a self-assembled structure that is related "epitaxially" to the aragonite

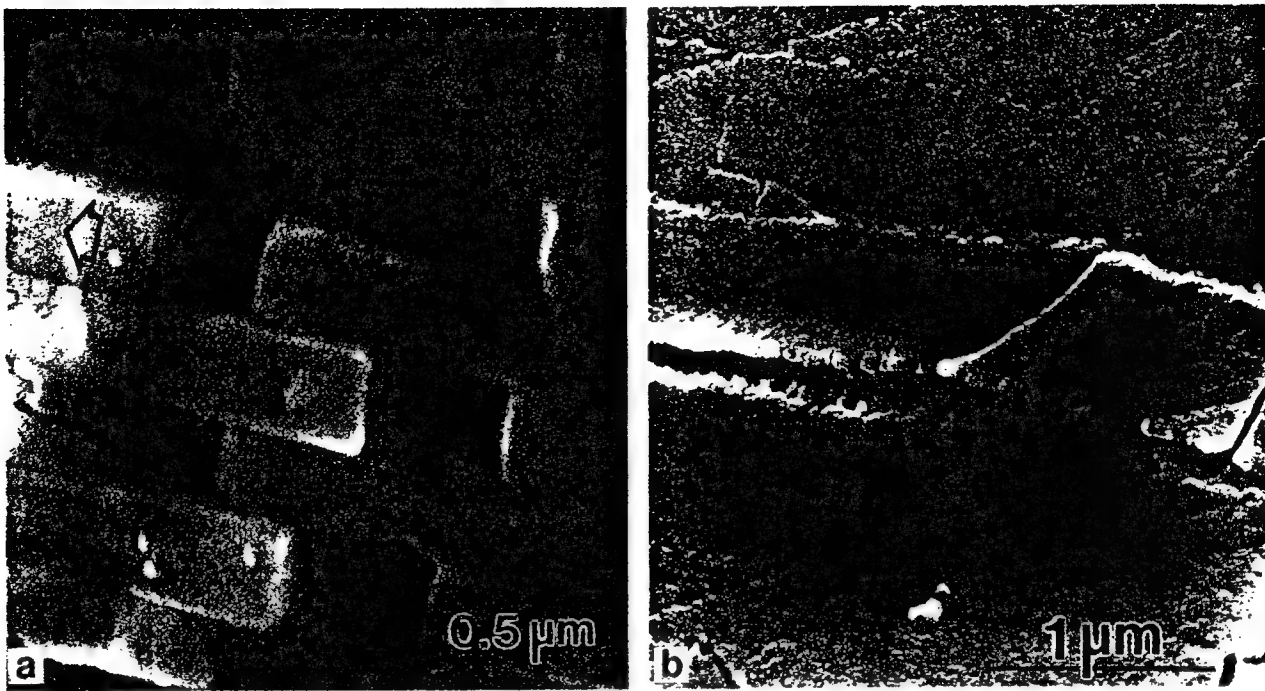


Fig. 8. SEM images revealing sliding of aragonite platelets (a) and ligament formation of organic phase (b), major toughening mechanisms. Arrows in (a) show direction of sliding, and in (b) they show the organic ligaments formed due to normal stresses.

lattice along the [001] projection (Sarikaya and Aksay, 1992; Sarikaya et al., 1992b).

In this investigation, each aragonite crystallite was analyzed separately and its crystallographic orientation relationship with respect to its neighbors, both on the same layer and across the thickness of the nacre, was established. Electron microdiffraction with an electron probe size as small as 50 nm diameter in a TEM allowed isolated diffraction patterns from individual aragonite crystal units enabling us to establish the overall crystallography of the inorganic component of the composite in three directions.

It was found that adjacent platelets belong to the same [001] zone axis, but there is a slight rotation among the platelets about this axis with respect to each other. The question remains whether there is any crystallographic relationship between the *a* and *b* axes in platelets on the same layer. The crystallographic relationship among the adjacent platelets in the face-on configuration analyzed by electron diffraction revealed that each platelet is actually twin-related to the one next to it with a twin plane of {110} type of the orthorhombic unit cell. In this scheme, the arrangement of the platelets indicates that all the platelets on the same layer are twin-related whether they share a boundary or not, constituting *first generation twins* since this twinning takes place at the largest spatial scale (Fig. 9 a,b). Further analysis indicates that each platelet consists of several domains which are crystallographically coupled (Fig. 9 c,d). Hence, again, diffrac-

tion patterns reveal two superimposed patterns that can be correlated with a twin relationship with {110} twin plane parallel to [001] direction of the unit cell, i.e., either (110) or (1 $\bar{1}$ 0) variants (Figure 9 e,f). In fact, the patterns recorded from all the domain boundaries show the same twin reflections, indicating that each domain is related to the one next to it by a {110} twin relation. Domains, therefore, constitute the *second generation twins*.

A platelet may have either four, 90°-, or six, 60°-, domains. In an ideal hexagonal shaped platelet with six twin-related domains, the angle between each pair of domains would be 60°. This is not possible, however, in aragonite lattice, since the outer edges of the platelets are parallel to {110} planes and the angle between each pair of planes—(110) and (1 $\bar{1}$ 0), for example—is 63.5°, leaving unaccounted for a 3.5°. This discrepancy induces strain during growth into the aragonite matrix and must be accommodated by some structural deformation, such as, in this case, nanometer-scale twins that form on {110} planes. These ultrafine twins are shown in Figure 10(a) formed on {110} planes at an angle of about 63.5° and are similar to the growth twins in geological minerals. These twins constitute the *third generation twins* since they occur at the smallest scale. It was found that a portion of the lattice stress created by the 3.5°-strain can also be accommodated by the misalignment of adjacent domains, as observed. However, this misalignment cannot account for all the strain accommodation, as the interfaces between the

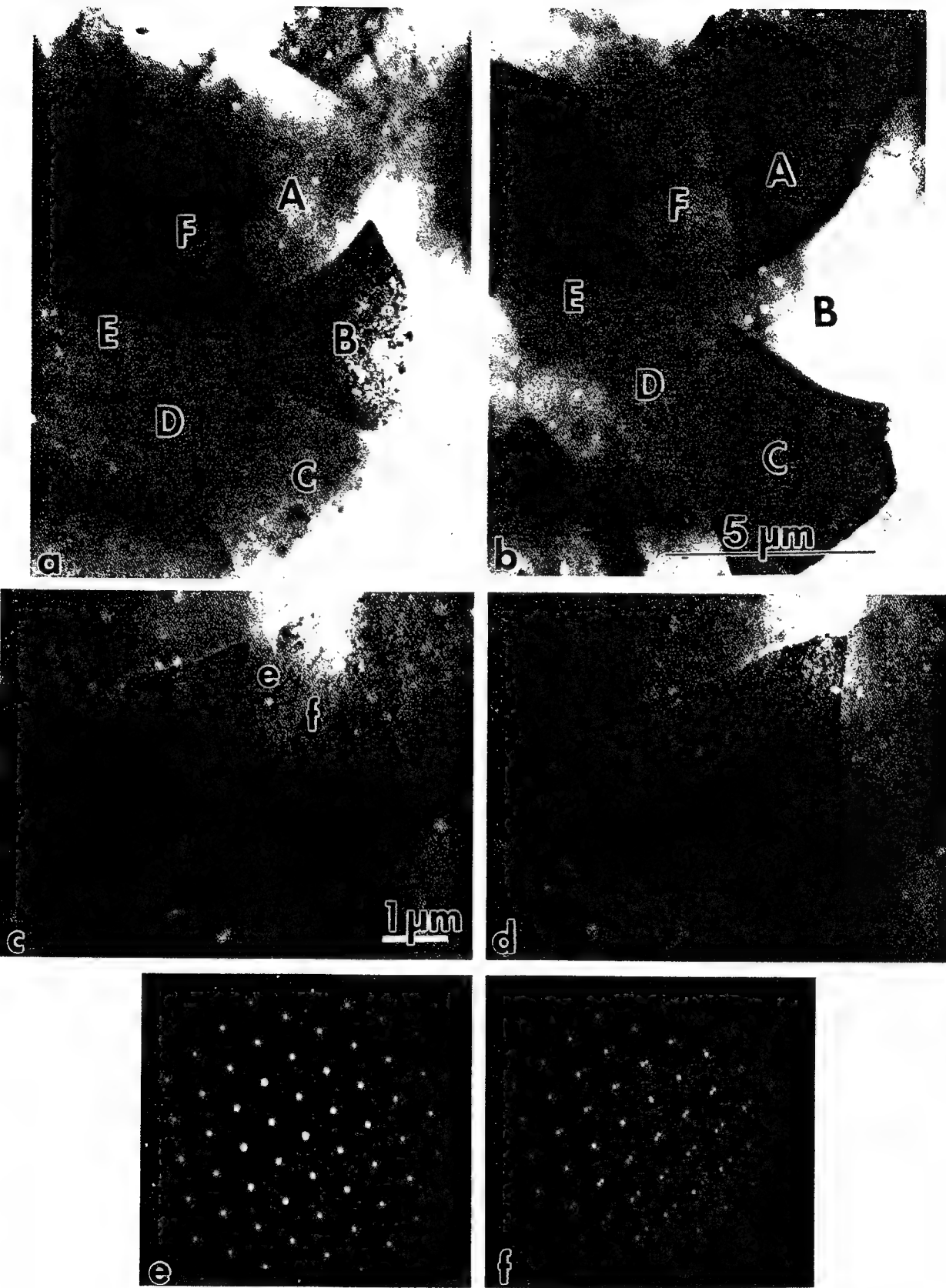


Fig. 9. TEM images of aragonite platelets viewed in face-on orientation before (a) and after (b) slight tilting display twin-contrast. Letters A,B,C,D,E, and F indicate aragonite platelets. Similarly, twinning also occurs between domains in a platelet (c-d). Electron diffraction patterns (e) from the interior of a domain, and (f) from the domain boundary. Arrows in (c) indicate location from which SAD patterns (e) and (f) were obtained.

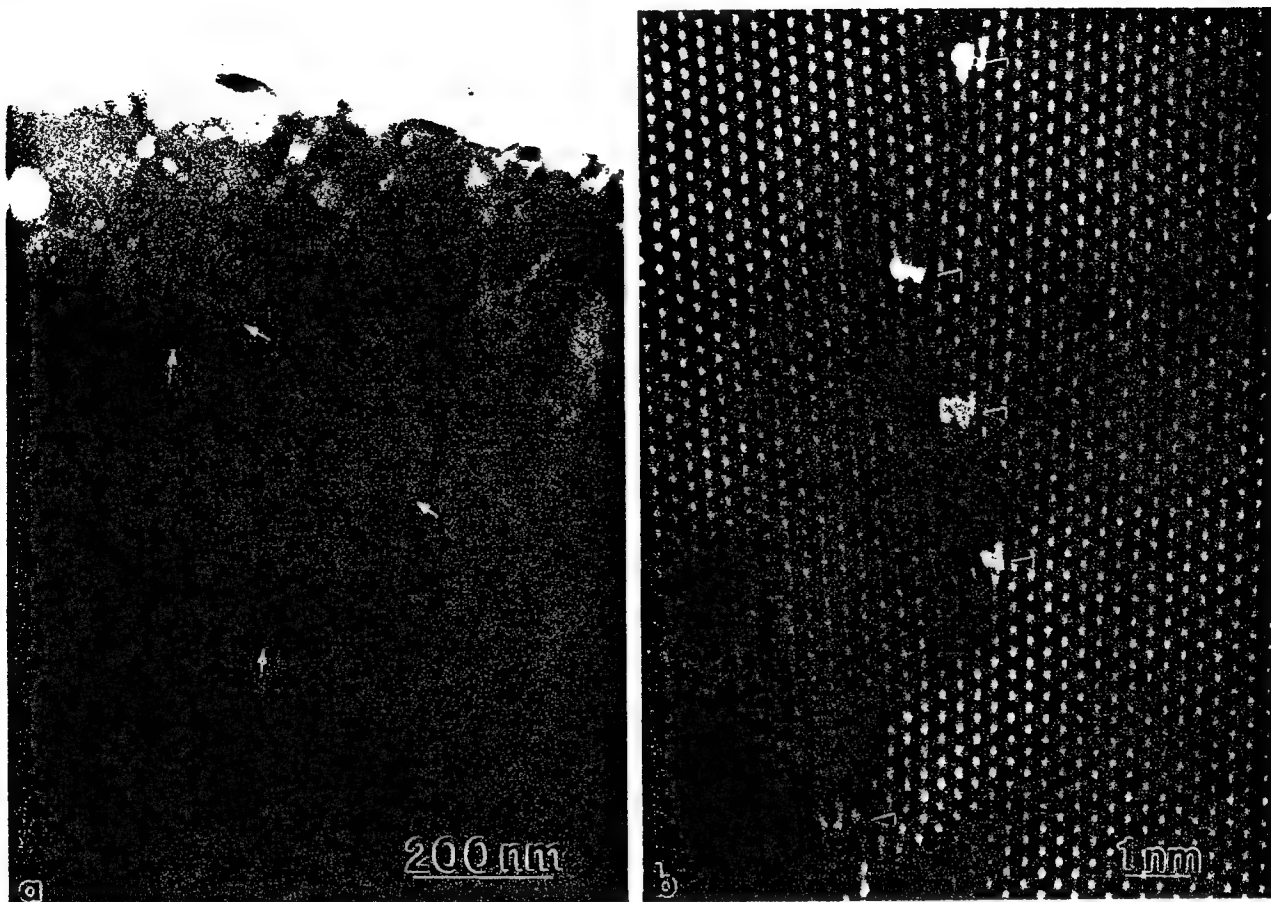


Fig. 10. (a) TEM—BF image of the nanoscale twins within an aragonite domain (Sarikaya and Aksay, 1992). (b) Atomic resolution image of a low angle boundary within a domain, showing that stresses are also accommodated by dislocations (arrows).

domains show a high degree of coherency. Local deformation within domains, such as low angle boundaries, as shown in Figure 10(b), may account for the accommodation of some of the internal stresses. Consequently, these three twin structures cover six orders of magnitude size scale from nanometer to submillimeter, and reveal for the first time a hierarchical structure in a biological hard tissue.

The geometrical and crystallographic model of aragonite platelets (Sarikaya and Aksay, 1992; Sarikaya et al., 1992b) discussed above is referred to as multiple tiling in mathematics (Grünbaum and Shephard, 1987). It appears that nature utilized this mathematical technique in nacre to form a highly ordered structure that is compatible with both the soft tissue and the crystalline structural constraints of the hard component. Furthermore, recent studies indicate that tiling may also play an important role in providing the overall shape of the nacre and its properties (Sarikaya and Aksay, 1992; Sarikaya et al., 1992b). The constraints that are developed as a result of the commensurate interface between the crystalline conformation of the

organic matrix proteins and crystalline ordering of the ions in the inorganic phase give rise to the hierarchical twin structure in the nacreous section of the mollusk shells. That is, the coupling between organic and inorganic crystalline structures results in a certain morphology of the inorganic phase, retaining the hierarchy of the defect structure in the CaCO_3 phase. Based on this crystallographic relationship, furthermore, even the growth pattern and shape of the overall shells may be described. There are significant implications of this result in biomimetic design of future materials. If the inorganic crystal units grow under the close scrutiny of the organic matrix, then in producing inorganic materials (thin films, small particles, bulk or laminated composites) all the important structural features of materials, such as shape, size, crystallography, and morphology, may be predicted based on the structural coupling between the organic template used and the knowledge of crystal structure of the desired inorganic phase. Future studies will explore these possibilities both studying the biological composites, such as nacre, and other sections of mollusks and echinoderms, and by

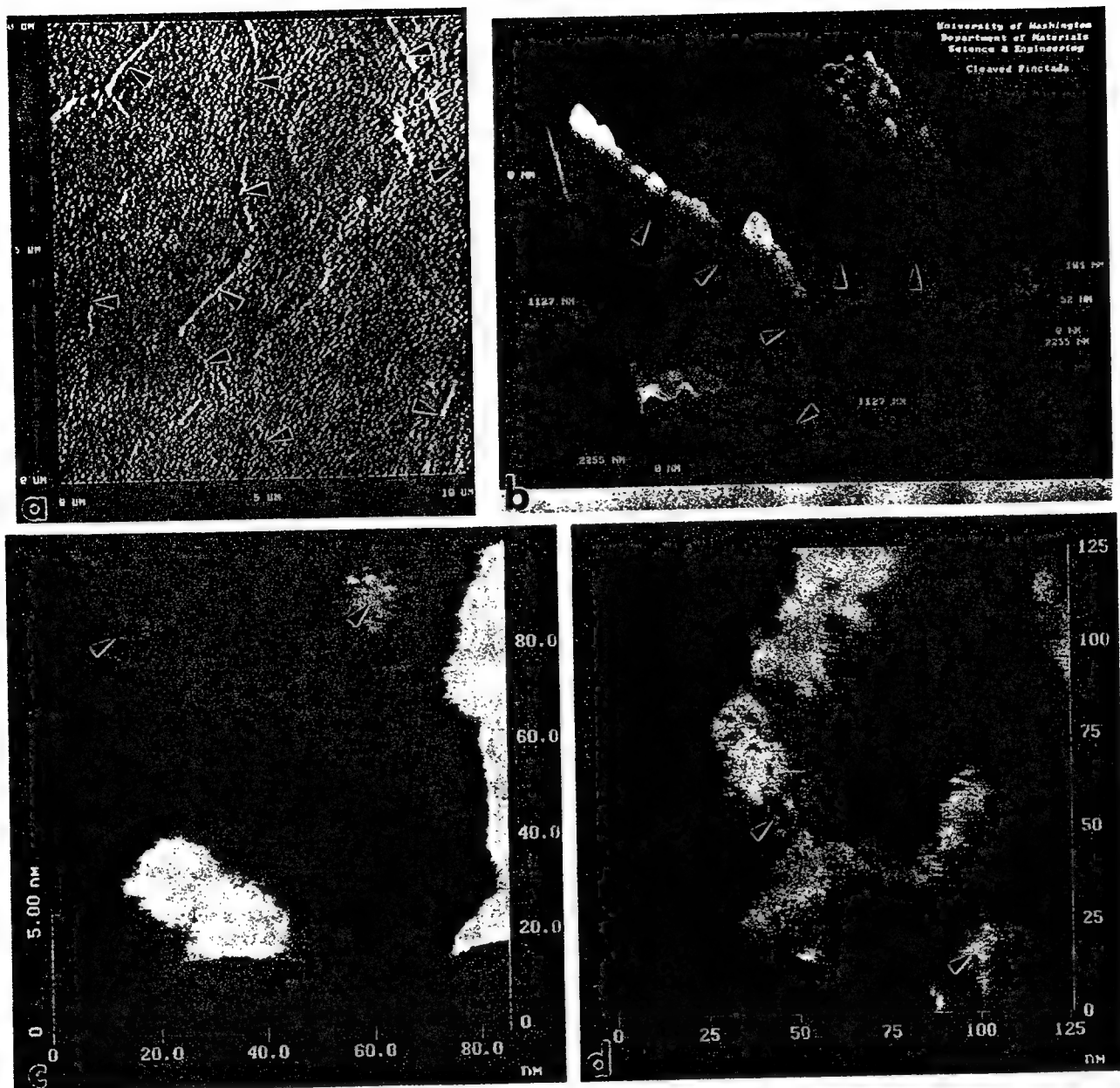


Fig. 11. AFM image of cleaved surface of the nacre section of a red abalone shell: The low magnification image in (a) shows the general view of the aragonite platelets with the platelet boundaries indicated by arrows. The image in (b) shows the detail of an interface between aragonite platelets (arrows). Corrugations in (b) are possibly due to

plastic deformation of the organic matrix during cleavage. Local ordering of corrugations at smaller length scale is discernible in the high magnification images (c) and (d). The origin of these corrugations, that have a separation of about 5 nm, is not yet known. Arrows in (c) and (d) show periodic organization of macromolecules.

CONCLUDING REMARKS AND FUTURE STUDIES

Biological composites were discussed in the context of their unique micro- and nano-architecture which result in excellent properties. Despite considerable effort in the field, our understanding of the mechanisms that operate in nacre making it a tough and strong composite, and current knowledge of the composition and

structure of the organic matrix and its structural relationship with the inorganic phase are still limited. Further investigation, therefore, is necessary in nacre, and other similar biomaterials reviewed here before their possible biomimetic applications. Based on the results from nacre, one of the widely investigated hard tissue, some of the major issues for future biomimetic research may be stated as follows: 1. On mechanical properties,

niques which might be specialized or involve all modes of microscopical analysis including imaging, diffraction, and spectroscopy, using light, X-rays, neutrons, or electrons as primary radiation. It will be possible only then to correlate structures at different length scales including their functions, and achieve design rules for synthesis of future biomimetic materials with tailored structures and properties.

ACKNOWLEDGMENTS

This work is supported by the Air Force Office of Scientific Research, Grant AFOSR-91-0281 and by a University Research Initiative through Army Research Office, Grant DAAL03-92-G-0241.

REFERENCES

- Addadi, L., and Weiner, S. (1990) Interaction between acidic macromolecules and structured crystal surfaces, stereochemistry and biominerization. *Mol. Cryst. Liq. Cryst.*, 13:305–322.
- Aksay, I.A., Baer, E., Sarikaya, M., and Tirrell, D.A., eds. (1992) Hierarchically Structured Materials. Vol. 255. Materials Research Society, Pittsburgh, PA.
- Alper, M., Calvert, P.D., Frankel, R., Rieke, P., and Tirrell, D.A., eds. (1991) Vol. 218. Materials Research Society, Pittsburgh, PA.
- Baer, E. (1986) Advanced polymers. *Sci. Am.*, 255:178–190.
- Baer, E., and Moet, A., eds. (1991) High Performance Polymers. Hanser, Munich.
- Baer, E., Cassidy, J.J., and Hiltner, A. (1988) Hierarchical structure of collagen and its relationship to the physical properties of tendon. In: Collagen: Biochemistry and Biomechanics. M.E. Nimi, ed. CRC Press, New York, pp. 177–199.
- Baer, E., Hiltner, A., and Morgan, R.J. (1992) Biological and synthetic hierarchical composites. *Physics Today*, October: pp. 60–67.
- Bazylinski, D.A., Frankel, R.B., Garrat-Reed, A., and Mann, S. (1991) Biominerization of iron sulfides in magnetotactic bacteria from sulfidic environments. In: Iron Biominerals. R.B. Frankel and R.P. Blakemore, eds. Plenum Press, New York, pp. 239–256.
- Berman, A. et al. (1988) Interaction of sea-urchin skeleton macromolecules with growing calcite crystals—A study of intercrystalline proteins. *Nature*, 331:546–548.
- Berman, A., Addadi, L., Leiserowitz, L., Weiner, S., Nelson, M., and Kvirk, A. (1990) A synchrotron X-ray study of a unique protein-calcite composite material. *Science*, 250:664–667.
- Blakemore, R.P. (1982) Magnetotactic bacteria. *Ann. Rev. of Microbiol.*, 36:217–238.
- Bouligand, Y. (1965) Sur une architecture torsadée repandue dans de nombreuses cuticules d'arthropodes. *C R Hebd. Séances Acad. Sci.*, 26:3665–3668.
- Brear, K., and Curry, J.D. (1976) Structure of the sea-urchin tooth. *J. Mat. Sci.*, 11:1977–1978.
- Currey, J.D. (1987) Biological composites. *J. Mat. Edu.*, 9:118–296.
- Dameron, C.T., Reese, R.N., Mehra, R.K., Kortan, A.R., Carroll, P.J., Steigerwald, L.E., Brus, M.L., and Winge, D.R. (1989) Biosynthesis of cadmium sulfide quantum semiconductor crystallites. *Nature*, 338:596–597.
- Dawridge, W. (1979) Mechanical Behavior of Ceramics. Cambridge University Press, London.
- Evans, A.G. (1988) High toughness ceramics. *J. Mat. Sci. Eng.*, A105/106:65–75.
- Evans, A.G., and Marshall, D.A. (1989) The mechanical behavior of ceramic matrix composites. *Acta. Met.*, 37:2567–2583.
- Fendler, J.H. (1982) Membranemimetic Chemistry. Wiley-Interscience, New York.
- Frankel, R., and Blakemore, R.P. eds. (1991) Iron Biominerals. Plenum, New York.
- Fulrath, R.M., and Pask, J.A., eds. (1966) Ceramic Microstructures. University of California Press, Berkeley.
- Gell, M., Duhi, D.H., and Giamei, A.F. (1980) High Temperature Superconductors: Relationships Between Properties, Structure, and Solid-State Chemistry. ASM-International, Metals Park, OH.
- Ghiradella, H., Aneshansley, D., Eisner, T., Silberglied, R.E., and Hinton, H.E. (1972) Ultraviolet reflection of male butterfly: Interference color caused by thin-layer elaboration of wing scales. *Science*, 178:1214–1217.
- Glimcher, J. (1981) On the form and function of bone: From molecules to organs. In: The Chemistry and Biology of Mineralized Biological Tissues: Wolff's Law Revisited. A. Veis, ed. Elsevier, New York, pp. 617–673.
- Gorby, Y.A., Beveridge, T.J., and Blakemore, R.P. (1988) Characterization of the bacterial magnetosome membrane. *J. Bacteriol.*, 170: 834–841.
- Gosline, M., DuMont, M.E., and Denny, M.W. (1986) Structure and properties of spiders' silk. *Endeavour*, 10:37–43.
- Grégoire, C. (1972) Structure of the molluscan shell. In: Chemical Zoology, M. Florkin and M. Scheer, eds. Academic Press, New York, pp. 45–102.
- Griffith, A. (1925) The phenomena of rupture and flow in solids. *Phil. Trans. CCXXI*, A:163–198.
- Grünbaum, B., and Shephard, G.C. (1987) Tilings and Patterns. W.H. Freeman, New York.
- Gunderson, S.L., and Schiavone, R.C. (1989) The insect exoskeleton: A natural structural material. *JOM*, 41:80–82.
- Gunnison, K., Sarikaya, M., Liu, J., and Aksay, I.A. (1992) Structure-mechanical property relationships in a biological ceramic-polymer composite: Nacre. In: Hierarchically Structured Materials, MRS Symp. Proc., Vol. 255. I.A. Aksay, E. Baer, M. Sarikaya, and D.A. Tirrell, eds. Materials Research Society, Pittsburgh, PA, pp. 171–183.
- Haasen, P. (1978) Physical Metallurgy. Cambridge University Press, London.
- Harrison, P.M., Artymiuk, P.J., Ford, G.C., Lawson, D.M., Smith, J.M.A., Trefry, A., and White, J.L. (1989) Ferritin: Function and structural design of an iron-storage protein. In: Biominerization: Chemical and Biochemical Perspectives. S. Mann, J. Webb, and R.J.P. Williams eds. VCH, Weinheim, Germany, pp. 257–294.
- Hull, D. (1981) An Introduction to Composite Materials. Cambridge University Press, London.
- Jackson, A.P., Vincent, J.F.V., and Turner, R.M. (1988) The mechanical design of nacre. *Proc. R. Soc. London (Biol.)*, B234:415–440.
- Jorgenson, J.D., Kitazawa, K., Tarascon, J.M., Thomson, M.S., and Torrance, J.B., eds. (1989) High Temperature Superconductors: Relationships Between Properties, Structure, and Solid-State Chemistry, Vol. 156. Materials Research Society, Pittsburgh, PA.
- Khanuja, S. (1991) Processing of Laminated B₄C-Polymer Laminated Composites. MS Thesis, University of Washington.
- Liu, J., Sarikaya, M., and Aksay, I.A. (1992) A hierarchically structured model composite: A TEM study of the hard tissue of red abalone. In: Hierarchically Structured Materials, MRS Symp. Proc., Vol. 255. I.A. Aksay, E. Baer, M. Sarikaya, and D.A. Tirrell, eds. Materials Research Society, Pittsburgh, PA, pp. 9–17.
- Lowenstam, H.A., and Weiner, S. (1989) On Biominerization. Oxford University Press, New York.
- Mann, S. (1988) Molecular recognition in biominerization. *Nature*, 33:119–123.
- Mann, S., Sparks, H.C., and Wade, W.J. (1990) Crystallo-chemical control of iron oxide biominerization. In: Iron Biominerals. R.B. Frankel and R.P. Blakemore, eds. Plenum, New York, pp. 21–49.
- Nakahara, H., Bevelander, G., and Kakei, M. (1982) Electron microscopic and amino acid studies on the outer and inner shell layers of *Haliotis rufescens*. *VENUS Jpn. J. Malac.*, 41:33–46.
- Neville, A. (1975) The Biology of Arthropod Cuticle. Springer and Verlag, Berlin.
- Rieke, P.C., Calvert, P.D., and Alper, M., eds. (1990) Materials Synthesis Using Biological Processes. Vol. 174. Materials Research Society, Pittsburgh, PA.
- Sarikaya, M., and Aksay, I.A. (1992) Nacre of abalone shell: A natural multifunctional nanolaminated ceramic-polymer composite material. In: Results and Problems in Cell Differentiation in Biopolymers. S. Case ed. Springer and Verlag, Amsterdam, pp. 1–25.
- Sarikaya, M., and Aksay, I.A. (1993a) Nacre: Properties, crystallography, morphology, and formation. In: Design and Processing of Materials by Biomimetics. M. Sarikaya and I.A. Aksay eds. American Institute of Physics, Washington, D.C., pp. 35–86.
- Sarikaya, M., and Aksay, I.A. eds. (1993b) Design and Processing of Materials by Biomimetics. American Institute of Physics, Washington, D.C.
- Sarikaya, M., Gunnison, K.E., Yasrebi, M., and Aksay, I.A. (1990) Mechanical Property-Microstructural Relationships in Abalone Shell. Vol. 174. Materials Research Society, Pittsburgh, PA, pp. 109–116.
- Sarikaya, M., Liu, J., and Aksay, I.A. (1992a) Structure of the sea-urchin teeth. unpublished research.

- Sarikaya, M., Liu, J., and Aksay, I.A. (1992b) unpublished results.
- Shaw, D.W., Bean, J.C., Keramidas, V.G., and Peercy, P.S., eds. (1989) Epitaxial Heterostructures. Vol. 198. Materials Research Society, Pittsburgh, PA.
- Shinjo, T., and Takada, T., eds. (1987) Metallic Superlattices, Elsevier, Amsterdam.
- Simkiss, K., and Wilbur, K.M. (1989) Biomimetication, Academic Press, New York.
- Tressler, R.E., and Bradt, R.C., eds. (1983) Deformation of Ceramic Materials, Plenum, New York.
- Veis, D.J., Albiner, T.M., Clohisy, J., Rahima, M., Sabsay, B., and Veis, A. (1986) Matrix proteins of the teeth of the sea urchin *Lytocrinus variegatus*. *J. Exp. Zool.*, 240:35-46.
- Wainwright, S., Briggs, W.D., Currey, J.D., and Gosline, J.M. (1976) Mechanical Design in Organisms. John Wiley and Sons, New York.
- Watabe, N. (1965) Studies in Shell Formation: Crystal-Matrix Relationships in the Inner layers of Molluscan Shells. *J. Ultrastr. Res.* 12:351-370.
- Weiner, S., and Traub, W. (1984) Macromolecules in mollusc shells and their functions in biomimetication. *Philos. Trans. R. Soc. Lond. Biol.* B304:425-434.
- Weiner, S., Talmon, Y., and Traub, W. (1983) Electron diffraction studies of molluscan shell organic matrices and their relationship to the mineral phase. *Int. J. Biol. Macromol.*, 5:325-328.
- Yasrebi, M., Kim, G.H., Milius, D.L., Sarikaya, M., and Aksay, I.A. (1990) Biomimetic processing of ceramics and ceramic-based composites. In: Better Ceramics Through Chemistry-IV. Vol. 180. C.J. Brinker, D.R. Ulrich, and B.J. Zelinski, eds. Materials Research Society, Pittsburgh, PA, pp. 625-635.
- Zackay, V.F., and Aaronson, H.I., eds. (1962) Decomposition of Austenite by Diffusional Processes. Interscience, New York.

M. Sarikaya, "Biological Composites: Ultimate Self-Assembled Materials," Proceedings of XIIIth International Congress of Electron Microscopy, ICEM 13, Paris, Vol. 3B: Applications in Biological Sciences (Les éditions de Physique, Paris, France, 1994) pp. 889-890.

Biological Composites: Ultimate Self Assembled Materials

M. Sarikaya

Department of Materials Science and Engineering, Roberts Hall, FB-10, University of Washington, Seattle, WA 98195, U.S.A.

Biological composites, such as bone, dentin, and mollusk shells, have complex but highly ordered structures (Currey (1987)). The interest in biological composites stems from the fact that these materials are self assembled in an hierarchical fashion from molecular to macro scale, and that the resulting assemblies have physical properties that far exceed those of current synthetic materials of similar elemental or phase compositions. The objective of biomimetics is to understand the structures and mechanisms of formation of biological composites with the aim of either mimicking the microstructures (biomimicking) or the processing (bioduplication) so as to synthesize novel materials for technological applications (Sarikaya and Aksay (1994)).

Some examples of biological hard tissues are shown in Figures 1 - 4 which present variety of nanostructures involving both organic and inorganic components in various configurations in significantly diverse organisms. Fig. 1 displays a string of magnetite, Fe_3O_4 (cubic), particles in magnetotactic bacteria. The particles form within closed biological sacs that regulate ion transport and control nucleation and growth (Blakemore and Frankel (1992)). The particles are single crystalline and have a perfect lattice (devoid of any defect), small (about 500 Å in dia., and hence paramagnetic), and their shapes are species specific. Fig. 2 displays distribution of fine (50 Å dia.) coherent MgCO_3 precipitates in a calcite (rhombohedral CaCO_3) matrix in a sea-urchin spine. The spine (0.5-1.0 mm in dia., and several cm long) is a "single" crystal but has an intricate microstructure (Liu and Sarikaya (1992)). The microstructure of the inner section of a nautilus (*Nautilus pompelius*) shell is given in Fig. 3 which displays a brick and mortar microarchitecture composed of aragonite (orthorhombic CaCO_3) platelets (0.5 μm thick and 5 μm edge-length) and a thin (100 Å) film of composite organic matrix. The microstructure is called nacre, or "mother-of-pearl," and can be frequently found in many mollusk species (for instance, gastropods, e.g., abalone, and bivalves, e.g., pearl oyster). The platelets can be represented mathematically as space filling multiple tiles that are crystallographically highly organized with the underlying organic matrix from nanometer to macroscale, resulting in nacre (98% inorganic) that has mechanical properties that far exceed high technology ceramics (Sarikaya and Aksay (1994)). Finally, HREM image of caribou antler is shown in Fig. 4 which displays ultrafine hydroxyapatite crystallites within a framework of collagenous organic matrix. The amount of inorganic particles can reach up to 50% of the structure resulting in toughness values exceeding even that of a mammalian bone.

In all these examples, formation, crystallography, shape, micro-and nanoarchitecture of the inorganic phase are controlled by an organic matrix that have many different configurations and are subject of study (Addadi and Weiner (1990) Mann (1990)). The major issues in biomimetics are: (i) type, amino acid composition and sequence, conformation, and spatial distribution of organic component, its self assembly and structural relationship with the inorganic phase; (ii) crystallography, spatial distribution, nucleation, and growth of the inorganic phase, and (iii) properties of biocomposites.

The microscopy in this multidisciplinary field is the single most important technique that would provide a better insight into the formation of hard tissues. For example, long-range conformation and assembly of organic matrix, including polysaccharides and proteins can be analyzed by AFM performed in liquids; macro scale structures can be imaged by light optical microscopy techniques (such as Brewster angle, confocal, fluorescence); X-ray microscopy, diffraction, and spectroscopy allows the determination of nanostructures; and electron microscopy imaging, diffraction, and spectroscopy provide information on crystallography, nanostructures, and elemental compositions. These will be addressed in the presentation.

1. Addadi L. and Weiner S. (1990) *Mol. Cryst. Liq. Cryst.* **13**, 305-322.
2. Blakemore R. P. and Frankel R. B. (eds.) (1992) *Iron Biominerals* (Pergamon, New York).
3. Currey J. (1987) *Biological Composites, J. Mater. Edu.* **9**, 118-296.
4. Liu J. and Sarikaya M. (1992) unpublished.
5. Mann S. (1988) *Nature* **33**, 119-123.
6. Sarikaya M. and Aksay I. A. (eds.) (1994) *Biomimetics: Design and Processing of Materials* (American Institute of Physics, New York).
7. The work is supported by Grants under #s AFOSR-92-0xxx and URI/ARO.

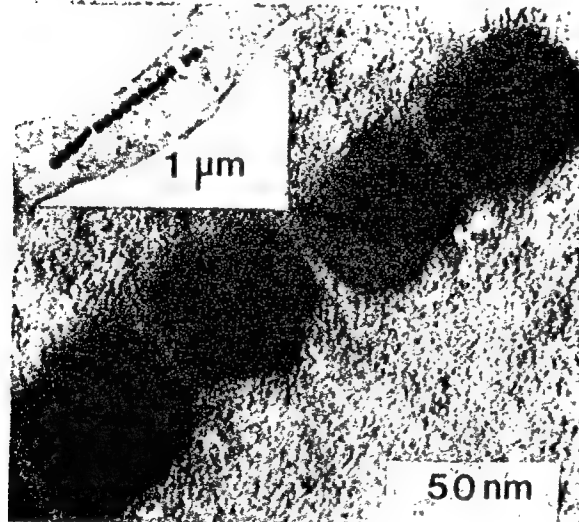


Figure 1: Magnetite particles that form in magnetotactic bacterium (inset).

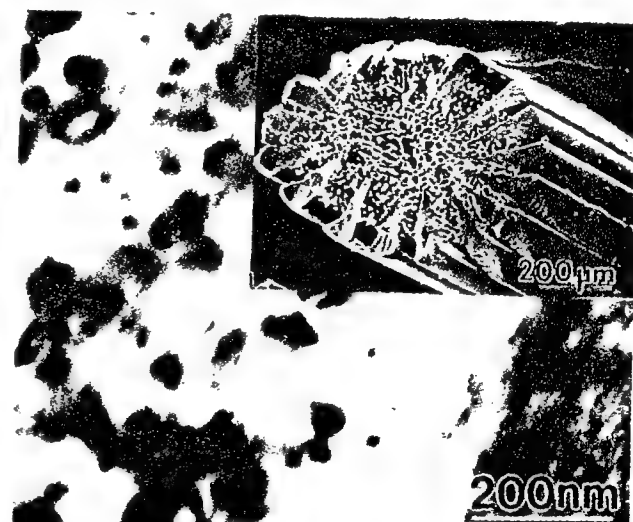


Figure 2: Nanostructure of sea urchin spine displays coherent MgCO_3 precipitates within CaCO_3 matrix (inset: SEM image of sea urchin).

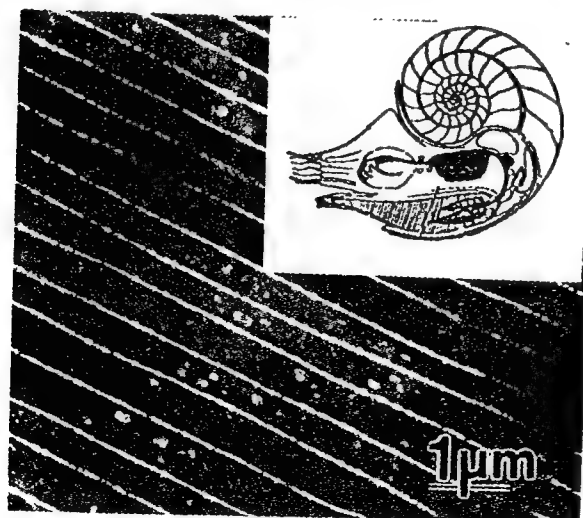


Figure 3: Edge-on view of brick and mortar structure of nacre of nautilus (inset).

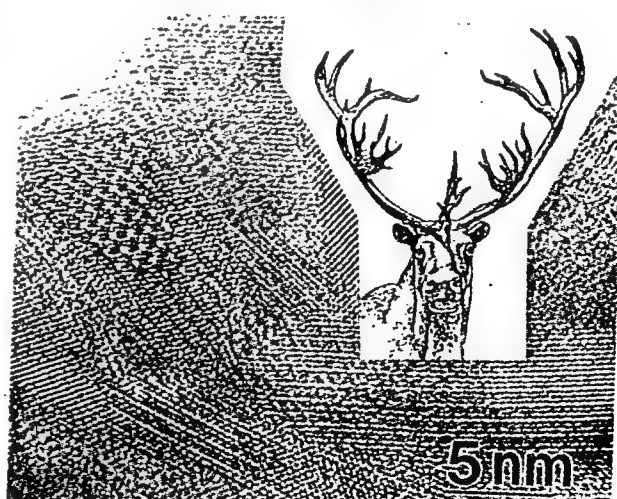


Figure 4: AREM image of caribou antler (inset) showing hydroxyapatite particles within collagenous matrix.

M. Sarikaya,
"Organic-Inorganic Interfaces In Layered Biological
Composites,"
Proceedings of 52nd Microscopy Society of America,
W. Bailey (ed.)
(San Francisco Press, San Francisco, CA, 1994)

ORGANIC-INORGANIC INTERFACES IN BIOLOGICAL COMPOSITES

Mehmet Sarikaya

Materials Science and Engineering, University of Washington, Seattle, WA 98195, USA

Biological hard tissues, such as bone, dentin, and mollusk shells, are composite materials incorporating an organic matrix and inorganic crystallites in a complex nano- and micro-architectural forms.¹ The interest of physical sciences in biological composites stems from the fact that these materials are self assembled in an hierarchical fashion from molecular to macro scale, and that the resulting assemblies have properties that far exceed those of current synthetic materials of similar elemental or phase compositions. The objective of biomimetics is to either mimick structures of biological composites, *biomimicking*, or use the synthesis methodologies of organisms to produce new materials, *bioduplication*.² In a biocomposite, substructure and crystallography of the inorganic component are highly ordered, its morphology and shape are species specific; these are all thought to be regulated by the organic matrix.³⁻⁴ The understanding of structural relationship between the organic and ceramic components of a biological composite, therefore, is fundamental both to the understanding of mechanisms of biomineralization and to biomimetic design and synthesis of novel engineering materials. These issues will be addressed in the present paper.

Several examples of biological hard tissues are given in Figures 1 through 4. Ultrafine magnetic particles (Fe_3O_4 : magnetite) form within magnetosomes (closed biological membranes) in magnetotactic bacteria. The particles are single crystalline, their size (average dia 500 Å) is within the single domain region, they have a perfect lattice (no defects), and their shape is species specific.⁵ The question involves how the organic sack controls ion transport and regulate the nucleation and growth of the particles. The second example is from sea urchins, which form "single" crystalline calcitic (CaCO_3 : rhombohedral) spines that are several centimeters long and a mm in diameter. Analysis by TEM reveals that the spines are actually polycrystalline with low-angle grain boundaries containing ultrafine MgCO_3 precipitates. The question here is how the organic matrix is involved in the evolution of the micro- and nano-structure of the spine that has highly intricate structure at the macro scale. The third example is from mollusk shells; in some species the inner section has a layered structure, called nacre, which is an alternating nanolaminate of aragonitic platelets (CaCO_3 : orthorhombic) and organic thin film (proteins and polysaccharides) covering these platelets, a structure commonly known as "mother of pearl." The highly organized structure has fracture toughness and strength properties that surpass high technology ceramics such as Si_3N_4 , ZrO_2 , SiC , and Al_2O_3 .⁶ In addition to being an integral part of the biocomposite, the organic matrix may be also involved in both the nucleation/growth, and the shape formation of the shell. Finally, in antler bone, ultrafine particles of $\text{CaH}(\text{PO}_4)_3$ form within a network of callogenous matrix, constituting 50% of the structure and providing toughness values that far surpass the mammalian skeletal bone. Again, the question is how the organic matrix, in the form of a scaffolding, is involved in the formation of the inorganic particles and their distribution.

Organic macromolecules (such as proteins and polysaccharides) may influence the formation of inorganic phases in several different ways: (i) Organic macromolecules may serve as nucleators (or seeds) for the formation of inorganic crystals of a certain crystal structure and composition;⁶ (ii) Self-assembled macromolecules with specific charge distribution, stereochemical and geometrical structures may serve as a template for inorganic phases;³ (iii) Macromolecules may regulate growth patterns of inorganic crystals by modifying their free-surfaces to control particle morphology;⁴ (iv) Macromolecules, or their fractions, may be occluded within inorganic crystals to control substructure, and hence, modify intrinsic materials properties; (v) Macromolecules may provide scaffolding with long-range order within which inorganic crystallites form; (vi) They may provide compartments to control size of the inorganic particles.⁵ In this presentation, current understanding of these issues will be discussed with examples from several biological and synthetic systems, and future direction will be addressed in the formation of synthetic materials with structures similar to biological composites.

1. J. Currey, *Biological Composites, J. Mater. Edu.* **9**, 118-296 (1987).
2. *Biomimetics: Design and Processing of Materials*, Sarikaya M. and Aksay I. A. (eds.) (American Institute of Physics, New York, 1994).
3. S. Mann, *Nature* **33**, 119-123 (1988).
4. L. Addadi and Weiner, *Mol. Cryst. Liq. Cryst.* **13**, 305-322 (1990).
5. *Iron Biominerals*, R. P. Blakemore and R. B. Frankel (eds.) (Pergamon, New York, 1992).
6. M. Sarikaya and I. A. Aksay, in:
7. Research is performed in collaboration with Prof. James Staley (Microbiology) and Prof. Clement Furlong (Medical Genetics) and supported by Air Force Office of Scientific Research under Grant # AFOSR-91-0281 and URI (Army Research Office) under Grant #DAAL03-92-G-0241.

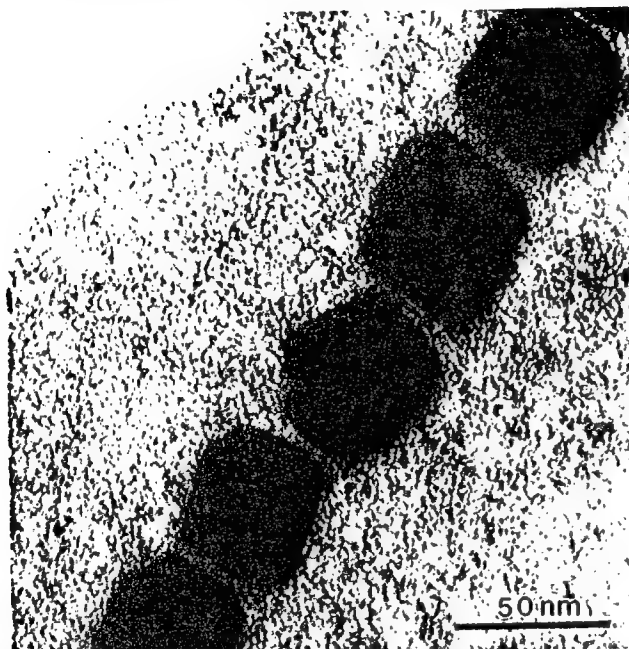


Fig. 1 - Magnetite particles in magnetotactic bacterium, *Aquaspirillum magnetotacticum*

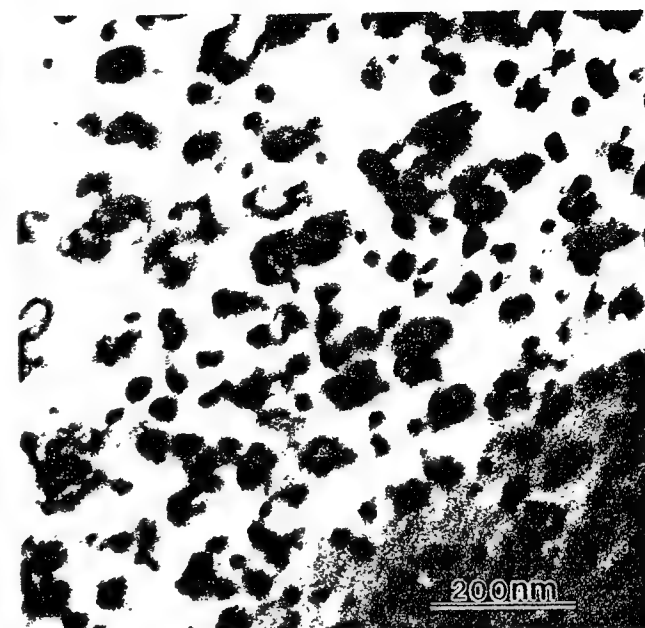


Fig. 2 - Structure of sea urchin spine displays coherent spherical $MgCO_3$ precipitates within $CaCO_3$ matrix.

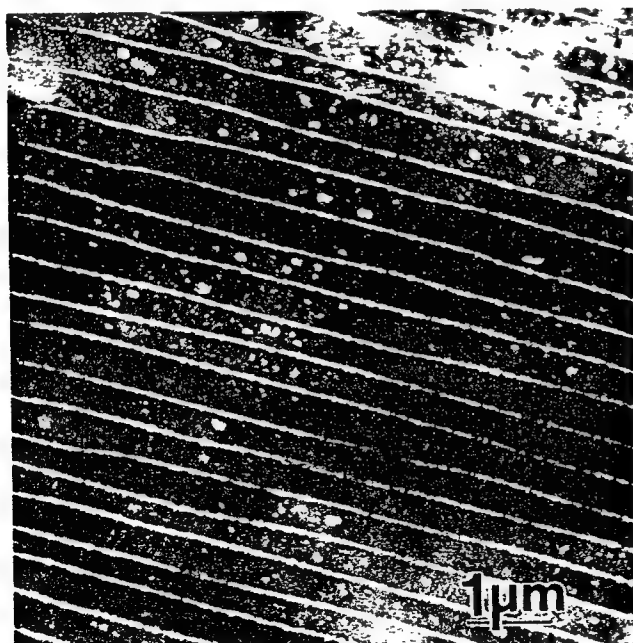


Fig. 3 - Edge-on view of brick and mortar structure of nacre of a cephalopod, *Nautilus pompelius*.

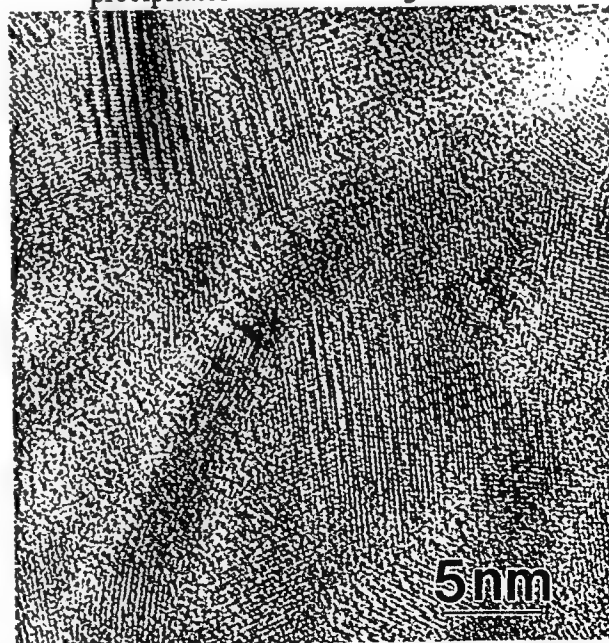


Fig. 4 - AREM image of caribou antler displays small particles of hydroxyapatite within a collagenous matrix.

M. Sarikaya,
"Nanodesign and Properties of a Biocomposite for
Biomimetics,"
Proc. of *Segundo Congreso Mexicano de Microscopia
Electronica*, edited by F. Gasga (1994) pp. SP2.

Mehmet Sarikaya

Materials Science and Engineering, University of Washington, Seattle, Washington 98195, USA

Biological hard tissues, e.g., bone, dentin, and mollusk shells, are composites of organic matrix and inorganic crystallites often forming hierarchical structures from nanometer to macro-scale. Biocomposite properties are superior to those of synthetic materials with similar phase compositions. In biomimetics, either structures are mimicked, *biomimicking*, or biological pathways are duplicated, *bioduplication*, in synthesizing novel technological materials. Structural relationships between organic and inorganic components is fundamental to both mechanisms of biominerization and to biomimetic design and synthesis of novel engineering materials. An overview will be given on structures, mechanical properties, and formation of biocomposites.

Unique microstructures and resulting properties in biocomposites can be inspirational sources for future materials.^{1,2} Based on this promise, this research group investigates structures of biocomposites to establish relationships with properties and to obtain processing strategies and microstructural design criteria for the development of new materials with novel properties.²

Biomaterials of engineering interest are mostly hard and stiff tissues, and small particles (Table - I).¹⁻⁴ Structure is composed of an intricately ordered crystalline inorganic phase (~95 vol. %) interspersed throughout an organic matrix which controls its formation.^{1,2,5,6} An example is shells of mollusks, e.g., gastropod, cephalopods, and bivalves, display two types of microstructures: prismatic (calcite) and nacreous (aragonite). Nacre, e.g., in *Haliotis rufescens*, is composed of stacked aragonite platelets (0.2 - 0.5 μm thick) arranged in brick and mortar microarchitecture with organic matrix (10 - 40 nm thick) forming a "glue" between the platelets (Fig. 1). As a result of this highly ordered, but simple, laminated-hierarchical structure, nacre exhibits an excellent combination of mechanical properties (Fig. 2). Average values of fracture toughness, K_{IC} , and flexural strength, σ_{F} , of nacre give about 20-30 times that of synthetic monolithic CaCO_3 and 2 to 3 times that of high technology ceramics. This result is the major driving force in producing ceramic-based composites with better mechanical properties than existing composites through nanoscale lamination based on lessons from biology (cermets in Fig. 2).²

Several toughening mechanisms in nacre are: (i) crack blunting/branching, (ii) microcrack formation, (iii) plate pull-out, (iv) crack bridging (ligament formation), and (v) sliding of CaCO_3 layers. Both sliding (Fig. 3(a)) and organic ligament formation between the layers (Fig. 3(b)) are major toughening mechanisms as they are the main energy absorption mechanisms during crack propagation. The high strength of nacre may be due to the size and structure of the aragonite platelets and the strong interfaces between the inorganic and the organic components.

Formation of nacre structure and its control by the organic macromolecules have to be understood for producing engineering structures based on biology. A theoretical model, supported by experiments, gives nucleator proteins organized, as seeds, in pseudo-hexagonal conformation for CaCO_3 formation which then grow by self-generation on successive layers separated by organic film consisting of proteins and polysaccharides (Fig. 4).² Growth in the lateral direction occurs with aragonite crystallites forming a 3-D multiple tiling with hierarchical structural twinning. The "seeding" mechanism, self-generative nucleation, and hierarchical crystallography of the inorganic are due to complex formation mechanisms that we, one day, desire to bioduplicate via self-assembling biomacromolecules extracted from mollusk shells used for biominerization.

References

1. J. D. Currey, "Biological Composites," *J. Mater. Edu.*, (1987) 9, 118.
2. M. Sarikaya and I. A. Aksay, Chp. 1, in: *Results and Problems in Cell Differentiation in Biopolymers*, S. Case (ed.) (Springer, Amsterdam, 1993) 1.
3. *On Biominerization*, H. A. Lowenstam and S. Weiner (Oxford University Press, New York, 1989).
4. *Iron Biominerals*, R. B. Frankel and R. P. Blakemore (eds.) (Plenum, New York, 1991).
5. L. Addadi and S. Weiner, *Mol. Cryst. Liq. Cryst.* (1990) 13, 305.
6. S. Mann, *Nature* (1988) 33, 119.
7. This work was supported by AFOSR and URI/ARO.

Table-I: Biocomposites, Structural-Design and Physical Properties

material/composite	example	structure	properties
small particles	bacterial algal	N	magnetic, opt.
ceramic/ceramic	sea-urchin	N	electronic,
ceramic/polymer	mollusk bone dentin	B N, H	mech. (wear) mech., ferroelastic " "
polymer/polymer			N, H mech., opt. ferroelastic,
laminated	cuticle	N, H	mech., opt.
fiber/matrix	tendon	N, H	mech., ferroelastic
fiber/fiber	silk	N	mech. (tensile)
liquid crystalline	mucus	N	rheological

N: nano; M: micro; B: both; H: hierarchical; opt.: Optical

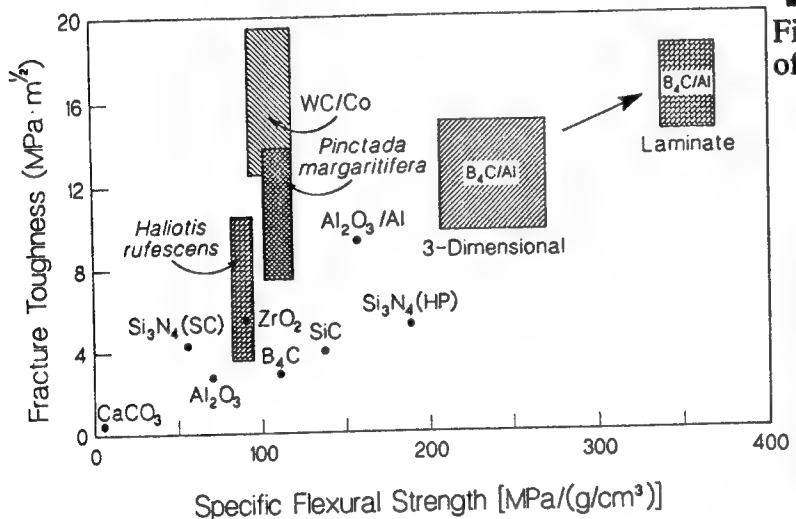


Fig. 2 -Properties of nacre, synthetic CaCO₃ and high technology ceramics and cermets.



Fig. 4 - Edge of abalone shell shows aragonite platelets, separated by organic membrane, that grow by self-generation on successive layers of nacre.

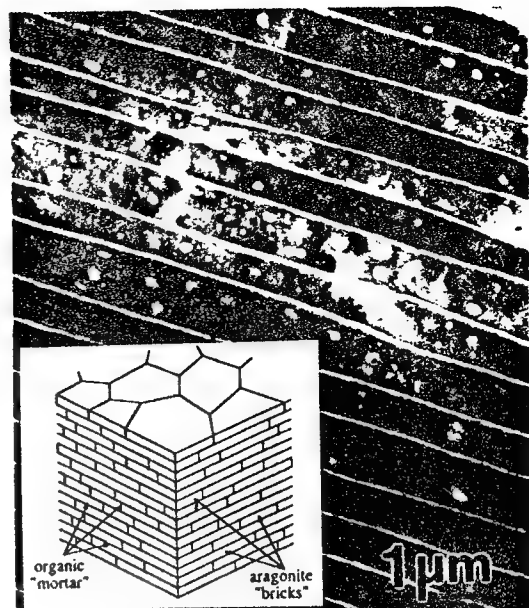


Fig. 1 -Brick and mortar microarchitecture of nacre and schematic illustration (inset).

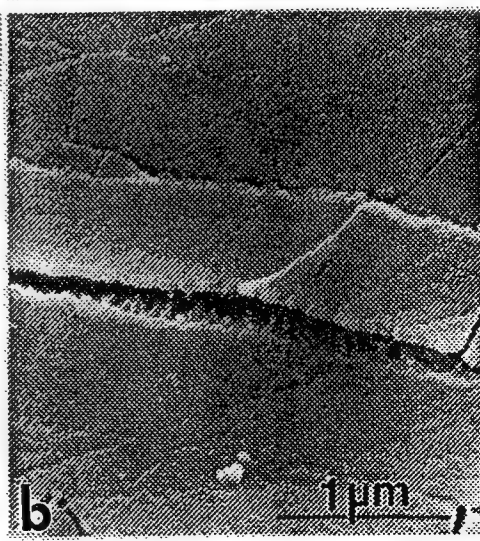
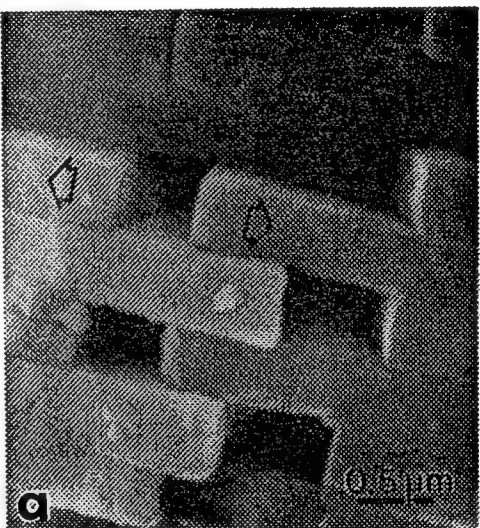


Fig. 3 - (a) Sliding of platelets and (b) ligament formation by the organic matrix between platelets.

APPENDIX-B

News Clippings

"Biomimetics: Creating Materials From Nature's Blueprints"

by Robin Eisner

The Scientist
July 8, 1991

RESEARCH

Biomimetics: Creating Materials From Nature's Blueprints

BY ROBIN EISNER

In order to design a 21st-century, impact-resistant substance, materials scientist Mehmet Sarikaya of the University of Washington in Seattle finds inspiration in a 500-million-year-old feat of evolution—the shell of a present-day mollusk, the abalone.

Following blueprints drawn from analysis of the microarchitecture of the shell, Sarikaya and colleague Ilhan Aksay have manufactured a prototype material that mimics the shell's laminar, protection-providing structure.

Sarikaya is one of growing number of materials researchers involved in biomimicking, or biomimetics—the study of the structure and function of biological materials and systems as models for materials design. According to materials scientist Aksay, also from the University of Washington, about 500 scientists in the United States are involved in some aspect of biomimicking, although they might not identify their specialty as such.

What they have in common is looking at nature as a guide to create the materials for the new machines, fabrics, and shelters of the next century. While biomimicking, per se, represents a small part of the federal government's current resurgence of interest in materials research, these scientists see their approach as crucial to the national technology development effort and as a source of opportunities for collaborations involving academic, industrial, and government scientists in disciplines as diverse as botany, aerospace, and condensed-matter physics.

Proponents of biomimetics say there are numerous economic, environmental, and scientific advantages to be gleaned from their approach to materials design. Sarikaya says that when the time comes to actually develop materials based on the biomimetic paradigm, around 15 to 20 years from now, "we will most likely use raw materials that are cheaper; energy costs will be lower, since many of the processes in nature take place at room temperature; and, to some extent, these materials we make will be biodegradable."

But the material, based on the shell, that Sarikaya and Aksay created in their laboratory at the University of Washington—a carbon, boron, and aluminum mixture—is not as tough or strong as they believe it can be. Although their new material is better than a similar substance composed of these elements, it is still not as good as the shell in these parameters.

Sarikaya and Aksay's material tested 1.3 times tougher and stronger than the standard carbon, boron, and aluminum mixture. But the shell's protein-and-calcium-carbonate-layered structure has hundred-fold superiority to the strength and toughness of its standard of comparison, calcium carbonate—the inorganic

salt that makes up 98 percent of the shell—alone. Since the scientists cannot directly measure their new material against the shell for these characteristics, because it would be like comparing apples and oranges, they must compare these magnitudes of difference. They are still off by at least a factor of 10.

To increase the toughness and strength of their biomimetics-produced material, they think they will have to make the component layers of their substance thinner. The mollusk somehow exudes its protein in a layer that is two hundred-millionths of a meter thick and places it upon a five ten-millionths of a meter layer of calcium carbonate. The University of Washington group can achieve thicknesses only on the order of a hundred-thousandth of a meter. Eventually, though, the group expects to overcome this limitation by layering both biologic and synthetic materials during manufacture.

According to researchers working in this area, the collaborations that are necessary for biomimetics to be successful will generate advances

SIGNIFICANT PAPERS IN BIOMIMETICS

J. Currey, "Biological Composites," *Journal of Materials Education*, 9(1-2):118-296, 1987.

E. Baer, A. Hiltner, H.D. Keith, "Hierarchical Structure in Polymeric Materials," *Science*, 235:1015-22, 1987.

L. Addadi, S. Weiner, "Interaction between Acidic Proteins and Crystals: Stereochemical Requirements in Biomimetication," *Proceedings of the National Academy of Sciences*, 82:4110-14, 1985.

S. Mann, et al., "Controlled Crystallization of CaCO₃ Under Stearic Acid Monolayers," *Nature*, 334:692-95, 1988.

for all the scientific disciplines concerned. Biologists, for example, will ask more fundamental questions about the nature of the organisms and systems they study in order to answer the questions that the chemists, physicists, and engineers pose when they do materials design.

"Biologists and technologists are finally coming to the realization that there is something to be gained by seriously working together," says Stephen Wainwright, a mechanical biologist at Duke University. Sarikaya adds: "There is no way a materials scientist will be able to do it on his or her own."

Amurthi Srinivasan, aerospace engineer at United Technologies in Hartford, Conn., and coeditor of *Biomimetics*, a journal that Plenum Press in New York expects to launch in the spring of 1992, says biomimetics will spawn new kinds of sci-



Sarikaya looks to a 500-million-year-old feat of evolution, a mollusk, in designing a 21st-century material.

tific instruments and approaches to materials manufacturing. "To truly understand materials in nature, we have to see them in their living state," he says. "Most of the measurements we make are unnatural, based on dead material. This field offers opportunities to design machines that can monitor life better. And once we understand how materials are made in living systems, we can then mimic the processes artificially and efficiently."

Wainwright says that biological materials and systems are multifunctional, adaptive, nonlinear, complex, and, in general, just "weird and wonderful" compared to somewhat simplistic synthetically created materials. Bone, for example, is far more complicated than metals, according to Srinivasan, and possesses remarkable abilities of structural adaptation to external loading. Bone differs not only from animal to animal, but also from place to place within the same animal. It changes over time, and under various loading conditions.

Wainwright says biomimetics is the single most exciting thing in science he has experienced in his life. "And I am turning 60 this year," he says. Since biological form and function will be the key to materials design, Wainwright feels that descriptive biology, the study of the structure of biological systems, will overcome its current poor reputation as a dead, 19th-century science. "It's going to take a lot of morphologists [descriptive biologists] out of the ivory tower of basic research into the area of applied research. It will open many doors for them," he says.

But the main disadvantage of this kind of research is related to its very advantage: Most biological systems operate at room temperature and

coordinate high-performance computing and education in the U.S.

For materials, "each agency is driven by different needs," says Aksay. "The Department of Energy, for example, is concerned about environmentally conscious materials processing. They are looking for materials and processes that are energy-conserving, nonpolluting, and recyclable. The Department of Defense, on the other hand, is interested in materials for weapons and for the Air Force. They are interested in airplanes that can lift off without a runway. The Navy wants materials that will protect their ships from corrosion. The National Institutes of Health want biomaterials that have medical applications."

Although the OSTP materials program will be included in the president's 1993 budget, the National Science Foundation has gotten a jump start in this initiative in the agency's 1992 budget. According to Jim Brown, division director of molecular biosciences at NSF, the agency expects an additional \$25 million for materials research in 1992 over its 1991 allocation of \$59 million. Of that new money, some \$7 million to \$9 million is slated for biomimicking-related research. In late March, the foundation sent out letters announcing the funds to 5,000 scientists. "We hoped to generate the development of collaborations for eventual proposal submissions," says Brown.

The same day that the OSTP made its announcement, the two senators from New Mexico, Democrat Jeff Bingaman and Republican Pete Domenici, introduced the Advanced Synthesis, Processing and Commercialization Act, which would provide \$475 million over the next five years for materials research partnerships among industry, academia, and federal laboratories. The bill allots an additional \$474 million for university-based efforts exclusively.

In late June, the Technology and Competitiveness Subcommittee of the House Committee on Science, Space, and Technology held a hearing focusing on ways to beef up materials science in the U.S. Among the issues the committee discussed with leaders in materials research were the status of materials technology, the consequences of foreign domination in this field, the question of involvement of federal labs in joint ventures with industry; and whether regulatory and safety concerns are impeding the development and commercialization of materials in the U.S.

Says a staffer on the subcommittee: "Materials are essential for the economic viability and competitiveness of American industry. If the U.S. loses out on this, which is the cornerstone for numerous other industries in the U.S., we are in trouble." And according to materials scientist Aksay, biomimicking will play a critical role in keeping America's edge. □

Heeding the Call of the Wild"

by Ivan Amato

in Research News Section

Science
253, 966-969 (30 August, 1991)

AMERICAN
ASSOCIATION FOR THE
ADVANCEMENT OF
SCIENCE

SCIENCE

30 AUGUST 1991

VOL. 253 ■ PAGES 941-1064

\$6.00



Heeding the Call of the Wild

Drawn by the engineering brilliance embodied in biological materials, a growing number of researchers and entrepreneurs are getting into the business of biomimicking

IF NATURE COULD FILE PATENTS ON THE miraculous materials it has devised, materials scientist Joseph Cappello and his fledgling San Diego company, Protein Polymer Technologies, Inc., might end up paying out a lot of royalties. Biology has two prior claims on the company's very first product—an adhesive for gluing living cells to Petri dishes and other surfaces. The adhesive, which mates a molecular motif from spider's silk with one from a common blood-plasma protein that binds living cells to one another, could make lab technicians' lives a lot easier, Cappello believes. And he isn't alone in his debt to nature. A biology-savvy community of materials scientists is pirating its ideas from the living world—so much so that if species other than our own could demand intellectual tribute, a host of academic and corporate researchers would have to start crediting their best inspirations to mollusks, insects, and even rodents.

Some members of the tribe—known as biomimetic researchers—are unabashedly striving to reverse-engineer the ancient biochemical secrets that enable marine mussels to make some of the strongest adhesives in all of the oceans. Others are attempting to mimic the chemical and engineering virtuosity embodied in the tough, hard shells of abalones. Still others are filching ideas about making lightweight composite materials from beetle exoskeletons. "Nature has these wonderful solutions and exquisite structures that are far beyond anything we have now," remarks Michael T. Marron, molecular biology program manager in the Office of Naval Research (ONR), which has funded biomimetic materials research since the mid-1980s.

Not every materials scientist is sanguine that the lessons of biology can be translated to high-volume industrial processes (see box on p. 968). But Marron and his peers have dedicated themselves to proving the skeptics wrong. They hope to push the performance envelope of materials—creating, say, more capable armor, extra-durable textiles, or lightweight composite materials for advanced aircraft—by imitating the molecular makeup, microscopic architecture, and manufacturing processes of biological materials.

As biomimetic researchers see it, much of their basic R&D has been done for them—

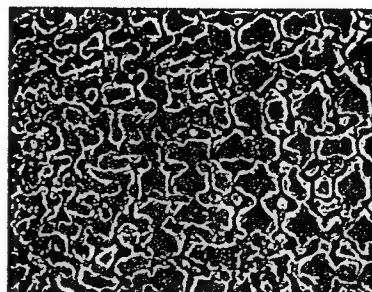
by the process of natural selection. "Nature has been developing materials for hundreds of millions of years," remarks Frederick L. Hedberg, program manager at the Air Force Office of Scientific Research (AFOSR), which oversees a modest biotechnology initiative that includes about \$500,000 for a handful of projects, among them

the development of paint-stripping enzymes, marine adhesives, and aircraft materials based on biological models. Over the eons, evolutionary selection pressure has put millions of biological materials through the test, leading to today's long catalogue of durable, strong, fracture-resistant, elastic, energy-absorbing, lubricating, self-repairing, self-assembling materials. Inferior materials went the way of unsuccessful species, notes George Haritos, associate director of AFOSR.

In that vast catalogue of biological materials, researchers have identified a common theme: They all reflect exquisitely precise control over composition and structure at every level, from atomic and molecular components through intermediate structures such as fibers and crystals up to visible objects such as tendons, bones, and skin. That multilevel control is a skill that materials scientists are eager to acquire. "Learning from these complicated hierarchical material systems is the goal," explains chemist Eric Baer of Case Western Reserve University.

As an example, Baer cites collagen, a protein-based material found in connective tissue, tendon, tooth, and bone. Collagen fibers are structured rather like cables made up of bunches of twisted wire strands, with each strand a protein molecule. Thanks to that structure, they are strong, flexible, and tough, since the breakage of individual strands or bunches leaves the structure as a whole intact. Materials scientists could build better properties into their products by imitating that sort of microscopic hierarchy, Baer says.

He isn't preaching slavish imitation, however. Biomimicry most often involves borrowing nature's design principles but execut-



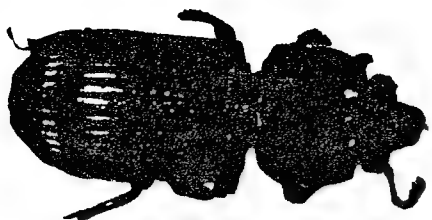
Crystal power. The porous, intricate structure of a sea urchin spine is actually a single crystal of calcite.

ing them in quite different materials (see opposite page). Stephen Gundersen of the University of Dayton Research Institute, for example, has been trying to imitate the multilayer construction that toughens the cuticle of the bess beetle, a biological composite turned up by one of Gundersen's colleagues during a literature search. But the

resulting biomimetic materials—possible prototypes for strong, failure-resistant, and lightweight aircraft composites—would be made of decidedly unbiological materials such as epoxy resin and carbon fibers. Similarly, Paul Calvert and his colleagues at the University of Arizona are using synthetic ceramics and polymers to mimic the intricate architecture of mineral and protein found in rat's tooth.

Translating such natural microstructures into lab-made materials, Gundersen, Calvert, and other biomimickers are finding, takes painstaking work. Standard laboratory techniques for making materials are ill-suited to giving researchers the kind of molecule-to-macromaterials control that results in something like collagen or insect cuticle. In making a material as simple as calcite (a form of calcium carbonate), for example, chemists and sea creatures couldn't be further apart at the moment. Chemists make calcite—the stuff of chalk and over-the-counter antacid pills—by precipitating it in bulk from a solution. The ions crystallize willy-nilly, most often into simple cubes. In sea urchins, a favorite object lesson for biomimicry researchers, calcite crystallization takes place within individual cells, which control the process to produce crystals with extremely intricate architectures: Witness the urchins' arrays of predator-deterring spines, each spine a single calcite crystal.

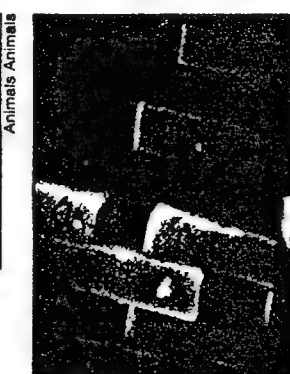
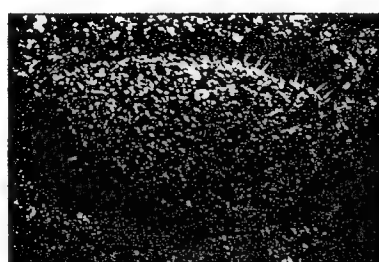
And that inspires biomimickers to learn not just what nature has done but how it does it, notes Stephen Mann, a chemist at the University of Bath who studies how organic structures resembling cell membranes can serve as precise templates for forming minerals. Mann, Ilhan Aksay and Mehmet Sarikaya



Sturdy as a VW bug? A bess beetle goes through life armored with an exoskeleton consisting of a protein matrix riddled with layers of chitin fibers, as shown in an electron micrograph (center).

The chitin layers are criss-crossed like the reinforcing plies in an old tire. The structure inspired a strong, lightweight composite (right) of epoxy polymer matrix with carbon reinforcing fibers.

Abalone architecture. In the tough inner layer of its shell (center right), an abalone lays down calcium carbonate crystals in a bricklike pattern with a mortar of organic polymers such as chitin. The resulting material is not only strong but also fracture resistant, since a fissure is forced to take a tortuous path through the layered structure. The synthetic analogue (far right) consists of multiple layers made of a boron-carbide/polypropylene mixture alternating with thinner layers of polypropylene.

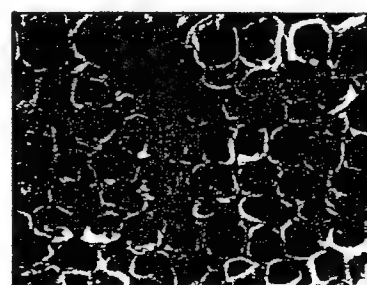


Rodent dentistry. Rats can gnaw through cans thanks to their tough, wear-resistant teeth. The secret lies in crossed rods of hydroxyapatite (a calcium compound that is also the main mineral in bone) embedded in

collagen, a biological polymer. The structure (center), has inspired a biomimetic material in which elongated particles of the mineral titania (TiO_2) are distributed through a polymer matrix (right).



Artificial wood grain. The cellular structure of Douglas fir wood (right) serves as a mold for depositing the ceramic precursor tetraethoxysilane. Water already within the cellulose of the cell walls hydrolyzes the precursor into a ceramic. Heating the preparation to 800 C gets rid of the cell material, leaving behind a cellular ceramic (far right)—strong but lighter than the monolithic material.



of the University of Washington, and others have been learning how to draw crystal precursors into tiny sacs or sheets made of phospholipids, the same kind of molecules that make up the membranes of living cells. The membranes serve as templates or, as Aksay prefers to call them, "nanoscale reaction vessels," for crystal growth. These scientists ultimately hope to use collections of such crystal-growing templates for controlling the size and shape of ceramic crystals and organizing them into technologically important forms—"elaborately structured ceramics, finely powdered catalysts, or single crystals of unusual shapes for electronic devices" are some of the possibilities Mann lists.

An important bonus, says Mann, is the fact that these tiny crystal factories work at normal temperatures and pressures. Indeed, that's typical for materials manufacturing modeled on biological processes. In contrast to the harsh conditions and toxic effluents of human manufacturing, living creatures make their own high-performance materials in aqueous environments, at low temperatures,

and under physiologically friendly conditions. As a result, Calvert points out, biomimetic material making could lead to more environmentally sound manufacturing methods.

Still, the minuscule reaction vessels in which living things make the hard parts of their anatomies often cook too slowly for the purposes of modern industry, says Dan Urry, a University of Alabama materials scientist whose 10 years of work with protein-based polymers led to his founding of Bioelastics Research, Ltd., in Birmingham 2 years ago. "The clam makes its shell over a long period of time," he points out. So after discovering the rules by which animals slowly make bones, teeth, shells, and spines, biomimetic ceramic researchers need to learn ways of speeding up these biominerization processes, he says. But Calvert suggests a simple remedy: using a feed solution more concentrated than the seawater from which marine animals extract the building blocks for their ceramics.

Researchers trying to harness biological polymer-making methods may face fewer hurdles in trying to scale up to industrial

production, notes synthetic chemist David Tirrell of the University of Massachusetts. For one thing, organisms, especially when working en masse, can churn out natural polymers such as proteins at a good clip. For another, the path has been smoothed by biotechnology researchers, who are already engineering bacteria to produce proteins. Now Tirrell and others are harnessing bacteria to make artificial materials—specialized biomimetic polymers. Equipped with genes for the chemical units of the novel materials, the bacteria act as minuscule polymer factories, working in parallel by the billions.

Two early fruits of this strategy are Protein Polymer Technologies' cell adhesion product and the candidate products of Urry's fledgling company. Urry and his colleagues are developing a series of epithelium-like materials with a molecular structure partially mimicking the elastin proteins found in blood vessels, lungs, and other tissues that repeatedly stretch and relax. The Navy is interested in trying out such materials as resorbable surgical implants; by providing a compliant layer between a patient's tissues, the implants might prevent the painful and sometimes dangerous "surgical adhesions" that often form after an operation.

The small scale of these ventures emphasizes how far research and development on biomimetic materials still has to go. For now, many researchers are driven more by the thrill of uncovering and trying to imitate the exquisite match between biological form and function than by the lure of the market. "These are early days yet," Mann stresses.

And like any field in its infancy, this one faces threats to its future. For example, Marron of the ONR fears industry may not be willing to face development periods that could last 5 years or more, poor prospects for short-term gains, and the lack of any guarantee that biomimetic products will ever catch on in a marketplace raised on conventional synthetic materials.

Marron and like-minded scientists are biased, of course, but they see the potential payoffs of their work as more than making up for such uncertainties. Pursued to its limit, the most enthusiastic of the tribe will argue, the approach could even expand the definition of materials beyond the inert substances the word now conjures. Julian Vincent, an expert in biological materials at the University of Reading, puts it this way: "If some of the techniques of nature could be exploited, self-designing, self-adjusting, and self-repairing structures could be developed." Vincent and his fellow biomimetic researchers will have to pull off heroic feats to justify this dream, but if they do, they will have imitated not just the structures but the very dynamism

No Easy Lessons in Nature

A researcher's role in life might be described as pushing the bounds of optimism. That doesn't mean, however, that the materials scientists who are trying to imitate the products and processes of nature think their task will be simple (see main text). But their efforts to be pragmatic strike Rustum Roy, a veteran materials scientist at Pennsylvania State University who is known for his outspokenness, as Pollyannaish. When it comes to the potential payoffs of biomimetic research, Roy also pushes the bounds—of pessimism. "Mimicking nature has the same chance as a snowball in hell," Roy told *Science*.

In a memo sent earlier this year to funding agencies—including the National Science Foundation, the Office of Naval Research, and the Air Force Office of Scientific Research (AFOSR)—and in other documents that have circulated throughout the materials science community, Roy has blasted the field. Exaggerated claims about the potential for mimicking biological materials and the technological promise it holds, he warns, can distort national goals for materials research.

Roy was prompted to write his memo by a research report and accompanying commentary that appeared in *Nature* on 24 January. He claimed the work—a biologically inspired experiment in which cadmium sulfide crystals were precipitated within a synthetic matrix—duplicated (without crediting) earlier studies published by him and others. The memo stressed that biomimetic materials researchers should scour the literature so as not to neglect crediting earlier researchers—a plea his fellow materials scientists mostly welcome. But Roy went on to question the concept of biomimetic materials as a whole.

As his complaint about credit shows, Roy himself has not been immune to the lure of biomimicking; in his ceramics research he has sometimes sought to duplicate natural mineralization processes. But those attempts, he says, taught him that the mild conditions biology uses—which enthusiasts tout as an added benefit of the biomimetic strategy—just don't allow materials to be synthesized fast enough for industrial purposes.

Many biomimickers acknowledge the need to find ways to accelerate natural processes, but they think it's too early to be discouraged. Besides, says AFOSR associate director George Haritos, "Nothing ventured, nothing gained."



Rustum Roy

■ I.A.

"Natureworks, Making Minerals the Biological Way"

by Elizabeth Pennisi

Science News
Feature Article

141-144, May 16, 1992.

"Natureworks, Making Minerals the Biological Way"

by Elizabeth Pennisi

Science News
Feature Article

141-144, May 16, 1992.



Natureworks

Making minerals the biological way

By ELIZABETH PENNISI

F

or beach lovers, the seashell symbolizes sand, surf and sun. Children quickly learn to tap its hidden talents. By putting one close to their ears, they can listen for that familiar ocean roar.

But for materials scientists, the seashell symbolizes something much more elusive. They cherish the seashell's integrity: Though made from simple stuff, mollusk shells are quite tough and strong. In fact, organisms create a whole host of hard materials, each suited to a particular purpose.

Out of seawater, oysters fashion pearls, the nautilus crafts chambered compartments, snails make intricately spiraled shells, sea urchins grow long, piercing spines and bacteria piece together internal compass needles that guide them to suitable environments (see sidebar, p.330). In a matter of hours, a hard, protective shell begins to encase a hen's developing egg. Vertebrates make bones that they repair and remodel throughout their lives and teeth sculpted to meet their particular grinding, gnashing, rip-

ping or munching needs.

Organisms fashion all these biomaterials with great precision and under conditions that would make many processing engineers envious. Over and over they demonstrate that whatever engineers can do, nature can do better and on a much finer scale. "We haven't tried the molecular engineering that exists in nature," says Arthur H. Heuer, a materials scientist at Case Western Reserve University in Cleveland.

As researchers strive to create and customize new materials, they come to appreciate the prolific artistry of biological systems. "The cells are really kind of amazing little workhorses," says David J. Fink, a chemical engineer with CollaTek, Inc., in Columbus, Ohio. Sometimes these cells work like master artists, taking years to create a finished product. Other times, they dash off a new layer of biomaterial quite quickly.

Slow growth yields layers of thin inorganic plates sandwiched in an even thinner organic matrix, a "glue" of proteins and other molecules, says Heuer. These layers lie parallel to the substrate upon which they form. With fast growth, the matrix and mineral build columns per-

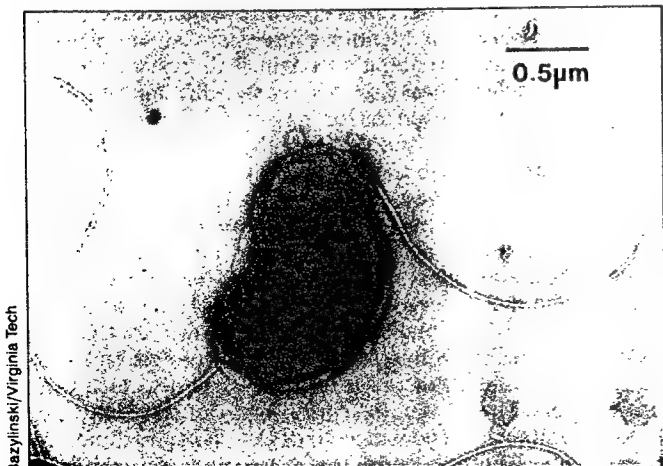
pendicular to the substrate surface. Each organism shapes this hard stuff while depositing it, often by incorporating building blocks into a hierarchical architecture that repeats itself from microscopic to macroscopic dimensions. Different levels of the hierarchy impart different properties to the finished material.

Biomaterials offer almost everything a materials scientist could want — without requiring any special processing environment. Seashells consist of calcium carbonate, the stuff of chalk. Yet "the toughness of the abalone and the pearl oyster is twice as high as any high-tech ceramics," says Mehmet Sarikaya, a materials scientist at the University of Washington in Seattle. "Also, the shells are tough and strong at the same time." Most synthetic materials fail because even tiny cracks grow, compromising the material's integrity. But in biomaterials, small cracks tend not to grow, says Arthur Veis, a biochemist at Northwestern University Dental School in Chicago.

By looking in great detail at the structure of a few biomaterials, Sarikaya, Veis and others have begun to fathom what makes the shell so tough and strong (SN: 12/9/89, p.383). At the March meeting of the American Physical Society in Indianapolis, Sarikaya described a recipe for mimicking nature that may help scientists improve synthetic materials. Eventually, he and others hope to learn enough of nature's secrets to duplicate what organisms seem to accomplish with so little effort.

"You know that a complex ceramic material got made somehow, so there's incentive to learning how that is done," says Fink. "The key is to be able to isolate and reconstruct what happens."

The secret lies in the way organisms



Electron micrograph shows bacterium with its chain of rectangular, membrane-enclosed magnetic particles, which help orient the microbe as it uses its two flagella to swim.

Bazylnski/Virginia Tech



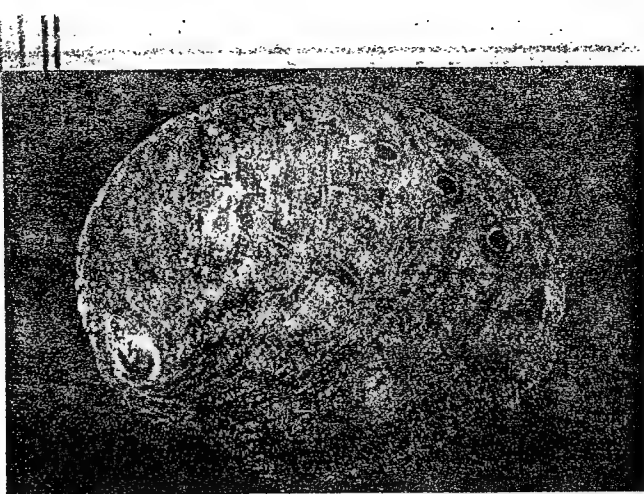
Photos: R. Tucker Abbott

put a mineral's molecules together. Organisms seem to rely on proteins and other large molecules to order inorganic molecules and to control the size and shape of the resulting crystal. Last month, geologists used the atomic force microscope to observe the formation of one such crystal, calcite (SN: 4/18/92, p.246). Other research groups are now working to determine which molecules direct that process.

"The kind of understanding that we will get from biology certainly will give us more insight into how to do a better job," says Heuer, who with several colleagues summarized current understanding of biominerization in the Feb. 28 SCIENCE. That understanding has developed only after years of effort.

S

ix years ago, while visiting the Olympic Peninsula in Washington, Sarikaya bought a red abalone shell from



a street vendor. The abalone survives for decades, adding about an inch a year to its armor until the shell measures about a foot across. The shell, a natural ceramic consisting of 95 percent inorganic material, fascinated Sarikaya. Until then, biologists had studied shell structure by first removing the inorganic component. Sarikaya wondered what he would see if he examined the shell from a materials scientist's perspective — with the inorganic part intact.

He and University of Washington colleague Ilhan A. Aksay observed that the shell consists of two layers. Calcite makes up a rough outer layer, while aragonite makes up the inorganic portion of the inner layer, called the nacre.

They expected abalone aragonite to resemble the aragonite found in metamorphic rock in Aragon, Spain. But the two versions looked quite different. This means that the abalone cell somehow controls crystal development — a feat that still eludes materials scientists, says Sarikaya.

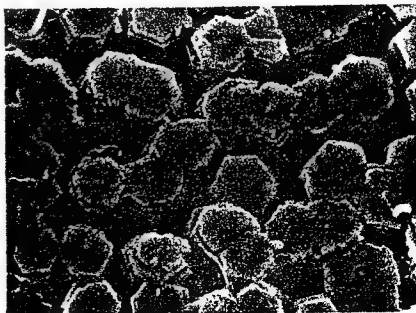
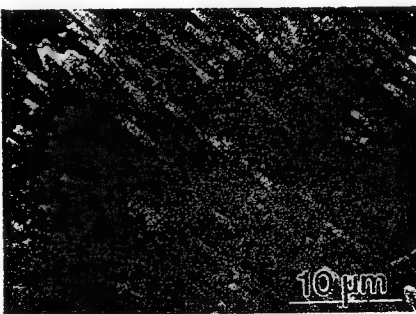
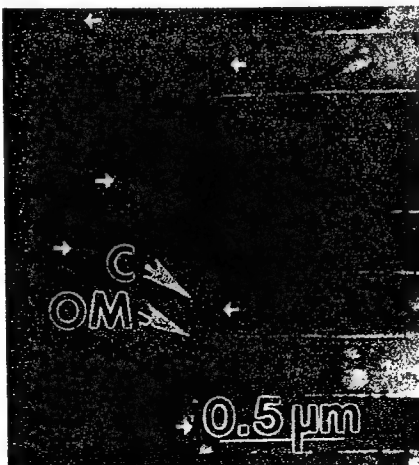
In abalone, they saw a brick-and-mortar configuration: stacked layers of

six-sided calcium carbonate bricks, with a thin organic "mortar" in between. Each brick layer is about 0.25 micron high, while the mortar ranges from 10 to 50 nanometers thick.

The mortar itself seems layered. Large, acidic, protein-like molecules surround a core, which probably consists of a tough carbohydrate substance called chitin. Giant soluble molecules form a top coating. The acidic molecules assemble themselves in such a way that they form a template for crystal growth, says Sarikaya.

To their surprise, the researchers also found this brick-and-mortar arrangement in the free-swimming chambered nautilus and in pearl oyster shells, even though these mollusks shape the material quite differently. "Although these organisms diverged [evolutionarily] from each other hundreds of millions of years ago, they have exactly the same structure at the nanometer level," says Sarikaya. The abalone makes flat, impact-resistant layers one-half-inch thick so that otters and other predators must work quite hard to crack the shell. The nautilus, a

Micrographs show side (top right) and face-on (bottom right) views of nacre's aragonite bricks, with a close-up of brick-and-mortar construction (below), made up of calcium (C) and organic matrix (OM).



Though quite different in appearance, the thick-shelled red abalone (near left) and the delicate nautilus (far left) build their shells in a similar way, one that materials scientists hope to mimic.

A biological orientation

Almost 800 years ago, Arabian sailors used a fish-shaped iron leaf suspended in water to guide their journeys northward on cloudy nights. But nature first harnessed Earth's magnetic field for navigation long before that. For millions of years, "magnetotactic" bacteria have made their own internal compasses.

Richard P. Blakemore, a microbiologist at the University of New Hampshire in Durham, discovered these organisms in mud samples almost 20 years ago, when he noticed that they tend to gather at the north end of water droplets. Since then, researchers have sought to understand how the bacteria make and use their microscopic compass needles. Recent interest in mimicking nature's handiwork has made some researchers wonder about recruiting these microbes to make magnetic particles for commercial applications.

"The bacteria are able to control the [particle's] size, shape and placement in the cells. This is submicron technology. We would like to know how they do it," says Richard B. Frankel, a biophysicist at California Polytechnic State University in San Luis Obispo.

Many kinds of bacteria make magnetic particles. Some make an iron sulfide crystal, such as greigite; others make magnetite, an iron oxide. Scientists are evaluating the phylogenetic relationship between these two types to understand better how — and how often — magnetic biomineratization evolved.

He thinks the magnetite makers collect iron and convert it to a stable iron oxide to create the magnetite crystal. But at least three species that have poor access to oxygen combine iron with sulfur instead, Frankel reported at the March 1991 meeting of the American Physical Society in Indianapolis. Iron accounts for 2 percent of the organism's total weight, making these bacteria "the most prodigious iron accumulators in the world," he says.

But each kind of bacterium customizes its particle, says Frankel. Some adopt cubic-octahedral arrangements, while others build six-sided or rectangular prisms. "This tells us that the mineralization part in these bacteria is very highly controlled," says Dennis A. Bazylinski at Virginia Polytechnic Institute and State University in Blacksburg.

"It's the equivalent of our producing bones and teeth. For a long time, people thought only higher organisms could do this [biomineratization]," says Frankel. But the closer researchers look, the more the microbial process seems to resemble that occurring in vertebrates. A membrane encases each particle, indicating that an organic component plays a key role in forming the inorganic

component. That membrane probably contains a protein that lures iron compounds out of solution and concentrates them inside the membrane.

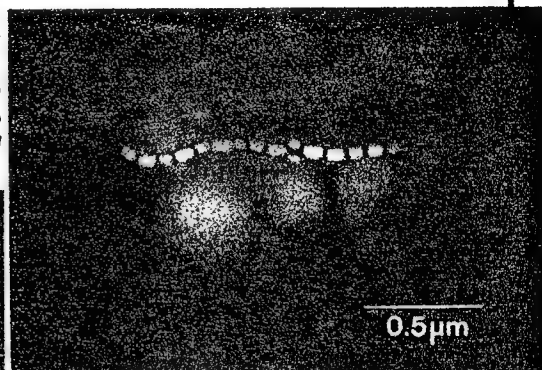
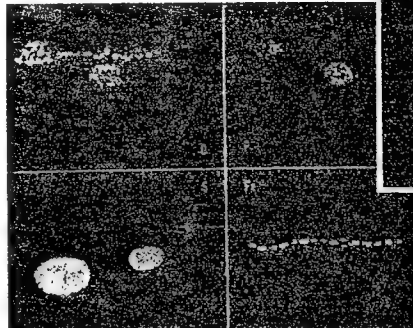
"What the membrane seems to do is not only regulate the deposition of the particle, but also control its position relative to the cell's other particles," says Frankel.

A microbe makes about 20 particles, each some 50 nanometers long — just big

them downward as well as poleward, Bazylinski explains. That downward tilt pulls them away from oxygen-rich surface water. Bazylinski and others suspect that when the bacteria sense favorable oxygen levels, they stop swimming.

Any bacterium with a genetic mutation that causes it to head the wrong way — such as south when it lives north of the equator — winds up in a hostile

Elemental X-ray map (below) shows how magnetotactic bacterium (right) concentrates iron (Fe) with oxygen (O) in magnetosomes and also packages up phosphorus (P) and sulfur (S).



Bazylinski/Virginia Tech

environment and dies. Experiments in which researchers placed bacteria in containers where the magnetic field was artificially reversed seem to bear out this idea. Within six weeks, the descendants switch the direction in which they swim, says Bazylinski. Thus, natural selection seems to segregate north-seekers in one hemisphere and south-seekers in the other.

But orientation may be a side benefit of particle formation, Bazylinski suggests. He believes some bacteria may oxidize the iron to get energy. In addition, iron sulfide particles may be important in the cycling of sulfur through the environment, he says.

Growing these bacteria in the lab has proved quite a challenge. To create the right environment, Bazylinski puts hydrogen sulfide in the bottom of a test tube, then seals it and lets the sulfide gas and the air spread out. Inside, an oxygen-sensitive strip turns pink, letting him know the location of the air-gas boundary. That's where he starts his colony of magnetotactic bacteria. "I've got six strains now," he says.

Most of the interest in these microbes stems from a fundamental amazement that such simple organisms can accomplish something as complex as magnetic orientation. So even though some scientists envision creating microbial factories to produce biomaterials, neither Frankel nor Bazylinski thinks bacterially grown magnetic particles will ever coat cassette or computer tapes. "You've got to grow hundreds of gallons of cells to make a little magnetite," Bazylinski says. "It's not worth it."

— E. Pennisi

relative of the octopus, keeps its highly curved shell paper-thin and builds in chambers filled with air to make its body buoyant. This shell holds up even at depths of 1,800 feet, where pressures reach 55 atmospheres.

Such different properties may arise from the way the organisms lay their bricks. Like many other biological systems, abalone nacre exists in a hierarchical arrangement, Sarikaya and several colleagues reported at last December's meeting of the Materials Research Society, held in Boston. The Seattle team determined this after looking at the orientation and makeup of each aragonite crystal — a 5-micron-wide hexagonal brick — with respect to its vertical and horizontal neighbors. They saw that the crystals are imperfect. Each brick contains "twinning" defects that divide the crystal into four to six wedges, and each wedge is the mirror image of the one next to it. The researchers find that twinning also exists on smaller and larger scales. Within each brick's wedges, 1- to 4-nanometer-wide regions twin with their neighbors; twinning also occurs between bricks.

"For the first time, we find a hierarchical structure for hard tissue in a biological material," Sarikaya told *SCIENCE News*. The twins are all touching each other, with no space in between. This hierarchy may confer abalone's toughness and strength. Sarikaya also thinks that similar defects somehow allow the nautilus to shape its developing shell and to make the highly curved chambers without sacrificing strength.

very small, discrete crystals that wind up confined within collagen fibrils, says Heuer.

As part of his 30-year quest to understand biomimetic mineralization, Northwestern's Veis thinks he has a crystallization protein in hand for dentin, which makes up the inner bulk of teeth. The protein has phosphorus-containing side chains that may act as templates for crystal formation. Different organisms seem to rely on different proteins. The protein in mollusks, for example, may use lots of amino acids with acidic side groups as templates. With these observations, some scientists have begun making their own template proteins, some of which cause crystal growth that resembles biomimetic crystallization, Veis notes.

To get a better grip on this process in other types of hard materials, Heuer, Arnold I. Caplan of Case Western Reserve and Jose L. Arias of the University of Chile in Santiago have chronicled the formation of chick eggshells. In about 20 hours, the cells in the lining of a hen's reproductive tract incorporate 2 grams of calcium carbonate into the rapidly forming shell. The process begins as egg white surrounds the yolk and then is cloaked by two fibrous membranes. The outer membrane seems critical to shell formation.

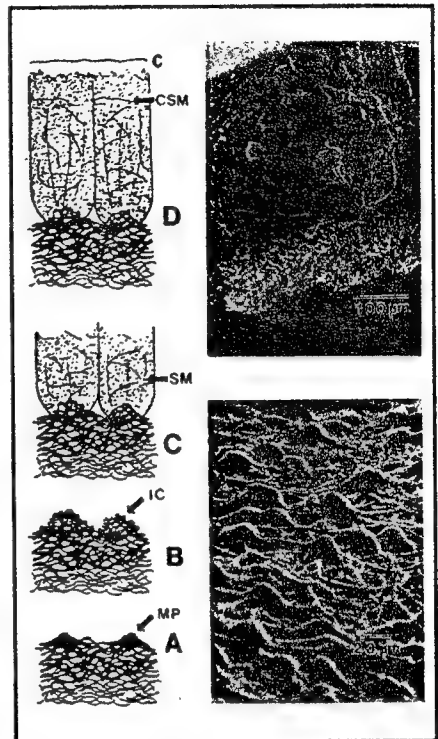
The scientists remove this outer membrane, which contains nodes of organic material thought to be the starting point for crystallization. Using the membrane as an organic film, they then examine details of mineralization.

Calcium carbonate crystals seem to grow up and out in all directions from the nodes. "When we grow calcium carbonate, it starts around the knobs but not between the knobs," says Fink, who is collaborating with the Cleveland group. As the crystals grow, organic molecules continue to assemble into the scaffolding that guides this growth.

In some experiments, the researchers added extracts from the organic matrix to the membrane preparation. The extract caused finer crystals to develop, they reported at last December's Materials Research Society meeting. They also think that at least one type of fibrous molecule, a collagen, may function by inhibiting biomimetic mineralization where it is not wanted. But like Sarikaya, they have yet to pin down the proteins that initiate mineral formation.

Sarikaya finds that by working backward, he can deduce the probable blueprint for the organic layer by the shape and structure of the crystals. On the basis of work done in part by Stephen Weiner at the Weizmann Institute of Science in Rehovot, Israel, and on his own observations of the aragonite microstructure, he hypothesizes that one type of protein, always folded the same way, is responsible and forms an orderly array. "They must organize in a pseudohexagonal fashion," he predicts.

Sarikaya has enlisted biologists to analyze the molecules, particularly proteins, present in this mortar. Once Clement E. Furlong, a geneticist at the University of Washington, knows which proteins are there, he can make antibodies for them. By labeling the antibodies, each of which attaches to a specific protein, Furlong can then determine which proteins wind up at the mineral-matrix interface and start the mineralization. Then he and microbiologist James T. Staley will genetically program bacteria



On an eggshell membrane's knobs (a, lower micrograph), calcium crystals form (b). Then a matrix (c) guides the building of calcite columns (d, top micrograph).

Now that they know what the abalone shell looks like on a microscopic scale, Sarikaya and his co-workers want to learn how the organism creates this hierarchy. Other researchers are investigating how other organisms build their bones, shells and teeth. "The key is that it's matrix-regulated," says Fink. "The matrix constrains the crystal in certain regions."

Proteins and carbohydrate-like molecules make up the organic mortar. These may set themselves up in an orderly formation such that one protein provides a flat surface. Chemical side groups stick out of the protein and cause dissolved molecules to precipitate and start forming a crystal. In teeth and mother-of-pearl, the matrix creates large biomimetic compartments where long crystals can form. But in bone, the compartments package the biomimetic in

to mass produce this protein. Once produced, the protein should provide a starting point for synthetic biomimetic mineralization, says Sarikaya.

This biological approach represents the cutting edge for materials scientists, who hope to duplicate, not just mimic, nature's artistry. "We want to use biology directly to do the chemical processing for us," says Paul D. Calvert, a materials scientist at the University of Arizona in Tucson. Someday, researchers may harness biomimetic mineralization to make entirely new materials with electrical, magnetic or optical properties as well as the sea-shell's toughness, adds Veis.

But achieving that goal is decades away. "People do not know where to start," says Sarikaya. "You need [experts in] five or six different disciplines to do significant research in this area."

"That's hard to do," he adds. □

Other News Clippings

To : Mehmet Sarikaya
from Keith Ritala

TECHNOLOGY

Nature at the Patent Office

Researchers look to fruit and nuts to find inspiration for the next generation of materials



MARYANN KOOPMAN

Horn of plenty: Biomimetics lifts ideas from potatoes, webs, mussels

The Stone Age. The Bronze Age. The Iron Age. The . . . Potato Age? OK, so it doesn't have quite the ring of its predecessors. But potatoes—not to mention beetle carapaces, iridescent blue mussels, abalone shells, apples and other natural bounty—could well form the basis of the next revolution in what the world is made of. Having taken petroleum-based plastics and fabrics just about as far as they can (and maybe farther than they should, as those who know the beauty of a polyester suit can attest), researchers in materials science are looking to nature for inspiration. The idea is not to fabricate bulletproof vests, tanks and jet wings out of lowly tubers, but rather to study natural products for clues to making materials stronger, more durable, more flexible. Their rallying cry: "Mussels are good for more than marinara sauce," as geneticist Ina Goldberg of Allied-Signal puts it.

She's not talking up the joys of *sauce moutarde*. Goldberg is trying to replicate the glue that allows these bivalves to stick to rocks in even the roughest seas. Chemists have yet to synthesize an adhesive that can withstand such conditions, but a glue that works in water would do wonders for building, to say nothing of dentistry. Last week Goldberg was in Boston, along with 3,800 other material boys and girls, for the annual meeting of the Materials

Research Society. That wasn't unusual—MRS meets in Boston every year. The surprise was that sprinkled among the usual metallurgists, ceramics mavens and plastics gurus were geneticists and zoologists. They had come to preach the wonders of biomimetics, the science of mimicking biological materials. "Nature comes up with solutions that are very novel and clever," says molecular biologist John Cordingley of the University of Wyoming. Its successes have survived millions of years of natural selection. Its failures are extinct. Says geneticist Steven Case of the University of Mississippi, "You can make something from scratch, or steal something that's already out there."

Even wood, edged out of skis and kitchen counters, may be poised for a comeback. Zoologist Julian Vincent of Reading University in England has created a fiber-glass-resin composite inspired by wood. It's lightweight but tough enough to absorb high-energy impacts from things like speeding bullets. Vincent thinks it would make a dandy material for bulletproof vests, now made from Kevlar. (Kevlar is derived from nylon, which comes from oil or coal.) Unlike Kevlar, this George's Wood can stop a bullet without bruising the body. Vincent is also studying the morphology of potatoes. He thinks that may serve as a model for a new kind of "hydraulic actua-

tor," a machine that uses fluid pressure to produce movement without friction-prone and easily snapped pistons.

Ever tried to shoot an abalone? Its shell is mostly chalk—calcium carbonate—which, as every school janitor knows, is not exactly shatterproof. The abalone shell's strength comes from the way the calcium is arranged. Crystals of chalk are held together with a sticky polymer that acts as glue. This brick-and-mortar arrangement is stronger and more resistant to fractures than solid chalk. Researchers at the University of Washington have imitated this design, with polypropylene for the glue, to produce an armor for tanks that resists impacts better than anything today. The army is testing it.

Silk alchemy: The rag trade long ago recognized the profits to be made from imitating silk, and now materials scientists have caught on. Silk still inside a spider dissolves in water—not a very useful property if the spider wants to catch flies on a rainy day. But spinning the silk into a web somehow makes it resist rain and snow like the toughest twine. Christopher Viney and colleagues at the University of Washington hope to perform the same sort of alchemy. The idea is to figure out how to make a fabric as strong and stiff as silk using simple water as the solvent (most fancy materials, like Kevlar, require a solution of red-hot sulfuric acid). Viney thinks this sort of silk-inspired synthetic could be useful as cables for suspension bridges or for protective clothing.

Other researchers have found inspiration for ultrastrong aircraft composites in the crisscrossing fibers of the common bess beetle's outer skeleton, and for the skin of tomorrow's aerospace plane (two hours from New York to Tokyo) in the light but strong covering of the horned beetle. At Reading, Vincent has been shattering walnuts—not for snacks but to understand what makes their shells so strong. Contrary to man's tendency to try to increase the strength of an object by adding more material, nature designs for strength by crafting a more complicated structure.

Don't expect nature to take out any patents just yet, though. "There's a long lag between taking some building block nature has perfected and using it in a different way to make something new," says Case. And some scientists, led by MRS president Rustum Roy of Pennsylvania State University, have blasted what they see as the exaggerated claims of biomimetics: Roy says natural materials take so long to synthesize that anything modeled on them just won't be practical on an industrial scale. Still, nature at least has what other inventors don't: a multi-million-year winning track record.

SHARON BEGLEY with
CAROLYN FRIDAY in Boston

Nature's materials

Unlocking the secrets to Charlotte's web

Ever since the first human cast an envious eye at a bird's ability to fly, people have looked to the natural world for ideas to imitate and shape to their own needs.

Today, armed with powerful computers, imaging devices and other advanced technologies, engineers and scientists from many disciplines have begun to take the closest look ever at how and why nature does what it does—at all levels, from individual molecules and cells to entire organisms.

That look will result in a revolution. Just as biotechnology is changing the way we fight disease and advance our health, another "bio" discipline—called biomimetics—will change the materials we use to work and live.

"We are on the brink of a materials revolution that will be on a par with the Iron Age and the Industrial Revolution," says Material Science and Engineering Professor Mehmet Sarikaya at the University of Washington (UW).

Biomimetics draws on some of the most powerful source material imaginable: hundreds of millions of years of evolution in which nature, slowly, painstakingly, has perfected or discarded creature after creature, adjusting and refining all life.

Even at its infancy, the field's possibilities are stunning:

- ships, aircraft, cars, clothes, buildings and yes, even picture windows made from materials that heal themselves when dented, hit, punctured or smashed;

- long bridges spanning waterways, suspended from glistening, lightweight cables no thicker than a garden hose yet possessing previously unknown strength, toughness and durability;

- thin, gel-like coatings that come in a tube and can be applied to human skin, giving police officers and fire-fighters instant protection from bullets and flames;

- ecologically ideal building con-

struction materials that can be instantly manufactured at room temperature from virtually whatever happens to be present in sufficient quantities—be it dirt, pine needles or chalk;

•and whole, complex chemical "factories" capable of rendering even the most toxic organic compounds harmless—located within the confines of a single organic cell.

How necessary is this revolution? Materials scientists say the world has taken petroleum-based plastics and fabrics about as far as possible.

"Basically, we're stuck," says Sarikaya, a pioneer in biomimetics. "The world needs lighter planes, lighter cars, lighter engines that can operate at much higher temperatures, and a host of other new materials. But today, we're still working with the ceramic materials we've had for the past 25 to 30 years, for example, and metals that have been around for 100 years."

UW Bioengineering Professor Christopher Viney half-jokingly puts it like this: "The challenge is to make things that are stiff and tough and have the right color and the right fatigue properties; that don't cost anything, won't hurt the environment and can be made out of beach sand."

Viney weaves his biomimetics research into lectures for incoming engineering students. First, he shows a slide of a helicopter made from Lego bricks. Next, he flashes up a slide of a tractor and crane, also built from Lego bricks. "I tell the students, 'Same Lego kit, exactly the same pieces. Different toys built from it.' And then I go on to explain that what nature offers us is a set of building blocks: 20 amino acids. And from these, all the proteins in the world—the millions of different types of proteins necessary to sustain every form of life on earth—are manufactured. But there are only 20 types of blocks in the starter kit. Just 20."

Viney and Sarikaya are among approximately 500 biomimeticians in the United States. The goal, the two agree, is not only to understand nature's

way of doing things, but to do nature one better—and perhaps faster. "The traditionalists say, 'If nature makes it, what's new?'" says Viney. "That's why I am very careful to say, we are selecting what we learn from nature—not trying to copy it exactly, because there would be no point in that."

Currently, Viney's main research interest is liquid crystals—substances suspended in a state somewhere between a solid crystal and a liquid. Millions of us wear artificial liquid crystals on our wrists: they make up the display screen for digital watches.

While liquid crystals may be commonplace in a watch, Viney and his colleagues surprised the scientific world when they wrote that silk secreted by silkworms and spiders owes its exceptional strength to temporarily becoming a liquid crystal. The team found that as the golden orb weaver spider secretes its webbing, molecules in the droplets align themselves in rod-like structures—passing through an interim phase in which they take on a semi-ordered structure. The result is a material that, when solidified, can support far more weight for its size than steel.

By understanding how spider silk works, Viney believes we may someday use this information to improve bulletproof vests and build stronger suspension bridges, for instance.

Viney and others involved in biomimetics often speak of "hierarchical microstructures." The same components can be reassembled again and again in things that may be very different from one another.

How different? As unlike, say, as multi-legged spiders and slimy slugs. Earlier this year, Viney, Bioengineering and Biostructure Professor Pedro Verdugo and UW graduate student Anne Huber became the first to report that there's much more to the mucus highway secreted by common banana slugs than previously thought.

Though mucus research lacks mass appeal, it can shed light on a host of human health problems, including cystic

L. G. Blanchard

fibrosis and other abnormalities in the reproductive and digestive tracts. To Viney and Verdugo, mucus is one of nature's most remarkable substances. Slugs use it not only for transportation, but also for protection—enabling them, for instance, to creep harmlessly along the edge of a razor blade.

Verdugo, who has studied mucus in a variety of species for nearly two decades, and other researchers had thought that the microstructure of mucus was much like a randomly tangled web of spaghetti—it's consistency dependent on the extent of tangling (the more tangled, the thicker). However, once released from the small granules in which it is stored inside the cell, slug mucus can swell up to 50 times its initial volume—so fast that researchers use the term “explosive.” In fact, mucus granules can expand from 10 to 500 microns in 15 to 20 milliseconds. And this had researchers stumped: How can something expand so fast, so efficiently, if it is as disorganized as a bowl of tangled spaghetti?

Now, much more is known, thanks to Viney and colleagues. Earlier this year, they showed that slug mucus is highly organized, not random. They found that before secretion, mucus molecules are stored in tightly packed, accordion-like bunches like jack-in-the-boxes. When secreted, the molecules—polymers with all the characteristics of liquid crystals—absorb water, expanding at high rates without involving high amounts of energy.

The tremendous range of expansion and condensation is what makes mucus one of nature's “very best inventions,” says Verdugo. Understanding the structure is the key to the design of new and highly efficient polymer gels. “Now we have a gateway to understanding how to develop new technology. We have the blueprints nature used, and we can re-engineer them in our own land.”

While much research remains, Verdugo, Viney and others foresee many potential inventions coming from biomimetic materials based on mucus. For example, they might foster new drug delivery systems for cancer patients, pollutant traps in sewage treatment plants, and water-based lubricants. And if mucus makes such an ideal highway for slugs, light rail might someday be

For its size, spider silk is stronger than steel

The Image Bank/Franklin Wagner

replaced by slime rail.

Another gastropod, the red abalone, absorbs much of Sarikaya's interest. Over the course of its life, this sea-dwelling creature produces an impact-resistant shell so hard it can be run over by a truck without breaking. But if the shell does get damaged in the natural world, it heals itself—and later, when its occupant dies, the shell readily biodegrades. Finally, the abalone and similar organisms manufacture their shells at sea-water temperature using a readily available ingredient: calcium carbonate, a.k.a. chalk.

Broken down into components, abalone shells are relatively simple, explains Sarikaya, much like a single Lego brick. When assembled, however, the components—ranging in size from molecules to millimeters—function together to provide a material well worth mimicking: one that incorporates superb properties of toughness and strength.

Using powerful electron microscopes, Sarikaya found beneath the shell's outer portion a section consisting of extremely thin layers of laminate. It's here that nature's masons are at work, as flat bricks of calcium carbonate are set off from one another in typical brick-wall fashion. The “mortar” holding them together consists of small amounts of organic matter, mostly proteins and sugars.

Sarikaya and colleagues tested the abalone's composite material and found that it has greater toughness and strength than conventional ceramics alone owing to its brick architecture and the organic mortar. The next step is to unlock how

the mollusk produces the proteins and sugar molecules that make up the mortar. Then they must discover how this material finds its way through the watery environment within the shell to the correct layer—and, once there, assembles itself exactly where it is needed.

To help break the secrets, Ilhan Aksay, at Princeton, and Sarikaya enlisted the help of genetic engineers. The team hopes to invent genetically engineered organic “templates.” With these plans, Sarikaya thinks he can grow technological materials the same way as an abalone produces its shell.

There even is the possibility of duplicating, perhaps using different materials, the abalone shell's ability to self-heal. Does this mean it could never be destroyed? Not to worry, says Sarikaya; science also will come up with a way to switch this capability on and off.

This concept and other as-yet-unanswered questions about biomimetics lead even its chief proponents to caution that the future is not now. But it is coming, and at a far faster speed than it took technology to travel from Kitty Hawk to Cape Canaveral.

Ah, but if we are going to take things from nature, how can we be sure nature is right? “You can't be,” answers Viney. “Nature has some ideas. That is, nature has optimized everything very nicely for what nature has to do. But this isn't always ‘right’ for biomimicking.”

Feathers not only help birds fly, Viney wrote a year ago, they also provide protection from bumps and bruises.

“Clearly there is a useful suggestion here. But the materials engineer who hurries to cover his automobile with feathers might be better off wearing them himself.”

About the author

L.G. Blanchard covers engineering for the UW Office of News and Information. He lives on Vashon Island, Washington.

Adapted and reprinted with permission from “Doing what comes naturally,” Columns, The University of Washington Alumni Magazine (Sept. 1993).

Tecnologia/I nuovi materiali

Su licenza di Dio

Tessuti in seta di ragno sintetica, guanti di scarafaggio, aerei in similcorno di rinoceronte: così gli scienziati cercano di copiare la natura.

Apparentemente non c'è molto in comune tra l'aereo invisibile usato dall'aviazione americana contro Saddam Hussein e un rinoceronte africano. Ma è una falsa impressione. C'è una parte del rinoceronte che di analogie con l'aereo invisibile ne ha tantissime: il corno. O meglio, la sua struttura. Come hanno recentemente scoperto i ricercatori che si occupano di creare nuovi materiali, le ali dell'aereo invisibile hanno una struttura quasi identica sia nell'aspetto che per caratteristiche a quella del tessuto osseo di cui è fatto il corno dei rinoceronti. Con una sola differenza: che i corni del rinoceronte sono in grado di autoripararsi in caso di rottura, evento abbastanza frequente tra questi grandi animali, che lo usano spesso per duellare tra loro. Mentre se si rompono le ali l'aereo invisibile cade. In futuro, tuttavia, gli scienziati sperano di riuscire a strappare il segreto dei corni autoriparanti alla natura. E di costruire così anche automobili, aerei e treni in grado di aggiustarsi da soli.

Come testimonia l'autorevole settima-

nale statunitense *Time*, non è questo il solo «brevetto» che la scienza cerca di rubare al creato. Gli scienziati di una particolare branca della biochimica, ribattezzata «biomimica» proprio perché il suo scopo è copiare la natura, stanno anche cercando di scoprire come fanno a essere così taglienti i denti dei topi, così elastiche le ragnatele, così appiccicosse le secrezioni delle cozze e così dure la corazzatura di alcuni insetti. Obiet-

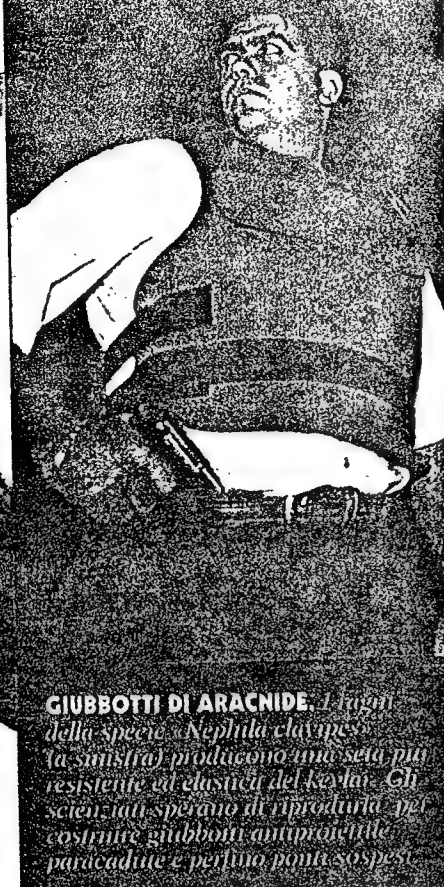
tivo: aprire la strada a una serie di nuovi materiali non più basati, come il nylon e la plastica, sul petrolio, ma sulle proteine prodotte dagli organismi viventi.

Raffinata da più di 4 miliardi di anni di evoluzione, la chimica delle proteine può in effetti insegnarci molte cose. Per produrre per esempio un tessuto come il kevlar, oggi l'uomo ha bisogno di grandi vasche di acido solforico concentrato e mantenuto ad alta pressione. I ragni della specie *Nephila clavipes*, studiati dal biologo americano Randy Lewis dell'università del Wyoming, sono capaci di produrre nella loro pancia una seta che non ha niente da invidiare al kevlar usando l'acqua come solvente e trasformando, non si sa bene come, proteine solubili in fibre insolubili. Lewis, che alleva decine di questi grossi ragni rosso-dorati ed estrae da ciascuno di loro, con una speciale macchi-

ALI CON LE CORNA.

Le corna dei rinoceronti (qui sono) hanno una struttura simile a quella delle ali dell'aereo invisibile (a destra). Con materiali simili si potranno costruire forse auto che si riparano da sole.





GIUBBOTTI DI ARACHIDE. I raggi della specie *Nephila clavipes* (a sinistra) producono una seta più resistente ed elastica del kevlar. Gli scienziati sperano di riprodurla per costruire giubbotti antiproiettile, paracadute e perfino ponti sospesi.

na, fino a 320 metri al giorno di seta per ragnatele, è convinto che un tessuto fatto con seta di ragni sarebbe più forte dell'acciaio, più elastico del nylon e più resistente del kevlar. Se si riuscisse a riprodurlo sinteticamente, un simile tessuto potrebbe servire per esempio per fabbricare giubbotti antiproiettile molto più sicuri di quelli attualmente usati, paracadute e perfino cavi per ponti sospesi. Mentre con la seta nella fase ancora liquida, come è nella pancia del ragni, si potrebbe fare, secondo Christopher Viney, un ricercatore dell'università di Washington, qualcosa di molto simile ai cristalli liquidi degli schermi digitali.

Un altro segreto della natura che ha attirato l'attenzione degli scienziati è la durissima madreperla di alcune conchiglie, le aliotide, più note come orecchie di mare. Vista al microscopio la madreperla delle orecchie di mare rivela una struttura simile a quella di alcune pareti rocciose stratificate. Gli strati di madreperla sono però fatti di carbonato di calcio estratto dall'acqua di mare, mentre il collante tra i vari strati è una miscela di proteine e zuccheri. «Gli ingre-

dienti in sé non sono niente di che», commenta Ilhan Aksay, della Princeton University, «ma la conchiglia è più dura delle più avanzate superceramiche costruite dall'uomo». Aksay e i suoi assistenti stanno pensando di copiare la struttura delle orecchie di mare utilizzando al posto del carbonato di calcio materiali come l'ossido di alluminio e il carburo di silicio che sono molto resistenti al calore ma tendono a rompersi facilmente. Sperando che i nuovi materiali accoppino la resistenza al calore alla durezza delle orecchie di mare.

Nei laboratori militari americani di Natick, nel Massachusetts, si sta studiando anche una proteina estratta dalla corazzza degli scarafaggi. Secondo David Kaplan, un ricercatore del centro, questa proteina, chiamata resilina, ha la proprietà, a differenza di altre gomme artificiali, di non gonfiarsi a contatto con sol-



DURA COME ROCCIA. La madreperla di una conchiglia (l'orecchia di mare a sinistra) ha la sua struttura al microscopio, e più resistente di qualsiasi ceramica artificiale.

venti organici. Guanti fatti con resina sarebbero insomma l'ideale per soldati che lavorano nei depositi di carburante o per addetti ai distributori di benzina.

Paul Calvert, infine, un ricercatore dell'università dell'Arizona, è alle prese con i denti dei topi. Il suo problema è quello di trovare qualcosa per eliminare il tallone d'Achille della ceramica: la fragilità agli urti. E per farlo Calvert pensa adesso di riprodurre, usando ossido di titanio, la struttura di una ceramica naturale resistentissima: come è appunto quella dei denti di topo.

Colture cellulari

In genere gli scienziati tendono a studiare la struttura dei materiali naturali per poterla poi riprodurre sinteticamente. Utilizzare direttamente questi materiali pone infatti non pochi problemi. Allevare milioni di rinoceronti è un obiettivo poco proponibile visto che sembra difficile tenerne in vita anche solo poche centinaia in Africa. Mentre per fare anche una sola cravatta in seta di ragni naturali ci vorrebbero almeno 500 ragni. «È probabilmente molti sarebbero troppo schizzinosi per indossarla», scherza John Fosline, uno zoologo dell'università della British Columbia. Senza contare che c'è una proprietà della seta di ragni che la renderebbe poco adatta per farne cravatte: tende a restringersi fino al 50 per cento in ambienti molto umidi.

Un esempio di come in futuro l'uomo potrà copiare la natura per fare nuovi materiali è una sostanza brevettata e fabbricata da una piccola azienda di San Diego, in California: la Protein Polymer Technologies. Il prodotto messo a punto dalla società californiana è un ibrido, composto di una proteina estratta dal baco da seta e da fibronectina, una proteina presente nel sangue che favorisce l'adesività delle cellule. Stesa su un foglio di plastica la nuova sostanza permette di creare un ambiente ideale per culture di cellule in laboratorio.

L'ibrido della Protein Polymer Technologies è il solo prodotto della biomimica già arrivato sul mercato. Fino a oggi la tecnologia ha aiutato la biologia molto più di quanto la biomimica abbia dato una mano ai tecnologi. Ma, sostengono gli esperti, le cose stanno per cambiare.

PROCESSO A MUCCOLI/ Comunità o lager?

RIVELAZIONI

TangentEni:
la verità su
40 anni di
soldi ai partiti



Tutte le
confessioni di
Larini su Craxi
e Martelli.



E le ultime
su Greganti,
Prandini,
Sbardella...

"UCCIDEVA COSÌ"
ESCLUSIVO:
PARLA IL PENTITO
CHE HA FATTO
CATTURARE RIINA

Bella
scatenata

L. 3.500

Sommario

Panorama 1405
Arnoldo Mondadori Editore

In copertina: fotografie di Gerbasi
e Granata Press Service



SILVANO LARINI. Tutti i verbali dell'ex latitante (p. 40).



GIULIANO AMATO. Gli italiani non lo amano più (p. 52).



CLAUDIA SCHIFFER. Top model dietro le quinte (p. 134).



BORIS ELTSIN. Dura battaglia per il potere (p. 90).

3 Forattini

ESCLUSIVO

- 8 «Riina lo l'accusa»
- 9 Identikit
- 11 Una first lady per il boss
- 12 Antimafia all'erta!
- 13 Mafia/lì giallo di Pino Greco. Lupara per due
- 14 San Giuseppe, salvaci tu

PRIMO PIANO

- 36 Fondi neri. TangentEni
- 39 Parla l'amministratore. Benvenuta la bufera
- 40 Le confessioni di Larini. Ciclone Silvano
- 42 Quando Florio pagava
- 43 Greganti. Quando il Signor G scriveva a Vienna
- 45 Anas/Le accuse a Prandini. Compra l'hotel, farai strada
- 46 Giù di sella, Fantini
- 46 Cirino spento
- 48 Mani pulite a Roma. All'università della mazzetta
- 50 Diari dal carcere/Carra. A San Vittore e ritorno

ITALIA

- 52 Governo. Processo ad Amato
- 54 L'ora dell'addio
- 56 Cossiga contro Scalfaro. Li chiamavano Trinità

- 58 Referendum/Cresce il fronte anti-Segni. Là dove il No suona
- 59 Pochi posson bastare
- 60 Indiscreto
- 61 Tipi italiani, di Paolo Guzzanti
- 62 Caso Muccilli. Santo e picchiatore
- 63 San Patrignano. Con i figli nel canile
- 69 Cooperazione. Quel piano vale un Perù
- 69 Immigrati. Stranieri o caporali?

IL CASO

- 70 È giusto tornare alla «cura maledetta»? Elettroshock
- 72 Come un pugno alla radio

INCHIESTA

- 74 Televisione/Quando i dibattiti si trasformano in pollai. Chicchitivù!
- 77 America. Video su misura
- 78 Gioco al massacro, di Furio Colombo

ESTERI

- 84 Francia/Verso le elezioni politiche. Guai ai vincitori
- 85 Dumas il siriano
- 87 Gran Bretagna. Carlo il rustico
- 88 Vaticano. Assolvete quel papa

SPECIALE ESTERI

- 90 Russia/I nostalgici alla riscossa. Ombre rosse
- 93 Russia. Attenti, c'è un nuovo Baffone, di Ilya Levin

CULTURA

- 108 Speciale/Grandi mostre di primavera. Marcel, istruzioni per l'uso, di Arturo Schwarz
- 113 Eredi o no
- 114 Parigi. Concerto per due
- 117 Matissemania
- 118 Barcellona/L'anno di Joan Miró. Cinquecento pezzi facili

SPETTACOLI

- 122 Registi/Perché i giovani battono i maestri. Film generation
- 123 Giovani registi? Carini, ma...
- 127 Paolo Rossi torna al teatro. Giullare col fiasco
- 128 L'idea? È nata all'osteria, di Paolo Rossi

SOCIETÀ'

- 134 Moda. Missione passerelle pulite
- 143 La neoparsimonia. M'accontento di poco
- 146 Naomi Campbell, intervista

SCIENZA

- 154 Epidemiologia/L'imprevisto ritorno di tre flagelli.
 - Mali da poveri
- 157 Virus viaggiatore
- 158 I nuovi materiali. Su licenza di Dio
- 162 Astronomia. Satellite della vita

MASS MEDIA

- 167 Pintor abbandona. Disenso Manifesto
- 170 Il primo seno di Tina

ECONOMIA

- 172 Verso il modello tedesco. Banca padrona
- 177 Gruppo Ferruzzi. Addio, provetta crudele
- 183 Lega delle cooperative. Pizza a colazione
- 187 Scuola/Le proposte della Confindustria. Operai con laurea, intervista con Giancarlo Lombardi
- 191 Recessione in Germania. Se fonde la locomotiva
- 193 Cosa rischia l'Italia

RUBRICHE

- 19 Il Cartellone
- 83 Diclamoci tutto, di Biagi
- 101 Turno di notte, di Furio Colombo
- 151 Il lato debole, di Cederna
- 199 Stile libero
- 218 Periscopio

FEBRUARY 1994

IEEE

the quarterly magazine
for up-and-coming engineers

Current status on:
**the Sea Moss Microship,
multimedia, FPGAs,**

THE INSTITUTE OF ELECTRICAL AND ELECTRONICS ENGINEERS, INC.

Nature's materials

Unlocking the secrets to Charlotte's web

Ever since the first human cast an envious eye at a bird's ability to fly, people have looked to the natural world for ideas to imitate and shape to their own needs.

Today, armed with powerful computers, imaging devices and other advanced technologies, engineers and scientists from many disciplines have begun to take the closest look ever at how and why nature does what it does—at all levels, from individual molecules and cells to entire organisms.

That look will result in a revolution. Just as biotechnology is changing the way we fight disease and advance our health, another "bio" discipline—called biomimetics—will change the materials we use to work and live.

"We are on the brink of a materials revolution that will be on a par with the Iron Age and the Industrial Revolution," says Material Science and Engineering Professor Mehmet Sarikaya at the University of Washington (UW).

Biomimetics draws on some of the most powerful source material imaginable: hundreds of millions of years of evolution in which nature, slowly, painstakingly, has perfected or discarded creature after creature, adjusting and refining all life.

Even at its infancy, the field's possibilities are stunning:

- ships, aircraft, cars, clothes, buildings and yes, even picture windows made from materials that heal themselves when dented, hit, punctured or smashed;

- long bridges spanning waterways, suspended from glistening, lightweight cables no thicker than a garden hose yet possessing previously unknown strength, toughness and durability;

- thin, gel-like coatings that come in a tube and can be applied to human skin, giving police officers and fire-fighters instant protection from bullets and flames;

- ecologically ideal building con-

struction materials that can be instantly manufactured at room temperature from virtually whatever happens to be present in sufficient quantities—be it dirt, pine needles or chalk;

- and whole, complex chemical "factories" capable of rendering even the most toxic organic compounds harmless—located within the confines of a single organic cell.

How necessary is this revolution? Materials scientists say the world has taken petroleum-based plastics and fabrics about as far as possible.

"Basically, we're stuck," says Sarikaya, a pioneer in biomimetics. "The world needs lighter planes, lighter cars, lighter engines that can operate at much higher temperatures, and a host of other new materials. But today, we're still working with the ceramic materials we've had for the past 25 to 30 years, for example, and metals that have been around for 100 years."

UW Bioengineering Professor Christopher Viney half-jokingly puts it like this: "The challenge is to make things that are stiff and tough and have the right color and the right fatigue properties, that don't cost anything, won't hurt the environment and can be made out of beach sand."

Viney weaves his biomimetics research into lectures for incoming engineering students. First, he shows a slide of a helicopter made from Lego bricks. Next, he flashes up a slide of a tractor and crane, also built from Lego bricks. "I tell the students, 'Same Lego kit, exactly the same pieces. Different toys built from it.' And then I go on to explain that what nature offers us is a set of building blocks: 20 amino acids. And from these, all the proteins in the world—the millions of different types of proteins necessary to sustain every form of life on earth—are manufactured. But there are only 20 types of blocks in the starter kit. Just 20."

Viney and Sarikaya are among approximately 500 biomimeticists in the United States. The goal, the two agree, is not only to understand nature's

way of doing things, but to do nature one better—and perhaps faster. "The traditionalists say, 'If nature makes it, what's new?'" says Viney. "That's why I am very careful to say, we are selecting what we learn from nature—not trying to copy it exactly, because there would be no point in that."

Currently, Viney's main research interest is liquid crystals—substances suspended in a state somewhere between a solid crystal and a liquid. Millions of us wear artificial liquid crystals on our wrists: they make up the display screen for digital watches.

While liquid crystals may be commonplace in a watch, Viney and his colleagues surprised the scientific world when they wrote that silk secreted by silkworms and spiders owes its exceptional strength to temporarily becoming a liquid crystal. The team found that as the golden orb weaver spider secretes its webbing, molecules in the droplets align themselves in rod-like structures—passing through an interim phase in which they take on a semi-ordered structure. The result is a material that, when solidified, can support far more weight for its size than steel.

By understanding how spider silk works, Viney believes we may someday use this information to improve bulletproof vests and build stronger suspension bridges, for instance.

Viney and others involved in biomimetics often speak of "hierarchical microstructures." The same components can be reassembled again and again in things that may be very different from one another.

How different? As unlike, say, as multi-legged spiders and slimy slugs. Earlier this year, Viney, Bioengineering and Biostructure Professor Pedro Verdugo and UW graduate student Anne Huber became the first to report that there's much more to the mucus highway secreted by common banana slugs than previously thought.

Though mucus research lacks mass appeal, it can shed light on a host of human health problems, including cystic

L. G. Blanchard

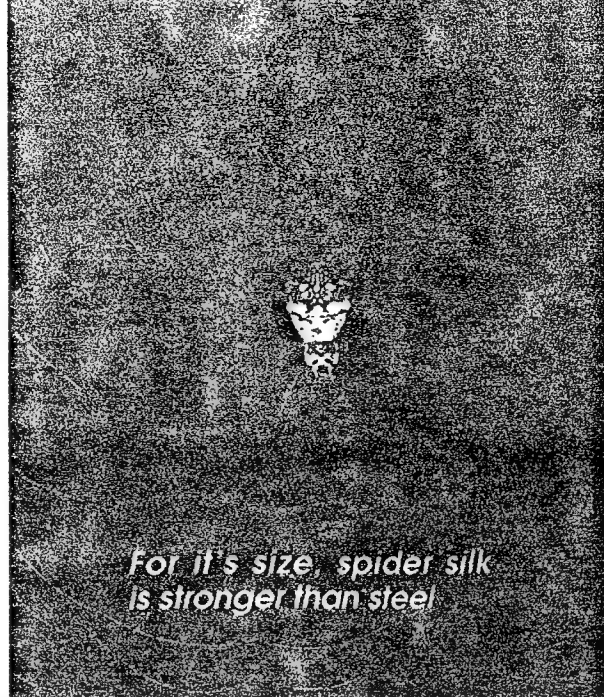
fibrosis and other abnormalities in the reproductive and digestive tracts. To Viney and Verdugo, mucus is one of nature's most remarkable substances. Slugs use it not only for transportation, but also for protection—enabling them, for instance, to creep harmlessly along the edge of a razor blade.

Verdugo, who has studied mucus in a variety of species for nearly two decades, and other researchers had thought that the microstructure of mucus was much like a randomly tangled web of spaghetti—it's consistency dependent on the extent of tangling (the more tangled, the thicker). However, once released from the small granules in which it is stored inside the cell, slug mucus can swell up to 50 times its initial volume—so fast that researchers use the term “explosive.” In fact, mucus granules can expand from 10 to 500 microns in 15 to 20 milliseconds. And this had researchers stumped: How can something expand so fast, so efficiently, if it is as disorganized as a bowl of tangled spaghetti?

Now, much more is known, thanks to Viney and colleagues. Earlier this year, they showed that slug mucus is highly organized, not random. They found that before secretion, mucus molecules are stored in tightly packed, accordion-like bunches like jack-in-the-boxes. When secreted, the molecules—polymers with all the characteristics of liquid crystals—absorb water, expanding at high rates without involving high amounts of energy.

The tremendous range of expansion and condensation is what makes mucus one of nature's “very best inventions,” says Verdugo. Understanding the structure is the key to the design of new and highly efficient polymer gels. “Now we have a gateway to understanding how to develop new technology. We have the blueprints nature used, and we can re-engineer them in our own land.”

While much research remains, Verdugo, Viney and others foresee many potential inventions coming from biomimetic materials based on mucus. For example, they might foster new drug delivery systems for cancer patients, pollutant traps in sewage treatment plants, and water-based lubricants. And if mucus makes such an ideal highway for slugs, light rail might someday be



For its size, spider silk is stronger than steel

The Image Bank/Franklin Wagner

replaced by slime rail.

Another gastropod, the red abalone, absorbs much of Sarikaya's interest. Over the course of its life, this sea-dwelling creature produces an impact-resistant shell so hard it can be run over by a truck without breaking. But if the shell does get damaged in the natural world, it heals itself—and later, when its occupant dies, the shell readily biodegrades. Finally, the abalone and similar organisms manufacture their shells at sea-water temperature using a readily available ingredient: calcium carbonate, a.k.a. chalk.

Broken down into components, abalone shells are relatively simple, explains Sarikaya, much like a single Lego brick. When assembled, however, the components—ranging in size from molecules to millimeters—function together to provide a material well worth mimicking: one that incorporates superb properties of toughness and strength.

Using powerful electron microscopes, Sarikaya found beneath the shell's outer portion a section consisting of extremely thin layers of laminate. It's here that nature's masons are at work, as flat bricks of calcium carbonate are set off from one another in typical brick-wall fashion. The “mortar” holding them together consists of small amounts of organic matter, mostly proteins and sugars.

Sarikaya and colleagues tested the abalone's composite material and found that it has greater toughness and strength than conventional ceramics alone owing to its brick architecture and the organic mortar. The next step is to unlock how

the mollusk produces the proteins and sugar molecules that make up the mortar. Then they must discover how this material finds its way through the watery environment within the shell to the correct layer—and, once there, assembles itself exactly where it is needed.

To help break the secrets, İlhan Aksay, at Princeton, and Sarikaya enlisted the help of genetic engineers. The team hopes to invent genetically engineered organic “templates.” With these plans, Sarikaya thinks he can grow technological materials the same way as an abalone produces its shell.

There even is the possibility of duplicating, perhaps using different materials, the abalone shell's ability to self-heal. Does this mean it could never be destroyed? Not to worry, says Sarikaya; science also will come up with a way to switch this capability on and off.

This concept and other as-yet-unanswered questions about biomimetics lead even its chief proponents to caution that the future is not now. But it is coming, and at a far faster speed than it took technology to travel from Kitty Hawk to Cape Canaveral.

Ah, but if we are going to take things from nature, how can we be sure nature is right? “You can't be,” answers Viney. “Nature has some ideas. That is, nature has optimized everything very nicely for what nature has to do. But this isn't always ‘right’ for biomimicking.”

Feathers not only help birds fly, Viney wrote a year ago, they also provide protection from bumps and bruises.

“Clearly there is a useful suggestion here. But the materials engineer who hurries to cover his automobile with feathers might be better off wearing them himself.”

About the author

L.G. Blanchard covers engineering for the UW Office of News and Information. He lives on Vashon Island, Washington.

Adapted and reprinted with permission from “Doing what comes naturally,” Columns, The University of Washington Alumni Magazine (Sept. 1993).

Stephen Gunderson, a scientist at the University of Dayton Research Institute, would like to know how a large, black insect called the bess beetle can turn sugar and protein into an outer shell that is lightweight yet strong, stiff, and damage resistant. University of Washington researcher Christopher Viney is trying to figure out how spiders can spin water-soluble protein molecules into insoluble silk threads that are tougher than Kevlar—the stuff of bulletproof vests. Princeton University's Ilhan Aksay and Mehmet Sarikaya of the University of Washington are studying the abalone in an attempt to understand how it can crystallize chalk from seawater, and turn that substance into a shell that has twice the strength of the most advanced ceramics.

Elsewhere, scientists are studying

other natural materials, including rat teeth that can gnaw through metal cans; walnut and coconut shells that resist cracking; rhinoceros horn with self-healing properties; and the super-sticky glue that mussels manufacture to attach themselves to the ocean floor.

The researchers' goal is to unlock one of nature's best-kept secrets: how living organisms can turn simple building blocks into materials that are superior to advanced synthetic composites manufactured from the latest high-tech materials.

It is all part of a new area of research called biomimetics—the study of the structure and function of biological substances as models for material design and manufacturing. Biomimetics, or biological mimicking, has attracted researchers from fields as seemingly unconnected as materials science, molecular biology, engineering,

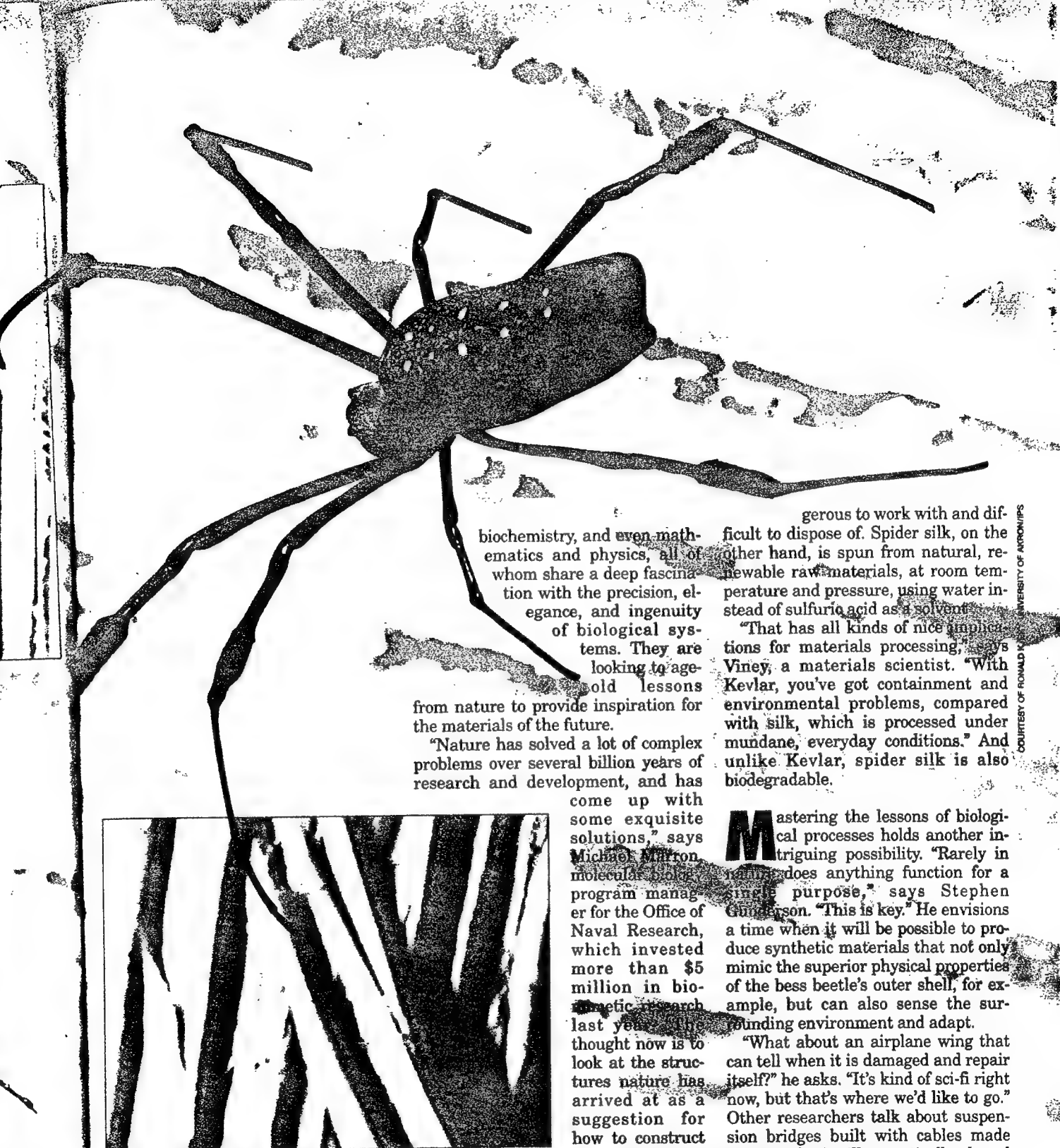
The bess beetle's sturdy shell is made from layers of fibers embedded in a protein matrix. At the microscopic level, it bears an uncanny resemblance to aerospace composites.



**Scientists are
creating new
materials by
copying the
structures of
beetle shells,
spider silk,
and rat teeth.**

BY TODD CAMPBELL

NATURE'S BUILDING BLOCKS



biochemistry, and even mathematics and physics, all of whom share a deep fascination with the precision, elegance, and ingenuity of biological systems. They are looking to age-old lessons

from nature to provide inspiration for the materials of the future.

"Nature has solved a lot of complex problems over several billion years of research and development, and has come up with some exquisite solutions," says Michael Marron, molecular biology program manager for the Office of Naval Research, which invested more than \$5 million in biomimetic research last year. "The thought now is to look at the structures nature has arrived at as a suggestion for how to construct new materials."

Following nature's lead may have advantages even beyond the promise of new substances with enhanced properties. Researchers believe that biomimetics will lead to compounds that are not only technologically superior, but are also environmentally benign. A synthetic fiber such as Kevlar, for example, is produced in vats of boiling sulfuric acid under very high pressure. The process is energy intensive, and the materials used are dan-

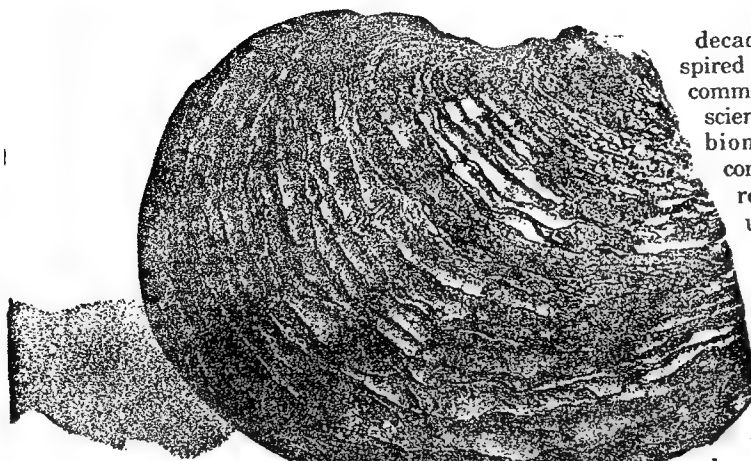
gerous to work with and difficult to dispose of. Spider silk, on the other hand, is spun from natural, renewable raw materials, at room temperature and pressure, using water instead of sulfuric acid as a solvent.

"That has all kinds of nice implications for materials processing," says Viney, a materials scientist. "With Kevlar, you've got containment and environmental problems, compared with silk, which is processed under mundane everyday conditions." And unlike Kevlar, spider silk is also biodegradable.

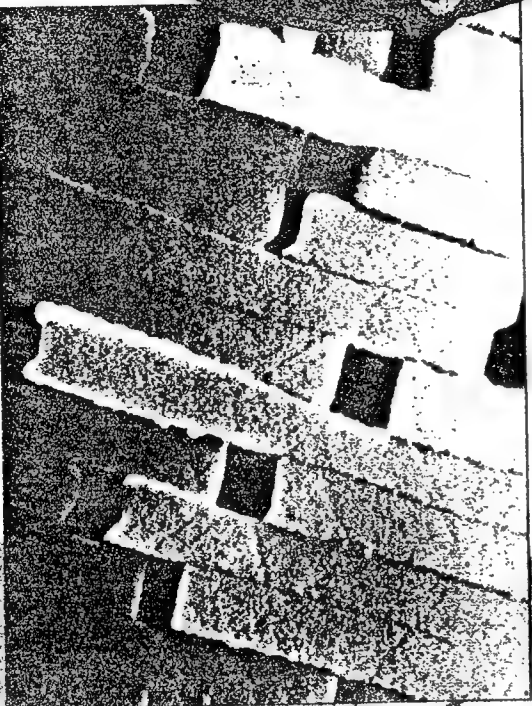
Mastering the lessons of biological processes holds another intriguing possibility. "Rarely in nature does anything function for a single purpose," says Stephen Gunderson. "This is key." He envisions a time when it will be possible to produce synthetic materials that not only mimic the superior physical properties of the bess beetle's outer shell, for example, but can also sense the surrounding environment and adapt.

"What about an airplane wing that can tell when it is damaged and repair itself?" he asks. "It's kind of sci-fi right now, but that's where we'd like to go." Other researchers talk about suspension bridges built with cables made from synthetic silk; genetically altered cells that grow new hard tissue to repair broken bones and replace missing teeth; drug delivery systems that can sense changes in the body and release precise amounts of drugs at specific locations; even miniature motors that draw their power from the same source as the human body, converting chemical energy into mechanical force. Wary of raising unreasonable expectations, researchers caution that it will be anywhere from five years to

Using water as a solvent, a spider called the golden orb weaver spins protein molecules into silk threads like the ones shown in this electron micrograph. Spider silk is tougher than Kevlar.



COURTESY OF KATE E.O. THORP, UNIVERSITY OF DAYTON RESEARCH INSTITUTE



The strong outer layer of calcium shell is composed of microscopic calcium carbonate "bricks" held together by an organic "mortar." This arrangement prevents cracks from forming, and makes the shell much less brittle than synthetic ceramics.

decades before bio-inspired materials become commonplace. For now, scientists in the field of biomimetics mostly concentrate on basic research aimed at uncovering the underlying rules governing the production of biological materials.

Their work has already led to an important new insight. What they

have discovered is that nature works with a small number of simple building blocks—sugars, proteins, minerals, and water—over which it exercises precise control at every level, from the arrangement of atoms into molecules, to the assembly of molecules into intermediate components such as fibers and crystals, up through to the final architecture of larger, multi-functional composite materials like wood, bone, or insect cuticle. The resulting natural structures are often breathtakingly complex and elegant.

The human approach to manufacturing synthetic materials is fundamentally different. Where nature works with simple materials and complex designs, humans start with a vast

number of advanced, complex compounds that are assembled in relatively simple ways. The microstructural control that is the norm in nature is still far beyond the capacity of human engineering.

Take the example of fiberglass. "By human standards it is a relatively complex material," says Stephen Wainwright, a mechanical biologist at Duke University who is considered one of the pioneers of biomimetics. "But there isn't a biological material in the world that is that simple."

In nature, a creature like the abalone is able to take a simple substance like chalk, which is not normally considered a useful structural material, and turn it into a surprisingly strong shell. Mehmet Sarikaya bought the abalone shell that inspired his research from a roadside stand while on a weekend trip in western Washington state. The battered and pitted shell does not look like a promising model for the materials of the future. But

when a team of researchers at the University of Washington looked at the shell with an electron microscope, they found a highly ordered brick-and-mortar configuration—layer upon layer of ultrathin calcium carbonate (chalk) platelets held together by an organic protein matrix just 10 billionths of a meter thick.

The microstructure of calcium carbonate endows the shell with an unexpected combination of properties: It has the strength of the most advanced synthetic ceramics, yet is not brittle like ceramics, which get their strength from the powerful chemical bonds that hold them together. Apply enough force to break these bonds, and the ceramic cracks. By contrast, the layered platelets of abalone resist the formation of cracks. "You don't get catastrophic failure in the abalone because the platelets slide on top of one another on the organic layer," says Sarikaya. "What we are saying is that the abalone shell deforms, and is behaving like a metal."

Sarikaya believes that, if he and his colleagues can design new substances using the principles they have gleaned from the abalone shell, they will be able to produce revolutionary new ceramic composites. The abalone shell's ordered structure increases the strength of calcium carbonate by a factor of 20, he says. "Would it be possible to increase the properties of current ceramic materials by even five times? That would be an incredible increase in strength, and we would have a new class of materials that would be far superior to anything we have today."

Sarikaya's team has developed a new material in which boron carbide, a ceramic, is suffused with aluminum. The aluminum appears to work in the same way as the organic protein matrix found in the abalone shell. The US Army has been testing the material as a possible new tank armor.

While Sarikaya's work with abalone shells promises to lead to new, high-performance ceramic materials, Stephen Gunderson's study of the structure of bess beetle cuticle may change the way composites are constructed for the aerospace industry. When Gunderson's colleagues at the University of Dayton Research Institute learned about his interest in insect exoskeletons as part of a search for new materials with potential aerospace applications, they brought him bugs. "My desk was inundated with insects," he recalls. "People would leave notes that said things like: 'This one ran into my windshield and didn't break.' One insect that found

at the end at scope, and so on by an 10 bil-

its way to his desk was the bess beetle. When viewed under an electron microscope, the bess beetle's cuticle shows a remarkable resemblance to the materials used in modern military aircraft. "We were amazed to see the similarity between its microstructure and some of the advanced composites we were working on," Gunderson says. Both are made of layers of fiber that are embedded in glue—sugar embedded in protein in the case of the beetle, graphite embedded in epoxy for synthetic materials. The layers are stacked to give strength and stiffness.

In synthetic composites, the lamination is a relatively simple, symmetrical design. Gunderson found that the lamination in the bess beetle cuticle is asymmetrical but highly ordered, with alternating layers precisely rotated so that the cuticle is formed from a pair of mingled spirals, what Gunderson calls a "dual helical lay-up."

Engineers who work with composites previously assumed that any structure made from an asymmetric layering would distort. But a panel made of a graphite epoxy composite following the beetle's architectural principles didn't warp. "It was so unsymmetrical that it was symmetric," says Gunderson. The resulting material proved to have better load-bearing characteristics and greater impact resistance than materials assembled in a traditional symmetric pattern.

But don't expect to fly in an airplane sheathed in a composite material that imitates the bess beetle's dual helical architecture anytime soon. While scientists like Gunderson are beginning to decipher some of nature's secrets, they are a long way from developing methods that will allow industry to mass-produce such materials. "We're still at the bottom rung of basic research," says Gunderson. "From the point we're at to actual use in an airplane is still years and years away."

Although the widespread use of biomimetic materials remains in the future, biomimetic research has already led to a number of patentable materials. At the University of Alabama, biophysicist Dan Urry has been studying elastin, a common protein found in skin and other elastic body tissue. He has developed a synthetic elastin that has been tested in rats and has proven to be extremely successful in preventing the formation of adhesions after surgery. Researchers at the University of Utah will use sheets of elastin to wrap an artificial heart they are developing.

By slightly modifying the same synthetic elastin, Urry has created a material that shows promise as a replacement for damaged tissue. "If you have a material with the same elasticity as normal tissue, you can make a temporary, synthetic scaffolding," Urry explains. Cells will be attracted to this scaffolding and grow, thus regenerating the damaged site. Such a material could even be used to fashion synthetic arteries. The same material also turns out to have super-absorbent properties. All told, 20 patents have been issued or are pending for the synthetic elastin developed by Urry's research team.

It remains to be seen whether Urry's flurry of patentable materials signals the beginning of a new era, in which materials inspired by natural models gradually replace the petroleum-based plastics and fabrics that have been the hallmark of most of this century's technology. And it is still too early to predict whether humankind, having evolved through the Stone Age, the Bronze Age, and the Iron Age, is on the precipice of the transition from the Oil Age into the Biomimetic Age.

At the very least, however, it seems clear that recent advances in a host of technologies ranging from electron microscopy to genetic engineering have allowed an adventurous group of scientific explorers to take a peek into the inner workings of nature. If they succeed in solving some of the fundamental mysteries that govern these natural processes, a scientific revolution could be just around the corner. **BS**

Seen here under magnification, a rat's tooth is made from rods of a calcium compound embedded in a fibrous protein called collagen. This structure makes the tooth wear-resistant and tough enough to gnaw through cans.



COURTESY OF J.W. BURDON & P.D. CALVERT, UNIVERSITY OF ARIZONA

ANIMALS, ANIMALS



DEPARTMENTS

EDITOR'S NOTE
4

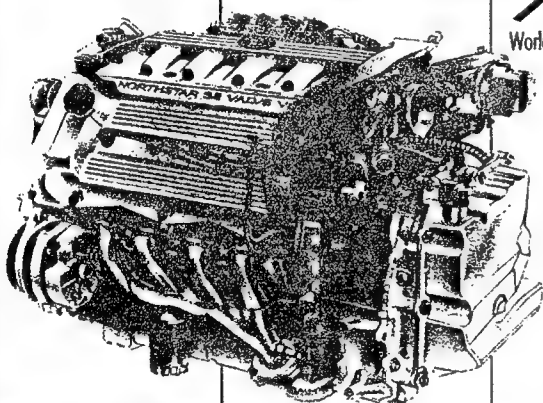
READERS TALK BACK
6

WHAT'S NEW
10

NEWSFRONTS

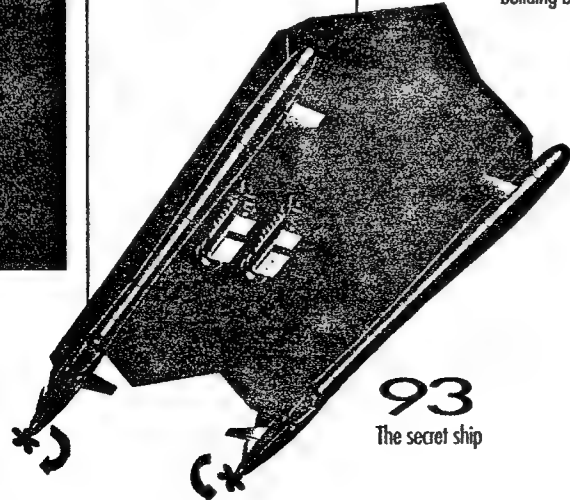
Science & Technology 25
Automotive 35
Electronics 45
Computers & Software 55
Home Technology 61

LOOKING BACK
134



84
Power for the future

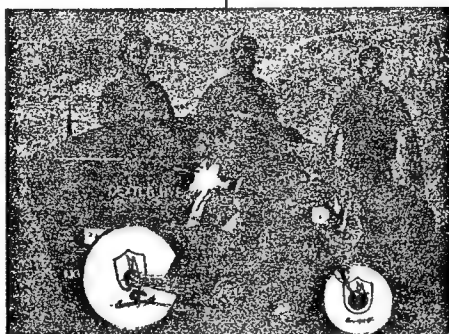
66
The outlook for hydrogen



93
The secret ship

Popular Science

THE WHAT'S NEW MAGAZINE



78
World's fastest bike



74
Nature's building blocks

FEATURES

THE OUTLOOK FOR HYDROGEN **66**

If the Utopian promise of a hydrogen economy remains unfulfilled, it's not for lack of effort. The concept continues to be a potent attraction, with vocal advocates.

NATURE'S BUILDING BLOCKS **74**

By copying such materials as beetle shells, spider silk, and rat teeth, scientists are creating new materials that are superior to the most advanced synthetics.

THE WORLD'S FASTEST BIKE **78**

An innovative semi-recumbent bicycle is pushing the speed frontier for human-powered vehicles.

AUTOTECH '94 **POWER FOR THE FUTURE** **84**

Domestic automakers are introducing fundamentally different engine designs. The new motors are smaller but more efficient, and with improved emissions.

THE SECRET SHIP **93**

A secret experiment in seagoing stealth glides into the light of day. The Navy's Sea Shadow is designed to be nearly invisible to radar.

ROAD WORK **98**

When your desk is an airplane tray table, it pays to plan ahead. Our itinerant editor introduces you to the perils and pleasures of computing on-the-go.

PREVIEW GUIDE **IMPORT CARS TO COME:** **1994-1997** **103**

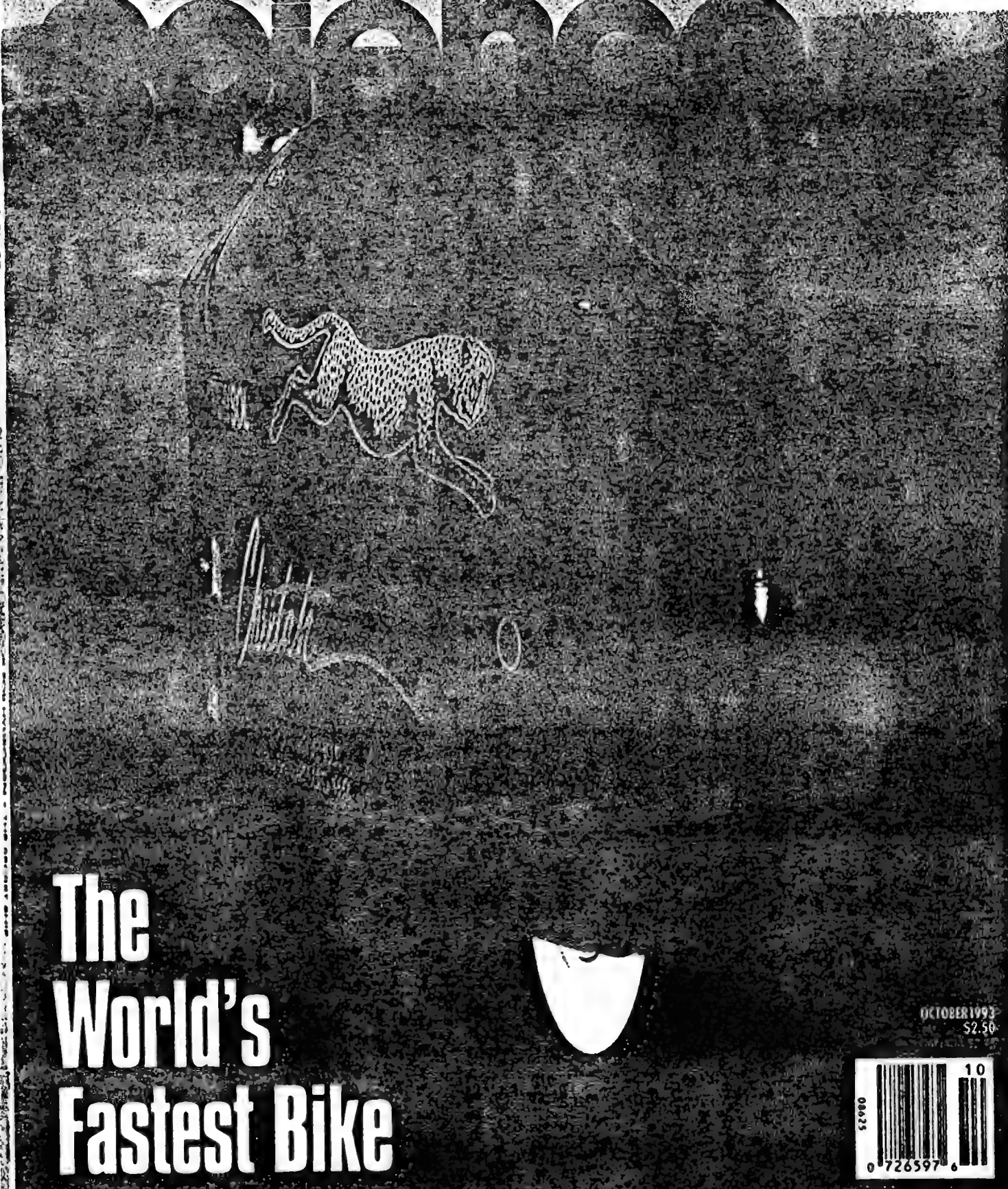
After years of U.S. expansion and high profitability, overseas car makers are now feeling the pressure. They're responding with higher performance, more efficient offerings.

A TIMES MIRROR MAGAZINE
FOUNDED IN 1872
VOLUME 243
NUMBER 4
COVER PHOTO BY JOHN B. CARNETT

POPULAR SCIENCE

A J. Ross Publishing Magazine

Hydrogen:
The Forever
Fuel



The World's
Fastest Bike

OCTOBER 1993
\$2.50



TECHNOLOGY

The mother of all pearls

DOUGLAS Adams wrote in the third part of his series the *Hitchhiker's Guide to the Galaxy*, "very few things actually get manufactured these days, because in an infinitely large universe . . . most things one could possibly imagine, and a lot of things one would rather not, grow somewhere." As an example, he described a forest where trees grow ratchet screwdrivers as fruit.

Adams may soon be proved right, but without going so far afield. Researchers are now trying to harness the way living organisms can produce useful inorganic materials. They hope to produce thin coatings which are tougher than any synthetic ceramic and microscopic magnets that could one day be used in tiny machines.

Synthesising these organically made materials, a process called biomimetics, is relatively easy, Mehmet Sarikaya of the University of Washington in Seattle told the American Physical Society meeting in Indianapolis last week. What he is trying to do is copy the organism's own manufacturing techniques, to avoid the expensive high temperatures and pressures of synthetic methods.

Sarikaya wants to make thin films of a

Daniel Clery, Indianapolis

material called nacre, more commonly known as mother-of-pearl. The material covers the inside of shells belonging to creatures such as abalone, nautilus and bivalves, and is twice as tough as any synthetic ceramic.



Oyster cult: synthetic nacre will be tougher than any ceramic

of a matrix of hexagonal prisms of calcium carbonate. The inside of the shell is coated with nacre which consists of flat hexagonal platelets of calcium carbonate laid down in a multilayered tiling pattern.

The cells of the abalone closest to the nacre layer produce proteins which are responsible for forming the nacre. The cells release the proteins into a thin layer of sea water between them and the shell. The water also contains calcium and carbonate ions and by some unknown process the proteins form these ions into platelets and cement them in place as a new layer of nacre.

Sarikaya has managed to isolate the proteins responsible for forming nacre and is about to set about identifying them.

Once he knows the identity of the proteins, he will find the gene responsible for producing them and, using genetic engineering, insert it in the bacterium *Escherichia coli*. This bacterium will then produce the proteins in usable quantities.

Sarikaya then hopes he will be able to cover objects with a tough coating of nacre by immersing them in a solution of the proteins and necessary ions. His work is only in its early stages and he does not expect to accomplish this for at least five years.

Meanwhile, Richard Frankel, of the Californian Polytechnic State University, is studying waterborne bacteria that find their way around with their own compasses. "They are a masterpiece of permanent magnet engineering," Frankel says.

Inside these "magnetotactic" bacteria are sacks made of a membrane that gathers iron and oxygen ions from the water to create particles of an oxide called magnetite, each of them just 50 nanometres across. Magnetite, also known as lodestone, was used by the ancient Greeks to make the earliest compasses but, as Frankel points out, bacteria discovered it millions of years earlier.

The bacteria produce particles of magnetite with a very precisely controlled size and shape. Each bacterium also links up about half a dozen particles in a chain which produces a stronger magnet.

These bacteria use the magnets to follow the flux lines of the Earth's magnetic field. One type of the bacterium only swims towards the magnetic pole, which in effect takes it downwards into deeper water. Another type can move up and down the flux line until it finds the best conditions.

Frankel has succeeded in removing the particles from the bacteria and removing the membrane sack around them. He is now analysing the protein in the sacks and hopes that this may make it possible to manufacture microscopic magnets to order, or particles of other ceramics. □

State of the arc for waste disposal

AMACHINE that can tear noxious chemicals apart into their constituent atoms was commissioned last week by Australia's largest herbicide manufacturers, Nufarm.

Inside the machine an electric arc is fired between two copper terminals in a tube filled with argon gas. The arc creates a plasma—a hot gas made up of atoms, ions and electrons—within which temperatures reach 10 000 to 15 000 °C, about twice as hot as the surface of the Sun.

Toxic organic chemicals—such as dioxins and polychlorinated biphenols (PCBs)—fed into this electric arc are blasted apart. By carefully controlling physical and chemical conditions, the elements can be recombined to form simple, and relatively harmless, compounds such as carbon dioxide, water and hydrochloric acid.

At present, Australia has no means of disposing of such hazardous wastes. They are shipped overseas for treatment in high-temperature incinerators. A panel of experts is touring the country exploring the potential for setting up an incinerator in Australia. But the idea has met stiff opposition (*New Scientist*, 8 June 1991, p 35).

The new technology was developed at the Division of Manufacturing Technology of the CSIRO, Australia's national research body. The critical problem was to find a means of ensuring that the stream of waste

passed through the hottest part of the arc.

This was solved by pumping the stream into the tube from the centre of the anode, the positive electrode. The shape of the arc is kept stable by an external magnetic field, which ensures the wastes always enter the hottest part of the arc. The CSIRO research group says that the plant destroys virtually all chemicals.

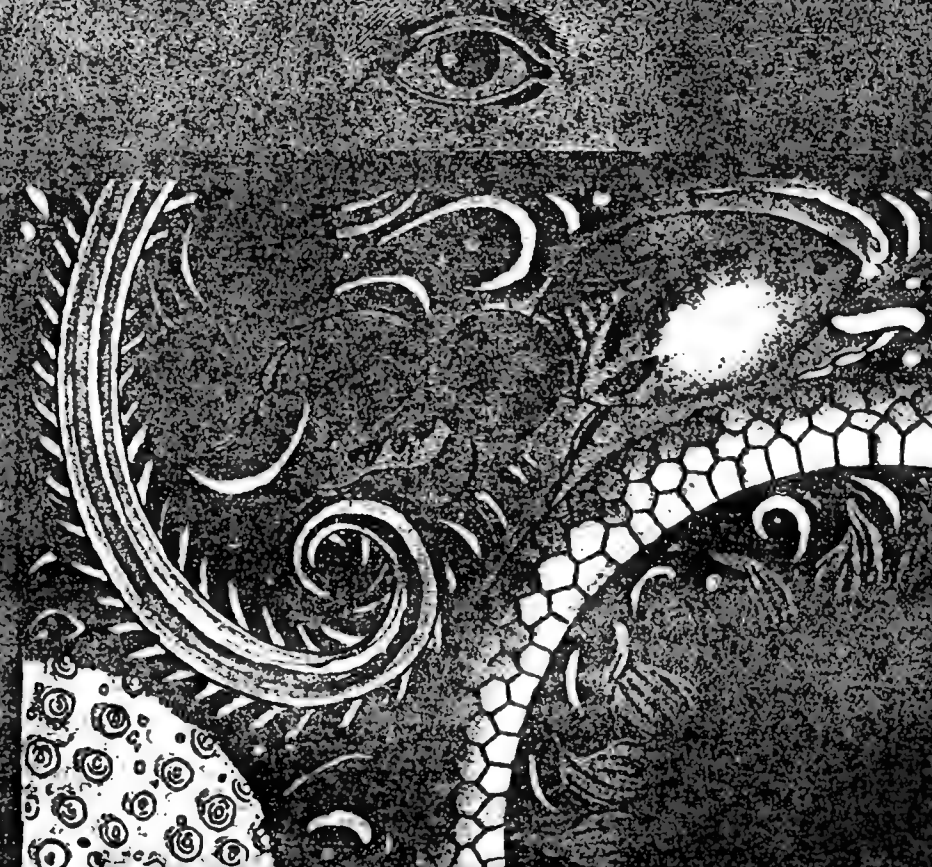
The reaction tube and associated equipment is compact enough to fit into a standard chemical production line, allowing wastes to be treated as they are produced. This saves the cost and hazard of moving them to a large central incinerator.

A company spokesman, Robert Reis, said Nufarm had selected the technology after examining about 20 other methods of disposal worldwide. It has spent about A\$2 million (£1 million) developing and installing the 200-kilowatt pilot unit, which can treat about 700 litres of waste.

The CSIRO research team calculates that the system will cost less than A\$2 a litre to operate, a considerable saving on the A\$5 to A\$6 a litre it presently costs to dispose of the waste. Rama Ramakrishnan, who heads the team, believes the system will be used with conventional technology to dispose only of the most intracable wastes. It may even be used in the destruction of US chemical weapons on Johnston Atoll in the Pacific. □

THE PRIVATE EYE

(S)X-LOOKING, THINKING BY ANALOG



A GUIDE TO DEVELOPING
THE INTERDISCIPLINARY MIND
HANDS-ON THINKING SKILLS,
CREATIVITY, SCIENTIFIC LITERACY.

THE PRIVATE EYE®

The Private Eye is a program about the drama and wonder of LOOKING CLOSELY at the world, THINKING BY ANALOGY, and CHANGING SCALE. It's also about THEORIZING. Designed to develop higher order thinking skills, creativity, and scientific literacy - across subjects, it's based on a simple set of "tools" that produce "gifted" results.

Hands-on, investigative, The Private Eye - using everyday objects, a jeweler's loupe, and simple questions - accelerates science, writing, art, math, and social studies; as well as vocational and technological education; it builds communication, problem solving, and concentration skills. For K-12 through life, all levels, The Private Eye develops "the interdisciplinary mind."

Cover illustration by Julie Paschus



The Private Eye® Project Seattle, Washington



51800



□ BIOMIMETICS: Nature as Engineer:

Biomimetics is the science of imitating nature to solve *analogous* human problems.

A FEW EXAMPLES:

Look for more after you've studied these. (See Velcro, opposite page.)

- **Barnacle Glue:** The glue of barnacles is under study by dentists for dental applications.
- **Grow a House, a Bridge, a...**

The Seattle Times, January 15, 1990
by Frederick Case

Chasing Nature's Engineers

Richland - You might think that highly trained scientists can't learn much from an ordinary nautilus sea shell or an old bone. But in all the exploding new multi-billion-dollar field of materials technology, possibly the most exciting development is biomimetics, the science of imitating nature.

Back in pre-Cambrian times, mollusks invented a way to shield their soft bodies by exuding a calcium-carbonate mixture that swiftly solidified into a marble-hard shell. Some 600 million years later, scientists in Washington are struggling to match the lowly shellfish's skill.

"We have a lot to learn," says Gary McVay, manager of the materials sciences department at Pacific Northwest laboratory [Richland, Washington]. "We humans think we're pretty smart, but when you look at what nature has evolved over millions of years it puts us to shame. Even spider webs are much stronger than steel."

The lab's aim is to help launch a new industrial era in which houses, bridges and even airplanes can be built by "growing" new shatterproof material called bioceramic.

• A Bricks-and-mortar world:

"Natureworks - Making minerals the biological way," by Elizabeth Pennisi, in *Science News*, May 16, 1992, gives a magnified look at the source of these investigations into "growing" bioceramics.

"The secret lies in the way organisms put a mineral's molecules together... and the size and shape of the resulting crystal."

A line of inquiry begins, typically, not with high powered, lab-only magnifiers, that can "see" the tiny, underlying crystalline structures of our world - but with a hands-on, natural scale experience of a material, looking closely with "eyes like loupes," using a field loupe if handy, thinking by analogy and theorizing based on those analogies. The *Science News* article offers this anecdote:

"Six years ago, while visiting the Olympic Peninsula in Washington, Sarikaya bought a red abalone shell from a street vendor. The abalone survives for decades, adding about an inch a year to its armor until the shell measures about a foot across. The shell, a natural ceramic consisting of 95 percent inorganic material, fascinated Sarikaya. ...Sarikaya wondered what he would see if he examined the shell from a materials scientist's perspective - with the inorganic part intact."

He found a brick-and-mortar configuration, and the mortar itself seemed layered. How does the abalone do it? Sarikaya's team is studying the abalone, Richland's labs are studying the barnacle, and other researchers are investigating how yet other organisms build their bones and shells and teeth.

• Spider Silk Vest

Stephen Lombardi has succeeded: "in engineering the gene for spider silk into a bacteria that produces a fiber stronger than a silkworm's

silk - indeed, far stronger than steel.

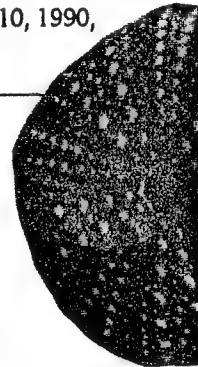
"Lombardi, who works at the Army's research laboratory in Natick, south of Boston, devised his method of replicating spider silk last spring.

"Spider silk has five to 10 times the tensile strength of steel and can be stretched about 18 percent without breaking. Because of its toughness, spider silk is likely to replace Kevlar as the military's choice for bulletproof vests, Lombardi said."

- Associated Press, *The Seattle Times*, 2/27/90.

• **Human Sonar:** Adam A. Jorgensen thought that if bats and owls can navigate through the darkness, their bio-technology could be applied to blind people. He's mimicked the natural sonar system - and patented a hand-held echolocation aid that will, when it's perfected, "enable a visually impaired person to learn to 'hear the distance' as skillfully as he or she can read Braille, Mr. Jorgensen said."

The New York Times, March 10, 1990, in the Patents section.



□ You, the Inventor the Designer, the Biomimetics Scientist:

In pairs or teams: loupe-analogy look at a natural object. As you loupe-look ask the usual loupe-look questions: "What else does that look like? What else does it remind me of?" and then add a slightly different version of the question: "What else is that *like* - that human beings need? Feel? Could use? Analogous to what? If the barnacle is attached by some kind of "glue," could it offer an improvement to current human glues?

Make up 10-20 analogies. List 5-10 analogy-based inventions or technologies or materials - however futuristic or



• Doing What Comes Naturally

*Plastic is Passé—The Secrets of Slug
Slime, Spider Spit and Mollusk
Shells Will Cause a Revolution in
What Our World is Made Of.*

by L.G. BLANCHARD



EVER SINCE THE FIRST HUMAN cast an envious eye at a bird's ability to fly, people have looked to the natural world for ideas to imitate and shape to their own needs.

Today, armed with powerful computers, imaging devices and other advanced technologies, engineers and scientists from many disciplines have begun to take the closest look ever at how and why nature does what it does — at all levels, from individual molecules and cells to entire organisms.

That look will result in a revolution, say engineering professors at the UW. Just as biotechnology is changing the way we fight disease and advance our health, another "bio" discipline — called "biomimetics" — will change the materials we use to work and live.

"We are on the brink of a materials revolution that will be on a par with the Iron Age and the Industrial Revolution," says Materials Science and Engineering Professor Mehmet Sarikaya. "We are leaping forward — we are not running — into a new era of materials. Within

Spider web photo © 1990, Darrell Gulin

the next century, I think biomimetics will significantly alter the way in which we live."

Biomimetics draws on some of the most powerful source material imaginable: hundreds of millions of years of evolution in which nature, slowly, painstakingly, has perfected or discarded creature after creature, adjusting and refining all life.

Reaching into nature's vast trove of time-tested, unpatented ideas — some of the very processes that have enabled the world to tick on quite nicely, thank you, for as long as it has — these researchers think they can figure out how to make useful things from materials that not only are stronger, tougher and superior to what we have today, but that also don't harm the environment or use excessive amounts of energy.

To this end, scientists at the UW College of Engineering and elsewhere have begun — barely, they concede — to take apart and analyze everyday marvels from the natural world: things as simple as how a spider spins its silk, a slug secretes its mucus, or an abalone grows its shell.

The payoff will not begin for a decade or two. But when it comes, brace yourself for what *Newsweek* last

For its size, spider silk is stronger than steel. UW scientists want to create materials with similar properties, which might lead to stronger suspension bridges.

December, in an article describing biomimetics at the UW, termed "the next revolution in what the world is made of."

Even at its infancy, the field's possibilities are stunning:

- ships, aircraft, cars, clothes, buildings and yes, even picture windows made from materials that heal themselves when dented, hit, punctured or smashed;
- long bridges spanning Puget Sound and other waterways, suspended from glistening, lightweight cables no thicker than a garden hose yet possessing previously unknown strength, toughness and durability;
- thin, gel-like coatings that come in a tube and can be applied to human skin, giving police officers and firefighters instant protection from bullets and flames;
- ecologically ideal building construction materials that can be instantly manufactured at room temperature from virtually whatever happens to be present in sufficient quantities — be it dirt, pine needles or chalk;
- and whole, complex chemical "factories" capable of rendering even the most toxic organic compounds harmless — located within the confines of a single organic cell.

How necessary is this revolution? Materials scientists say the world has taken petroleum-based plastics and fabrics about as far as possible. But the need for new, tougher, stronger, lighter and more energy efficient and environmentally sound materials is ever present.

"Basically, we're stuck," says Sarikaya, a pioneer in biomimetics. "The world needs lighter planes, lighter

cars, lighter engines that can operate at much higher temperatures, and a host of other new materials. But today, we're still working with the ceramic materials we've had for the past 25 to 30 years, for example, and metals that have been around for 100 years."

UW Bioengineering Professor Christopher Viney half-jokingly puts it like this: "The challenge is to make things that are stiff and tough and have the right color and the right fatigue properties, that don't cost anything, won't hurt the environment and can be made out of beach sand."

Viney, who also is an adjunct professor in materials science and a 1992 UW Distinguished Teaching award-winner, weaves his biomimetics research into lectures for incoming engineering students. First, he shows a slide of a helicopter made from Lego bricks. He asks the students to describe what they see. "They always respond the same way," says Viney. "They either say it's a helicopter, Lego bricks, gears or some such thing — but I never get the answer I'm trying to lead them to."

Next, he flashes up a slide of a tractor and crane, also built from Lego bricks. "I tell the students, 'Same Lego kit, exactly the same pieces. Different toys built from it.' And then I go on to explain that what nature offers us is a set of building blocks: 20 amino acids. And from these, all the proteins in the world — the millions of different types of proteins necessary to sustain every form of life on earth — are manufactured. But there are only 20 types of blocks in the starter kit. Just 20.

"The idea is to bring nature into the repertoire of tools for inspiration and get ideas for how to proceed," he continues. "Nature didn't teach us to make those things, but there are some really neat starting materials lying around."

"We are on the brink of a materials revolution that will be on a par with the Iron Age and the Industrial Revolution."

Viney and Sarikaya are among approximately 500 biomimeticians in the United States — a field where the U.S. is the undisputed world leader. The goal, the two agree, is not only to understand nature's way of doing things, but to do nature one better — and perhaps faster. "The traditionalists say, 'If nature makes it, what's new?'" says Viney. "That's why I am very careful to say, we are selecting what we learn from nature — not trying to copy it exactly, because there would be no point in that."

Currently, Viney's main research interest is liquid crystals — substances suspended in a state somewhere between a solid crystal and a liquid. Millions of us wear artificial liquid crystals on our wrists: they make up the display screen for digital watches.

While liquid crystals may be commonplace in a watch, Viney and his colleagues surprised the scientific world when they wrote that silk secreted by silkworms

gives it the ability to give exceptional strength to temporarily becoming a liquid crystal. The 1991 report, published in *Nature*, was co-authored by UW graduate student Keven Kerkam, and colleagues from the U.S. Army Research, Development and Engineering Center.

The team found that as the golden orb weaver spider secretes its webbing, molecules in the droplets align themselves in rod-like structures — passing through an interim phase in which they take on a semi-ordered structure. The result is a material that, when solidified, can support far more weight for its size than steel.

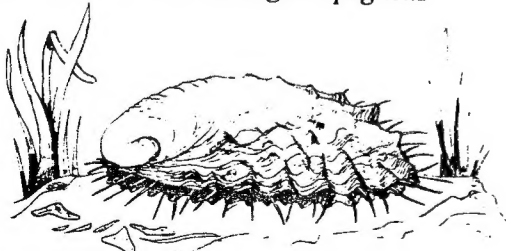
By understanding how spider silk works, Viney believes we may someday use this information to improve bulletproof vests and build stronger suspension bridges, for instance.

Viney and others involved in biomimetics often speak of "hierarchical microstructures," which are like a catalog of Lego constructions. The same components can be assembled and reassembled again and again in things that may be very different from one another.

How different? As unlike, say, as multi-legged spiders and slimy slugs. Earlier this year, Viney, Bioengineering and Biostucture Professor Pedro Verdugo and UW graduate student Anne Huber became the first to report that there's much more to the mucus highway secreted by common banana slugs than previously thought.

Though mucus research lacks mass appeal, it can shed light on a host of human health problems, including cystic fibrosis and other abnormalities in the reproductive and digestive tracts. To Viney and Verdugo, mucus is one of nature's most remarkable substances. Slugs use it not only for transportation, but also for protection — enabling them, for instance, to creep harmlessly along the edge of a razor blade.

Verdugo, who has studied mucus in a variety of species for nearly two decades, and other researchers had thought that the microstructure of mucus was much like a randomly tangled web of spaghetti — its consistency dependent on the extent of tangling (the more tangled, the thicker). However, once released from the small granules in which it is stored inside the cell, slug mucus can swell up to 50 times its initial volume — so fast that researchers use the term "explosive." In fact, mucus granules can expand from 10 to 500 microns in 15 to 20 milliseconds. And this had researchers stumped: How can something expand so fast, so efficiently, if it is as disorganized as a bowl of tangled spaghetti?



Shell game: UW scientists are studying the red abalone, *Haliotis rufescens*, found along the coast of Southern California and Baja California. Drawing courtesy of Mehmet Sarikaya.



Bricks and mortar: At top, an electron microscope enlarges a section of an abalone shell 10,000 times, showing the brick-and-mortar architecture. At bottom, an electron microscope image of a fracture surface suggests that the shell is tough and strong. Photos courtesy of Mehmet Sarikaya.

Now, much more is known, thanks to Viney and colleagues. Earlier this year, they showed that slug mucus is highly organized, not random. They found that before secretion, mucus molecules are stored in tightly packed, accordion-like bunches like jack-in-the-boxes. When secreted, the molecules — polymers with all the characteristics of liquid crystals — absorb water, expanding at high rates without involving high amounts of energy.

The tremendous range of expansion and condensation is what makes mucus one of nature's "very best inventions," says Verdugo. Understanding the structure is the key to the design of new and highly efficient polymer gels. "Now we have a gateway to understanding how to develop new technology. We have the blueprints nature used, and we can re-engineer them in our own land."

While much research remains, Verdugo, Viney and others foresee many potential inventions coming from biomimetic materials based on mucus. For example, they might foster new drug delivery systems for cancer patients, pollutant traps in sewage treatment plants, and water-based lubricants. And if mucus makes such an ideal highway for slugs, light rail might someday be replaced by slime rail.

Another gastropod, the red abalone, absorbs much of Sarikaya's interest. Over the course of its life, this sea-dwelling creature produces an impact-resistant shell so hard it can be run over by a truck without breaking. But if the shell does get damaged in the natural world, it heals itself — and later, when its occupant dies, the shell readily biodegrades. Finally, the abalone and similar organisms manufacture their shells at sea-water temperature using a readily available ingredient: calcium carbonate, a.k.a. chalk.

Broken down into components, abalone shells are

relatively simple, explains Sarikaya, much like a single Lego brick. When assembled, however, the components — ranging in size from molecules to millimeters — function together to provide a material well worth mimicking: one that incorporates superb properties of toughness and strength.

It's how these components, these bricks, are put together that makes the shell a miracle material. Using powerful electron microscopes, Sarikaya found beneath the shell's outer portion a section consisting of extremely thin layers of laminate. It's here that nature's masons are at work, as flat bricks of calcium carbonate are set off from one another in typical brick-wall fashion. The "mortar" holding them together consists of small amounts of organic matter, mostly proteins and sugars.

Sarikaya and colleagues tested the abalone's composite material and found that it has greater toughness and strength than conventional ceramics alone, owing to its brick architecture and the organic mortar. The next step is to unlock how the mollusk produces the proteins and sugar molecules that make up the mortar. Then they must discover how this material finds its way through the watery environment within the shell to the correct layer — and, once there, assembles itself exactly where it is needed.

To help break the secrets, Ilhan Aksay, formerly at the UW and now at Princeton, and Sarikaya enlisted the help of genetic engineers on the faculty of the UW School of Medicine: Medical Geneticist Clement Furlong

and Microbiologist James Staley. The team hopes to invent genetically engineered organic "templates." With these plans Sarikaya thinks he can grow technological materials the same way as an abalone produces its shell.

THERE EVEN IS THE possibility of duplicating, perhaps using different materials, the abalone shell's ability to self-heal. Does this mean it could never be destroyed? Not to worry, says Sarikaya; science also will come up with a way to switch this capability on and off.

This concept and other as-yet-unanswered questions about biomimetics lead even its chief proponents to caution that the future is not now. But it is coming, and at a far faster speed than it took technology to travel from Kitty Hawk to Cape Canaveral.

Ah, but if we are going to take things from nature, how can we be sure nature is right? "You can't be," answers Viney. "Nature has some ideas. That is, nature has optimized everything very nicely for what nature has to do. But this isn't always 'right' for biomimicking."

Feathers not only help birds fly, Viney wrote earlier this year, they also provide protection from bumps and bruises.

"Clearly, there is a useful suggestion here. But the materials engineer who hurries to cover his automobile with feathers might be better off wearing them himself."

L.G. Blanchard covers engineering for the UW Office of News and Information. He lives on Vashon Island.

Husky Apples in a gift pack

Available now, a unique product that offers you the ability to share a little bit of Washington with all your special friends, business associates or just someone you care a great deal about.

Maybe yourself!

Order today!
Call anytime between
5:30 a.m. and 5 p.m.

Mondays thru Friday

1-800-260-5520

or fax us at

(509) 558-4798

or mail your order to:

Taplett's Apples

P.O. Box 2522

Wenatchee, WA 98807

Price: \$12 plus
shipping included in
WA, OR and CA.

Other continental

states at \$3.95

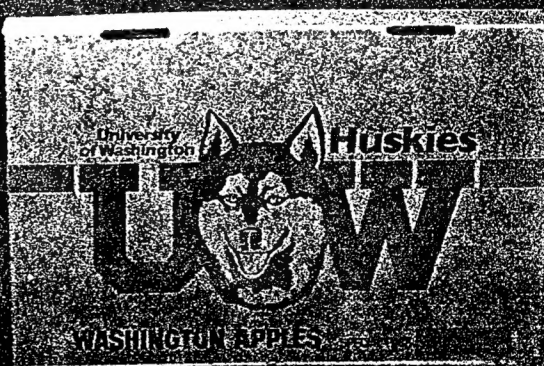
Alaska and Hawaii at

\$27 plus shipping

call for quote.

Orders shipped within

7 days of receipt of order.



Ask about our
100 years of
Husky football
print offer.

A Very Tempting Offer from Taplett Fruit